

STATE OF NEW MEXICO

DEPARTMENT OF ENERGY, MINERALS, AND NATURAL RESOURCES
OIL CONSERVATION COMMISSION

APPLICATION OF THE NEW MEXICO OIL
CONSERVATION DIVISION TO ADOPT 19.15.27 NMAC
AND 19.15.28 NMAC, AND TO AMMEND 19.15.7 NMAC,
19.15.18 NMAC, AND 19.15.19 NMAC; STATEWIDE

CASE NO. 21528

ENVIRONMENTAL DEFENSE FUND'S LIST OF EXHIBITS – VOLUME I

1. *Santa Fe Exploration Co. v. Oil Conservation Comm'n of State of N.M.*, 835 P.2d 819 (1992)
2. *Swepi, LP v. Mora County*, N.M., 81 F.Supp.3d 1075, 1196 (D.NM 2015)
3. *El Paso Natural Gas Co. v. Oil Conservation Comm'n*, 414 P.2d 496 (1966)
4. EDF's proposed redline of OCD rules.
5. Resume of Jon Goldstein
6. Executive Order 2019-003 on Addressing Climate Change and Energy Waste Prevention (Jan. 29, 2019)
7. New Mexico Climate Strategy, Initial Recommendations and Status Update (2019)
8. New Mexico Climate Strategy, 2020 Progress and Recommendations
9. New Mexico Oil & Gas Data, New Analysis Reveals Persistent Problem (updated November 2020), <https://www.edf.org/nm-oil-gas/>
10. Resume of David R. Lyon, Ph.D.
11. Wuebbles, Donald et al., U.S. Glob. Change Research Program, *Climate Science Special Report (CSSR)* (fifth order draft) (final clearance June 28, 2017), https://science2017.globalchange.gov/downloads/CSSR2017_FullReport.pdf
12. Myhre, Gunnar et al., *Anthropogenic and Natural Radiative Forcing in: Climate Change 2013: The Physical Science Basis*. Contribution of Working Group I to the Fifth Assessment Report of the Intergovernmental Panel on Climate Change, ch. 8, https://www.ipcc.ch/site/assets/uploads/2018/02/WG1AR5_Chapter08_FINAL.pdf.
13. Bradbury, James et al., Dep't of Energy, Office of Energy Policy and Systems Analysis, *Greenhouse Gas Emissions and Fuel Use within the Natural Gas Supply Chain – Sankey Diagram Methodology* at 10 (July 2015), https://www.energy.gov/sites/prod/files/2015/07/f24/QER%20Analysis%20-%20Fuel%20Use%20and%20GHG%20Emissions%20from%20the%20Natural%20Gas%20System%2C%20Sankey%20Diagram%20Methodology_0.pdf
14. Atmospheric Lifetime and Global Warming Potential Defined (updated November 2020), <https://www.epa.gov/climateleadership/atmospheric-lifetime-and-global-warming-potential-defined>
15. U.S. Climate Change Science Programs Synthesis and Assessment Product 3.2, *Climate Projections Based on Emissions Scenarios for Long-Lived and Short Lived Radiatively Active Gases and Aerosols* at 64-65 (2008)

16. *Methane: The Other Important Greenhouse Gas*, EDF (accessed Dec. 15, 2020), <https://www.edf.org/methane-other-important-greenhouse-gas>
17. Alvarez, Ramon A. et al, *Assessment of Methane Emissions from the U.S. Oil and Gas Supply Chain*, 361 *SCIENCE* 186-88 (2018), <https://science.sciencemag.org/content/361/6398/186>
18. Omara, Mark et al., *Methane Emissions from Natural Gas Production Sites in the United States: Data Synthesis and National Estimate*, 52 *ENVIRON. SCI. TECHNOL.* 12915-25 (2018), <https://pubs.acs.org/doi/abs/10.1021/acs.est.8b03535>
19. Schneising, Oliver et al., *Remote Sensing of Methane Leakage from Natural Gas and Petroleum Systems Revisited*, 20 *ATMOS. CHEM. PHYS.* 9169-82 (2020), <https://acp.copernicus.org/articles/20/9169/2020/>
20. Robertson, Anna M et al., *New Mexico Permian Basin Measured Well Pad Methane Emissions Are a Factor of 5–9 Times Higher Than U.S. EPA Estimates*, 54, 21 *ENVIRON. SCI. TECHNOL.*, 13926-13934, 2020
21. Rutherford, Jeffrey S. et al., *Closing the Gap: Explaining Persistent Underestimation by US Oil and Natural Gas Production-Segment Methane Inventories*, *EARTHARXIV* (in review), <https://eartharxiv.org/repository/object/1793/download/3784/>

Exhibit 1

JUSTIA

Laws & Legal Resources.

Receive free daily summaries of new opinions from the **New Mexico Supreme Court.**

Santa Fe Exploration Co. v. OIL CONS. COM'N

835 P.2d 819 (1992)

114 N.M. 103

SANTA FE EXPLORATION COMPANY, Petitioner-Appellant, v. OIL CONSERVATION COMMISSION OF the STATE OF NEW MEXICO, Respondent-Appellee, and STEVENS OPERATING CORPORATION, Petitioner-Cross-Appellant, v. OIL CONSERVATION COMMISSION OF the STATE OF NEW MEXICO, Respondent-Cross-Appellee.

No. 19707.

Supreme Court of New Mexico.

July 27, 1992.

*821 Padilla & Snyder, Ernest L. Padilla, Santa Fe, Brown, Maroney & Oaks Hartline, K. Douglas Perrin, Dallas, Tex., for appellant.

Robert G. Stovall, Santa Fe, for Oil Conservation Com'n.

Campbell, Carr, Berge & Sheridan, William F. Carr, Santa Fe, for Stevens Operating Corp.

OPINION

BACA, Justice.

This appeal involves a series of orders issued by the New Mexico Oil Conservation Commission (the "Commission") and the New Mexico Oil Conservation Division (the "Division"). These orders established and govern the production of oil from the North King Camp Devonian Pool (the "Pool") in which appellant, Santa Fe Exploration Company ("Santa Fe"), and cross-appellant, Stevens Operating Corporation ("Stevens"), owned interests. After the Division approved Stevens's request to drill a *822 well at an unorthodox location and limited production from the well, both Santa Fe and Stevens petitioned the Commission for a de novo review. After consolidation of the petitions, the Commission, in its final order, approved the Stevens well, placed restrictions on Stevens's production from this well, and limited oil production from the entire Pool. Pursuant to NMSA 1978, Section 70-2-25 (Repl.Pamp. 1987), both Santa Fe and Stevens appealed the final order of the Commission to the district court, which affirmed. Both parties appeal the decision of the district court. We note jurisdiction under Section 70-2-25 and affirm.

I

In December 1988, at the request of Santa Fe, the Division issued Order No. R-8806, which established the Pool and the rules and regulations governing operation of the Pool. These rules established standard well spacings and a standard unit size of 160 acres; regulated the distances that wells could be placed from other wells, the Pool boundary, other standard units, and quarter-section lines; set production limits for wells in the Pool; and outlined procedures for obtaining exceptions to the rules. The order also approved Santa Fe's Holstrom Federal Well No. 1 (the "Holstrom well") for production, which Santa Fe began producing at the rate of 200 barrels per day.

In April 1989, Curry and Thornton ("Curry"), predecessors in interest to Stevens, applied to the Division to drill a well in the Pool and for an exception to the standard spacing and well location rules. Curry requested the non-standard spacing because it claimed that geologic conditions would not allow for production of oil from their lease from an orthodox well location. Santa Fe^[1] opposed the application, claiming that the well would impair its correlative rights to oil in the Pool. In its Order No. R-8917, the Division approved Curry's application to drill the well at the unorthodox location but imposed a production penalty

limiting the amount of oil that Curry could produce from the well to protect correlative rights of other lease holders in the Pool.

In May, Stevens, which had replaced Curry as an operator in the Pool, applied to the Division for an amendment to Order No. R-8917. Stevens requested that, instead of drilling the well authorized by Order No. R-8917, it be allowed to enter an existing abandoned well and drill directionally to a different location. The requested well, if approved and drilled, would also be at an unorthodox location. Santa Fe opposed the amendment and objected to the original production penalty, which it contended should have allowed less production from the Stevens well. The Division approved Stevens's application and issued Order No. R-8917-A amending Order No. R-8917. The amended order, while allowing directional drilling to an unorthodox location, required Stevens to otherwise meet the requirements of the original order, including the original production penalty.

Stevens proceeded to drill the well authorized by the amended order. When the well failed to produce oil, Stevens contacted the Division Director and requested approval to re-drill the well to a different location and depth. The Director permitted Stevens to continue drilling at its own risk and subject to subsequent orders to be entered after notice to all affected parties and a hearing. Stevens drilled and completed this well (the "Deemar well") and filed an application for a de novo hearing by the Commission to approve production from the well and to consider the production penalty. See NMSA 1978, § 70-2-13 (Repl.Pamp. 1987) (decisions by the Director may be heard de novo by the Commission). Santa Fe also filed an application for a de novo hearing opposing Stevens's application or, in the alternative, urging that a production penalty be assessed against the Stevens well.

The Commission consolidated the petitions and, after notice to the parties and a *823 hearing, entered Order No. R-9035. This order estimated the total amount of oil in the Pool and the amount of oil under each of the three tracts in the Pool.[2] The order set the total allowable production from the Pool at the existing production rate of 235 barrels per day, [3] and allocated production to the two wells in accordance with the relative percentages of oil underlying each of the three tracts. Under this formula, Stevens was allowed to produce 49 barrels per day from its Deemar well, Santa Fe was allowed to produce 125 barrels per day from its Holstrom well, and the undeveloped tract left in the Pool would be allowed to produce 61 barrels per day, if developed. The order also allowed the production to be increased to 1030 barrels per day if all operators voluntarily agreed to unitized operation of the Pool.

Pursuant to NMSA 1978, Section 70-2-25(A), both Santa Fe and Stevens applied to the Commission for a rehearing. Santa Fe contended that the second attempt at directional

drilling was unlawful; that it was denied due process and equal protection by the ex parte contact between Stevens and the Division Director; that the findings of the Commission apportioning production were not supported by the evidence; that the reduction of production was not supported by the evidence and was erroneous, capricious, and contrary to law; and that the unitization was illegal and confiscatory to Santa Fe. Stevens argued that the order was contrary to law because it would result in the drilling of an unnecessary well on the undeveloped tract, which would result in waste; that the order was arbitrary, capricious, unreasonable, and contrary to law because it exceeded the Commission's statutory authority; that the order violated its due process rights; and that the findings regarding recoverable reserves were contrary to the evidence and arbitrary and capricious. When the Commission took no action on the applications for rehearing, the petition was presumed to be denied and each party appealed to the district court, which consolidated the appeals. See NMSA 1978, § 70-2-25.

On appeal to the district court, Santa Fe contended that Order No. R-9035 was arbitrary and capricious, that it was not supported by substantial evidence, that the Commission exceeded its statutory authority, and that the Commission Chairman's bias against Santa Fe denied it due process. Stevens contended that the order was arbitrary, capricious, and unreasonable; that it was contrary to law; and that it denied Stevens's rights to due process. The trial court, after a review of the evidence presented at the Commission's hearings, affirmed the Commission's order. The trial court also dismissed, with prejudice, Santa Fe's contention of bias.

Pursuant to Section 70-2-25, both Santa Fe and Stevens appeal the district court decision to this Court. Santa Fe contends (1) that it was denied procedural due process because the Commission was biased; (2) that the district court erred when it failed to consider the question of bias; (3) that the Division violated its own regulations and procedures; (4) that the Commission abused its discretion when it lowered allowable production from the Pool; and (5) that the Commission decision was not supported by the evidence and was arbitrary and capricious. Stevens contends (1) that the Commission exceeded its authority when it reduced allowable production in an attempt to unitize operation of the Pool; (2) that the order violated the Commission's statutory duty to prevent waste; (3) that the order was not supported by substantial evidence; and (4) that its rights to due process were violated. Because of a substantial overlap of issues *824 raised by Santa Fe and Stevens, we consolidate these issues and address the following: (1) whether the Commission's actions violated due process rights of either Santa Fe or Stevens; (2) whether by issuing Order No. R-9035 the Commission exceeded its statutory authority or violated any of its own rules;

U.S. 232, 77 S. Ct. 752, 1 L. Ed. 2d 796 (1957), claims that this is a violation of substantive due process. We disagree. As discussed in Section VI, *infra*, the Commission did not act in an arbitrary or capricious manner. Moreover, as demonstrated in Section IV, *infra*, the Commission's actions were consistent with its statutory duties to prevent waste and protect the correlative rights of other producers in the Pool.

IV

The next issue that we address is whether the Commission exceeded its statutory authority or violated its rules when it issued Order No. R-9035. Both Santa Fe and Stevens contend that Order No. R-9035, while not requiring unitization, effectively unitizes operation of the Pool. They argue that the Commission does not have the statutory authority to require unitization of the Pool because, under the Statutory Unitization Act, NMSA 1978, Sections 70-7-1 to -21 (Repl.Pamp. 1987), unitization is available only in fields that are in the secondary or tertiary recovery phase. They assert that, because the Commission order effectively unitizes the Pool, a field in the primary development phase, the Commission exceeded its statutory authority. In addition, Santa Fe contends that the Commission violated its own rules when it allowed Stevens's second directional drilling attempt and that Order No. 9035 is void. The Commission argues that its actions were proper under the Oil and Gas Act, NMSA 1978, Sections 70-2-1 to -38 (Repl.Pamp. 1987 & Cum.Supp. 1991), and argues that the Statutory Unitization Act is inapplicable to the instant case.

A

"The Oil Conservation Commission is a creature of statute, expressly defined, limited and empowered by the laws creating it." *Continental Oil Co. v. Oil Conservation Comm'n*, 70 N.M. 310, 318, 373 P.2d 809, 814 (1962). The Oil and Gas Act gives the Commission and the Division the two major duties: the prevention of waste and the protection of correlative rights. NMSA 1978, § 70-2-11(A); *Continental Oil Co.*, 70 N.M. at 323, 373 P.2d at 817. Correlative rights are defined as

the opportunity afforded * * * to the owner of each property in a pool to produce without waste his just and equitable share of the oil * * * in the pool, being an amount, so far as can be practicably determined and so far as can be practicably obtained without waste, substantially in the proportion that the quantity of recoverable oil * * * under the property bears to the total recoverable oil * * * in the pool and, for such purpose, to use his just and equitable share of the reservoir energy.

NMSA 1978, § 70-2-33(H). In addition to its ordinary meaning, waste is defined to include "the locating, spacing, drilling, equipping, operating or producing, of any well or wells in a manner to reduce or tend to reduce the total quantity of crude petroleum oil * * * ultimately recovered from any pool." NMSA 1978, § 70-2-3(A).

The broad grant of power given to the Commission to protect correlative rights and prevent waste allows the Commission "to require wells to be drilled, operated and produced in such manner as to prevent injury to neighboring leases or properties." NMSA 1978, § 70-2-12(B) (7). In addition, the Division and the Commission are "empowered to make and enforce rules, regulations and orders, and to do whatever may be reasonably necessary to carry out the purpose of this act, whether or not indicated or specified in any section hereof." NMSA 1978, § 70-2-11.

In the instant case, evidence presented to the Commission indicated that the Pool was located under three separate tracts of land. *829 The Commission was called upon to determine the total amount of oil in the Pool and the proportionate share underlying each tract. Stevens's Deemar well was located so that it could produce oil from the top portion of the Pool, thereby avoiding waste that would have occurred unless the well was allowed. However, the well was located so that it could effectively drain the entire Pool. The Commission, charged with the protection of correlative rights of the other lease owners in the Pool, placed a production penalty on the well to protect these rights. Thus, the Commission attempted to avoid waste while protecting correlative rights. We hold that, under the facts of this case, the Commission did not exceed the broad statutory authority granted by the Oil and Gas Act.

Moreover, we are unpersuaded by the argument of both Stevens and Santa Fe that the Statutory Unitization Act prohibits the Commission's actions. They argue that, by enacting the Statutory Unitization Act, the legislature intended to limit the availability of forced unitization to secondary and tertiary recovery only. Both Santa Fe and Stevens quote the following language from the Statutory Unitization Act to support their argument:

It is the intention of the legislature that the Statutory Unitization Act apply to any type of operation that will substantially increase the recovery of oil above the amount that would be recovered by primary recovery alone and not to what the industry understands as exploratory units.

Section 70-7-1 (emphasis added by Stevens and Santa Fe). They assert that this section precludes unitization of a field in primary production such as the Pool. We disagree.

We read the above quoted language from Section 70-7-1 merely to say that the Statutory Unitization Act is not applicable to fields in their primary production phase, such as the Pool in the instant case. Nothing contained in the Statutory Unitization Act, including the above quoted section, however, limits the authority of the Commission to regulate oil production from a pool under the Oil and Gas Act. The Commission still must protect correlative rights of lease holders in the Pool while preventing waste. The Commission still has broad authority "to do whatever may be reasonably necessary to carry out the purpose of this act, whether or not indicated or specified in any section hereof." NMSA 1978, § 70-2-11(A). As discussed above, in the instant case the Commission's actions were within its statutory authority. We hold that the circumstances of this case do not implicate the Statutory Unitization Act and that the Commission's actions in effectively unitizing operation of the Pool were an appropriate exercise of its statutory authority under the Oil and Gas Act.

B

Santa Fe contends that, by issuing Order No. R-9035, the Commission abused its discretion by failing to follow the rules and regulations established by Order No. R-8806. That order established the Pool and set out special rules and regulations designed to prevent waste and protect correlative rights.[4] The order also established notice and hearing requirements before the Commission could allow a non-standard well to be drilled in the Pool. Santa Fe contends that, by allowing Stevens to drill a well at a non-standard location, i.e., to within 70 feet of Santa Fe's lease line, without prior notice and a hearing, the Commission violated its own rules. Santa Fe also contends that lowering the allowable production from the Holstrom well to 125 barrels of oil per day without adequate notice is a violation of these rules. Santa Fe concludes that, because Order No. 9035 was issued in a manner inconsistent with these rules, the order is void and Order Nos. 8917 and 8917-A should be reinstated. We disagree.

*830 The Commission's actions in this case did not violate the Commission's rules established by Order No. 8806. While the Director did allow Stevens to make a second attempt to drill a well at an unorthodox location without notice to other lease holders in the Pool, the other lease holders had notice of the subsequent hearing to determine whether this well would be allowed to produce oil. In addition, this action was designed to further the Director's statutory duty to prevent waste by preventing added expense in the development of the field. Moreover, the Director could have approved drilling the second Stevens attempt at the hearing that it held prior to issuing Order No. 8917-A. Thus, the

Exhibit 2

SWEPI, LP v. Mora County

81 F. Supp. 3d 1075 (D.N.M. 2015)
Decided Jan 19, 2015

No. CIV 14–0035 JB/SCY.

01-19-2015

SWEPI, LP, a Delaware Limited Partnership, Plaintiff, v. MORA COUNTY, NEW MEXICO; Mora County Board of County Commissioners; Paula A. Garcia, Mora County Commissioner; John P. Olivas, Mora County Commissioner; and Alfonso J. Griego, Mora County Commissioner, Defendants, and La Merced de Santa Getrudis de Lo de Mora, a Land Grant; and Jacobo E. Pacheco, an Individual, Defendant–Intervenors.

Bradford C. Berge, Larry J. Montañó, John C. Anderson, Michael H. Feldewert, Holland & Hart, LLP, Santa Fe, NM, for Plaintiff. Nancy Ruth Long, Justin W. Miller, Long Komer & Associates, P.A., Santa Fe, NM, for Defendants. Jeff H. Haas, Law Offices of Nanasi & Haas, Santa Fe, NM, for Defendants/Defendant–Intervenors.

JAMES O. BROWNING, District Judge.

1087*1087

Bradford C. Berge, Larry J. Montañó, John C. Anderson, Michael H. Feldewert, Holland & Hart, LLP, Santa Fe, NM, for Plaintiff.

Nancy Ruth Long, Justin W. Miller, Long Komer & Associates, P.A., Santa Fe, NM, for Defendants.

Jeff H. Haas, Law Offices of Nanasi & Haas, Santa Fe, NM, for Defendants/Defendant–Intervenors.

MEMORANDUM OPINION AND ORDER

JAMES O. BROWNING, District Judge.

THIS MATTER comes before the Court on SWEPI's Motion for Partial Judgment on the Pleadings, filed May 31, 2014 (Doc. 21)(“Motion”). The Court held a hearing on November 3, 2014. The primary issues are: (i) whether the Court may consider evidence outside the pleadings to determine issues of justiciability; (ii) whether Plaintiff SWEPI, LP has standing to bring its claims; (iii) whether SWEPI, LP's claims are ripe; (iv) whether SWEPI, LP can bring a claim for a violation of the Supremacy Clause of article 6 of the Constitution of the United States of America; (v) whether the Mora County, N.M., Ordinance 2013–10 (2013), filed January 10, 2014 (Doc. 1–1)(“Ordinance”), violates the Supremacy Clause; (vi) whether the Ordinance violates SWEPI, LP's substantive due-process rights; (vii) whether the Ordinance violates the Equal Protection Clause of Fourteenth Amendment to the Constitution of the United States; (viii) whether the Ordinance violates the First Amendment to the Constitution of the United States; (ix) whether the Defendants have the authority to enforce zoning regulations on New Mexico state land; (ix) whether New Mexico state law preempts the entire

field of oil-and-gas production; (x) whether the Ordinance conflicts with state law; and (xi) whether the valid provisions of the Ordinance can be severed from the invalid provisions. Because the Court may consider evidence outside the pleadings for issues of justiciability, the Court will consider outside evidence solely to determine standing and ripeness. SWEPI, LP has suffered an injury in fact and thus has standing to bring each of its claims. Additionally, because the Ordinance has already been enacted, and because SWEPI, LP would suffer harm if the Court delayed considering its claims, each of SWEPI, LP's claims are ripe, except for its claim under the Takings Clause of the Fifth Amendment to the Constitution of the United States. SWEPI, LP has not sought just compensation for its takings claim through a state inverse condemnation action, and, as such, it is not ripe. SWEPI, LP may bring its claim under the Supremacy Clause, because it can bring
 1088 independent claims through a [42 U.S.C. § 1983](#) action and under the constitutional *1088 provisions that it asserts trumps the Ordinance. Also, the Ordinance violates the Supremacy Clause by conflicting with federal law, and certain provisions must be invalidated. The Ordinance does not, however, violate SWEPI, LP's substantive due-process rights, because the Defendants had a legitimate state interest for enacting the Ordinance. For the same reason, the Ordinance does not violate the Equal Protection Clause. The Ordinance violates the First Amendment by chilling protected First Amendment activities. The Defendants lack the authority to enforce zoning laws on New Mexico state lands, and thus, may not enforce the Ordinance on state lands. Because there is room for concurrent jurisdiction between state and local laws, New Mexico state law does not preempt the entire field of oil-and-gas production. The Ordinance, however, conflicts with New Mexico state law by banning hydrocarbon extraction activities, and certain provisions must be invalidated. Finally, the invalid provisions are not severable from the remaining valid provisions, and the Ordinance, in its entirety, must be invalidated. The Court will, thus, grant the Motion in part and deny it in part, and will invalidate the Ordinance.

FACTUAL BACKGROUND

In deciding a motion for judgment on the pleadings that a plaintiff filed, the Court may consider only “ ‘allegations of fact [that] are admitted or not controverted in the pleadings’ ” so that “ ‘only questions of law remain to be decided by the district court.’ ” *Kellar v. U.S. Dep't of Veteran's Affairs*, No. CIV 08–0761 WYD/KLM, [2009 WL 1706719](#), at *1 (D.Colo. June 17, 2009) (Daniel, C.J.) (quoting 5C Charles A. Wright & Arthur R. Miller, *Federal Practice and Procedure: Civil* § 1367 (3d ed.2004)). The Court will, thus, in connection with this motion for judgment on the pleadings, state and consider only those facts alleged in the Complaint for Declaratory and Injunctive Relief and Damages, filed January 10, 2014 (Doc. 1)(“Complaint”), which the Defendants did not deny in the Answer to Complaint, filed March, 13, 2014 (Doc. 9)(“Answer”). The Court's previous Memorandum Opinion and Order provides a fuller statement of the allegations in the Complaint, including allegations which the Defendants deny. *See SWEPI, LP v. Mora Cnty.*, No. CIV 14–0035 JB/SCY, [2014 WL 6983288](#), at *1–11 (D.N.M. Dec. 5, 2014) (Browning, J.).

1. *The Parties.*

SWEPI, LP filed the Complaint, seeking an injunction to prohibit the Defendants from enforcing the Ordinance and seeking monetary damages. *See* Complaint ¶ 2, at 2; Answer ¶ 2, at 2. SWEPI, LP entered into an oil-and-gas lease with the State of New Mexico through a lease dated August 1, 2010. *See* Complaint ¶ 5, at 2; Answer ¶ 5, at 2 (“Defendants admit that a copy of a lease dated August 1, 2010 between the State of New Mexico and SWEPI is attached to the Complaint as exhibit 3.”). *See also* Oil and Gas Lease between SWEPI LP and the
 1089 State of New Mexico, dated August 1, 2010, filed January 1, 2014 (Doc. 1–3)(“Aug. 1, 2010, Lease”).¹ *1089 Mora County, New Mexico, is a political subdivision of the State of New Mexico. *See* Complaint ¶ 8, at 3. The Mora County Board of Commissioners is the governing body responsible for exercising the powers that the

state lands, but it would be a violation for the Defendants to enforce the Ordinance on state lands. Accordingly, invalidation of the Ordinance is not warranted; however, the Court will enjoin the Defendants from enforcing the Ordinance on state lands.³⁹ *1193 **B STATE LAW PREEMPTS THE ORDINANCE.**

³⁹ While the Court is willing to issue a permanent injunction, enjoining the Defendants from enforcing the Ordinance on state lands, because the Court will invalidate the Ordinance, in its entirety, such an injunction would be moot.

New Mexico state law impliedly preempts the Ordinance, because it conflicts with state law. State law may either expressly or impliedly preempt a county ordinance. *See San Pedro Mining Corp. v. Bd. of Cnty. Comm'rs*, 1996–NMCA–002, ¶ 9, 121 N.M. 194, 909 P.2d 754, 758. To expressly preempt local laws, the State “legislature must clearly state its intention to do so.” *Rancho Lobo, Ltd. v. Devargas*, 303 F.3d at 1201. There are two doctrines under which state law may impliedly preempt a local law: (i) field preemption; and (ii) conflict preemption. *See San Pedro Mining Corp. v. Bd. of Cnty. Comm'rs*, 1996–NMCA–002, ¶ 11, 121 N.M. 194, 909 P.2d 754. Field preemption occurs when “it is evident from the language of the New Mexico law at issue that the legislature ‘clearly intended to preempt a governmental area.’ ” *Rancho Lobo, Ltd. v. Devargas*, 303 F.3d at 1204 (quoting *Casuse v. City of Gallup*, 1987–NMSC–112, ¶ 6, 106 N.M. 571, 746 P.2d 1103, 1105). Conflict preemption examines “whether the ordinance permits an act the general law prohibits, or prohibits an act the general law permits.” *Rancho Lobo, Ltd. v. Devargas*, 303 F.3d at 1205 (citing *Inc. Cnty. of Los Alamos v. Montoya*, 1989–NMCA–004, ¶ 16, 108 N.M. 361, 772 P.2d 891 (“Rather, the tests are whether the stricter requirements of the ordinance conflict with state law, and whether the ordinance permits an act the general law prohibits, or prohibits an act the general law permits.”)). Merely requiring greater restrictions than state law, however, does not necessarily make the ordinance invalid. *See Inc. Cnty. of Los Alamos v. Montoya*, 1989–NMCA–004, ¶ 16, 108 N.M. 361, 772 P.2d 891. SWEPI, LP argues that state law impliedly preempts the Ordinance through either field or conflict preemption. State law does not entirely preempt the oil-and-gas field. The Ordinance conflicts, however, with state law and is, thus, invalid because of conflict preemption.

1. *New Mexico State Law Does Not Impliedly Preempt the Entire Oil–And–Gas Field.*

New Mexico state law does not impliedly preempt the entire oil-and-gas field. SWEPI, LP directs the Court to a 1986 New Mexico Attorney General advisory letter in which the Attorney General opined that the entire field of oil-and-gas regulation was occupied by the State—*i.e.* the State of New Mexico impliedly preempted the entire oil-and-gas field. *See Motion at 20* (citing N.M. Att’y Gen. Op. 86–2, 1986 WL 220334). However, “Attorney General opinions and advisory letters do not have the force of law.” *United States v. Reese*, 2014–NMSC–013, ¶ 36, 326 P.3d 454, 462. Moreover, the advisory letter is almost thirty years old, and there has been intervening case law that indicates that field preemption does not apply.⁴⁰ *1194 In the advisory letter, the Attorney General’s Office, through Assistant Attorney General Barbara G. Stephenson, considered whether the County of Santa Fe could regulate oil-and-gas operations. *See N.M. Att’y Gen. Op. 86–2, 1986 WL 220334, at *1.* Ms. Stephenson opined that it could not regulate oil-and-gas operations, because the county regulations conflicted with Oil Conservation Division regulations, and because “the county is preempted from adopting zoning regulations relating to oil and gas production.” N.M. Att’y Gen. Op. 86–2, 1986 WL 220334, at *1. Specifically, Ms. Stephenson opined that “[t]he legislature has vested” the regulation of oil-and-gas production with the Oil Conservation Division “with the intention that the state agency occupy the entire field of regulation.” N.M. Att’y Gen. Op. 86–2, 1986 WL 220334, at *1. Ms. Stephenson noted that the county has only those powers that the Legislature provides, and that the county’s zoning authority is subject to statutory or

constitutional limitations. *See* N.M. Att'y Gen. Op. 86–2, 1986 WL 220334, at *2. Ms. Stephenson opined that one such limitation comes from Section 70–2–36 of the New Mexico Statutes Annotated. *See* N.M. Att'y Gen. Op. 86–2, 1986 WL 220334, at *2.

⁴⁰ Several additional concerns caution against relying on the advisory letter. First, the letter appears to be an informal “advisory letter” rather than a formal Attorney General Opinion. During his time in office, New Mexico Attorney General, Paul Bardacke, the Attorney General in 1986, issued very few formal Attorney General Opinions. *See* Hal Stratton & Paul Farley, *Office of the Attorney General State of New Mexico: History, Powers & Responsibilities 1846–1990* 119 (1990)(showing that, in 1986, less than five Official Attorney General Opinions were issued while over seventy-five were issued in 1987, after Mr. Bardacke left office). Second, and related to the first, Mr. Bardacke did not sign the 1986 advisory letter. *See* N.M. Att'y Gen. Op. 86–2, 1986 WL 220334, at *1. Assistant Attorney General Barbara G. Stephenson signed it. *See* N.M. Att'y Gen. Op. 86–2, 1986 WL 220334, at *3. The lack of the New Mexico Attorney General's signature on the letter cautions against giving too much weight to the letter.

A. The [Oil Conservation Division] shall have, and is hereby given, jurisdiction and authority over all matters relating to the conservation of oil and gas and the prevention of waste of potash as a result of oil and gas operations in this state. It shall have jurisdiction, authority and control of and over all persons, matters or things necessary or proper to enforce effectively the provisions of this act or any other law of this state relating to the conservation of oil and gas and the prevention of waste of potash as a result of oil and gas operations.

N.M. Att'y Gen. Op. 86–2, 1986 WL 220334, at *2 (quoting [N.M. Stat. Ann. § 70–2–36](#))(emphasis in N.M. Att'y Gen. Op. 86–2 but not in source). Based on this statute, Ms. Stephenson concluded that the Oil Conservation Division, “therefore, occupies the entire area of oil and gas regulation and a county cannot, by ordinance, attempt to regulate this area.” N.M. Att'y Gen. Op. 86–2, 1986 WL 220334, at *2. The Attorney General discussed cases from Washington, Missouri, and Alaska in which the courts found that the state law preempted the areas of prison construction, location of intercity electric transmission lines, subdivisions, and mobile home construction standards. *See* N.M. Att'y Gen. Op. 86–2, 1986 WL 220334, at *2 (citing *Snohomish Cnty. v. State of Washington*, [97 Wash.2d 646, 648 P.2d 430](#) (1982) (en banc) (prison location); *Union Elec. Co. v. City of Crestwood*, [562 S.W.2d 344](#) (Mo.1978) (en banc) (location of intercity electric transmission lines); *Kenai Peninsula Borough v. Kenai Peninsula Bd. of Realtors, Inc.*, [652 P.2d 471](#) (Alaska 1982) (subdivisions); *Snohomish Cnty. v. Thompson*, [19 Wash.App. 768, 577 P.2d 627](#) (1978)). Additionally, Ms. Stephenson opined that the county ordinance was further invalid, because it “applies requirements to oil and gas production beyond those imposed by OCD and thus prohibits, that which OCD permits.” N.M. Att'y Gen. Op. 86–2, 1986 WL 220334, at *3. Finally, Ms. Stephenson concluded that “[c]oncurrent jurisdiction does not appear possible.” N.M. Att'y Gen. Op. 86–2, 1986 WL 220334, at *3.

¹¹⁹⁵ Since the Attorney General's Office issued the advisory letter, New Mexico ¹¹⁹⁵ courts and the Tenth Circuit have reined in New Mexico's field-preemption doctrine. In *San Pedro Mining Corp. v. Board of County Commissioners*, the Court of Appeals of New Mexico considered whether the New Mexico Mining Act, [N.M. Stat. Ann. §§ 69–36–1](#) through [69–36–20](#), preempts a county's ability to regulate mining activity within its jurisdiction. *See* 1996–NMCA–002, ¶ 4, [121 N.M. 194, 909 P.2d 754](#). The Court of Appeals of New Mexico first concluded that the Mining Act does not expressly preempt local mining ordinances. *See* 1996–NMCA–002, ¶ 10, [121 N.M. 194, 909 P.2d 754](#). Concerning implied field preemption, the Court of Appeals of New

Mexico noted that the Mining Act's, and subsequent regulations', primary focus is on “the minimization of damage to the land being mined.” 1996–NMCA–002, ¶ 12, [121 N.M. 194, 909 P.2d 754](#). The Court of Appeals of New Mexico noted, however, that

neither the Act nor the regulations contain any mention of development issues with which local governments are traditionally concerned, such as traffic congestion, increased noise, possible nuisance created by blasting or fugitive dust, compatibility of mining use with the use made of surrounding land, appropriate distribution of land use and development, and the effect of the mining activity on surrounding property values.

1996–NMCA–002, ¶ 12, [121 N.M. 194, 909 P.2d 754](#). The Court of Appeals of New Mexico concluded that, “[t]herefore, there is room for concurrent jurisdiction and regulation, with the County's ordinance regulating aspects of the mining activity that concern off-site safety, compatibility with surrounding property uses, and other matters left unaddressed by the Act and regulations.” 1996–NMCA–002, ¶ 12, [121 N.M. 194, 909 P.2d 754](#). Because there was room for concurrent regulation between a county and the Mining Act, the Court of Appeals of New Mexico held that the Mining Act and subsequent regulations do not completely preempt the mining field. *See* 1996–NMCA–002, ¶ 14, [121 N.M. 194, 909 P.2d 754](#). The Court of Appeals of New Mexico noted that portions of Santa Fe County's ordinance may conflict with the Mining Act, and thus be preempted under conflict preemption, but, because the plaintiff argued only that the ordinance, as a whole, was preempted, the court did not consider which individual provisions might be preempted through conflict preemption. *See* 1996–NMCA–002, ¶ 13, [121 N.M. 194, 909 P.2d 754](#).

In *Rancho Lobo, Ltd. v. Devargas*, the Tenth Circuit considered whether the New Mexico Forest Conservation Act, [N.M. Stat. Ann. §§ 68–2–1 through 68–2–34](#), preempted a New Mexico county's “Timber Harvest Ordinance.” *See* [303 F.3d at 1197](#). The Tenth Circuit, in an opinion that the Honorable Mary B. Briscoe, United States Circuit Judge for the Tenth Circuit, authored, and Judges Ebel and McKay joined, held that the Conservation Act did not preempt the ordinance. *See* [303 F.3d at 1207](#). The Tenth Circuit noted that there was some support for the argument that the Conservation Act impliedly preempted the entire field; specifically, the Conservation Act created the Forestry Division and granted it with sweeping powers to make rules and regulations concerning timber harvests, and the Forestry Division's regulations were comprehensive. *See* [303 F.3d at 1204](#). The Tenth Circuit concluded, however, that the Conservation Act was “very similar” to the Mining Act in *San Pedro Mining Corp. v. Board of County Commissioners*. [303 F.3d at 1204](#). Both acts, it noted, “did not really address the kinds of development issues ‘with which local governments are traditionally concerned.’ ” [303 F.3d at 1204](#) (quoting ¹¹⁹⁶ *San Pedro Mining Corp. v. Bd. of Cnty. Comm'rs*, 1996–NMCA–002, ¶ 12, [121 N.M. 194, 909 P.2d 754](#)). Specifically, the Tenth Circuit stated that the “Conservation Act's primary focus is the minimization of damage to the permitted land,” while

the main focus of the Timber Harvest Ordinance is on local issues, such as the amelioration of damage to the surrounding property as the result of timber harvesting, including issues such as the effect of the timber harvest on economic development and local employment, water quality and availability, soil protection, archeological, historic and cultural resources, abatement of noise, dust, smoke and traffic, hours of operation, compatibility with adjacent land uses, cumulative effect when combined with existing harvests.

Rancho Lobo, Ltd. v. Devargas, [303 F.3d at 1204–05](#). The Tenth Circuit concluded that, because the Conservation Act “left room for concurrent jurisdiction over local forestry issues,” the Conservation Act does not impliedly preempt “the entire field of regulation relating to timber harvesting in New Mexico.” [303 F.3d at](#)

1205. As for conflict preemption, the plaintiff argued, and the district court concluded, that, because the Conservation Act permits clear cutting⁴¹ but the county ordinance prohibits it, the ordinance conflicts with state law. *See* 303 F.3d at 1205. The Tenth Circuit, however, held that, because the Conservation Act did not create a right to clear cutting or state that clear cutting is permitted, the ordinance's prohibition did not conflict with Conservation Act. *See* 303 F.3d at 1205.

⁴¹ “Clearcutting, clearfelling, or clearcut logging is a forestry/logging practice in which most or all trees in an area are uniformly cut down.” *Clearcutting*, Wikipedia.org, <http://en.wikipedia.org/wiki/Clearcutting> (last visited Jan. 14, 2014).

The Oil and Gas Act is focused primarily on the prevention of waste and the drilling and maintenance of oil-and-gas wells. The Oil and Gas Act prohibits the production or handling of oil and gas in a manner that constitutes or results in waste. *See* N.M. Stat. Ann. § 70–2–2. Waste is interpreted with its ordinary meaning, and the Oil and Gas Act also provides a number of specific examples that can be summed up as the inefficient, excessive, or improper use of oil and gas. *See* N.M. Stat. Ann. § 70–2–3. The Oil and Gas Act provides the Oil Conservation Division with a number of powers concerning the regulation of drilling for, and producing, oil and gas. *See* N.M. Stat. Ann. § 70–2–12. The Oil and Gas Act, however, does not address “the kinds of ... issues ‘with which local governments are traditionally concerned.’ ” *Rancho Lobo, Ltd. v. Devargas*, 303 F.3d at 1204 (quoting *San Pedro Mining Corp. v. Bd. of Cnty. Comm'rs*, 1996–NMCA–002, ¶ 12, 121 N.M. 194, 909 P.2d 754). The Oil and Gas Act does not address issues such as traffic that oil-and-gas production creates; noise limitations for production near residential areas; potential nuisance issues from sound, dust, or chemical run-off; or the impact of oil-and-gas production on neighboring properties.⁴² There is thus “room for concurrent regulation” by Mora County. *Rancho Lobo, Ltd. v. Devargas*, 303 F.3d at 1200. Because there is room for concurrent regulation, State law does not preempt the entire oil-and-gas field. ¹¹⁹⁷ *See Rancho Lobo, Ltd. v. Devargas*, 303 F.3d at 1204–05 ; *San Pedro Mining Corp. v. Bd. of Cnty. Comm'rs*, 1996–NMCA–002, ¶ 12, 121 N.M. 194, 909 P.2d 754.

⁴² The Surface Owners Protection Act, N.M. Stat. Ann. §§ 70–12–1 through 70–12–10, provides protections to surface owners, but the definition of “surface owner” is limited to the “person who holds legal or equitable title ... to the surface of the real property on which the operator has the legal right to conduct oil and gas operations.” N.M. Stat. Ann. § 70–12–3(D). Consequently, it does not apply to neighboring properties.

In the 1986 advisory letter, Assistant Attorney General Stephenson focused on the Oil Conservation Division's authority and jurisdiction in concluding that the Oil and Gas Act preempted the entire oil-and-gas field. *See* N.M. Att'y Gen. Op. 86–2, 1986 WL 220334, at *2. That the Legislature has authorized the Oil Conservation Commission to pass regulations and has passed extensive regulations does not change the conclusion that there is no field preemption. Both the Mining Act and the Conservation Act created state agencies with the authority to enact extensive regulations. *See* N.M. Stat. Ann. § 69–36–6 (creating the Mining Commission); N.M. Stat. Ann. § 69–36–7 (providing the Mining Commission with authority to enact regulations); N.M. Stat. Ann. § 68–2–16 (noting that the Forestry Division has the authority to enforce and enact rules and regulations). The existence of a state agency with regulatory authority, however, did not lead the Tenth Circuit or the Court of Appeals of New Mexico to conclude that the Mining Act or the Conservation Act preempted their respective fields. *See Rancho Lobo, Ltd. v. Devargas*, 303 F.3d at 1204–05 ; *San Pedro Mining Corp. v. Bd. of Cnty. Comm'rs*, 1996–NMCA–002, ¶ 12, 121 N.M. 194, 909 P.2d 754. Similarly, the existence of the Oil Conservation Division, and its abilities to enact and enforce regulations, does not cause the Oil and Gas Act to

Exhibit 3

Laws & Legal Resources.

Receive free daily summaries of new opinions from the **New Mexico Supreme Court.**

El Paso Natural Gas Co. v. Oil Conservation Com'n

414 P.2d 496 (1966)

76 N.M. 268

EL PASO NATURAL GAS COMPANY, a corporation, Pan American Petroleum Corporation, a Corporation, Marathon Oil Company, a corporation, and Sunset International Petroleum Corporation, a corporation, petitioners-appellants, v. OIL CONSERVATION COMMISSION of New Mexico, Jack M. Campbell, Chairman, E.S. Walker, Member, A.L. Porter, Jr., Member and Secretary, and Consolidated Oil & Gas, Inc., a corporation, Respondents-Appellees.

No. 7727.

Supreme Court of New Mexico.

May 16, 1966.

Seth, Montgomery, Federici & Andrews, Santa Fe, for El Paso Natural Gas Co. and Sunset International Petroleum Corp.

Ben R. Howell, Garrett C. Whitworth, El Paso, Tex., for El Paso Natural Gas Co.

Atwood & Malone, Roswell, J.K. Smith, Fort Worth, Tex., for Pan American Petroleum Corp.

Kent Hampton, Findlay, Ohio, for Marathon Oil Co.

Boston E. Witt, Atty. Gen., J.M. Durrett, Jr., Sp. Asst. Atty. Gen., Santa Fe, for Oil Conservation Commission.

Kellahin & Fox, Santa Fe, Holme, Roberts, More & Owen, Ted P. Stockmar, Denver, Colo., for Consolidated Oil & Gas, Inc.

NOBLE, Justice.

Consolidated Oil & Gas, Inc. requested a change in the proration formula in the Basin-Dakota gas pool from the existing "25-75" formula (25% acreage plus 75% acreage, times deliverability) to a "60-40" formula. The Oil Conservation Commission originally denied the change, but on rehearing, limited to the question of recoverable reserves in the pool, reversed its decision, ordered the change, and adopted the "60-40" formula. The Commission then denied a requested rehearing. The Commission's order was reviewed and affirmed by the district court of San Juan County. This appeal is from the judgment of the district court.

The district court reviewed only the record of the administrative hearing and concluded as a matter of law that the Commission's order was substantially supported by the evidence and by applicable law. This court, in reviewing the judgment, in the first instance, makes the same review of the Commission's action as did the district court. *Reynolds v. Wiggins*, 74 N.M. 670, 397 P.2d 469; *Kelley v. Carlsbad Irrigation District*, 71 N.M. 464, 379 P.2d 763.

As in *Continental Oil Co. v. Oil Conservation Com'n*, 70 N.M. 310, 373 P.2d 809, the Commission was concerned with a formula allocating production among the various producers from the gas pool allocation of the correlative rights. It is agreed that the duty of the Commission in this case is identical with that in *Continental*, but the parties are not in complete agreement as to what *Continental* requires. Its proper interpretation requires us to again consider the statutes with which we were concerned in that case and which are controlling here. Since the pertinent statutory provisions were quoted at length in *Continental Oil Co. v. Oil Conservation Com'n*, *supra*, we shall not restate them in detail.

Recognizing the need and right of the state; in the interest of the public welfare, to prevent waste of an irreplaceable natural resource, the legislature enacted those laws *498 authorizing the Commission to exercise control over oil and gas wells by limiting the total production in the pool, and making it the duty of the Commission to protect the correlative rights of all producers so far as it can be accomplished without waste to the pool. Sections 65-3-1 to 65-3-29, N.M.S.A. 1953. A review of the history of our oil and gas legislation reveals the primary concern in eliminating and preventing waste in the pool so far as it can practicably be done, and next the protection of the correlative rights of the producers from the pool. The legislature spelled out the duty of the Commission to limit production in such manner as to prevent waste, while affording:

"* * * to the owner of each property in the pool the opportunity to produce his just and equitable share of the * * * gas * * * in the pool, being an amount, * * * so far as such can be practicably obtained without waste, substantially in the proportion that the quantity of the recoverable * * * gas * * * under such property bears to the total recoverable * * * gas * * * in the pool, * * *" (§ 65-3-14(a), N.M.S.A. 1953) (Emphasis added).

Continental Oil Co. v. Oil Conservation Commission, *supra*, made clear those purposes and requirements.

The disagreement in this case arises from a difference of opinion as to the proper construction of language in Continental, saying that the statute requires the Commission to determine certain foundational matters without which the correlative rights of the various owners cannot be fixed, and, specifically, respecting those foundational matters:

"* * * Therefore, the commission, by 'basic conclusions of fact' (or what might be termed 'findings'), must determine, insofar as practicable, (1) the amount of recoverable gas under each producer's tract; (2) the total amount of recoverable gas in the pool; (3) the proportion that (1) bears to (2); and (4) what portion of the arrived at proportion can be recovered without waste. * * *"

The appellants argue that those four findings are jurisdictional in the sense that absent any one of them, the Commission lacked authority to consider or change any production formula. While the parties agree that the first three "basic" facts were specifically found, the appellees assert and appellants deny that a percentage determination was made of "what portion of the arrived at proportion" can be recovered without waste. Thus, the main thrust of appellants' argument is directed to the contention that the Commission lacked jurisdiction to change the allocation formula.

We did not, in Continental, say that the four basic findings must be determined in advance of testing the result under an existing or proposed allocation formula. Actually, what we said was:

"* * * That the extent of the correlative rights must be determined before the commission can act to protect them is manifest."

In addition, however, Continental observed that the Commission should so far as practicable prevent drainage between tracts which is not equalized by counter-drainage and to so regulate as to permit owners to utilize their share of pool energy. While Continental stated the four basic findings which the Commission must make before it can change a production formula, we were not concerned with the language in which the findings must be couched. What we said is that a proposed new formula must be shown to have been "based on the amounts of recoverable gas in the pool and under the tracts, insofar as those amounts can be practicably determined and obtained without waste." We then, in effect, said that such findings need not be in the language of the opinion but that they or their equivalents are necessary requisites to the validity of an order replacing a formula in current use. It is, accordingly, apparent that we must consider the Commission's findings to determine whether findings in *499 the language of Continental or their equivalent were adopted. We think they were.

The statute, in requiring the allocation order to afford each owner the opportunity to produce his just and equitable share of the recoverable gas in the pool, "so far as such can be practicably obtained without waste," of course, requires the adoption of an allocation formula which will permit the owners to produce as nearly as possible their percentage of the recoverable gas in the pool, with as little waste as can practicably be accomplished. It is obvious to us that each different allocation formula will allow the tract owners to produce a different percentage of the total gas in the pool. Having determined (1) the amount of recoverable gas under each tract, and (2) the total amount of recoverable gas in the pool, the ideal formula would be one that would permit each owner to recover all of that proportion which the gas underlying his tract bears to the total in the pool. But, since the legislature has required the Commission to protect the pool against waste, it must then test the different proposed formulae against the percentage which (1) bears to (2) to determine which one will permit the tract owner to most nearly produce its percentage of the total gas in the pool with the least waste. When that has been done, then the portion which the gas underlying each tract bears to the total recoverable gas in the pool which can be produced with the least waste can be determined. It is this latter figure which determines the formula that will permit the greater number of owners the opportunity to recover the greatest

amount allowable under the applicable statutes. We think the Commission made that determination in this instance.

The Commission termed the relationship between the percentage of total pool allowable apportioned to each tract by a formula, as compared to those percentages of total pool reserves, the A/R factor. It, thus, based each formula on the amounts of recoverable gas in the pool and under the tracts insofar as those amounts can be practicably determined, as Continental requires it to do. Applying the statute and the rule of Continental, the Commission determined that it must then select the allocation formula that will allow the maximum number of wells in the pool to produce as nearly as possible their complete percentage of the pool reserves. The Commission then made the required test applying both the "25-75" and the "60-40" formulae and determined that neither correlative rights nor waste were being adequately protected under the "25-75" formula but that both would be more nearly protected insofar as can be practicably determined under the "60-40" formula, and found the percentage that each owner could produce of the total pool reserves. It was further determined by the Commission that the "60-40" formula will, insofar as it is practicable to do so, afford to each owner the opportunity to use his just and equitable share of the reserve energy and prevent drainage between producing tracts which is not equalized by counter drainage.

It is true that the order in this instance did not, in the express language of the Continental Oil Company decision, find the "portion of the arrived at proportion" which "can be recovered without waste." However, our review of the Commission's findings reveals that it did make the requested findings in language equivalent to that required by Continental and did adopt a formula in compliance with statutory requirements. We think the findings as a whole determine that the percentage set forth in Schedule J constitute the "portion of the arrived at proportion" which can be recovered by each owner without waste. We agree with the district court that the Commission made those basic findings necessary to authorize it to change the production formula and that its Order R-2259-B is valid.

It follows that the judgment appealed from should be affirmed.

It is so ordered.

CHAVEZ and COMPTON, JJ., concur.

Exhibit 4

TITLE 19 **NATURAL RESOURCES AND WILDLIFE**
CHAPTER 15 **OIL AND GAS**
PART 27 **VENTING AND FLARING OF NATURAL GAS**

19.15.27.1 **ISSUING AGENCY:** Oil Conservation Commission.
[19.15.27.1 NMAC – N, xx/xx/xx]

19.15.27.2 **SCOPE:** 19.15.27 NMAC applies to persons engaged in oil and gas development and production within New Mexico.
[19.15.27.2 NMAC – N, xx/xx/xx]

19.15.27.3 **STATUTORY AUTHORITY:** 19.15.27 NMAC is adopted pursuant to the Oil and Gas Act, Section 70-2-6, Section 70-2-11 and Section 70-2-12 NMSA 1978.
[19.15.27.3 NMAC – N, xx/xx/xx]

19.15.27.4 **DURATION:** Permanent.
[19.15.27.4 NMAC – N, xx/xx/xx]

19.15.27.5 **EFFECTIVE DATE:** [DATE], unless a later date is cited at the end of a section.
[19.15.27.5 NMAC – N, xx/xx/xx]

19.15.27.6 **OBJECTIVE:** To regulate the venting and flaring of natural gas from wells and production equipment and facilities to prevent waste and protect correlative rights, public health and the environment.
[19.15.27.6 NMAC – N, xx/xx/xx]

19.15.27.7 **DEFINITIONS:** Definitions shall have the meaning specified in 19.15.2 NMAC except as specified below.

A. **“Air Pollution Control Equipment”** means a combustion device or vapor recovery unit.

B. **“ALARM”** means advanced leak and repair monitoring technology for detecting natural gas or crude oil leaks or releases that is not required by applicable state or federal law, rule, or regulation, and which the division has approved as eligible to earn a credit against the reported volume of lost natural gas pursuant to Paragraph (3) of Subsection B of 19.15.27.9 NMAC.

C. **“Average daily production”** has the same meaning as in Subsection A of 19.15.6.7 NMAC.

D. **“AVO”** means audio, visual or olfactory.

E. **“Completion operations”** means the period that begins with the initial perforation of the well in the completed interval and concludes on the earlier of 30 days after commencement of initial flowback or when permanent production equipment is first placed into service.

F. **“Certify”** means signed by an official with accountability over the operations or activities subject to the certification or submission.

G. **“Drilling operations”** means the period that begins when a well is spud and concludes when casing and cementing has been completed and casing slips have been set to install the tubing head.

H. **“Drill out”** means the process of removing the plugs placed during hydraulic fracturing or refracturing. Drill-out ends after the removal of all stage plugs and the initial wellbore clean-up.

I. **“Exploratory well”** means a well located in the spacing unit the closest boundary of which is two miles or more from:

(1) the outer boundary of a defined pool that has produced oil and gas from the formation to which the well is or will be drilled

(2) an existing gathering pipeline defined in 19.15.28 NMAC.

J. **“Emergency”** means a temporary, infrequent, and unavoidable event in which the loss of natural gas is uncontrollable or necessary to avoid a risk of an immediate and substantial adverse impact on safety, public health, or the environment, but does not include an event arising from or related to:

(1) the operator’s failure to install appropriate equipment of sufficient capacity to accommodate the anticipated or actual rate and pressure of production;

Deleted: A

Deleted: 8

Deleted: 10

Deleted: B

Deleted: C

Deleted: D

Deleted: E

Deleted: F

Deleted: Delineation

Deleted: G

(2) the operator's failure to limit production when the production rate exceeds the capacity of the related equipment or natural gas gathering system as defined in 19.15.28 NMAC, or exceeds the sales contract volume of natural gas;

(3) scheduled maintenance;

(4) venting or flaring of natural gas for more than four hours that is caused by an emergency, unscheduled maintenance, or malfunction of a natural gas gathering system as defined in 19.15.28 NMAC;

(5) the operator's negligence, including a recurring equipment failure;

or

(6) three or more emergencies experienced by the operator within the preceding 60 days, unless the division determines the operator could not have reasonably anticipated the current event and it was beyond the operator's control.

K. "Flowback" means the process of allowing fluids and entrained solids to flow from a well following stimulation, either in preparation for a subsequent phase of treatment or in preparation for cleanup and placing the well into production. Flowback ends when all temporary flowback equipment is removed from service. Flowback does not include drill-out.

L. "Flowback Fluid" means the gases, liquids, and entrained solids flowing from a well after drilling or hydraulic fracturing or refracturing.

M. "Flare" or "Flaring" means the controlled combustion of natural gas in a device designed for that purpose.

N. "Flare stack" means an appropriately designed stack equipped with a burner used for the combustion and disposal of natural gas.

O. "Gas-to-oil ratio (GOR)" for purposes of 19.15.27 NMAC means the ratio of natural gas to oil in the production stream expressed in standard cubic feet of natural gas per barrel of oil.

P. "Initial flowback" means the period during completion operations that begins with the onset of flowback and concludes when it is technically feasible for a separator to function.

Q. "Malfunction" means a sudden, unavoidable failure or breakdown of equipment beyond the reasonable control of the operator that substantially disrupts operations and requires correction, but does not include a failure or breakdown that is caused entirely or in part by poor maintenance, careless operation, or other preventable equipment failure or breakdown.

R. "N₂" means nitrogen gas.

S. "Natural gas" means a gaseous mixture of hydrocarbon compounds, primarily composed of methane, and includes both casinghead gas and gas as defined in 19.15.2 NMAC.

T. "Production operations" means the period that begins on the earlier of 31 days following the commencement of initial flowback or when permanent production equipment is placed into service and concludes when the well is plugged and abandoned.

U. "Producing in paying quantities" means the production of a quantity of oil and gas that yields revenue in excess of operating expenses.

V. "Separation flowback" means the period during completion operations that begins when it is technically feasible for a separator to function and concludes on the earlier of 30 days after the commencement of initial flowback or when permanent production equipment is placed into service.

W. "Vent" or "Venting" means the release of uncombusted natural gas to the atmosphere.

[19.15.27.7 NMAC – N, xx/xx/xx]

19.15.27.8 VENTING AND FLARING OF NATURAL GAS:

A. Venting and flaring of natural gas during drilling, completion or production operations constitutes waste and is prohibited except as authorized in Subsections B, C and D of 19.15.27.8 NMAC. The operator has a general duty to maximize the recovery of natural gas and to minimize the release of natural gas to the atmosphere. During drilling, completion and production operations, the operator shall flare natural gas rather than vent natural gas except when flaring is technically infeasible or would pose a risk to safe operations or personnel safety, and venting is a safer alternative than flaring.

B. Venting and flaring during drilling operations.

(1) The operator shall capture or combust natural gas if technically feasible using best industry practices and control technologies.

(2) A flare stack shall be located at a minimum of 100 feet from the nearest surface hole location, shall be properly sized, enclosed and equipped with an automatic ignition system or continuous pilot.

Deleted: The term flowback also means the fluids and entrained solids flowing from a well after drilling or hydraulic fracturing or refracturing.

Formatted: Font: Not Bold

Formatted: Normal

Deleted: H

Formatted: Font: (Default) Times New Roman

Formatted: Font: Not Bold

Deleted: M

Deleted: I

Deleted: N

Deleted: J

Deleted: O

Deleted: K

Deleted: P

Deleted: L

Deleted: M

Deleted: Q

Deleted: R

Deleted: N

Deleted: S

Deleted: O

Deleted: T

Deleted: P

Deleted: U

Deleted: Q

Deleted: V

Deleted: R

Deleted: and

(3) In an emergency or malfunction, the operator may vent natural gas to avoid a risk of an immediate and substantial adverse impact on safety, public health or the environment. The operator shall report natural gas vented or flared during an emergency or malfunction to the division pursuant to Paragraph (1) of Subsection G of 19.15.27.8 NMAC.

C. Venting and flaring during completion and recompletion operations.

(1) During initial flowback, the operator ~~must direct all fluids to flowback vessels and collect and control emissions from each flowback vessel on and after the date of initial flowback by routing emissions to an operating air pollution control equipment that achieves a hydrocarbon control efficiency of at least 95%. If a combustion device is used, it must have a design destruction efficiency of at least 98% for hydrocarbons.~~

(a) Owners or operators must use enclosed, vapor-tight flowback vessels with an appropriate pressure relief system to be used only as necessary to ensure safety.

(b) Flowback vessels must be inspected, tested, and refurbished where necessary to ensure the flowback vessel is vapor-tight prior to receiving flowback.

(c) Flares used to control emissions from flowback vessels and pressure relief systems must be equipped with an automatic igniter or continuous pilot.

(2) During separation flowback, the operator shall capture and route natural gas:

(a) to a gas flowline or collection system, reinjecting it into the well, or use on-site as a fuel source or for another purpose that a purchased fuel or raw material would serve; or

(b) to a flare if routing the natural gas to a gas flowline or collection system, reinjecting it into the well, or using it on-site as a fuel source or other purpose that a purchased fuel or raw material would pose a risk to safe operation or personnel safety, provided that the flare is properly sized and equipped with an automatic igniter or continuous pilot.

(3) If N₂ or H₂S concentrations in natural gas exceeds the gathering pipeline specifications, the operator may flare the natural gas for 60 days or until the N₂ or H₂S concentrations meet the pipeline specifications, whichever is sooner, provided that:

(a) the flare stack is properly sized and equipped with an automatic igniter or continuous pilot;

(b) the operator analyzes the natural gas samples twice per week;

(c) the operator routes the natural gas samples twice per week;

(d) the operator provides the pipeline specifications and natural gas analyses to the

division upon request.

D. Venting and flaring during production operations. The operator shall not vent or flare natural gas except:

(1) to the extent authorized by a valid federally enforceable air quality permit issued by the New Mexico environment department;

(2) during an emergency or malfunction, but only to avoid a risk of an immediate and substantial adverse impact on safety, public health, or the environment. The operator shall notify the division of venting or flaring resulting from an emergency pursuant to Paragraph (1) of Subsection G of 19.15.27.8 NMAC.

(3) to unload or clean-up liquid holdup in a well to atmospheric pressure, provided

(a) ~~the operator uses an automated control system, such as a plunger lift, where technically feasible and optimizes the system to minimize the venting of natural gas;~~

(b) the operator does not vent after the well achieves a stabilized rate and pressure;

(c) for liquids unloading by manual purging, when the operator remains present on-site until the end of unloading, takes all reasonable actions to achieve a stabilized rate and pressure at the earliest practical time and takes all reasonable actions to minimize venting to the maximum extent practicable; or

(d) during downhole well maintenance, only when the operator uses a workover rig, swabbing rig, coiled tubing unit or similar specialty equipment and minimizes the venting of natural gas to the extent that it does not pose a risk to safe operations and personnel safety and is consistent with best management practices;

(e) ~~the operator must notify the division at least 48 hours prior to conducting unloading or well clean-up activities, except where the operator must act more quickly in order to minimize waste of natural gas. In these cases, the operator must notify the division as soon as possible prior to conducting unloading or well clean-up activities; or~~

(5) during the first 12 months of production from an exploratory well, or as extended by the division for good cause shown, provided:

Formatted: Space After: 8 pt, Line spacing: Multiple 1.08 li

Deleted: is routed to the flowback vessel by

Deleted: shall route flowback fluids into a

Formatted: Font:

Deleted: completion or storage tank and commence operation of a separator as soon as it is technically feasible for a separator to function.

Formatted: Font: (Default) Times New Roman

Deleted: b

Deleted: ¶

→→→(c)→ for a well equipped with a plunger lift system or an automated control system, the operator optimizes the system to minimize the venting of natural gas;

Deleted: o

Deleted: s

Deleted: OCD

Deleted: If the 48 hour notification would prevent the operator from conducting the least environmental impactful unloading or well clean-up activities

Deleted: , then

Deleted: shall

Deleted: OCD

Deleted: 4

Deleted: tion

Deleted: delineation

(a) the operator proposes and the division approves the well as an exploratory well
 (b) the operator is in compliance with its statewide gas capture requirements; and
 (c) if an exploratory well is capable of producing in paying quantities within 60
days of the division's approval, the operator submits an updated form C-129 to the division, including a natural gas management plan and timeline for connecting the well to a natural gas gathering system. If it is not possible for the operators to determine if a well is capable of producing in paying quantities within 60 days, the operator may seek approval for an extension of time, not to exceed 12 months; or
 (6) during the following activities unless prohibited by applicable state or federal law, rule, or regulation for the emission of hydrocarbons and volatile organic compounds:
 (a) gauging or sampling of a storage tank or other low-pressure production vessel;
 (b) loading out liquids from a storage tank or other low-pressure production vessel to a transport vehicle;
 (c) scheduled repair and maintenance, including blowing down and depressurizing production equipment to perform repair and maintenance;
 (d) normal operation of a gas-activated pneumatic controller or pump;
 (e) normal operation of a storage tank or other low-pressure production vessel, but not including venting from a thief hatch that has not been fully and timely closed or from a seal that is not maintained on an established schedule;
 (f) a bradenhead test taking no longer than 30 minutes, if practicable.
 (g) a packer leakage test;
 (h) a production test that does not exceed 24 hours unless the division requires or approves a longer test period; or
 (i) when N2 or H2S concentrations in natural gas exceeds the gathering pipeline specifications, provided the operator analyzes natural gas samples twice per week to determine whether the specifications have been achieved, routes the natural gas into a gathering pipeline as soon as the pipeline specifications are met and provides the pipeline specifications and natural gas analyses to the division upon request.

E. Performance standards for separation, storage tank and flare equipment.

(1) The operator shall design completion and production separation equipment and storage tanks for maximum throughput and pressure to maximize hydrocarbon recovery and minimize excess natural gas flashing and vapor accumulation.
 (2) The operator shall equip a permanent storage tank associated with production operations that is installed after {effective date of rule} with an automatic gauging system that reduces the venting of natural gas.
 (3) The operator shall combust natural gas in a flare stack that is properly sized and designed for and operated at maximum efficiency.
 (a) A flare stack installed or replaced after May 31, 2021 shall be equipped with an automatic ignitor or continuous pilot.
 (b) A flare stack installed before June 1, 2021 shall be retrofitted with an automatic ignitor or continuous pilot or technology that alerts the operator that the flare has malfunctioned no later than six months after {effective date of rule}.
 (c) Notwithstanding subsection E(3)(b), a flare stack located at a well with an average daily production of equal to or less than 10 barrels of oil or 60,000 cubic feet of natural gas shall be equipped with an automatic ignitor or continuous pilot no later than 12 months after {effective date of the rule}.
 (4) A flare stack located at a well spud after {effective date of rule} shall be securely anchored and located at least 100 feet from the well and storage tanks.
 (5) The operator shall conduct an AVO inspection on the frequency specified below to confirm that all production equipment is operating properly and there are no leaks or releases except as allowed in Subsection D of 19.15.27.8 NMAC.
 (a) During an AVO inspection the operator shall inspect all components, including flare stacks, thief hatches, closed vent systems, pumps, compressors, pressure relief devices, valves, lines, flanges, connectors, and associated piping to identify defects, leaks, and releases by:
 (i) visually inspecting for cracks and holes; loose connections; leaks, broken and missing caps; broken, damaged seals and gaskets; broken, missing and open hatches; broken, missing and open access covers and closure devices; and to ensure a flare stack is operating in conformance with its design.
 (ii) listening for pressure and liquid leaks; and
 (iii) smelling for unusual and strong odors.

- Deleted: delineation
- Deleted: ion
- Deleted: delineation
- Deleted: 12 months
- Deleted: 5

- Deleted: 18
- Deleted: A
- Formatted: Font: (Default) Times New Roman
- Deleted: if the flare stack is replaced after

- (b) The operator shall conduct an AVO inspection weekly:
 - (i) during the first year of production; and
 - (ii) on a well with an average daily production greater than 10 barrels of oil or 60,000 cubic feet of natural gas.
- (c) The operator shall conduct an AVO inspection weekly if it is on site, and in no case less than once per calendar month with at least 20 calendar days between inspections:
 - (i) on a well with an average daily production equal to or less than 10 barrels of oil or 60,000 cubic feet of natural gas; and
 - (ii) on shut-in, temporarily abandoned, or inactive wells.
- (d) The operators shall make and keep a record of each AVO inspection for not less than five years and make such record available for inspection by the division upon request.
- (7) Subject to the division's prior written approval, the operator may use a remote or automated monitoring technology to detect leaks and releases in lieu of an AVO inspection.
- (8) Operators shall submit to the Division an engineer's certification that all flares or combustors will have sufficient and consistent gas flow and heat content to achieve the manufacturer's design destruction efficiency.
- (9) All flaring during completions and production shall be done with an enclosed device that has a design destruction efficiency of 98%.

F. Measurement of vented and flared natural gas.

- (1) The operator shall measure the volume of natural gas that it vents, flares or beneficially uses during drilling, completion, and production operations regardless of the reason or authorization for such venting or flaring.
- (2) The operator shall install equipment on flowlines that are piped from equipment such as high pressure separators, heater treaters and vapor recovery units to measure the volume of natural gas vented and flared from a well authorized by an APD issued after May 31, 2021 that has an average daily production greater than 10 barrels of oil or 60,000 cubic feet of natural gas.
- (3) Measuring equipment shall be an orifice meter or other measurement device or technology such as a thermal mass or ultrasonic flow meter approved by the division that, at the time of installation, complies with the accuracy ratings and design standards for the measurement of natural gas, such as the American petroleum institute, international organization for standards, or American gas association.
- (4) Measuring equipment shall not be designed or equipped with a manifold that allows the diversion of natural gas around the metering element except for the sole purpose of inspecting and servicing the measurement equipment.
- (5) For an event for which metering is not practicable, such as low pressure venting and flaring, the operator ~~shall calculate~~ the volume of vented and flared natural gas using the methodologies specified by the U.S. EPA Greenhouse Gas Reporting Rule (40 CFR Part 98 Subpart W, § 98.233) or other established methodologies specified by the division. If the division determines that no established methodology is available for a particular source of venting or flaring, it may authorize the operator to estimate the volume of vented or flared gas using the best information available to the operator.
- (6) The operator shall install additional measuring equipment whenever the division determines that the existing measuring equipment is not sufficient to measure the volume of vented and flared natural gas.

G. Reporting of vented or flared gas.

- (1) **Venting or flaring caused by emergency or malfunction, or of long duration.**
 - (a) The operator shall notify the division of venting or flaring that exceeds 50 MCF in volume and either results from an emergency or malfunction, or lasts eight hours or more cumulatively within any 24-hour period by filing a form C-129 with the division as follows:
 - (i) for venting or flaring that equals or exceeds 50 MCF but less than 500 MCF, notify the appropriate division district office in writing by filing a form C-129 no later than 15 days following discovery or commencement of venting or flaring.
 - (ii) for venting or flaring that equals or exceeds 500 MCF or otherwise qualifies as a major release as defined in 19.15.29.7 NMAC, notify the appropriate division district office verbally or by e-mail as soon as possible and no later than 24 hours following discovery or commencement of venting or flaring and provide the information required in form C-129. No later than 15 days following the discovery or commencement of venting or flaring, the operator shall file a form C-129 that verifies, updates, or corrects the verbal or e-mail notification; and

- Deleted:** may estimate
- Formatted:** Font: (Default) Times New Roman
- Formatted:** Font: (Default) Times New Roman
- Deleted:** → For a well that does not require measuring equipment, the operator shall estimate the volume of vented and flared natural gas based on the result of an annual GOR test for that well reported on form C-116.¶
- Deleted:** (7)→
- Deleted:** or GOR test

(iii) no later than 15 days following the termination of venting or flaring, notify the appropriate division district office by filing a form C-129.

(b) The operator shall provide and certify the accuracy of the following information in the form C-129:

- (i) operator's name;
- (ii) name and type of facility;
- (iii) equipment involved;
- (iv) analysis of vented or flared natural gas;
- (v) date(s) and time(s) that venting or flaring was discovered or commenced and terminated;
- (vi) measured or estimated volume of vented or flared natural gas;
- (vii) cause and nature of venting or flaring;
- (viii) steps taken to limit the duration and magnitude of venting or flaring;

and

- (ix) corrective actions taken to eliminate the cause and recurrence of venting or flaring.

(c) At the division's request, the operator shall provide and certify additional information by the specified date.

(d) The operator shall file a form C-141 instead of a form C-129 for the release of a liquid during venting or flaring that is or may be a major or minor release under 19.15.29.7 NMAC.

(2) Monthly reporting of vented and flared natural gas. The operator shall report the volume of vented and flared natural gas for each month in each category listed below. Beginning June 2021, the operator shall submit quarterly reports in a format specified by the division. Beginning January 2022, the operator shall submit a form C-115B monthly on or before the 15th day of the second month following the month in which it vented or flared natural gas. The operator shall specify whether it estimated or measured each reported volume. In filing the initial report, the operator shall provide the methodology (measured or estimated using calculations and industry standard factors) used to report the volumes and shall report changes in the methodology on future forms. The operator shall make and keep records of the measurements and estimates, including records showing how it calculated the estimates, for no less than five years and make such records available for inspection by the division upon request. The categories are:

- (a) emergency;
- (b) non-scheduled maintenance or malfunction;
- (c) routine repair and maintenance, including blowdown and depressurization;
- (d) routine downhole maintenance, including operation of workover rigs, swabbing rigs, coiled tubing units and similar specialty equipment;
- (e) manual liquid unloading;
- (f) uncontrolled storage tanks;
- (g) insufficient availability or capacity in a natural gas gathering system during separation phase of completion operations or production operations;
- (h) natural gas quality that is not suitable for transportation and processing because of N₂ or H₂S concentrations;
- (i) venting as a result of normal operation of pneumatic controllers and pumps, unless the operator vents or flares less than 500,000 cubic feet per year of natural gas;
- (j) improperly closed or maintained thief hatches that are routed to a flare or control device;
- (k) venting or flaring in excess of four hours that is caused by an emergency, unscheduled maintenance or malfunction of a natural gas gathering system as defined in 19.15.28 NMAC; and
- (l) other not described above.

(3) The operator shall report the lost natural gas for each month on a volumetric and percentage basis on form C-115B.

- (a) To calculate the lost natural gas on a volumetric basis, the operator shall deduct the volume of natural gas sold, used for beneficial use, vented or flared during an emergency, and vented or flared because it was not suitable for transportation or processing, from the natural gas produced.
- (b) To calculate the lost natural gas on a percentage basis, the operator shall add the volume of natural gas sold, used for beneficial use, vented or flared during an emergency and vented or flared

- Deleted: ¶

because it was not suitable for transportation or processing, and divide by the total volume of natural gas produced.

(4) The operator shall report the vented and flared natural gas on a volumetric and percentage basis to all royalty owners in the mineral estate being produced by the well on a monthly basis, keep such reports for not less than five years and make such records available for inspection by the division upon request.

(5) Upon request by the division, the operator, at its own expense, shall retain a third-party approved by the division to verify any data or information collected or reported pursuant to Subsections F and G of 19.15.27.8 NMAC and make recommendations to correct or improve the collection and reporting of data and information, submit a report of the verification and recommendations to the division by the specified date, and implement the recommendations in the manner approved by the division.

(6) Upon the New Mexico environment department's request, the operator shall promptly provide a copy of any form filed pursuant to 19.15.27 NMAC.
[19.15.27.8 NMAC – N, xx/xx/xx]

19.15.27.9 STATEWIDE NATURAL GAS CAPTURE REQUIREMENTS:

A. Statewide natural gas capture requirements. Commencing January 1, 2022, the operator shall reduce the annual volume of vented and flared natural gas in order to capture ninety-eight percent of the natural gas produced from its wells in each of two reporting areas, one north and one south of the Township 10 North line, by December 31, 2026. The division shall calculate and publish each operator's baseline natural gas capture rate based on the operator's 2021 monthly data reported on form C-115B. In each calendar year between January 1, 2022 and December 31, 2026, the operator shall increase the percentage of natural gas captured based on the following formula: (2021 baseline loss rate minus two percent) divided by five.

(1) The following table provides examples of the formula based on a range of baseline natural gas capture rates.

Baseline Natural Gas Capture Rate	Minimum Required Annual Natural Gas Capture Percentage Increase
90-98%	0-1.6%
80-89%	>1.6-3.6%
70-79%	>3.6-5.6%
0-69%	>5.6-19.6%

(2) If the operator's baseline capture rate is less than sixty percent, the operator shall submit by the specified date to the division for approval a plan to meet the minimum required annual capture percentage increase.

(3) An operator that acquires one or more wells from another operator shall comply with its statewide natural gas capture requirements for the acquired well(s) no later than December 1, 2026 unless the division approves a later date.

B. Accounting. No later than February 15 each year beginning in 2022 and each year thereafter, the operator shall submit a report certifying compliance with its statewide gas capture requirements. The operator's volume of vented and flared natural gas shall be counted as produced natural gas and excluded from the volume of natural gas sold or used for beneficial use in the calculation of its statewide natural gas capture requirements, except that:

(1) the operator may exclude from the volume of produced natural gas the volume of natural gas vented and flared pursuant to Subparagraphs (a) and (h) of Paragraph (2) of Subsection G of 19.15.27.8 NMAC for which the operator timely filed, and the division approved, a form C-129.

(2) the operator may exclude the volume of produced natural gas the volume of natural gas reported as a beneficial use or vented or flared from an ~~exploratory well~~ and reported on the operator's form C-115.

(3) An operator that used a division-approved ALARM technology to monitor for leaks and releases may obtain a credit against the volume of lost natural gas if it discovered the leak or release using the ALARM technology and the operator:

- (a) isolated the leak or release within 48 hours following field verification;
- (b) repaired the leak or release within 15 days following field verification
- (c) timely notified the division by filing a form C-129 or form C-141;
- (d) timely reported the volume of natural gas leaked or released on form C-

115 as an ALARM event pursuant to Subparagraph (n) of Paragraph (2) of Subsection F of 19.15.28.8 NMAC; and

Deleted: delineation

(d) used ALARM monitoring technology as a routine and on-going aspect of its waste-reduction practices.

(i) For discrete waste-reduction practices such as aerial methane monitoring, the operator must use the technology at least twice per year; and

(ii) for waste-reduction practices such as automated emissions monitoring systems that operate routinely or continuously, the division will determine the required frequency of use.

(4) An operator may file an application with the division for a credit against its volume of lost natural gas that identifies:

(a) use ALARM technology used to discover the leak or release;

(b) the dates on which the leak or release was discovered, field-verified, isolated

and repaired;

(c) the method used to measure, calculate, or estimate the volume of natural gas leaked or released, which method shall be consistent with the quantification requirements specified under 19.15.27.8(F);

(d) a description and the date of each action taken to isolate and repair the leak or release;

(e) visual documentation or other verification of discovery, isolation and repair of the leak or release;

(f) a certification that the operator did not know or have reason to know of the leak or release before discovery using ALARM technology; and

(g) a description of how the operator used ALARM technology as a routine and on-going aspect of its waste-reduction practices.

(5) For each leak or release reported by an operator that meets the requirements of Paragraphs (3) and (4) of Subsection B of 29.15.28.10 NMAC, the division, in its sole discretion, may approve a credit that the operator can apply against its reported volume of lost natural gas as follows:

(a) a credit of forty percent of the volume of natural gas discovered and isolated within 48 hours of discovery and timely repaired;

(b) an additional credit of twenty percent if the operator uses ALARM technology no less than once per calendar quarter as a routine and on-going aspect of its waste-reduction practices.

(6) A division-approved ALARM credit shall:

(a) be used only by the operator who submitted the application pursuant to Paragraph (4) of Subsection B of 29.15.27.10 NMAC;

(b) not be transferred to or used by another operator, including a parent, subsidiary, related entity, or person acquiring the well;

(c) be used only once; and

(d) expire 24 months after division approval.

C. Third-party verification. Upon request by the division, the operator, at its own expense, shall retain a third-party approved by the division to verify any data or information collected or reported pursuant to Subsections F and G of 19.15.27.8 NMAC or Subsection B(4) of 19.15.27.9 NMAC and make recommendations to correct or improve the collection and reporting of data and information, submit a report of the verification and recommendations to the division by the specified date, and implement the recommendations in the manner approved by the division.

D. Natural gas management plan.

(1) After May 31, 2021, the operator shall file a natural gas management plan with each APD for a new or recompleted well, including exploratory wells. The operator may file a single natural gas management plan for multiple wells drilled or recompleted from a single well pad or that will be connected to a central delivery point. The natural gas management plan shall describe the actions that the operator will take at each proposed well to meet its statewide natural gas capture requirements and to comply with the requirements of Subsections A through F of 19.15.27.8 NMAC, including for each well:

(a) the operator's name and OGRID number;

(b) the name, API number, location and footage;

(c) the anticipated dates of drilling, completion and first production;

(d) any anticipated safety risks that will require the operator to allow natural gas to escape during drilling;

(e) a description of operational best practices that will be used to minimize venting during active and planned maintenance;

Deleted: and

Deleted: Paragraph (4) of

Deleted: and

(f) procedures the operator will employ to reduce the frequency of well liquids unloading events; and

(g) anticipated volumes of liquids and gas production and a description of how separation equipment will be sized to optimize gas capture.

(2) An operator that, at the time it submits an APD for a new or recompletion well, is not in compliance with its statewide natural gas capture requirements shall also include the following information in the natural gas management plan:

(a) the anticipated volume of produced natural gas in units of MCFD for the first year of production;

(b) the existing natural gas gathering system the operator has contracted or anticipates contracting with to gather the natural gas, including

(i) the name of the natural gas gathering system operator;

(ii) the name and location of the natural gas gathering system;

(iii) a map of the natural gas gathering system as built or as planned if it has

not yet been built; and

(iv) the maximum daily capacity of the natural gas gathering system to which the well will be connected; and;

(c) the operator's plans for connecting the well to the natural gas gathering system, including:

(i) the anticipated date on which the natural gas gathering system will be available to gather the natural gas produced from the well;

(ii) whether, at the time of application, the natural gas gathering system has existing capacity to gather the anticipated natural gas production volume from the well; and

(iii) whether the operator anticipates the operator's existing well(s) connected to the same natural gas gathering system will continue to be able to meet anticipated increases in line pressure caused by the well and the operator's plan to manage increased line pressure.

(3) The operator may submit a request asserting confidentiality for information specified in Paragraph (2) of Subsection D of 19.15.27.9 NMAC, which the division will review in accordance with Section 71-2-8 NMSA 1978.

(4) The operator shall certify that it has determined based on the available information at the time of submitting the natural gas management plan either:

(a) it will be able to connect the well to a natural gas gathering system in the general area with sufficient capacity to transport one hundred percent of the volume of natural gas the operator anticipates the well will produce commencing on the date of first production, taking into account the current and anticipated volumes of produced natural gas from other wells connected to the pipeline gathering system; or

(b) it will not be able to connect to a natural gas gathering system in the general area with sufficient capacity to transport one hundred percent of the volume of natural gas the operator anticipates the well will produce commencing on the date of first production, taking into account the current and anticipated volumes of produced natural gas from other wells connected to the pipeline gathering system.

(5) If the operator determines it will not be able to connect a natural gas gathering system in the general area with sufficient capacity to transport one hundred percent of the anticipated volume of natural gas produced on the date of first production from the well, the operator shall submit a venting and flaring plan to the division that evaluates the potential alternative uses for the natural gas until a natural gas gathering system is available, including:

(a) power generation on lease;

(b) power generation for grid;

(c) compression on lease;

(d) liquids removal on lease;

(e) reinjection for underground storage;

(f) reinjection for temporary storage;

(g) reinjection for storage;

(h) reinjection for enhanced oil recovery;

(i) fuel cell production; and

(j) other alternative uses for putting the gas to beneficial use approved by the

division.

Formatted: Font: (Default) Times New Roman, 10 pt

(6) If, at any time after the operator submits the natural gas management plan and before the well is spud:

(a) the operator becomes aware that the natural gas gathering system it planned to connect the well to has become unavailable or will not have capacity to transport one hundred percent of the production from the well, no later than 20 days after becoming aware of such information, the operator shall submit for the division's approval a new or revised venting and flaring plan containing the information specified in Paragraph (4) of Subsection D of 19.15.27.9 NMAC; and

(b) the operator becomes aware that it has become out of compliance with the statewide natural gas capture requirements, no later than 20 days after becoming aware of such information, the operator shall submit for the division's approval a new or revised natural gas management plan containing the information specified in Paragraph (2) of Subsection D of 19.15.27.9 NMAC.

(7) If the operator does not make a certification or fails to submit an adequate venting and flaring plan, or if the operator is not in compliance with its statewide natural gas capture requirements, or if the division determines that the operator will not have adequate natural gas takeaway capacity at the time a well will be spud, the division ~~will~~:

- (a) deny the APD; or
- (b) conditionally approve the APD.

[19.15.27.9 NMAC – N, xx/xx/xx]

Deleted: may

Formatted: Font: (Default) Times New Roman

Exhibit 5

JON GOLDSTEIN

408 Stickney St.
PO Box 401
Lyons, CO 80540
(505) 603-8522

jonw.goldstein@gmail.com

ENERGY AND ENVIRONMENTAL POLICY EXPERIENCE:

Environmental Defense Fund, Boulder, CO

2012-Present

DIRECTOR, REGULATORY & LEGISLATIVE AFFAIRS/SENIOR ENERGY POLICY MANAGER

- Led efforts to improve oil and gas environmental regulations in the Rocky Mountain region -- including a specific focus on New Mexico, Utah and Wyoming -- through extensive in-state work establishing and maintaining relationships with industry, environmental groups, and regulators
- Managed EDF's multifaceted, multiyear, multi-million dollar campaign to pass and defend strong Bureau of Land Management regulations designed to limit methane emissions from oil and gas development on all federal and tribal lands
- Spearheaded EDF's involvement in Wyoming's development of nationally-leading air quality and groundwater testing rules

American Wind Energy Association, Washington, DC

2011-2012

DIRECTOR OF PUBLIC AFFAIRS

- Led press relations, messaging and rapid response efforts for the American wind industry's major trade group
- Managed AWEA's issue campaigns including extensive work on siting issues such as avian impacts, noise and community acceptance and involvement
- Responsible for personnel management and budgetary issues as well as assistance in managing and leading the department and the organization as a member of AWEA's Senior Management Team

New Mexico Energy, Minerals and Natural Resources Department, Santa Fe, NM

2010

CABINET SECRETARY

- Led a diverse regulatory and land management agency with 550 employees and a \$75 million annual budget
- Appointed by Governor Bill Richardson and confirmed by the New Mexico State Senate as one of the youngest cabinet secretaries in state history
- Oversaw the state's efforts to promote renewable energy, improve regulation of the oil & gas and mining industries and increase the number and quality of state parks
- Managed departmental communications with the Governor, Chief of Staff, other state agencies and members of the state legislature
- Served on the New Mexico Renewable Energy Transmission Authority and Finance Authority

New Mexico Environment Department, Santa Fe, NM

2007-2009

DEPUTY CABINET SECRETARY

- Oversaw day-to-day operations and acted as Chief of Staff for a 700 employee regulatory agency with a more than \$100 million annual budget
- Led policy development in areas including climate change and proposed coal-fired power plants, water and wastewater infrastructure investments, opposition to federal environmental rollbacks, uranium mining, tribal relations, international border issues and environmental justice
- Served as a member of New Mexico's Green Jobs Cabinet and Water Cabinet
- Named State Liaison to the U.S. Nuclear Regulatory Commission by Governor Richardson

CHAIRMAN, New Mexico Water Quality Control Commission (2007-2009)

- Heard appeals and issued decisions on cases including Clean Water Act water quality standards, Los Alamos National Laboratory permitting and native fish restoration
- Increased Tribal representation on the Commission

CHAIRMAN, New Mexico Mining Commission (2009)

- Elected Chair of the state's rulemaking body for the New Mexico Mining Act
- Successfully passed new, more protective uranium mining regulations

DIVISION DIRECTOR

- Managed the New Mexico Environment Department's largest division with more than 200 employees and a \$22 million annual budget
- Crafted strong environmental enforcement actions and negotiated major settlements that led to improved environmental safeguards for all New Mexicans
- Directed implementation of radioactive and hazardous waste clean-up under a fence-to-fence order with the U.S. Department of Energy's Los Alamos National Laboratory
- Served as the state's representative to the DOE's State and Tribal Government Working Group

New Mexico Governor Bill Richardson, Santa Fe, NM

2005-2007

DEPUTY COMMUNICATIONS DIRECTOR

- Led message development and handled all media issues in policy areas including energy, environment and health
- Wrote speeches, press releases and assisted in policy development in a demanding media environment during historic re-election and presidential campaigns
- Staffed the Governor during meetings with the Democratic Governors Association and Democratic Leadership Council
- Set up media opportunities, wrote talking points and staffed the Governor during interviews with outlets including CNN's Larry King Live, Fox News, NPR, The New York Times, The Washington Post, *Piolin por la Mañana*, and The Los Angeles Times

New Mexico Environment Department, Santa Fe, NM

2003-2005

COMMUNICATIONS DIRECTOR

- Enabled positive coverage of Governor Richardson's environmental policies including cover stories in the *High Country News* and numerous positive editorials
- Coordinated media for the largest environmental settlement in state history (\$320 million) with the Public Service Company of New Mexico, historic clean up order signing with the Los Alamos National Laboratory, and the nation's strongest regulations protecting late-night retail workers
- Executive Producer and co-writer of the half hour "Water Warning" program aired on Public Broadcasting stations to raise awareness of water quality issues in New Mexico
- Negotiated a legal agreement placing disposal prohibitions and enforceable limits on radioactive waste storage at a URENCO-owned uranium enrichment facility

Richardson for Governor, Albuquerque, NM

Fall 2002

SPECIAL EVENTS COORDINATOR

- Planned, orchestrated and executed political rallies in diverse communities across New Mexico during Bill Richardson's successful campaign for Governor
- Messaging work on environmental issues including script writing for a radio advertisement recorded by Robert Redford
- Cultivated relationships with elected officials and community leaders

JOURNALISM EXPERIENCE:

The Baltimore Sun, Baltimoresun.com, Baltimore, MD

2000-2002

BUSINESS EDITOR/REPORTER

- Designed and conceived the business news page of the Baltimore *Sun's* Web site including coverage of regional economic news and the technology industry
- Covered local political, crime and general news on tight deadlines
- Reported, wrote and photographed a multiday series of stories on the U.S. Coast Guard's underfunded search and rescue efforts

Time Magazine/Time Digital, New York, NY

1996-1998

REPORTER/EDITOR

- Researched and wrote profiles of Congressional candidates during the 1996 cycle
- Covered new technology with a focus on the intersection of technology and culture
- Wrote feature stories on Disney's efforts to build a wired planned community and led the magazine's annual effort to rank the world's top 50 cyber elite

EDUCATION:

- PRINCETON UNIVERSITY**, Woodrow Wilson School of Public and International Affairs, Princeton, NJ 2011
- Master in Public Policy (MPP) with a Certificate in Science, Technology and Environmental Policy (STEP)
 - Co-recipient of the *MPP Award* for outstanding academic achievement and commitment to public service
- TRINITY COLLEGE**, Hartford, CT 1996
- Bachelor of Arts Degree, Major: History (honors); Minor: The Classical Tradition
 - Elected to the *Phi Beta Kappa* and *Pi Gamma Mu* national academic honor societies

GRADUATE RESEARCH AND OTHER EXPERIENCE:

Author of "How to Build a Better Sepulcher: Lessons Learned from the Waste Isolation Pilot Project"

Published in the scholarly journal: *Bulletin of the Atomic Scientists* – September, 2011

- Conducted independent research and analysis of the three decade long process that went into locating the world's only operating deep geologic repository for radioactive waste in Carlsbad, New Mexico
- Developed concrete recommendations for applying these lessons to other radioactive waste disposal efforts in Europe and Asia as well as at the Yucca Mountain repository in Nevada

Plutonium & Radioactive Waste Politics in East Asia Policy Workshop

Princeton University, Woodrow Wilson School, Fall 2010, taught by Dr. Frank von Hippel

- Worked with a small team of Woodrow Wilson graduate students to produce a report on the politics and policies surrounding nuclear fuel reprocessing and interim nuclear waste storage issues in East Asia
- Traveled to Beijing and Tokyo to interview Chinese and Japanese government officials, scholars, nuclear energy experts, environmental activists and utility managers
- Led the presentation of the report and its recommendations to high level officials from the U.S. Department of State and the U.S. Department of Energy in Washington, DC

Board Member, State Review of Oil and Natural Gas Environmental Regulations (STRONGER) 2016-Present

Volunteer Member, EDF Diversity Committee and Co-Chair, Environmental Justice Subcommittee 2012-Present

Board Chair, Conservation Voters New Mexico Education Fund, Santa Fe, NM 2012-2014

Board Member, Chupadero Mutual Domestic Water and Sewage Corp., Santa Fe, NM 2012-2014

National Finalist, White House Fellows Program, Washington, DC 2011

Exhibit 6



EXECUTIVE ORDER 2019-003

EXECUTIVE ORDER ON ADDRESSING CLIMATE CHANGE AND ENERGY WASTE PREVENTION

I. Background and Purpose

To further New Mexico's responsibility and opportunity to build a clean energy future for our people, limit adverse climate change impacts that harm our natural and cultural heritage, prevent the waste of New Mexico energy resources and reduce pollution that threatens human health, I hereby issue this Executive Order.

II. Climate Change

WHEREAS, climate change creates new risks and exacerbates existing vulnerabilities in communities across New Mexico and presents growing challenges for human health and safety, quality of life, and the rate of economic growth.

WHEREAS, in a special report authored by the United Nations and World Meteorological Organization Intergovernmental Panel on Climate Change ("IPCC"), it was found that the planet has as little as 12 years to take meaningful climate action in order to limit the increase in global average temperature to 1.5°C – the level necessary to forestall dramatic climatic changes that will further imperil our water supplies.

WHEREAS, carbon dioxide, methane, nitrous oxide, hydrofluorocarbons (HFCs), perfluorocarbons, and sulfur hexafluoride are recognized as the six greenhouse gases contributing to climate change.

WHEREAS, in 2009, the U.S. Environmental Protection Agency ("EPA") found that these "six greenhouse gases taken in combination endanger both the public health and the public welfare of current and future generations."

WHEREAS, in May 2010, the National Research Council, the operating arm of the National Academy of Sciences, published an assessment which concluded that "climate change is occurring, is caused largely by human activities, and poses significant risks for - and in many cases is already affecting - a broad range of human and natural systems."

WHEREAS, carbon dioxide is emitted through the combustion of fossil fuels for electricity generation and for combustion-engine vehicles.

WHEREAS, the U.S. Energy Information Administration finds that the transportation sector is the largest anthropogenic source of carbon dioxide emissions in the United States.

WHEREAS, methane is a powerful greenhouse gas, 84 times more effective at trapping heat than carbon dioxide over a 20-year timeframe.



WHEREAS, the oil and gas industry is the largest industrial source of methane emissions.

WHEREAS, HFCs are potent greenhouse gases used in the refrigeration, air conditioning, and foam industries, for which alternatives are readily available and approved for use by the EPA.

WHEREAS, governments and global industries have expressed widespread support for a global transition to alternatives to HFCs, as agreed to in the 2016 Kigali Amendment to the Montreal Protocol.

WHEREAS, New Energy Conservation Code templates are developed by the International Code Council every three years. New Mexico adopted and is using the 2009 International Energy Conservation Code (IECC), which puts the state three full code cycles behind. As newer, safer, and more durable building materials, technologies, and techniques become more commonplace, they are voted on and incorporated into the model energy code.

WHEREAS, energy codes create safe, resilient, and habitable structures based on building science and physics principals for heat, air, and moisture transfer—all of which have real and significant impacts on human lives and health; they also can cut utility bills in buildings.

WHEREAS, low- and zero-emission vehicles can provide long-term public health, environmental, and climate benefits.

WHEREAS, federal rollbacks of climate protections, waste prevention, and clean air rules have made it imperative for New Mexico to act to protect our citizens and our economy from the damages of climate change impacts.

WHEREAS, emissions, venting, flaring, and leaks of natural gas by New Mexico's oil and gas industry results in the waste of an important source of domestic energy to the tune of an estimated \$244 million per year.

WHEREAS, oil and gas production growth in the New Mexico Permian Basin resulted in an 18% increase in venting and flaring volumes during the first seven months of 2018 compared to 2017 according to official state statistics.

WHEREAS, efforts to reduce methane emissions throughout New Mexico will have a significant climate benefit as well as prevent the waste of energy resources.

WHEREAS, science, innovation, collaboration and compliance efforts can prevent waste, methane emissions and improve air quality while creating jobs for New Mexicans.

III. Directives

NOW, THEREFORE, by the authority vested in me as Governor by the Constitution and laws of the State of New Mexico, IT IS ORDERED:

1. The State of New Mexico will support the 2015 Paris Agreement Goals by joining the U.S. Climate Alliance. New Mexico's objective is to achieve a statewide reduction in greenhouse gas emissions of at least 45% by 2030 as compared to 2005 levels.
2. The Secretary (or designee) of each state agency shall serve on an interagency Climate Change Task Force which is hereby established. The Secretary (or designee) of the Energy, Minerals and Natural Resources Department ("EMNRD") and the Environment Department ("NMED") shall serve as the Co-Chairs, convening meetings, facilitating stakeholder participation, and providing strategic direction for achieving the above goals in developing a New Mexico Climate Strategy document.
3. All State Agencies shall evaluate the impacts of climate change on their programs and operations and integrate climate change mitigation and adaptation practices into their programs and operations. The agencies shall share these actions with the Climate Change Task Force for inclusion into the New Mexico Climate Strategy document.
4. EMNRD and NMED shall work with stakeholders on legislation to increase the New Mexico renewable portfolio standard ("RPS") and increase New Mexico's energy efficiency standards for electric utilities.
5. The Climate Change Task Force shall evaluate policies and regulatory strategies to achieve reductions in greenhouse gas pollution, consistent with the targets set out above, across all categories of emission sources. Such policies and regulatory strategies shall include, but not be limited to, the following:
 - a. Adoption of a comprehensive market-based program that sets emission limits to reduce carbon dioxide, and other greenhouse gas pollution across New Mexico;
 - b. Adoption of approaches to reduce greenhouse gas and criteria pollutant emissions from light-duty vehicles sold in state, including Low Emission Vehicle (LEV) emission standards and Zero Emission Vehicle (ZEV) performance standards;
 - c. Adoption of building codes; and
 - d. Collaboration with the Renewable Energy Transmission Authority (RETA) to identify transmission corridors needed to transport the state's renewable electricity to market.
6. EMNRD and NMED shall jointly develop a statewide, enforceable regulatory framework to secure reductions in oil and gas sector methane emissions and to prevent waste from new and existing sources and enact such rules as soon as practicable.
7. EMNRD and NMED shall coordinate as much as possible with the New Mexico State Land Office and federal bureaus and agencies that manage land and natural resources in New Mexico to help advance the priorities identified in this Executive Order.
8. The Climate Change Task Force will develop a *New Mexico Climate Strategy* document with initial recommendations and a status update, where applicable, to the Governor by September 15, 2019.

IV. Disclaimer

Nothing in this Executive Order is intended to create a private right of action to enforce any provision of this Order or to mandate the undertaking of any particular action pursuant to this Order; nor is this Order intended to diminish or expand any existing legal rights or remedies.

THIS ORDER supersedes any other previous orders, proclamations, or directives in conflict. This Executive Order shall take effect immediately and shall remain in effect until such time as it is rescinded by the Governor.

ATTEST:

DONE AT THE EXECUTIVE OFFICE
THIS 29th DAY OF JANUARY, 2019

Maggie Toulouse Oliver

WITNESS MY HAND AND THE GREAT
SEAL OF THE STATE OF NEW MEXICO

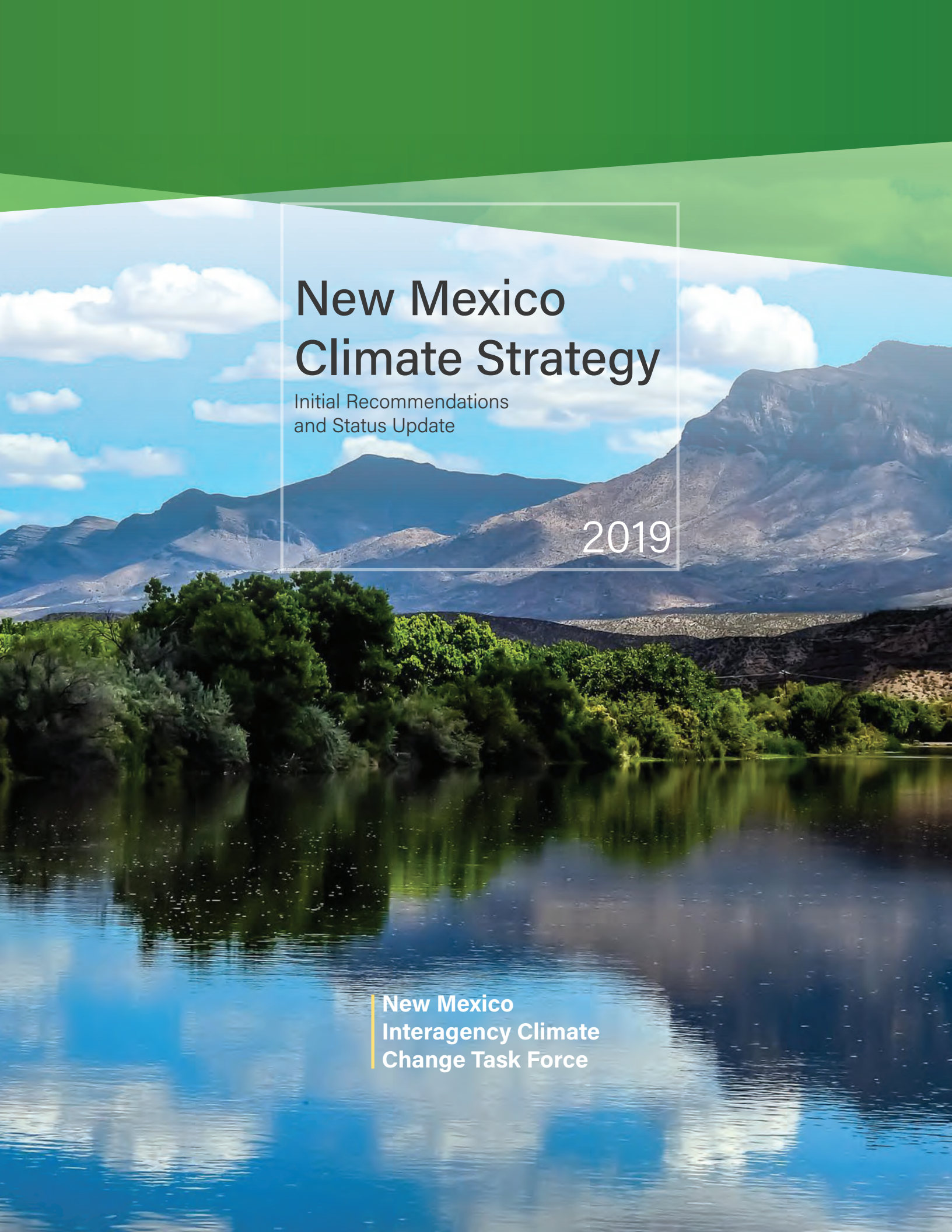
MAGGIE TOULOUSE OLIVER
SECRETARY OF STATE



Michelle Lujan Grisham

MICHELLE LUJAN GRISHAM
GOVERNOR

Exhibit 7



New Mexico Climate Strategy

Initial Recommendations
and Status Update

2019

New Mexico
Interagency Climate
Change Task Force



Table of Contents

The Governor’s Message	3
Science and Data	4
Reducing Greenhouse Gas Levels	8
Electricity Sector	9
Transportation Sector	11
Industrial Sector	13
Built Environment Sector	15
Natural and Working Lands Sector	18
Cross-Sector Emissions Reductions: Market Mechanisms	19
Adaptation and Resilience	21
Economic Transition	21
Public Health	22
Emergency Preparedness and Management	23
Water Availability	25
Conclusions	26

Bluewater Lake State Park – which are open for public use.

- NMDOT and EMNRD’s State Parks Division are in the process of installing charging stations at additional locations.

Electric vehicle adoption is accelerating. To stay on top of the evolving transportation landscape, we have formed two groups to drive our future actions in the right direction. The first of these is an EV Working Group, composed of state agencies, utilities, electric co-ops, the vehicle industry, and advocacy groups, convened by EMNRD. The second is a multi-agency EV Climate Action Team comprised of EMNRD, NMED, New Mexico Department of Transportation (NMDOT), New Mexico Tourism Department, New Mexico Tax and Revenue Department, and GSD, which is developing partnerships with educational institutions, utilities, automobile manufacturers, and vehicle dealerships to increase EV market penetration. For example, the Team will review the progress of installing charging infrastructure across the state after NMED distributes the next round of funding for projects that improve air quality related to transportation in late 2020, and then assess where New Mexico and its REV West partners need to fill in charging infrastructure gaps on major highways.

Industrial Sector

The industrial sector, including oil and gas production, is the largest source of greenhouse gas emissions in New Mexico. Emissions from the oil and gas industry are 57% of industrial emissions: given current production trends, these emissions are likely to grow absent new regulations. Methane emissions, which the EPA estimates are 25 times more potent than CO₂ emissions, are a large but addressable part of total oil and gas emissions. In addition, the state loses at

least \$10 million each year in revenue when methane is vented or flared – it is an expensive waste of a resource, as well as a major contributor to climate change. These factors make reducing methane emissions from oil and gas through a statewide methane regulatory framework the highest priority for New Mexico.

Reducing Oil and Gas Sector Methane Emissions

NMED and EMNRD both regulate the oil and gas sector and are working together to develop a “statewide, enforceable regulatory framework to secure reductions in oil and gas sector methane emissions and to prevent waste from new and existing sources and enact such rules as soon as practicable” as mandated in Governor Michelle Lujan Grisham’s Executive Order 2019-003. The agencies have unique yet complementary jurisdictions. NMED regulates air pollution under the state Air Quality Control Act, while EMNRD regulates the waste of a resource under the state Oil and Gas Act.

Methane from the oil and natural gas industry is emitted alongside with other pollutants: volatile organic compounds (VOCs) and “air toxics” that include benzene, toluene, ethylbenzene, and xylene. VOCs are a key ingredient in creating ground-level ozone (smog).

The state Air Quality Control Act requires the state to develop a plan and regulations to reduce ozone precursors – VOCs (Volatile Organic Compounds) and NO_x (Oxides of Nitrogen) – in areas where monitored ozone levels are greater than 95% of the National Ambient Air Quality Standard (NAAQS) for ozone. Seven counties in New Mexico are approaching 95% of the ozone standard of 70 parts per billion (ppb): Bernalillo, Chavez, Dona Ana, Eddy, Lea, Rio Arriba, and San Juan Counties. Bernalillo County has its own regulatory authority for air quality and will not be included in these rules. To reduce the ozone levels in the remaining six counties, NMED is developing rules

targeting VOC and NO_x reductions. The reductions in VOCs will collaterally reduce methane. This will be the first time that NMED regulates VOCs and methane beyond federal requirements.

The New Mexico Oil and Gas Act governs EMNRD's Oil Conservation Division (OCD) on methane matters. The Oil and Gas Act directs OCD to prevent waste, protect correlative rights, and protect public health and the environment.

Specifically, the Oil and Gas Act prohibits "waste" from oil and gas production, and the OCD has a "no vent or flare" rule in place. Rule 19.15.18.12(A) NMAC, titled "Casinghead Gas" states that, "An operator shall not flare or vent casinghead gas produced from a well after 60 days following the well's completion." However, there are multiple exceptions to the rule. Operators tend to operate within the exceptions of the rule instead of the intent, making additional regulation necessary.

NMED and EMNRD conducted extensive stakeholder engagement during the summer of 2019 to seek feedback on effective ways to prevent methane pollution and waste. In addition, to gain a deeper technical perspective on methane emissions and waste, the agencies established a Methane Advisory Panel (MAP) consisting of 27 stakeholders who possess technical expertise related to the oil and natural gas industry. MAP members are professionals with specific areas of practice, including petroleum engineers, chemical and life scientists, environmental attorneys, and public administrators. Individuals from Los Alamos National Laboratory, Colorado State University, and the New Mexico Institute of Mining and Technology are providing technical assistance throughout the MAP process. A draft technical report stemming from the MAP efforts will be available for public review and comment prior to December 20, 2019. The focus of this report is methane controls in the production (upstream) and midstream industry sectors of the oil and natural gas value chain.⁷

MAP Meeting Topics

- Process overview and available data and studies
- Completions and stimulations
- Workovers and liquids unloading
- Dehydrators, separators, and heater treaters
- Compressors and engines
- Pneumatic controllers and pumps
- Infrastructure planning and gathering lines
- Venting and flaring
- Produced water tank storage vessels
- Closed loop systems
- Leak detection and repair
- MAP summary and next steps

MAP Member Affiliations

Aztec Well Service
 Center for Civic Policy
 Chaco Canyon Coalition
 Chevron Corp.
 Conoco Phillips Company
 Devon Energy
 DJR Energy
 Earthworks
 Enduring Resources LLC
 Environmental Defense Fund
 EOG Resources, Inc.
 Epic Energy
 Hanson Operating Company
 Hilcorp Energy Company
 Lucid Energy Group
 Marathon Oil
 Merrion Oil and Gas Corp.
 Mewbourne Oil Company
 New Mexico Environmental Law Center
 Occidental Petroleum Corp.
 San Juan Citizens Alliance
 Sierra Club
 Western Environmental Law Center
 Whiptail Midstream
 XTO Energy, Inc

⁷ Production includes well drilling and subsequent operations that support mineral extraction. Once the oil or natural gas has left the well site, it is put into gathering pipelines that transport the gas. Compressor/gathering and boosting stations push the natural gas through the lines to a natural gas processing plant where the methane gas is separated from the natural gas liquids such as propane, butane, and pentane. The midstream sector encompasses the moment that the gas leaves the well site through the processing.

After the MAP meetings conclude, NMED and EMNRD will host follow-up public meetings to discuss the information gathered on options for reducing methane pollution and waste so far. After the public meetings, NMED and EMNRD will develop draft rules that will be available for public comment prior to going before their respective rulemaking bodies in 2020. There will be public hearings in front of the Environmental Improvement Board for NMED rules to reduce VOC/methane pollution and in front of the Oil Conservation Commission for EMNRD rules to reduce methane waste.

HFC Regulations

Hydrofluorocarbons (HFCs) are a component of the industrial sector's greenhouse gas emissions profile. HFCs are gaseous compounds used as refrigerants in air conditioning systems and refrigerators, blowing agents in foams, propellants in medicinal aerosols, and cleaning agents. HFCs contain carbon, fluorine, hydrogen, and water vapor. Unlike the generation of refrigerants that preceded them (phased out by the 1987 Montreal Protocol), they do not damage the ozone layer.

However, HFCs are powerful greenhouse gases, with a warming potential 1,300 to 3,700 times greater than an equivalent amount of CO₂. Some states, including California, Vermont, and Washington, have set targets to reduce HFC emissions by as much as 40% by 2030. Other states, like New York, Connecticut, and Maryland, are developing rules based on California's regulations.

NMED is writing rules to mitigate HFC emissions and HFC use in New Mexico. These rules will be published as early as 2021.

Built Environment Sector

The built environment – buildings, roads, and other structures built by people – are a source of greenhouse gas emissions in two ways: the energy they use and the resources they require during construction. The strategies that we will use to reduce emissions from the built environment will also reduce emissions from all other sectors. Energy efficiency and better building codes reduce electricity emissions as well as emissions from heating and cooling buildings. Infrastructure investments, like new road design, creating more pedestrian and bicycle access, and improving our water and wastewater systems, reduce emissions across all sectors.

Energy Efficiency and Building Codes

Energy efficiency – using less energy to accomplish our everyday activities – is a way to reduce greenhouse gas emissions from the electricity and built environment sectors without changing how we live our everyday lives. While using LED lightbulbs, energy-efficient appliances, and installing better insulated windows are a great place to start reducing energy use, there is a lot more that we can do.

Current New Mexico law requires utilities to offer programs to improve energy efficiency in residential and commercial customers' buildings. To complement this existing law, we need to expand the availability of energy-efficient housing and appliances to low-income and disadvantaged New Mexicans. We also need to continue to update the Efficient Use of Energy Act, making sure that the method utilities use to measure energy efficiency cost-effectiveness is the fairest it can be, bringing energy efficiency upgrades and benefits to more New Mexicans – while saving them money and improving their comfort and health.⁸

When new buildings are constructed, or major renovations are made to an older building, contractors

⁸ New Mexico currently uses the utility cost test to determine whether energy efficiency improvements are cost effective (and therefore eligible for utility efficiency program funding), which does not account for benefits to participants and ratepayers. The total resource cost test includes these benefits and its use expands available measures and benefits for participants.

Exhibit 8

2020



New Mexico Climate Strategy

2020 Progress and Recommendations

New Mexico Interagency Climate Change Task Force

Table of Contents

The Governor's Message	4
Science and Data	6
Science	6
Data	6
Reducing Greenhouse Gas Levels	10
Electricity Sector	11
Transportation Sector	14
Industrial Sector	18
Built Environment Sector	20
Natural and Working Lands Sector	24
Cross-Sector Emissions Reductions	27
Adaptation and Resilience	28
Economic Transition	28
Public Health	32
Emergency Management and Infrastructure Resilience	33
Water and Natural Resource Resilience	34
Moving New Mexico Forward	38



The Governor's Message

Governor Michelle Lujan Grisham



In just the eighteen months since I signed Executive Order 2019-003 on Addressing Climate Change and Energy Waste Prevention, we have made significant progress on our agenda. This annual report provides updates on my administration's policies to advance our goals as well as sobering reminders of the work ahead.

In an unprecedented year, dominated by the coronavirus pandemic, our work to address climate change has not stopped because the need to address climate change has not gone away – just the opposite. Our record-breaking fire season is just one reminder that tackling climate change must be one of our top priorities.

Implementation of the Energy Transition Act (ETA) – our signature legislation driving electric sector emission reductions - is progressing. We anticipate 1,346 megawatts (MW) of renewables will have come online between ETA passage in March 2019 and the end of 2020, for both in-state use and exports. This is almost twice the amount of new renewables that came online in the prior two years between March 2017 and March 2019, highlighting the importance of state leadership.

At the same time, new building codes have been adopted that will save new homeowners up to \$400 per year on energy costs while reducing emissions. The Solar Market Development Tax Credit, passed in the 2020 legislative session, is expanding solar affordability and growing New Mexico's solar industry by investing up to \$8 million per year through a 10% tax credit on new solar systems. The tax credit makes solar panel installation more affordable and will save New Mexicans money over time by reducing electric bills.

New Mexico is also making progress in the transportation sector. This year, the state awarded \$4.6 million in Volkswagen Settlement funds for 43 projects including electric vehicle charging infrastructure, new electric transit buses, electric and alternate-fueled school buses, and alternate-fueled solid waste vehicles. Utilities are also filing electric vehicle and charging infrastructure plans with the Public Regulation Commission to further spur electric vehicle adoption and infrastructure deployment. Clean cars and hydrofluorocarbon (HFC) rules are scheduled for next year, giving us additional goals to work for to reduce emissions in the transportation sector.



Our Departments have also made significant progress on our methane and natural gas waste and volatile organic compounds (VOC) rules. Final rules that will curb emissions from our state's largest source of greenhouse gas emissions—the oil and gas industry—are expected this fall.

We're also taking this progress and translating it into jobs. Economic Development Department programs invested over \$5.8 million in clean energy and emissions monitoring companies that will help us reach our climate goals while generating over 300 jobs in New Mexico.

We are rising to the challenge even as we confront the twin crises of climate change and COVID-19. State government is evolving and increasing its leadership by looking at everything from our buildings and fleets to procurement and budget policies. Agencies are leveraging all the resources we have to increase staff time on this important work and gear up for the next phase of action.

Even in the midst of a global pandemic, it is critical to keep thinking and talking and acting on climate change. Our bold action at the state level is in stark contrast to the failure of our federal government to put into place a national policy on climate change. In the context of COVID-19, we must go beyond "getting back to normal" in our recovery and instead think about how we can cultivate a better, cleaner future for New Mexico.

We are on the right track and we will not let up. Even as we continue work on our established policy priorities, we are looking ahead to how we can be more aggressive in tackling difficult sectors — oil and gas, transportation — and implementing broader market mechanisms. We are staffing up and building tools to expand our adaptation and resilience work with input from local and tribal governments and communities around the state.

I am encouraged by the progress we have made thus far and look forward to pushing ahead on our ambitious and important climate change agenda. We cannot afford to stand still in our fight to combat climate change. Our future depends on winning this fight.



Michelle Lujan Grisham

SCIENCE & DATA

Science

Climate scientists identified warming of 1.5 degrees Celsius as the point where climate change becomes severely dangerous to human life and society. We must continue our decisive action now to do our part to stay under 1.5 degrees Celsius and avoid the worst effects of climate change.¹ New Mexico is already experiencing negative climate change impacts. Just this summer, Truth or Consequences saw extensive flooding during heavy monsoon storms and the Medio Fire in the Santa Fe National Forest burned over 3,000 acres, blanketing much of the region in smoke and haze. Science tells us to expect more flash flooding and wildfires, as well as hotter and longer summers, more intense storms, and more frequent droughts.

We expect less predictable and robust harvests of our agricultural products, and changes in the health of New Mexicans – who are experiencing higher rates of asthma and heat-related illnesses. All of these changes bring economic, human, and natural costs. Warmer year-round temperatures mean additional energy costs to keep residences and businesses cool throughout the year. Declining air and water quality are disrupting natural habitats and ecosystems, leading to bark beetle infestations, fish habitat reduction, and fewer alpine meadows. Climate change also threatens our critical infrastructure, including roads, overpasses, bridges, and rail; electrical power distribution systems; drinking water and sewer pipes; and flood control and drainage systems. We must reaffirm our commitment to rapid and ambitious action to avert continued climate change impacts to public health, our environment, and our communities.²

Data

A new study from Colorado State University (CSU) conducted in 2020 analyzed New Mexico's greenhouse gas emissions in detail, giving us the best estimates to date of our recent and projected emissions.³ Unlike previously reported emissions estimates, this study relied on extensive New Mexico-specific data sources, including sources for the difficult-to-measure oil and gas sector. The results of this study are reflected in our understanding of New Mexico's emissions profile throughout this report.

Key findings from the CSU inventory of New Mexico greenhouse gas emissions:

- The oil and gas sector generated 60 million metric tons (MMT) of greenhouse gas emissions in 2018, nearly four times more than previously estimated based on national data.
- Transportation is still the second-largest source of emissions, followed by electricity generation.
- Natural and working lands emissions, while uncertain due to data limitations, may have been a net source of emissions in 2018 rather than absorbing more emissions than they produced. This is due to several factors including wildfire and changes in land use that cause deforestation.

¹IPCC, 2018: Summary for Policymakers. In: Global Warming of 1.5°C. An IPCC Special Report on the impacts of global warming of 1.5°C above pre-industrial levels and related global greenhouse gas emission pathways, in the context of strengthening the global response to the threat of climate change, sustainable development, and efforts to eradicate poverty [Masson- Delmotte, V., P. Zhai, H.-O. Pörtner, D. Roberts, J. Skea, P.R. Shukla, A. Pirani, W. Moufouma-Okia, C. Péan, R. Pidcock, S. Connors, J.B.R. Matthews, Y. Chen, X. Zhou, M.I. Gomis, E. Lonnoy, T. Maycock, M. Tignor, and T. Waterfield (eds.)]. In Press.

²Funk, J., Barnett-Loro, C., Rising, M., & Dayette, J. (2016). Confronting Climate Change in New Mexico: action needed today to prepare the state for a hotter, drier future. Union of Concerned Scientists. Retrieved from <https://www.ucsusa.org/sites/default/files/attach/2016/04/Climate-Change-New-Mexico-fact-sheet.pdf>

³Sharad Bharadwaj et al., "New Mexico Greenhouse Gas (GHG) Emissions Inventory and Forecast" (Prepared for Center for the New Energy Economy at Colorado State University by Energy and Environmental Economics, Inc., October 27, 2020), <https://cnee.colostate.edu/repowering-western-economy/>.

Exhibit 9

New Mexico Oil & Gas Data

[Overview](#) | [Analytics](#) | [Explorer](#) | [Modeling Tool](#) | [Methodology](#)

New analysis reveals persistent methane problem

Updated November 2020

Using peer-reviewed satellite data and methods in tandem with extensive research studies, scientists at EDF have estimated oil and gas methane emissions across New Mexico to be over 1.1 million metric tons per year.

Persistent emissions in the state's Permian Basin, combined with insufficient management of leaks and wasteful venting and flaring practices, are the major contributing factors. These avoidable emissions are generating tangible impacts to New Mexico's economy, public health and climate.

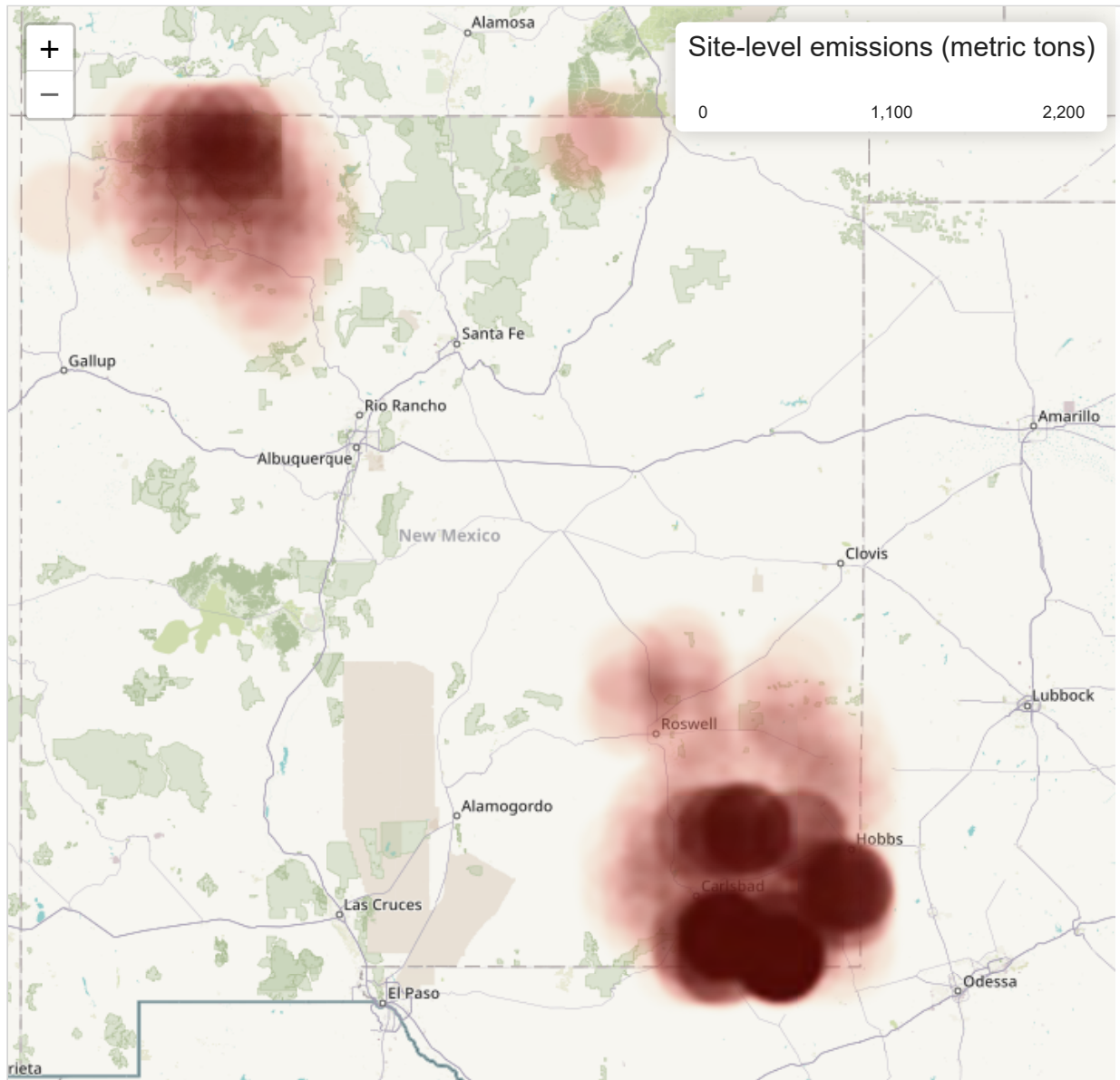
Thanks to the incredible scope and frequency of satellite observation along with extensive and ongoing [field research](#) by EDF in the Permian Basin, scientists now have an unprecedented view into oilfield emissions in New Mexico and what will be required to reduce them.

This analysis models the proposed solutions put forward by New Mexico's Environment Department and Energy Minerals and Natural Resources Department to reduce emissions, and finds that, as written, they would exempt the vast majority of

New Mexico Oil & Gas Data

[Overview](#) | [Analytics](#) | [Explorer](#) | [Modeling Tool](#) | [Methodology](#)

in other oil and gas producing regions, and finds that New Mexico has an opportunity to eliminate about 56% of statewide methane emissions from oil and gas with nation-leading regulations.



Methane emissions density across New Mexico

Source: see [methodology](#).

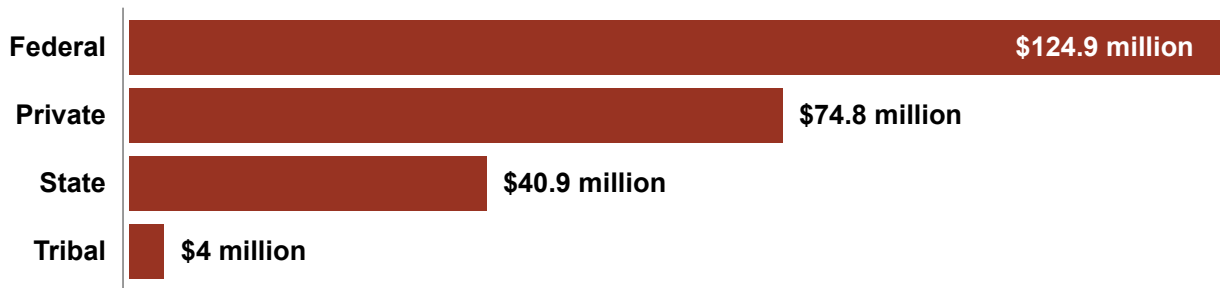
Key findings

Economic losses:

- Flaring, venting and leaks lead to the loss of at least **\$271 million** worth of natural gas in New Mexico every year.

New Mexico Oil & Gas Data

[Overview](#) | [Analytics](#) | [Explorer](#) | [Modeling Tool](#) | [Methodology](#)



Value of wasted gas by land type (dollars) – total: \$271 million/year

Values do not sum to the total because Gathering/Boosting and Abandoned Wells emissions are not apportioned to land types.

Source: see [methodology](#).

Public health risks:

- Oil and gas emissions contribute to poor local air quality. EDF’s analysis shows that **more than 337,500 metric tons of volatile organic compounds (VOCs)** are emitted annually from oil and gas sites across the state. These include various air toxics and smog-forming pollutants that can cause respiratory illness among other acute and chronic health problems – especially among children and the elderly.
- New Mexico’s largest oil and gas producing regions are struggling with increasing ozone pollution levels, which threaten to push some areas – like San Juan and Eddy counties – beyond federal air quality standards.

Environmental impact:

- EDF estimates that statewide methane emissions from upstream oil and gas sites total more than 1.1 million metric tons a year, which has the same short-term climate impact as 25 coal plants or 21 million automobiles. These emissions are about 5 times higher than what EPA emissions data suggest.
- Leaks, equipment malfunctions and other avoidable issues are responsible for the majority of emissions, contributing to climate change and wasting a valuable natural resource.

Crafting solutions:

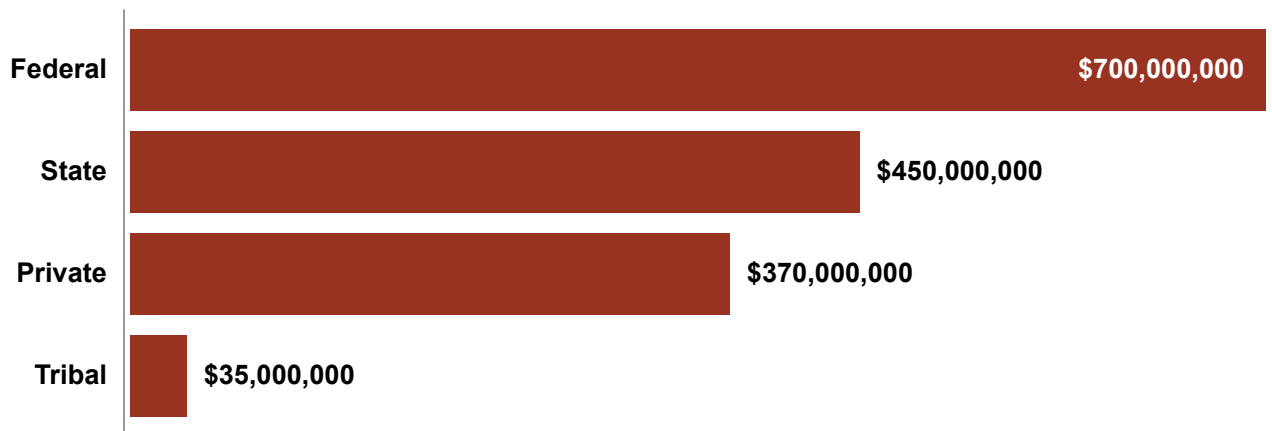
Gov. Michelle Lujan Grisham has made tackling New Mexico’s methane challenge a priority for her administration, and has an opportunity to strengthen rules put forward

New Mexico Oil & Gas Data

[Overview](#) | [Analytics](#) | [Explorer](#) | [Modeling Tool](#) | [Methodology](#)

and potential-to-emit thresholds and could be easily and cost effectively closed to ensure all wells in the state are covered. Together, the state's proposed regulations would reduce only 20.6% of methane and 19.2% of VOCs from oil and gas.

Proven, [cost-effective solutions](#) are readily available – in the form of requirements like better leak management practices and other control technologies – and a comprehensive package of policies could reduce emissions by about 56% by 2030, saving more than \$1.6 billion worth of natural gas.



Value of natural gas saved by 2030 if comprehensive regulations are enacted – total: \$1,600,000,000

Source: see [methodology](#).

[Report home page](#) | [Technical specification](#) | [Project overview and contact information »](#)

New Mexico Oil & Gas Data

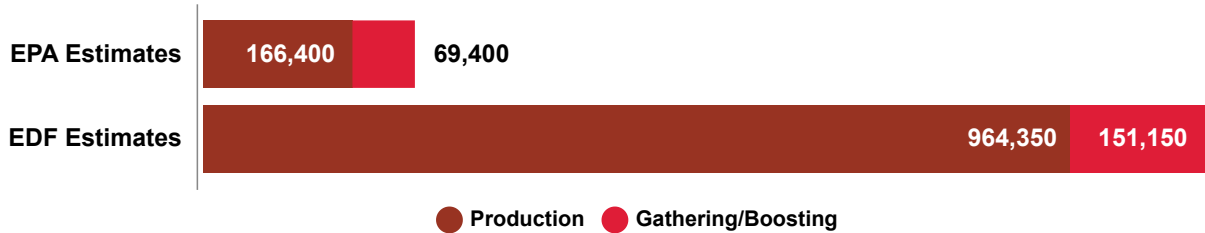
Overview | **Analytics** | Explorer | Modeling Tool | Methodology

Emissions | State Revenue | Wells & Production

Methane and Air Toxics

EDF analyzed New Mexico emissions using a combination of satellite readings from the Permian Basin – collected from the European Space Agency’s Tropospheric Monitoring Instrument – and peer-reviewed data and methods from a 2018 [Science](#) study. The complete [methodology](#) for this analysis is available for review.

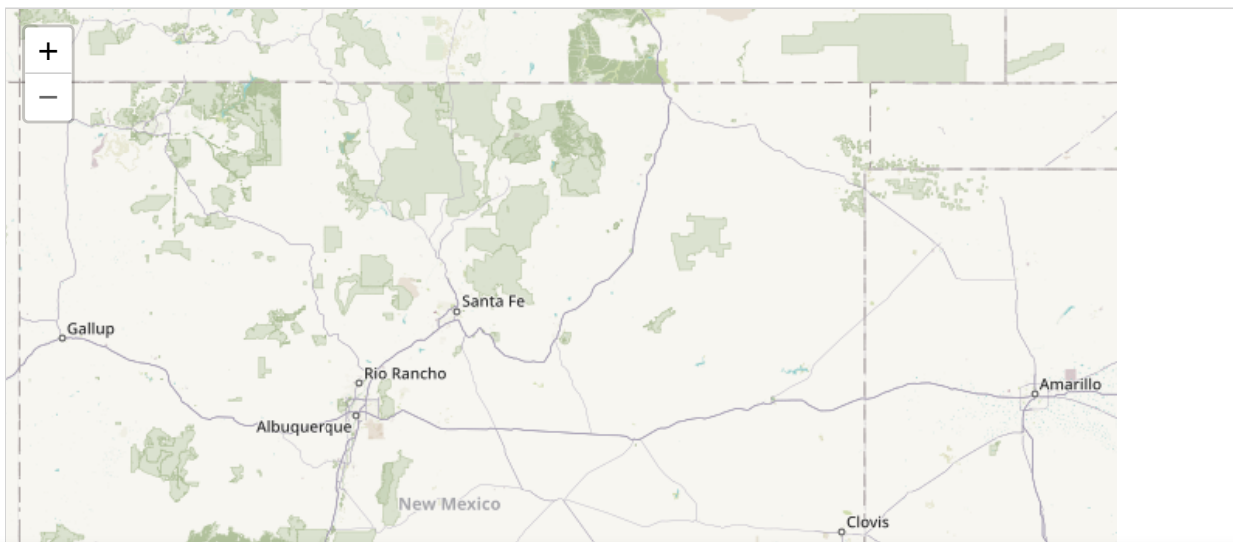
Total methane emissions - 1,116,000 metric tons in 2019



EPA estimates are calculated from basin-level emissions reported by operators to the EPA Greenhouse Gas Reporting Program. They are based primarily on emission factors and engineering equations rather than measurement data.

Source: 2019 emissions estimates, see [methodology](#).

Emissions per county, methane & VOCs (in metric tons)



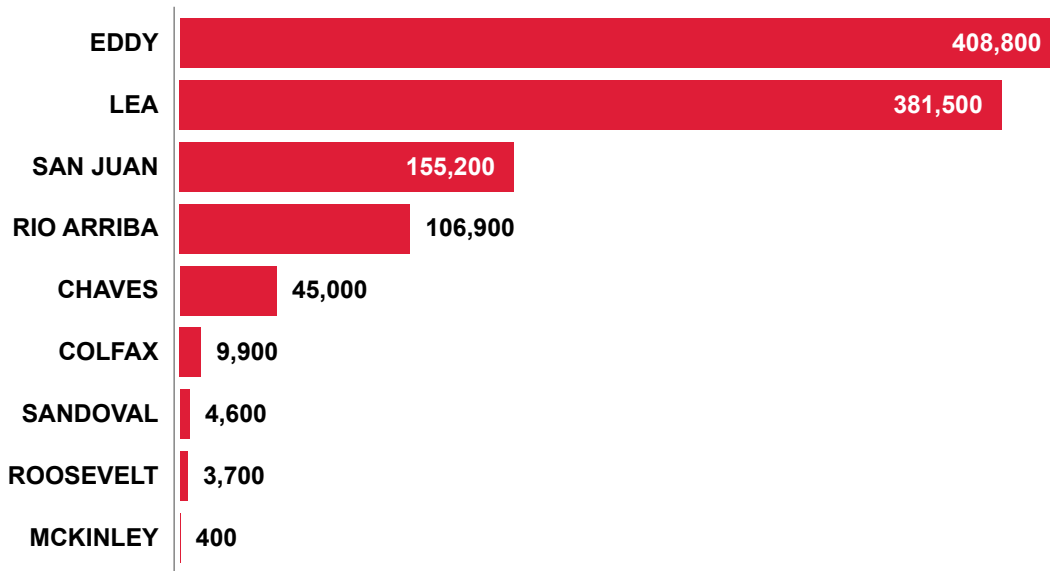
New Mexico Oil & Gas Data

Overview | **Analytics** | Explorer | Modeling Tool | Methodology



Source: 2019 emissions estimates, see [methodology](#).

Methane emissions by county (metric tons)

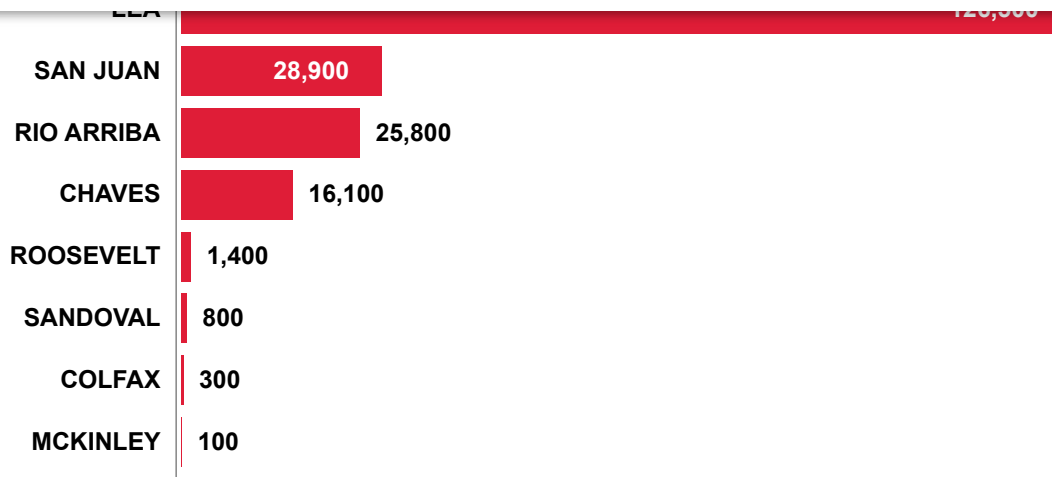


Source: 2019 emissions estimates, see [methodology](#).

VOC Emissions by county – total: 337,500 metric tons

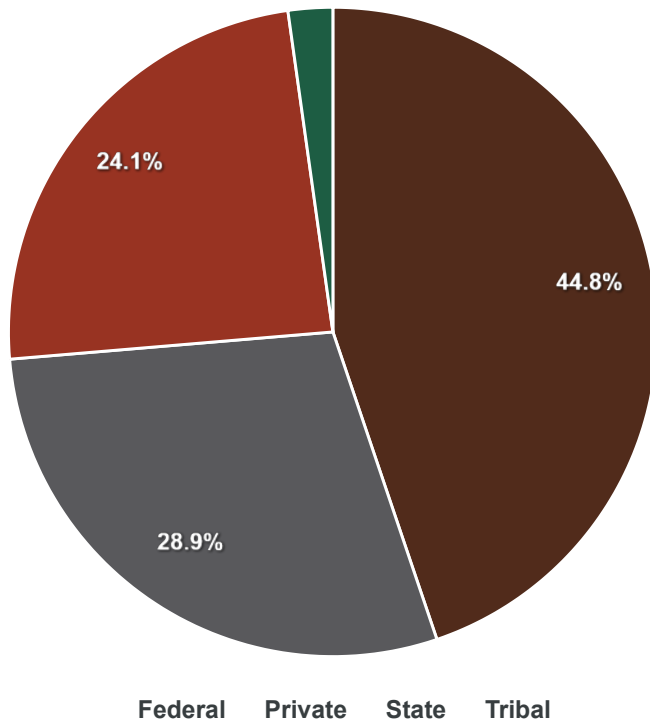
New Mexico Oil & Gas Data

Overview | **Analytics** | Explorer | Modeling Tool | Methodology



Source: 2019 emissions estimates, see [methodology: Western Regional Air Partnership \(WRAP\)](#).

Emissions by Land Ownership

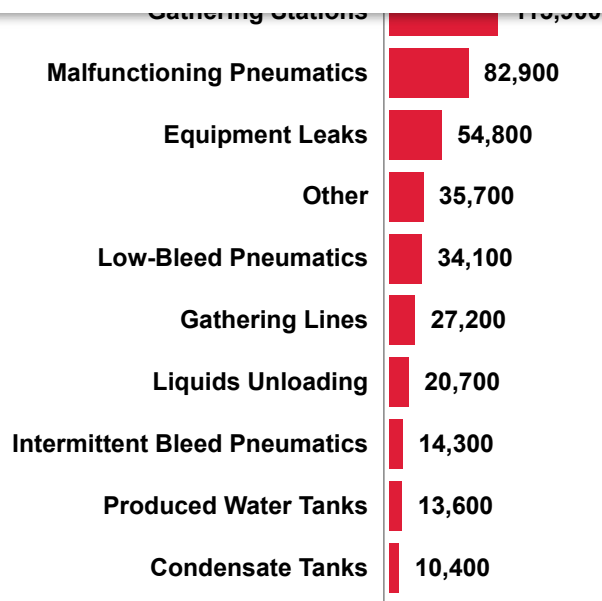


Source: 2019 emissions estimates, see [methodology: U.S. Bureau of Land Management](#)

Top methane emission sources (metric tons)

New Mexico Oil & Gas Data

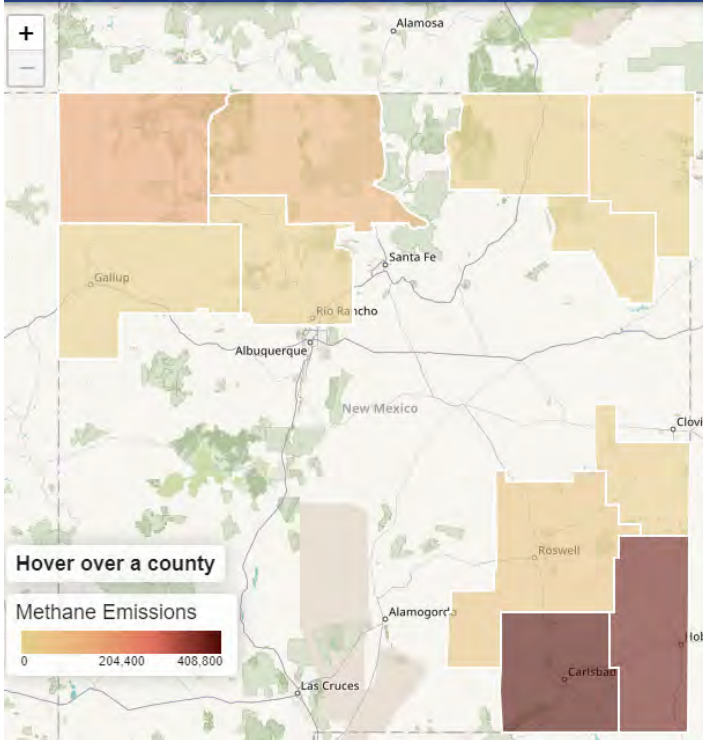
[Overview](#) | [Analytics](#) | [Explorer](#) | [Modeling Tool](#) | [Methodology](#)



Abnormal emissions were determined from the difference of total site-level emissions and our best estimate of emissions by source category. This category includes emissions from malfunctions and otherwise avoidable conditions that may be associated with other source categories.

Source: 2019 emissions estimates, see [methodology](#).

[Report home page](#) | [Technical specification](#) | [Project overview and contact information »](#)



DATA LAYERS

BASEMAP

- Counties
- Well Locations
- Well Sites: Covered
- Well Sites: Exempt

Emissions

- Methane Emissions
- Ozone
- NOAA Flaring Sites

New Mexico Oil & Gas Data

Overview | Analytics | Explorer | **Modeling Tool** | Methodology

Modeling Tool: Evaluating Options for Reducing Emissions

How to use this tool [i](#)

Select options

Pollutants

- Methane
 VOC

Timeframe

- 2020-2025
 2020-2030

Predicted Emissions – Methane: 2020–2025

No State Controls	8,200,000 metric tons
Modeled scenario	8,200,000 metric tons
Emissions reduced	0.00% reduction of 0 metric tons

Level of Controls:

Quick select

- No State Controls
 State Proposal
 Comprehensive Controls

EMISSIONS BY COUNTY

SAVED GAS

EARNED REVENUE

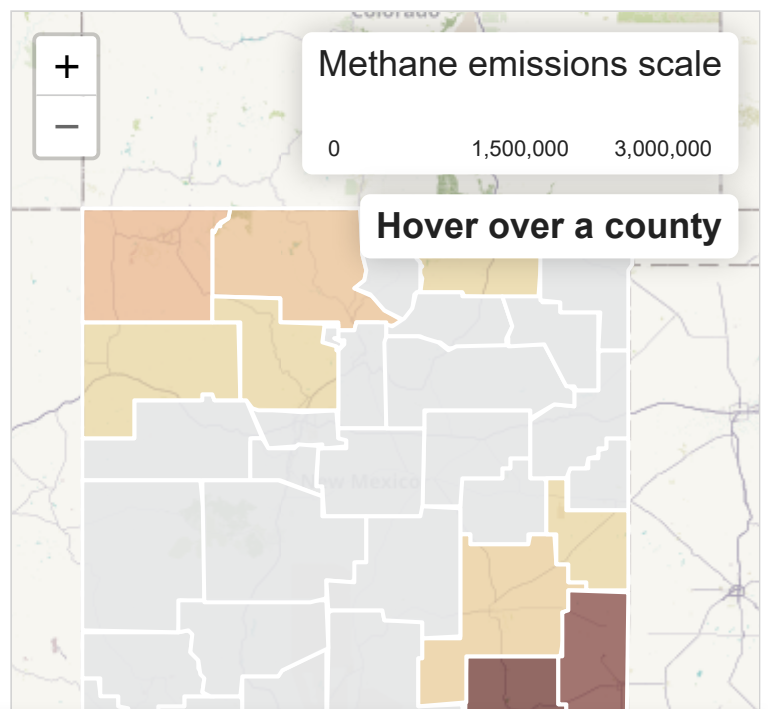
EARNED REVENUE BY TYPE

* Assumes federal NSPS standards (2018 Reconsideration) for new wells are in effect

Or select controls by source:

Source	Estimated Emissions (metric tons) Existing Sources / New Sources (metric tons)	Reduction Potential
+ Leaks	200,000 / 170,000	0
+ Abnormal Conditions i	2,100,000 / 3,200,000	0
+ Malfunctioning Pneumatic Controller	240,000 / 380,000	0
+ Gathering Stations	390,000 / 380,000	0
+ Low-bleed Pneumatic Controller	100,000 / 140,000	0

Methane Emissions by County



New Mexico Oil & Gas Data

[Overview](#) | [Analytics](#) | [Explorer](#) | **[Modeling Tool](#)** | [Methodology](#)

+ Liquids Unloading	76,000 / 56,000	0	
+ Associated Gas Flaring	7,700 / 18,000	0	
+ Associated Gas Venting	6,300 / 15,000	0	

[Report home page](#) | [Technical specification](#) | [Project overview and contact information »](#)

New Mexico Oil & Gas Data

[Overview](#) | [Analytics](#) | [Explorer](#) | [Modeling Tool](#) | **[Methodology](#)**

Methodology

EDF Estimate: Method for estimating upstream oil & gas methane emissions

Environmental Defense Fund estimated total annual methane emissions from upstream oil and gas (O&G) sites in New Mexico, including well pads, gathering stations and gathering pipelines. Emissions were estimated for the year 2019 using a combination of site-level measurement data from previously published studies and satellite measurements from a recent paper.

Emissions were estimated using two different methods: a basin-level (or top-down) estimate and a source-level (bottom-up) estimate.

Basin-level production emissions

Production emissions were estimated for the Permian, San Juan and Raton basins using different methods.

For the San Juan and Raton basins, baseline emissions estimates were developed for 2017, described here, and then adjusted for 2019. We obtained 2017 active well counts and production data from Enverus/DrillingInfo, a subscription database that compiles well data from regulatory agencies including the New Mexico Oil Conservation Division. We grouped wells into production sites based on reported surface wellhead locations and a 50-meter cluster radius. Total production-site emissions by county were estimated by multiplying site counts by site-level emission factors (EFs).

EFs were calculated with a gas production dependent, log-normal equation based on the methods outlined in [Alvarez et al 2018](#), section S.1.1. The underlying data are from >400 site-level measurements from six U.S. basins (Barnett, Fayetteville, Marcellus, Uintah, Upper Green River, Denver-Julesburg). In summary, maximum likelihood,

New Mexico Oil & Gas Data

[Overview](#) | [Analytics](#) | [Explorer](#) | [Modeling Tool](#) | **[Methodology](#)**

New Mexico, Alvarez et al 2018 reports that analogous estimates of San Juan Basin 2015 emissions agree closely with basin-level, aircraft-based measurements from the region ([Smith et al 2017](#)), suggesting that this combined dataset is broadly representative of the region. For the San Juan and other smaller basins, the central estimate EF of $1.5 \text{ kg CH}_4 \text{ h}^{-1}$ was applied

This process yielded basin-level emissions for the San Juan and Raton basins for 2017. Emissions for 2019 were calculated by multiplying the 2017 basin-level emissions by the ratio of 2019 to 2017 gas production (production was relatively constant in both basins).

For the Permian, emissions estimates were based on satellite measurements from the Tropospheric Monitoring Instrument (TROPOMI) (Zhang et al. 2020). Zhang et al. found a natural gas leakage rate of 4.1% for the Delaware sub-basin of the Permian from May 2018 to March 2019. We assume this leakage rate is constant for all of 2019. Using 2019 production data from Enverus/DrillingInfo and an assumed methane content of 78.8%, we calculate basin-wide emissions for the Permian to be 740,000 metric tons of methane in 2019.

Emissions by source category

Emissions by source category had previously been calculated for each basin for 2017, incorporating EPA Greenhouse Gas Reporting Program (GHGRP) data as described below. When the 2019 inventory was being compiled, GHGRP was not yet available for 2019 (it has since been released). Therefore, to update this analysis to 2019, the relative contribution of each source category to the total basin-wide emissions was assumed to remain constant between 2017 and 2019. Thus, the 2019 emissions totals were multiplied by the percent contributions for each source category to yield source-level estimates for 2019 for each basin.

EDF estimated production emissions by source category using a combination of data sources, including the EPA GHGRP and previously published measurement studies. Source-level emissions were estimated using similar methods as reported in Alvarez et al 2018 for the alternative inventory (section S1.4). In summary, GHGRP data were analyzed with a statistical model that uses production data and reported basin-level

New Mexico Oil & Gas Data

[Overview](#) | [Analytics](#) | [Explorer](#) | [Modeling Tool](#) | **[Methodology](#)**

The difference between basin-level and aggregate source-level emissions was attributed to “abnormal process conditions” (see Zavala-Araiza et al. 2017). This includes malfunctions and other issues that lead to high emission rates that are not accounted for by traditional source-level inventory methods. It is important to note that our source-level emission estimates are intended to approximate how empirically derived total emissions are allocated among sources based on independent, source-level data. Our “abnormal process conditions” category may include additional emissions that are released from reported source categories like tanks due to potential issues with GHGRP data, such as systematically underreported control efficiencies.

Gathering and boosting

For the gathering and boosting segment, total methane emissions from gathering stations, pipelines, and blowdowns were estimated according to the methods outlined in Alvarez et al 2018, section S.1.1. In summary, we estimated station emissions from gas production and percentage loss rates based on ~100 previously published site-level measurements (Marchese et al 2015). As reported in Alvarez et al, the loss rates from Marchese et al were adjusted slightly upward (~17%) to account for sites above the sampled range. Gathering blowdown emissions were based on episodic emissions reported in Marchese et al. Gathering pipeline emissions were based on EPA Greenhouse Gas Inventory EFs; these EFs are based on data from local distribution pipeline leaks and are highly uncertain.

Estimating VOCs

EDF estimated the total annual emissions of volatile organic compounds (VOCs) based on the estimated methane emissions inventory. In order to account for variations in gas composition across the state, EDF converted methane to VOCs using basin and source-specific CH₄:VOC ratios from a 2016 Western Regional Air Partnership (WRAP) report.

Additional documentation on this analysis is available.

New Mexico Oil & Gas Data

[Overview](#) | [Analytics](#) | [Explorer](#) | [Modeling Tool](#) | **[Methodology](#)**

EPA Greenhouse Gas Reporting Program if their annual greenhouse gas emissions exceed 25,000 metric tons CO₂e. For onshore production and gathering and boosting (G&B), emissions are reported at the basin level. As basins often cross state boundaries, the US EPA is unable to provide precise state-level emission estimates. For the 2019 reporting year, there were 83 onshore production and 62 G&B facilities reporting emissions in three basins located at least partially within New Mexico counties: the Permian, San Juan, and Las Vegas-Raton. EDF estimated reported emissions attributable to New Mexico by allocating basin-level emissions by the fraction of 2019 O&G energy production from the New Mexico portion of each basin (35%, 68% and 23%, respectively).

Lost Revenue: Method for estimating lost revenue from methane emissions and flared natural gas

Well sites were categorized based on land ownership: federal, state, private, or tribal (using BLM New Mexico surface ownership data). Well sites were further classified to identify sites on state trust lands. (Not all state lands are included in the state trust, and the state trust includes wells where subsurface ownership belongs to the state trust and surface ownership to a different entity. See New Mexico State Land Office).

Site-level production emissions were then summed for each land type (federal, state, private, tribal and state trust) to generate production percentages by land type. Because flared gas volumes are included in the revenue calculation (described below), vented and flared production emissions are set to zero to avoid double counting. Combustion emissions are also set to zero as these emissions are often seen as necessary. Methane emissions are converted to volumes of natural gas using a volumetric-methane content value of 78.8% for production emissions.

Flared gas volumes are from the NOAA VIIRS 2018 dataset (2019 data is not yet available. As flaring has increased from 2018 to 2019, the choice of 2018 is conservative). Flare locations were categorized based on land ownership, using the same methodology and land ownership data described above. Flared volumes were then summed for each land type: federal, state, private, tribal, and state trust. The

New Mexico Oil & Gas Data

[Overview](#) | [Analytics](#) | [Explorer](#) | [Modeling Tool](#) | **[Methodology](#)**

following assumptions (see [Oil and Natural Gas Taxing in New Mexico](#)):

- The royalty rate for production on federal lands is 12.5%, of which 49% is returned to the state.
- The royalty rate for production on state trust lands varies by lease. An economist for natural resources on the New Mexico Legislative Finance Committee estimated (via a private phone call) that on average, the royalty rate is 19% for natural gas.
- The following taxes are assessed on gas production on all land types:
 - 4% emergency school tax
 - 3.75% severance tax
 - 0.24% conservation tax
 - Approximately 1% ad valorem tax (slight differences based on land type)
- Any allowable deductions (of which there are many) are ignored in this analysis, and the lost revenue values should be viewed as estimates.
- Federal royalties (of which 49% are returned to the state) are already assessed on flared gas from federal lands in the Permian basin. This value was subtracted from the federal lost state revenue estimate.
- Revenue is calculated based on a \$2.57/MMBtu natural gas price (the average 2019 Henry Hub gas price) using a heat value of natural gas of 1,037 Btu/ft³ to convert natural gas volumes (Henry Hub U.S. natural gas heat content).

Projecting emissions through 2025

Using the EDF estimated inventory, we projected emissions forward under a Business as Usual (BAU) scenario, using the Rystad oil and gas production projections for New Mexico, to generate the best available representation of future changes in BAU methane emissions.

We then assigned a growth profile (Oil, Gas, or Oil & Gas) for each source category based on the most representative resource projection. For example, fugitive leak emissions were tied to total oil & gas projections, while compressors were tied to the natural gas projections. Using this method, we were able to project forward the estimated emissions for each source category under a BAU scenario.

Additionally, we used DrillingInfo to establish a turnover rate of existing to new wells year-to-year by examining recent well turnover rates in New Mexico. We calculated an

New Mexico Oil & Gas Data

[Overview](#) | [Analytics](#) | [Explorer](#) | [Modeling Tool](#) | **[Methodology](#)**

In addition to the updates to the inventory and underlying data, an earlier version of the tool (released July 2019) contained an error in emissions projections that has been corrected in this version.

Calculating reductions from the state's proposed rules

EDF conducted an analysis of the potential impacts of the proposed New Mexico Environment Department (NMED) and Oil Conservation Division (OCD) rules. Percent reductions were estimated for each source category. However, the NMED rule contains two exemptions for wells that apply to both those with a potential-to-emit (PTE) of less than 15 tons per year (TPY) of VOCs and stripper wells on both the number of facilities that would be subject to the rule's control requirements. Per our analysis, the exemptions carve out 95% of wellheads and production sites in the six counties subject to the proposed NMED rule and a significant percent of emissions. This percent exempted was applied in the model when determining the impact of the state's proposed rules.

EDF analyzed the impact of the low producing well exemption by examining the number of facilities in the NMED permit/NOI database (<https://gis.web.env.nm.gov/oem/?map=methane>) and calculating the number of facilities that fall below the proposed PTE threshold. NMED requires facilities with regulated emissions above 25 TPY to have an air permit. Oil and gas facilities are required to submit a Notice of Intent (NOI) if they have regulated air contaminant emissions above 10 TPY. The permit and NOI database includes potential to emit (PTE) for VOC emissions; use of these data shows that 2,398 wellheads and production sites have a VOC PTE above 15 TPY VOC. Using data from DrillingInfo, EDF determined the total number of oil and gas facilities in New Mexico to be roughly 43,100. Therefore, roughly 95% of wellheads and production sites in NM will be below the 15 TPY VOC threshold and will be exempted from the rule.

To calculate the impact of the stripper well exemption on the number of covered facilities, EDF pulled well data from Enverus/DrillingInfo. Wells were clustered into well sites based on a 50 m radius. Average oil production (bbl/day) and average gas production (Mcf/day) were calculated on a per well basis. If the average oil production

New Mexico Oil & Gas Data

[Overview](#) | [Analytics](#) | [Explorer](#) | [Modeling Tool](#) | **[Methodology](#)**

Covered and exempt well sites are shown in the Explorer tab of this digital report.

Location data for covered well sites were taken directly from the NMED permit/NOI database for those well sites with PTE above 15 TPY. These data were overlaid with the well site location data from Enverus/DrillingInfo in order to display both covered and exempted well sites.

[Report home page](#) | [Technical specification](#) | [Project overview and contact information »](#)

Exhibit 10

David R. Lyon, Ph.D.

Environmental Defense Fund
301 Congress Avenue, Suite 1300
Austin, TX 78701
(512) 691-3414
dlyon@edf.org
<https://www.edf.org/people/david-lyon>

EDUCATION

University of Arkansas, Fayetteville, AR

Ph.D. in Environmental Dynamics (May 2016)

- Dissertation: *Quantifying, Assessing, and Mitigating Methane Emissions from Super-emitters in the Oil and Gas Supply Chain*
- Honors: 4.0 GPA; Doctoral Academy Fellowship

University of Kentucky, Lexington, KY

M.S. in Forestry (May 2004)

- Thesis: *Persistent Effects of Eastern Redcedar on Calcareous Glade Soils and Plant Community*
- Honors: 4.0 GPA; Garden Club of America 2003 Fellowship in Ecological Restoration

Hendrix College, Conway, AR

B.A. in Biology with Chemistry Minor (June 2002)

- Honors: 3.95 GPA; Summa Cum Laude with Distinction; Phi Beta Kappa
-

WORK EXPERIENCE

Environmental Defense Fund, Austin, TX

Scientist (March 2014 – present)

- Contribute to the design, planning, execution, and analysis of EDF-sponsored research studies on quantifying methane emissions from the oil and gas supply chain
- Advise internal and external projects on innovative approaches for leak detection and mitigation
- Prepare and review manuscripts for submission to peer-reviewed journals
- Communicate science and advocacy through presentations, briefings, and media interviews
- Provide scientific expertise to other EDF programs and external groups

Environmental Defense Fund, Austin, TX

Research Analyst (June 2012 – March 2014)

- Research, analyze, synthesize, and interpret data related to oil and gas methane emissions

- Analyze, interpret, and communicate data to policymakers, industry, the scientific community, and other stakeholders in support of EDF advocacy on environmental policy
- Write reports, blogs, and other communication materials for general audiences

University of Arkansas at Little Rock, Little Rock, AR

Part-time Lecturer (January 2012 – May 2012)

- Taught senior-level environmental science course *Fundamentals of Air Pollution*

Arkansas Department of Environmental Quality, North Little Rock, AR

Environmental Program Coordinator (January 2009 – May 2012)

- Obtained EPA funding, managed project, and authored report on a study to develop an emissions inventory and monitor air quality impacts of natural gas development in the Fayetteville Shale
- Managed \$500,000 project to develop and implement a web-based emissions inventory reporting system for a multi-state consortium of environmental agencies
- Led the state's air pollution emissions inventory program, which included approximately 175 regulated facilities and several nonpoint emission source categories
- Analyzed emissions data and produced reports for the agency and public
- Analyzed current and proposed federal air regulations to assist agency planning
- Supervised up to four staff

University of Arkansas, Fayetteville, AR

Graduate Assistant (August 2004 – December 2008)

- Performed research on the effects of nutrient enrichment on stream carbon cycling
- Assisted students in general ecology laboratory

University of Kentucky, Lexington, KY

Graduate Assistant (June 2002 – June 2004)

- Performed research in restoration ecology and soil biogeochemistry of calcareous glades
- Taught dendrology and tree species identification to undergraduate students

PUBLICATIONS

Lyon, D. R. (2016). Methane emissions from the natural gas supply chain. In: Kaden, D.A. and Rose, T.L. eds. *Environmental and Health Issues in Unconventional Oil and Gas Development*. Elsevier. pp. 33-48.

Lyon, D. R., Alvarez, R. A., Zavala-Araiza, D., Brandt, A. R., Jackson, R. B., & Hamburg, S. P. (2016). Aerial surveys of elevated hydrocarbon emissions from oil and gas production sites. *Environmental Science & Technology*, 50 (9), pp 4877–4886, DOI: 10.1021/acs.est.6b00705.

Lyon, D. R., Zavala-Araiza, D., Alvarez, R. A., Harriss, R., Palacios, V., Lan, X., ... & Herndon, S. C. (2015). Constructing a spatially resolved methane emission inventory for the Barnett Shale region. *Environmental science & technology*, 49(13), 8147-8157.

- Alvarez, R. A., Zavala-Araiza, D., Lyon, D. R., Allen, D. T., Barkley, Z. R., Brandt, A. R., ... & Kort, E. A. (2018). Assessment of methane emissions from the US oil and gas supply chain. *Science*, eaar7204.
- Ravikumar, A.P., Sreedhara, S., Wang, J., Englander, J., Roda-Stuart, D., Bell, C., Zimmerle, D., Lyon, D., Mogstad, I., Ratner, B. and Brandt, A.R. (2019). Single-blind inter-comparison of methane detection technologies—results from the Stanford/EDF Mobile Monitoring Challenge. *Elementa*, 7(1).
- Fox, T.A., Ravikumar, A.P., Hugenholtz, C.H., Zimmerle, D., Barchyn, T.E., Johnson, M., Lyon, D. and Taylor, T. (2019.) A methane emissions reduction equivalence framework for alternative leak detection and repair programs. *Elementa*, 7(1).
- Hajny, K., Salmon, O.E., Rudek, J., Lyon, D.R., Stuff, A.A., Stirm, B.H., Kaeser, R., Floerchinger, C., Conley, S.A., Smith, M.L. and Shepson, P.B. (2019). Observations of Methane Emissions from Natural Gas-Fired Power Plants. *Environmental Science & Technology*, 53 (15), 8976-8984.
- Englander, J. G., Brandt, A. R., Conley, S., Lyon, D. R., & Jackson, R. B. (2018). Aerial Interyear Comparison and Quantification of Methane Emissions Persistence in the Bakken Formation of North Dakota, USA. *Environmental science & technology*, 52(15), 8947-8953.
- Lavoie, T. N., Shepson, P. B., Cambaliza, M. O., Stirm, B. H., Conley, S., Mehrotra, S., ... & Lyon, D. (2017). Spatiotemporal variability of methane emissions at oil and natural gas operations in the Eagle Ford Basin. *Environmental science & technology*, 51(14), 8001-8009.
- Lavoie, T. N., Shepson, P. B., Gore, C. A., Stirm, B. H., Kaeser, R., Wulle, B., Lyon, D. & Rudek, J. (2017). Assessing the methane emissions from natural gas-fired power plants and oil refineries. *Environmental science & technology*, 51(6), 3373-3381.
- Zavala-Araiza, D., Alvarez, R. A., Lyon, D. R., Allen, D. T., Marchese, A. J., Zimmerle, D. J., & Hamburg, S. P. (2017). Super-emitters in natural gas infrastructure are caused by abnormal process conditions. *Nature communications*, 8, 14012.
- Alvarez, R. A., Lyon, D. R., Marchese, A. J., Robinson, A. L., & Hamburg, S. P. (2016). Possible malfunction in widely used methane sampler deserves attention but poses limited implications for supply chain emission estimates. *Elementa*, 4.
- Marrero, J. E., Townsend-Small, A., Lyon, D. R., Tsai, T. R., Meinardi, S., & Blake, D. R. (2016). Estimating Emissions of Toxic Hydrocarbons from Natural Gas Production Sites in the Barnett Shale Region of Northern Texas. *Environmental Science & Technology*, 50(19), 10756-10764.
- Lamb, B. K., Cambaliza, M. O., Davis, K. J., Edburg, S. L., Ferrara, T. W., Floerchinger, C., ... & Lyon, D. R. (2016). Direct and indirect measurements and modeling of methane emissions in Indianapolis, Indiana. *Environmental Science & Technology*, 50(16), 8910-8917.

- Townsend-Small, A., Ferrara, T. W., Lyon, D. R., Fries, A. E., & Lamb, B. K. (2016). Emissions of coalbed and natural gas methane from abandoned oil and gas wells in the United States. *Geophysical Research Letters*, 43(5), 2283-2290, DOI: 10.1002/2015GL067623.
- Zavala-Araiza, D., Lyon, D. R., Alvarez, R. A., Davis, K. J., Harriss, R., Herndon, S. C., ... & Marchese, A. J. (2015). Reconciling divergent estimates of oil and gas methane emissions. *Proceedings of the National Academy of Sciences*, 112(51), 15597-15602, DOI: 10.1073/pnas.1522126112
- Zavala-Araiza, D.; Lyon, D. R.; Alvarez, R. A.; Palacios, V.; Harriss, R.; Lan, X.; Talbot, R.; Hamburg, S. P. (2015). Towards a Functional Definition of Methane Super-Emitters: Application to Natural Gas Production Sites. *Environmental Science & Technology*, 49, DOI: 10.1021/acs.est.5b00133.
- Karion, A.; Sweeney, C.; Kort, E. A.; Shepson, P. B.; Brewer, A.; Cambaliza, M. O. L.; Conley, S.; Davis, K. J.; Deng, A.; Hardesty, M.; Herndon, S. C.; Lauvaux, T.; Lavoie, T.; Lyon, D. R.; Newberger, T.; Petron, G.; Rella, C.; Smith, M.; Wolter, S.; Yacovitch, T.; Tans, P. (2015). Aircraft-based estimate of total methane emissions from the Barnett Shale region. *Environmental Science & Technology*, 49, DOI: 10.1021/acs.est.5b00217.
- Yacovitch, T. I.; Herndon, S. C.; Pétron, G.; Kofler, J.; Lyon, D. R. ; Zahniser, M. S.; Kolb, C. E. (2015). Mobile Laboratory Observations of Methane Emissions in the Barnett. *Environmental Science & Technology*, 49, DOI: 10.1021/es506352j.
- Lavoie, T. N.; Shepson, P. B.; Cambaliza, M. O. L.; Stirm, B. H.; Karion, A.; Sweeney, C.; Yacovitch, T. I.; Herndon, S. C.; Lan, X.; Lyon, D. R. (2015). Aircraft-Based Measurements of Point Source Methane Emissions in the Barnett Shale Basin. *Environmental Science & Technology*, 49, DOI: 10.1021/acs.est.5b00410.
- Harriss, R.; Alvarez, R. A.; Lyon, D. R.; Zavala-Araiza, D.; Nelson, D.; Hamburg, S. P. (2015). Using Multi-Scale Measurements to Improve Methane Emission Estimates from Oil and Gas Operations in the Barnett Shale Region, Texas. *Environmental Science & Technology*, 49, DOI: 10.1021/acs.est.5b02305.

Exhibit 11

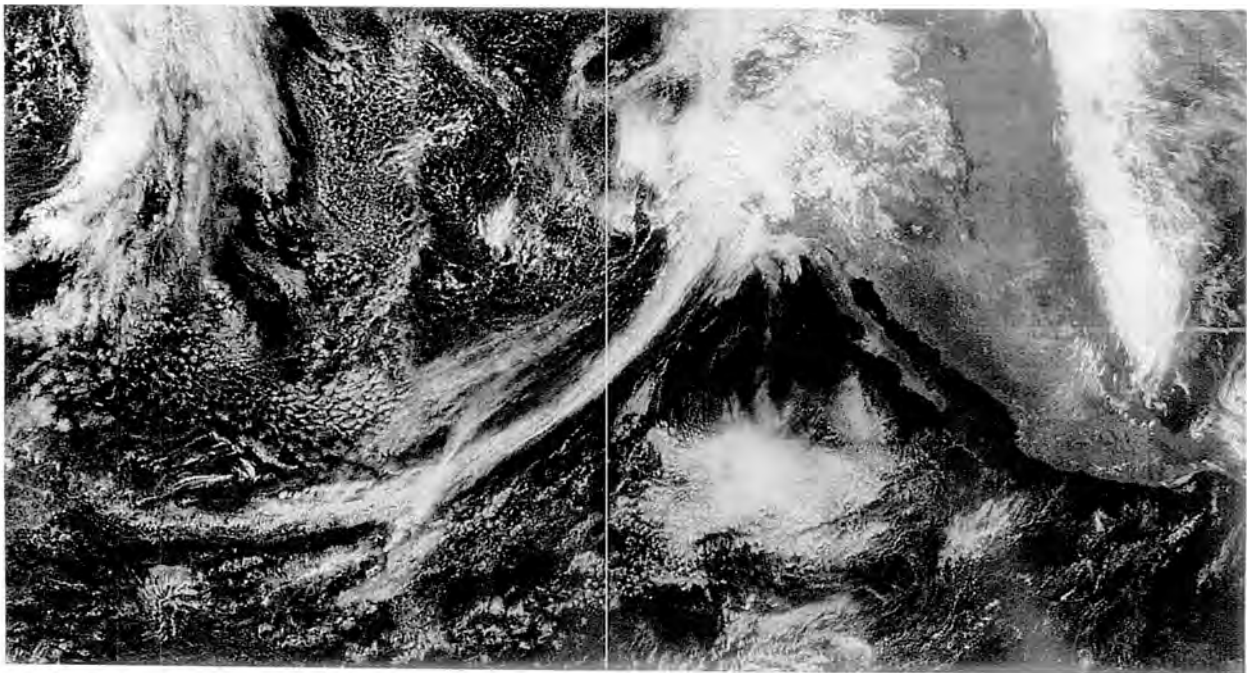


U.S. Global Change
Research Program

CLIMATE SCIENCE SPECIAL REPORT

Fourth National Climate Assessment | Volume I

CLIMATE SCIENCE SPECIAL REPORT



Fourth National Climate Assessment | Volume I



U.S. Global Change
Research Program

Available on-line at: <science2017.globalchange.gov>

This document responds to requirements of Section 106 of the U.S. Global Change Research Act of 1990 (P.L. 101-606, <<http://www.globalchange.gov/about/legal-mandate>>). It does not express any regulatory policies of the United States or any of its agencies, or make any findings of fact that could serve as predicates of regulatory action. Agencies must comply with required statutory and regulatory processes before they could rely on any statements in the document or by the USGCRP as basis for regulatory action.

This document was prepared in compliance with Section 515 of the Treasury and General Government Appropriations Act for Fiscal Year 2001 (P.L. 106-554) and information quality guidelines issued by the Department of Commerce / National Oceanic and Atmospheric Administration pursuant to Section 515 (<http://www.cio.noaa.gov/services_programs/info_quality.html>). For purposes of compliance with Section 515, this document is deemed a “highly influential scientific assessment” (HISA). The report graphics follow the ISO 19115 standard which includes the necessary information to achieve reproducibility.

In all cases, permissions were secured by the U.S. Government to use and/or adapt copyrighted material contained in this document. High-resolution art is available at science2017.globalchange.gov/, with accompanying captions providing source and credit information.

First published 2017

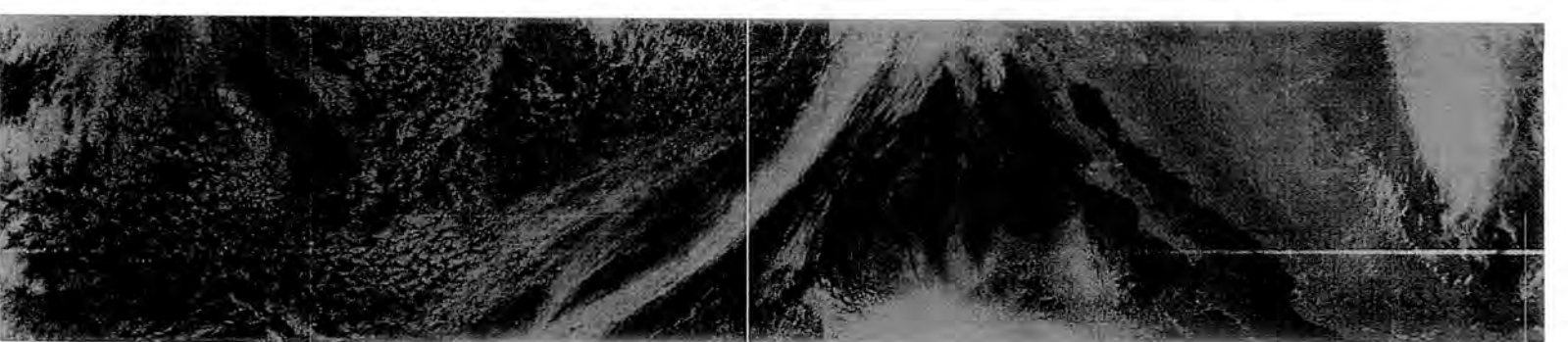
Recommended Citation for Report

USGCRP, 2017: *Climate Science Special Report: Fourth National Climate Assessment, Volume I* [Wuebbles, D.J., D.W. Fahey, K.A. Hibbard, D.J. Dokken, B.C. Stewart, and T.K. Maycock (eds.)]. U.S. Global Change Research Program, Washington, DC, USA, 470 pp., doi: 10.7930/J0J964J6.

Image Credit

Front Cover: Atmospheric rivers are relatively long, narrow regions in the atmosphere – like rivers in the sky – that transport most of the water vapor outside of the tropics. When an atmospheric river makes landfall, extreme precipitation and flooding can often result. The cover features a natural-color image of conditions over the northeastern Pacific on 20 February 2017, helping California and the American West emerge from a 5-year drought in stunning fashion. Some parts of California received nearly twice as much rain in a single deluge as normally falls in the preceding 5 months (October–February). The visualization was generated by Jesse Allen (NASA Earth Observatory) using data from the Visible Infrared Imaging Radiometer Suite (VIIRS) on the Suomi National Polar-orbiting Partnership (NPP) satellite.

Chapter Banners: Special thanks to the NASA Earth Observatory team for the non-captioned data products incorporated into chapter titles and web banners throughout the Climate Science Special Report.



CSSR Writing Team

Coordinating Lead Authors

Donald J. Wuebbles, National Science Foundation and
U.S. Global Change Research Program – University
of Illinois

David W. Fahey, NOAA Earth System Research
Laboratory
Kathy A. Hibbard, NASA Headquarters

Lead Authors

Jeff R. Arnold, U.S. Army Corps of Engineers
Benjamin DeAngelo, NOAA Climate Program Office
Sarah Doherty, University of Washington
David R. Easterling, NOAA National Centers for
Environmental Information
James Edmonds, Pacific Northwest National Laboratory
Timothy Hall, NASA Goddard Institute for Space Studies
Katharine Hayhoe, Texas Tech University
Forrest M. Hoffman, Oak Ridge National Laboratory
Radley Horton, Columbia University
Deborah Huntzinger, Northern Arizona University
Libby Jewett, NOAA Ocean Acidification Program
Thomas Knutson, NOAA Geophysical Fluid Dynamics
Lab
Robert E. Kopp, Rutgers University
James P. Kossin, NOAA National Centers for
Environmental Information

Kenneth E. Kunkel, North Carolina State University
Allegra N. LeGrande, NASA Goddard Institute for Space Studies
L. Ruby Leung, Pacific Northwest National Laboratory
Wieslaw Maslowski, Naval Postgraduate School
Carl Mears, Remote Sensing Systems
Judith Perlwitz, NOAA Earth System Research Laboratory
Anastasia Romanou, Columbia University
Benjamin M. Sanderson, National Center for Atmospheric
Research
William V. Sweet, NOAA National Ocean Service
Patrick C. Taylor, NASA Langley Research Center
Robert J. Trapp, University of Illinois at Urbana-Champaign
Russell S. Vose, NOAA National Centers for Environmental
Information
Duane E. Waliser, NASA Jet Propulsion Laboratory
Michael F. Wehner, Lawrence Berkeley National Laboratory
Tristram O. West, DOE Office of Science

Review Editors

Linda O. Mearns, National Center for Atmospheric
Research
Ross J. Salawitch, University of Maryland

Christopher P. Weaver, USEPA

Contributing Authors

Richard Alley, Pennsylvania State University
C. Taylor Armstrong, NOAA Ocean Acidification
Program
John Bruno, University of North Carolina
Shallin Busch, NOAA Ocean Acidification Program
Sarah Champion, North Carolina State University
Imke Durre, NOAA National Centers for Environmental
Information
Dwight Gledhill, NOAA Ocean Acidification Program
Justin Goldstein, U.S. Global Change Research Program
– ICF
Boyin Huang, NOAA National Centers for
Environmental Information

Hari Krishnan, Lawrence Berkeley National Laboratory
Lisa Levin, University of California – San Diego
Frank Muller-Karger, University of South Florida
Alan Rhoades, University of California – Davis
Laura Stevens, North Carolina State University
Liqiang Sun, North Carolina State University
Eugene Takle, Iowa State University
Paul Ullrich, University of California – Davis
Eugene Wahl, NOAA National Centers for Environmental
Information
John Walsh, University of Alaska – Fairbanks

climate change as well (see Ch. 15: Potential Surprises).^{172, 173} Connections to subarctic ocean variations and the Atlantic Meridional Overturning Circulation have not been conclusively established and require further investigation (see Ch. 13: Ocean Changes).

11.3.3 Permafrost–Carbon Feedback

Alaska and arctic permafrost characteristics have responded to increased temperatures and reduced snow cover in most regions since the 1980s.¹³⁰ The permafrost warming rate varies regionally; however, colder permafrost is warming faster than warmer permafrost.^{37, 174} This feature is most evident across Alaska, where permafrost on the North Slope is warming more rapidly than in the interior. Permafrost temperatures across the North Slope at various depths ranging from 39 to 65 feet (12 to 20 meters) have warmed between 0.3° and 1.3°F (0.2° and 0.7°C) per decade over the observational period (Figure 11.5).¹⁷⁵ Permafrost active layer thickness increased across much of the Arctic while showing strong regional

variations.^{37, 180, 176} Further, recent geologic survey data indicate significant permafrost thaw slumping in northwestern Canada and across the circumpolar Arctic that indicate significant ongoing permafrost thaw, potentially priming the region for more rapid thaw in the future.¹⁷⁷ Continued degradation of permafrost and a transition from continuous to discontinuous permafrost is expected over the 21st century.^{37, 178, 179}

Permafrost contains large stores of carbon. Though the total contribution of these carbon stores to global methane emission is uncertain, Alaska's permafrost contains rich and vulnerable organic carbon soils.^{99, 179, 180} Thus, warming Alaska permafrost is a concern for the global carbon cycle as it provides a possibility for a significant and potentially uncontrollable release of carbon, complicating the ability to limit global temperature increases. Current methane emissions from Alaskan arctic tundra and boreal forests contribute a small fraction of the global methane (CH₄) budget.¹⁸¹ Howev-

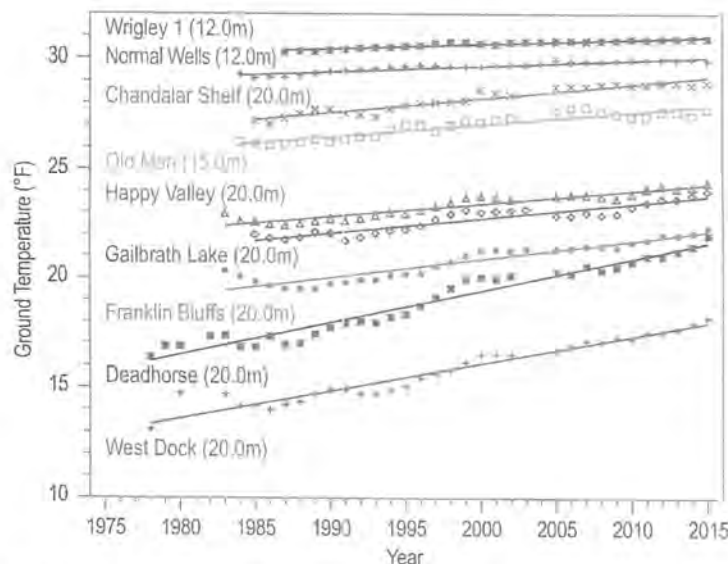


Figure 11.5: Time series of annual mean permafrost temperatures (units: °F) at various depths from 39 to 65 feet (12 to 20 meters) from 1977 through 2015 at several sites across Alaska, including the North Slope continuous permafrost region (purple/blue/green shades), and the discontinuous permafrost (orange/pink/red shades) in Alaska and northwestern Canada. Solid lines represent the linear trends drawn to highlight that permafrost temperatures are warming faster in the colder, coastal permafrost regions than the warmer interior regions. (Figure Source: adapted from Romanovsky et al. 2016;¹⁷⁵ © American Meteorological Society, used with permission.)

er, gas flux measurements have directly measured the release of CO₂ and CH₄ from arctic permafrost.¹⁸² Recent measurements indicate that cold season methane emissions (after snowfall) are greater than summer emissions in Alaska, and methane emissions in upland tundra are greater than in wetland tundra.¹⁸³

The permafrost–carbon feedback represents the additional release of CO₂ and CH₄ from thawing permafrost soils providing additional radiative forcing, a source of a potential surprise (Ch. 15: Potential Surprises).¹⁸⁴ Thawing permafrost makes previously frozen organic matter available for microbial decomposition, producing CO₂ and CH₄. The specific condition under which microbial decomposition occurs, aerobic or anaerobic, determines the proportion of CO₂ and CH₄ released. This distinction has potentially significant implications, as CH₄ has a 100-year global warming potential 35 times that of CO₂.¹⁸⁵ Emerging science indicates that 3.4 times more carbon is released under aerobic conditions than anaerobic conditions, and 2.3 times more carbon after accounting for the stronger greenhouse effect of CH₄.¹⁸⁶ Additionally, CO₂ and CH₄ production strongly depends on vegetation and soil properties.¹⁸⁴

Combined data and modeling studies indicate a positive permafrost–carbon feedback with a global sensitivity between –14 and –19 GtC per °C (approximately –25 to –34 GtC per °F) soil carbon loss^{187, 188} resulting in a total 120 ± 85 GtC release from permafrost by 2100 and an additional global temperature increase of 0.52° ± 0.38°F (0.29° ± 0.21°C) by the permafrost–carbon feedback.¹⁸⁹ More recently, Chadburn et al.¹⁹⁰ infer a –4 million km² per °C (or approximately 858,000 mi² per °F) reduction in permafrost area to globally averaged warming at stabilization by constraining climate models with the observed spatial distribution of permafrost; this sensitivity is 20% higher

than previous studies. In the coming decades, enhanced high-latitude plant growth and its associated CO₂ sink should partially offset the increased emissions from permafrost thaw;^{179, 189, 191} thereafter, decomposition is expected to dominate uptake. Permafrost thaw is occurring faster than models predict due to poorly understood deep soil, ice wedge, and thermokarst processes.^{188, 192, 193} Additionally, uncertainty stems from the surprising uptake of methane from mineral soils.¹⁹⁴ There is *high confidence* in the positive sign of the permafrost–carbon feedback, but *low confidence* in the feedback magnitude.

11.3.4 Methane Hydrate Instability

Significant stores of CH₄, in the form of methane hydrates (also called clathrates), lie within and below permafrost and under the global ocean on continental margins. The estimated total global inventory of methane hydrates ranges from 500 to 3,000 GtC^{195, 196, 197} with a central estimate of 1,800 GtC.¹⁹⁸ Methane hydrates are solid compounds formed at high pressures and cold temperatures, trapping methane gas within the crystalline structure of water. Methane hydrates within upper continental slopes of the Pacific, Atlantic, and Gulf of Mexico margins and beneath the Alaskan arctic continental shelf may be vulnerable to small increases in ocean temperature.^{197, 198, 199, 200, 201, 202, 203}

Rising sea levels and warming oceans have a competing influence on methane hydrate stability.^{199, 204} Studies indicate that the temperature effect dominates and that the overall influence is *very likely* a destabilizing effect.¹⁹⁸ Projected warming rates for the 21st century Arctic Ocean are not expected to lead to sudden or catastrophic destabilization of seafloor methane hydrates.²⁰⁵ Recent observations indicate increased CH₄ emission from the arctic seafloor near Svalbard; however, these emissions are not reaching the atmosphere.^{198, 206}



171. Yang, Q., T.H. Dixon, P.G. Myers, J. Bonin, D. Chambers, and M.R. van den Broeke, 2016: Recent increases in Arctic freshwater flux affects Labrador Sea convection and Atlantic overturning circulation. *Nature Communications*, **7**, 10525. <http://dx.doi.org/10.1038/ncomms10525>
172. Liu, W., S.-P. Xie, Z. Liu, and J. Zhu, 2017: Overlooked possibility of a collapsed Atlantic Meridional Overturning Circulation in warming climate. *Science Advances*, **3**, e1601666. <http://dx.doi.org/10.1126/sciadv.1601666>
173. Smeed, D.A., G.D. McCarthy, S.A. Cunningham, E. Frajka-Williams, D. Rayner, W.E. Johns, C.S. Meinen, M.O. Baringer, B.I. Moat, A. Duchez, and H.L. Bryden, 2014: Observed decline of the Atlantic meridional overturning circulation 2004–2012. *Ocean Science*, **10**, 29–38. <http://dx.doi.org/10.5194/os-10-29-2014>
174. Romanovsky, V.E., S.L. Smith, H.H. Christiansen, N.I. Shiklomanov, D.A. Streletskiy, D.S. Drozdov, G.V. Malkova, N.G. Oberman, A.L. Kholodov, and S.S. Marchenko, 2015: [The Arctic] Terrestrial permafrost [in “State of the Climate in 2014”]. *Bulletin of the American Meteorological Society*, **96** (12), S139–S141. <http://dx.doi.org/10.1175/2015BAMSStateoftheClimate.1>
175. Romanovsky, V.E., S.L. Smith, K. Isaksen, N.I. Shiklomanov, D.A. Streletskiy, A.L. Kholodov, H.H. Christiansen, D.S. Drozdov, G.V. Malkova, and S.S. Marchenko, 2016: [The Arctic] Terrestrial permafrost [in “State of the Climate in 2015”]. *Bulletin of the American Meteorological Society*, **97**, S149–S152. <http://dx.doi.org/10.1175/2016BAMSStateoftheClimate.1>
176. Shiklomanov, N.E., D.A. Streletskiy, and F.E. Nelson, 2012: Northern Hemisphere component of the global Circumpolar Active Layer Monitory (CALM) program. In *Proceedings of the 10th International Conference on Permafrost*, Salekhard, Russia. Kane, D.L. and K.M. Hinkel, Eds., 377–382. http://research.iarc.uaf.edu/NICOP/proceedings/10th/TICOP_voll.pdf
177. Kokelj, S.V., T.C. Lantz, J. Tunnicliffe, R. Segal, and D. Lacelle, 2017: Climate-driven thaw of permafrost preserved glacial landscapes, northwestern Canada. *Geology*, **45**, 371–374. <http://dx.doi.org/10.1130/g38626.1>
178. Grosse, G., S. Goetz, A.D. McGuire, V.E. Romanovsky, and E.A.G. Schuur, 2016: Changing permafrost in a warming world and feedbacks to the Earth system. *Environmental Research Letters*, **11**, 040201. <http://dx.doi.org/10.1088/1748-9326/11/4/040201>
179. Schuur, E.A.G., A.D. McGuire, C. Schadel, G. Grosse, J.W. Harden, D.J. Hayes, G. Hugelius, C.D. Koven, P. Kuhry, D.M. Lawrence, S.M. Natali, D. Olefeldt, V.E. Romanovsky, K. Schaefer, M.R. Turetsky, C.C. Treat, and J.E. Vonk, 2015: Climate change and the permafrost carbon feedback. *Nature*, **520**, 171–179. <http://dx.doi.org/10.1038/nature14338>
180. Tarnocai, C., J.G. Canadell, E.A.G. Schuur, P. Kuhry, G. Mazhitova, and S. Zimov, 2009: Soil organic carbon pools in the northern circumpolar permafrost region. *Global Biogeochemical Cycles*, **23**, GB2023. <http://dx.doi.org/10.1029/2008GB003327>
181. Chang, R.Y.-W., C.E. Miller, S.J. Dinardo, A. Karion, C. Sweeney, B.C. Daube, J.M. Henderson, M.E. Mountain, J. Eluszkiewicz, J.B. Miller, L.M.P. Bruhwiler, and S.C. Wofsy, 2014: Methane emissions from Alaska in 2012 from CARVE airborne observations. *Proceedings of the National Academy of Sciences*, **111**, 16694–16699. <http://dx.doi.org/10.1073/pnas.1412953111>
182. Schuur, E.A.G., J.G. Vogel, K.G. Crummer, H. Lee, J.O. Sickman, and T.E. Osterkamp, 2009: The effect of permafrost thaw on old carbon release and net carbon exchange from tundra. *Nature*, **459**, 556–559. <http://dx.doi.org/10.1038/nature08031>
183. Zona, D., B. Gioli, R. Commane, J. Lindaas, S.C. Wofsy, C.E. Miller, S.J. Dinardo, S. Dengel, C. Sweeney, A. Karion, R.Y.-W. Chang, J.M. Henderson, P.C. Murphy, J.P. Goodrich, V. Moreaux, A. Liljedahl, J.D. Watts, J.S. Kimball, D.A. Lipson, and W.C. Oechel, 2016: Cold season emissions dominate the Arctic tundra methane budget. *Proceedings of the National Academy of Sciences*, **113**, 40–45. <http://dx.doi.org/10.1073/pnas.1516017113>
184. Treat, C.C., S.M. Natali, J. Ernakovich, C.M. Iversen, M. Lupascu, A.D. McGuire, R.J. Norby, T. Roy Chowdhury, A. Richter, H. Šantrůčková, C. Schädel, E.A.G. Schuur, V.L. Sloan, M.R. Turetsky, and M.P. Waldrop, 2015: A pan-Arctic synthesis of CH₄ and CO₂ production from anoxic soil incubations. *Global Change Biology*, **21**, 2787–2803. <http://dx.doi.org/10.1111/gcb.12875>
185. Myhre, G., D. Shindell, F.-M. Bréon, W. Collins, J. Fuglestedt, J. Huang, D. Koch, J.-F. Lamarque, D. Lee, B. Mendoza, T. Nakajima, A. Robock, G. Stephens, T. Takemura, and H. Zhang, 2013: Anthropogenic and natural radiative forcing. *Climate Change 2013: The Physical Science Basis. Contribution of Working Group I to the Fifth Assessment Report of the Intergovernmental Panel on Climate Change*. Stocker, T.F., D. Qin, G.-K. Plattner, M. Tignor, S.K. Allen, J. Boschung, A. Nauels, Y. Xia, V. Bex, and P.M. Midgley, Eds. Cambridge University Press, Cambridge, United Kingdom and New York, NY, USA, 659–740. <http://www.climatechange2013.org/report/full-report/>
186. Schädel, C., M.K.F. Bader, E.A.G. Schuur, C. Biasi, R. Bracho, P. Capek, S. De Baets, K. Diakova, J. Ernakovich, C. Estop-Aragones, D.E. Graham, I.P. Hartley, C.M. Iversen, E. Kane, C. Knoblauch, M. Lupascu, P.J. Martikainen, S.M. Natali, R.J. Norby, J.A. O'Donnell, T.R. Chowdhury, H. Šantrůčková, G. Shaver, V.L. Sloan, C.C. Treat, M.R. Turetsky, M.P. Waldrop, and K.P. Wickland, 2016: Potential carbon emissions dominated by carbon dioxide from thawed permafrost soils. *Nature Climate Change*, **6**, 950–953. <http://dx.doi.org/10.1038/nclimate3054>



Exhibit 12

8

Anthropogenic and Natural Radiative Forcing

Coordinating Lead Authors:

Gunnar Myhre (Norway), Drew Shindell (USA)

Lead Authors:

François-Marie Bréon (France), William Collins (UK), Jan Fuglestedt (Norway), Jianping Huang (China), Dorothy Koch (USA), Jean-François Lamarque (USA), David Lee (UK), Blanca Mendoza (Mexico), Teruyuki Nakajima (Japan), Alan Robock (USA), Graeme Stephens (USA), Toshihiko Takemura (Japan), Hua Zhang (China)

Contributing Authors:

Borgar Aamaas (Norway), Olivier Boucher (France), Stig B. Dalsøren (Norway), John S. Daniel (USA), Piers Forster (UK), Claire Granier (France), Joanna Haigh (UK), Øivind Hodnebrog (Norway), Jed O. Kaplan (Switzerland/Belgium/USA), George Marston (UK), Claus J. Nielsen (Norway), Brian C. O'Neill (USA), Glen P. Peters (Norway), Julia Pongratz (Germany), Michael Prather (USA), Venkatachalam Ramaswamy (USA), Raphael Roth (Switzerland), Leon Rotstayn (Australia), Steven J. Smith (USA), David Stevenson (UK), Jean-Paul Vernier (USA), Oliver Wild (UK), Paul Young (UK)

Review Editors:

Daniel Jacob (USA), A.R. Ravishankara (USA), Keith Shine (UK)

This chapter should be cited as:

Myhre, G., D. Shindell, F.-M. Bréon, W. Collins, J. Fuglestedt, J. Huang, D. Koch, J.-F. Lamarque, D. Lee, B. Mendoza, T. Nakajima, A. Robock, G. Stephens, T. Takemura and H. Zhang, 2013: Anthropogenic and Natural Radiative Forcing. In: *Climate Change 2013: The Physical Science Basis. Contribution of Working Group I to the Fifth Assessment Report of the Intergovernmental Panel on Climate Change* [Stocker, T.F., D. Qin, G.-K. Plattner, M. Tignor, S.K. Allen, J. Boschung, A. Nauels, Y. Xia, V. Bex and P.M. Midgley (eds.)]. Cambridge University Press, Cambridge, United Kingdom and New York, NY, USA.

Table of Contents

Executive Summary 661

8.1 Radiative Forcing 664

8.1.1 The Radiative Forcing Concept 664

Box 8.1: Definition of Radiative Forcing and Effective Radiative Forcing 665

Box 8.2: Grouping Forcing Compounds by Common Properties 668

8.1.2 Calculation of Radiative Forcing due to Concentration or Emission Changes 668

8.2 Atmospheric Chemistry 669

8.2.1 Introduction 669

8.2.2 Global Chemistry Modelling in Coupled Model Intercomparison Project Phase 5 670

8.2.3 Chemical Processes and Trace Gas Budgets 670

8.3 Present-Day Anthropogenic Radiative Forcing 675

8.3.1 Updated Understanding of the Spectral Properties of Greenhouse Gases and Radiative Transfer Codes 675

8.3.2 Well-mixed Greenhouse Gases 676

8.3.3 Ozone and Stratospheric Water Vapour 679

8.3.4 Aerosols and Cloud Effects 682

8.3.5 Land Surface Changes 686

8.4 Natural Radiative Forcing Changes: Solar and Volcanic 688

8.4.1 Solar Irradiance 688

8.4.2 Volcanic Radiative Forcing 691

Box 8.3: Volcanic Eruptions as Analogues 693

8.5 Synthesis of Global Mean Radiative Forcing, Past and Future 693

8.5.1 Summary of Radiative Forcing by Species and Uncertainties 694

8.5.2 Time Evolution of Historical Forcing 698

8.5.3 Future Radiative Forcing 700

8.6 Geographic Distribution of Radiative Forcing 702

8.6.1 Spatial Distribution of Current Radiative Forcing 702

8.6.2 Spatial Evolution of Radiative Forcing and Response over the Industrial Era 705

8.6.3 Spatial Evolution of Radiative Forcing and Response for the Future 708

8.7 Emission Metrics 710

8.7.1 Metric Concepts 710

Box 8.4: Choices Required When Using Emission Metrics 711

8.7.2 Application of Metrics 716

References 721

Appendix 8.A: Lifetimes, Radiative Efficiencies and Metric Values 731

Frequently Asked Questions

FAQ 8.1 How Important Is Water Vapour to Climate Change? 666

FAQ 8.2 Do Improvements in Air Quality Have an Effect on Climate Change? 684

Supplementary Material

Supplementary Material is available in online versions of the report.

8.7 Emission Metrics

8.7.1 Metric Concepts

8.7.1.1 Introduction

To quantify and compare the climate impacts of various emissions, it is necessary to choose a climate parameter by which to measure the effects; that is, RF, temperature response, and so forth. Thus, various choices are needed for the steps down the cause–effect chain from emissions to climate change and impacts (Figure 8.27 and Box 8.4). Each step in the cause effect chain requires a modelling framework. For assessments and evaluation one may—as an alternative to models that explicitly include physical processes resulting in forcing and responses—apply simpler measures or *metrics* that are based on results from complex models. Metrics are used to quantify the contributions to climate change of emissions of different substances and can thus act as ‘exchange rates’ in multi-component policies or comparisons of emissions from regions/countries or sources/sectors. Metrics are also used in areas such as Life Cycle Assessments and Integrated Assessment Modelling (e.g., by IPCC WGIII).

Metrics can be given in *absolute* terms (e.g., K kg^{-1}) or in *relative* terms by normalizing to a reference gas — usually CO_2 . To transform the effects of different emissions to a common scale — often called ‘ CO_2 equivalent emissions’—the emission (E_i) of component i can be multiplied with the adopted normalized metric (M_i): $M_i \times E_i = \text{CO}_2\text{-eq}_i$. Ideally, the climate effects of the calculated CO_2 equivalent emissions should be the same regardless of the mix of components emitted. However, different components have different physical properties, and a metric that establishes equivalence with regard to one effect cannot guarantee equivalence with regard to other effects and over extended time periods, for example, Lauder et al. (2013), O’Neill (2000), Smith and Wigley (2000), Fuglestedt et al. (2003).

Metrics do not define goals and policy—they are tools that enable evaluation and implementation of multi-component policies (i.e., which emissions to abate). The most appropriate metric will depend on which aspects of climate change are most important to a particular application, and different climate policy goals may lead to different conclusions about what is the most suitable metric with which to implement that policy, for example, Plattner et al. (2009); Tol et al. (2012). Metrics that have been proposed include physical metrics as well as more comprehensive metrics that account for both physical and economic dimensions (see 8.7.1.5 and WGIII, Chapter 3).

This section provides an assessment that focuses on the scientific aspects and utility of emission metrics. Extending such an assessment to include more policy-oriented aspects of their performance and usage such as simplicity, transparency, continuity, economic implications of usage of one metric over another, and so forth, is not given here as this is beyond the scope of WGI. However, consideration of such aspects is vital for user-assessments. In the following, the focus is on the more well-known Global Warming Potential (GWP) and Global Temperature change Potential (GTP), though other concepts are also briefly discussed.

8.7.1.2 The Global Warming Potential Concept

The Global Warming Potential (GWP) is defined as the time-integrated RF due to a pulse emission of a given component, relative to a pulse emission of an equal mass of CO_2 (Figure 8.28a and formula). The GWP was presented in the First IPCC Assessment (Houghton et al., 1990), stating ‘It must be stressed that there is no universally accepted methodology for combining all the relevant factors into a single global warming potential for greenhouse gas emissions. A simple approach has been adopted here to illustrate the difficulties inherent in the concept, ...’. Further, the First IPCC Assessment gave no clear physical interpretation of the GWP.

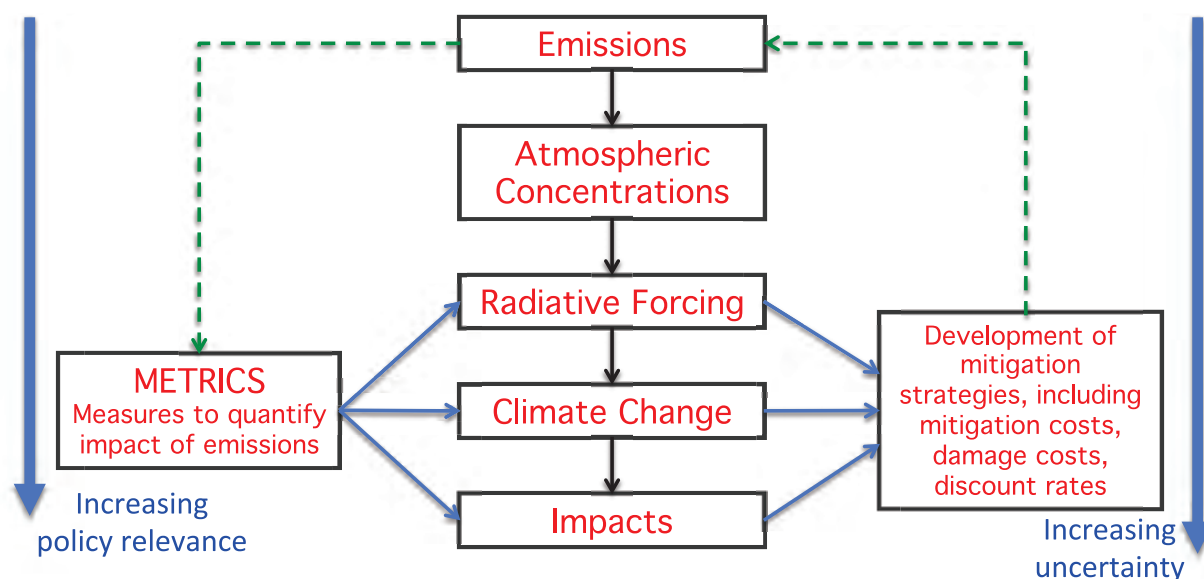


Figure 8.27 | The cause–effect chain from emissions to climate change and impacts showing how metrics can be defined to estimate responses to emissions (left) and for development of multi-component mitigation (right). The relevance of the various effects increases downwards but at the same time the uncertainty also increases. The dotted line on the left indicates that effects and impacts can be estimated directly from emissions, while the arrows on the right side indicate how these estimates can be used in development of strategies for reducing emissions. (Adapted from Fuglestedt et al., 2003, and Plattner et al., 2009.)

Box 8.4 | Choices Required When Using Emission Metrics

Time frames: One can apply a *backward-looking* (i.e., historical) or a *forward-looking* perspective on the responses to emissions. In the forward-looking case one may use pulses of emissions, sustained emissions or emission scenarios. All choices of emission perturbations are somewhat artificial and idealized, and different choices serve different purposes. One may use the *level* (e.g., degrees Celsius) or *rate of change* (e.g., degrees Celsius per decade). Furthermore, the effects of emissions may be estimated at a particular time or be integrated over time up to a chosen time horizon. Alternatively, discounting of future effects may be introduced (i.e., a weighting of effects over time).

Type of effect or end-point: Radiative forcing, temperature change or sea level change, for example, could be examined (Figure 8.27). Metrics may also include eco/biological or socioeconomic damages. The choice of climate impact parameters is related to which aspects of climate change are considered relevant for interpretation of ‘dangerous anthropogenic interference with the climate system’ (UNFCCC Article 2).

Spatial dimension for emission and response: Equal-mass emissions of NTCFs from different regions can induce varying global mean climate responses, and the climate response also has a regional component irrespective of the regional variation in emissions. Thus, metrics may be given for region of *emission* as well as region of *response*.

Some of the choices involved in metrics are scientific (e.g., type of model, and how processes are included or parameterized in the models). Choices of time frames and climate impact are policy-related and cannot be based on science alone, but scientific studies can be used to analyse different approaches and policy choices.

A direct interpretation is that the GWP is an index of the total energy added to the climate system by a component in question relative to that added by CO₂. However, the GWP does not lead to equivalence with temperature or other climate variables (Fuglestedt et al., 2000, 2003; O’Neill, 2000; Daniel et al., 2012; Smith and Wigley, 2000; Tanaka et al., 2009). Thus, the name ‘Global Warming Potential’ may be somewhat misleading, and ‘relative cumulative forcing index’ would be more appropriate. It can be shown that the GWP is approximately equal to the ratio (normalizing by the similar expression for CO₂) of the *equilibrium temperature response due to a sustained emission* of the species or to the *integrated temperature response for a pulse emission* (assuming efficacies are equal for the gases that are compared; O’Neill, 2000; Prather, 2002; Shine et al., 2005a; Peters et al., 2011a; Azar and Johansson, 2012).

The GWP has become the default metric for transferring emissions of different gases to a common scale; often called ‘CO₂ equivalent emissions’ (e.g., Shine, 2009). It has usually been integrated over 20, 100 or 500 years consistent with Houghton et al. (1990). Note, however that Houghton et al. presented these time horizons as ‘candidates for discussion [that] should not be considered as having any special significance’. The GWP for a time horizon of 100 years was later adopted as a metric to implement the multi-gas approach embedded in the United Nations Framework Convention on Climate Change (UNFCCC) and made operational in the 1997 Kyoto Protocol. The choice of time horizon has a strong effect on the GWP values — and thus also on the calculated contributions of CO₂ equivalent emissions by component, sector or nation. There is no scientific argument for selecting 100 years compared with other choices (Fuglestedt et al., 2003; Shine, 2009). The choice of time horizon is a value judgement because it depends

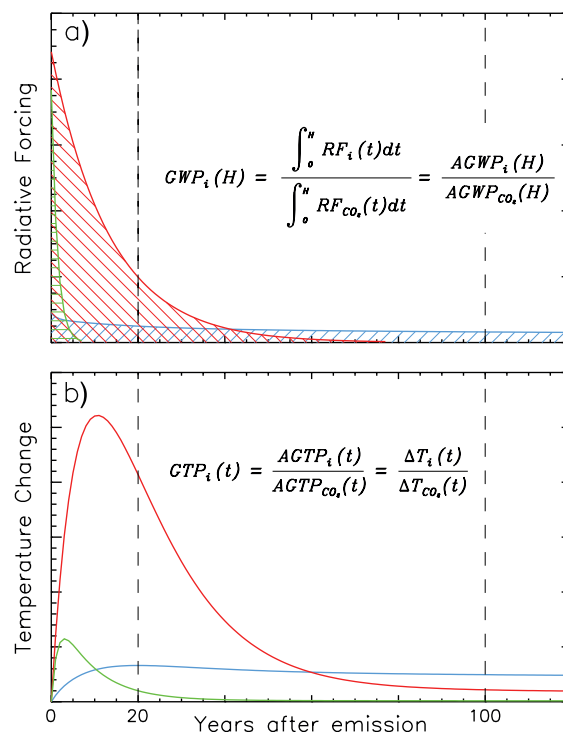


Figure 8.28 | (a) The Absolute Global Warming Potential (AGWP) is calculated by integrating the RF due to emission pulses over a chosen time horizon; for example, 20 and 100 years (vertical lines). The GWP is the ratio of AGWP for component *i* over AGWP for the reference gas CO₂. The blue hatched field represents the integrated RF from a pulse of CO₂, while the green and red fields represent example gases with 1.5 and 13 years lifetimes, respectively. (b) The Global Temperature change Potential (GTP) is based on the temperature response at a selected year after pulse emission of the same gases; e.g., 20 or 100 years (vertical lines). See Supplementary Material Section 8.SM.11 for equations for calculations of GWP and GTP.

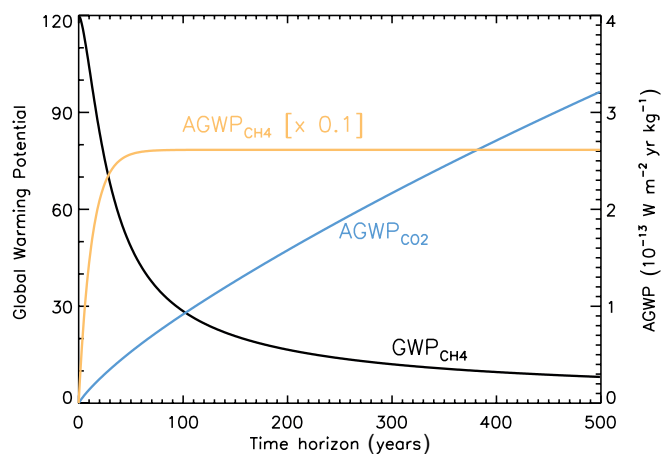


Figure 8.29 | Development of AGWP- CO_2 , AGWP- CH_4 and GWP- CH_4 with time horizon. The yellow and blue curves show how the AGWPs changes with increasing time horizon. Because of the integrative nature the AGWP for CH_4 (yellow curve) reaches a constant level after about five decades. The AGWP for CO_2 continues to increase for centuries. Thus the ratio which is the GWP (black curve) falls with increasing time horizon.

on the relative weight assigned to effects at different times. Other important choices include the background atmosphere on which the GWP calculations are superimposed, and the way indirect effects and feedbacks are included (see Section 8.7.1.4).

For some gases the variation in GWP with time horizon mainly reflects properties of the reference gas, not the gas for which the GWP is calculated. The GWP for NTCFs decreases with increasing time horizon, as GWP is defined with the integrated RF of CO_2 in the denominator. As shown in Figure 8.29, after about five decades the development in the GWP for CH_4 is almost entirely determined by CO_2 . However, for long-lived gases (e.g., SF_6) the development in GWP is controlled by both the increasing integrals of RF from the long-lived gas and CO_2 .

8.7.1.3 The Global Temperature change Potential Concept

Compared to the GWP, the Global Temperature change Potential (GTP; Shine et al., 2005a) goes one step further down the cause–effect chain (Figure 8.27) and is defined as the *change in global mean surface temperature at a chosen point in time* in response to an emission pulse—relative to that of CO_2 . Whereas GWP is integrated in time (Figure 8.28a), GTP is an end-point metric that is based on temperature change for a selected year, t , (see Figure 8.28b with formula). Like for the GWP, the impact from CO_2 is normally used as reference, hence, for a component i , $\text{GTP}(t)_i = \text{AGTP}(t)_i / \text{AGTP}(t)_{\text{CO}_2} = \Delta T(t)_i / \Delta T(t)_{\text{CO}_2}$, where AGTP is the absolute GTP giving temperature change per unit emission (see Supplementary Material Section 8.SM.11 for equations and parameter values). Shine et al. (2005a) presented the GTP for both pulse and sustained emission changes based on an energy balance model as well as analytical equations. A modification was later introduced (Shine et al., 2007) in which the time horizon is determined by the proximity to a target year as calculated by using scenarios and climate models (see Section 8.7.1.5).

Like GWP, the GTP values can be used for weighting the emissions to obtain ‘ CO_2 equivalents’ (see Section 8.7.1.1). This gives the

temperature effects of emissions relative to that of CO_2 for the chosen time horizon. As for GWP, the choice of time horizon has a strong effect on the metric values and the calculated contributions to warming.

In addition, the AGTP can be used to calculate the global mean temperature change due to any given emission scenario (assuming linearity) using a convolution of the emission scenarios and AGTP $_i$:

$$\Delta T(t) = \sum_i \int_0^t E_i(s) \text{AGTP}_i(t-s) ds \quad (8.1)$$

where i is component, t is time, and s is time of emission (Berntsen and Fuglestedt, 2008; Peters et al., 2011b; Shindell et al., 2011).

By accounting for the climate sensitivity and the exchange of heat between the atmosphere and the ocean, the GTP includes physical processes that the GWP does not. The GTP accounts for the slow response of the (deep) ocean, thereby prolonging the response to emissions beyond what is controlled by the decay time of the atmospheric concentration. Thus the GTP includes both the atmospheric adjustment time scale of the component considered and the response time scale of the climate system.

The GWP and GTP are fundamentally different by construction and different numerical values can be expected. In particular, the GWPs for NTCFs, over the same time frames, are higher than GTPs due to the integrative nature of the metric. The GTP values can be significantly affected by assumptions about the climate sensitivity and heat uptake by the ocean. Thus, the relative uncertainty ranges are wider for the GTP compared to GWP (see Section 8.7.1.4). The additional uncertainty is a typical trade-off when moving along the cause–effect chain to an effect of greater societal relevance (Figure 8.27). The formulation of the ocean response in the GTP has a substantial effect on the values; thus its characterization also represents a trade-off between simplicity and accuracy. As for GWP, the GTP is also influenced by the background atmosphere, and the way indirect effects and feedbacks are included (see Section 8.7.1.4).

8.7.1.4 Uncertainties and Limitations related to Global Warming Potential and Global Temperature change Potential

The uncertainty in the numerator of GWP; that is, the AGWP $_i$ (see formula in Figure 8.28a) is determined by uncertainties in lifetimes (or perturbation lifetimes) and radiative efficiency. Inclusion of indirect effects increases uncertainties (see below). For the reference gas CO_2 , the uncertainty is dominated by uncertainties in the *impulse response function* (IRF) that describes the development in atmospheric concentration that follows from an emission pulse (Joos et al., 2013); see Box 6.2 and Supplementary Material Section 8.SM.12. The IRF is sensitive to model representation of the carbon cycle, pulse size and background CO_2 concentrations and climate.

Based on a multi-model study, Joos et al. (2013) estimate uncertainty ranges for the time-integrated IRF for CO_2 to be $\pm 15\%$ and $\pm 25\%$ (5 to 95% uncertainty range) for 20- and 100-year time horizons, respectively. Assuming quadratic error propagation, and $\pm 10\%$ uncertainty in radiative efficiency, the uncertainty ranges in AGWP for CO_2 were estimated to be $\pm 18\%$ and $\pm 26\%$ for 20 and 100 years. These

uncertainties affect all metrics that use CO₂ as reference. Reisinger et al. (2010) and Joos et al. (2013) show that these uncertainties increase with time horizon.

The same factors contribute to uncertainties in the GTP, with an additional contribution from the parameters describing the ocean heat uptake and climate sensitivity. In the first presentation of the GTP, Shine et al. (2005a) used one time constant for the climate response in their analytical expression. Improved approaches were used by Boucher and Reddy (2008), Collins et al. (2010) and Berntsen and Fuglestedt (2008) that include more explicit representations of the deep ocean that increased the long-term response to a pulse forcing. Over the range of climate sensitivities from AR4, GTP₅₀ for BC was found to vary by a factor of 2, the CH₄ GTP₅₀ varied by about 50%, while for N₂O essentially no dependence was found (Fuglestedt et al., 2010). AGTPs for CO₂ were also calculated in the multi-model study by Joos et al. (2013). They found uncertainty ranges in AGTP that are much larger than for AGWP; ±45% and ±90% for 20 and 100 years (5 to 95% uncertainty range). These uncertainty ranges also reflect the signal-to-noise ratio, and not only uncertainty in the physical mechanisms.

There are studies combining uncertainties in various input parameters. Reisinger et al. (2011) estimated the uncertainty in the GWP for CH₄ and found an uncertainty of –30 to +40% for the GWP₁₀₀ and –50 to +75% for GTP₁₀₀ of CH₄ (for 5 to 95% of the range). Boucher (2012) performed a Monte Carlo analysis with uncertainties in perturbation lifetime and radiative efficiency, and for GWP₁₀₀ for CH₄ (assuming a constant background atmosphere) he found ±20%, and –40 to +65 for GTP₁₀₀ (for 5 to 95% uncertainty range).

Here we estimate uncertainties in GWP values based on the uncertainties given for radiative efficiencies (Section 8.3.1), perturbation lifetimes, indirect effects and in the AGWP for the reference gas CO₂ (see Supplementary Material Section 8.SM.12). For CH₄ GWP we estimate an uncertainty of ±30% and ±40% for 20- and 100-year time horizons, respectively (for 5 to 95% uncertainty range). The uncertainty is dominated by AGWP for CO₂ and indirect effects. For gases with lifetimes of a century or more the uncertainties are of the order of ±20% and ±30% for 20- and 100-year horizons. The uncertainty in GWPs for gases with lifetimes of a few decades is estimated to be of the order of ±25% and ±35% for 20 and 100 years. For shorter-lived gases, the uncertainties in GWPs will be larger (see Supplementary Material Section 8.SM.12 for a discussion of contributions to the total uncertainty.) For GTP, few uncertainty estimates are available in the literature. Based on the results from Joos et al. (2013), Reisinger et al. (2010) and Boucher (2012) we assess the uncertainty to be of the order of ±75% for the CH₄ GTP₁₀₀.

The metric values are also strongly dependent on which processes are included in the definition of a metric. Ideally all indirect effects (Sections 8.2 and 8.3) should be taken into account in the calculation of metrics. The indirect effects of CH₄ on its own lifetime, tropospheric ozone and stratospheric water have been traditionally included in its GWP. Boucher et al. (2009) have quantified an indirect effect on CO₂ when fossil fuel CH₄ is oxidized in the atmosphere. Shindell et al. (2009) estimated the impact of reactive species emissions on both gaseous and aerosol forcing species and found that ozone precursors,

including CH₄, had an additional substantial climate effect because they increased or decreased the rate of oxidation of SO₂ to sulphate aerosol. Studies with different sulphur cycle formulations have found lower sensitivity (Collins et al., 2010; Fry et al., 2012). Collins et al. (2010) postulated an additional component to their GWPs and GTPs for ozone precursors due to the decreased productivity of plants under higher levels of surface ozone. This was estimated to have the same magnitude as the ozone and CH₄ effects. This effect, however, has so far only been examined with one model. In a complex and interconnected system, feedbacks can become increasingly complex, and uncertainty of the magnitude and even direction of feedback increases the further one departs from the primary perturbation, resulting in a trade-off between completeness and robustness, and hence utility for decision-making.

Gillett and Matthews (2010) included climate–carbon feedbacks in calculations of GWP for CH₄ and N₂O and found that this increased the values by about 20% for 100 years. For GTP of CH₄ they found an increase of ~80%. They used numerical models for their studies and suggest that climate–carbon feedbacks should be considered and parameterized when used in simple models to derive metrics. Collins et al. (2013) parameterize the climate-carbon feedback based on Friedlingstein et al. (2006) and Arora et al. (2013) and find that this more than doubles the GTP₁₀₀ for CH₄. Enhancement of the GTP for CH₄ due to carbon–climate feedbacks may also explain the higher GTP values found by Reisinger et al. (2010).

The inclusion of indirect effects and feedbacks in metric values has been inconsistent in the IPCC reports. In SAR and TAR, a carbon model without a coupling to a climate model was used for calculation of IRF for CO₂ (Joos et al., 1996), while in AR4 climate-carbon feedbacks were included for the CO₂ IRF (Plattner et al., 2008). For the time horizons 20 and 100 years, the AGWP_{CO2} calculated with the Bern3D-LPJ model is, depending on the pulse size, 4 to 5% and 13 to 15% lower, respectively, when carbon cycle–climate feedbacks are not included (Joos et al., 2013). While the AGWP for the reference gas CO₂ included climate–carbon feedbacks, this is not the case for the non-CO₂ gas in the numerator of GWP, as recognized by Gillett and Matthews (2010), Joos et al. (2013), Collins et al. (2013) and Sarofim (2012). This means that the GWPs presented in AR4 may underestimate the relative impacts of non-CO₂ gases. The different inclusions of feedbacks partially represent the current state of knowledge, but also reflect inconsistent and ambiguous definitions. In calculations of AGWP for CO₂ in AR5 we use the IRF for CO₂ from Joos et al. (2013) which includes climate–carbon feedbacks. Metric values in AR5 are presented both with and without including climate–carbon feedbacks for non-CO₂ gases. This feedback is based on the carbon-cycle response in a similar set of models (Arora et al., 2013) as used for the reference gas (Collins et al., 2013).

The effect of including this feedback for the non-reference gas increases with time horizon due to the long-lived nature of the initiated CO₂ perturbation (Table 8.7). The relative importance also increases with decreasing lifetime of the component, and is larger for GTP than GWP due to the integrative nature of GWP. We calculate an increase in the CH₄ GWP₁₀₀ of 20%. For GTP₁₀₀, however, the changes are much larger; of the order of 160%. For the shorter time horizons (e.g., 20 years) the effect of including this feedback is small (<5%) for both GWP

Table 8.7 | GWP and GTP with and without inclusion of climate–carbon feedbacks (cc fb) in response to emissions of the indicated non-CO₂ gases (climate-carbon feedbacks in response to the reference gas CO₂ are always included).

	Lifetime (years)		GWP ₂₀	GWP ₁₀₀	GTP ₂₀	GTP ₁₀₀
CH ₄ ^b	12.4 ^a	No cc fb	84	28	67	4
		With cc fb	86	34	70	11
HFC-134a	13.4	No cc fb	3710	1300	3050	201
		With cc fb	3790	1550	3170	530
CFC-11	45.0	No cc fb	6900	4660	6890	2340
		With cc fb	7020	5350	7080	3490
N ₂ O	121.0 ^a	No cc fb	264	265	277	234
		With cc fb	268	298	284	297
CF ₄	50,000.0	No cc fb	4880	6630	5270	8040
		With cc fb	4950	7350	5400	9560

Notes:

Uncertainties related to the climate–carbon feedback are large, comparable in magnitude to the strength of the feedback for a single gas.

^a Perturbation lifetime is used in the calculation of metrics.

^b These values do not include CO₂ from methane oxidation. Values for fossil methane are higher by 1 and 2 for the 20 and 100 year metrics, respectively (Table 8.A.1).

and GTP. For the more long-lived gases the GWP₁₀₀ values increase by 10 to 12%, while for GTP₁₀₀ the increase is 20 to 30%. Table 8.A.1 gives metric values including the climate–carbon feedback for CO₂ only, while Supplementary Material Table 8.SM.16 gives values for all halocarbons that include the climate–carbon feedback. Though uncertainties in the carbon cycle are substantial, it is *likely* that including the climate–carbon feedback for non-CO₂ gases as well as for CO₂ provides a better estimate of the metric value than including it only for CO₂.

Emission metrics can be estimated based on a constant or variable background climate and this influences both the adjustment times and the concentration–forcing–temperature relationships. Thus, all metric values will need updating due to changing atmospheric conditions as well as improved input data. In AR5 we define the metric values with respect to a constant present-day condition of concentrations and climate. However, under non-constant background, Joos et al. (2013) found decreasing CO₂ AGWP₁₀₀ for increasing background levels (up to 23% for RCP8.5). This means that GWP for all non-CO₂ gases (except CH₄ and N₂O) would increase by roughly the same magnitude. Reisinger et al. (2011) found a reduction in AGWP for CO₂ of 36% for RCP8.5 from 2000 to 2100 and that the CH₄ radiative efficiency and AGWP also decrease with increasing CH₄ concentration. Accounting for both effects, the GWP₁₀₀ for CH₄ would increase by 10 to 20% under low and mid-range RCPs by 2100, but would decrease by up to 10% by mid-century under the highest RCP. While these studies have focused on the background levels of GHGs, the same issues apply for temperature. Olivé et al. (2012) find different temperature IRFs depending on the background climate (and experimental set up).

User related choices (see Box 8.4) such as the time horizon can greatly affect the numerical values obtained for CO₂ equivalents. For a change in time horizon from 20 to 100 years, the GWP for CH₄ decreases by a factor of approximately 3 and its GTP by more than a factor of 10. Short-lived species are most sensitive to this choice. Some approaches have removed the time horizon from the metrics (e.g., Boucher, 2012), but discounting is usually introduced which means that a discount rate

r (for the weighting function e^{-rt}) must be chosen instead. The choice of discount rate is also value based (see WGIII, Chapter 3).

For NTCFs the metric values also depend on the location and timing of emission and whether regional or global metrics are used for these gases is also a choice for the users. Metrics are usually calculated for pulses, but some studies also give metric values that assume constant emissions over the full time horizon (e.g., Shine et al., 2005a; Jacobson, 2010). It is important to be aware of the idealized assumption about constant future emissions (or change in emissions) of the compound being considered if metrics for sustained emissions are used.

8.7.1.5 New Metric Concepts

New metric concepts have been developed both to modify physical metrics to address shortcomings as well as to replace them with metrics that account for economic dimensions of problems to which metrics are applied. Modifications to physical metrics have been proposed to better represent CO₂ emissions from bioenergy, regional patterns of response, and for peak temperature limits.

Emissions of CO₂ from the combustion of biomass for energy in national emission inventories are currently assumed to have no net RF, based on the assumption that these emissions are compensated by biomass regrowth (IPCC, 1996). However, there is a time lag between combustion and regrowth, and while the CO₂ is resident in the atmosphere it leads to an additional RF. Modifications of the GWP and GTP for bioenergy (GWP_{bio}, GTP_{bio}) have been developed (Cherubini et al., 2011; Cherubini et al., 2012). The GWP_{bio} give values generally between zero (current default for bioenergy) and one (current for fossil fuel emissions) (Cherubini et al., 2011), and negative values are possible for GTP_{bio} due to the fast time scale of atmospheric–ocean CO₂ exchange relative to the growth cycle of biomass (Cherubini et al., 2012). GWP_{bio} and GTP_{bio} have been used in only a few applications, and more research is needed to assess their robustness and applicability. Metrics for biogeophysical effects, such as albedo changes, have been proposed (Betts, 2000; Rotenberg and Yakir, 2010), but as for NTCFs regional variations

are important (Claussen et al., 2001) and the RF concept may not be adequate (Davin et al., 2007).

New concepts have also been developed to capture information about regional patterns of responses and cancelling effects that are lost when global mean metrics are used. The use of nonlinear damage functions to capture information on the spatial pattern of responses has been explored (Shine et al., 2005b; Lund et al., 2012). In addition, the Absolute Regional Temperature Potential (ARTP) (Shindell, 2012; Collins et al., 2013) has been developed to provide estimates of impacts at a sub-global scale. ARTP gives the time-dependent temperature response in four latitude bands as a function of the regional forcing imposed in all bands. These metrics, as well as new regional precipitation metrics (Shindell et al., 2012b), require additional studies to determine their robustness.

Alternatives to the single basket approach adopted by the Kyoto Protocol are a component-by-component approach or a multi-basket approach (Rypdal et al., 2005; Daniel et al., 2012; Sarofim, 2012; Jackson, 2009). Smith et al. (2012) show how peak temperature change is constrained by *cumulative emissions* (see 12.5.4) for gases with long lifetimes and *emissions rates* for shorter-lived gases (including CH_4). Thus, they divide gases into two baskets and present two metrics that can be used for estimating peak temperature for various emission scenarios. This division of gases into the two baskets is sensitive to the time of peak temperature in the different scenarios. The approach uses time invariant metrics that do not account for the timing of emissions relative to the target year. The choice of time horizon is implicit in the scenario assumed and this approach works only for a peak scenario.

A number of new metrics have been developed to add economic dimensions to purely physically based metrics such as the GWP and GTP. The use of physical metrics in policy contexts has been criticized by economists (Reilly and Richards, 1993; Schmalensee, 1993; Hammitt et al., 1996; Reilly et al., 1999; Bradford, 2001; De Cara et al., 2008). A prominent use of metrics is to set relative prices of gases when implementing a multi-gas policy. Once a particular policy has been agreed on, economic metrics can address policy goals more directly than physical metrics by accounting not only for physical dimensions but also for economic dimensions such as mitigation costs, damage costs and discount rates (see WGIII, Chapter 3; Deuber et al., 2013).

For example, if mitigation policy is set within a *cost-effectiveness* framework with the aim of making the least cost mix of emissions reductions across components to meet a global temperature target, the 'price ratio' (Manne and Richels, 2001), also called the Global Cost Potential (GCP) (Tol et al., 2012), most directly addresses the goal. The choice of target is a policy decision; metric values can then be calculated based on an agreed upon target. Similarly, if policy is set within a *cost-benefit* framework, the metric that directly addresses the policy goal is the ratio of the marginal damages from the emission of a gas (i.e., the damage costs to society resulting from an incremental increase in emissions) relative to the marginal damages of an emission of CO_2 , known as the Global Damage Potential (GDP) (Kandlikar, 1995). Both types of metrics are typically determined within an integrated climate–economy model, since they are affected both by the response of the climate system as well as by economic factors.

If other indexes, such as the GWP, are used instead of an economic cost-minimizing index, costs to society will increase. Cost implications at the project or country level could be substantial under some circumstances (Godal and Fuglestvedt, 2002; Shine, 2009; Reisinger et al., 2013). However, under idealized conditions of full participation in mitigation policy, the increase is relatively small at the global level, particularly when compared to the cost savings resulting from a multi- (as opposed to single-) gas mitigation strategy even when based on an imperfect metric (O'Neill, 2003; Aaheim et al., 2006; Johansson et al., 2006; Johansson, 2012; Reisinger et al., 2013; Smith et al., 2013).

Purely physical metrics continue to be used in many contexts due at least in part to the added uncertainties in mitigation and damage costs, and therefore in the values of economic metrics (Boucher, 2012). Efforts have been made to view purely physical metrics such as GWPs and GTPs as approximations of economic indexes. GTPs, for example, can be interpreted as an approximation of a Global Cost Potential designed for use in a cost-effectiveness setting (Shine et al., 2007; Tol et al., 2012). Quantitative values for time-dependent GTPs reproduce in broad terms several features of the Global Cost Potential such as the rising value of metrics for short-lived gases as a climate policy target is approached (Tanaka et al., 2013). Figure 8.30 shows how contributions of N_2O , CH_4 and BC to warming in the target year changes over time. The contributions are given relative to CO_2 and show the effects of emission occurring at various times. Similarly, GWPs can be interpreted as approximations of the Global Damage Potential designed for a cost–benefit framework (Tol et al., 2012). These interpretations of the GTP and GWP imply that using even a purely physical metric in an economic policy context involves an implicit economic valuation.

In both cases, a number of simplifying assumptions must be made for these approximations to hold (Tol et al., 2012). For example, in the case of the GWP, the influence of emissions on RF, and therefore implicitly on costs to society, beyond the time horizon is not taken into account, and there are substantial numerical differences between GWP and GDP values (Marten and Newbold, 2012). In the case of the GTP, the influence of emissions on temperature change (and costs) is

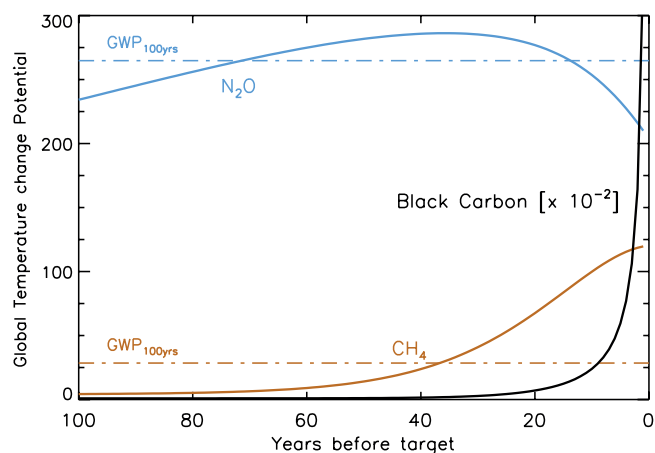


Figure 8.30 | Global Temperature change Potential (GTP(t)) for CH_4 , nitrous oxide and BC for each year from year of emission to the time at which the temperature change target is reached. The (time-invariant) GWP_{100} is also shown for N_2O and CH_4 for comparison.

included only at the time the target is reached, but not before nor after. Other metrics have been developed to more closely approximate GCPs or GDPs. The Cost-Effective Temperature Potential (CETP) reproduces values of the GCP more closely than does the GTP (Johansson, 2012). It is similar to the GTP but accounts for post-target temperature effects based on an assumption about how to value costs beyond the time the target is reached. Metrics have also been proposed that take into account forcing or temperature effects that result from emissions trajectories over broad time spans, and that behave similarly to GCP and GTP (Tanaka et al., 2009; Manning and Reisinger, 2011) or to GWP (e.g., O'Neill, 2000; Peters et al., 2011a; Gillett and Matthews, 2010; Azar and Johansson, 2012).

8.7.1.6 Synthesis

In the application and evaluation of metrics, it is important to distinguish between two main sources of variation in metric values. While scientific choices of input data have to be made, there are also choices involving value judgements. For some metrics such choices are not always explicit and transparent. The choice of metric type and time horizon will for many components have a much larger effect than improved estimates of input parameters and can have strong effects on perceived impacts of emissions and abatement strategies.

In addition to progress in understanding of GWP, new concepts have been introduced or further explored since AR4. Time variant metrics introduce more dynamical views of the temporal contributions that accounts for the proximity to a prescribed target (in contrast to the traditional static GWP). Time variant metrics can be presented in a format that makes changing metric values over time predictable.

As metrics use parameters further down the cause effect chain the metrics become in general more policy relevant, but at the same time the uncertainties increase. Furthermore, metrics that account for regional variations in sensitivity to emissions or regional variation in response could give a very different emphasis to various emissions. Many species, especially NTCFs, produce distinctly regionally heterogeneous RF and climate response patterns. These aspects are not accounted for in the commonly used global scale metrics.

The GWPs and GTPs have had inconsistent treatment of indirect effects and feedbacks. The GWPs reported in AR4 include climate–carbon feedbacks for the reference gas CO₂ but not for the non-CO₂ gases. Such feedbacks may have significant impacts on metrics and should be treated consistently. More studies are needed to assess the importance of consistent treatment of indirect effects/feedbacks in metrics.

The weighting of effects over time—choice of time horizon in the case of GWP and GTP—is value based. Discounting is an alternative, which also includes value judgements and is equally controversial. The weighting used in the GWP is a weight equal to one up to the time horizon and zero thereafter, which is not in line with common approaches for evaluation of future effects in economics (e.g., as in WGIII, Chapter 3). Adoption of a fixed horizon of e.g., 20, 100 or 500 years will inevitably put no weight on the long-term effect of CO₂ beyond the time horizon (Figure 8.28 and Box 6.1). While GWP integrates the effects up to a chosen time horizon the GTP gives the temperature just for one

chosen year with no weight on years before or after. The most appropriate metric depends on the particular application and which aspect of climate change is considered relevant in a given context. The GWP is not directly related to a temperature limit such as the 2°C target (Manne and Richels, 2001; Shine et al., 2007; Manning and Reisinger, 2011; Smith et al., 2012; Tol et al., 2012; Tanaka et al., 2013), whereas some economic metrics and physical end-point metrics like the GTP may be more suitable for this purpose.

To provide metrics that can be useful to the users and policymakers a more effective dialog and discussion on three topics is needed: (1) which applications particular metrics are meant to serve; (2) how comprehensive metrics need to be in terms of indirect effects and feedbacks, and economic dimensions; and—related to this (3) how important it is to have simple and transparent metrics (given by analytical formulations) versus more complex model-based and thus model-dependent metrics. These issues are also important to consider in a wider disciplinary context (e.g., across the IPCC Working Groups). Finally, it is important to be aware that all metric choices, even 'traditional' or 'widely used' metrics, contain implicit value judgements as well as large uncertainties.

8.7.2 Application of Metrics

8.7.2.1 Metrics for Carbon Dioxide, Methane, Nitrous Oxide, Halocarbons and Related Compounds

Updated (A)GWP and (A)GTP values for CO₂, CH₄, N₂O, CFCs, HCFCs, bromofluorocarbons, halons, HFCs, PFCs, SF₆, NF₃, and related halogen-containing compounds are given for some illustrative and tentative time horizons in Tables 8.7, 8.A.1 and Supplementary Material Table 8.SM.16. The input data and methods for calculations of GWPs and GTPs are documented in the Supplementary Material Section 8.SM.13. Indirect GWPs that account for the RF caused by depletion of stratospheric ozone (consistent with Section 8.3.3) are given for selected gases in Table 8.A.2.

The *confidence* in the ability to provide useful metrics at time scales of several centuries is *very low* due to nonlinear effects, large uncertainties for multi-century processes and strong assumptions of constant background conditions. Thus, we do not give metric values for longer time scales than 100 years (see discussion in Supplementary Material Section 8.SM.11). However, these time scales are important to consider for gases such as CO₂, SF₆ and PFCs. For CO₂, as much as 20 to 40% of the initial increase in concentration remains after 500 years. For PFC-14, 99% of an emission is still in the atmosphere after 500 years. The effects of emissions on these time scales are discussed in Chapter 12.

The GWP values have changed from previous assessments due to new estimates of lifetimes, impulse response functions and radiative efficiencies. These are updated due to improved knowledge and/or changed background levels. Because CO₂ is used as reference, any changes for this gas will affect all metric values via AGWP changes. Figure 8.31 shows how the values of radiative efficiency (RE), integrated impulse response function (IRF) and consequentially AGWP for CO₂ have changed from earlier assessments relative to AR5 values. The net effect of change in RE and IRF is an increase of approximately 1% and

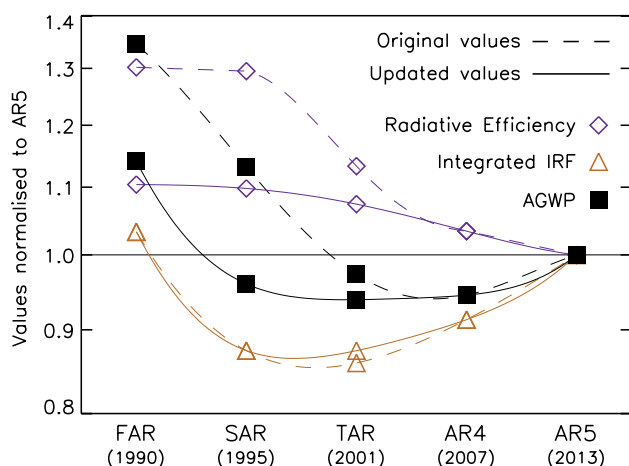


Figure 8.31 | Changes in the radiative efficiency (RE), integrated impulse response function (IRF) and Absolute Global Warming Potential (AGWP) for CO₂ for 100 years from earlier IPCC Assessment Reports normalized relative to the values given in AR5. The 'original' values are calculated based on the methods explained or value reported in each IPCC Assessment Report. The 'updated' values are calculated based on the methods used in AR5, but the input values from each Assessment Report. The difference is primarily in the formula for the RE, which was updated in TAR. The different integrated IRF in TAR relates to a different parameterisation of the same IRF (WMO, 1999). Changes represent both changes in scientific understanding and a changing background atmospheric CO₂ concentration (note that y-axis starts from 0.8). The lines connecting individual points are meant as a visual guide and not to represent the values between different Assessment Reports.

6% from AR4 to AR5 in AGWP for CO₂ for 20 and 100 years, respectively (see Supplementary Material Section 8.SM.12). These increases in the AGWP of the reference gas lead to corresponding decreases in the GWPs for all non-CO₂ gases. Continued increases in the atmospheric levels of CO₂ will lead to further changes in GWPs (and GTPs) in the future.

To understand the factors contributing to changes relative to AR4, comparisons are made here using the AR5 values that include climate-carbon feedbacks for CO₂ only. Relative to AR4 the CH₄ AGWP has changed due to changes in perturbation lifetime, a minor change in RE due to an increase in background concentration, and changes in the estimates of indirect effects. The indirect effects on O₃ and stratospheric H₂O are accounted for by increasing the effect of CH₄ by 50% and 15%, respectively (see Supplementary Material Table 8.SM.12). The ozone effect has doubled since AR4 taking into account more recent studies as detailed in Sections 8.3.3 and 8.5.1. Together with the changes in AGWP for CO₂ the net effect is increased GWP values of CH₄.

The GWPs for N₂O are lower here compared to AR4. A longer perturbation lifetime is used in AR5, while the radiative efficiency is lower due to increased abundances of CH₄ and N₂O. In addition, the reduction in CH₄ via stratospheric O₃, UV fluxes and OH levels due to increased N₂O abundance is included in GWPs and GTP. Owing to large uncertainties related to altitude of changes, we do not include the RF from stratospheric ozone changes as an indirect effect of N₂O.

Lifetimes for most of the halocarbons are taken from WMO (2011) and many of these have changed from AR4. The lifetimes of CFC-114, CFC-115 and HCF-161 are reduced by approximately 40%, while HFC-152

is reduced by one third. Among the hydrofluoroethers (HFEs) there are also several large changes in lifetimes. In addition, substantial updates of radiative efficiencies are made for several important gases; CFC-11, CFC-115, HCFC-124, HCFC-225cb, HFC-143a, HFC-245fa, CCl₄, CHCl₃, and SF₆. The radiative efficiency for carbon tetrachloride (CCl₄) is higher now and the GWP₁₀₀ has increased by almost 25% from AR4. Uncertainties in metric values are given in Section 8.7.1.4. See also Supplementary Material Section 8.SM.12 and footnote to Table 8.A.1. As can be seen from Table 8.A.2, some ODS have strong indirect effects through stratospheric ozone forcing, which for some of the gases reduce their net GWP₁₀₀ values substantially (and for the halons, to large negative values). Note that, consistent with Section 8.3.3, the uncertainties are large; ±100% for this indirect effect.

When climate-carbon feedbacks are included for both the non-CO₂ and reference gases, all metric values increase relative to the methodology used in AR4, sometimes greatly (Table 8.7, Supplementary Material Table 8.SM.16). Though the uncertainties range for these metric values is greater, as uncertainties in climate-carbon feedbacks are substantial, these calculations provide a more consistent methodology.

8.7.2.2 Metrics for Near-Term Climate Forcers

The GWP concept was initially used for the WMGHGs, but later for NTCFs as well. There are, however, substantial challenges related to calculations of GWP (and GTP) values for these components, which is reflected in the large ranges of values in the literature. Below we present and assess the current status of knowledge and quantification of metrics for various NTCFs.

8.7.2.2.1 Nitrogen oxides

Metric values for NO_x usually include the short-lived ozone effect, CH₄ changes and the CH₄-controlled O₃ response. NO_x also causes RF through nitrate formation, and via CH₄ it affects stratospheric H₂O and through ozone it influences CO₂. In addition, NO_x affects CO₂ through nitrogen deposition (fertilization effect). Due to high reactivity and the many nonlinear chemical interactions operating on different time scales, as well as heterogeneous emission patterns, calculation of *net* climate effects of NO_x is difficult. The net effect is a balance of large opposing effects with very different temporal behaviours. There is also a large spread in values among the regions due to variations in chemical and physical characteristics of the atmosphere.

As shown in Table 8.A.3 the GTP and GWP values are very different. This is due to the fundamentally different nature of these two metrics (see Figure 8.28) and the way they capture the temporal behaviour of responses to NO_x emissions. Time variation of GTP for NO_x is complex, which is not directly seen by the somewhat arbitrary choices of time horizon, and the net GTP is a fine balance between the contributing terms. The general pattern for NO_x is that the short-lived ozone forcing is always positive, while the CH₄-induced ozone forcing and CH₄ forcing are always negative (see Section 8.5.1). Nitrate aerosols from NO_x emission are not included in Table 8.A.3. For the GTP, all estimates for NO_x from surface sources give a negative net effect. As discussed in Section 8.7.1.4 Collins et al. (2010) and Shindell et al. (2009) implemented further indirect effects, but these are not included in Table

8.A.3 due to large uncertainties. The metric estimates for NO_x reflect the level of knowledge, but they also depend on experimental design, treatment of transport processes, and modelling of background levels. The multi-model study by Fry et al. (2012) shows the gaseous chemistry response to NO_x is relatively robust for European emissions, but that the uncertainty is so large that for some regions of emissions it is not possible to conclude whether NO_x causes cooling or warming.

8.7.2.2.2 Carbon monoxide and volatile organic compounds

Emissions of carbon monoxide (CO) and volatile organic compounds (VOCs) lead to production of ozone on short time scales. By affecting OH and thereby the levels of CH_4 they also initiate a positive long-term ozone effect. With its lifetime of 2 to 3 months, the effect of CO emissions is less dependent on location than is the case for NO_x (see Table 8.A.4). There is also less variation across models. However, Collins et al. (2010) found that inclusion of vegetation effects of O_3 increased the GTP values for CO by 20 to 50%. By including aerosol responses Shindell et al. (2009) found an increase in GWP_{100} by a factor of ~ 2.5 . CO of fossil origin will also have a forcing effect by contributing to CO_2 levels. This effect adds 1.4 to 1.6 to the GWP_{100} for CO (Daniel and Solomon, 1998; Derwent et al., 2001). (The vegetation and aerosol effects are not included in the numbers in Table 8.A.4.)

VOC is not a well-defined group of hydrocarbons. This group of gases with different lifetimes is treated differently across models by lumping or using representative key species. However, the spread in metric values in Table 8.A.5 is moderate across regions, with highest values for emissions in South Asia (of the four regions studied). The effects via ozone and CH_4 cause warming, and the additional effects via interactions with aerosols and via the O_3 – CO_2 link increase the warming effect further. Thus, the net effects of CO and VOC are less uncertain than for NO_x for which the net is a residual between larger terms of opposite sign. However, the formation of SOAs is usually not included in metric calculations for VOC, which introduces a cooling effect and increased uncertainty.

8.7.2.2.3 Black carbon and organic carbon

Most of the metric values for BC in the literature include the aerosol–radiation interaction and the snow/ice albedo effect of BC, though whether external or internal mixing is used varies between the studies. Bond et al. (2011) calculate GWPs and find that when the albedo effect is included the values increase by 5 to 15%. Studies have shown, however, that the climate response per unit forcing to this mechanism is stronger than for WMGHG (see Section 7.5).

Bond et al. (2013) assessed the current understanding of BC effects and calculated GWP and GTP for BC that includes aerosol–radiation interaction, aerosol–cloud interactions and albedo. As shown in Table 8.A.6 the uncertainties are wide for both metrics (for 90% uncertainty range) reflecting the current challenges related to understanding and quantifying the various effects (see Sections 7.5, 8.3.4 and 8.5.1). Their aerosol–radiation interaction effect is about 65% of the total effect while the albedo effect is approximately 20% of the aerosol–radiation interaction effect. Based on two studies (Rypdal et al., 2009; Bond et al., 2011), the GWP and GTP metrics were found to vary with

the region where BC is emitted by about $\pm 30\%$. For larger regions of emissions, Collins et al. (2013) calculated GWPs and GTPs for the direct effect of BC and found somewhat lower variations among the regions.

Several studies have focused on the effects of emissions of BC and OC from different regions (Bauer et al., 2007; Koch et al., 2007; Naik et al., 2007; Reddy and Boucher, 2007; Rypdal et al., 2009). However, examination of results from these models (Fuglestedt et al., 2010) reveals that there is not a robust relationship between the region of emission and the metric value — hence, regions that yield the highest metric value in one study, do not, in general, do so in the other studies.

The metric values for OC are quite consistent across studies, but fewer studies are available (see Table 8.A.6). A brief overview of metric values for other components is given in the Supplementary Material Section 8.SM.14.

8.7.2.2.4 Summary of status of metrics for near-term climate forcers

The metrics provide a format for comparing the magnitudes of the various emissions as well as for comparing effects of emissions from different regions. They can also be used for comparing results from different studies. Much of the spread in results is due to differences in experimental design and how the models treat physical and chemical processes. Unlike most of the WMGHGs, many of the NTCFs are tightly coupled to the hydrologic cycle and atmospheric chemistry, leading to a much larger spread in results as these are highly complex processes that are difficult to validate on the requisite small spatial and short temporal scales. The confidence level is lower for many of the NTCF compared to WMGHG and much lower where aerosol–cloud interactions are important (see Section 8.5.1). There are particular difficulties for NO_x , because the net impact is a small residual of opposing effects with quite different spatial distributions and temporal behaviour. Although climate–carbon feedbacks for non- CO_2 emissions have not been included in the NTCF metrics (other than CH_4) presented here, they can greatly increase those values (Collins et al., 2013) and likely provide more realistic results.

8.7.2.3 Impact by Emitted Component

We now use the metrics evaluated here to estimate climate impacts of various components (in a forward looking perspective). Figure 8.32 shows global anthropogenic emissions of some selected components weighted by the GWP and GTP. The time horizons are chosen as examples and illustrate how the perceived impacts of components—relative to the impact of the reference gas—vary strongly as function of impact parameter (integrated RF in GWP or end-point temperature in GTP) and with time horizon.

We may also calculate the temporal development of the temperature responses to pulse or sustained emissions using the AGTP metric. Figure 8.33 shows that for a one-year pulse the impacts of NTCF decay quickly owing to their atmospheric adjustment times even if effects are prolonged due to climate response time (in the case of constant emissions the effects reach approximately constant levels since the emissions are replenished each year, except for CO_2 , which has a fraction

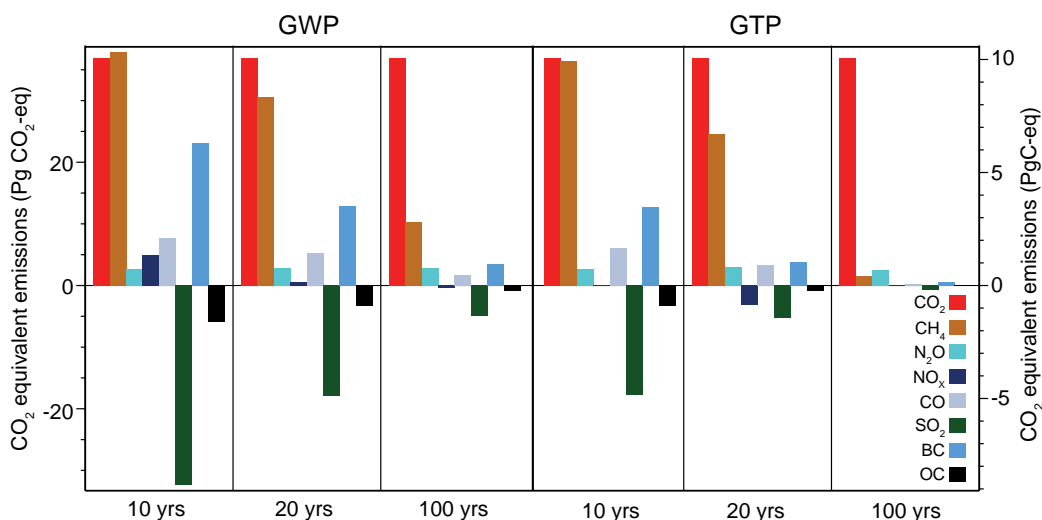


Figure 8.32 | Global anthropogenic emissions weighted by GWP and GTP for chosen time horizons (aerosol–cloud interactions are not included). Emission data for 2008 are taken from the EDGAR database. For BC and OC emissions for 2005 are from Shindell et al. (2012a). The units are ‘CO₂ equivalents’ which reflects equivalence only in the impact parameter of the chosen metric (integrated RF over the chosen time horizon for GWP; temperature change at the chosen point in time for GTP), given as Pg(CO₂)_{eq} (left axis) and given as PgC_{eq} (right axis). There are large uncertainties related to the metric values and consequentially also to the calculated CO₂ equivalents (see text).

remaining in the atmosphere on time scales of centuries). Figure 8.33 also shows how some components have strong short-lived effects of both signs while CO₂ has a weaker initial effect but one that persists to create a long-lived warming effect. Note that there are large uncertainties related to the metric values (as discussed in Section 8.7.1.4); especially for the NTCFs.

These examples show that the outcome of comparisons of effects of emissions depends strongly on choice of time horizon and metric type. Such end-user choices will have a strong influence on the calculated contributions from NTCFs versus WMGHGs or non-CO₂ versus CO₂ emissions. Thus, each specific analysis should use a design chosen in light of the context and questions being asked.

8.7.2.4 Metrics and Impacts by Sector

While the emissions of WMGHGs vary strongly between sectors, the climate impacts of these gases are independent of sector. The latter is not the case for chemically active and short-lived components, due to the dependence of their impact on the emission location. Since most sectors have multiple co-emissions, and for NTCFs some of these are warming while others are cooling, the net impact of a given sector requires explicit calculations. Since AR4, there has been significant progress in the understanding and quantification of climate impacts of NTCFs from sectors such as transportation, power production and biomass burning (Berntsen and Fuglestvedt, 2008; Skeie et al., 2009; Stevenson and Derwent, 2009; Lee et al., 2010; Unger et al., 2010; Dahlmann et al., 2011). Supplementary Material Table 8.SM.18 gives an overview of recent published metric values for various components by sector.

The impact from sectors depends on choice of metric, time horizon, pulse versus sustained emissions and forward versus backward looking perspective (see Section 8.7.1 and Box 8.4). Unger et al. (2010) calculated RF for a set of components emitted from each sector. RF at chosen points in time (20 and 100 years) for *sustained* emissions was used by Unger et al. (2010) as the metric for comparison. This is comparable

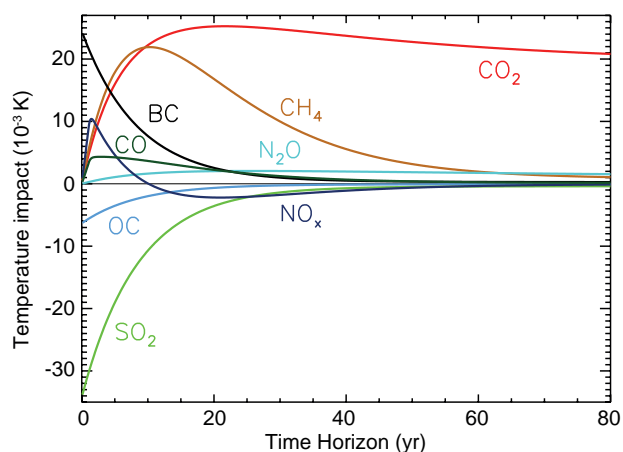


Figure 8.33 | Temperature response by component for total anthropogenic emissions for a 1-year pulse. Emission data for 2008 are taken from the EDGAR database and for BC and OC for 2005 from Shindell et al. (2012a). There are large uncertainties related to the AGTP values and consequentially also to the calculated temperature responses (see text).

to using integrated RF up to the chosen times for *pulse* emissions (as in GWPs). Such studies are relevant for policymaking that focuses on regulating the *total activity* of a sector or for understanding the contribution from a sector to climate change. On the other hand, the fixed mix of emissions makes it less general and relevant for emission scenarios. Alternatively, one may adopt a component-by-component view which is relevant for policies directed towards specific components (or sets of components, as controlling an individual pollutant in isolation is usually not practical). But this view will not capture interactions and non-linearities within the suite of components emitted by most sectors. The effects of specific emission control technologies or policies or projected societal changes on the mix of emissions is probably the most relevant type of analysis, but there are an enormous number of possible actions and regional details that could be investigated. Henze et al. (2012) demonstrate a method for providing highly spatially resolved

estimates of forcing per component, and caution that RF aggregated over regions or sectors may not represent the impacts of emissions changes on finer scales.

Metrics for individual land-based sectors are often similar to the global mean metric values (Shindell et al., 2008). In contrast, metrics for emissions from aviation and shipping usually show large differences from global mean metric values (Table 8.A.3 versus Table 8.SM.18). Though there can sometimes be substantial variation in the impact of land-based sectors across regions, and for a particular region even from one sector to another, variability between different land-based sources is generally smaller than between land, sea and air emissions.

NO_x from aviation is one example where the metric type is especially important. GWP_{20} values are positive due to the strong response of short-lived ozone. Reported GWP_{100} and GTP_{100} values are of either sign, however, due to the differences in balance between the individual effects modelled. Even if the models agree on the net effect of NO_x , the individual contributions can differ significantly, with large uncertainties stemming from the relative magnitudes of the CH_4 and O_3 responses (Myhre et al., 2011) and the background tropospheric concentrations of NO_x (Holmes et al., 2011; Stevenson and Derwent, 2009). Köhler et al. (2013), find strong regional sensitivity of ozone and CH_4 to NO_x particularly at cruise altitude. Generally, they find the strongest effects at low latitudes. For the aviation sector contrails and contrail induced cirrus are also important. Based on detailed studies in the literature, Fuglestedt et al. (2010) produced GWP and GTP for contrails, water vapor and contrail-induced cirrus.

The GWP and GTPs for NO_x from shipping are strongly negative for all time horizons. The strong positive effect via O_3 due to the low- NO_x environment into which ships generally emit NO_x is outweighed by the stronger effect on CH_4 destruction due to the relatively lower latitudes of these emissions compared to land-based sources.

In addition to having large emissions of NO_x the shipping sector has large emission of SO_2 . The direct GWP_{100} for shipping ranges from -11 to -43 (see Supplementary Material Table 8.SM.18). Lauer et al. (2007) reported detailed calculations of the indirect forcing specifically for this sector and found a wide spread of values depending on the emission inventory. Righi et al. (2011) and Peters et al. (2012) calculate indirect effects that are 30 to 50% lower than the indirect forcing reported by Lauer et al. (2007). The values from Shindell and Faluvegi (2010) for SO_2 from power generation are similar to those for shipping.

Although the various land transport sectors often are treated as one aggregate (e.g., road transport) there are important subdivisions. For instance, Bond et al. (2013) points out that among the BC-rich sectors they examined, diesel vehicles have the most clearly positive net impact on forcing. Studies delving even further have shown substantial differences between trucks and cars, gasoline and diesel vehicles, and low-sulphur versus high-sulphur fuels. Similarly, for power production there are important differences depending on fuel type (coal, oil, gas; e.g., Shindell and Faluvegi, 2010).

In the assessment of climate impacts of current emissions by sectors we give examples and apply a forward-looking perspective on effects

in terms of temperature change. The AGTP concept can be used to study the effects of the various components for chosen time horizons. A single year's worth of current global emissions from the energy and industrial sectors have the largest contributions to warming after 100 years (see Figure 8.34a). Household fossil fuel and biofuel, biomass burning and on-road transportation are also relatively large contributors to warming over 100-year time scales. Those same sectors, along with sectors that emit large amounts of CH_4 (animal husbandry, waste/landfills and agriculture), are most important over shorter time horizons (about 20 years; see Figure 8.34b).

Analysing climate change impacts by using the net effect of particular activities or sectors may—compared to other perspectives—provide more insight into how societal actions influence climate. Owing to large variations in mix of short- and long-lived components, as well as cooling and warming effects, the results will also in these cases depend strongly on choice of time horizon and climate impact parameter. Improved understanding of aerosol–cloud interactions, and how those are attributed to individual components is clearly necessary to refine estimates of sectoral or emitted component impacts.

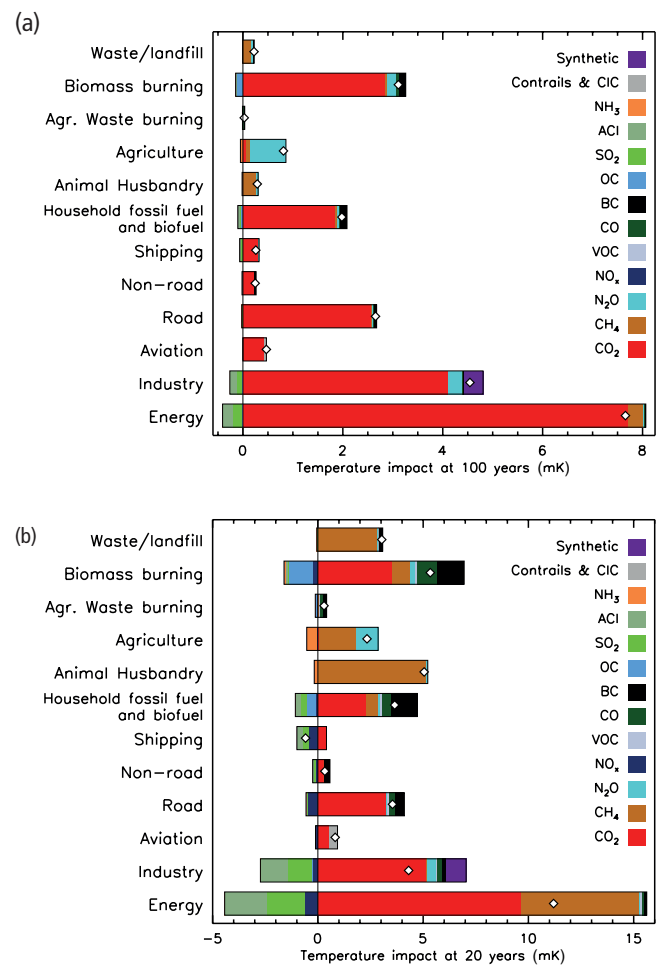


Figure 8.34 | Net global mean temperature change by source sector after (a) 100 and (b) 20 years (for 1-year pulse emissions). Emission data for 2008 are taken from the EDGAR database. For BC and OC anthropogenic emissions are from Shindell et al. (2012a) and biomass burning emissions are from Lamarque et al. (2010), see Supplementary Material Section 8.SM.17. There are large uncertainties related to the AGTP values and consequentially also to the calculated temperature responses (see text).

References

- Aaheim, A., J. Fuglestedt, and O. Godal, 2006: Costs savings of a flexible multi-gas climate policy. *Energy J. (Special Issue No. 3)*, 485–501.
- Abreu, J., J. Beer, F. Steinhilber, S. Tobias, and N. Weiss, 2008: For how long will the current grand maximum of solar activity persist? *Geophys. Res. Lett.*, **35**, L20109.
- Ackerley, D., B. B. Booth, S. H. E. Knight, E. J. Highwood, D. J. Frame, M. R. Allen, and D. P. Rowell, 2011: Sensitivity of twentieth-century Sahel rainfall to sulfate aerosol and CO₂ forcing. *J. Clim.*, **24**, 4999–5014.
- Allan, W., H. Struthers, and D. C. Lowe, 2007: Methane carbon isotope effects caused by atomic chlorine in the marine boundary layer: Global model results compared with Southern Hemisphere measurements. *J. Geophys. Res. Atmos.*, **112**, D04306.
- Ammann, C. M., and P. Naveau, 2003: Statistical analysis of tropical explosive volcanism occurrences over the last 6 centuries. *Geophys. Res. Lett.*, **30**, 1210.
- Ammann, C. M., and P. Naveau, 2010: A statistical volcanic forcing scenario generator for climate simulations. *J. Geophys. Res. Atmos.*, **115**, D05107.
- Anchukaitis, K. J., B. M. Buckley, E. R. Cook, B. I. Cook, R. D. D'Arrigo, and C. M. Ammann, 2010: Influence of volcanic eruptions on the climate of the Asian monsoon region. *Geophys. Res. Lett.*, **37**, L22703.
- Andersen, M., D. Blake, F. Rowland, M. Hurley, and T. Wallington, 2009: Atmospheric chemistry of sulfuranyl fluoride: Reaction with OH radicals, Cl atoms and O₃, atmospheric lifetime, IR spectrum, and global warming potential. *Environ. Sci. Technol.*, **43**, 1067–1070.
- Andersen, M., V. Andersen, O. Nielsen, S. Sander, and T. Wallington, 2010: Atmospheric chemistry of HCF₂O(CF₂CF₂O)(x)CF₂H (x=2–4): Kinetics and mechanisms of the chlorine-atom-initiated oxidation. *Chemphyschem*, **11**, 4035–4041.
- Andrews, T., and P. M. Forster, 2008: CO₂ forcing induces semi-direct effects with consequences for climate feedback interpretations. *Geophys. Res. Lett.*, **35**, L04802.
- Andrews, T., M. Doutriaux-Boucher, O. Boucher, and P. M. Forster, 2011: A regional and global analysis of carbon dioxide physiological forcing and its impact on climate. *Clim. Dyn.*, **36**, 783–792.
- Andrews, T., J. Gregory, M. Webb, and K. Taylor, 2012a: Forcing, feedbacks and climate sensitivity in CMIP5 coupled atmosphere-ocean climate models. *Geophys. Res. Lett.*, **39**, L09712.
- Andrews, T., P. Forster, O. Boucher, N. Bellouin, and A. Jones, 2010: Precipitation, radiative forcing and global temperature change. *Geophys. Res. Lett.*, **37**, doi:10.1029/2010GL043991, L14701.
- Andrews, T., M. Ringer, M. Doutriaux-Boucher, M. Webb, and W. Collins, 2012b: Sensitivity of an Earth system climate model to idealized radiative forcing. *Geophys. Res. Lett.*, **39**, L10702.
- Antuña, J. C., A. Robock, G. Stenchikov, J. Zhou, C. David, J. Barnes, and L. Thomason, 2003: Spatial and temporal variability of the stratospheric aerosol cloud produced by the 1991 Mount Pinatubo eruption. *J. Geophys. Res. Atmos.*, **108**, 4624.
- Archibald, A. T., M. E. Jenkin, and D. E. Shallcross, 2010: An isoprene mechanism intercomparison. *Atmos. Environ.*, **44**, 5356–5364.
- Archibald, A. T., et al., 2011: Impacts of HO(x) regeneration and recycling in the oxidation of isoprene: Consequences for the composition of past, present and future atmospheres. *Geophys. Res. Lett.*, **38**, L05804.
- Arnold, T., et al., 2013: Nitrogen trifluoride global emissions estimated from updated atmospheric measurements. *Proc. Natl. Acad. Sci. U.S.A.*, **110**, 2029–2034.
- Arora, V. K., and A. Montenegro, 2011: Small temperature benefits provided by realistic afforestation efforts. *Nature Geosci.*, **4**, 514–518.
- Arora, V. K., et al., 2013: Carbon-concentration and carbon-climate feedbacks in CMIP5 Earth system models. *J. Clim.*, **26**, 5289–5314.
- Ashmore, M. R., 2005: Assessing the future global impacts of ozone on vegetation. *Plant Cell Environ.*, **28**, 949–964.
- Azar, C., and D. J. A. Johansson, 2012: On the relationship between metrics to compare greenhouse gases—the case of IGTP, GWP and SGTP. *Earth Syst. Dynam.*, **3**, 139–147.
- Baasandorj, M., A. R. Ravishankara, and J. B. Burkholder, 2011: Atmospheric chemistry of (Z)-CF₃CH=CHCF₃: OH radical reaction rate coefficient and global warming potential. *J. Phys. Chem. A*, **115**, 10539–10549.
- Baasandorj, M., G. Knight, V. Papadimitriou, R. Talukdar, A. Ravishankara, and J. Burkholder, 2010: Rate coefficients for the gas-phase reaction of the hydroxyl radical with CH₂=CHF and CH₂=CF₂. *J. Phys. Chem. A*, **114**, 4619–4633.
- Bala, G., K. Caldeira, M. Wickett, T. J. Phillips, D. B. Lobell, C. Delire, and A. Mirin, 2007: Combined climate and carbon-cycle effects of large-scale deforestation. *Proc. Natl. Acad. Sci. U.S.A.*, **104**, 6550–6555.
- Balinas, S., and R. Jastrow, 1990: Evidence for long-term brightness changes of solar-type stars. *Nature*, **348**, 520–523.
- Ball, W., Y. Unruh, N. Krivova, S. Solanki, T. Wenzler, D. Mortlock, and A. Jaffe, 2012: Reconstruction of total solar irradiance 1974–2009. *Astron. Astrophys.*, **541**, A27.
- Ban-Weiss, G., L. Cao, G. Bala, and K. Caldeira, 2012: Dependence of climate forcing and response on the altitude of black carbon aerosols. *Clim. Dyn.*, **38**, 897–911.
- Barnes, C. A., and D. P. Roy, 2008: Radiative forcing over the conterminous United States due to contemporary land cover land use albedo change. *Geophys. Res. Lett.*, **35**, L09706.
- Bathiany, S., M. Claussen, V. Brovkin, T. Raddatz, and V. Gayler, 2010: Combined biogeophysical and biogeochemical effects of large-scale forest cover changes in the MPI earth system model. *Biogeosciences*, **7**, 1383–1399.
- Bauer, S., D. Koch, N. Unger, S. Metzger, D. Shindell, and D. Streets, 2007: Nitrate aerosols today and in 2030: A global simulation including aerosols and tropospheric ozone. *Atmos. Chem. Phys.*, **7**, 5043–5059.
- Bekki, S., J. A. Pyle, W. Zhong, R. Toumi, J. D. Haigh, and D. M. Pyle, 1996: The role of microphysical and chemical processes in prolonging the climate forcing of the Toba eruption. *Geophys. Res. Lett.*, **23**, 2669–2672.
- Bellouin, N., J. Rae, A. Jones, C. Johnson, J. Haywood, and O. Boucher, 2011: Aerosol forcing in the Climate Model Intercomparison Project (CMIP5) simulations by HadGEM2-ES and the role of ammonium nitrate. *J. Geophys. Res. Atmos.*, **116**, D20206.
- Bernier, P. Y., R. L. Desjardins, Y. Karimi-Zindashty, D. Worth, A. Beaudoin, Y. Luo, and S. Wang, 2011: Boreal lichen woodlands: A possible negative feedback to climate change in eastern North America. *Agr. Forest Meteorol.*, **151**, 521–528.
- Berntsen, T., and J. Fuglestedt, 2008: Global temperature responses to current emissions from the transport sectors. *Proc. Natl. Acad. Sci. U.S.A.*, **105**, 19154–19159.
- Berntsen, T. K., et al., 1997: Effects of anthropogenic emissions on tropospheric ozone and its radiative forcing. *J. Geophys. Res. Atmos.*, **102**, 28101–28126.
- Betts, R., 2000: Offset of the potential carbon sink from boreal forestation by decreases in surface albedo. *Nature*, **408**, 187–190.
- Betts, R. A., P. D. Falloon, K. K. Goldewijk, and N. Ramankutty, 2007: Biogeophysical effects of land use on climate: Model simulations of radiative forcing and large-scale temperature change. *Agr. Forest Meteorol.*, **142**, 216–233.
- Biasutti, M., and A. Giannini, 2006: Robust Sahel drying in response to late 20th century forcings. *Geophys. Res. Lett.*, **33**, L11706.
- Blowers, P., K. F. Tetrault, and Y. Trujillo-Morehead, 2008: Global warming potential predictions for hydrofluoroethers with two carbon atoms. *Theor. Chem. Acc.*, **119**, 369–381.
- Blowers, P., D. Moline, K. Tetrault, R. Wheeler, and S. Tuchawena, 2007: Prediction of radiative forcing values for hydrofluoroethers using density functional theory methods. *J. Geophys. Res. Atmos.*, **112**, D15108.
- Boer, G. J., and B. Yu, 2003: Climate sensitivity and response. *Clim. Dyn.*, **20**, 415–429.
- Bollasina, M. A., Y. Ming, and V. Ramaswamy, 2011: Anthropogenic aerosols and the weakening of the South Asian summer monsoon. *Science*, **334**, 502–505.
- Bond, T., C. Zarzycki, M. Flanner, and D. Koch, 2011: Quantifying immediate radiative forcing by black carbon and organic matter with the Specific Forcing Pulse. *Atmos. Chem. Phys.*, **11**, 1505–1525.
- Bond, T. C., et al., 2007: Historical emissions of black and organic carbon aerosol from energy-related combustion, 1850–2000. *Global Biogeochem. Cycles*, **21**, Gb2018.
- Bond, T. C., et al., 2013: Bounding the role of black carbon in the climate system: A scientific assessment. *J. Geophys. Res. Atmos.*, **118**, doi:10.1002/jgrd.50171, 5380–5552.
- Bonfils, C., and D. Lobell, 2007: Empirical evidence for a recent slowdown in irrigation-induced cooling. *Proc. Natl. Acad. Sci. U.S.A.*, **104**, 13582–13587.
- Bonfils, C. J. W., T. J. Phillips, D. M. Lawrence, P. Cameron-Smith, W. J. Riley, and Z. M. Subin, 2012: On the influence of shrub height and expansion on northern high latitude climate. *Environ. Res. Lett.*, **7**, 015503.

- Booth, B., N. Dunstone, P. Halloran, T. Andrews, and N. Bellouin, 2012: Aerosols implicated as a prime driver of twentieth-century North Atlantic climate variability. *Nature*, **485**, 534–534.
- Boucher, O., 2012: Comparison of physically- and economically-based CO₂-equivalences for methane. *Earth Syst. Dyn.*, **3**, 49–61.
- Boucher, O., and J. Haywood, 2001: On summing the components of radiative forcing of climate change. *Clim. Dyn.*, **18**, 297–302.
- Boucher, O., and M. Reddy, 2008: Climate trade-off between black carbon and carbon dioxide emissions. *Energy Policy*, **36**, 193–200.
- Boucher, O., P. Friedlingstein, B. Collins, and K. P. Shine, 2009: The indirect global warming potential and global temperature change potential due to methane oxidation. *Environ. Res. Lett.*, **4**, 044007.
- Bourassa, A. E., et al., 2012: Large volcanic aerosol load in the stratosphere linked to Asian monsoon transport. *Science*, **337**, 78–81.
- Bourassa, A. E., et al., 2013: Response to Comments on “Large Volcanic Aerosol Load in the Stratosphere Linked to Asian Monsoon Transport”. *Science*, **339**, 6120.
- Bowman, D., et al., 2009: Fire in the Earth System. *Science*, **324**, 481–484.
- Bowman, K. W., et al., 2013: Evaluation of ACCMIP outgoing longwave radiation from tropospheric ozone using TES satellite observations. *Atmos. Chem. Phys.*, **13**, 4057–4072.
- Bradford, D., 2001: Global change – Time, money and tradeoffs. *Nature*, **410**, 649–650.
- Bravo, I., et al., 2010: Infrared absorption spectra, radiative efficiencies, and global warming potentials of perfluorocarbons: Comparison between experiment and theory. *J. Geophys. Res. Atmos.*, **115**, D24317.
- Brovkin, V., et al., 2010: Sensitivity of a coupled climate-carbon cycle model to large volcanic eruptions during the last millennium. *Tellus B*, **62**, 674–681.
- Calvin, K., et al., 2012: The role of Asia in mitigating climate change: Results from the Asia modeling exercise. *Energ. Econ.*, **34**, S251–S260.
- Campra, P., M. Garcia, Y. Canton, and A. Palacios-Orueta, 2008: Surface temperature cooling trends and negative radiative forcing due to land use change toward greenhouse farming in southeastern Spain. *J. Geophys. Res. Atmos.*, **113**, D18109.
- Carlton, A. G., R. W. Pinder, P. V. Bhawe, and G. A. Pouliot, 2010: To what extent can biogenic SOA be controlled? *Environ. Sci. Technol.*, **44**, 3376–3380.
- Carslaw, K. S., O. Boucher, D. V. Spracklen, G. W. Mann, J. G. L. Rae, S. Woodward, and M. Kulmala, 2010: A review of natural aerosol interactions and feedbacks within the Earth system. *Atmos. Chem. Phys.*, **10**, 1701–1737.
- Chang, W. Y., H. Liao, and H. J. Wang, 2009: Climate responses to direct radiative forcing of anthropogenic aerosols, tropospheric ozone, and long-lived greenhouse gases in Eastern China over 1951–2000. *Adv. Atmos. Sci.*, **26**, 748–762.
- Chen, W. T., A. Nenes, H. Liao, P. J. Adams, J. L. F. Li, and J. H. Seinfeld, 2010: Global climate response to anthropogenic aerosol indirect effects: Present day and year 2100. *J. Geophys. Res. Atmos.*, **115**, D12207.
- Cherubini, F., G. Guest, and A. Strömman, 2012: Application of probability distributions to the modelling of biogenic CO₂ fluxes in life cycle assessment. *Global Change Biol.*, **4**, doi:10.1111/j.1757-1707.2011.01156.x, 784–798.
- Cherubini, F., G. Peters, T. Berntsen, A. Stromman, and E. Hertwich, 2011: CO₂ emissions from biomass combustion for bioenergy: Atmospheric decay and contribution to global warming. *Global Change Biol. Bioenerg.*, **3**, 413–426.
- Chung, C. E., and V. Ramanathan, 2006: Weakening of North Indian SST gradients and the monsoon rainfall in India and the Sahel. *J. Clim.*, **19**, 2036–2045.
- Clark, H. L., M. L. Cathala, H. Teysseire, J. P. Cammas, and V. H. Peuch, 2007: Cross-tropopause fluxes of ozone using assimilation of MOZAIC observations in a global CTM. *Tellus B*, **59**, 39–49.
- Clarke, A. D., and K. J. Noone, 1985: Soot in the Arctic Snowpack—A cause for perturbations in radiative-transfer. *Atmos. Environ.*, **19**, 2045–2053.
- Claussen, M., V. Brovkin, and A. Ganopolski, 2001: Biogeophysical versus biogeochemical feedbacks of large-scale land cover change. *Geophys. Res. Lett.*, **28**, 1011–1014.
- Cofala, J., M. Amann, Z. Klimont, K. Kupiainen, and L. Hoglund-Isaksson, 2007: Scenarios of global anthropogenic emissions of air pollutants and methane until 2030. *Atmos. Environ.*, **41**, 8486–8499.
- Collins, W., R. Derwent, C. Johnson, and D. Stevenson, 2002: The oxidation of organic compounds in the troposphere and their global warming potentials. *Clim. Change*, **52**, 453–479.
- Collins, W. D., et al., 2006: Radiative forcing by well-mixed greenhouse gases: Estimates from climate models in the Intergovernmental Panel on Climate Change (IPCC) Fourth Assessment Report (AR4). *J. Geophys. Res. Atmos.*, **111**, D14317.
- Collins, W. J., S. Sitch, and O. Boucher, 2010: How vegetation impacts affect climate metrics for ozone precursors. *J. Geophys. Res. Atmos.*, **115**, D23308.
- Collins, W. J., M. M. Fry, H. Yu, J. S. Fuglestedt, D. T. Shindell, and J. J. West, 2013: Global and regional temperature-change potentials for near-term climate forcings. *Atmos. Chem. Phys.*, **13**, 2471–2485.
- Conley, A. J., J. F. Lamarque, F. Vitt, W. D. Collins, and J. Kiehl, 2013: PORT, a CESM tool for the diagnosis of radiative forcing. *Geosci. Model Dev.*, **6**, 469–476.
- Cooper, O. R., et al., 2010: Increasing springtime ozone mixing ratios in the free troposphere over western North America. *Nature*, **463**, 344–348.
- Cox, P. M., et al., 2008: Increasing risk of Amazonian drought due to decreasing aerosol pollution. *Nature*, **453**, 212–215.
- Crook, J., and P. Forster, 2011: A balance between radiative forcing and climate feedback in the modeled 20th century temperature response. *J. Geophys. Res. Atmos.*, **116**, D17108.
- Crowley, T. J., and M. B. Unterman, 2013: Technical details concerning development of a 1200 yr proxy index for global volcanism. *Earth Syst. Sci. Data*, **5**, 187–197.
- Crutzen, P., 1973: Discussion of chemistry of some minor constituents in stratosphere and troposphere. *Pure Appl. Geophys.*, **106**, 1385–1399.
- Dahlmann, K., V. Grewe, M. Ponater, and S. Matthes, 2011: Quantifying the contributions of individual NO_x sources to the trend in ozone radiative forcing. *Atmos. Environ.*, **45**, 2860–2868.
- Daniel, J., and S. Solomon, 1998: On the climate forcing of carbon monoxide. *J. Geophys. Res. Atmos.*, **103**, 13249–13260.
- Daniel, J., S. Solomon, and D. Abritton, 1995: On the evaluation of halocarbon radiative forcing and global warming potentials. *J. Geophys. Res. Atmos.*, **100**, 1271–1285.
- Daniel, J., E. Fleming, R. Portmann, G. Velders, C. Jackman, and A. Ravishankara, 2010: Options to accelerate ozone recovery: Ozone and climate benefits. *Atmos. Chem. Phys.*, **10**, 7697–7707.
- Daniel, J., S. Solomon, T. Sanford, M. McFarland, J. Fuglestedt, and P. Friedlingstein, 2012: Limitations of single-basket trading: Lessons from the Montreal Protocol for climate policy. *Clim. Change*, **111**, 241–248.
- Davin, E., N. de Noblet-Ducoudre, and P. Friedlingstein, 2007: Impact of land cover change on surface climate: Relevance of the radiative forcing concept. *Geophys. Res. Lett.*, **34**, L13702.
- Davin, E. L., and N. de Noblet-Ducoudre, 2010: Climatic impact of global-scale deforestation: Radiative versus nonradiative processes. *J. Clim.*, **23**, 97–112.
- De Cara, S., E. Galco, and P. Jayet, 2008: The global warming potential paradox: Implications for the design of climate policy. In: *Design of Climate Policy* [R. Guesnerie and H. Tulkens (eds.)]. The MIT Press, Cambridge, MA, USA, pp. 359–384.
- de la Torre, L., et al., 2006: Solar influence on Northern Annular Mode spatial structure and QBO modulation. *Part. Accel. Space Plasma Phys. Sol. Radiat. Earth. Atmos. Clim.*, **37**, 1635–1639.
- de Noblet-Ducoudre, N., et al., 2012: Determining robust impacts of land-use-induced land cover changes on surface climate over North America and Eurasia: Results from the first set of LUCID experiments. *J. Clim.*, **25**, 3261–3281.
- DeAngelis, A., F. Dominguez, Y. Fan, A. Robock, M. D. Kustu, and D. Robinson, 2010: Evidence of enhanced precipitation due to irrigation over the Great Plains of the United States. *J. Geophys. Res. Atmos.*, **115**, D15115.
- DeLand, M., and R. Cebula, 2012: Solar UV variations during the decline of Cycle 23. *J. Atmos. Sol. Terres. Phys.*, **77**, 225–234.
- Delaygue, G., and E. Bard, 2011: An Antarctic view of Beryllium-10 and solar activity for the past millennium. *Clim. Dyn.*, **36**, 2201–2218.
- Deligne, N. I., S. G. Coles, and R. S. J. Sparks, 2010: Recurrence rates of large explosive volcanic eruptions. *J. Geophys. Res. Sol. Earth*, **115**, B06203.
- den Elzen, M., et al., 2005: Analysing countries' contribution to climate change: Scientific and policy-related choices. *Environ. Sci. Policy*, **8**, 614–636.
- Denman, K. L., et al., 2007: Couplings between changes in the climate system and biogeochemistry. In: *Climate Change 2007: The Physical Science Basis. Contribution of Working Group I to the Fourth Assessment Report of the Intergovernmental Panel on Climate Change* [Solomon, S., D. Qin, M. Manning, Z. Chen, M. Marquis, K. B. Averyt, M. Tignor and H. L. Miller (eds.)] Cambridge University Press, Cambridge, United Kingdom and New York, NY, USA, 499–587.

- Dentener, F., et al., 2006: The global atmospheric environment for the next generation. *Environ. Sci. Technol.*, **40**, 3586–3594.
- Derwent, R., W. Collins, C. Johnson, and D. Stevenson, 2001: Transient behaviour of tropospheric ozone precursors in a global 3-D CTM and their indirect greenhouse effects. *Clim. Change*, **49**, 463–487.
- Deuber, O., G. Luderer, and O. Edenhofer, 2013: Physico-economic evaluation of climate metrics: A conceptual framework. *Environ. Sci. Policy*, **29**, 37–45.
- Dewitte, S., D. Crommelynck, S. Mekaoui, and A. Joukoff, 2004: Measurement and uncertainty of the long-term total solar irradiance trend. *Solar Phys.*, **224**, 209–216.
- Dickinson, R., 1975: Solar variability and lower atmosphere. *Bull. Am. Meteorol. Soc.*, **56**, 1240–1248.
- Doherty, S. J., S. G. Warren, T. C. Grenfell, A. D. Clarke, and R. E. Brandt, 2010: Light-absorbing impurities in Arctic snow. *Atmos. Chem. Phys.*, **10**, 11647–11680.
- Doutriaux-Boucher, M., M. Webb, J. Gregory, and O. Boucher, 2009: Carbon dioxide induced stomatal closure increases radiative forcing via a rapid reduction in low cloud. *Geophys. Res. Lett.*, **36**, doi:10.1029/2008GL036273, L02703.
- Ehhalt, D. H., and L. E. Heidt, 1973: Vertical profiles of CH₄ in troposphere and stratosphere. *J. Geophys. Res.*, **78**, 5265–5271.
- Eliseev, A. V., and I. I. Mokhov, 2011: Effect of including land-use driven radiative forcing of the surface albedo of land on climate response in the 16th–21st centuries. *Izvestiya Atmos. Ocean. Phys.*, **47**, 15–30.
- Engel, A., et al., 2009: Age of stratospheric air unchanged within uncertainties over the past 30 years. *Nature Geosci.*, **2**, 28–31.
- Erykin, A., and A. Wolfendale, 2011: Cosmic ray effects on cloud cover and their relevance to climate change. *J. Atmos. Sol. Terres. Phys.*, **73**, 1681–1686.
- Ermolli, I., K. Matthes, T. Dudok de Wit, N. A. Krivova, K. Tourpali, M. Weber, Y. C. Unruh, L. Gray, U. Langematz, P. Pilewskie, E. Rozanov, W. Schmutz, A. Shapiro, S. K. Solanki, and T. N. Woods, 2013: Recent variability of the solar spectral irradiance and its impact on climate modelling. *Atmospheric Chemistry and Physics*, **13**, 3945–3977.
- Esper, J., and F. H. Schweingruber, 2004: Large-scale treeline changes recorded in Siberia. *Geophys. Res. Lett.*, **31**, L06202.
- Eyring, V., et al., 2010a: Sensitivity of 21st century stratospheric ozone to greenhouse gas scenarios. *Geophys. Res. Lett.*, **37**, L16807.
- Eyring, V., et al., 2010b: Multi-model assessment of stratospheric ozone return dates and ozone recovery in CCMVal-2 models. *Atmos. Chem. Phys.*, **10**, 9451–9472.
- Fan, F. X., M. E. Mann, and C. M. Ammann, 2009: Understanding changes in the Asian summer monsoon over the past millennium: Insights from a long-term coupled model simulation. *J. Clim.*, **22**, 1736–1748.
- FAO, 2012: State of the world's forests. Food and Agriculture Organization of the United Nations, Rome, Italy, 60 pp.
- Feng, X., and F. Zhao, 2009: Effect of changes of the HITRAN database on transmittance calculations in the near-infrared region. *J. Quant. Spectrosc. Radiat. Transfer*, **110**, 247–255.
- Feng, X., F. Zhao, and W. Gao, 2007: Effect of the improvement of the HITRAN database on the radiative transfer calculation. *J. Quant. Spectrosc. Radiat. Transfer*, **108**, 308–318.
- Findell, K. L., E. Shevliakova, P. C. D. Milly, and R. J. Stouffer, 2007: Modeled impact of anthropogenic land cover change on climate. *J. Clim.*, **20**, 3621–3634.
- Fioletov, V. E., G. E. Bodeker, A. J. Miller, R. D. McPeters, and R. Stolarski, 2002: Global and zonal total ozone variations estimated from ground-based and satellite measurements: 1964–2000. *J. Geophys. Res. Atmos.*, **107**, 4647.
- Fiore, A. M., et al., 2009: Multimodel estimates of intercontinental source-receptor relationships for ozone pollution. *J. Geophys. Res. Atmos.*, **114**, D04301.
- Fischer, E. M., J. Luterbacher, E. Zorita, S. F. B. Tett, C. Casty, and H. Wanner, 2007: European climate response to tropical volcanic eruptions over the last half millennium. *Geophys. Res. Lett.*, **34**, L05707.
- Fishman, J., et al., 2010: An investigation of widespread ozone damage to the soybean crop in the upper Midwest determined from ground-based and satellite measurements. *Atmos. Environ.*, **44**, 2248–2256.
- Flanner, M. G., C. S. Zender, J. T. Randerson, and P. J. Rasch, 2007: Present-day climate forcing and response from black carbon in snow. *J. Geophys. Res. Atmos.*, **112**, D11202.
- Fletcher, C. G., P. J. Kushner, A. Hall, and X. Qu, 2009: Circulation responses to snow albedo feedback in climate change. *Geophys. Res. Lett.*, **36**, L09702.
- Fomin, B. A., and V. A. Falaleeva, 2009: Recent progress in spectroscopy and its effect on line-by-line calculations for the validation of radiation codes for climate models. *Atmos. Oceanic Opt.*, **22**, 626–629.
- Forster, P., and K. Shine, 1997: Radiative forcing and temperature trends from stratospheric ozone changes. *J. Geophys. Res. Atmos.*, **102**, 10841–10855.
- Forster, P., et al., 2005: Resolution of the uncertainties in the radiative forcing of HFC-134a. *J. Quant. Spectrosc. Radiat. Transfer*, **93**, 447–460.
- Forster, P., et al., 2007: Changes in Atmospheric Constituents and in Radiative Forcing. In: *Climate Change 2007: The Physical Science Basis. Contribution of Working Group I to the Fourth Assessment Report of the Intergovernmental Panel on Climate Change* [Solomon, S., D. Qin, M. Manning, Z. Chen, M. Marquis, K. B. Averyt, M. Tignor and H. L. Miller (eds.)] Cambridge University Press, Cambridge, United Kingdom and New York, NY, USA, 129–234.
- Forster, P., et al., 2011a: Evaluation of radiation scheme performance within chemistry climate models. *J. Geophys. Res. Atmos.*, **116**, D10302.
- Forster, P. M., T. Andrews, P. Good, J. M. Gregory, L. S. Jackson, and M. Zelinka, 2013: Evaluating adjusted forcing and model spread for historical and future scenarios in the CMIP5 generation of climate models. *J. Geophys. Res. Atmos.*, **118**, 1139–1150.
- Forster, P. M., et al., 2011b: Stratospheric changes and climate. In: *Scientific Assessment of Ozone Depletion: 2010*. Global Ozone Research and Monitoring Project—Report No. 52, World Meteorological Organization, Geneva, Switzerland, 516 pp.
- Fortuin, J. P. F., and H. Kelder, 1998: An ozone climatology based on ozonesonde and satellite measurements. *J. Geophys. Res. Atmos.*, **103**, 31709–31734.
- Foukal, P., and J. Lean, 1988: Magnetic modulation of solar luminosity by photospheric activity. *Astrophys. J.*, **328**, 347–357.
- Fowler, D., et al., 2009: Atmospheric composition change: Ecosystems-atmosphere interactions. *Atmos. Environ.*, **43**, 5193–5267.
- Frame, T., and L. Gray, 2010: The 11-yr solar cycle in ERA-40 data: An update to 2008. *J. Clim.*, **23**, 2213–2222.
- Freckleton, R., E. Highwood, K. Shine, O. Wild, K. Law, and M. Sanderson, 1998: Greenhouse gas radiative forcing: Effects of averaging and inhomogeneities in trace gas distribution. *Q. J. R. Meteorol. Soc.*, **124**, 2099–2127.
- Friedlingstein, P., et al., 2006: Climate-carbon cycle feedback analysis: Results from the C(4)MIP model intercomparison. *J. Clim.*, **19**, 3337–3353.
- Frohlich, C., 2006: Solar irradiance variability since 1978—Revision of the PMOD composite during solar cycle 21. *Space Sci. Rev.*, **125**, 53–65.
- Frohlich, C., 2009: Evidence of a long-term trend in total solar irradiance. *Astron. Astrophys.*, **501**, L27–L30.
- Frolicher, T. L., F. Joos, and C. C. Raible, 2011: Sensitivity of atmospheric CO₂ and climate to explosive volcanic eruptions. *Biogeosciences*, **8**, 2317–2339.
- Fromm, M., G. Nedoluha, and Z. Charvat, 2013: Comment on “Large Volcanic Aerosol Load in the Stratosphere Linked to Asian Monsoon Transport”. *Science*, **339**, 647–c.
- Fry, M., et al., 2012: The influence of ozone precursor emissions from four world regions on tropospheric composition and radiative climate forcing. *J. Geophys. Res. Atmos.*, **117**, D07306.
- Fuglestedt, J., T. Berntsen, O. Godal, and T. Skodvin, 2000: Climate implications of GWP-based reductions in greenhouse gas emissions. *Geophys. Res. Lett.*, **27**, 409–412.
- Fuglestedt, J., T. Berntsen, O. Godal, R. Sausen, K. Shine, and T. Skodvin, 2003: Metrics of climate change: Assessing radiative forcing and emission indices. *Clim. Change*, **58**, 267–331.
- Fuglestedt, J. S., et al., 2010: Transport impacts on atmosphere and climate: Metrics. *Atmos. Environ.*, **44**, 4648–4677.
- Fung, I., J. John, J. Lerner, E. Matthews, M. Prather, L. P. Steele, and P. J. Fraser, 1991: 3-Dimensional model synthesis of the global methane cycle. *J. Geophys. Res. Atmos.*, **96**, 13033–13065.
- Gaillard, M. J., et al., 2010: Holocene land-cover reconstructions for studies on land cover-climate feedbacks. *Clim. Past*, **6**, 483–499.
- Gao, C. C., A. Robock, and C. Ammann, 2008: Volcanic forcing of climate over the past 1500 years: An improved ice core-based index for climate models. *J. Geophys. Res. Atmos.*, **113**, D23111.
- García, R. R., W. J. Randel, and D. E. Kinnison, 2011: On the determination of age of air trends from atmospheric trace species. *J. Atmos. Sci.*, **68**, 139–154.
- Gerlach, T., 2011: Volcanic versus anthropogenic carbon dioxide. *Eos*, **92**, 201–202.
- Gettelman, A., J. Holton, and K. Rosenlof, 1997: Mass fluxes of O₃, CH₄, N₂O and CF₂Cl₂ in the lower stratosphere calculated from observational data. *J. Geophys. Res. Atmos.*, **102**, 19149–19159.

- Gillett, N., and H. Matthews, 2010: Accounting for carbon cycle feedbacks in a comparison of the global warming effects of greenhouse gases. *Environ. Res. Lett.*, **5**, 034011.
- Ginoux, P., D. Garbuzov, and N. C. Hsu, 2010: Identification of anthropogenic and natural dust sources using Moderate Resolution Imaging Spectroradiometer (MODIS) Deep Blue level 2 data. *J. Geophys. Res. Atmos.*, **115**, D05204.
- Godal, O., and J. Fuglestedt, 2002: Testing 100-year global warming potentials: Impacts on compliance costs and abatement profile. *Clim. Change*, **52**, 93–127.
- Goosse, H., et al., 2006: The origin of the European “Medieval Warm Period”. *Clim. Past*, **2**, 99–113.
- Granier, C., et al., 2011: Evolution of anthropogenic and biomass burning emissions of air pollutants at global and regional scales during the 1980–2010 period. *Clim. Change*, **109**, 163–190.
- Gray, L., S. Rumbold, and K. Shine, 2009: Stratospheric temperature and radiative forcing response to 11-year solar cycle changes in irradiance and ozone. *J. Atmos. Sci.*, **66**, 2402–2417.
- Gray, L., et al., 2010: Solar influences on climate. *Rev. Geophys.*, **48**, RG4001.
- Gregory, J., and M. Webb, 2008: Tropospheric adjustment induces a cloud component in CO₂ forcing. *J. Clim.*, **21**, 58–71.
- Gregory, J., et al., 2004: A new method for diagnosing radiative forcing and climate sensitivity. *Geophys. Res. Lett.*, **31**, L03205.
- Gregory, J. M., 2010: Long-term effect of volcanic forcing on ocean heat content. *Geophys. Res. Lett.*, **37**, L22701.
- Grewe, V., 2007: Impact of climate variability on tropospheric ozone. *Sci. Tot. Environ.*, **374**, 167–181.
- Gusev, A. A., 2008: Temporal structure of the global sequence of volcanic eruptions: Order clustering and intermittent discharge rate. *Phys. Earth Planet. Inter.*, **166**, 203–218.
- Haigh, J., 1994: The role of stratospheric ozone in modulating the solar radiative forcing of climate. *Nature*, **370**, 544–546.
- Haigh, J., 1999: A GCM study of climate change in response to the 11-year solar cycle. *Q. J. R. Meteorol. Soc.*, **125**, 871–892.
- Haigh, J. D., 1996: The impact of solar variability on climate. *Science*, **272**, 981–984.
- Hall, J., and G. Lockwood, 2004: The chromospheric activity and variability of cycling and flat activity solar-analog stars. *Astrophys. J.*, **614**, 942–946.
- Hallquist, M., et al., 2009: The formation, properties and impact of secondary organic aerosol: Current and emerging issues. *Atmos. Chem. Phys.*, **9**, 5155–5236.
- Hammit, J., A. Jain, J. Adams, and D. Wuebbles, 1996: A welfare-based index for assessing environmental effects of greenhouse-gas emissions. *Nature*, **381**, 301–303.
- Hansen, J., and L. Nazarenko, 2004: Soot climate forcing via snow and ice albedos. *Proc. Natl. Acad. Sci. U.S.A.*, **101**, 423–428.
- Hansen, J., et al., 2005: Efficacy of climate forcings. *J. Geophys. Res. Atmos.*, **110**, D18104.
- Hansen, J., et al., 2007: Climate simulations for 1880–2003 with GISS modelE. *Clim. Dyn.*, **29**, 661–696.
- Harder, J., J. Fontenla, P. Pilewskie, E. Richard, and T. Woods, 2009: Trends in solar spectral irradiance variability in the visible and infrared. *Geophys. Res. Lett.*, **36**, L07801.
- Harrison, R., and M. Ambaum, 2010: Observing Forbush decreases in cloud at Shetland. *J. Atmos. Sol. Terres. Phys.*, **72**, 1408–1414.
- Haywood, J., and M. Schulz, 2007: Causes of the reduction in uncertainty in the anthropogenic radiative forcing of climate between IPCC (2001) and IPCC (2007). *Geophys. Res. Lett.*, **34**, L20701.
- Haywood, J. M., et al., 2010: Observations of the eruption of the Sarychev volcano and simulations using the HadGEM2 climate model. *J. Geophys. Res. Atmos.*, **115**, D21212.
- Heathfield, A., C. Anastasi, A. McCulloch, and F. Nicolaisen, 1998: Integrated infrared absorption coefficients of several partially fluorinated ether compounds: CF₃OCF₂H, CF₂HOOCF₂H, CH₃OCF₂CF₂H, CH₃OCF₂CFClH, CH₃CH₂OCF₂CF₂H, CF₃CH₂OCF₂CF₂H AND CH₂=CHCH₂OCF₂CF₂H. *Atmos. Environ.*, **32**, 2825–2833.
- Hegg, D. A., S. G. Warren, T. C. Grenfell, S. J. Doherty, T. V. Larson, and A. D. Clarke, 2009: Source attribution of black carbon in Arctic snow. *Environ. Sci. Technol.*, **43**, 4016–4021.
- Hegglin, M. I., and T. G. Shepherd, 2009: Large climate-induced changes in ultraviolet index and stratosphere-to-troposphere ozone flux. *Nature Geosci.*, **2**, 687–691.
- Helama, S., M. Fauria, K. Mielikainen, M. Timonen, and M. Eronen, 2010: Sub-Milankovitch solar forcing of past climates: Mid and late Holocene perspectives. *Geol. Soc. Am. Bull.*, **122**, 1981–1988.
- Henze, D. K., et al., 2012: Spatially refined aerosol direct radiative forcing efficiencies. *Environ. Sci. Technol.*, **46**, 9511–9518.
- Hohne, N., et al., 2011: Contributions of individual countries’ emissions to climate change and their uncertainty. *Clim. Change*, **106**, 359–391.
- Holmes, C., Q. Tang, and M. Prather, 2011: Uncertainties in climate assessment for the case of aviation NO. *Proc. Natl. Acad. Sci. U.S.A.*, **108**, 10997–11002.
- Holmes, C. D., M. J. Prather, O. A. Sovde, and G. Myhre, 2013: Future methane, hydroxyl, and their uncertainties: Key climate and emission parameters for future predictions. *Atmos. Chem. Phys.*, **13**, 285–302.
- Horowitz, L. W., 2006: Past, present, and future concentrations of tropospheric ozone and aerosols: Methodology, ozone evaluation, and sensitivity to aerosol wet removal. *J. Geophys. Res. Atmos.*, **111**, D22211.
- Houghton, J. T., G. J. Jenkins, and J. J. Ephraums (eds.), 1990: *Climate Change. The IPCC Scientific Assessment*. Cambridge University Press, Cambridge, United Kingdom and New York, NY, USA, 364 pp.
- Hoyle, C., et al., 2011: A review of the anthropogenic influence on biogenic secondary organic aerosol. *Atmos. Chem. Phys.*, **11**, 321–343.
- Hsu, J., and M. J. Prather, 2009: Stratospheric variability and tropospheric ozone. *J. Geophys. Res. Atmos.*, **114**, D06102.
- Huang, J., Q. Fu, W. Zhang, X. Wang, R. Zhang, H. Ye, and S. Warren, 2011: Dust and black carbon in seasonal snow across northern China. *Bull. Am. Meteorol. Soc.*, **92**, 175–181.
- Huijnen, V., et al., 2010: The global chemistry transport model TM5: Description and evaluation of the tropospheric chemistry version 3.0. *Geosci. Model Dev.*, **3**, 445–473.
- Hurst, D. F., et al., 2011: Stratospheric water vapor trends over Boulder, Colorado: Analysis of the 30 year Boulder record. *J. Geophys. Res. Atmos.*, **116**, D02306.
- Hurt, G. C., et al., 2006: The underpinnings of land-use history: Three centuries of global gridded land-use transitions, wood-harvest activity, and resulting secondary lands. *Global Change Biol.*, **12**, 1208–1229.
- Iacono, M. J., J. S. Delamere, E. J. Mlawer, M. W. Shephard, S. A. Clough, and W. D. Collins, 2008: Radiative forcing by long-lived greenhouse gases: Calculations with the AER radiative transfer models. *J. Geophys. Res. Atmos.*, **113**, D13103.
- Ineson, S., A. A. Scaife, J. R. Knight, J. C. Manners, N. J. Dunstone, L. J. Gray, and J. D. Haigh, 2011: Solar forcing of winter climate variability in the Northern Hemisphere. *Nature Geosci.*, **4**, 753–757.
- IPCC, 1996: *Revised 1996 IPCC Guidelines for National Greenhouse Gas Inventories*. Intergovernmental Panel of Climate Change.
- Isaksen, I., et al., 2009: Atmospheric composition change: Climate-chemistry interactions. *Atmos. Environ.*, **43**, 5138–5192.
- Ito, A., and J. E. Penner, 2005: Historical emissions of carbonaceous aerosols from biomass and fossil fuel burning for the period 1870–2000. *Global Biogeochem. Cycles*, **19**, Gb2028.
- Jackson, S., 2009: Parallel pursuit of near-term and long-term climate mitigation. *Science*, **326**, 526–527.
- Jacobson, M., 2010: Short-term effects of controlling fossil-fuel soot, biofuel soot and gases, and methane on climate, Arctic ice, and air pollution health. *J. Geophys. Res. Atmos.*, **115**, D14209.
- Jacobson, M., 2012: Investigating cloud absorption effects: Global absorption properties of black carbon, tar balls, and soil dust in clouds and aerosols. *J. Geophys. Res. Atmos.*, **117**, D06205.
- Javadi, M., O. Nielsen, T. Wallington, M. Hurley, and J. Owens, 2007: Atmospheric chemistry of 2-ethoxy-3,3,4,4,5-pentafluorotetra-hydro-2,5-bis[1,2,2,2-tetrafluoro-1-(trifluoromethyl)ethyl]-furan: Kinetics, mechanisms, and products of CL atom and OH radical initiated oxidation. *Environ. Sci. Technol.*, **41**, 7389–7395.
- Jin, M. L., R. E. Dickinson, and D. L. Zhang, 2005: The footprint of urban areas on global climate as characterized by MODIS. *J. Clim.*, **18**, 1551–1565.
- Jin, Y., and D. P. Roy, 2005: Fire-induced albedo change and its radiative forcing at the surface in northern Australia. *Geophys. Res. Lett.*, **32**, L13401.
- Jin, Y. F., J. T. Randerson, M. L. Goulden, and S. J. Goetz, 2012: Post-fire changes in net shortwave radiation along a latitudinal gradient in boreal North America. *Geophys. Res. Lett.*, **39**, L13403.
- Johansson, D., 2012: Economics- and physical-based metrics for comparing greenhouse gases. *Clim. Change*, **110**, 123–141.
- Johansson, D., U. Persson, and C. Azar, 2006: The cost of using global warming potentials: Analysing the trade off between CO₂, CH₄ and N₂O. *Clim. Change*, **77**, doi:10.1007/s10584-006-9054-1, 291–309.

- Jones, G., M. Lockwood, and P. Stott, 2012: What influence will future solar activity changes over the 21st century have on projected global near-surface temperature changes? *J. Geophys. Res. Atmos.*, **117**, D05103.
- Jones, G. S., J. M. Gregory, P. A. Stott, S. F. B. Tett, and R. B. Thorpe, 2005: An AOGCM simulation of the climate response to a volcanic super-eruption. *Clim. Dyn.*, **25**, 725–738.
- Joos, F., M. Bruno, R. Fink, U. Siegenthaler, T. Stocker, and C. LeQuere, 1996: An efficient and accurate representation of complex oceanic and biospheric models of anthropogenic carbon uptake. *Tellus B*, **48**, 397–417.
- Joos, F., et al., 2013: Carbon dioxide and climate impulse response functions for the computation of greenhouse gas metrics: A multi-model analysis. *Atmos. Chem. Phys.*, **13**, 2793–2825.
- Joshi, M., and J. Gregory, 2008: Dependence of the land-sea contrast in surface climate response on the nature of the forcing. *Geophys. Res. Lett.*, **35**, L24802.
- Joshi, M. M., and G. S. Jones, 2009: The climatic effects of the direct injection of water vapour into the stratosphere by large volcanic eruptions. *Atmos. Chem. Phys.*, **9**, 6109–6118.
- Kandlikar, M., 1995: The relative role of trace gas emissions in greenhouse abatement policies. *Energ. Policy*, **23**, 879–883.
- Kaplan, J. O., K. M. Krumhardt, E. C. Ellis, W. F. Ruddiman, C. Lemmen, and K. K. Goldewijk, 2011: Holocene carbon emissions as a result of anthropogenic land cover change. *Holocene*, **21**, 775–791.
- Kasischke, E. S., and J. E. Penner, 2004: Improving global estimates of atmospheric emissions from biomass burning. *J. Geophys. Res. Atmos.*, **109**, D14501.
- Kawase, H., T. Nagashima, K. Sudo, and T. Nozawa, 2011: Future changes in tropospheric ozone under Representative Concentration Pathways (RCPs). *Geophys. Res. Lett.*, **38**, L05801.
- Kawase, H., M. Abe, Y. Yamada, T. Takemura, T. Yokohata, and T. Nozawa, 2010: Physical mechanism of long-term drying trend over tropical North Africa. *Geophys. Res. Lett.*, **37**, L09706.
- Kirkby, J., 2007: Cosmic rays and climate. *Surv. Geophys.*, **28**, 333–375.
- Kirkby, J., et al., 2011: Role of sulphuric acid, ammonia and galactic cosmic rays in atmospheric aerosol nucleation. *Nature*, **476**, 429–433.
- Kleinman, L. I., P. H. Daum, Y. N. Lee, L. J. Nunnermacker, S. R. Springston, J. Weinstein-Lloyd, and J. Rudolph, 2001: Sensitivity of ozone production rate to ozone precursors. *Geophys. Res. Lett.*, **28**, 2903–2906.
- Knutti, R., et al., 2008: A review of uncertainties in global temperature projections over the twenty-first century. *J. Clim.*, **21**, 2651–2663.
- Koch, D., and A. D. Del Genio, 2010: Black carbon semi-direct effects on cloud cover: Review and synthesis. *Atmos. Chem. Phys.*, **10**, 7685–7696.
- Koch, D., T. Bond, D. Streets, N. Unger, and G. van der Werf, 2007: Global impacts of aerosols from particular source regions and sectors. *J. Geophys. Res. Atmos.*, **112**, D02205.
- Koch, D., S. Menon, A. Del Genio, R. Ruedy, I. Alienov, and G. A. Schmidt, 2009a: Distinguishing aerosol impacts on climate over the past century. *J. Clim.*, **22**, 2659–2677.
- Koch, D., et al., 2011: Coupled aerosol-chemistry-climate twentieth-century transient model investigation: Trends in short-lived species and climate responses. *J. Clim.*, **24**, 2693–2714.
- Koch, D., et al., 2009b: Evaluation of black carbon estimations in global aerosol models. *Atmos. Chem. Phys.*, **9**, 9001–9026.
- Koehler, M. O., G. Raedel, K. P. Shine, H. L. Rogers, and J. A. Pyle, 2013: Latitudinal variation of the effect of aviation NO_x emissions on atmospheric ozone and methane and related climate metrics. *Atmos. Environ.*, **64**, 1–9.
- Koffi, B., et al., 2012: Application of the CALIOP layer product to evaluate the vertical distribution of aerosols estimated by global models: AeroCom phase I results. *J. Geophys. Res. Atmos.*, **117**, D10201.
- Kopp, G., and J. Lean, 2011: A new, lower value of total solar irradiance: Evidence and climate significance. *Geophys. Res. Lett.*, **38**, L01706.
- Kratz, D., 2008: The sensitivity of radiative transfer calculations to the changes in the HITRAN database from 1982 to 2004. *J. Quant. Spectrosc. Radiat. Transfer*, **109**, 1060–1080.
- Kravitz, B., and A. Robock, 2011: Climate effects of high-latitude volcanic eruptions: Role of the time of year. *J. Geophys. Res. Atmos.*, **116**, D01105.
- Kravitz, B., A. Robock, and A. Bourassa, 2010: Negligible climatic effects from the 2008 Okmok and Kasatochi volcanic eruptions. *J. Geophys. Res. Atmos.*, **115**, D00L05.
- Kravitz, B., et al., 2011: Simulation and observations of stratospheric aerosols from the 2009 Sarychev volcanic eruption. *J. Geophys. Res. Atmos.*, **116**, D18211.
- Kristjansson, J. E., T. Iversen, A. Kirkevåg, O. Seland, and J. Debernard, 2005: Response of the climate system to aerosol direct and indirect forcing: Role of cloud feedbacks. *J. Geophys. Res. Atmos.*, **110**, D24206.
- Krivova, N., L. Vieira, and S. Solanki, 2010: Reconstruction of solar spectral irradiance since the Maunder minimum. *J. Geophys. Res. Space Phys.*, **115**, A12112.
- Kueppers, L. M., M. A. Snyder, and L. C. Sloan, 2007: Irrigation cooling effect: Regional climate forcing by land-use change. *Geophys. Res. Lett.*, **34**, L03703.
- Kuroda, Y., and K. Kodera, 2005: Solar cycle modulation of the southern annular mode. *Geophys. Res. Lett.*, **32**, L13802.
- Kvalevåg, M. M., G. Myhre, G. Bonan, and S. Levis, 2010: Anthropogenic land cover changes in a GCM with surface albedo changes based on MODIS data. *Int. J. Climatol.*, **30**, 2105–2117.
- Lacis, A. A., D. J. Wuebbles, J. A. Logan, 1990: Radiative forcing of climate by changes in the vertical-distribution of ozone, *J. Geophys. Res.*, **95**, 9971–9981.
- Lamarque, J., et al., 2011: Global and regional evolution of short-lived radiatively-active gases and aerosols in the Representative Concentration Pathways. *Clim. Change*, **109**, 191–212.
- Lamarque, J., et al., 2010: Historical (1850–2000) gridded anthropogenic and biomass burning emissions of reactive gases and aerosols: Methodology and application. *Atmos. Chem. Phys.*, **10**, 7017–7039.
- Lamarque, J. F., et al., 2013: The Atmospheric Chemistry and Climate Model Intercomparison Project (ACCMIP): Overview and description of models, simulations and climate diagnostics. *Geosci. Model Dev.*, **6**, 179–206.
- Lau, K. M., M. K. Kim, and K. M. Kim, 2006: Asian summer monsoon anomalies induced by aerosol direct forcing: The role of the Tibetan Plateau. *Clim. Dyn.*, **26**, 855–864.
- Lauder, A. R., I. G. Enting, J. O. Carter, N. Clisby, A. L. Cowie, B. K. Henry, and M. R. Raupach, 2013: Offsetting methane emissions—An alternative to emission equivalence metrics. *Int. J. Greenh. Gas Control*, **12**, 419–429.
- Lauer, A., V. Eyring, J. Hendricks, P. Jockel, and U. Lohmann, 2007: Global model simulations of the impact of ocean-going ships on aerosols, clouds, and the radiation budget. *Atmos. Chem. Phys.*, **7**, 5061–5079.
- Lawrence, P. J., and T. N. Chase, 2010: Investigating the climate impacts of global land cover change in the community climate system model. *Int. J. Climatol.*, **30**, 2066–2087.
- Lean, J., 2000: Evolution of the sun's spectral irradiance since the Maunder Minimum. *Geophys. Res. Lett.*, **27**, 2425–2428.
- Lean, J., and M. Deland, 2012: How does the sun's spectrum vary? *J. Clim.*, **25**, 2555–2560.
- Lee, D. S., et al., 2010: Transport impacts on atmosphere and climate: Aviation. *Atmos. Environ.*, **44**, 4678–4734.
- Lee, J., D. Shindell, and S. Hameed, 2009: The influence of solar forcing on tropical circulation. *J. Clim.*, **22**, 5870–5885.
- Lee, R., M. Gibson, R. Wilson, and S. Thomas, 1995: Long-term total solar irradiance variability during sunspot cycle-22. *J. Geophys. Res. Space Phys.*, **100**, 1667–1675.
- Lee, X., et al., 2011: Observed increase in local cooling effect of deforestation at higher latitudes. *Nature*, **479**, 384–387.
- Lee, Y. H., et al., 2013: Evaluation of preindustrial to present-day black carbon and its albedo forcing from Atmospheric Chemistry and Climate Model Intercomparison Project (ACCMIP). *Atmos. Chem. Phys.*, **13**, 2607–2634.
- Legras, B., O. Mestre, E. Bard, and P. Yiou, 2010: A critical look at solar-climate relationships from long temperature series. *Clim. Past*, **6**, 745–758.
- Leibensperger, E. M., L. J. Mickley, and D. J. Jacob, 2008: Sensitivity of US air quality to mid-latitude cyclone frequency and implications of 1980–2006 climate change. *Atmos. Chem. Phys.*, **8**, 7075–7086.
- Leibensperger, E. M., et al., 2012a: Climatic effects of 1950–2050 changes in US anthropogenic aerosols—Part 1: Aerosol trends and radiative forcing. *Atmos. Chem. Phys.*, **12**, 3333–3348.
- Leibensperger, E. M., et al., 2012b: Climatic effects of 1950–2050 changes in US anthropogenic aerosols—Part 2: Climate response. *Atmos. Chem. Phys.*, **12**, 3349–3362.
- Lelieveld, J., et al., 2008: Atmospheric oxidation capacity sustained by a tropical forest. *Nature*, **452**, 737–740.
- Levy, H., 1971: Normal atmosphere—Large radical and formaldehyde concentrations predicted. *Science*, **173**, 141–143.
- Liao, H., W. T. Chen, and J. H. Seinfeld, 2006: Role of climate change in global predictions of future tropospheric ozone and aerosols. *J. Geophys. Res. Atmos.*, **111**, D12304.

- Lockwood, M., 2010: Solar change and climate: An update in the light of the current exceptional solar minimum. *Proc. R. Soc. London A*, **466**, 303–329.
- Lockwood, M., and C. Frohlich, 2008: Recent oppositely directed trends in solar climate forcings and the global mean surface air temperature. II. Different reconstructions of the total solar irradiance variation and dependence on response time scale. *Proc. R. Soc. London A*, **464**, 1367–1385.
- Lockwood, M., A. Rouillard, and I. Finch, 2009: The rise and fall of open solar flux during the current grand solar maximum. *Astrophys. J.*, **700**, 937–944.
- Logan, J. A., 1999: An analysis of ozonesonde data for the troposphere: Recommendations for testing 3-D models and development of a gridded climatology for tropospheric ozone. *J. Geophys. Res. Atmos.*, **104**, 16115–16149.
- Logan, J. A., M. J. Prather, S. C. Wofsy, and M. B. McElroy, 1981: Tropospheric chemistry—A global perspective. *J. Geophys. Res. Oceans Atmos.*, **86**, 7210–7254.
- Logan, J. A., et al., 2012: Changes in ozone over Europe: Analysis of ozone measurements from sondes, regular aircraft (MOZAIC) and alpine surface sites. *J. Geophys. Res. Atmos.*, **117**, D09301.
- Lohila, A., et al., 2010: Forestation of boreal peatlands: Impacts of changing albedo and greenhouse gas fluxes on radiative forcing. *J. Geophys. Res. Biogeosci.*, **115**, G04011.
- Lohmann, U., et al., 2010: Total aerosol effect: Radiative forcing or radiative flux perturbation? *Atmos. Chem. Phys.*, **10**, 3235–3246.
- Long, C. N., E. G. Dutton, J. A. Augustine, W. Wiscombe, M. Wild, S. A. McFarlane, and C. J. Flynn, 2009: Significant decadal brightening of downwelling shortwave in the continental United States. *J. Geophys. Res. Atmos.*, **114**, D00D06.
- Long, D., and M. Collins, 2013: Quantifying global climate feedbacks, responses and forcing under abrupt and gradual CO₂ forcing. *Clim. Dyn.*, **41**, 2471–2479.
- Lu, P., H. Zhang, and X. Jing, 2012: The effects of different HITRAN versions on calculated long-wave radiation and uncertainty evaluation. *Acta Meteorol. Sin.*, **26**, 389–398.
- Lu, Z., Q. Zhang, and D. G. Streets, 2011: Sulfur dioxide and primary carbonaceous aerosol emissions in China and India, 1996–2010. *Atmos. Chem. Phys.*, **11**, 9839–9864.
- Lund, M., T. Berntsen, J. Fuglestedt, M. Ponater, and K. Shine, 2012: How much information is lost by using global-mean climate metrics? an example using the transport sector. *Clim. Change*, **113**, 949–963.
- MacFarling Meure, C., et al., 2006: Law Dome CO₂, CH₄ and N₂O ice core records extended to 2000 years BP. *Geophys. Res. Lett.*, **33**, L14810.
- MacMynowski, D., H. Shin, and K. Caldeira, 2011: The frequency response of temperature and precipitation in a climate model. *Geophys. Res. Lett.*, **38**, L16711.
- Mader, J. A., J. Staehelin, T. Peter, D. Brunner, H. E. Rieder, and W. A. Stahel, 2010: Evidence for the effectiveness of the Montreal Protocol to protect the ozone layer. *Atmos. Chem. Phys.*, **10**, 12161–12171.
- Mahowald, N. M., et al., 2010: Observed 20th century desert dust variability: Impact on climate and biogeochemistry. *Atmos. Chem. Phys.*, **10**, 10875–10893.
- Mann, M., M. Cane, S. Zebiak, and A. Clement, 2005: Volcanic and solar forcing of the tropical Pacific over the past 1000 years. *J. Clim.*, **18**, 447–456.
- Manne, A., and R. Richels, 2001: An alternative approach to establishing trade-offs among greenhouse gases. *Nature*, **410**, 675–677.
- Manning, M., and A. Reisinger, 2011: Broader perspectives for comparing different greenhouse gases. *Philos. Trans. R. Soc. London A*, **369**, 1891–1905.
- Marenco, A., H. Gouget, P. Nedelec, J. P. Pages, and F. Karcher, 1994: Evidence of a long-term increase in tropospheric ozone from PIC Du Midi Data Series—Consequences—Positive radiative forcing. *J. Geophys. Res. Atmos.*, **99**, 16617–16632.
- Marten, A. L., and S. C. Newbold, 2012: Estimating the social cost of non-CO₂ GHG emissions: Methane and nitrous oxide. *Energ. Policy*, **51**, 957–972.
- Matthews, H. D., A. J. Weaver, K. J. Meissner, N. P. Gillett, and M. Eby, 2004: Natural and anthropogenic climate change: Incorporating historical land cover change, vegetation dynamics and the global carbon cycle. *Clim. Dyn.*, **22**, 461–479.
- McComas, D., R. Ebert, H. Elliott, B. Goldstein, J. Gosling, N. Schwadron, and R. Skoug, 2008: Weaker solar wind from the polar coronal holes and the whole Sun. *Geophys. Res. Lett.*, **35**, L18103.
- McLandress, C., T. G. Shepherd, J. F. Scinocca, D. A. Plummer, M. Sigmond, A. I. Jonsson, and M. C. Reader, 2011: Separating the dynamical effects of climate change and ozone depletion. Part II. Southern Hemisphere troposphere. *J. Clim.*, **24**, 1850–1868.
- Meinshausen, M., T. Wigley, and S. Raper, 2011a: Emulating atmosphere-ocean and carbon cycle models with a simpler model, MAGICC6—Part 2: Applications. *Atmos. Chem. Phys.*, **11**, 1457–1471.
- Meinshausen, M., et al., 2011b: The RCP greenhouse gas concentrations and their extensions from 1765 to 2300. *Clim. Change*, **109**, 213–241.
- Mercado, L. M., N. Bellouin, S. Sitoh, O. Boucher, C. Huntingford, M. Wild, and P. M. Cox, 2009: Impact of changes in diffuse radiation on the global land carbon sink. *Nature*, **458**, 1014–1017.
- Merikanto, J., D. Spracklen, G. Mann, S. Pickering, and K. Carslaw, 2009: Impact of nucleation on global CCN. *Atmos. Chem. Phys.*, **9**, 8601–8616.
- Mickley, L. J., E. M. Leibensperger, D. J. Jacob, and D. Rind, 2012: Regional warming from aerosol removal over the United States: Results from a transient 2010–2050 climate simulation. *Atmos. Environ.*, **46**, 545–553.
- Miller, G. H., et al., 2012: Abrupt onset of the Little Ice Age triggered by volcanism and sustained by sea-ice/ocean feedbacks. *Geophys. Res. Lett.*, **39**, L02708.
- Miller, R. L., I. Tegen, and J. Perlwitz, 2004: Surface radiative forcing by soil dust aerosols and the hydrologic cycle. *J. Geophys. Res. Atmos.*, **109**, D04203.
- Mills, M. J., O. B. Toon, R. P. Turco, D. E. Kinnison, and R. R. Garcia, 2008: Massive global ozone loss predicted following regional nuclear conflict. *Proc. Natl. Acad. Sci. U.S.A.*, **105**, 5307–5312.
- Ming, Y., and V. Ramaswamy, 2012: Nonlocal component of radiative flux perturbation. *Geophys. Res. Lett.*, **39**, L22706.
- Ming, Y., V. Ramaswamy, and G. Persad, 2010: Two opposing effects of absorbing aerosols on global-mean precipitation. *Geophys. Res. Lett.*, **37**, L13701.
- Ming, Y., V. Ramaswamy, and G. Chen, 2011: A model investigation of aerosol-induced changes in boreal winter extratropical circulation. *J. Clim.*, **24**, 6077–6091.
- Ming, Y., V. Ramaswamy, L. J. Donner, V. T. J. Phillips, S. A. Klein, P. A. Ginoux, and L. W. Horowitz, 2007: Modeling the interactions between aerosols and liquid water clouds with a self-consistent cloud scheme in a general circulation model. *J. Atmos. Sci.*, **64**, 1189–1209.
- Mirme, S., A. Mirme, A. Minikin, A. Petzold, U. Horrak, V.-M. Kerminen, and M. Kulmala, 2010: Atmospheric sub-3 nm particles at high altitudes. *Atm. Chem. Phys.*, **10**, 437–451.
- Montzka, S. A., E. J. Dlugokencky, and J. H. Butler, 2011: Non-CO₂ greenhouse gases and climate change. *Nature*, **476**, 43–50.
- Morrill, J., L. Floyd, and D. McMullin, 2011: The solar ultraviolet spectrum estimated using the Mg II Index and Ca II K disk activity. *Solar Physics*, **269**, 253–267.
- Muhle, J., et al., 2009: Sulfuryl fluoride in the global atmosphere. *J. Geophys. Res. Atmos.*, **114**, D05306.
- Mulitza, S., et al., 2010: Increase in African dust flux at the onset of commercial agriculture in the Sahel region. *Nature*, **466**, 226–228.
- Murphy, D., and D. Fahey, 1994: An estimate of the flux of stratospheric reactive nitrogen and ozone into the troposphere. *J. Geophys. Res. Atmos.*, **99**, 5325–5332.
- Myhre, G., M. M. Kvalevåg, and C. B. Schaaf, 2005a: Radiative forcing due to anthropogenic vegetation change based on MODIS surface albedo data. *Geophys. Res. Lett.*, **32**, L21410.
- Myhre, G., E. J. Highwood, K. P. Shine, and F. Stordal, 1998: New estimates of radiative forcing due to well mixed greenhouse gases. *Geophys. Res. Lett.*, **25**, 2715–2718.
- Myhre, G., Y. Govaerts, J. M. Haywood, T. K. Berntsen, and A. Lattanzio, 2005b: Radiative effect of surface albedo change from biomass burning. *Geophys. Res. Lett.*, **32**, L20812.
- Myhre, G., J. Nilsen, L. Gulstad, K. Shine, B. Rognerud, and I. Isaksen, 2007: Radiative forcing due to stratospheric water vapour from CH₄ oxidation. *Geophys. Res. Lett.*, **34**, L01807.
- Myhre, G., et al., 2011: Radiative forcing due to changes in ozone and methane caused by the transport sector. *Atmos. Environ.*, **45**, 387–394.
- Myhre, G., et al., 2013: Radiative forcing of the direct aerosol effect from AeroCom Phase II simulations. *Atmos. Chem. Phys.*, **13**, 1853–1877.
- Nagai, T., B. Liley, T. Sakai, T. Shibata, and O. Uchino, 2010: Post-Pinatubo evolution and subsequent trend of the stratospheric aerosol layer observed by mid-latitude lidars in both hemispheres. *Sola*, **6**, 69–72.
- Naik, V., D. L. Mauzerall, L. W. Horowitz, M. D. Schwarzkopf, V. Ramaswamy, and M. Oppenheimer, 2007: On the sensitivity of radiative forcing from biomass burning aerosols and ozone to emission location. *Geophys. Res. Lett.*, **34**, L03818.

- Nair, U. S., D. K. Ray, J. Wang, S. A. Christopher, T. J. Lyons, R. M. Welch, and R. A. Pielke, 2007: Observational estimates of radiative forcing due to land use change in southwest Australia. *J. Geophys. Res. Atmos.*, **112**, D09117.
- Neely, R. R., et al., 2013: Recent anthropogenic increases in SO₂ from Asia have minimal impact on stratospheric aerosol. *Geophys. Res. Lett.*, **40**, 999–1004.
- O'ishi, R., A. Abe-Ouchi, I. Prentice, and S. Sitch, 2009: Vegetation dynamics and plant CO₂ responses as positive feedbacks in a greenhouse world. *Geophys. Res. Lett.*, **36**, L11706.
- O'Neill, B., 2000: The jury is still out on global warming potentials. *Clim. Change*, **44**, 427–443.
- O'Neill, B., 2003: Economics, natural science, and the costs of global warming potentials—An editorial comment. *Clim. Change*, **58**, 251–260.
- Oleson, K. W., G. B. Bonan, and J. Feddema, 2010: Effects of white roofs on urban temperature in a global climate model. *Geophys. Res. Lett.*, **37**, L03701.
- Olivié, D. J. L., G. Peters, and D. Saint-Martin, 2012: Atmosphere response time scales estimated from AOGCM experiments. *J. Climate*, **25**, 7956–7972.
- Olsen, S. C., C. A. McLinden, and M. J. Prather, 2001: Stratospheric N₂O–NO_y system: Testing uncertainties in a three-dimensional framework. *J. Geophys. Res.*, **106**, 28771.
- Oreopoulos, L., et al., 2012: The Continual Intercomparison of Radiation Codes: Results from Phase I. *J. Geophys. Res. Atmos.*, **117**, D06118.
- Osterman, G. B., et al., 2008: Validation of Tropospheric Emission Spectrometer (TES) measurements of the total, stratospheric, and tropospheric column abundance of ozone. *J. Geophys. Res. Atmos.*, **113**, D15516.
- Otterå, O. H., M. Bentsen, H. Drange, and L. L. Suo, 2010: External forcing as a metronome for Atlantic multidecadal variability. *Nature Geosci.*, **3**, 688–694.
- Özdoğan, M., A. Robock, and C. J. Kucharik, 2013: Impacts of a nuclear war in South Asia on soybean and maize production in the Midwest United States. *Clim. Change*, **116**, 373–387.
- Parrish, D. D., D. B. Millet, and A. H. Goldstein, 2009: Increasing ozone in marine boundary layer inflow at the west coasts of North America and Europe. *Atmos. Chem. Phys.*, **9**, 1303–1323.
- Paulot, F., J. D. Crouse, H. G. Kjaergaard, A. Kurten, J. M. St. Clair, J. H. Seinfeld, and P. O. Wennberg, 2009: Unexpected epoxide formation in the gas-phase photooxidation of isoprene. *Science*, **325**, 730–733.
- Paynter, D., and V. Ramaswamy, 2011: An assessment of recent water vapor continuum measurements upon longwave and shortwave radiative transfer. *J. Geophys. Res. Atmos.*, **116**, D20302.
- Pechony, O., and D. Shindell, 2010: Driving forces of global wildfires over the past millennium and the forthcoming century. *Proc. Natl. Acad. Sci. U.S.A.*, **107**, 19167–19170.
- Peeters, J., T. L. Nguyen, and L. Vereecken, 2009: HO(x) radical regeneration in the oxidation of isoprene. *Phys. Chem. Chem. Phys.*, **11**, 5935–5939.
- Penn, M., and W. Livingston, 2006: Temporal changes in sunspot umbral magnetic fields and temperatures. *Astrophys. J.*, **649**, L45–L48.
- Penner, J., L. Xu, and M. Wang, 2011: Satellite methods underestimate indirect climate forcing by aerosols. *Proc. Natl. Acad. Sci. U.S.A.*, **108**, 13404–13408.
- Penner, J., et al., 2006: Model intercomparison of indirect aerosol effects. *Atmos. Chem. Phys.*, **6**, 3391–3405.
- Perlwitz, J., and R. L. Miller, 2010: Cloud cover increase with increasing aerosol absorptivity: A counterexample to the conventional semidirect aerosol effect. *J. Geophys. Res. Atmos.*, **115**, D08203.
- Persad, G. G., Y. Ming, and V. Ramaswamy, 2012: Tropical tropospheric-only responses to absorbing aerosols. *J. Clim.*, **25**, 2471–2480.
- Peters, G., B. Aamaas, T. Berntsen, and J. Fuglestedt, 2011a: The integrated global temperature change potential (iGTP) and relationships between emission metrics. *Environ. Res. Lett.*, **6**, 044021.
- Peters, G. P., B. Aamaas, M. T. Lund, C. Solli, and J. S. Fuglestedt, 2011b: Alternative “Global Warming” metrics in life cycle assessment: A case study with existing transportation data. *Environ. Sci. Technol.*, **45**, 8633–8641.
- Peters, K., P. Stier, J. Quaas, and H. Grassl, 2012: Aerosol indirect effects from shipping emissions: Sensitivity studies with the global aerosol-climate model ECHAM-HAM. *Atmos. Chem. Phys.*, **12**, 5985–6007.
- Philipona, R., K. Behrens, and C. Ruckstuhl, 2009: How declining aerosols and rising greenhouse gases forced rapid warming in Europe since the 1980s. *Geophys. Res. Lett.*, **36**, L02806.
- Pinto, J. P., R. P. Turco, and O. B. Toon, 1989: Self-limiting physical and chemical effects in volcanic-eruption clouds. *J. Geophys. Res. Atmos.*, **94**, 11165–11174.
- Pitman, A. J., et al., 2009: Uncertainties in climate responses to past land cover change: First results from the LUCID intercomparison study. *Geophys. Res. Lett.*, **36**, L14814.
- Plattner, G.-K., T. Stocker, P. Midgley, and M. Tignor, 2009: IPCC Expert Meeting on the Science of Alternative Metrics: Meeting Report. IPCC Working Group I, Technical Support Unit.
- Plattner, G. K., et al., 2008: Long-term climate commitments projected with climate-carbon cycle models. *J. Clim.*, **21**, 2721–2751.
- Pongratz, J., C. Reick, T. Raddatz, and M. Claussen, 2008: A reconstruction of global agricultural areas and land cover for the last millennium. *Global Biogeochem. Cycles*, **22**, Gb3018.
- Pongratz, J., C. H. Reick, T. Raddatz, and M. Claussen, 2010: Biogeophysical versus biogeochemical climate response to historical anthropogenic land cover change. *Geophys. Res. Lett.*, **37**, L08702.
- Pongratz, J., T. Raddatz, C. H. Reick, M. Esch, and M. Claussen, 2009: Radiative forcing from anthropogenic land cover change since AD 800. *Geophys. Res. Lett.*, **36**, L02709.
- Pozzer, A., et al., 2012: Effects of business-as-usual anthropogenic emissions on air quality. *Atmos. Chem. Phys.*, **12**, 6915–6937.
- Prather, M., 2002: Lifetimes of atmospheric species: Integrating environmental impacts. *Geophys. Res. Lett.*, **29**, 2063.
- Prather, M., and J. Hsu, 2010: Coupling of nitrous oxide and methane by global atmospheric chemistry. *Science*, **330**, 952–954.
- Prather, M. J., 1998: Time scales in atmospheric chemistry: Coupled perturbations to N₂O, NO_y, and O₃. *Science*, **279**, 1339–1341.
- Prather, M. J., C. D. Holmes, and J. Hsu, 2012: Reactive greenhouse gas scenarios: Systematic exploration of uncertainties and the role of atmospheric chemistry. *Geophys. Res. Lett.*, **39**, L09803.
- Puma, M. J., and B. I. Cook, 2010: Effects of irrigation on global climate during the 20th century. *J. Geophys. Res. Atmos.*, **115**, D16120.
- Quaas, J., O. Boucher, N. Bellouin, and S. Kinne, 2011: Which of satellite- or model-based estimates is closer to reality for aerosol indirect forcing? *Proc. Natl. Acad. Sci. U.S.A.*, **108**, E1099.
- Quaas, J., et al., 2009: Aerosol indirect effects—general circulation model intercomparison and evaluation with satellite data. *Atmos. Chem. Phys.*, **9**, 8697–8717.
- Rajakumar, B., R. Portmann, J. Burkholder, and A. Ravishankara, 2006: Rate coefficients for the reactions of OH with CF₃CH₂CH₃ (HFC-263fb), CF₃CHFCH₂F (HFC-245eb), and CHF₂CHFCH₂F (HFC-245ea) between 238 and 375 K. *J. Phys. Chem. A*, **110**, 6724–6731.
- Ramanathan, V., and G. Carmichael, 2008: Global and regional climate changes due to black carbon. *Nature Geosci.*, **1**, 221–227.
- Ramanathan, V., et al., 2005: Atmospheric brown clouds: Impacts on South Asian climate and hydrological cycle. *Proc. Natl. Acad. Sci. U.S.A.*, **102**, 5326–5333.
- Ramaswamy, V., et al., 2001: Radiative forcing of climate change. In: *Climate Change 2001: The Scientific Basis. Contribution of Working Group I to the Third Assessment Report of the Intergovernmental Panel on Climate Change* [J. T. Houghton, Y. Ding, D. J. Griggs, M. Noguer, P. J. van der Linden, X. Dai, K. Maskell and C. A. Johnson (eds.)]. Cambridge University Press, Cambridge, United Kingdom and New York, NY, USA, 349–416.
- Randel, W., and F. Wu, 2007: A stratospheric ozone profile data set for 1979–2005: Variability, trends, and comparisons with column ozone data. *J. Geophys. Res. Atmos.*, **112**, D06313.
- Randles, C. A., and V. Ramaswamy, 2008: Absorbing aerosols over Asia: A Geophysical Fluid Dynamics Laboratory general circulation model sensitivity study of model response to aerosol optical depth and aerosol absorption. *J. Geophys. Res. Atmos.*, **113**, D21203.
- Rasch, P. J., et al., 2008: An overview of geoengineering of climate using stratospheric sulphate aerosols. *Philos. Trans. R. Soc. A*, **366**, 4007–4037.
- Ravishankara, A. R., J. S. Daniel, and R. W. Portmann, 2009: Nitrous oxide (N₂O): The dominant ozone-depleting substance emitted in the 21st century. *Science*, **326**, 123–125.
- Rechid, D., T. Raddatz, and D. Jacob, 2009: Parameterization of snow-free land surface albedo as a function of vegetation phenology based on MODIS data and applied in climate modelling. *Theor. Appl. Climatol.*, **95**, 245–255.
- Reddy, M., and O. Boucher, 2007: Climate impact of black carbon emitted from energy consumption in the world's regions. *Geophys. Res. Lett.*, **34**, L11802.
- Reilly, J., et al., 1999: Multi-gas assessment of the Kyoto Protocol. *Nature*, **401**, 549–555.

- Reilly, J. M., and K. R. Richards, 1993: Climate-change damage and the trace-gas-index issue. *Environ. Resour. Econ.*, **3**, 41–61.
- Reisinger, A., M. Meinshausen, and M. Manning, 2011: Future changes in global warming potentials under representative concentration pathways. *Environ. Res. Lett.*, **6**, 024020.
- Reisinger, A., M. Meinshausen, M. Manning, and G. Bodeker, 2010: Uncertainties of global warming metrics: CO₂ and CH₄. *Geophys. Res. Lett.*, **37**, L14707.
- Reisinger, A., P. Havlik, K. Riahi, O. Vliet, M. Obersteiner, and M. Herrero, 2013: Implications of alternative metrics for global mitigation costs and greenhouse gas emissions from agriculture. *Clim. Change*, **117**, 677–690.
- Righi, M., C. Klinger, V. Eyring, J. Hendricks, A. Lauer, and A. Petzold, 2011: Climate impact of biofuels in shipping: global model studies of the aerosol indirect effect. *Environ. Sci. Technol.*, **45**, 3519–3525.
- Rigozo, N., E. Echer, L. Vieira, and D. Nordemann, 2001: Reconstruction of Wolf sunspot numbers on the basis of spectral characteristics and estimates of associated radio flux and solar wind parameters for the last millennium. *Sol. Phys.*, **203**, 179–191.
- Rigozo, N., D. Nordemann, E. Echer, M. Echer, and H. Silva, 2010: Prediction of solar minimum and maximum epochs on the basis of spectral characteristics for the next millennium. *Planet. Space Sci.*, **58**, 1971–1976.
- Robock, A., 2000: Volcanic eruptions and climate. *Rev. Geophys.*, **38**, 191–219.
- Robock, A., 2010: New START, Eyjafjallajökull, and Nuclear Winter. *Eos*, **91**, 444–445.
- Robock, A., L. Oman, and G. L. Stenchikov, 2007a: Nuclear winter revisited with a modern climate model and current nuclear arsenals: Still catastrophic consequences. *J. Geophys. Res. Atmos.*, **112**, D13107.
- Robock, A., L. Oman, and G. L. Stenchikov, 2008: Regional climate responses to geoengineering with tropical and Arctic SO₂ injections. *J. Geophys. Res. Atmos.*, **113**, D16101.
- Robock, A., L. Oman, G. L. Stenchikov, O. B. Toon, C. Bardeen, and R. P. Turco, 2007b: Climatic consequences of regional nuclear conflicts. *Atmos. Chem. Phys.*, **7**, 2003–2012.
- Robock, A., C. M. Ammann, L. Oman, D. Shindell, S. Levis, and G. Stenchikov, 2009: Did the Toba volcanic eruption of similar to 74 ka BP produce widespread glaciation? *J. Geophys. Res. Atmos.*, **114**, D10107.
- Rogelj, J., et al., 2011: Emission pathways consistent with a 2 degrees C global temperature limit. *Nature Clim. Change*, **1**, 413–418.
- Roscoe, H. K., and J. D. Haigh, 2007: Influences of ozone depletion, the solar cycle and the QBO on the Southern Annular Mode. *Q. J. R. Meteorol. Soc.*, **133**, 1855–1864.
- Rotenberg, E., and D. Yakir, 2010: Contribution of semi-arid forests to the climate system. *Science*, **327**, 451–454.
- Rothman, L., 2010: The evolution and impact of the HITRAN molecular spectroscopic database. *J. Quant. Spectrosc. Radiat. Transfer*, **111**, 1565–1567.
- Rotstajn, L., and J. Penner, 2001: Indirect aerosol forcing, quasi forcing, and climate response. *J. Clim.*, **14**, 2960–2975.
- Rotstajn, L. D., and U. Lohmann, 2002: Tropical rainfall trends and the indirect aerosol effect. *J. Clim.*, **15**, 2103–2116.
- Rotstajn, L. D., B. F. Ryan, and J. E. Penner, 2000: Precipitation changes in a GCM resulting from the indirect effects of anthropogenic aerosols. *Geophys. Res. Lett.*, **27**, 3045–3048.
- Rottman, G., 2006: Measurement of total and spectral solar irradiance. *Space Sci. Rev.*, **125**, 39–51.
- Ruckstuhl, C., et al., 2008: Aerosol and cloud effects on solar brightening and the recent rapid warming. *Geophys. Res. Lett.*, **35**, L12708.
- Russell, C., J. Luhmann, and L. Jian, 2010: How unprecedented a solar minimum? *Rev. Geophys.*, **48**, RG2004.
- Rypdal, K., N. Rive, T. Berntsen, Z. Klimont, T. Mideksa, G. Myhre, and R. Skeie, 2009: Costs and global impacts of black carbon abatement strategies. *Tellus B.*, **61**, 625–641.
- Rypdal, K., et al., 2005: Tropospheric ozone and aerosols in climate agreements: Scientific and political challenges. *Environ. Sci. Policy*, **8**, 29–43.
- Salby, M. L., E. A. Titova, and L. Deschamps, 2012: Changes of the Antarctic ozone hole: Controlling mechanisms, seasonal predictability, and evolution. *J. Geophys. Res. Atmos.*, **117**, D10111.
- Sarofim, M., 2012: The GTP of methane: Modeling analysis of temperature impacts of methane and carbon dioxide reductions. *Environ. Model. Assess.*, **17**, 231–239.
- Sato, M., J. E. Hansen, M. P. McCormick, and J. B. Pollack, 1993: Stratospheric aerosol optical depths, 1850–1990. *J. Geophys. Res. Atmos.*, **98**, 22987–22994.
- Schaaf, C., et al., 2002: First operational BRDF, albedo nadir reflectance products from MODIS. *Remote Sens. Environ.*, **83**, 135–148.
- Schmalensee, R., 1993: Comparing greenhouse gases for policy purposes. *Energy J.*, **14**, 245–256.
- Schmidt, A., K. S. Carslaw, G. W. Mann, M. Wilson, T. J. Breider, S. J. Pickering, and T. Thordarson, 2010: The impact of the 1783–1784 AD Laki eruption on global aerosol formation processes and cloud condensation nuclei. *Atmos. Chem. Phys.*, **10**, 6025–6041.
- Schmidt, A., et al., 2012: Importance of tropospheric volcanic aerosol for indirect radiative forcing of climate. *Atmos. Chem. Phys.*, **12**, 7321–7339.
- Schmidt, G., et al., 2011: Climate forcing reconstructions for use in PMIP simulations of the last millennium (v1.0). *Geosci. Model Dev.*, **4**, 33–45.
- Schneider, D. P., C. M. Ammann, B. L. Otto-Bliesner, and D. S. Kaufman, 2009: Climate response to large, high-latitude and low-latitude volcanic eruptions in the Community Climate System Model. *J. Geophys. Res. Atmos.*, **114**, D15101.
- Schultz, M. G., et al., 2008: Global wildland fire emissions from 1960 to 2000. *Global Biogeochem. Cycles*, **22**, Gb2002.
- Seinfeld, J. H., and S. N. Pandis, 2006: *Atmospheric Chemistry and Physics: From Air Pollution to Climate Change*. John Wiley & Sons, Hoboken, NJ, USA.
- Self, S., and S. Blake, 2008: Consequences of explosive supereruptions. *Elements*, **4**, 41–46.
- Sharma, S., D. Lavoue, H. Cachier, L. Barrie, and S. Gong, 2004: Long-term trends of the black carbon concentrations in the Canadian Arctic. *J. Geophys. Res. Atmos.*, **109**, D15203.
- Shibata, K., and K. Kodera, 2005: Simulation of radiative and dynamical responses of the middle atmosphere to the 11-year solar cycle. *J. Atmos. Sol. Terres. Phys.*, **67**, 125–143.
- Shindell, D., and G. Faluvegi, 2009: Climate response to regional radiative forcing during the twentieth century. *Nature Geosci.*, **2**, 294–300.
- Shindell, D., and G. Faluvegi, 2010: The net climate impact of coal-fired power plant emissions. *Atmos. Chem. Phys.*, **10**, 3247–3260.
- Shindell, D., G. Schmidt, M. Mann, D. Rind, and A. Waple, 2001: Solar forcing of regional climate change during the maunder minimum. *Science*, **294**, 2149–2152.
- Shindell, D., G. Faluvegi, A. Lacis, J. Hansen, R. Ruedy, and E. Aguilar, 2006a: Role of tropospheric ozone increases in 20th-century climate change. *J. Geophys. Res. Atmos.*, **111**, D08302.
- Shindell, D., G. Faluvegi, R. Miller, G. Schmidt, J. Hansen, and S. Sun, 2006b: Solar and anthropogenic forcing of tropical hydrology. *Geophys. Res. Lett.*, **33**, L24706.
- Shindell, D., M. Schulz, Y. Ming, T. Takemura, G. Faluvegi, and V. Ramaswamy, 2010: Spatial scales of climate response to inhomogeneous radiative forcing. *J. Geophys. Res. Atmos.*, **115**, D19110.
- Shindell, D., et al., 2008: Climate forcing and air quality change due to regional emissions reductions by economic sector. *Atmos. Chem. Phys.*, **8**, 7101–7113.
- Shindell, D., et al., 2011: Climate, health, agricultural and economic impacts of tighter vehicle-emission standards. *Nature Clim. Change*, **1**, 59–66.
- Shindell, D., et al., 2013a: Attribution of historical ozone forcing to anthropogenic emissions. *Nature Clim. Change*, **3**, 567–570.
- Shindell, D., et al., 2012a: Simultaneously mitigating near-term climate change and improving human health and food security. *Science*, **335**, 183–189.
- Shindell, D. T., 2012: Evaluation of the absolute regional temperature potential. *Atmos. Chem. Phys.*, **12**, 7955–7960.
- Shindell, D. T., A. Voulgarakis, G. Faluvegi, and G. Milly, 2012b: Precipitation response to regional radiative forcing. *Atmos. Chem. Phys.*, **12**, 6969–6982.
- Shindell, D. T., G. Faluvegi, D. M. Koch, G. A. Schmidt, N. Unger, and S. E. Bauer, 2009: Improved attribution of climate forcing to emissions. *Science*, **326**, 716–718.
- Shindell, D. T., et al., 2006c: Simulations of preindustrial, present-day, and 2100 conditions in the NASA GISS composition and climate model G-PUCCINI. *Atmos. Chem. Phys.*, **6**, 4427–4459.
- Shindell, D. T., et al., 2013b: Interactive ozone and methane chemistry in GISS-E2 historical and future climate simulations. *Atmos. Chem. Phys.*, **13**, 2653–2689.
- Shindell, D. T., et al., 2013c: Radiative forcing in the ACCMIP historical and future climate simulations. *Atmos. Chem. Phys.*, **13**, 2939–2974.
- Shine, K., 2009: The global warming potential—the need for an interdisciplinary retrieval. *Clim. Change*, **96**, 467–472.
- Shine, K., J. Cook, E. Highwood, and M. Joshi, 2003: An alternative to radiative forcing for estimating the relative importance of climate change mechanisms. *Geophys. Res. Lett.*, **30**, 2047.

- Shine, K., J. Fuglestedt, K. Hailemariam, and N. Stuber, 2005a: Alternatives to the global warming potential for comparing climate impacts of emissions of greenhouse gases. *Clim. Change*, **68**, 281–302.
- Shine, K., T. Berntsen, J. Fuglestedt, and R. Sausen, 2005b: Scientific issues in the design of metrics for inclusion of oxides of nitrogen in global climate agreements. *Proc. Natl. Acad. Sci. U.S.A.*, **102**, 15768–15773.
- Shine, K., T. Berntsen, J. Fuglestedt, R. Skeie, and N. Stuber, 2007: Comparing the climate effect of emissions of short- and long-lived climate agents. *Philos. Trans. R. Soc. A*, **365**, 1903–1914.
- Shine, K. P., I. V. Ptashnik, and G. Raedel, 2012: The water vapour continuum: Brief history and recent developments. *Surv. Geophys.*, **33**, 535–555.
- Siddaway, J. M., and S. V. Petelina, 2011: Transport and evolution of the 2009 Australian Black Saturday bushfire smoke in the lower stratosphere observed by OSIRIS on Odin. *J. Geophys. Res. Atmos.*, **116**, D06203.
- Sitch, S., P. M. Cox, W. J. Collins, and C. Huntingford, 2007: Indirect radiative forcing of climate change through ozone effects on the land-carbon sink. *Nature*, **448**, 791–794.
- Skeie, R., T. Berntsen, G. Myhre, K. Tanaka, M. Kvalevag, and C. Hoyle, 2011a: Anthropogenic radiative forcing time series from pre-industrial times until 2010. *Atmos. Chem. Phys.*, **11**, 11827–11857.
- Skeie, R., T. Berntsen, G. Myhre, C. Pedersen, J. Strom, S. Gerland, and J. Ogren, 2011b: Black carbon in the atmosphere and snow, from pre-industrial times until present. *Atmos. Chem. Phys.*, **11**, 6809–6836.
- Skeie, R. B., J. Fuglestedt, T. Berntsen, M. T. Lund, G. Myhre, and K. Rypdal, 2009: Global temperature change from the transport sectors: Historical development and future scenarios. *Atmos. Environ.*, **43**, 6260–6270.
- Smith, E., and A. Balogh, 2008: Decrease in heliospheric magnetic flux in this solar minimum: Recent Ulysses magnetic field observations. *Geophys. Res. Lett.*, **35**, L22103.
- Smith, S., and M. Wigley, 2000: Global warming potentials: 1. Climatic implications of emissions reductions. *Clim. Change*, **44**, 445–457.
- Smith, S., J. Karas, J. Edmonds, J. Eom, and A. Mizrahi, 2013: Sensitivity of multi-gas climate policy to emission metrics. *Clim. Change*, **117**, 663–675.
- Smith, S. M., J. A. Lowe, N. H. A. Bowerman, L. K. Gohar, C. Huntingford, and M. R. Allen, 2012: Equivalence of greenhouse-gas emissions for peak temperature limits. *Nature Clim. Change*, **2**, 535–538.
- Snow-Kropla, E., J. Pierce, D. Westervelt, and W. Trivittayanurak, 2011: Cosmic rays, aerosol formation and cloud-condensation nuclei: Sensitivities to model uncertainties. *Atmos. Chem. Phys.*, **11**, 4001–4013.
- Solanki, S., and N. Krivova, 2004: Solar irradiance variations: From current measurements to long-term estimates. *Sol. Phys.*, **224**, 197–208.
- Solomon, S., 1999: Stratospheric ozone depletion: A review of concepts and history. *Rev. Geophys.*, **37**, 275–316.
- Solomon, S., J. S. Daniel, R. R. Neely, J. P. Vernier, E. G. Dutton, and L. W. Thomason, 2011: The persistently variable “background” stratospheric aerosol layer and global climate change. *Science*, **333**, 866–870.
- Son, S. W., N. F. Tandon, L. M. Polvani, and D. W. Waugh, 2009: Ozone hole and Southern Hemisphere climate change. *Geophys. Res. Lett.*, **36**, L15705.
- Soukharev, B., and L. Hood, 2006: Solar cycle variation of stratospheric ozone: Multiple regression analysis of long-term satellite data sets and comparisons with models. *J. Geophys. Res. Atmos.*, **111**, D20314.
- Søvde, O., C. Hoyle, G. Myhre, and I. Isaksen, 2011: The HNO₃ forming branch of the HO₂ + NO reaction: Pre-industrial-to-present trends in atmospheric species and radiative forcings. *Atmos. Chem. Phys.*, **11**, 8929–8943.
- Steinhilber, F., J. Beer, and C. Frohlich, 2009: Total solar irradiance during the Holocene. *Geophys. Res. Lett.*, **36**, L19704.
- Stenchikov, G., A. Robock, V. Ramaswamy, M. D. Schwarzkopf, K. Hamilton, and S. Ramachandran, 2002: Arctic Oscillation response to the 1991 Mount Pinatubo eruption: Effects of volcanic aerosols and ozone depletion. *J. Geophys. Res. Atmos.*, **107**, 4803.
- Stenchikov, G., T. L. Delworth, V. Ramaswamy, R. J. Stouffer, A. Wittenberg, and F. R. Zeng, 2009: Volcanic signals in oceans. *J. Geophys. Res. Atmos.*, **114**, D16104.
- Stephens, G. L., N. B. Wood, and L. A. Pakula, 2004: On the radiative effects of dust on tropical convection. *Geophys. Res. Lett.*, **31**, L23112.
- Stevenson, D., and R. Derwent, 2009: Does the location of aircraft nitrogen oxide emissions affect their climate impact? *Geophys. Res. Lett.*, **36**, L17810.
- Stevenson, D. S., et al., 2013: Tropospheric ozone changes, radiative forcing and attribution to emissions in the Atmospheric Chemistry and Climate Model Intercomparison Project (ACCMIP). *Atmos. Chem. Phys.*, **13**, 3063–3085.
- Stevenson, D. S., et al., 2006: Multimodel ensemble simulations of present-day and near-future tropospheric ozone. *J. Geophys. Res. Atmos.*, **111**, D08301.
- Stiller, G. P., et al., 2012: Observed temporal evolution of global mean age of stratospheric air for the 2002 to 2010 period. *Atmos. Chem. Phys.*, **12**, 3311–3331.
- Stothers, R. B., 2007: Three centuries of observation of stratospheric transparency. *Clim. Change*, **83**, 515–521.
- Struthers, H., et al., 2011: The effect of sea ice loss on sea salt aerosol concentrations and the radiative balance in the Arctic. *Atmos. Chem. Phys.*, **11**, 3459–3477.
- Swann, A. L. S., I. Y. Fung, and J. C. H. Chiang, 2012: Mid-latitude afforestation shifts general circulation and tropical precipitation. *Proc. Natl. Acad. Sci. U.S.A.*, **109**, 712–716.
- Swingedouw, D., L. Terray, C. Cassou, A. Voldoire, D. Salas-Melia, and J. Servonnat, 2011: Natural forcing of climate during the last millennium: Fingerprint of solar variability. *Clim. Dyn.*, **36**, 1349–1364.
- Takemura, T., 2012: Distributions and climate effects of atmospheric aerosols from the preindustrial era to 2100 along Representative Concentration Pathways (RCPs) simulated using the global aerosol model SPRINTARS. *Atmos. Chem. Phys.*, **12**, 11555–11572.
- Tanaka, K., D. Johansson, B. O’Neill, and J. Fuglestedt, 2013: Emission metrics under the 2°C climate stabilization. *Clim. Change Lett.*, **117**, 933–941.
- Tanaka, K., B. O’Neill, D. Rokityanskiy, M. Obersteiner, and R. Tol, 2009: Evaluating Global Warming Potentials with historical temperature. *Clim. Change*, **96**, 443–466.
- Taraborrelli, D., et al., 2012: Hydroxyl radical buffered by isoprene oxidation over tropical forests. *Nature Geosci.*, **5**, 190–193.
- Taylor, P. C., R. G. Ellingson, and M. Cai, 2011: Seasonal variations of climate feedbacks in the NCAR CCSM3. *J. Clim.*, **24**, 3433–3444.
- Textor, C., et al., 2006: Analysis and quantification of the diversities of aerosol life cycles within AeroCom. *Atmos. Chem. Phys.*, **6**, 1777–1813.
- Thomason, L., and T. Peter, 2006: Assessment of Stratospheric Aerosol Properties (ASAP). *SPARC Reports/WCRP-124, WMO/TD- No. 1295*, SPARC Report No. 4.
- Thompson, D. W. J., S. Solomon, P. J. Kushner, M. H. England, K. M. Grise, and D. J. Karoly, 2011: Signatures of the Antarctic ozone hole in Southern Hemisphere surface climate change. *Nature Geosci.*, **4**, 741–749.
- Thonicke, K., A. Spessa, I. C. Prentice, S. P. Harrison, L. Dong, and C. Carmona-Moreno, 2010: The influence of vegetation, fire spread and fire behaviour on biomass burning and trace gas emissions: Results from a process-based model. *Biogeosciences*, **7**, 1991–2011.
- Tilmes, S., et al., 2012: Technical Note: Ozonesonde climatology between 1995 and 2011: Description, evaluation and applications. *Atmos. Chem. Phys.*, **12**, 7475–7497.
- Timmreck, C., 2012: Modeling the climatic effects of large explosive volcanic eruptions. *Climate Change*, **3**, 545–564.
- Timmreck, C., et al., 2010: Aerosol size confines climate response to volcanic super-eruptions. *Geophys. Res. Lett.*, **37**, L24705.
- Tol, R., T. Berntsen, B. O’Neill, J. Fuglestedt, and K. Shine, 2012: A unifying framework for metrics for aggregating the climate effect of different emissions. *Environ. Res. Lett.*, **7**, 044006.
- Toon, O. B., A. Robock, and R. P. Turco, 2008: Environmental consequences of nuclear war. *Physics Today*, **61**, 37–42.
- Trenberth, K. E., and A. Dai, 2007: Effects of Mount Pinatubo volcanic eruption on the hydrological cycle as an analog of geoengineering. *Geophys. Res. Lett.*, **34**, L15702.
- Tsigrasidou, K., and M. Kanakidou, 2007: Secondary organic aerosol importance in the future atmosphere. *Atmos. Environ.*, **41**, 4682–4692.
- UNEP, 2011: Near-term Climate Protection and Clean Air Benefits: Actions for Controlling Short-Lived Climate Forcers. United Nations Environment Programme (UNEP), 78 pp.
- Unger, N., T. C. Bond, J. S. Wang, D. M. Koch, S. Menon, D. T. Shindell, and S. Bauer, 2010: Attribution of climate forcing to economic sectors. *Proc. Natl. Acad. Sci. U.S.A.*, **107**, 3382–3387.
- van der Molen, M. K., B. J. J. M. van den Hurk, and W. Hazeleger, 2011: A dampened land use change climate response towards the tropics. *Clim. Dyn.*, **37**, 2035–2043.
- van der Werf, G. R., et al., 2010: Global fire emissions and the contribution of deforestation, savanna, forest, agricultural, and peat fires (1997–2009). *Atmos. Chem. Phys.*, **10**, 11707–11735.

- van Vuuren, D., J. Edmonds, M. Kainuma, K. Riahi, and J. Weyant, 2011: A special issue on the RCPs. *Clim. Change*, **109**, 1–4.
- Van Vuuren, D. P., et al., 2008: Temperature increase of 21st century mitigation scenarios. *Proc. Natl. Acad. Sci. U.S.A.*, **105**, 15258–15262.
- Vasekova, E., E. Drage, K. Smith, and N. Mason, 2006: FTIR spectroscopy and radiative forcing of octafluorocyclobutane and octofluorocyclopentene. *J. Quant. Spectrosc. Radiat. Transfer*, **102**, 418–424.
- Velders, G. J. M., D. W. Fahey, J. S. Daniel, M. McFarland, and S. O. Andersen, 2009: The large contribution of projected HFC emissions to future climate forcing. *Proc. Natl. Acad. Sci. U.S.A.*, **106**, 10949–10954.
- Vernier, J. P., L. W. Thomason, T. D. Fairlie, P. Minnis, R. Palikonda, and K. M. Bedka, 2013: Comment on “Large Volcanic Aerosol Load in the Stratosphere Linked to Asian Monsoon Transport”. *Science*, **339**, 647-d.
- Vernier, J. P., et al., 2011: Major influence of tropical volcanic eruptions on the stratospheric aerosol layer during the last decade. *Geophys. Res. Lett.*, **38**, L12807.
- Vial, J., J.-L. Dufresne, and S. Bony, 2013: On the interpretation of inter-model spread in CMIP5 climate sensitivity estimates. *Clim. Dyn.*, doi:10.1007/s00382-013-1725-9, in press.
- Volz, A., and D. Kley, 1988: Evaluation of the Montsouris Series of ozone measurements made in the 19th century. *Nature*, **332**, 240–242.
- Voulgarakis, A., and D. T. Shindell, 2010: Constraining the sensitivity of regional climate with the use of historical observations. *J. Clim.*, **23**, 6068–6073.
- Voulgarakis, A., et al., 2013: Analysis of present day and future OH and methane lifetime in the ACCMIP simulations. *Atmos. Chem. Phys.*, **13**, 2563–2587.
- Wang, C., D. Kim, A. Ekman, M. Barth, and P. Rasch, 2009: Impact of anthropogenic aerosols on Indian summer monsoon. *Geophys. Res. Lett.*, **36**, L21704.
- Wang, M., and J. E. Penner, 2009: Aerosol indirect forcing in a global model with particle nucleation. *Atmos. Chem. Phys.*, **9**, 239–260.
- Wang, X., S. J. Doherty, and J. Huang, 2013: Black carbon and other light-absorbing impurities in snow across Northern China. *J. Geophys. Res. Atmos.*, **118**, 1471–1492.
- Wang, Y., J. Lean, and N. Sheeley, 2005: Modeling the sun’s magnetic field and irradiance since 1713. *Astrophys. J.*, **625**, 522–538.
- Warren, S., and W. Wiscombe, 1980: A model for the spectral albedo of snow. 2. Snow containing atmospheric aerosols. *J. Atmos. Sci.*, **37**, 2734–2745.
- Weiss, R., J. Muhle, P. Salameh, and C. Harth, 2008: Nitrogen trifluoride in the global atmosphere. *Geophys. Res. Lett.*, **35**, L20821.
- Wenzler, T., S. Solanki, and N. Krivova, 2009: Reconstructed and measured total solar irradiance: Is there a secular trend between 1978 and 2003? *Geophys. Res. Lett.*, **36**, L11102.
- Wilcox, L., K. Shine, and B. Hoskins, 2012: Radiative forcing due to aviation water vapour emissions. *Atmos. Environ.*, **63**, 1–13.
- Wild, M., 2009: How well do IPCC-AR4/CMIP3 climate models simulate global dimming/brightening and twentieth-century daytime and nighttime warming? *J. Geophys. Res. Atmos.*, **114**, D00D11.
- Wild, O., 2007: Modelling the global tropospheric ozone budget: Exploring the variability in current models. *Atmos. Chem. Phys.*, **7**, 2643–2660.
- Wild, O., and P. I. Palmer, 2008: How sensitive is tropospheric oxidation to anthropogenic emissions? *Geophys. Res. Lett.*, **35**, L22802.
- Wild, O., M. Prather, and H. Akimoto, 2001: Indirect long-term global radiative cooling from NO_x emissions. *Geophys. Res. Lett.*, **28**, 1719–1722.
- Williams, K. D., A. Jones, D. L. Roberts, C. A. Senior, and M. J. Woodage, 2001: The response of the climate system to the indirect effects of anthropogenic sulfate aerosol. *Clim. Dyn.*, **17**, 845–856.
- Willson, R., and A. Mordvinov, 2003: Secular total solar irradiance trend during solar cycles 21–23. *Geophys. Res. Lett.*, **30**, 1199.
- WMO, 1999: *Scientific Assessment of Ozone Depletion: 1998*. Global Ozone Research and Monitoring Project. Report No. 44. World Meteorological Organization, Geneva, Switzerland.
- WMO, 2011: *Scientific Assessment of Ozone Depletion: 2010*. Global Ozone Research and Monitoring Project-Report. World Meteorological Organisation, Geneva, Switzerland, 516 pp.
- Worden, H., K. Bowman, S. Kulawik, and A. Aghedo, 2011: Sensitivity of outgoing longwave radiative flux to the global vertical distribution of ozone characterized by instantaneous radiative kernels from Aura-TES. *J. Geophys. Res. Atmos.*, **116**, D14115.
- Worden, H., K. Bowman, J. Worden, A. Eldering, and R. Beer, 2008: Satellite measurements of the clear-sky greenhouse effect from tropospheric ozone. *Nature Geosci.*, **1**, 305–308.
- Wright, J., 2004: Do we know of any Maunder minimum stars? *Astron. J.*, **128**, 1273–1278.
- Wu, S. L., L. J. Mickley, D. J. Jacob, J. A. Logan, R. M. Yantosca, and D. Rind, 2007: Why are there large differences between models in global budgets of tropospheric ozone? *J. Geophys. Res. Atmos.*, **112**, D05302.
- Xia, L. L., and A. Robock, 2013: Impacts of a nuclear war in South Asia on rice production in Mainland China. *Clim. Change*, **116**, 357–372.
- Ye, H., R. Zhang, J. Shi, J. Huang, S. G. Warren, and Q. Fu, 2012: Black carbon in seasonal snow across northern Xinjiang in northwestern China. *Environ. Res. Lett.*, **7**, 044002.
- Young, P. J., et al., 2013: Pre-industrial to end 21st century projections of tropospheric ozone from the Atmospheric Chemistry and Climate Model Intercomparison Project (ACCMIP). *Atmos. Chem. Phys.*, **13**, 2063–2090.
- Zanchettin, D., et al., 2012: Bi-decadal variability excited in the coupled ocean-atmosphere system by strong tropical volcanic eruptions. *Clim. Dyn.*, **39**, 419–444.
- Zarzycki, C. M., and T. C. Bond, 2010: How much can the vertical distribution of black carbon affect its global direct radiative forcing? *Geophys. Res. Lett.*, **37**, L20807.
- Zeng, G., J. A. Pyle, and P. J. Young, 2008: Impact of climate change on tropospheric ozone and its global budgets. *Atmos. Chem. Phys.*, **8**, 369–387.
- Zeng, G., O. Morgenstern, P. Braesicke, and J. A. Pyle, 2010: Impact of stratospheric ozone recovery on tropospheric ozone and its budget. *Geophys. Res. Lett.*, **37**, L09805.
- Zhang, H., G. Y. Shi, and Y. Liu, 2005: A comparison between the two line-by-line integration algorithms. *Chin. J. Atmos. Sci.*, **29**, 581–593.
- Zhang, H., G. Shi, and Y. Liu, 2008: The effects of line-wing cutoff in LBL integration on radiation calculations. *Acta Meteorol. Sin.*, **22**, 248–255.
- Zhang, H., J. Wu, and P. Luc, 2011: A study of the radiative forcing and global warming potentials of hydrofluorocarbons. *J. Quant. Spectrosc. Radiat. Transfer*, **112**, 220–229.
- Zhang, X. B., et al., 2007: Detection of human influence on twentieth-century precipitation trends. *Nature*, **448**, 461–465.
- Zhong, Y., G. H. Miller, B. L. Otto-Bliessner, M. M. Holland, D. A. Bailey, D. P. Schneider, and A. Geirsdottir, 2011: Centennial-scale climate change from decadal-paced explosive volcanism: A coupled sea ice-ocean mechanism. *Clim. Dyn.*, **37**, 2373–2387.
- Ziemke, J. R., S. Chandra, G. J. Labow, P. K. Bhartia, L. Froidevaux, and J. C. Witte, 2011: A global climatology of tropospheric and stratospheric ozone derived from Aura OMI and MLS measurements. *Atmos. Chem. Phys.*, **11**, 9237–9251.

Appendix 8.A: Lifetimes, Radiative Efficiencies and Metric Values

Table 8.A.1 | Radiative efficiencies (REs), lifetimes/adjustment times, AGWP and GWP values for 20, 50 and 100 years. Climate-carbon feedbacks are included for CO₂ while no climate feedbacks are included for the other components (see discussion in Sections 8.7.1.4 and 8.7.2.1, Supplementary Material and notes below the table; Supplementary Material Table 8.SM.16 gives analogous values including climate-carbon feedbacks for non-CO₂ emissions). For a complete list of chemical names and CAS numbers, and for accurate replications of metric values, see Supplementary Material Section 8.SM.13 and references therein.

Acronym, Common Name or Chemical Name	Chemical Formula	Lifetime (Years)	Radiative Efficiency (W m ⁻² ppb ⁻¹)	AGWP 20-year (W m ⁻² yr kg ⁻¹)	GWP 20-year	AGWP 100-year (W m ⁻² yr kg ⁻¹)	GWP 100-year	AGTP 20-year (K kg ⁻¹)	GTP 20-year	AGTP 50-year (K kg ⁻¹)	GTP 50-year	AGTP 100-year (K kg ⁻¹)	GTP 100-year
Carbon dioxide	CO ₂	see*	1.37e-5	2.49e-14	1	9.17e-14	1	6.84e-16	1	6.17e-16	1	5.47e-16	1
Methane	CH ₄	12.4 [†]	3.63e-4	2.09e-12	84	2.61e-12	28	4.62e-14	67	8.69e-15	14	2.34e-15	4
Fossil methane†	CH ₄	12.4 [†]	3.63e-4	2.11e-12	85	2.73e-12	30	4.68e-14	68	9.55e-15	15	3.11e-15	6
Nitrous Oxide	N ₂ O	121 [†]	3.00e-3	6.58e-12	264	2.43e-11	265	1.89e-13	277	1.74e-13	282	1.28e-13	234
Chlorofluorocarbons													
CFC-11	CCl ₃ F	45.0	0.26	1.72e-10	6900	4.28e-10	4660	4.71e-12	6890	3.01e-12	4890	1.28e-12	2340
CFC-12	CCl ₂ F ₂	100.0	0.32	2.69e-10	10,800	9.39e-10	10,200	7.71e-12	11,300	6.75e-12	11,000	4.62e-12	8450
CFC-13	CClF ₃	640.0	0.25	2.71e-10	10,900	1.27e-09	13,900	7.99e-12	11,700	8.77e-12	14,200	8.71e-12	15,900
CFC-113	CCl ₂ FCClF ₂	85.0	0.30	1.62e-10	6490	5.34e-10	5820	4.60e-12	6730	3.85e-12	6250	2.45e-12	4470
CFC-114	CClF ₂ CClF ₂	190.0	0.31	1.92e-10	7710	7.88e-10	8590	5.60e-12	8190	5.56e-12	9020	4.68e-12	8550
CFC-115	CClF ₂ CF ₃	1,020.0	0.20	1.46e-10	5860	7.03e-10	7670	4.32e-12	6310	4.81e-12	7810	4.91e-12	8980
Hydrochlorofluorocarbons													
HCFC-21	CHCl ₂ F	1.7	0.15	1.35e-11	543	1.35e-11	148	1.31e-13	192	1.59e-14	26	1.12e-14	20
HCFC-22	CHClF ₂	11.9	0.21	1.32e-10	5280	1.62e-10	1760	2.87e-12	4200	5.13e-13	832	1.43e-13	262
HCFC-122	CHCl ₂ CF ₂ Cl	1.0	0.17	5.43e-12	218	5.43e-12	59	4.81e-14	70	6.25e-15	10	4.47e-15	8
HCFC-122a	CHFClCFCl ₂	3.4	0.21	2.36e-11	945	2.37e-11	258	2.91e-13	426	2.99e-14	48	1.96e-14	36
HCFC-123	CHCl ₂ CF ₃	1.3	0.15	7.28e-12	292	7.28e-12	79	6.71e-14	98	8.45e-15	14	6.00e-15	11
HCFC-123a	CHClFCl ₂ Cl	4.0	0.23	3.37e-11	1350	3.39e-11	370	4.51e-13	659	4.44e-14	72	2.81e-14	51
HCFC-124	CHClFCl ₂	5.9	0.20	4.67e-11	1870	4.83e-11	527	7.63e-13	1120	7.46e-14	121	4.03e-14	74
HCFC-132c	CH ₂ FClCFCl ₂	4.3	0.17	3.07e-11	1230	3.10e-11	338	4.27e-13	624	4.14e-14	67	2.58e-14	47
HCFC-141b	CH ₂ CCl ₂ F	9.2	0.16	6.36e-11	2550	7.17e-11	782	1.27e-12	1850	1.67e-13	271	6.09e-14	111
HCFC-142b	CH ₂ CClF ₂	17.2	0.19	1.25e-10	5020	1.82e-10	1980	3.01e-12	4390	8.46e-13	1370	1.95e-13	356
HCFC-225ca	CHCl ₂ CF ₂ CF ₃	1.9	0.22	1.17e-11	469	1.17e-11	127	1.17e-13	170	1.38e-14	22	9.65e-15	18
HCFC-225cb	CHClFCl ₂ CClF ₂	5.9	0.29	4.65e-11	1860	4.81e-11	525	7.61e-13	1110	7.43e-14	120	4.01e-14	73
(E)-1-Chloro-3,3,3-trifluoroprop-1-ene	trans-CF ₃ CH=CHCl	26.0 days	0.04	1.37e-13	5	1.37e-13	1	1.09e-15	2	1.54e-16	<1	1.12e-16	<1

(continued on next page)

Table 8.A.1 (continued)

Acronym, Common Name or Chemical Name	Chemical Formula	Lifetime (Years)	Radiative Efficiency ($W m^{-2} ppb^{-1}$)	AGWP 20-year ($W m^{-2} yr kg^{-1}$)	GWP 20-year	AGWP 100-year ($W m^{-2} yr kg^{-1}$)	GWP 100-year	AGTP 20-year ($K kg^{-1}$)	GTP 20-year	AGTP 50-year ($K kg^{-1}$)	GTP 50-year	AGTP 100-year ($K kg^{-1}$)	GTP 100-year
Hydrofluorocarbons													
HFC-23	CHF_3	222.0	0.18	$2.70e-10$	10,800	$1.14e-09$	12,400	$7.88e-12$	11,500	$7.99e-12$	13,000	$6.95e-12$	12,700
HFC-32	CH_2F_2	5.2	0.11	$6.07e-11$	2430	$6.21e-11$	677	$9.32e-13$	1360	$8.93e-14$	145	$5.17e-14$	94
HFC-41	CH_3F	2.8	0.02	$1.07e-11$	427	$1.07e-11$	116	$1.21e-13$	177	$1.31e-14$	21	$8.82e-15$	16
HFC-125	CHF_2CF_3	28.2	0.23	$1.52e-10$	6090	$2.91e-10$	3170	$3.97e-12$	5800	$1.84e-12$	2980	$5.29e-13$	967
HFC-134	CHF_2CHF_2	9.7	0.19	$8.93e-11$	3580	$1.02e-10$	1120	$1.82e-12$	2660	$2.54e-13$	412	$8.73e-14$	160
HFC-134a	CH_2FCF_3	13.4	0.16	$9.26e-11$	3710	$1.19e-10$	1300	$2.09e-12$	3050	$4.33e-13$	703	$1.10e-13$	201
HFC-143	CH_2FCHF_2	3.5	0.13	$3.00e-11$	1200	$3.01e-11$	328	$3.76e-13$	549	$3.82e-14$	62	$2.49e-14$	46
HFC-143a	CH_3CF_3	47.1	0.16	$1.73e-10$	6940	$4.41e-10$	4800	$4.76e-12$	6960	$3.12e-12$	5060	$1.37e-12$	2500
HFC-152	CHF_2CHF_2F	0.4	0.04	$1.51e-12$	60	$1.51e-12$	16	$1.25e-14$	18	$1.71e-15$	3	$1.24e-15$	2
HFC-152a	CH_3CHF_2	1.5	0.10	$1.26e-11$	506	$1.26e-11$	138	$1.19e-13$	174	$1.47e-14$	24	$1.04e-14$	19
HFC-161	CH_3CH_2F	66.0 days	0.02	$3.33e-13$	13	$3.33e-13$	4	$2.70e-15$	4	$3.76e-16$	<1	$2.74e-16$	<1
HFC-227ca	$CF_3CF_2CHF_2$	28.2	0.27	$1.27e-10$	5080	$2.42e-10$	2640	$3.31e-12$	4830	$1.53e-12$	2480	$4.41e-13$	806
HFC-227ea	$CF_3CHF_2CF_3$	38.9	0.26	$1.34e-10$	5360	$3.07e-10$	3350	$3.61e-12$	5280	$2.12e-12$	3440	$7.98e-13$	1460
HFC-236cb	$CH_2FCF_2CF_3$	13.1	0.23	$8.67e-11$	3480	$1.11e-10$	1210	$1.94e-12$	2840	$3.92e-13$	636	$1.01e-13$	185
HFC-236ea	$CHF_2CHF_2CF_3$	11.0	0.30 ^a	$1.03e-10$	4110	$1.22e-10$	1330	$2.18e-12$	3190	$3.53e-13$	573	$1.06e-13$	195
HFC-236fa	$CF_3CH_2CF_3$	242.0	0.24	$1.73e-10$	6940	$7.39e-10$	8060	$5.06e-12$	7400	$5.18e-12$	8400	$4.58e-12$	8380
HFC-245ca	$CH_2FCF_2CHF_2$	6.5	0.24 ^b	$6.26e-11$	2510	$6.56e-11$	716	$1.07e-12$	1570	$1.09e-13$	176	$5.49e-14$	100
HFC-245cb	$CF_3CF_2CH_3$	47.1	0.24	$1.67e-10$	6680	$4.24e-10$	4620	$4.58e-12$	6690	$3.00e-12$	4870	$1.32e-12$	2410
HFC-245ea	$CHF_2CHF_2CHF_2$	3.2	0.16 ^c	$2.15e-11$	863	$2.16e-11$	235	$2.59e-13$	378	$2.70e-14$	44	$1.79e-14$	33
HFC-245eb	$CH_2FCH_2CF_3$	3.1	0.20 ^c	$2.66e-11$	1070	$2.66e-11$	290	$3.15e-13$	460	$3.31e-14$	54	$2.20e-14$	40
HFC-245fa	$CHF_2CH_2CF_3$	7.7	0.24	$7.29e-11$	2920	$7.87e-11$	858	$1.35e-12$	1970	$1.51e-13$	245	$6.62e-14$	121
HFC-263fb	$CH_3CH_2CF_3$	1.2	0.10 ^c	$6.93e-12$	278	$6.93e-12$	76	$6.31e-14$	92	$8.02e-15$	13	$5.70e-15$	10
HFC-272ca	$CH_3CF_2CH_3$	2.6	0.07	$1.32e-11$	530	$1.32e-11$	144	$1.46e-13$	213	$1.61e-14$	26	$1.09e-14$	20
HFC-329p	$CHF_2CF_2CF_2CF_3$	28.4	0.31	$1.13e-10$	4510	$2.16e-10$	2360	$2.94e-12$	4290	$1.37e-12$	2220	$3.96e-13$	725
HFC-365mfc	$CH_3CF_2CH_2CF_3$	8.7	0.22	$6.64e-11$	2660	$7.38e-11$	804	$1.30e-12$	1890	$1.62e-13$	262	$6.24e-14$	114
HFC-43-10mee	$CF_3CHFCH_2CF_2CF_3$	16.1	0.42 ^b	$1.08e-10$	4310	$1.51e-10$	1650	$2.54e-12$	3720	$6.62e-13$	1070	$1.54e-13$	281
HFC-1132a	$CH_2=CF_2$	4.0 days	0.004 ^d	$3.87e-15$	<1	$3.87e-15$	<1	$3.08e-17$	<1	$4.35e-18$	<1	$3.18e-18$	<1
HFC-1141	$CH_2=CHF$	2.1 days	0.002 ^d	$1.54e-15$	<1	$1.54e-15$	<1	$1.23e-17$	<1	$1.73e-18$	<1	$1.27e-18$	<1
(Z)-HFC-1225ye	$CF_3CF=CHF(Z)$	8.5 days	0.02	$2.14e-14$	<1	$2.14e-14$	<1	$1.70e-16$	<1	$2.40e-17$	<1	$1.76e-17$	<1
(E)-HFC-1225ye	$CF_3CF=CHF(E)$	4.9 days	0.01	$7.25e-15$	<1	$7.25e-15$	<1	$5.77e-17$	<1	$8.14e-18$	<1	$5.95e-18$	<1
(Z)-HFC-1234ze	$CF_3CH=CHF(Z)$	10.0 days	0.02	$2.61e-14$	1	$2.61e-14$	<1	$2.08e-16$	<1	$2.93e-17$	<1	$2.14e-17$	<1
HFC-1234yf	$CF_3CF=CH_2$	10.5 days	0.02	$3.22e-14$	1	$3.22e-14$	<1	$2.57e-16$	<1	$3.62e-17$	<1	$2.65e-17$	<1
(E)-HFC-1234ze	$trans-CF_3CH=CHF$	16.4 days	0.04	$8.74e-14$	4	$8.74e-14$	<1	$6.98e-16$	<1	$9.82e-17$	<1	$7.18e-17$	<1
(Z)-HFC-1336	$CF_3CH=CHF(Z)$	22.0 days	0.07 ^d	$1.54e-13$	6	$1.54e-13$	2	$1.23e-15$	2	$1.73e-16$	<1	$1.26e-16$	<1

(continued on next page)

Table 8.A.1 (continued)

Acronym, Common Name or Chemical Name	Chemical Formula	Lifetime (Years)	Radiative Efficiency (W m ⁻² ppb ⁻¹)	AGWP 20-year (W m ⁻² yr kg ⁻¹)	GWP 20-year	AGWP 100-year (W m ⁻² yr kg ⁻¹)	GWP 100-year	AGTP 20-year (K kg ⁻¹)	GTP 20-year	AGTP 50-year (K kg ⁻¹)	GTP 50-year	AGTP 100-year (K kg ⁻¹)	GTP 100-year
HFC-1243zf	C ₂ F ₅ CH=CH ₂	7.0 days	0.01	1.37e-14	1	1.37e-14	<1	1.09e-16	<1	1.53e-17	<1	1.12e-17	<1
HFC-1345zfc	C ₂ F ₅ CH=CH ₂	7.6 days	0.01	1.15e-14	<1	1.15e-14	<1	9.19e-17	<1	1.30e-17	<1	9.48e-18	<1
3,3,4,4,5,5,6,6-Nonafluorohex-1-ene	C ₆ F ₉ CH=CH ₂	7.6 days	0.03	1.25e-14	<1	1.25e-14	<1	9.92e-17	<1	1.40e-17	<1	1.02e-17	<1
3,3,4,4,5,5,6,6,7,7,8,8-Tridecafluorooct-1-ene	C ₈ F ₁₃ CH=CH ₂	7.6 days	0.03	9.89e-15	<1	9.89e-15	<1	7.87e-17	<1	1.11e-17	<1	8.12e-18	<1
3,3,4,4,5,5,6,6,7,7,8,8,9,9,10,10,10-Hep-tadecafluorodec-1-ene	C ₈ F ₁₇ CH=CH ₂	7.6 days	0.03	8.52e-15	<1	8.52e-15	<1	6.79e-17	<1	9.57e-18	<1	7.00e-18	<1
Chlorocarbons and Hydrochlorocarbons													
Methyl chloroform	CH ₃ CCl ₃	5.0	0.07	1.44e-11	578	1.47e-11	160	2.17e-13	317	2.07e-14	34	1.22e-14	22
Carbon tetrachloride	CCl ₄	26.0	0.17	8.69e-11	3480	1.59e-10	1730	2.24e-12	3280	9.68e-13	1570	2.62e-13	479
Methyl chloride	CH ₃ Cl	1.0	0.01 ^a	1.12e-12	45	1.12e-12	12	9.93e-15	15	1.29e-15	2	9.20e-16	2
Methylene chloride	CH ₂ Cl ₂	0.4	0.03 ^b	8.18e-13	33	8.18e-13	9	6.78e-15	10	9.26e-16	2	6.72e-16	1
Chloroform	CHCl ₃	0.4	0.08	1.50e-12	60	1.50e-12	16	1.25e-14	18	1.70e-15	3	1.24e-15	2
1,2-Dichloroethane	CH ₂ ClCH ₂ Cl	65.0 days	0.01	8.24e-14	3	8.24e-14	<1	6.67e-16	<1	9.29e-17	<1	6.77e-17	<1
Bromocarbons, Hydrobromocarbons and Halons													
Methyl bromide	CH ₃ Br	0.8	0.004	2.16e-13	9	2.16e-13	2	1.87e-15	3	2.47e-16	<1	1.78e-16	<1
Methylene bromide	CH ₂ Br ₂	0.3	0.01	9.31e-14	4	9.31e-14	1	7.66e-16	1	1.05e-16	<1	7.65e-17	<1
Halon-1201	CHBrF ₂	5.2	0.15	3.37e-11	1350	3.45e-11	376	5.17e-13	756	4.96e-14	80	2.87e-14	52
Halon-1202	CBr ₂ F ₂	2.9	0.27	2.12e-11	848	2.12e-11	231	2.43e-13	356	2.61e-14	42	1.75e-14	32
Halon-1211	CBrClF ₂	16.0	0.29	1.15e-10	4590	1.60e-10	1750	2.70e-12	3950	6.98e-13	1130	1.62e-13	297
Halon-1301	CBF ₃	65.0	0.30	1.95e-10	7800	5.77e-10	6290	5.46e-12	7990	4.16e-12	6750	2.28e-12	4170
Halon-2301	CH ₂ BrCF ₃	3.4	0.14	1.59e-11	635	1.59e-11	173	1.96e-13	286	2.01e-14	33	1.32e-14	24
Halon-2311 / Halothane	CHBrClCF ₃	1.0	0.13	3.77e-12	151	3.77e-12	41	3.35e-14	49	4.34e-15	7	3.10e-15	6
Halon-2401	CHBrCF ₃	2.9	0.19	1.68e-11	674	1.68e-11	184	1.94e-13	283	2.07e-14	34	1.39e-14	25
Halon-2402	CBF ₂ CBF ₂	20.0	0.31	8.59e-11	3440	1.35e-10	1470	2.12e-12	3100	7.08e-13	1150	1.66e-13	304
Fully Fluorinated Species													
Nitrogen trifluoride	NF ₃	500.0	0.20	3.19e-10	12,800	1.47e-09	16,100	9.39e-12	13,700	1.02e-11	16,500	9.91e-12	18,100
Sulphur hexafluoride	SF ₆	3,200.0	0.57	4.37e-10	17,500	2.16e-09	23,500	1.29e-11	18,900	1.47e-11	23,800	1.54e-11	28,200
(Trifluoromethyl) sulphur pentafluoride	SF ₅ CF ₃	800.0	0.59	3.36e-10	13,500	1.60e-09	17,400	9.93e-12	14,500	1.10e-11	17,800	1.11e-11	20,200
Sulphuryl fluoride	SO ₂ F ₂	36.0	0.20	1.71e-10	6840	3.76e-10	4090	4.58e-12	6690	2.55e-12	4140	9.01e-13	1650
PFC-14	CF ₄	50,000.0	0.09	1.22e-10	4880	6.08e-10	6630	3.61e-12	5270	4.12e-12	6690	4.40e-12	8040
PFC-116	C ₂ F ₆	10,000.0	0.25	2.05e-10	8210	1.02e-09	11,100	6.07e-12	8880	6.93e-12	11,200	7.36e-12	13,500
PFC-c216	c-C ₃ F ₆	3,000.0	0.23 [*]	1.71e-10	6850	8.44e-10	9200	5.06e-12	7400	5.74e-12	9310	6.03e-12	11,000
PFC-218	C ₃ F ₈	2,600.0	0.28	1.66e-10	6640	8.16e-10	8900	4.91e-12	7180	5.56e-12	9010	5.83e-12	10,700
PFC-318	c-C ₄ F ₈	3,200.0	0.32	1.77e-10	7110	8.75e-10	9540	5.25e-12	7680	5.96e-12	9660	6.27e-12	11,500

(continued on next page)

Table 8.A.1 (continued)

Acronym, Common Name or Chemical Name	Chemical Formula	Lifetime (Years)	Radiative Efficiency (W m ⁻² ppb ⁻¹)	AGWP 20-year (W m ⁻² yr kg ⁻¹)	GWP 20-year	AGWP 100-year (W m ⁻² yr kg ⁻¹)	GWP 100-year	AGTP 20-year (K kg ⁻¹)	GTP 20-year	AGTP 50-year (K kg ⁻¹)	GTP 50-year	AGTP 100-year (K kg ⁻¹)	GTP 100-year
PFC-31-10	C ₄ F ₁₀	2,600.0	0.36	1.71e-10	6870	8.44e-10	9200	5.08e-12	7420	5.75e-12	9320	6.02e-12	11,000
Perfluorocyclopentene	c-C ₅ F ₈	31.0 days	0.08 ^f	1.71e-13	7	1.71e-13	2	1.37e-15	2	1.92e-16	<1	1.40e-16	<1
PFC-41-12	n-C ₅ F ₁₂	4,100.0	0.41	1.58e-10	6350	7.84e-10	8550	4.69e-12	6860	5.33e-12	8650	5.62e-12	10,300
PFC-51-14	n-C ₆ F ₁₄	3,100.0	0.44	1.47e-10	5890	7.26e-10	7910	4.35e-12	6370	4.94e-12	8010	5.19e-12	9490
PFC-61-16	n-C ₇ F ₁₆	3,000.0	0.50	1.45e-10	5830	7.17e-10	7820	4.31e-12	6290	4.88e-12	7920	5.13e-12	9380
PFC-71-18	C ₈ F ₁₈	3,000.0	0.55	1.42e-10	5680	6.99e-10	7620	4.20e-12	6130	4.76e-12	7710	5.00e-12	9140
PFC-91-18	C ₁₀ F ₁₈	2,000.0	0.55	1.34e-10	5390	6.59e-10	7190	3.98e-12	5820	4.49e-12	7290	4.68e-12	8570
Perfluorodecalin (cis)	Z-C ₁₀ F ₁₈	2,000.0	0.56	1.35e-10	5430	6.64e-10	7240	4.01e-12	5860	4.52e-12	7340	4.72e-12	8630
Perfluorodecalin (trans)	E-C ₁₀ F ₁₈	2,000.0	0.48	1.18e-10	4720	5.77e-10	6290	3.48e-12	5090	3.93e-12	6380	4.10e-12	7500
PFC-1114	CF ₂ =CF ₂	1.1 days	0.002	2.68e-16	<1	2.68e-16	<1	2.13e-18	<1	3.00e-19	<1	2.20e-19	<1
PFC-1216	CF ₃ CF=CF ₂	4.9 days	0.01	6.42e-15	<1	6.42e-15	<1	5.11e-17	<1	7.21e-18	<1	5.27e-18	<1
Perfluorobuta-1,3-diene	CF ₂ =CFCF=CF ₂	1.1 days	0.003	3.29e-16	<1	3.29e-16	<1	2.61e-18	<1	3.69e-19	<1	2.70e-19	<1
Perfluorobut-1-ene	CF ₃ CF ₂ CF=CF ₂	6.0 days	0.02	8.38e-15	<1	8.38e-15	<1	6.67e-17	<1	9.41e-18	<1	6.88e-18	<1
Perfluorobut-2-ene	CF ₃ CF=CFCF ₃	31.0 days	0.07	1.62e-13	6	1.62e-13	2	1.30e-15	2	1.82e-16	<1	1.33e-16	<1
Halogenated Alcohols and Ethers													
HFE-125	CHF ₂ OCF ₃	119.0	0.41	3.10e-10	12,400	1.14e-09	12,400	8.91e-12	13,000	8.14e-12	13,200	5.97e-12	10,900
HFE-134 (HG-00)	CHF ₂ OCHF ₂	24.4	0.44	2.90e-10	11,600	5.10e-10	5560	7.42e-12	10,800	3.02e-12	4900	7.83e-13	1430
HFE-143a	CH ₃ OCF ₃	4.8	0.18	4.72e-11	1890	4.80e-11	523	6.95e-13	1020	6.66e-14	108	3.99e-14	73
HFE-227ea	CF ₃ CHFOCF ₃	51.6	0.44	2.22e-10	8900	5.92e-10	6450	6.15e-12	8980	4.22e-12	6850	1.98e-12	3630
HCFE-235ca2 (enflurane)	CHF ₂ OCF ₂ CHFCl	4.3	0.41	5.30e-11	2120	5.35e-11	583	7.36e-13	1080	7.14e-14	116	4.44e-14	81
HCFE-235da2 (isoflurane)	CHF ₂ OCHClCF ₃	3.5	0.42	4.49e-11	1800	4.50e-11	491	5.62e-13	822	5.72e-14	93	3.73e-14	68
HFE-236ca	CHF ₂ OCF ₂ CHF ₂	20.8	0.56 ^g	2.42e-10	9710	3.89e-10	4240	6.03e-12	8820	2.10e-12	3400	4.98e-13	912
HFE-236ea2 (desflurane)	CHF ₂ OCHF ₂ CF ₃	10.8	0.45	1.39e-10	5550	1.64e-10	1790	2.93e-12	4280	4.64e-13	753	1.42e-13	260
HFE-236fa	CF ₃ CH ₂ OCF ₃	7.5	0.36	8.35e-11	3350	8.98e-11	979	1.53e-12	2240	1.68e-13	273	7.54e-14	138
HFE-245cb2	CF ₃ CF ₂ OCH ₃	4.9	0.33	5.90e-11	2360	6.00e-11	654	8.77e-13	1280	8.40e-14	136	4.99e-14	91
HFE-245fa1	CHF ₂ CH ₂ OCF ₃	6.6	0.31	7.22e-11	2900	7.59e-11	828	1.25e-12	1820	1.27e-13	206	6.35e-14	116
HFE-245fa2	CHF ₂ OCH ₂ CF ₃	5.5	0.36	7.25e-11	2910	7.45e-11	812	1.15e-12	1670	1.10e-13	179	6.21e-14	114
2,2,3,3,3-Pentafluoropropan-1-ol	CF ₃ CF ₂ CH ₂ OH	0.3	0.14	1.72e-12	69	1.72e-12	19	1.42e-14	21	1.95e-15	3	1.42e-15	3
HFE-254cb1	CH ₃ OCF ₂ CHF ₂	2.5	0.26	2.76e-11	1110	2.76e-11	301	2.99e-13	438	3.34e-14	54	2.28e-14	42
HFE-263fb2	CF ₃ CH ₂ OCH ₃	23.0 days	0.04	1.22e-13	5	1.22e-13	1	9.72e-16	1	1.37e-16	<1	9.98e-17	<1
HFE-263m1	CF ₃ OCH ₂ CH ₃	0.4	0.13	2.70e-12	108	2.70e-12	29	2.25e-14	33	3.06e-15	5	2.22e-15	4
3,3,3-Trifluoropropan-1-ol	CF ₃ CH ₂ CH ₂ OH	12.0 days	0.02	3.57e-14	1	3.57e-14	<1	2.85e-16	<1	4.01e-17	<1	2.93e-17	<1
HFE-329mcc2	CHF ₂ CF ₂ OCF ₂ CF ₃	22.5	0.53	1.68e-10	6720	2.81e-10	3070	4.23e-12	6180	1.59e-12	2580	3.93e-13	718
HFE-338mmz1	(CF ₃) ₂ CHOCHF ₂	21.2	0.44	1.48e-10	5940	2.40e-10	2620	3.70e-12	5410	1.31e-12	2130	3.14e-13	575

(Continued on next page)

Table 8.A.1 (continued)

Acronym, Common Name or Chemical Name	Chemical Formula	Lifetime (Years)	Radiative Efficiency (W m ⁻² ppb ⁻¹)	AGWP 20-year (W m ⁻² yr kg ⁻¹)	GWP 20-year	AGWP 100-year (W m ⁻² yr kg ⁻¹)	GWP 100-year	AGTP 20-year (K kg ⁻¹)	GTP 20-year	AGTP 50-year (K kg ⁻¹)	GTP 50-year	AGTP 100-year (K kg ⁻¹)	GTP 100-year
HFE-338mcf2	CF ₃ CH ₂ OCHF ₂ CF ₃	7.5	0.44	7.93e-11	3180	8.52e-11	929	1.45e-12	2120	1.60e-13	259	7.16e-14	131
Sevoflurane (HFE-347mmz1)	(CF ₃) ₂ CHOCHF ₂ F	2.2	0.32	1.98e-11	795	1.98e-11	216	2.06e-13	302	2.37e-14	38	1.64e-14	30
HFE-347mcc3 (HFE-7000)	CH ₃ OCHF ₂ CF ₂ CF ₃	5.0	0.35	4.78e-11	1910	4.86e-11	530	7.18e-13	1050	6.87e-14	111	4.05e-14	74
HFE-347mcf2	CHF ₂ CH ₂ OCHF ₂ CF ₃	6.6	0.42	7.45e-11	2990	7.83e-11	854	1.29e-12	1880	1.31e-13	212	6.55e-14	120
HFE-347pcf2	CHF ₂ CF ₂ OCH ₂ CF ₃	6.0	0.48 ^h	7.86e-11	3150	8.15e-11	889	1.30e-12	1900	1.27e-13	206	6.81e-14	124
HFE-347mmy1	(CF ₃) ₂ CFOCH ₃	3.7	0.32	3.32e-11	1330	3.33e-11	363	4.27e-13	624	4.28e-14	69	2.76e-14	51
HFE-356mcc3	CH ₃ OCHF ₂ CHF ₂ CF ₃	3.8	0.30	3.53e-11	1410	3.55e-11	387	4.60e-13	673	4.58e-14	74	2.94e-14	54
HFE-356mff2	CF ₃ CH ₂ OCH ₂ CF ₃	105.0 days	0.17	1.54e-12	62	1.54e-12	17	1.26e-14	18	1.74e-15	3	1.26e-15	2
HFE-356pcf2	CHF ₂ CH ₂ OCHF ₂ CHF ₂	5.7	0.37	6.40e-11	2560	6.59e-11	719	1.03e-12	1500	9.97e-14	162	5.50e-14	101
HFE-356pcf3	CHF ₂ OCH ₂ CF ₂ CHF ₂	3.5	0.38	4.08e-11	1640	4.09e-11	446	5.11e-13	747	5.20e-14	84	3.39e-14	62
HFE-356pcc3	CH ₃ OCHF ₂ CF ₂ CHF ₂	3.8	0.32	3.77e-11	1510	3.79e-11	413	4.91e-13	718	4.89e-14	79	3.14e-14	57
HFE-356mmz1	(CF ₃) ₂ CHOCH ₃	97.1 days	0.15	1.25e-12	50	1.25e-12	14	1.02e-14	15	1.41e-15	2	1.02e-15	2
HFE-365mcf3	CF ₃ CF ₂ CH ₂ OCH ₃	19.3 days	0.05	8.51e-14	3	8.51e-14	<1	6.80e-16	<1	9.56e-17	<1	6.99e-17	<1
HFE-365mcf2	CF ₃ CF ₂ OCH ₂ CH ₃	0.6	0.26 ⁱ	5.35e-12	215	5.35e-12	58	4.53e-14	66	6.10e-15	10	4.40e-15	8
HFE-374pcf2	CHF ₂ CF ₂ OCH ₂ CH ₃	5.0	0.30	5.65e-11	2260	5.75e-11	627	8.48e-13	1240	8.12e-14	132	4.79e-14	88
4,4,4-Trifluorobutane-1-ol	CF ₃ (CH ₂) ₂ CH ₂ OH	4.0 days	0.01	1.73e-15	<1	1.73e-15	<1	1.38e-17	<1	1.94e-18	<1	1.42e-18	<1
2,2,3,3,4,4,5,5-Octafluorocyclopentanol	-(CF ₂) ₄ CH(OH)-	0.3	0.16	1.18e-12	47	1.18e-12	13	9.67e-15	14	1.33e-15	2	9.69e-16	2
HFE-43-10pcccl24 (H-Galden 1040x, HG-11)	CHF ₂ OCHF ₂ OCF ₂ OCHF ₂	13.5	1.02	2.00e-10	8010	2.58e-10	2820	4.52e-12	6600	9.46e-13	1530	2.38e-13	436
HFE-449s1 (HFE-7100)	C ₆ F ₉ OCH ₃	4.7	0.36	3.80e-11	1530	3.86e-11	421	5.54e-13	809	5.32e-14	86	3.21e-14	59
n-HFE-7100	n-C ₆ F ₉ OCH ₃	4.7	0.42	4.39e-11	1760	4.45e-11	486	6.39e-13	934	6.14e-14	99	3.70e-14	68
i-HFE-7100	i-C ₆ F ₉ OCH ₃	4.7	0.35	3.68e-11	1480	3.73e-11	407	5.35e-13	783	5.14e-14	83	3.10e-14	57
HFE-569sf2 (HFE-7200)	C ₆ F ₉ OC ₂ H ₅	0.8	0.30	5.21e-12	209	5.21e-12	57	4.52e-14	66	5.97e-15	10	4.29e-15	8
n-HFE-7200	n-C ₆ F ₉ OC ₂ H ₅	0.8	0.35 ⁱ	5.92e-12	237	5.92e-12	65	5.14e-14	75	6.78e-15	11	4.87e-15	9
i-HFE-7200	i-C ₆ F ₉ OC ₂ H ₅	0.8	0.24	4.06e-12	163	4.06e-12	44	3.52e-14	52	4.65e-15	8	3.34e-15	6
HFE-236ca12 (HG-10)	CHF ₂ OCHF ₂ OCHF ₂	25.0	0.65	2.75e-10	11,000	4.91e-10	5350	7.06e-12	10,300	2.94e-12	4770	7.75e-13	1420
HFE-338pcc13 (HG-01)	CHF ₂ OCHF ₂ CF ₂ OCHF ₂	12.9	0.86	2.10e-10	8430	2.67e-10	2910	4.69e-12	6860	9.28e-13	1500	2.42e-13	442
1,1,1,3,3,3-Hexafluoropropan-2-ol	(CF ₃) ₂ CHOH	1.9	0.26	1.67e-11	668	1.67e-11	182	1.66e-13	243	1.97e-14	32	1.38e-14	25
HG-02	HF ₂ C-(OCF ₂ CF ₂) ₂ -OCF ₂ H	12.9	1.24 ⁱ	1.97e-10	7900	2.50e-10	2730	4.40e-12	6430	8.70e-13	1410	2.27e-13	415
HG-03	HF ₂ C-(OCF ₂ CF ₂) ₃ -OCF ₂ H	12.9	1.76 ⁱ	2.06e-10	8270	2.62e-10	2850	4.60e-12	6730	9.10e-13	1480	2.37e-13	434
HG-20	HF ₂ C-(OCF ₂) ₂ -OCF ₂ H	25.0	0.92 ⁱ	2.73e-10	10,900	4.86e-10	5300	7.00e-12	10,200	2.91e-12	4730	7.68e-13	1400
HG-21	HF ₂ C-OCF ₂ CF ₂ OCF ₂ OCF ₂ OCF ₂ H	13.5	1.71 ⁱ	2.76e-10	11,100	3.57e-10	3890	6.23e-12	9110	1.31e-12	2120	3.29e-13	602

(continued on next page)

Table 8.A.1 (continued)

Acronym, Common Name or Chemical Name	Chemical Formula	Lifetime (Years)	Radiative Efficiency (W m ⁻² ppb ⁻¹)	AGWP 20-year (W m ⁻² yr kg ⁻¹)	GWP 20-year	AGWP 100-year (W m ⁻² yr kg ⁻¹)	GWP 100-year	AGTP 20-year (K kg ⁻¹)	GTP 20-year	AGTP 50-year (K kg ⁻¹)	GTP 50-year	AGTP 100-year (K kg ⁻¹)	GTP 100-year
HG-30	HF ₂ C-(OCF ₂) ₃ -OCF ₂ H	25.0	1.65 ¹	3.77e-10	15,100	6.73e-10	7330	9.68e-12	14,100	4.03e-12	6530	1.06e-12	1940
1-Ethoxy-1,1,2,2,3,3,3-heptafluoropropane	CF ₃ CF ₂ CF ₂ OCH ₂ CH ₃	0.8	0.28 ¹	5.56e-12	223	5.56e-12	61	4.80e-14	70	6.36e-15	10	4.57e-15	8
Fluoroxene	CF ₃ CH ₂ OCH=CH ₂	3.6 days	0.01 ¹	4.97e-15	<1	4.97e-15	<1	3.95e-17	<1	5.58e-18	<1	4.08e-18	<1
1,1,2,2-Tetrafluoro-1-(fluoromethoxy)ethane	CH ₂ FOCF ₂ CF ₂ H	6.2	0.34 ¹	7.68e-11	3080	7.99e-11	871	1.29e-12	1880	1.28e-13	207	6.68e-14	122
2-Ethoxy-3,3,4,4,5-pentafluorotetrahydro-2,5-bis(1,2,2,2-tetrafluoro-1-(trifluoromethyl)ethyl)-furan	C ₁₂ H ₅ F ₁₉ O ₂	1.0	0.49 ¹	5.09e-12	204	5.09e-12	56	4.53e-14	66	5.86e-15	10	4.19e-15	8
Fluoro(methoxy)methane	CH ₃ OCH ₂ F	73.0 days	0.07 ⁹	1.15e-12	46	1.15e-12	13	9.34e-15	14	1.30e-15	2	9.46e-16	2
Difluoro(methoxy)methane	CH ₂ OCHF ₂	1.1	0.17 ⁹	1.32e-11	528	1.32e-11	144	1.18e-13	173	1.52e-14	25	1.08e-14	20
Fluoro(fluoromethoxy)methane	CH ₂ FOCH ₂ F	0.9	0.19 ⁹	1.20e-11	479	1.20e-11	130	1.05e-13	153	1.37e-14	22	9.84e-15	18
Difluoro(fluoromethoxy)methane	CH ₂ FOCHF ₂	3.3	0.30 ⁹	5.65e-11	2260	5.66e-11	617	6.88e-13	1010	7.11e-14	115	4.69e-14	86
Trifluoro(fluoromethoxy)methane	CH ₂ FOCF ₃	4.4	0.33 ⁹	6.82e-11	2730	6.89e-11	751	9.59e-13	1400	9.27e-14	150	5.72e-14	105
HG'-01	CH ₃ OCF ₂ CF ₂ OCH ₃	2.0	0.29	2.03e-11	815	2.03e-11	222	2.06e-13	301	2.42e-14	39	1.68e-14	31
HG'-02	CH ₂ O(CF ₂ CF ₂ O) ₂ CH ₃	2.0	0.56	2.16e-11	868	2.16e-11	236	2.19e-13	320	2.57e-14	42	1.79e-14	33
HG'-03	CH ₃ O(CF ₂ CF ₂ O) ₃ CH ₃	2.0	0.76	2.03e-11	812	2.03e-11	221	2.05e-13	299	2.41e-14	39	1.67e-14	31
HFE-329me3	CF ₃ CFHCF ₂ OCF ₃	40.0	0.48	1.79e-10	7170	4.17e-10	4550	4.85e-12	7090	2.89e-12	4690	1.12e-12	2040
3,3,4,4,5,5,6,6,7,7,7-Undecafluoroheptan-1-ol	CF ₃ (CF ₂) ₄ CH ₂ CH ₂ OH	20.0 days	0.06	3.91e-14	2	3.91e-14	<1	3.12e-16	<1	4.39e-17	<1	3.21e-17	<1
3,3,4,4,5,5,6,6,7,7,8,8,9,9-Pentadecafluorononan-1-ol	CF ₃ (CF ₂) ₆ CH ₂ CH ₂ OH	20.0 days	0.07	3.00e-14	1	3.00e-14	<1	2.40e-16	<1	3.37e-17	<1	2.46e-17	<1
3,3,4,4,5,5,6,6,7,7,8,8,9,9,10,10,11,11-Nonadecafluorodecan-1-ol	CF ₃ (CF ₂) ₈ CH ₂ CH ₂ OH	20.0 days	0.05	1.72e-14	<1	1.72e-14	<1	1.37e-16	<1	1.93e-17	<1	1.41e-17	<1
2-Chloro-1,1,2-trifluoro-1-methoxyethane	CH ₃ OCF ₂ CHCl	1.4	0.21	1.12e-11	449	1.12e-11	122	1.05e-13	153	1.31e-14	21	9.24e-15	17
PFPMIE (perfluoropolymethylisopropyl ether)	CF ₃ OCF(CF ₃)CF ₂ OCF ₂ OCF ₃	800.0	0.65	1.87e-10	7500	8.90e-10	9710	5.52e-12	8070	6.11e-12	9910	6.15e-12	11,300
HFE-216	CF ₃ OCF=CF ₂	8.4 days	0.02	1.92e-14	<1	1.92e-14	<1	1.53e-16	<1	2.15e-17	<1	1.58e-17	<1
Trifluoromethyl formate	HCOOCF ₃	3.5	0.31 ¹	5.37e-11	2150	5.39e-11	588	6.73e-13	984	6.85e-14	111	4.47e-14	82
Perfluoroethyl formate	HCOOCF ₂ CF ₃	3.5	0.44 ¹	5.30e-11	2130	5.32e-11	580	6.64e-13	971	6.76e-14	110	4.41e-14	81
Perfluoropropyl formate	HCOOCF ₂ CF ₂ CF ₃	2.6	0.50 ¹	3.45e-11	1380	3.45e-11	376	3.80e-13	555	4.19e-14	68	2.85e-14	52
Perfluorobutyl formate	HCOOCF ₂ CF ₂ CF ₂ CF ₃	3.0	0.56 ¹	3.59e-11	1440	3.59e-11	392	4.19e-13	613	4.45e-14	72	2.97e-14	54
2,2,2-Trifluoroethyl formate	HCOOCH ₂ CF ₃	0.4	0.16 ¹	3.07e-12	123	3.07e-12	33	2.55e-14	37	3.48e-15	6	2.52e-15	5
3,3,3-Trifluoropropyl formate	HCOOCH ₂ CH ₂ CF ₃	0.3	0.13 ¹	1.60e-12	64	1.60e-12	17	1.31e-14	19	1.80e-15	3	1.31e-15	2
1,2,2,2-Tetrafluoroethyl formate	HCOOCHFCF ₃	3.2	0.35 ¹	4.30e-11	1720	4.31e-11	470	5.17e-13	755	5.39e-14	87	3.57e-14	65
1,1,1,3,3,3-Hexafluoropropan-2-yl formate	HCOOCH(CF ₃) ₂	3.2	0.33 ¹	3.05e-11	1220	3.05e-11	333	3.66e-13	535	3.81e-14	62	2.53e-14	46
Perfluorobutyl acetate	CH ₃ COOCF ₂ CF ₂ CF ₂ CF ₃	21.9 days	0.12 ¹	1.52e-13	6	1.52e-13	2	1.21e-15	2	1.71e-16	<1	1.25e-16	<1
Perfluoropropyl acetate	CH ₃ COOCF ₂ CF ₂ CF ₃	21.9 days	0.11 ¹	1.59e-13	6	1.59e-13	2	1.27e-15	2	1.78e-16	<1	1.30e-16	<1
Perfluoroethyl acetate	CH ₃ COOCF ₂ CF ₃	21.9 days	0.10 ¹	1.89e-13	8	1.89e-13	2	1.51e-15	2	2.12e-16	<1	1.55e-16	<1
Trifluoromethyl acetate	CH ₃ COOCF ₃	21.9 days	0.07 ¹	1.90e-13	8	1.90e-13	2	1.52e-15	2	2.14e-16	<1	1.56e-16	<1

(continued on next page)

Table 8.A.1 (continued)

Acronym, Common Name or Chemical Name	Chemical Formula	Lifetime (Years)	Radiative Efficiency (W m ⁻² ppb ⁻¹)	AGWP 20-year (W m ⁻² yr kg ⁻¹)	GWP 20-year	AGWP 100-year (W m ⁻² yr kg ⁻¹)	GWP 100-year	AGTP 20-year (K kg ⁻¹)	GTP 20-year	AGTP 50-year (K kg ⁻¹)	GTP 50-year	AGTP 100-year (K kg ⁻¹)	GTP 100-year
Methyl carbonylfluoride	FCOOCH ₃	1.8	0.07 [†]	8.74e-12	350	8.74e-12	95	8.60e-14	126	1.03e-14	17	7.21e-15	13
1,1-Difluoroethyl carbonofluoride	FCOOCF ₂ CH ₃	0.3	0.17 [†]	2.46e-12	99	2.46e-12	27	2.02e-14	30	2.78e-15	5	2.02e-15	4
1,1-Difluoroethyl 2,2,2-trifluoroacetate	CF ₃ COOCF ₂ CH ₃	0.3	0.27 [†]	2.83e-12	113	2.83e-12	31	2.33e-14	34	3.20e-15	5	2.32e-15	4
Ethyl 2,2,2-trifluoroacetate	CF ₃ COOCH ₂ CH ₃	21.9 days	0.05 [†]	1.26e-13	5	1.26e-13	1	1.00e-15	1	1.41e-16	<1	1.03e-16	<1
2,2,2-Trifluoroethyl 2,2,2-trifluoroacetate	CF ₃ COOCH ₂ CF ₃	54.8 days	0.15 [†]	6.27e-13	25	6.27e-13	7	5.06e-15	7	7.07e-16	1	5.15e-16	<1
Methyl 2,2,2-trifluoroacetate	CF ₃ COOCH ₃	0.6	0.18 [†]	4.80e-12	192	4.80e-12	52	4.08e-14	60	5.47e-15	9	3.95e-15	7
Methyl 2,2-difluoroacetate	HCF ₂ COOCH ₃	40.1 days	0.05 [†]	3.00e-13	12	3.00e-13	3	2.41e-15	4	3.38e-16	<1	2.47e-16	<1
Difluoromethyl 2,2,2-trifluoroacetate	CF ₃ COOCHF ₂	0.3	0.24 [†]	2.48e-12	99	2.48e-12	27	2.04e-14	30	2.81e-15	5	2.04e-15	4
2,2,3,3,4,4,4-Heptafluorobutan-1-ol	C ₃ F ₇ CH ₂ OH	0.6	0.20	3.10e-12	124	3.10e-12	34	2.61e-14	38	3.52e-15	6	2.55e-15	5
1,1,2-Trifluoro-2-(trifluoromethoxy)-ethane	CHF ₂ CHFOCF ₃	9.8	0.35	9.91e-11	3970	1.14e-10	1240	2.03e-12	2960	2.88e-13	467	9.74e-14	178
1-Ethoxy-1,1,2,3,3,3-hexafluoropropane	CF ₃ CHFCF ₂ OCH ₂ CH ₃	0.4	0.19	2.14e-12	86	2.14e-12	23	1.77e-14	26	2.43e-15	4	1.76e-15	3
1,1,1,2,2,3,3-Heptafluoro-3-(1,2,2,2-tetrafluoroethoxy)-propane	CF ₃ CF ₂ CF ₂ OCHFCF ₃	67.0	0.58	1.98e-10	7940	5.95e-10	6490	5.57e-12	8140	4.29e-12	6960	2.39e-12	4380
2,2,3,3-Tetrafluoro-1-propanol	CHF ₂ CF ₂ CH ₂ OH	91.3 days	0.11	1.19e-12	48	1.19e-12	13	9.72e-15	14	1.35e-15	2	9.79e-16	2
2,2,3,3,4,4-Hexafluoro-1-butanol	CF ₃ CHFCF ₂ CH ₂ OH	94.9 days	0.19	1.56e-12	63	1.56e-12	17	1.27e-14	19	1.76e-15	3	1.28e-15	2
2,2,3,3,4,4-Heptafluoro-1-butanol	CF ₃ CF ₂ CF ₂ CH ₂ OH	0.3	0.16	1.49e-12	60	1.49e-12	16	1.23e-14	18	1.69e-15	3	1.23e-15	2
1,1,2,2-Tetrafluoro-3-methoxy-propane	CHF ₂ CF ₂ CH ₂ OCH ₃	14.2 days	0.03	4.82e-14	2	4.82e-14	<1	3.84e-16	<1	5.41e-17	<1	3.96e-17	<1
perfluoro-2-methyl-3-pentanone	CF ₃ CF ₂ C(O)CF(CF ₃) ₂	7.0 days	0.03	9.14e-15	<1	9.14e-15	<1	7.27e-17	<1	1.03e-17	<1	7.51e-18	<1
3,3,3-Trifluoro-propanal	CF ₃ CH ₂ CHO	2.0 days	0.004	9.86e-16	<1	9.86e-16	<1	7.84e-18	<1	1.11e-18	<1	8.10e-19	<1
2-Fluoroethanol	CH ₃ FCH ₂ OH	20.4 days	0.02	8.07e-14	3	8.07e-14	<1	6.45e-16	<1	9.07e-17	<1	6.63e-17	<1
2,2-Difluoroethanol	CHF ₂ CH ₂ OH	40.0 days	0.04	2.78e-13	11	2.78e-13	3	2.23e-15	3	3.12e-16	<1	2.28e-16	<1
2,2,2-Trifluoroethanol	CF ₃ CH ₂ OH	0.3	0.10	1.83e-12	73	1.83e-12	20	1.50e-14	22	2.07e-15	3	1.50e-15	3
1,1'-Oxybis[2-(difluoromethoxy)-1,1,2,2-tetrafluoroethane	HCF ₂ O(CF ₂ CF ₂ O) ₂ CF ₂ H	26.0	1.15 [*]	2.47e-10	9910	4.51e-10	4920	6.38e-12	9320	2.75e-12	4460	7.45e-13	1360
1,1,3,3,4,4,6,6,7,7,9,10,10,12,12,12-hexa-decafluoro-2,5,8,11-tetraoxadodecane	HCF ₂ O(CF ₂ CF ₂ O) ₃ CF ₂ H	26.0	1.43 [*]	2.26e-10	9050	4.12e-10	4490	5.83e-12	8520	2.51e-12	4080	6.81e-13	1250
1,1,3,3,4,4,6,6,7,7,9,10,10,12,12,13,13,15,15-eico-safluoro-2,5,8,11,14-Pentaoxapentadecane	HCF ₂ O(CF ₂ CF ₂ O) ₄ CF ₂ H	26.0	1.46 [*]	1.83e-10	7320	3.33e-10	3630	4.71e-12	6880	2.03e-12	3300	5.50e-13	1010

Notes:

For CH₄ we estimate an uncertainty of ±30% and ±40% for 20- and 100-year time horizon, respectively (for 90% uncertainty range). The uncertainty is dominated by AGWP for CO₂ and indirect effects. The uncertainty in GWP for N₂O is estimated to ±20% and ±30% for 20- and 100-year time horizon, with the largest contributions from CO₂. The uncertainty in GWP for HFC-134a is estimated to ±25% and ±35% for 20- and 100-year time horizons while for CFC-11 the GWP the corresponding numbers are approximately ±20% and ±35% (not accounting for the indirect effects). For CFC-12 the corresponding numbers are ±20 and ±30. The uncertainties estimated for HFC-134a and CFC-11 are assessed as representative for most other gases with similar or longer lifetimes. For shorter-lived gases, the uncertainties will be larger. For GTP, few estimates are available in the literature. The uncertainty is assessed to be of the order of ±75% for the methane GTP₁₀₀.

* No single lifetime can be given. The impulse response function for CO₂ from Joos et al. (2013) has been used. See also Supplementary Material Section 8.SM.11.

† Perturbation lifetime is used in calculation of metrics, not the lifetime of the atmospheric burden.

(Continued on next page)

Table 8.A.1 Notes (continued)

- † Metric values for CH₄ of fossil origin include the oxidation to CO₂ (based on Boucher et al., 2009). In applications of these values, inclusion of the CO₂ effect of fossil methane must be done with caution to avoid any double-counting because CO₂ emissions numbers are often based on total carbon content. Methane values without the CO₂ effect from fossil methane are thus appropriate for fossil methane sources for which the carbon has been accounted for elsewhere, or for biospheric methane sources for which there is a balance between CO₂ taken up by the biosphere and CO₂ produced from CH₄ oxidization. The addition effect on GWP and GTP represents lower limits from Boucher et al. (2009) and assume 50% of the carbon is deposited as formaldehyde to the surface and is then lost. The upper limit in Boucher et al. (2009) made the assumption that this deposited formaldehyde was subsequently further oxidized to CO₂.
- a RE is unchanged since AR4.
 - b RE is unchanged since AR4 except the absolute forcing is increased by a factor of 1.04 to account for the change in the recommended RE of CFC-11.
 - c Based on Rajakumar et al. (2006) (lifetime correction factor has been applied to account for non-homogeneous horizontal and vertical mixing).
 - d Based on instantaneous RE from Baasandorj et al. (2010); Baasandorj et al. (2011) (correction factors have been applied to account for stratospheric temperature adjustment and non-homogeneous horizontal and vertical mixing).
 - e Based on instantaneous RE from *ab initio* study of Bravo et al. (2010) (a factor 1.10 has been applied to account for stratospheric temperature adjustment).
 - f Based on average instantaneous RE reported in literature (Vasekova et al., 2006; Bravo et al., 2010) (correction factors have been applied to account for stratospheric temperature adjustment and non-homogeneous horizontal and vertical mixing).
 - g Based on instantaneous RE from *ab initio* studies of Blowers et al. (2007, 2008) (correction factors have been applied to account for stratospheric temperature adjustment and non-homogeneous horizontal and vertical mixing).
 - h Based on instantaneous RE from Heathfield et al. (1998) (correction factors have been applied to account for stratospheric temperature adjustment and non-homogeneous horizontal and vertical mixing).
 - i Note that calculation of RE is based on calculated (*ab initio*) absorption cross-section and uncertainties are therefore larger than for calculations using experimental absorption cross section.
 - j Based on instantaneous RE from Javadi et al. (2007) (correction factors have been applied to account for stratospheric temperature adjustment and non-homogeneous horizontal and vertical mixing).
 - k Based on instantaneous RE from Andersen et al. (2010) (correction factors have been applied to account for stratospheric temperature adjustment and non-homogeneous horizontal and vertical mixing).

The GTP values are calculated with a temperature impulse response function taken from Boucher and Reddy (2008). See also Supplementary Material Section 8.SM.11.

Table 8.A.2 | Halocarbon indirect GWPs from ozone depletion using the EESC-based method described in WMO (2011), adapted from Daniel et al. (1995). A radiative forcing in year 2011 of -0.15 (-0.30 to 0.0) $W m^{-2}$ relative to preindustrial times is used (see Section 8.3.3). Uncertainty on the indirect AGWPs due to the ozone forcing uncertainty is $\pm 100\%$.

Gas	GWP ₁₀₀
CFC-11	-2640
CFC-12	-2100
CFC-113	-2150
CFC-114	-914
CFC-115	-223
HCFC-22	-98
HCFC-123	-37
HCFC-124	-46
HCFC-141b	-261
HCFC-142b	-152
CH ₃ CCl ₃	-319
CCl ₄	-2110
CH ₃ Br	-1250
Halon-1211	-19,000
Halon-1301	-44,500
Halon-2402	-32,000
HCFC-225ca	-40
HCFC-225cb	-60

Table 8.A.3 | GWP and GTP for NO_x from surface sources for time horizons of 20 and 100 years from the literature. All values are on a per kilogram of nitrogen basis. Uncertainty for numbers from Fry et al. (2012) and Collins et al. (2013) refer to $1-\alpha$. For the reference gas CO₂, RE and IRF from AR4 are used in the calculations. The GWP₁₀₀ and GTP₁₀₀ values can be scaled by 0.94 and 0.92, respectively, to account for updated values for the reference gas CO₂. For 20 years the changes are negligible.

	GWP		GTP	
	H = 20	H = 100	H = 20	H = 100
NO _x East Asia ^a	6.4 (± 38.1)	-5.3 (± 11.5)	-55.6 (± 23.8)	-1.3 (± 2.1)
NO _x EU + North Africa ^a	-39.4 (± 17.5)	-15.6 (± 5.8)	-48.0 (± 14.9)	-2.5 (± 1.3)
NO _x North America ^a	-2.4 (± 30.3)	-8.2 (± 10.3)	-61.9 (± 27.8)	-1.7 (± 2.1)
NO _x South Asia ^a	-40.7 (± 88.3)	-25.3 (± 29.0)	-124.6 (± 67.4)	-4.6 (± 5.1)
NO _x four above regions ^a	-15.9 (± 32.7)	-11.6 (± 10.7)	-62.1 (± 26.2)	-2.2 (± 2.1)
Mid-latitude NO _x ^c	-43 to +23	-18 to +1.6	-55 to -37	-2.9 to -0.02
Tropical NO _x ^c	43 to 130	-28 to -10	-260 to -220	-6.6 to -5.4
NO _x global ^b	19	-11	-87	-2.9
NO _x global ^d	-108 \pm 35	-31 \pm 10		
	-335 \pm 110	-95 \pm 31		
	-560 \pm 279	-159 \pm 79		

Notes:

^a Fry et al. (2012) (updated by including stratospheric H₂O) and Collins et al. (2013).

^b Fuglestedt et al. (2010); based on Wild et al. (2001).

^c Fuglestedt et al. (2010).

^d Shindell et al. (2009). Three values are given: First, without aerosols, second, direct aerosol effect included (sulfate and nitrate), third, direct and indirect aerosol effects included. Uncertainty ranges from Shindell et al. (2009) are given for 95% confidence levels.

Table 8.A.4 | GWP and GTP for CO for time horizons of 20 and 100 years from the literature. Uncertainty for numbers from Fry et al. (2012) and Collins et al. (2013) refer to $1-\sigma$. For the reference gas CO₂, RE and IRF from AR4 are used in the calculations. The GWP₁₀₀ and GTP₁₀₀ values can be scaled by 0.94 and 0.92, respectively, to account for updated values for the reference gas CO₂. For 20 years the changes are negligible.

	GWP		GTP	
	H = 20	H = 100	H = 20	H = 100
CO East Asia ^a	5.4 (±1.7)	1.8 (±0.6)	3.5 (±1.3)	0.26 (±0.12)
CO EU + North Africa ^a	4.9 (±1.5)	1.6 (±0.5)	3.2 (±1.2)	0.24 (±0.11)
CO North America ^a	5.6 (±1.8)	1.8 (±0.6)	3.7 (±1.3)	0.27 (±0.12)
CO South Asia ^a	5.7 (±1.3)	1.8 (±0.4)	3.4 (±1.0)	0.27 (±0.10)
CO four regions above ^a	5.4 (±1.6)	1.8 (±0.5)	3.5 (±1.2)	0.26 (±0.11)
CO global ^b	6 to 9.3	2 to 3.3	3.7 to 6.1	0.29 to 0.55
CO global ^c	7.8 ± 2.0	2.2 ± 0.6		
	11.4 ± 2.9	3.3 ± 0.8		
	18.6 ± 8.3	5.3 ± 2.3		

Notes:

^a Fry et al. (2012) (updated by including stratospheric H₂O) and Collins et al. (2013).

^b Fuglestedt et al. (2010).

^c Shindell et al. (2009). Three values are given: First, without aerosols, second, direct aerosol effect included, third, direct and indirect aerosol effects included. Uncertainty ranges from Shindell et al. (2009) are given for 95% confidence levels.

Table 8.A.5 | GWP and GTP for VOCs for time horizons of 20 and 100 years from the literature. Uncertainty for numbers from Fry et al. (2012) and Collins et al. (2013) refer to $1-\sigma$. For the reference gas CO₂, RE and IRF from AR4 are used in the calculations. The GWP₁₀₀ and GTP₁₀₀ values can be scaled by 0.94 and 0.92, respectively, to account for updated values for the reference gas CO₂. For 20 years the changes are negligible.

	GWP		GTP	
	H = 20	H = 100	H = 20	H = 100
VOC East Asia ^a	16.3 (±6.4)	5.0 (±2.1)	8.4 (±4.6)	0.7 (±0.4)
VOC EU + North Africa ^a	18.0 (±8.5)	5.6 (±2.8)	9.5 (±6.5)	0.8 (±0.5)
VOC North America ^a	16.2 (±9.2)	5.0 (±3.0)	8.6 (±6.4)	0.7 (±0.5)
VOC South Asia ^a	27.8 (±5.6)	8.8 (±1.9)	15.7 (±5.0)	1.3 (±0.5)
VOC four regions above	18.7 (±7.5)	5.8 (±2.5)	10.0 (±5.7)	0.9 (±0.5)
VOC global ^b	14	4.5	7.5	0.66

Notes:

^a Fry et al. (2012) (updated by including stratospheric H₂O) and Collins et al. (2013).

^b Fuglestedt et al. (2010) based on Collins et al. (2002).

The values are given on a per kilogram of C basis.

Table 8.A.6 | GWP and GTP from the literature for BC and OC for time horizons of 20 and 100 years. For the reference gas CO₂, RE and IRF from AR4 are used in the calculations. The GWP₁₀₀ and GTP₁₀₀ values can be scaled by 0.94 and 0.92, respectively, to account for updated values for the reference gas CO₂. For 20 years the changes are negligible.

	GWP		GTP	
	H = 20	H = 100	H = 20	H = 100
BC total, global ^c	3200 (270 to 6200)	900 (100 to 1700)	920 (95 to 2400)	130 (5 to 340)
BC (four regions) ^d	1200 ± 720	345 ± 207	420 ± 190	56 ± 25
BC global ^a	1600	460	470	64
BC aerosol–radiation interaction +albedo, global ^b	2900 ± 1500	830 ± 440		
OC global ^a	–240	–69	–71	–10
OC global ^b	–160 (–60 to –320)	–46 (–18 to –19)		
OC (4 regions) ^d	–160 ± 68	–46 ± 20	–55 ± 16	–7.3±2.1

Notes:

^a Fuglestedt et al. (2010).

^b Bond et al. (2011). Uncertainties for OC are asymmetric and are presented as ranges.

^c Bond et al. (2013). Metric values are given for total effect.

^d Collins et al. (2013). The four regions are East Asia, EU + North Africa, North America and South Asia (as also given in Fry et al., 2012). Only aerosol–radiation interaction is included.

Exhibit 13

Greenhouse Gas Emissions and Fuel Use within the Natural Gas Supply Chain – Sankey Diagram Methodology

James Bradbury, Zachary Clement, and Adrian Down

Office of Energy Policy and Systems Analysis

U.S. Department of Energy

July, 2015

Acknowledgements

The authors are grateful for excellent technical reviews and other contributions provided by several individuals. Within the Department of Energy, input was provided by Judi Greenwald, Elke Hodson and Diana Bauer. External reviewers included the following individuals: Melissa Weitz, Environmental Protection Agency; Tim Skone, National Energy Technology Laboratory; Garvin Heath, National Renewable Energy Laboratory; Joel Bluestein, ICF International; Richard Meyer, American Gas Association; Fiji George, Southwestern Energy; Ramon Alvarez, Environmental Defense Fund. Amy Sweeney, from the Energy Information Administration, was particularly helpful with understanding the survey forms that are used for EIA's natural gas system data. Finally, Matt Antes, Anna Mosby and Keith Jamison of Energetics Incorporated provided editing support and technical review. These reviewers helped to make this report as technically sound as possible; however, any remaining errors or omissions are those of the authors.

Contents

Overview	4
1.0 Introduction and Terminology	4
1.1 Data Sources and Uncertainty	5
1.2 Natural Gas Composition	5
2.0 Emissions and Fuel Use throughout Natural Gas Infrastructure, by Volume	6
2.1 Production.....	6
2.2 Processing	8
2.3 Transmission and Storage	8
2.4 Distribution	9
2.5 Consumer End Use	9
3.0 Greenhouse Gas Emissions from the Natural Gas System, by Mass	9
3.1 Production.....	10
3.2 Processing	11
3.3 Transmission and Storage	12
3.4 Distribution	13
3.5 Consumer End Use Combustion	13
<i>Appendix 1: Natural gas flaring associated with crude oil production</i>	<i>14</i>
<i>Appendix 2: Natural gas mass and volume conversions.....</i>	<i>15</i>
<i>Appendix 3: CO₂ emissions from natural gas combustion</i>	<i>16</i>
A3.1 CO ₂ emissions from combustion of methane in natural gas	16
A3.2 CO ₂ emissions from combustion of non-methane hydrocarbons in natural gas	16
A3.3 Total CO ₂ emissions from natural gas combustion.....	16
<i>Appendix 4: Data from figures</i>	<i>18</i>
Endnotes	20

Overview

Substantial quantities of methane (CH₄) and carbon dioxide (CO₂) emissions occur throughout the natural gas infrastructure. In 2012, approximately 155 million metric tons CO₂ equivalent (MMt CO₂e) of CH₄ were emitted as a result of inadvertent leakage and routine venting. In the same year, the natural gas industry emitted a similar amount of CO₂ (approximately 164 MMt CO₂e), primarily from the combustion of natural gas that is used as a fuel for compression and flared gas but also from the removal of non-hydrocarbon gases from raw gas by processing plants. Combined, these “midstream” and “upstream” emissions from natural gas infrastructure accounted for approximately 20% of total 2012 greenhouse gas (GHG) emissions from natural gas systems; the other 80% of GHG emissions from natural gas result from gas combustion by end-use consumers. The Sankey diagrams in this paper examine these emissions in some detail, focusing in particular on the production, processing, transmission and storage, and distribution segments of natural gas infrastructure.

1.0 Introduction and Terminology

Natural gas infrastructure produces, processes, transports, stores, and distributes natural gas. However, not all of the raw natural gas reaches consumers. For example, when raw gas is extracted from geologic reservoirs through production processes, it frequently contains impurities that need to be removed before it is marketable for use as a fuel or feedstock. Furthermore, as natural gas travels through production, processing, transmission, distribution, and compression facilities, small portions are routinely used as fuel, vented, flared, or inadvertently leaked to the atmosphere. This paper describes the analytical and methodological bases for three diagrams of the losses and emissions from these processes, in terms of natural gas volumes and associated GHG emissions.

Common terminology used throughout this paper includes the following:

- **Natural gas system:** Natural gas production, transmission and storage, processing, distribution, and end-use consumption.
- **Natural gas infrastructure:** Natural gas production, transmission and storage, processing, and distribution. This term does not include consumption of natural gas by end-use consumers.
- **Fuel use:** Natural gas’s use as a fuel at various points throughout natural gas infrastructure. The primary use is to drive natural gas compression equipment, through combustion in engines or turbines. More than 8% of U.S. natural gas consumption in 2012 was used in gas infrastructure as “lease and plant fuel” and for “pipeline and distribution use.”¹
- **Venting:** The deliberate or routine release of natural gas into the atmosphere. Venting includes blowdowns (e.g., when gas is evacuated from a section of pipeline for the purpose of conducting tests, repairs, or maintenance), emissions from pneumatic devices (which operate natural gas-driven controllers and natural gas-driven pumps, both of which emit natural gas as a function of routine operation), and the emissions of non-hydrocarbon gases (including CO₂), which are removed from the raw natural gas during processing.

- **Flaring:** A method of disposing of natural gas that cannot be economically used on site or transported via pipeline. The gas is burned using flares, usually at production sites or at gas processing plants (EIA, 2015).
- **Fugitive emissions:** Leaked natural gas, which includes losses of natural gas from natural gas infrastructure that occur inadvertently as a result of malfunctioning or aging equipment (e.g., damaged seals or loose fittings).

Three Sankey diagrams* are presented below, along with discussion of the data, calculations, and assumptions that were used to develop the diagrams. The diagrams illustrate the scale of emissions from various parts of the natural gas system, with a particular focus on emissions from natural gas infrastructure upstream of end-use consumers. The first diagram (Figure 1) presents this information in terms of volume of natural gas, measured in billion cubic feet (Bcf). The second and third diagrams (Figures 2 and 3) present comparable information in terms of GHG emissions and CO₂e units. For the purposes of this analysis, natural gas infrastructure is broken into four distinct stages/segments upstream of end-use consumers: production, processing, transmission and storage, and distribution.† For the purposes of this analysis, production facilities include gathering and boosting equipment that enables the transportation of natural gas from the well pad to processing facilities.‡ The term “end-use consumers” includes the residential, commercial, industrial, vehicle fuel, and electric power sectors.

1.1 Data Sources and Uncertainty

All of the data used for this analysis are derived from the U.S. Energy Information Administration (EIA) website and the U.S. Environmental Protection Agency’s (EPA’s) 2014 GHG inventory report. The specific data used for each part of the analysis are discussed in detail below. This analysis includes only data from 2012, which are the most recently available. EPA estimates the 95% confidence interval for their estimate of 2012 CH₄ emissions from the natural gas sector to be 125.2 to 201.1 MMT (equivalent to teragrams [Tg]) CO₂e, which is -19% to +30% of their most probable value of 154.6 MMT CO₂e.^{2,5} EIA does not provide uncertainty estimates for their data. Though the data presented here represent the vast majority of GHG emissions from natural gas infrastructure, this analysis does not constitute a life cycle analysis. For example, emissions associated with diesel equipment operating at production sites or electricity generation that powers electric drive natural gas compressors are not accounted for here.

1.2 Natural Gas Composition

Raw natural gas comprises methane and other gases. The composition of raw natural gas varies regionally and is dependent on the source of the gas. Gas composition varies depending on the geology

* Sankey diagrams are a type of flow diagram in which the width of the arrows is proportionate to the size of the represented flow. In this case, the flow quantities represent emissions.

† This analysis does not include transfers to and from natural gas storage, as net transfers to and from storage are assumed to balance over time.

‡ This scope is consistent with how emissions are reported by EPA and also how fuel use (i.e., “lease fuel”) is reported by the EIA.

⁵ As explained below, this assumes a global warming potential of 25 for methane.

of the source rock (regional or play** -specific results are beyond the scope of this study).³ Table 1 shows nationally averaged natural gas composition, by mass, before and after processing to refine the gas and increase the methane content (“production” and “pipeline quality” natural gas, respectively).

Table 1: Natural gas composition by mass, before and after processing.⁴

Component	Production	Pipeline Quality
CH ₄ (Methane)	78.3%	92.8%
NMVOOC (Non-Methane Volatile Organic Compounds)	17.8%	5.54%
N ₂ (Nitrogen)	1.77%	0.55%
CO ₂ (Carbon Dioxide)	1.51%	0.47%
H ₂ S (Hydrogen Sulfide)	0.5%	0.01%
H ₂ O (Water)	0.12%	0.01%

2.0 Emissions and Fuel Use throughout Natural Gas Infrastructure, by Volume

This section describes the methodology that was used to calculate the volume of natural gas that is used as fuel, vented, flared, and leaked from each segment of natural gas infrastructure. Figure 1 shows that the volume of natural gas that is emitted or used as fuel by the infrastructure itself is much smaller than the volume that is delivered to consumers. Note that data in the text and figures may not always match exactly, due to rounding.

2.1 Production

2.1.1 Flaring and venting

At the production stage, the volume of natural gas that was flared or vented in 2012 was 212.848 Bcf.^{5,††} Flaring and venting take place at multiple stages throughout natural gas infrastructure. However, EIA only reports flared and/or vented gas from the production segment.^{††} The volume of natural gas that EIA reports as flared, which is used in this analysis, includes some natural gas that is produced from crude oil wells. The percentage of EIA’s natural gas flaring volume attributable to crude oil production varies by year, but could be over 50%, as shown in Appendix 1.

** A “play” is defined as a set of known or postulated oil and or gas accumulations sharing similar geologic, geographic, and temporal properties, such as source rock, migration pathways, timing, trapping mechanism, and hydrocarbon type.

†† The United Nations Global Gas Flaring Reduction program reported 7.1 bcm, or 251 Bcf, of flared gas in the United States in 2011, as estimated from satellite data.

†† EIA reports volumes of “vented and flared” natural gas. However, EPA reports methane emissions associated with vented natural gas separately from CO₂ emissions associated with flared natural gas. Therefore, Figure 1 includes some overlap (i.e., double counting) with respect to the relatively small *volumes* of “flared and vented” emissions (which are from EIA) and the methane emissions (which are converted from EPA data). This is an issue only for volumes of natural gas presented in Figure 1; subsequent figures do not include any double-counted data.

2.1.2 Methane emissions

EPA reports that 1,992 gigagrams (Gg) of methane were emitted from the production segment of natural gas infrastructure in 2012.⁶ This mass of methane is converted to a corresponding volume of natural gas as follows. First, mass of methane is converted to mass of natural gas using the methane composition in the “production” column of Table 1:

$$1,992 \text{ Gg methane} / 0.783 = 2,544 \text{ Gg natural gas}$$

Mass of natural gas is then converted to volume using the conversion factors (see Appendix 2 for development):

$$2,544 \text{ Gg natural gas} * 41.239 = 82,148 \text{ MMcf natural gas} = 82.15 \text{ Bcf natural gas}$$

Figure 1. Volumes of natural gas consumption for fuel, emissions, and delivered to consumers, 2012^{7,8,§§}

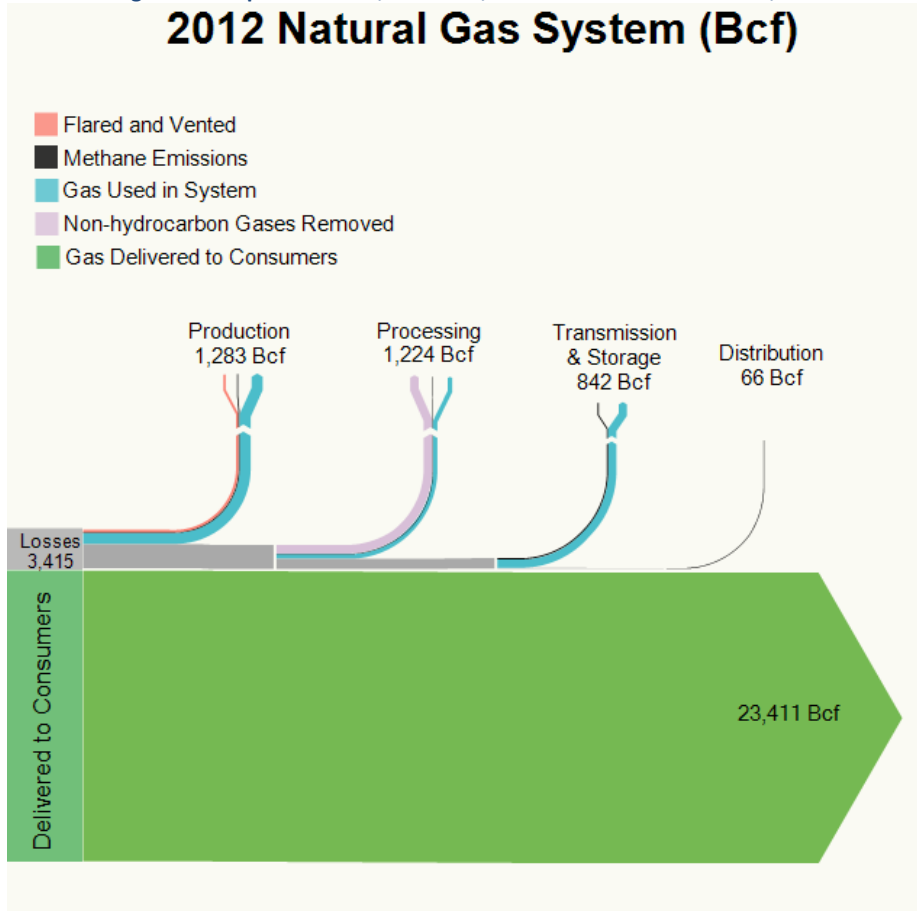


Diagram includes natural gas at varying stages of composition. The hydrocarbon composition of natural gas changes with the removal of non-hydrocarbon gases during the processing stage. This change in composition (and volume) resulting from processing is represented in the diagram with the removal of non-hydrocarbon gases.

^{§§} Natural gas used in the production stage (i.e., “lease fuel”) includes some activities associated with oil wells. Flaring and venting data also reflect these activities occurring at both oil and natural gas wells. Otherwise, all data in Figure 1 reflect fuel use and emissions that are exclusively associated with the natural gas system. For context, note that EIA estimated that “associated natural gas” production (gas produced along with oil) made up roughly 10% of total U.S. dry gas production in 2012 (according to the 2014 Annual Energy Outlook).

2.1.3 Natural gas fuel use

In addition to consumption by the electric power sector and other end-use consumers, EIA's website reports "Natural Gas Consumption by End Use" for "lease fuel," "plant fuel," and "pipeline and distribution use." EIA defines lease fuel as "natural gas used in well, field, and lease operations, such as gas used in drilling operations, heaters, dehydrators, and field compressors." For the purpose of the following analysis, "lease fuel" is considered to be natural gas combusted within the production stage of natural gas infrastructure. The volume of natural gas that was combusted as lease fuel in 2012 was 987,957 MMcf (987.957 Bcf).⁹

2.2 Processing

2.2.1 Non-hydrocarbon gas removal

The volume of non-hydrocarbon gases (CO₂, helium, hydrogen sulfide, nitrogen, etc.) that were removed during natural gas processing in 2012 was 768.598 Bcf.¹⁰ These non-hydrocarbon gases are part of the raw natural gas that is extracted at wellheads, and they are removed through processing to reduce impurities and to raise the hydrocarbon content of pipeline-quality natural gas. Non-hydrocarbon gases removed during processing are typically vented to the atmosphere, which can include venting of CO₂ (included in red line in Figure 1).

2.2.2 Methane emissions

EPA reports that 892 Gg of methane was emitted by natural gas processing facilities in 2012.¹¹ This volume of methane was converted to a volume of natural gas using the same conversion process used for fugitive emissions from the production sector (Section 2.1.2), the only difference being the different hydrocarbon composition of processed natural gas. The composition of process-stage natural gas is assumed to be a weighted average of pre-processed (32%) and post-processed (68%) natural gas:¹²

$$892 \text{ Gg methane} / (0.783 * 0.32 + 0.928 * 0.68) = 961 \text{ Gg natural gas}$$

$$961 \text{ Gg natural gas} * (41.239 * 0.32 + 49.703 * 0.68) = 47,550 \text{ MMcf natural gas} = 47.55 \text{ Bcf natural gas}$$

2.2.3 Natural gas fuel use for processing

EIA defines "plant fuel" as "natural gas used as fuel in natural gas processing plants." For the purpose of this analysis, "plant fuel" is considered to be the natural gas combusted by processing plants. The volume of natural gas combusted as "plant fuel" in 2012 was 408,316 MMcf (408.316 Bcf).¹³

2.3 Transmission and Storage

2.3.1 Methane emissions

EPA reports that 2,071 Gg of methane was emitted from the transmission and storage stage in 2012.¹⁴ This was converted to a volume of natural gas using the same conversion process used for fugitive emissions from the processing sector (Section 2.2.2):

$$2,071 \text{ Gg methane} / 0.928 = 2,231 \text{ Gg natural gas}$$

$$2,231 \text{ Gg natural gas} * 49.703 = 110,920 \text{ MMcf natural gas} = 110.92 \text{ Bcf natural gas}$$

2.3.2 Natural gas fuel use

EIA's natural gas "pipeline and distribution use" is assumed to be the natural gas that is combusted in the transmission and storage segment. The volume of natural gas that was combusted for transmission and distribution in 2012 was 730,790 MMcf (730.79 Bcf).¹⁵

2.4 Distribution

Distribution systems are located downstream of city gates and distribute pipeline-quality natural gas to residential, commercial, and industrial customers. *** There is very little natural gas used as fuel by natural gas distribution companies. Though EIA reports "pipeline and distribution use" of natural gas together, for the purposes of this exercise, it is assumed that all of this gas is used as a fuel for transmission and storage (including liquefied natural gas storage) and that none is used for local distribution.

2.4.1 Methane emissions

The EPA reports that 1,231 Gg of fugitive methane was emitted from distribution systems in 2012.¹⁶ This was converted to a volume of natural gas using the same conversion process used for fugitive emissions from the processing sector (Section 2.2.2):

$$1,231 \text{ Gg methane} / 0.928 = 1,338 \text{ Gg natural gas}$$

$$1,338 \text{ Gg natural gas} * 49.703 = 65,930 \text{ MMcf natural gas} = 65.93 \text{ Bcf natural gas}$$

2.5 Consumer End Use

End-use combustion is the largest component of natural gas consumption in the natural gas system. The amount of natural gas consumed by end users in 2012 was 23,411,423 MMcf (23,411 Bcf).¹⁷

3.0 Greenhouse Gas Emissions from the Natural Gas System, by Mass

Each type of natural gas fuel use, leakage, and venting from the natural gas system has associated greenhouse gas (GHG) emissions, either from fugitive emissions and venting, release of naturally occurring CO₂ from raw natural gas, or CO₂ created by combusting natural gas. The Sankey diagram in Figure 2 shows the magnitudes of the GHG emissions associated with each stage and the sources of emissions, presented in terms of CO₂ equivalents. The Sankey diagram in Figure 3 shows the same GHG emissions shown in Figure 2, in addition to GHG emissions associated with end uses of natural gas by consumers. Note that data in the text and figures may not always match exactly, due to rounding.

Methane is a potent greenhouse gas; it is more than 25 times more potent a GHG than CO₂¹⁸ on a 100-year basis. Global-warming potential (GWP) is commonly used to quantify the globally averaged relative

*** Natural gas used by electric generation units and other large industrial facilities is generally delivered directly from the transmission network (as opposed to being purchased from local distribution companies), and this gas does not pass through city gates.

radiative forcing of GHGs relative to CO₂⁺⁺⁺ (i.e., CO₂ equivalent).¹⁹ The CO₂ equivalent of methane leakage is equal to the quantity (in grams, or other unit of mass) of methane leaked multiplied by a factor representing the GWP of methane. In this analysis, a GWP of 25⁺⁺⁺ for methane was used to be consistent with EPA.

3.1 Production

3.1.1 Flaring and venting of “non-combustion CO₂”

The EPA inventory reports “non-combustion” CO₂, which, at the production site, is primarily the result of flaring. The resulting GHG emissions from flaring are 13,662.6 Gg of CO₂ (13.66 MMT CO₂).²⁰ EPA also reports 930.6 Gg of CO₂ (0.93 MMT CO₂)²¹ from other non-combustion sources.

3.1.2 Methane emissions

EPA reports that 1,992 Gg of methane were emitted from natural gas production facilities in 2012.²² This mass of methane is converted to an equivalent mass of CO₂ emissions using the GWP of methane:

$$1,992 \text{ Gg methane} * 25 = 49,800 \text{ Gg CO}_2\text{e} = 49.8 \text{ MMT CO}_2\text{e}$$

3.1.3 Natural gas fuel use

As in the analysis for Figure 1, EIA’s “lease fuel” is considered to be the natural gas combusted by production facilities. The volume of natural gas that was combusted as “lease fuel” in 2012 was 987,957 MMcf (987.957 Bcf).²³ This was converted to a mass of natural gas using the conversion factor developed in Appendix 2:

$$987,957 \text{ MMcf of natural gas} / 41.239 = 23,956.9 \text{ Gg natural gas}$$

⁺⁺⁺ GWP is a general concept that can be applied to any greenhouse gas. The Intergovernmental Panel on Climate Change (Climate Change 2013: The Physical Science Basis. Contribution of Working Group I to the Fifth Assessment Report of the Intergovernmental Panel on Climate Change; Chapter 8: Anthropogenic and Natural Radiative Forcing) describes GWP as “the time-integrated radiative forcing due to a pulse emission of a given component, relative to a pulse emission of an equal mass of CO₂.”

⁺⁺⁺ Calculating the GWP of a GHG depends on many factors, including the length of time over which the GWP is evaluated and whether additional climate feedback mechanisms are included. The Intergovernmental Panel on Climate Change’s Fifth Assessment Report (AR5) uses a GWP of 84 methane evaluated over a 20-year time horizon (86 with additional climate feedbacks), and 28 when evaluated over a 100-year time horizon (34 with additional climate feedbacks) (Intergovernmental Panel on Climate Change, Climate Change 2013: The Physical Science Basis. Contribution of Working Group I to the Fifth Assessment Report of the Intergovernmental Panel on Climate Change, page 714, Table 8.7). Including the climate impacts of oxidation of methane from fossil sources increases the GWP of methane by 1 on a 20-year time horizon (to 87) and 2 on a 100-year time horizon (to 36). The uncertainty in these GWP values is estimated to be ±30% and ±40% for 20- and 100-year time horizon, respectively (for 90% uncertainty range), resulting primarily from uncertainties in the long-term climate impact of CO₂ and the indirect climate feedbacks associated with methane. The GWP value of 25 used in this analysis is from the 2007 version of the IPCC report (AR4). Climate-carbon feedback effects were not used in calculating GWP values for GHGs other than CO₂ in the 2007 IPCC report (including the GWP for methane used in this report), but climate-carbon feedback effects are included in calculating the GWP of all GHGs in the more recent IPCC report (AR5). As noted in IPCC’s documentation for AR5, the inclusion of climate-carbon feedbacks introduces additional uncertainty of +/- 20% to the GWP factors. So, while the inclusion of climate-carbon feedbacks in the more recent IPCC GWP values does more consistently account for broader impacts from GHG emissions, it introduces further uncertainty. The 100-year GWP of 25 is used by the EPA in its GHG inventory.

The mass of CO₂ resulting from natural gas combustion is calculated in Appendix 3:
 23,956.9 Gg natural gas combusted * 2.70 = 64,683 Gg CO₂e = 64.68 MMT CO₂e

3.2 Processing

3.2.1 Non-hydrocarbon gas removal

EPA reports 21,403.6 Gg of CO₂ is released during the processing stage.²⁴ Venting from non-hydrocarbon gas removal^{§§§} accounts for 99.7% of these process-related (i.e. non-combustion) CO₂ emissions.

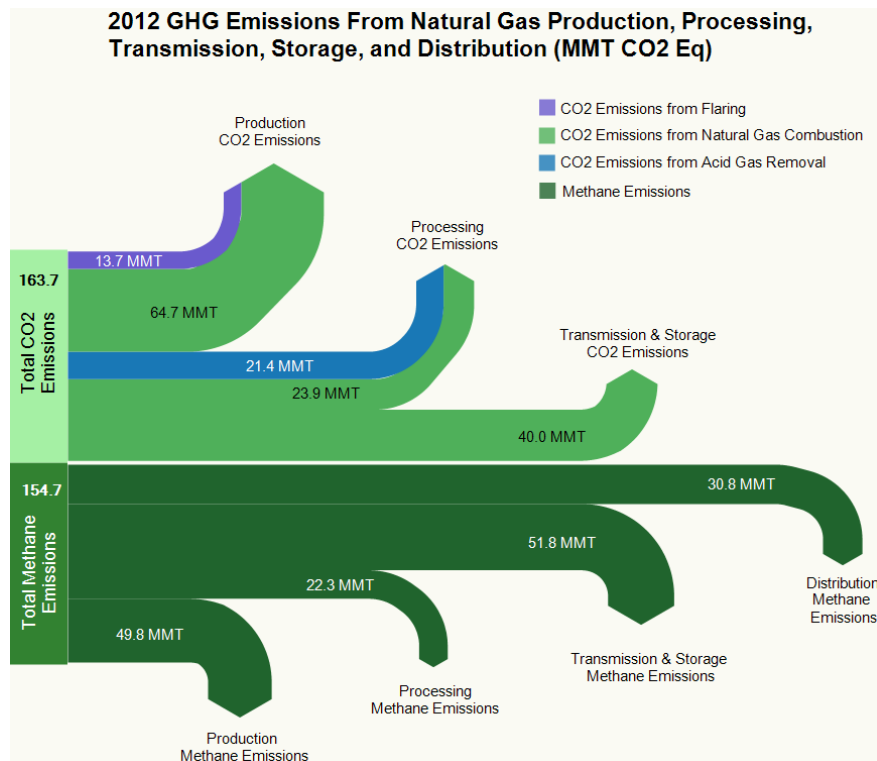
21,403.6 Gg of CO₂ = 21.4 MMT CO₂e

3.2.2 Methane emissions

EPA reports that 892 Gg of methane were emitted from the processing stage in 2012.²⁵ This mass of methane is converted to an equivalent mass of CO₂ emissions using the GWP of methane:

892 Gg methane * 25 = 22,300 Gg CO₂e = 22.3 MMT CO₂e

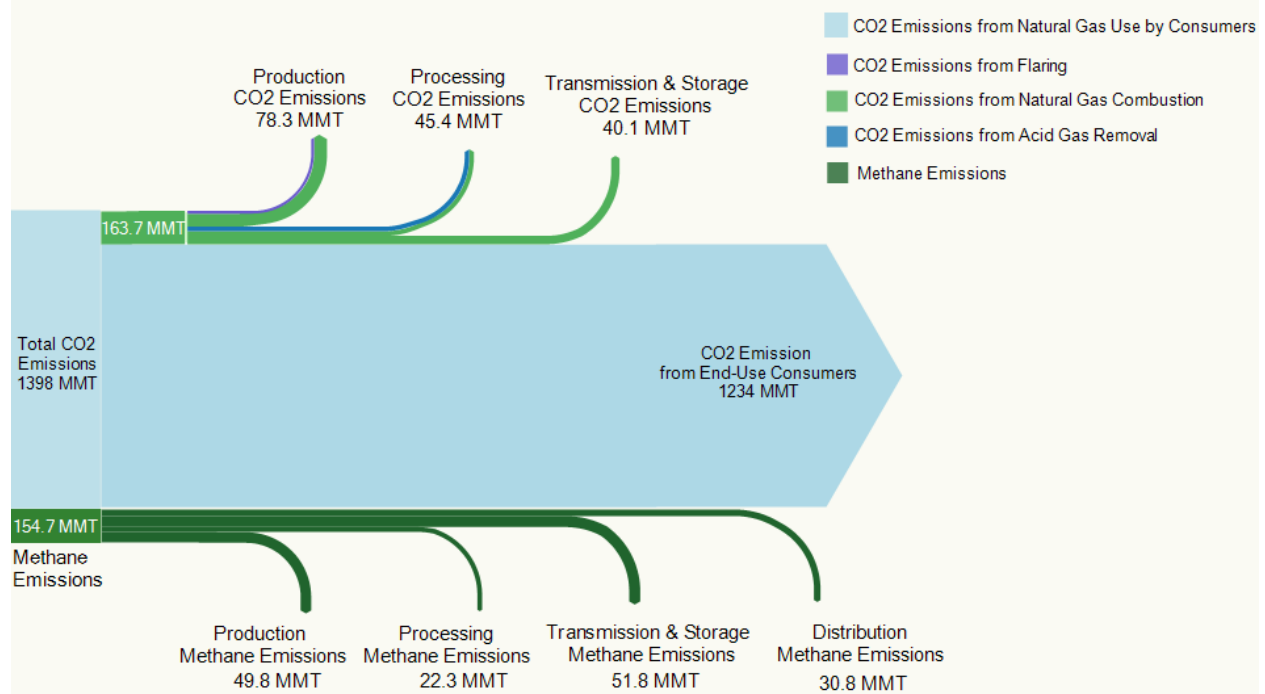
Figure 2. 2012 GHG emissions from natural gas production, processing, transmission, storage, and distribution. Note that this figure does not show GHG emissions from end-use consumers (see Figure 3 for image of all GHGs from natural gas systems).^{26,27,28}



^{§§§} EPA reports “non-combustion CO₂ emissions” but specifies that 99.7% of these emissions are due to “acid gas removal.” EPA uses the phrase “acid gas removal” to denote the process called “non-hydrocarbon gas removal” in this analysis.

Figure 3: 2012 GHG emissions from natural gas production, processing, transmission, storage, and distribution compared with GHG emissions from end-use consumers of natural gas.^{29,30}

2012 GHG Emissions From Natural Gas (MMT CO₂ Eq)



3.2.3 Natural gas fuel use

As in the previous section, EIA's "plant fuel" is considered to be the volume of natural gas combusted by processing plants. The volume of natural gas that was combusted as "plant fuel" in 2012 was 408,316 MMcf (408.316 Bcf).³¹ This was converted to a mass of natural gas using the conversion factor developed in Appendix 2, taking into account the change in composition that occurs when gas is processed:

$$408,316 \text{ MMcf of natural gas} * (2.70 / 41.239 * 0.36 + 2.72 / 49.703 * 0.64) = 23.92 \text{ MMT CO}_2\text{e}$$

3.3 Transmission and Storage

3.3.1 Methane emissions

EPA reports that 2,071 Gg of methane were emitted from the transmission and storage stage in 2012.^{32,****} This mass of methane is converted to an equivalent mass of CO₂ emissions using the GWP of methane:

$$2,071 \text{ Gg methane} * 25 = 51,775 \text{ Gg CO}_2\text{e} = 51.78 \text{ MMT CO}_2\text{e}$$

3.3.2 Natural gas fuel use

EIA's natural gas "pipeline and distribution use" is assumed to be the volume of natural gas that is combusted in the transmission and storage segment. The volume of natural gas that was combusted for

**** EPA also reports 63 Gg of non-combustion CO₂ emissions from the transmission and storage sector. These emissions are very small relative to those shown in Figures 2 and 3 and were omitted for legibility.

transmission and distribution in 2012 was 730.79 Bcf.³³ This was converted to a mass of natural gas using the same conversion used for natural gas fuel use in the processing segment:

$$730,790 \text{ MMcf of natural gas} / 49.703 = 14,703.1 \text{ Gg natural gas}$$

The mass of CO₂ resulting from natural gas combustion is calculated in Appendix 3:

$$15,736.7 \text{ Gg natural gas combusted} * 2.72 = 39,992 \text{ Gg CO}_2\text{e} = 39.99 \text{ MMT CO}_2\text{e}$$

3.4 Distribution

3.4.1 Methane emissions

EPA reports that 1,231 Gg of methane were emitted from distribution systems in 2012.^{34,****} This mass of methane is converted to an equivalent mass of CO₂ emissions using the GWP of methane:

$$1,231 \text{ Gg methane} * 25 = 30,775 \text{ Gg CO}_2\text{e} = 30.78 \text{ MMT CO}_2\text{e}$$

3.5 Consumer End Use Combustion

End-use combustion is the largest source of CO₂ emissions associated with the natural gas life cycle, as shown in Figure 3. Specifically, EIA reports 1,362.49 MMT CO₂ emissions associated with natural gas combustion.³⁵ Total CO₂e emissions from consumer end-use combustion were estimated as the difference between total natural gas combustion CO₂ emissions and CO₂ emissions from natural gas combustion within the natural gas supply chain:

$$1,362.49 \text{ Gg CO}_2 - 64.68 \text{ Gg CO}_2 - 23.92 \text{ Gg CO}_2 - 39.99 \text{ Gg CO}_2 = 1,233.9 \text{ Gg CO}_2$$

Note, total CO₂ emissions from natural gas broadly is the combination of emissions from combustion (1,362.49 MMT CO₂), plus emissions from non-hydrocarbon gas removal (21.4 MMT CO₂) and from flaring (13.66 MMT CO₂), resulting in the following: 1397.6 MMT CO₂.

**** EPA also reports 37 Gg of non-combustion CO₂ emissions from the distribution sector. Similar to the transmission and distribution sector, these emissions were omitted from Figures 2 and 3 for legibility.

Appendix 1: Natural gas flaring associated with crude oil production

Natural gas that is co-produced with crude oil and natural gas liquids can be flared intentionally near production sites. This can occur as a result of infrastructure constraints that limit the ability of producers to transport natural gas to market at profitable rates. The Bakken shale in North Dakota and the Eagle Ford shale in Texas are two areas with high rates of natural gas flaring, which, for the purpose of this analysis, is assumed to be associated with oil production.

As shown in Table 2, flaring in North Dakota and the Eagle Ford shale are estimated to account for more than half of natural gas flaring in the United States in 2012. The state-wide flaring numbers for North Dakota are assumed to be wholly associated with oil production in the Bakken shale, as the Bakken is the dominant shale play in North Dakota. Flaring numbers in the Eagle Ford shale are assumed to be wholly associated with oil production in that basin. These data form the basis for the estimate of the national percentage of flaring associated with oil production shown in the last row. This estimate likely includes some flaring associated with natural gas production in North Dakota and excludes oil-associated flaring in other states and other parts of Texas. Additional analysis beyond the scope of this study would be needed to more precisely attribute national totals of natural gas flaring to oil, natural gas liquids, or natural gas production wells.

Table 2: Flaring (in Bcf), for North Dakota and the Eagle Ford shale in particular, compared to flaring for the entire U.S. natural gas system.

	2011	2012	2013
US total (EIA)³⁶	209 ^{37,****}	213	260
North Dakota total³⁸	57	90	115
Texas total³⁹	35	48	77
Eagle Ford total⁴⁰	14	21	
Estimated oil associated flaring (ND + Eagle Ford, bcf)	71	111	
Estimated oil associated flaring (% of US total flaring)	34%	52%	

**** For comparison, the World Bank estimates that 251 Bcf of natural gas was flared in the U.S., in 2011 (data for years after 2011 are not yet available).

Appendix 2: Natural gas mass and volume conversions

This appendix develops factors for converting natural gas volumes to mass, accounting for average compositions and densities of natural gas components.

The density of natural gas was calculated based on the gas composition shown in Tables 1 and 3. These compositions were weighted by the densities of individual compounds in Table 1.

Table 3. Densities of natural gas components.⁴¹

Component	Density (kg/m³)
Methane	0.656
Ethane	1.356
Propane	2.010
iso-Butane	2.510
n-Butane	2.480
N ₂	1.251
CO ₂	1.977
H ₂ S	1.360
H ₂ O	0.804

For example:

Pipeline quality density = (methane density x 92.8%) + (ethane density x 3.7%) + (propane density x 0.9%) etc.

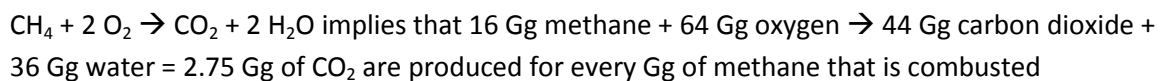
The resulting density conversions are 41.239 MMcf per Gg of natural gas before processing and 49.703 MMcf per Gg after processing.

Appendix 3: CO₂ emissions from natural gas combustion

The following subsections explain the methodologies used to determine the amount of CO₂ emissions resulting from a given quantity of natural gas as a fuel source in the natural gas supply chain. EIA provides natural gas fuel use in terms of volumes of natural gas. The following three appendices describe, in three steps, the conversion factors that were used to convert from a volume of natural gas combustion to resulting CO₂ emissions.

A3.1 CO₂ emissions from combustion of methane in natural gas

The CO₂ emissions from methane used for combustion in the natural gas supply chain were calculated using the following reaction:



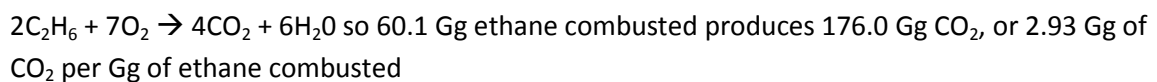
A3.2 CO₂ emissions from combustion of non-methane hydrocarbons in natural gas

The CO₂ emissions from combustion of non-methane hydrocarbons in natural gas were calculated assuming the following higher-chain hydrocarbon composition of natural gas:

Table 4. Non-methane hydrocarbon composition of natural gas, by mass.⁴²

Component	Production	Pipeline quality
Ethane	12.0 %	3.7 %
Propane	3.0 %	0.9 %
Butane	1.7 %	0.5 %
Pentane	0.7 %	0.2 %
Hexane	0.4 %	0.1 %
Total non-methane	17.8 %	5.5 %

Chemical equations were developed for each of the five non-methane components listed in Table 4. For example, considering ethane:



This process was repeated for all five hydrocarbons, and the results were weighted according to the pipeline quantities in Table 4. The resulting weighted average is 2.96 Gg CO₂ generated per Gg of non-methane hydrocarbons combusted, which is slightly higher than the 2.93 Gg of CO₂ per Gg of ethane combusted due to the small contributions of propane and other non-methane hydrocarbons. The result of 2.96 Gg CO₂ per Gg of non-methane hydrocarbons is the same using both the production and pipeline quality gas composition weighting.

A3.3 Total CO₂ emissions from natural gas combustion

The total CO₂ emissions from natural gas comprise the sum of emissions from the combustion of the methane and non-methane components, plus the release of non-combustion CO₂ contained in the

natural gas. These sources of GHG emissions were weighted based on the natural gas composition in Table 1. For pre-processed natural gas:

$$2.75 \text{ Gg CO}_2/\text{Gg CH}_4 \times 78.3\% + 2.96 \text{ Gg CO}_2/\text{Gg HC} \times 17.8\% + 1 \text{ Gg CO}_2/\text{Gg CO}_2 \times 1.51\% \\ = 2.70 \text{ Gg CO}_2/\text{Gg NG}$$

For pipeline quality natural gas:

$$2.75 \text{ Gg CO}_2/\text{Gg CH}_4 \times 92.8\% + 2.96 \text{ Gg CO}_2/\text{Gg HC} \times 5.54\% + 1 \text{ Gg CO}_2/\text{Gg CO}_2 \times 0.47\% \\ = 2.72 \text{ Gg CO}_2/\text{Gg NG}$$

Appendix 4: Data from figures

Table 5. Summary of data and methodology for Figure 1. ^{§§§§}

<u>Stage</u>	<u>Given</u>	<u>Units</u>	<u>Conversions</u>	<u>NG (Bcf)</u>
Production				1,282.95
flaring and venting ⁴³	212,848	MMcf of NG	MMcf NG -> Bcf NG	212.85
fuel use ⁴⁴	987,957	MMcf of NG	MMcf NG -> Bcf NG	987.96
fugitive emissions ⁴⁵	1,992	Gg of CH ₄	Gg CH ₄ -> Gg NG -> MMcf NG -> Bcf NG	82.15
Processing				1,224.46
gas removal ⁴⁶	768,598	MMcf of gases removed	MMcf gases removed -> Bcf gases removed	768.60
fuel use ⁴⁷	408,316	MMcf of NG	MMcf NG -> Bcf NG	408.32
fugitive emissions ⁴⁸	892	Gg of CH ₄	Gg CH ₄ -> Gg NG -> MMcf NG -> Bcf NG	47.55
Transmission and storage				841.71
fuel use ⁴⁹	730,790	MMcf of NG	MMcf NG -> Bcf NG	730.79
fugitive emissions ⁵⁰	2071	Gg of CH ₄	Gg CH ₄ -> Gg NG -> MMcf NG -> Bcf NG	110.92
Distribution				65.93
fugitive emissions ⁵¹	1,231	Gg of CH ₄	Gg CH ₄ -> Gg NG -> MMcf NG -> Bcf NG	65.93
Consumer end use⁵²	23,411,423	MMcf of NG	MMcf NG -> Bcf NG	23,411.42

^{§§§§} Note that data in this table may not always match exactly with data in the figures, due to rounding.

Table 6: Summary of data and methodology for Figures 2 and 3. ****

<u>Stage</u>	<u>Given</u>	<u>Units</u>	<u>Conversions</u>	<u>CO₂e (Tg)</u>
Production				128.15
flaring and venting ⁵³	13,662.6	Gg of CO ₂ eq	Gg CO ₂ eq -> Tg CO ₂ eq	13.66
fuel use ⁵⁴	987,957	MMcf of NG	MMcf NG -> Gg NG -> Gg CO ₂ eq -> Tg CO ₂ eq	64.68
fugitive emissions ⁵⁵	1992	Gg of CH ₄	Gg CH ₄ -> Gg CO ₂ eq -> Tg CO ₂ eq	49.80
Processing				67.68
gas removal ⁵⁶	21,403.6	Gg of CO ₂ eq	Gg CO ₂ eq -> Tg CO ₂ eq	21.40
other non-combustion ⁵⁷	65.2	Gg of CO ₂ eq	Gg CO ₂ eq -> Tg CO ₂ eq	0.07
fuel use ⁵⁸	408,316	MMcf of NG	MMcf NG -> Gg NG -> Gg CO ₂ eq -> Tg CO ₂ eq	23.92
fugitive emissions ⁵⁹	892	Gg of CH ₄	Gg CH ₄ -> Gg CO ₂ eq -> Tg CO ₂ eq	22.30
Transmission and storage				91.77
non-combustion ⁶⁰	63.4	Gg of CO ₂ eq	Gg CO ₂ eq -> Tg CO ₂ eq	0.06
fuel use ⁶¹	730,790	MMcf of NG	MMcf NG -> Gg NG -> Gg CO ₂ eq -> Tg CO ₂ eq	39.99
fugitive emissions ⁶²	2071	Gg of CH ₄	Gg CH ₄ -> Gg CO ₂ eq -> Tg CO ₂ eq	51.78
Distribution				30.82
non-combustion ⁶³	36.8	Gg of CO ₂ eq	Gg CO ₂ eq -> Tg CO ₂ eq	0.04
fugitive emissions ⁶⁴	1,231	Gg of CH ₄	Gg CH ₄ -> Gg CO ₂ eq -> Tg CO ₂ eq	30.78
Consumer end-use⁶⁵		Tg CO ₂ from combustion	Tg CO ₂ combustion - Tg CO ₂ process emissions	1,233.91

**** Note that data in this table may not always match exactly with data in the figures, due to rounding.

Endnotes

- ¹ U.S. Energy Information Administration. 2014. *Natural Gas Consumption by End Use*. http://www.eia.gov/dnav/ng/ng_cons_sum_dcu_nus_a.htm
- ² U.S. Environmental Protection Agency. 2014. Inventory of U.S. Greenhouse Gas Emissions and Sinks: 1990–2012. <http://www.epa.gov/climatechange/ghgemissions/usinventoryreport.html>
- ³ Gautier, D.L., Dolton, G.L., Takahashi, K.I., and Varnes, K.L., eds., 1996, 1995 National assessment of United States oil and gas resources--results, methodology, and supporting data: U.S. Geological Survey Digital Data Series 30, Release 2.
- ⁴ National Energy Technology Laboratory, 2012. Role of Alternative Energy Sources: Natural Gas Technology Assessment.
- ⁵ U.S. Energy Information Administration. 2014. Natural Gas Gross Withdrawals and Production. Vented and Flared. http://www.eia.gov/dnav/ng/ng_prod_sum_a_EPG0_vgv_mmcf_a.htm
- ⁶ U.S. Environmental Protection Agency. 2014. Inventory of U.S. Greenhouse Gas Emissions and Sinks: 1990–2012. <http://www.epa.gov/climatechange/ghgemissions/usinventoryreport.html>
- ⁷ U.S. Energy Information Administration. 2014. *Natural Gas Consumption by End Use*. http://www.eia.gov/dnav/ng/ng_cons_sum_dcu_nus_a.htm
- ⁸ U.S. Environmental Protection Agency. 2014. Inventory of U.S. Greenhouse Gas Emissions and Sinks: 1990–2012. <http://www.epa.gov/climatechange/ghgemissions/usinventoryreport.html>
- ⁹ U.S. Energy Information Administration. 2014. Natural Gas Consumption by End Use. http://www.eia.gov/dnav/ng/ng_cons_sum_dcu_nus_a.htm
- ¹⁰ U.S. Energy Information Administration. 2014. Natural Gas Gross Withdrawals and Production. Nonhydrocarbon Gases Removed. http://www.eia.gov/dnav/ng/ng_prod_sum_a_epg0_vrn_mmcf_a.htm
- ¹¹ U.S. Environmental Protection Agency. 2014. Inventory of U.S. Greenhouse Gas Emissions and Sinks: 1990–2012. <http://www.epa.gov/climatechange/ghgemissions/usinventoryreport.html>
- ¹² Tim Skone, National Energy Technology Laboratory, personal communication.
- ¹³ U.S. Energy Information Administration. 2014. Natural Gas Consumption by End Use. http://www.eia.gov/dnav/ng/ng_cons_sum_dcu_nus_a.htm
- ¹⁴ U.S. Environmental Protection Agency. 2014. Inventory of U.S. Greenhouse Gas Emissions and Sinks: 1990–2012. <http://www.epa.gov/climatechange/ghgemissions/usinventoryreport.html>
- ¹⁵ U.S. Energy Information Administration. 2014. Natural Gas Consumption by End Use. http://www.eia.gov/dnav/ng/ng_cons_sum_dcu_nus_a.htm
- ¹⁶ U.S. Environmental Protection Agency. 2014. Inventory of U.S. Greenhouse Gas Emissions and Sinks: 1990–2012. <http://www.epa.gov/climatechange/ghgemissions/usinventoryreport.html>
- ¹⁷ U.S. Energy Information Administration. 2014. *Natural Gas Consumption by End Use*. http://www.eia.gov/dnav/ng/ng_cons_sum_dcu_nus_a.htm
- ¹⁸ Intergovernmental Panel on Climate Change, 2013. Climate Change 2013: The Physical Science Basis. Contribution of Working Group I to the Fifth Assessment Report of the Intergovernmental Panel on Climate Change; Chapter 8: Anthropogenic and Natural Radiative Forcing. https://www.ipcc.ch/pdf/assessment-report/ar5/wg1/WG1AR5_Chapter08_FINAL.pdf
- ¹⁹ U.S. Environmental Protection Agency. 2014. Inventory of U.S. Greenhouse Gas Emissions and Sinks: 1990–2012. <http://www.epa.gov/climatechange/ghgemissions/usinventoryreport.html>
- ²⁰ U.S. Environmental Protection Agency. 2014. Inventory of U.S. Greenhouse Gas Emissions and Sinks: 1990–2012. <http://www.epa.gov/climatechange/ghgemissions/usinventoryreport.html>
- ²¹ U.S. Environmental Protection Agency. 2014. Inventory of U.S. Greenhouse Gas Emissions and Sinks: 1990–2012. <http://www.epa.gov/climatechange/ghgemissions/usinventoryreport.html>

-
- ²² U.S. Environmental Protection Agency. 2014. Inventory of U.S. Greenhouse Gas Emissions and Sinks: 1990–2012. <http://www.epa.gov/climatechange/ghgemissions/usinventoryreport.html>
- ²³ U.S. Energy Information Administration. 2014. Natural Gas Consumption by End Use. http://www.eia.gov/dnav/ng/ng_cons_sum_dcu_nus_a.htm
- ²⁴ U.S. Environmental Protection Agency. 2014. Inventory of U.S. Greenhouse Gas Emissions and Sinks: 1990–2012. <http://www.epa.gov/climatechange/ghgemissions/usinventoryreport.html>
- ²⁵ U.S. Environmental Protection Agency. 2014. Inventory of U.S. Greenhouse Gas Emissions and Sinks: 1990–2012. <http://www.epa.gov/climatechange/ghgemissions/usinventoryreport.html>
- ²⁶ U.S. Energy Information Administration. 2014. Natural Gas Consumption by End Use. http://www.eia.gov/dnav/ng/ng_cons_sum_dcu_nus_a.htm
- ²⁷ U.S. Energy Information Administration. 2014. Natural Gas Gross Withdrawals and Production. Vented and Flared. http://www.eia.gov/dnav/ng/ng_prod_sum_a_EPG0_vgv_mmc_f_a.htm
- ²⁸ U.S. Environmental Protection Agency. 2014. Inventory of U.S. Greenhouse Gas Emissions and Sinks: 1990–2012. <http://www.epa.gov/climatechange/ghgemissions/usinventoryreport.html>
- ²⁹ U.S. Energy Information Administration. 2014. *Natural Gas Consumption by End Use*. http://www.eia.gov/dnav/ng/ng_cons_sum_dcu_nus_a.htm
- ³⁰ U.S. Environmental Protection Agency. 2014. Inventory of U.S. Greenhouse Gas Emissions and Sinks: 1990–2012. <http://www.epa.gov/climatechange/ghgemissions/usinventoryreport.html>
- ³¹ U.S. Energy Information Administration. 2014. Natural Gas Consumption by End Use. http://www.eia.gov/dnav/ng/ng_cons_sum_dcu_nus_a.htm
- ³² U.S. Environmental Protection Agency. 2014. Inventory of U.S. Greenhouse Gas Emissions and Sinks: 1990–2012. <http://www.epa.gov/climatechange/ghgemissions/usinventoryreport.html>
- ³³ U.S. Energy Information Administration. 2014. Natural Gas Consumption by End Use. http://www.eia.gov/dnav/ng/ng_cons_sum_dcu_nus_a.htm
- ³⁴ U.S. Environmental Protection Agency. 2014. Inventory of U.S. Greenhouse Gas Emissions and Sinks: 1990–2012. <http://www.epa.gov/climatechange/ghgemissions/usinventoryreport.html>
- ³⁵ U.S. Energy Information Administration. 2014. Carbon Dioxide Emissions from Energy Consumption by Source. http://www.eia.gov/totalenergy/data/monthly/pdf/sec12_3.pdf
- ³⁶ EIA, 2014. "Natural Gas Withdrawals and Production." Accessed Dec. 19, 2014. <http://www.epa.gov/climatechange/Downloads/ghgemissions/US-GHG-Inventory-2014-Annex-3-Additional-Source-or-Sink-Categories.pdf>
- ³⁷ World Bank, 2014. "Estimated Flared Volumes from Satellite Data, 2007-2011." Accessed Dec. 19, 2014. <http://web.worldbank.org/WBSITE/EXTERNAL/TOPICS/EXTOGMC/EXTGGFR/0,,contentMDK:22137498~menuPK:3077311~pagePK:64168445~piPK:64168309~theSitePK:578069,00.html>
- ³⁸ North Dakota Department of Mineral Resources, 2014. "North Dakota Monthly Gas Production and Sales" <https://www.dmr.nd.gov/oilgas/stats/Gas1990ToPresent.pdf>
- ³⁹ Railroad Commission of Texas, 2014. "Production values." Accessed Dec. 19, 2014. <http://www.rrc.state.tx.us/oil-gas/research-and-statistics/production-data>
- ⁴⁰ Tedesco, John and Hiller, Jennifer. "Up in Flames: Flares in Eagle Ford shale wasting natural gas." San Antonio Express News. Accessed Dec. 19, 2014. <http://www.expressnews.com/business/eagleford/item/Up-in-Flames-Day-1-Flares-in-Eagle-Ford-Shale-32626.php%E2%80%9DUp%20in%20Flames>
- ⁴¹ National Energy Technology Laboratory, 2012. Role of Alternative Energy Sources: Natural Gas Technology Assessment.
- ⁴² National Energy Technology Laboratory, 2012. Role of Alternative Energy Sources: Natural Gas Technology Assessment.
- ⁴³ U.S. Energy Information Administration. 2014. Natural Gas Gross Withdrawals and Production. Vented and Flared. http://www.eia.gov/dnav/ng/ng_prod_sum_a_EPG0_vgv_mmc_f_a.htm

-
- ⁴⁴ U.S. Energy Information Administration. 2014. *Natural Gas Consumption by End Use*. http://www.eia.gov/dnav/ng/ng_cons_sum_dcu_nus_a.htm
- ⁴⁵ U.S. Environmental Protection Agency. 2014. Inventory of U.S. Greenhouse Gas Emissions and Sinks: 1990–2012. <http://www.epa.gov/climatechange/ghgemissions/usinventoryreport.html>, [Table 3-44](#)
- ⁴⁶ U.S. Energy Information Administration. 2014. Natural Gas Gross Withdrawals and Production. Nonhydrocarbon Gases Removed. http://www.eia.gov/dnav/ng/ng_prod_sum_a_epg0_vrn_mmcf_a.htm
- ⁴⁷ U.S. Energy Information Administration. 2014. *Natural Gas Consumption by End Use*. http://www.eia.gov/dnav/ng/ng_cons_sum_dcu_nus_a.htm
- ⁴⁸ U.S. Environmental Protection Agency. 2014. Inventory of U.S. Greenhouse Gas Emissions and Sinks: 1990–2012. <http://www.epa.gov/climatechange/ghgemissions/usinventoryreport.html>, [Table 3-44](#)
- ⁴⁹ U.S. Energy Information Administration. 2014. *Natural Gas Consumption by End Use*. http://www.eia.gov/dnav/ng/ng_cons_sum_dcu_nus_a.htm
- ⁵⁰ U.S. Environmental Protection Agency. 2014. Inventory of U.S. Greenhouse Gas Emissions and Sinks: 1990–2012. <http://www.epa.gov/climatechange/ghgemissions/usinventoryreport.html>, [Table 3-44](#)
- ⁵¹ U.S. Environmental Protection Agency. 2014. Inventory of U.S. Greenhouse Gas Emissions and Sinks: 1990–2012. <http://www.epa.gov/climatechange/ghgemissions/usinventoryreport.html>, [Table 3-44](#)
- ⁵² U.S. Energy Information Administration. 2014. *Natural Gas Consumption by End Use*. http://www.eia.gov/dnav/ng/ng_cons_sum_dcu_nus_a.htm
- ⁵³ U.S. Environmental Protection Agency. 2014. Inventory of U.S. Greenhouse Gas Emissions and Sinks: 1990–2012. <http://www.epa.gov/climatechange/ghgemissions/usinventoryreport.html>, [Annex 3.5, Table A-143](#)
- ⁵⁴ U.S. Energy Information Administration. 2014. *Natural Gas Consumption by End Use*. http://www.eia.gov/dnav/ng/ng_cons_sum_dcu_nus_a.htm
- ⁵⁵ U.S. Environmental Protection Agency. 2014. Inventory of U.S. Greenhouse Gas Emissions and Sinks: 1990–2012. <http://www.epa.gov/climatechange/ghgemissions/usinventoryreport.html>, [3-44](#)
- ⁵⁶ U.S. Environmental Protection Agency. 2014. Inventory of U.S. Greenhouse Gas Emissions and Sinks: 1990–2012. <http://www.epa.gov/climatechange/ghgemissions/usinventoryreport.html>, [Annex 3.5](#)
- ⁵⁷ U.S. Environmental Protection Agency. 2014. Inventory of U.S. Greenhouse Gas Emissions and Sinks: 1990–2012. <http://www.epa.gov/climatechange/ghgemissions/usinventoryreport.html>, [Annex 3.5](#)
- ⁵⁸ U.S. Energy Information Administration. 2014. *Natural Gas Consumption by End Use*. http://www.eia.gov/dnav/ng/ng_cons_sum_dcu_nus_a.htm
- ⁵⁹ U.S. Environmental Protection Agency. 2014. Inventory of U.S. Greenhouse Gas Emissions and Sinks: 1990–2012. <http://www.epa.gov/climatechange/ghgemissions/usinventoryreport.html>, [Table 3-44](#)
- ⁶⁰ U.S. Environmental Protection Agency. 2014. Inventory of U.S. Greenhouse Gas Emissions and Sinks: 1990–2012. <http://www.epa.gov/climatechange/ghgemissions/usinventoryreport.html>, [Annex 3.5](#)
- ⁶¹ U.S. Energy Information Administration. 2014. *Natural Gas Consumption by End Use*. http://www.eia.gov/dnav/ng/ng_cons_sum_dcu_nus_a.htm
- ⁶² U.S. Environmental Protection Agency. 2014. Inventory of U.S. Greenhouse Gas Emissions and Sinks: 1990–2012. <http://www.epa.gov/climatechange/ghgemissions/usinventoryreport.html>, [Table 3-44](#)
- ⁶³ U.S. Environmental Protection Agency. 2014. Inventory of U.S. Greenhouse Gas Emissions and Sinks: 1990–2012. <http://www.epa.gov/climatechange/ghgemissions/usinventoryreport.html>, [Annex 3.5](#)
- ⁶⁴ U.S. Environmental Protection Agency. 2014. Inventory of U.S. Greenhouse Gas Emissions and Sinks: 1990–2012. <http://www.epa.gov/climatechange/ghgemissions/usinventoryreport.html>, [Table 3-44](#)
- ⁶⁵ U.S. Energy Information Administration. 2014. *Natural Gas Consumption by End Use*. http://www.eia.gov/dnav/ng/ng_cons_sum_dcu_nus_a.htm

Exhibit 14

An official website of the United States government.



Atmospheric Lifetime and Global Warming Potential Defined

Atmospheric Lifetime (years)

Each of these gases can remain in the atmosphere for different amounts of time, ranging from a few years to thousands of years. All of these gases remain in the atmosphere long enough to become well mixed, meaning that the amount that is measured in the atmosphere is roughly the same all over the world, regardless of the source of the emissions.

Global Warming Potential (100 year)

Global Warming Potential Describes Impact of Each Gas

Certain greenhouse gases (GHGs) are more effective at warming Earth ("thickening the blanket") than others. The two most important characteristics of a GHG in terms of climate impact are how well the gas absorbs energy (preventing it from immediately escaping to space), and how long the gas stays in the atmosphere.

The Global Warming Potential (GWP) for a gas is a measure of the total energy that a gas absorbs over a particular period of time (usually 100 years), compared to carbon dioxide.^[1] The larger the GWP, the more warming the gas causes. For example, methane's 100-year GWP is 21, which means that methane will cause 21 times as much warming as an equivalent mass of carbon dioxide over a 100-year time period.^[2]

- Carbon dioxide (CO₂) has a GWP of 1 and serves as a baseline for other GWP values. CO₂ remains in the atmosphere for a very long time - changes in atmospheric CO₂ concentrations persist for thousands of years.
- Methane (CH₄) has a GWP more than 20 times higher than CO₂ for a 100-year time scale. CH₄ emitted today lasts for only about a decade in the atmosphere, on average.^[3] However, on a pound-for-pound basis, CH₄ absorbs more energy than CO₂, making its GWP higher.
- Nitrous Oxide (N₂O) has a GWP 300 times that of CO₂ for a 100-year timescale. N₂O emitted today remains in the atmosphere for more than 100 years, on average.^[3]

Chlorofluorocarbons (CFCs), hydrofluorocarbons (HFCs), hydrochlorofluorocarbons (HCFCs), perfluorocarbons (PFCs), and sulfur hexafluoride (SF₆) are sometimes called high-GWP gases because, for a given amount of mass, they trap substantially more heat than CO₂.

- [1]Solomon, S., D. Qin, M. Manning, R.B. Alley, T. Berntsen, N.L. Bindoff, Z. Chen, A. Chidthaisong, J.M. Gregory, G.C. Hegerl, M. Heimann, B. Hewitson, B.J. Hoskins, F. Joos, J. Jouzel, V. Kattsov, U. Lohmann, T. Matsuno, M. Molina, N. Nicholls, J. Overpeck, G. Raga, V. Ramaswamy, J. Ren, M. Rusticucci, R. Somerville, T.F. Stocker, P. Whetton, R.A. Wood and D. Wratt (2007). Technical Summary. In: *Climate Change 2007: The Physical Science Basis. EXIT Contribution of Working Group I to the Fourth Assessment Report of the Intergovernmental Panel on Climate Change* [Solomon, S., D. Qin, M. Manning, Z. Chen, M. Marquis, K.B. Averyt, M. Tignor and H.L. Miller (eds.)]. Cambridge University Press, Cambridge, United Kingdom and New York, NY, USA.
- [2]Forster, P., V. Ramaswamy, P. Artaxo, T. Berntsen, R. Betts, D.W. Fahey, J. Haywood, J. Lean, D.C. Lowe, G. Myhre, J. Nganga, R. Prinn, G. Raga, M. Schulz and R. Van Dorland (2007). Changes in Atmospheric Constituents and in Radiative Forcing. In: *Climate Change 2007: The Physical Science Basis. EXIT Contribution of Working Group I to the Fourth Assessment Report of the Intergovernmental Panel on Climate Change* [Solomon, S., D. Qin, M. Manning, Z. Chen, M. Marquis, K.B. Averyt, M. Tignor and H.L. Miller (eds.)]. Cambridge University Press, Cambridge, United Kingdom and New York, NY, USA.
- [3]NRC (2010). *Advancing the Science of Climate Change. EXIT* National Research Council. The National Academies Press, Washington, DC, USA.

LAST UPDATED ON NOVEMBER 18, 2020

Exhibit 15



Climate Projections Based on Emissions Scenarios for Long-Lived and Short-Lived Radiatively Active Gases and Aerosols

U.S. Climate Change Science Program
Synthesis and Assessment Product 3.2

September 2008

FEDERAL EXECUTIVE TEAM

Director, Climate Change Science Program	William J. Brennan
Director, Climate Change Science Program Office	Peter A. Schultz
Lead Agency Principal Representative to CCSP; Deputy Under Secretary of Commerce for Oceans and Atmosphere, National Oceanic and Atmospheric Administration.....	Mary M. Glackin
Product Lead, Geophysical Fluid Dynamics Laboratory, National Oceanic and Atmospheric Administration.....	Hiram Levy II
Synthesis and Assessment Product Advisory Group Chair; Associate Director, EPA National Center for Environmental Assessment.....	Michael W. Slimak
Synthesis and Assessment Product Coordinator, Climate Change Science Program Office	Fabien J.G. Laurier
Special Advisor, National Oceanic and Atmospheric Administration	Chad A. McNutt

EDITORIAL AND PRODUCTION TEAM

Chair	Hiram Levy II, NOAA/GFDL
Scientific Editor	Jessica Blunden, STG, Inc.
Scientific Editor	Anne M. Waple, STG, Inc.
Scientific Editor	Christian Zamarra, STG, Inc.
Technical Advisor	David J. Dokken, USGCRP
Graphic Design Lead	Sara W. Veasey, NOAA
Graphic Design Co-Lead.....	Deborah B. Riddle, NOAA
Designer	Brandon Farrar, STG, Inc.
Designer	Glenn M. Hyatt, NOAA
Designer	Deborah Misch, STG, Inc.
Copy Editor.....	Anne Markel, STG, Inc.
Copy Editor.....	Lesley Morgan, STG, Inc.
Copy Editor.....	Susan Osborne, STG, Inc.
Copy Editor.....	Susanne Skok, STG, Inc.
Copy Editor.....	Mara Sprain, STG, Inc.
Copy Editor.....	Brooke Stewart, STG, Inc.
Technical Support.....	Jesse Enloe, STG, Inc.

This Synthesis and Assessment Product, described in the U.S. Climate Change Science Program (CCSP) Strategic Plan, was prepared in accordance with Section 515 of the Treasury and General Government Appropriations Act for Fiscal Year 2001 (Public Law 106-554) and the information quality act guidelines issued by the Department of Commerce and NOAA pursuant to Section 515 <<http://www.noaanews.noaa.gov/stories/iq.htm>>. The CCSP Interagency Committee relies on Department of Commerce and NOAA certifications regarding compliance with Section 515 and Department guidelines as the basis for determining that this product conforms with Section 515. For purposes of compliance with Section 515, this CCSP Synthesis and Assessment Product is an “interpreted product” as that term is used in NOAA guidelines and is classified as “highly influential”. This document does not express any regulatory policies of the United States or any of its agencies, or provide recommendations for regulatory action.



Climate Projections Based on Emissions Scenarios for Long-Lived and Short-Lived Radiatively Active Gases and Aerosols

Synthesis and Assessment Product 3.2
Report by the U.S. Climate Change Science Program
and the Subcommittee on Global Change Research

EDITED BY:

Hiram Levy II, Drew Shindell, Alice Gilliland,
Larry W. Horowitz, and M. Daniel Schwarzkopf

SCIENCE EDITOR: Anne M. Waple

RECOMMENDED CITATIONS**For the Report as a whole:**

CCSP, 2008: *Climate Projections Based on Emissions Scenarios for Long-Lived and Short-Lived Radiatively Active Gases and Aerosols*. A Report by the U.S. Climate Change Science Program and the Subcommittee on Global Change Research. H. Levy II, D.T. Shindell, A. Gilliland, M.D. Schwarzkopf, L.W. Horowitz, (eds.). Department of Commerce, NOAA's National Climatic Data Center, Washington, D.C., USA, 100 pp.

For the Preface:

Levy II, H., D.T. Shindell, A. Gilliland, M.D. Schwarzkopf, L.W. Horowitz, 2008: Preface in *Climate Projections Based on Emissions Scenarios for Long-Lived and Short-Lived Radiatively Active Gases and Aerosols*. H. Levy II, D.T. Shindell, A. Gilliland, M.D. Schwarzkopf, L.W. Horowitz, (eds.). A Report by the U.S. Climate Change Science Program and the Subcommittee on Global Change Research, Washington, D.C.

For the Executive Summary:

Levy II, H., D.T. Shindell, A. Gilliland, M.D. Schwarzkopf, L.W. Horowitz, 2008: Executive Summary in *Climate Projections Based on Emissions Scenarios for Long-Lived and Short-Lived Radiatively Active Gases and Aerosols*. H. Levy II, D.T. Shindell, A. Gilliland, M.D. Schwarzkopf, L.W. Horowitz, (eds.). A Report by the U.S. Climate Change Science Program and the Subcommittee on Global Change Research, Washington, D.C.

For Chapter 1:

Levy II, H., D.T. Shindell, A. Gilliland, M.D. Schwarzkopf, L.W. Horowitz, 2008: Introduction in *Climate Projections Based on Emissions Scenarios for Long-Lived and Short-Lived Radiatively Active Gases and Aerosols*. H. Levy II, D.T. Shindell, A. Gilliland, M.D. Schwarzkopf, L.W. Horowitz, (eds.). A Report by the U.S. Climate Change Science Program and the Subcommittee on Global Change Research, Washington, D.C.

For Chapter 2:

Levy II, H., D. T. Shindell, T. Wigley, 2008: Climate Projections From Well-Mixed Greenhouse Gas Stabilization Scenarios in *Climate Projections Based on Emissions Scenarios for Long-Lived and Short-Lived Radiatively Active Gases and Aerosols*. H. Levy II, D.T. Shindell, A. Gilliland, M.D. Schwarzkopf, L.W. Horowitz, (eds.). A Report by the U.S. Climate Change Science Program and the Subcommittee on Global Change Research, Washington, D.C.

For Chapter 3:

Shindell, D.T., H. Levy II, A. Gilliland, M.D. Schwarzkopf, L.W. Horowitz, 2008: Climate Change From Short-Lived Emissions Due to Human Activities in *Climate Projections Based on Emissions Scenarios for Long-Lived and Short-Lived Radiatively Active Gases and Aerosols*. H. Levy II, D.T. Shindell, A. Gilliland, M.D. Schwarzkopf, L.W. Horowitz, (eds.). A Report by the U.S. Climate Change Science Program and the Subcommittee on Global Change Research, Washington, D.C.

For Chapter 4:

Levy II, H., D.T. Shindell, A. Gilliland, 2008: Findings, Issues, Opportunities, and Recommendations in *Climate Projections Based on Emissions Scenarios for Long-Lived and Short-Lived Radiatively Active Gases and Aerosols*. H. Levy II, D.T. Shindell, A. Gilliland, M.D. Schwarzkopf, L.W. Horowitz, (eds.). A Report by the U.S. Climate Change Science Program and the Subcommittee on Global Change Research, Washington, D.C.

For Appendix A:

Levy II, H., T. Wigley, 2008: IPCC 4th Assessment Climate Projections in *Climate Projections Based on Emissions Scenarios for Long-Lived and Short-Lived Radiatively Active Gases and Aerosols*. H. Levy II, D.T. Shindell, A. Gilliland, M.D. Schwarzkopf, L.W. Horowitz, (eds.). A Report by the U.S. Climate Change Science Program and the Subcommittee on Global Change Research, Washington, D.C.



very poorly known, is probably the most critical. Many aspects of the particle-cloud interaction are not well quantified, and hence the effect was left out entirely in the GFDL and CCSM simulations. The GISS model used a highly parameterized approach that is quite crude. The modeling community as a whole cannot yet produce a credible characterization of the climate response to particle/cloud interactions. Moreover, the measurements needed to guide this characterization do not yet exist. All mainstream climate models

(including those participating in this study) are currently either ignoring it, or strongly constraining the model response. Attempts have been made using satellite and ground-based observations to improve the characterization of the indirect effect, but major limitations remain.

As discussed in Section 3.2.4, observations of aerosol optical depth¹⁰ are best able to constrain the total extinction (absorption plus scattering) of sunlight by all particles under clear-sky conditions, but not to identify the effect of individual particles which may scatter (cool) or absorb (warm). Improved measurements of extinction and absorption may allow those two classes of particles to be separated, but will not solve the fundamental problem of determining their relative individual importance. As seen in this and other studies, models exhibit a wide range of relative contributions to total aerosol optical depth from the various natural and anthropogenic particles (Figure 3.2). Thus, the direct radiative effect of changes in a particular particle can be substantially different among models depending upon the relative importance of that particle.

¹⁰ Aerosol optical depth is a measure of the fraction of the sun's radiation at a given wavelength absorbed or scattered by particles while that radiation passes through the atmosphere.

Additionally, particles are not independent of one another. They mix together, a process that is only beginning to be incorporated in composition and climate models. In these studies, for example, the GISS model included the influence of sulfate particles sticking to dust, which can decrease the sulfate radiative forcing, by ~40 percent between 2000 and 2030 (Bauer *et al.*, 2007), but the sticking rates are quite uncertain. Mixing of other particle types is also highly uncertain, but is known to occur in the atmosphere and would also affect the magnitude of particle radiative forcings.

Another process that influences the effect of particles on climate is their uptake of water vapor, which alters their size and optical properties. This process is now included in all state-of-the-art comprehensive climate models. As the uptake varies exponentially with relative humidity, small differences in treatment of this process have the potential to cause large discrepancies. However, our analysis in Chapter 3 (*e.g.*, Table 3.7) suggests that the differences induced by this process may be small relative to the others we have just discussed.

4.3.3 Climate and Air Quality Policy Interdependence

Chapter 3 exposes major uncertainties in the climate impacts of short-lived gases and particles that will have to be addressed in future research. We raise important issues linking air quality control and global warming, but are unable to provide conclusive answers. We are able, however, to identify key questions that must be addressed by future research.

Most future sources of short-lived gases and particles result from the same combustion processes responsible for the increases in atmospheric carbon dioxide. However, while reductions in their emissions are currently driven by local and regional air pollution issues that can be addressed independently of any reductions in carbon dioxide emissions, in the future a unified approach could effectively address both climate and air quality issues. Furthermore, the climate responses to emissions changes in short-lived pollutants can be felt much more quickly because of shorter atmospheric lifetimes. The good news is that there is at least one clear win-win solution for climate (less warming) and



air quality (less pollution): methane reduction. Decreases in methane emissions lead to reduced levels of lower atmospheric ozone, thereby improving air quality; and both the direct methane and indirect ozone decreases lead to reduced global warming (Fiore *et al.*, 2002; Shindell *et al.*, 2005; West and Fiore, 2005; West *et al.*, 2006). Reductions in emissions of carbon monoxide or volatile organic compounds (VOCs) have similar effects, namely leading to reduced abundances of both methane and ozone (Bernsten *et al.*, 2005; Shindell *et al.*, 2005; West *et al.*, 2006; West *et al.*, 2007), therefore providing additional win-win strategies for improvement of climate and air quality. Reductions in black carbon particles and nitrogen oxide are potentially win-win as well, but the climate impact of reductions in their emissions is uncertain. On the other hand, the reduction of sulfur and organic carbon particles results in a reduction of cooling and increased global warming.

The cases of black carbon (soot) and nitrogen oxide gases are illustrative of the complexities of this issue. A major source of soot is the burning of biofuel, the sources of which are primarily animal and human waste as well as crop residue, all of which are considered carbon dioxide neutral (*i.e.*, the cycle of production and combustion does not lead to a net increase in atmospheric carbon dioxide). Current suggested replacements result in the release of fossil carbon dioxide. Therefore this reduction in biofuel burning, while reducing the emission of soot, will increase the net emission of carbon dioxide. The actual net climate response from reduced use of biofuel is not clear. The case of nitrogen oxides appears to be approximately neutral for climate, though clearly a strong win for air quality. Reducing nitrogen oxides reduces ozone, which reduces warming. However, reductions in both lead to reduced hydroxyl radicals and therefore an increased level of methane, which increases warming.

There clearly are win-win, win-uncertain, and win-lose situations regarding climate and actions taken to improve air quality. We are not making any policy recommendations in Synthesis and Assessment Product 3.2, but we do identify the policy relevant scientific issues. At this time we can not provide any quantita-

tively definitive scientific answers beyond the well known facts that the decrease of sulfur and organic carbon particles, both of which cool the climate, will increase global warming, while decreased methane, carbon monoxide, and volatile organics will decrease global mean warming. Decreases in the burning of biofuel, as well as decreased emissions of nitrogen oxides, are more complex and the net result is not clear at this time.

4.4 RESEARCH OPPORTUNITIES AND RECOMMENDATIONS

This last section of the report is a call for focused scientific research in emissions projections, radiative forcing, chemical composition modeling and regional downscaling. Particular emphasis needs to be paid to the future emissions scenarios for sulfur dioxide, black carbon particles and nitrogen oxides, to the indirect radiative forcing by particles, and to a number of ambiguities in current treatments of transport, deposition, and chemistry.

4.4.1 Emissions Scenario Development

Future climate studies must seriously address the very difficult issue of producing realistic and consistent 100-year emissions scenarios for short-lived gases and particles that include a wide range of socio-economic and development pathways and are driven by local and regional air quality actions taken around the globe.

The current best projections used in this report and in the Fourth Assessment Report of the IPCC do not even agree on whether black carbon particle and nitrogen oxide emissions trends continue to increase or decrease. While all the current sulfur dioxide emissions projections used in this study assume that emissions in 2100 will be less than at present, how much less is quite uncertain, and all of these projected decreases by 2100 may well be wrong. Part of the reason for the different emission inventories used here and in the IPCC studies was that the integrated assessment models did not recognize that these gases and particles were necessarily important when the scenarios were first constructed. Clarification of the challenges associated with emissions projections (not a simple matter of improving quantitative skill, as these



- models. *Journal of Geophysical Research*, **111**, D18101, doi:10.1029/2005JD006323.
- Mitchell**, J.F.B., R.A. Davis, W.J. Ingram, and C.A. Senior, 1995: On surface temperature, greenhouse gases, and aerosols: models and observations. *Journal of Climate*, **8(10)**, 2364-2386.
- Nakićenović**, N. and R. Swart (eds.), 2000: *Special Report on Emissions Scenarios*. A special report of Working Group III of the Intergovernmental Panel on Climate Change. Cambridge University Press, Cambridge, UK, and New York, 599 pp.
- Nolte**, C.G., A.B. Gilliland, C. Hogrefe, and L.J. Mickley, 2008: Linking global to regional models to assess future climate impacts on surface ozone levels in the United States. *Journal of Geophysical Research*, **113**, D14307, doi:10.1029/2007JD008497.
- Olivier**, J.G.J. and J.J.M. Berdowski, 2001: Global emissions sources and sinks. In: *The Climate System* [Berdowski, J., R. Guicherit and B.-J. Heij (eds.)]. A.A. Balkema Publishers/Swets & Zeitlinger Publishers, Lisse, The Netherlands, pp. 33-78.
- Pincus**, R. and M. Baker, 1994: Precipitation, solar absorption, and albedo susceptibility in marine boundary layer clouds. *Nature*, **372(6503)**, 250-252.
- Ramaswamy**, V. and C.-T. Chen, 1997: Linear additivity of climate response for combined albedo and greenhouse perturbations. *Geophysical Research Letters*, **24(5)**, 567-570.
- Ramaswamy**, V., O. Boucher, J. Haigh, D. Hauglustaine, J. Haywood, G. Myhre, T. Nakajima, G.Y. Shi, and S. Solomon, 2001: Radiative forcing of climate change. In: *Climate Change 2001: The Basis*. Contribution of Working Group I to the Third Assessment Report of the Intergovernmental Panel on Climate Change [Houghton, J. T., Y. Ding, D.J. Griggs, M. Noguer, P.J. van der Linden, X. Dai, K. Maskell, and C.A. Johnson (eds.)]. Cambridge University Press, Cambridge, UK, and New York, pp. 349-416.
- Schmidt**, G.A., R. Ruedy, J.E. Hansen, I. Aleinov, N. Bell, M. Bauer, S. Bauer, B. Cairns, V. Canuto, Y. Cheng, A. Del Genio, G. Faluvegi, A.D. Friend, T.M. Hall, Y. Hu, M. Kelley, N.Y. Kiang, D. Koch, A.A. Lacis, J. Lerner, K.K. Lo, R.L. Miller, L. Nazarenko, V. Oinas, J. Perlwitz, J. Perlwitz, D. Rind, A. Romanou, G.L. Russell, M. Sato, D.T. Shindell, P.H. Stone, S. Sun, N. Tausnev, D. Thresher, and M.-S. Yao, 2006: Present day atmospheric simulations using GISS ModelE: comparison to in-situ, satellite and reanalysis data. *Journal of Climate*, **19(2)**, 153-192.
- Schulz**, M., C. Textor, S. Kinne, Y. Balkanski, S. Bauer, T. Bernsten, T. Berglen, O. Boucher, F. Dentener, S. Guibert, I.S.A. Isaksen, T. Iversen, D. Koch, A. Kirkevåg, X. Liu, V. Montanaro, G. Myhre, J.E. Penner, G. Pitari, S. Reddy, Ø. Seland, P. Stier, and T. Takemura, 2006: Radiative forcing by aerosols as derived from the AeroCom present-day and pre-industrial simulations. *Atmospheric Chemistry and Physics*, **6(12)**, 5225-5246.
- Shindell**, D.T., G. Faluvegi, and N. Bell, 2003: Preindustrial-to-present-day radiative forcing by tropospheric ozone from improved simulations with the GISS chemistry-climate GCM. *Atmospheric and Chemical Physics*, **3(5)**, 1675-1702.
- Shindell**, D.T., B.P. Walter, and G. Faluvegi, 2004: Impacts of climate change on methane emissions from wetlands. *Geophysical Research Letters*, **31(21)**, L21202, doi:10.1029/2004GL021009.
- Shindell**, D.T., G. Faluvegi, A. Lacis, J.E. Hansen, R. Ruedy, and E. Aguilar, 2006a: The role of tropospheric ozone increases in 20th century climate change. *Journal of Geophysical Research*, **111(D8)**, D08302, , doi:10.1029/2005JD006348.
- Shindell**, D.T., G. Faluvegi, N. Unger, E. Aguilar, G.A. Schmidt, D. Koch, S.E. Bauer, and R.L. Miller, 2006b: Simulations of preindustrial, present-day, and 2100 conditions in the NASA GISS composition and climate model G-PUCCINI. *Atmospheric Chemistry and Physics*, **6**, 4427-4459.
- Shindell**, D.T., G. Faluvegi, S.E. Bauer, D.M. Koch, N. Unger, S. Menon, R.L. Miller, G.A. Schmidt, and D.G. Streets, 2007: Climate response to projected changes in short-lived species under an A1B scenario from 2000-2050 in the GISS climate model. *Journal of Geophysical Research*, **112(D20)**, D20103, doi:10.1029/2007JD008753.
- Shindell**, D.T., H. Levy II, M.D. Schwarzkopf, L.W. Horowitz, J.-F. Lamarque, and G. Faluvegi, 2008: Multi-model projections of climate change from short-lived emissions due to human activities. *Journal of Geophysical Research*, **113**, D11109, doi:10.1029/2007JD009152.
- Stevenson**, D.S., F.J. Dentener, M. G. Schultz, K. Ellingsen, T.P.C. van Noije, O. Wild, G. Zeng, M. Amann, C.S. Atherton, N. Bell, D.J. Bergmann, I. Bey, T. Butler, J. Cofala, W.J. Collins, R.G. Derwent, R.M. Doherty, J. Drevet, H.J. Eskes, A.M. Fiore, M. Gauss, D.A. Hauglustaine, L.W. Horowitz, I.S.A. Isaksen, M.C. Krol, J.-F. Lamarque, M.G. Lawrence, V. Montanaro, J.-F. Müller, G. Pitari, M.J. Prather, J.A. Pyle, S. Rast, J.M. Rodriguez, M.G. Sanderson, N.H. Savage, D.T. Shindell, S.E. Strahan, K. Sudo, and S. Szopa, 2006: Multi-model ensemble simulations of present-day and near-future tropospheric ozone. *Journal of Geophysical Research*, **111(D8)**, D08301, doi:10.1029/2005JD006338.

- Stewart**, R.W., S. Hameed, and J.P. Pinto, 1977: Photochemistry of the tropospheric ozone. *Journal of Geophysical Research*, **82(21)**, 3134-3140.
- Stouffer**, R.J., 2004: Time scales of climate response. *Journal of Climate*, **17(1)**, 209-217.
- Stouffer**, R.J., T.L. Delworth, K.W. Dixon, R. Gudgel, I. Held, R. Hemler, T. Knutson, M.D. Schwarzkopf, M.J. Spelman, M.W. Winton, A.J. Broccoli, H-C. Lee, F. Zeng, and B. Soden, 2006: GFDL's CM2 global coupled climate models. Part IV: Idealized climate response. *Journal of Climate*, **19(5)**, 723-740.
- Streets**, D., T.C. Bond, T. Lee, and C. Jang, 2004: On the future of carbonaceous aerosol emissions. *Journal of Geophysical Research*, **109(D24)**, doi:10.1029/2004JD004902.
- Twomey**, S., 1974: Pollution and the planetary albedo. *Atmospheric Environment*, **8(12)**, 1251-1256.
- Unger**, N., D.T. Shindell, D.M. Koch, and D.G. Streets, 2008: Air pollution radiative forcing from emissions sectors at 2030. *Journal of Geophysical Research*, **113**, D02306, doi:10.1029/2007JD008683.
- Van der Werf**, G.R., J.T. Randerson, G.J. Collatz, and L. Giglio, 2003: Carbon emissions from in tropical and subtropical ecosystems. *Global Change Biology*, **9(4)**, 547-562.
- Woodward**, S., D.L. Roberts, and R.A. Betts, 2005: A simulation of the effect of climate change-induced on mineral dust aerosol. *Geophysical Research Letters*, **32(18)**, L18810, doi:10.1029/2005GL023482.
- Atmospheric Concentrations**. Sub-report 2.1A of Synthesis and Assessment Product 2.1 by the U.S. Climate Change Science Program and the Subcommittee on Global Change Research. Department of Energy, of Biological & Environmental Research, Washington, DC, 154 pp.
- Fan**, S-M., L.W. Horowitz, H. Levy II, and W.J. Moxim, 2004: Impact of air pollution on wet deposition of mineral dust aerosols. *Geophysical Research Letters*, **31(2)**, L02104, doi:10.1029/2003GL018501.
- Fiore**, A.M., D.J. Jacob, B.D. Field, D.G. Streets, S.D. Fernandes, and C. Jang, 2002: Linking ozone pollution and climate change: The case for controlling methane. *Geophysical Research Letters*, **29(19)**, 1919, doi:10.1029/2002GL015601.
- Hegerl**, G.C., F.W. Zwiers, P. Braconnot, N.P. Gillett, Y. Luo, J.A. Marengo Orsini, N. Nicholls, J.E. Penner, and P.A. Scott, 2007: Understanding and attributing climate change. In: *Climate Change 2007: The Physical Science Basis*. Contribution of Working Group I to the Fourth Assessment Report (AR4) of the Intergovernmental Panel on Climate Change [Solomon, S., D. Qin, M. Manning, Z. Chen, M. Marquis, K.B. Averyt, M. Tignor and H.L. Miller (eds.)]. Cambridge University Press, Cambridge, UK and New York, pp. 663-745.
- IPCC** (Intergovernmental Panel on Climate Change) 2007: *Climate Change 2007: The Physical Science Basis*. Contribution of Working Group I to the Fourth Assessment Report (AR4) of the Intergovernmental Panel on Climate Change [Solomon, S., D. Qin, M. Manning, Z. Chen, M. Marquis, K.B. Averyt, M. Tignor, and H.L. Miller (eds.)]. Cambridge University Press, Cambridge, UK, and New York, 996 pp.
- Mahowald**, N.M. and C. Luo, 2003: A less dusty future? *Geophysical Research Letters*, **30(17)**, doi:10.1029/2003GL017880.
- Shindell**, D.T., G. Faluvegi, N. Bell, and G.A. Schmidt, 2005: An emissions-based view of climate forcing by methane and tropospheric ozone. *Geophysical Research Letters*, **32**, L04803, doi:10.1029/2004GL021900.
- Streets**, D., T.C. Bond, T. Lee, and C. Jang, 2004: On the future of carbonaceous aerosol emissions. *Journal of Geophysical Research*, **109(D24)**, D24212, doi:10.1029/2004JD004902.
- West**, J.J. and A.M. Fiore, 2005: Management of tropospheric ozone by reducing methane emissions. *Environmental Science & Technology*, **39**, 4685-4691.
- West**, J.J., A.M. Fiore, L.W. Horowitz, and D.L. Mauzerall, 2006: Global health of mitigating ozone pollution with meth-

CHAPTER 4 REFERENCES

- Bauer**, S.E. and D. Koch, 2005: Impact of heterogeneous sulfate formation at mineral dust surfaces on aerosol loads and radiative forcing in the Goddard Institute for Space Studies general circulation model. *Journal of Geophysical Research*, **110(D17)**, D17202, doi:10.1029/2005JD005870.
- Bauer**, S.E., D. Koch, N. Unger, S.M. Metzger, D.T. Shindell, and D. Streets, 2007: Nitrate aerosols today and in 2030: importance relative to other aerosol species and tropospheric ozone. *Atmospheric Chemistry and Physics*, **7(19)**, 5043-5059.
- Berntsen**, T.K., J.S. Fuglestedt, M.M. Joshi, K.P. Shine, N. Stuber, M. Ponater, R. Sausen, D.A. Hauglustaine, and L. Li, 2005: Response of climate to regional emissions of ozone precursors: sensitivities and warming potentials. *Tellus B*, **57(4)**, 283-304.
- Clarke**, L., J. Edmonds, H. Jacoby, H. Pitcher, J. Reilly, and R. Richels, 2007: *Scenarios of Greenhouse Gas Emissions and*

ane emission controls. *Proceedings of the National Academy of Sciences*, **103(11)**, 3988-3993.

West, J.J., A.M. Fiore, V. Naik, L.W. Horowitz, M.D. Schwarzkopf, and D.L. Mauzerall, 2007: Ozone air quality and radiative forcing consequences of changes in ozone precursor emissions. *Geophysical Research Letters*, **34**, L06806, doi:10.1029/2006GL029173.

Woodward, S., D.L. Roberts, and R.A. Betts, 2005: A simulation of the effect of climate change-induced on mineral dust aerosol. *Geophysical Research Letters*, **32(18)**, L18810, doi:10.1029/2005GL023482.

APPENDIX A REFERENCES

Clarke, L., J. Edmonds, H. Jacoby, H. Pitcher, J. Reilly, and R. Richels, 2007: *Scenarios of Greenhouse Gas Emissions and Atmospheric Concentrations*. Sub-report 2.1A of Synthesis and Assessment Product 2.1 by the U.S. Climate Change Science Program and the Subcommittee on Global Change Research. Department of Energy, of Biological & Environmental Research, Washington, DC, 154 pp.

CCSP (Climate Change Science Program), 2008: *Weather and Climate Extremes in a Changing Climate: Regions of Focus: North America, Hawaii, Caribbean, and U.S. Islands*. [Karl, T.R., G.A. Meehl, C.D. Miller, S.J. Hassol, A.M. Waple, and W.L. Murray (eds.)]. Synthesis and Assessment Product 3.3. U.S. Climate Change Science Program, Washington, DC, 164 pp.

Dai, A., G.A. Meehl, W.M. Washington, T.M.L. Wigley, and J.M. Arblaster, 2001a: Ensemble simulation of century climate changes: business as usual vs. CO₂ stabilization. *Bulletin of the American Meteorological Society*, **82(11)**, 2377-2388.

Dai, A., T.M.L. Wigley, G.A. Meehl, and W.M. Washington, 2001b: Effects of stabilizing atmospheric CO₂ on global climate in the next two centuries. *Geophysical Research Letters*, **28(23)**, 4511-4514.

Emanuel, K., R. Sundararajan, and J. Williams, 2008: Hurricanes and global warming: results from downscaling IPCC AR4 simulations. *Bulletin of American Meteorological Society*, **89(3)**, 347-367.

Knutson, T.R., J.J. Sirutis, S.T. Garner, G.A. Vecchi, and I.M. Held, 2008: Simulated reduction in Atlantic hurricane frequency under century warming conditions. *Nature Geoscience*, **1(6)**, 359-364.

Meehl, G.A., T.F. Stocker, W.D. Collins, P. Friedlingstein, A.T. Gaye, J.M. Gregory, A. Kitoh, R. Knutti, J.M. Murphy, A. Noda, S.C.B. Raper, I.G. Watterson, A.J. Weaver and Z.-C. Zhao, 2007: Global climate projections. In: *Climate Change 2007: The Physical Basis*. Contribution of Working Group I to the Fourth Assessment Report (AR4) of the Intergovernmental Panel on Climate Change [Solomon, S., D. Qin, M. Manning, Z. Chen, M. Marquis, K.B. Averyt, M. Tignor, and H.L. Miller (eds.)]. Cambridge University Press, Cambridge, UK, and New York, pp. 747-845.

Wigley, T.M.L., R. Richels, and J.A. Edmonds, 2007: Overshoot pathways to CO₂ stabilization in a multi-gas context. In: *Human Induced Climate Change: An Interdisciplinary Assessment* [Schlesinger, M., F.C. de la Chesnaye, H. Kheshgi, C.D. Kolstad, J. Reilly, J.B. Smith, and T. Wilson (eds.)]. Cambridge University Press, Cambridge, UK, pp. 84-92.

APPENDIX B REFERENCES

Church, J.A. and J.M. Gregory, 2001: Changes in sea level. In: *Climate Change 2001: The Basis*. Contribution of Working Group I to the Third Assessment Report of the Intergovernmental Panel on Climate Change [Houghton, J.T., Y. Ding, D.J. Griggs, M. Noguer, P.J. van der Linden, X. Dai, K. Maskell, and C.A. Johnson (eds.)]. Cambridge University Press, Cambridge, UK, and New York, pp. 639-693.

Cubasch, U. and G.A. Meehl, 2001: Projections for future climate change. In: *Climate Change 2001: The Basis*. Contribution of Working Group I to the Third Assessment Report of the Intergovernmental Panel on Climate Change [Houghton, J.T., Y. Ding, D.J. Griggs, M. Noguer, P.J. van der Linden, X. Dai, K. Maskell, and C.A. Johnson (eds.)]. Cambridge University Press, Cambridge, UK, and New York, pp. 525-582.

Harvey, L.D.D., J. Gregory, M. Hoffert, A. Jain, M. Lal, R. Leemans, S.B.C. Raper, T.M.L. Wigley, and J. de Wolde, 1997: *An Introduction to Simple Climate Models Used in the IPCC Second Assessment Report*. IPCC technical paper 2 [Houghton, J.T., L.G. Meira Filho, D.J. Griggs, and M. Noguer (eds.)]. Intergovernmental Panel on Climate Change, Geneva, Switzerland, 50 pp.

Hoffert, M.L., A.J. Callegari, and C.-T. Hsieh, 1980: The role of deep sea heat storage in the secular response to climate forcing. *Journal of Geophysical Research*, **85(C11)**, 6667- 6679.

IPCC (Intergovernmental Panel on Climate Change), 2001: *Climate Change 2001: The Basis*. Contribution of Working Group I to the Third Assessment Report of the Intergovernmental Panel on Climate Change [Houghton, J.T., Y. Ding, D.J. Griggs, M. Noguer, P.J. van der Linden, X. Dai,

Contact Information

1717 Pennsylvania Avenue, NW
Suite 250
Washington, DC 20006
202-223-6262 (voice)
202-223-3065 (fax)

The Climate Change Science Program incorporates the U.S. Global Change Research Program and the Climate Change Research Initiative.

To obtain a copy of this document, place an order at the Global Change Research

<http://www.gcrio.org/orders>

Climate Change Science Program and the Subcommittee on Global Change Research

William Brennan, Chair
Department of Commerce
National Oceanic and Atmospheric Administration
Acting Director, Climate Change Science Program

Jack Kaye, Vice Chair
National Aeronautics and Space Administration

Allen Dearry
Department of Health and Human Services

Jerry Elwood
Department of Energy

Mary Glackin
National Oceanic and Atmospheric Administration

Patricia Gruber
Department of Defense

William Hohenstein
Department of Agriculture

Linda Lawson
Department of Transportation

Mark Myers
U.S. Geological Survey

Timothy Killeen
National Science Foundation

Patrick Neale
Smithsonian Institution

Jacqueline Schafer
U.S. Agency for International Development

Joel Scheraga
Environmental Protection Agency

Harlan Watson
Department of State

EXECUTIVE OFFICE AND OTHER LIAISONS

Stephen Eule
Department of Energy
Director, Climate Change Technology Program

Katharine Gebbie
National Institute of Standards & Technology

Stuart Levenbach

Margaret McCalla

Rob Rainey
Council on Environmental Quality

Daniel Walker
Technology Policy



U.S. Climate Change Science Program
1717 Pennsylvania Avenue, NW • Suite 250 • Washington, D.C. 20006 USA
1-202-223-6262 (voice) • 1-202-223-3065 (fax)
<http://www.climatechange.gov>



Exhibit 16

[Our Work](#)[Get Involved](#)[About](#)[Donate](#)

Methane: The other important greenhouse gas

Methane is the primary component of natural gas — a common fuel source.

Why are we concerned about it?

If methane leaks into the air before being used — from a leaky pipe, for instance — it absorbs the sun's heat, warming the atmosphere. For this reason, it's considered a greenhouse gas, like carbon dioxide.

Why is it as critical to address as carbon dioxide?

In the first two decades after its release, methane is 84 times more potent than carbon dioxide. We must address both types of emissions if we want to reduce the impact of climate change.

While methane doesn't linger as long in the atmosphere as carbon dioxide, it is initially far more devastating to the climate because of how effectively it absorbs heat.

Because methane is so potent, and because we have solutions that reduce emissions, addressing methane is the fastest, most effective way to slow the rate of warming now.

Where is it coming from?

Methane can come from many sources, both natural and manmade. One major source of manmade methane emissions is the global oil and gas industry.

At least 25%

of today's global warming is caused by manmade methane emissions *

How do we fix the methane problem?

Until recently, little was known about where leaks were occurring, or the best way to fix them. In 2012, we kicked off a research series to better pinpoint leaks, and to find solutions.

A [summary of our 16 studies](#) of the whole U.S. supply chain shows methane emissions are significantly higher than we thought, reinforcing that major reductions from this sector are urgently needed.

In May 2016, the EPA finalized the first-ever national rule to directly limit methane emissions from oil and gas operations, unlocking a new opportunity to reduce climate pollution. We're working to defend these and related federal standards, which are under attack.

A closer look: Explore local leaks

Raising awareness about the scale and impact of methane leaks is essential to developing effective policy.

Our pilot project with Google Earth Outreach helps visualize the climate-damaging leaks found within local communities.

Act when it matters most

Every day **more than 60 people sign up** for news and alerts, to find out when their support helps most. Will you join them? (Read our [privacy policy](#).)

Sign up

Sources

* EDF calculation based on IPCC AR5 WGI Chapter 8.

“By emitting just a little bit of methane, mankind is greatly accelerating the rate of climatic change.”



[Steve Hamburg](#), EDF Chief Scientist

In-depth resources

- **Study series:** [U.S. methane emissions 60 percent higher than we thought](#)
- **Report:** [How reducing methane emissions creates jobs](#)
- **Study:** [Cost-effective solutions for reducing methane leaks](#)
- **Blog:** [Our experts' commentary](#)

Media contact

Lauren Whittenberg

(512) 691-3437 (office)

(512) 784-2161 (cell)

[Email](#)



About EDF

[CONTACT US](#)

[OFFICES](#)

[CAREERS](#)

Resources

[BLOGS](#)

[REPORTS AND PUBLICATIONS](#)

[FOR THE MEDIA](#)

Members

[BECOME A MEMBER](#)

[VISIT MYEDF](#)

[GET INVOLVED](#)

Exhibit 17

GREENHOUSE GASES

Assessment of methane emissions from the U.S. oil and gas supply chain

Ramón A. Alvarez^{1*}, Daniel Zavala-Araiza¹, David R. Lyon¹, David T. Allen², Zachary R. Barkley³, Adam R. Brandt⁴, Kenneth J. Davis³, Scott C. Herndon⁵, Daniel J. Jacob⁶, Anna Karion⁷, Eric A. Kort⁸, Brian K. Lamb⁹, Thomas Lauvaux³, Joannes D. Maasakkers⁶, Anthony J. Marchese¹⁰, Mark Omara¹, Stephen W. Pacala¹¹, Jeff Peischl^{12,13}, Allen L. Robinson¹⁴, Paul B. Shepson¹⁵, Colm Sweeney¹³, Amy Townsend-Small¹⁶, Steven C. Wofsy⁶, Steven P. Hamburg¹

Methane emissions from the U.S. oil and natural gas supply chain were estimated by using ground-based, facility-scale measurements and validated with aircraft observations in areas accounting for ~30% of U.S. gas production. When scaled up nationally, our facility-based estimate of 2015 supply chain emissions is 13 ± 2 teragrams per year, equivalent to 2.3% of gross U.S. gas production. This value is ~60% higher than the U.S. Environmental Protection Agency inventory estimate, likely because existing inventory methods miss emissions released during abnormal operating conditions. Methane emissions of this magnitude, per unit of natural gas consumed, produce radiative forcing over a 20-year time horizon comparable to the CO₂ from natural gas combustion. Substantial emission reductions are feasible through rapid detection of the root causes of high emissions and deployment of less failure-prone systems.

Methane (CH₄) is a potent greenhouse gas, and CH₄ emissions from human activities since preindustrial times are responsible for 0.97 W m⁻² of radiative forcing, as compared to 1.7 W m⁻² for carbon dioxide (CO₂) (1). CH₄ is removed from the atmosphere much more rapidly than CO₂; thus, reducing CH₄ emissions can effectively reduce the near-term rate of warming (2). Sharp growth in U.S. oil and natural gas (O/NG) production beginning around 2005 (3) raised concerns about the climate impacts of increased natural gas use (4, 5). By 2012, disagreement among published estimates of CH₄ emissions from U.S. natural gas operations led to a broad consensus that additional data were needed to better characterize emission rates (4–7). A large body of field measurements made between 2012 and 2016 (table S1) has markedly improved understanding of the sources and magnitude of CH₄ emissions from the industry's operations. Brandt *et al.* summarized the early literature (8); other assessments incorporated elements of recent data (9–11). This work synthesizes recent studies to provide an improved overall assessment of emissions from

the O/NG supply chain, which we define to include all operations associated with O/NG production, processing, and transport (materials and methods, section S1.0) (12).

Measurements of O/NG CH₄ emissions can be classified as either top-down (TD) or bottom-up (BU). TD studies quantify ambient methane enhancements using aircraft, satellites, or tower networks and infer aggregate emissions from all contributing sources across large geographies. TD estimates for nine O/NG production areas have been reported to date (table S2). These areas are distributed across the U.S. (fig. S1) and account for ~33% of natural gas, ~24% of oil production, and ~14% of all wells (13). Areas sampled in TD studies also span the range of hydrocarbon characteristics (predominantly gas, predominantly oil, or mixed), as well as a range of production characteristics such as well productivity and maturity. In contrast, BU studies generate regional, state, or national emission estimates by aggregating and extrapolating measured emissions from individual pieces of equipment, operations, or facilities, using measurements made directly at the emission point or, in the case of facilities, directly downwind.

Recent BU studies have been performed on equipment or facilities that are expected to represent the vast majority of emissions from the O/NG supply chain (table S1). In this work, we integrate the results of recent facility-scale BU studies to estimate CH₄ emissions from the U.S. O/NG supply chain, and then we validate the results using TD studies (materials and methods). The probability distributions of our BU methodology are based on observed facility-level emissions, in contrast to the component-by-component approach used for conventional inventories. We thus capture enhancements pro-

duced by all sources within a facility, including the heavy tail of the distribution. When the BU estimate is developed in this manner, direct comparison of BU and TD estimates of CH₄ emissions in the nine basins for which TD measurements have been reported indicates agreement between methods, within estimated uncertainty ranges (Fig. 1).

Our national BU estimate of total CH₄ emissions in 2015 from the U.S. O/NG supply chain is $13 (+2.1/-1.6, 95\% \text{ confidence interval})$ Tg CH₄/year (Table 1). This estimate of O/NG CH₄ emissions can also be expressed as a production-normalized emission rate of 2.3% (+0.4%/-0.3%) by normalizing by annual gross natural gas production [33 trillion cubic feet (13), with average CH₄ content of 90 volume %]. Roughly 85% of national BU emissions are from production, gathering, and processing sources, which are concentrated in active O/NG production areas.

Our assessment does not update emissions from local distribution and end use of natural gas, owing to insufficient information addressing this portion of the supply chain. However, recent studies suggest that local distribution emissions exceed the current inventory estimate (14–16), and that end-user emissions might also be important. If these findings prove to be representative, overall emissions from the natural gas supply chain would increase relative to the value in Table 1 (materials and methods, section S1.5).

Our BU method and TD measurements yield similar estimates of U.S. O/NG CH₄ emissions in 2015, and both are significantly higher than the corresponding estimate in the U.S. Environmental Protection Agency's Greenhouse Gas Inventory (EPA GHGI) (Table 1 and materials and methods, section S1.3) (17). Discrepancies between TD estimates and the EPA GHGI have been reported previously (8, 18). Our BU estimate is 63% higher than the EPA GHGI, largely due to a more than twofold difference in the production segment (Table 1). The discrepancy in production sector emissions alone is ~4 Tg CH₄/year, an amount larger than the emissions from any other O/NG supply chain segment. Such a large difference cannot be attributed to expected uncertainty in either estimate: The extremal ends of the 95% confidence intervals for each estimate differ by 20% (i.e., ~12 Tg/year for the lower bound of our BU estimate can be compared to ~10 Tg/year for the upper bound of the EPA GHGI estimate).

We believe the reason for such large divergence is that sampling methods underlying conventional inventories systematically underestimate total emissions because they miss high emissions caused by abnormal operating conditions (e.g., malfunctions). Distributions of measured emissions from production sites in BU studies are invariably “tail-heavy,” with large emission rates measured at a small subset of sites at any single point in time (19–22). Consequently, the most likely hypothesis for the difference between the EPA GHGI and BU estimates derived from facility-level measurements is that measurements used to develop GHGI emission factors

¹Environmental Defense Fund, Austin, TX, USA. ²University of Texas at Austin, Austin, TX, USA. ³The Pennsylvania State University, University Park, PA, USA. ⁴Stanford University, Stanford, CA, USA. ⁵Aerodyne Research Inc., Billerica, MA, USA. ⁶Harvard University, Cambridge, MA, USA. ⁷National Institute of Standards and Technology, Gaithersburg, MD, USA. ⁸University of Michigan, Ann Arbor, MI, USA. ⁹Washington State University, Pullman, WA, USA. ¹⁰Colorado State University, Fort Collins, CO, USA. ¹¹Princeton University, Princeton, NJ, USA. ¹²University of Colorado, CIRES, Boulder, CO, USA. ¹³NOAA Earth System Research Laboratory, Boulder, CO, USA. ¹⁴Carnegie Mellon University, Pittsburgh, PA, USA. ¹⁵Purdue University, West Lafayette, IN, USA. ¹⁶University of Cincinnati, Cincinnati, OH, USA.

*Corresponding author. Email: ralvarez@edf.org

undersample abnormal operating conditions encountered during the BU work. Component-based inventory estimates like the GHGI have been shown to underestimate facility-level emissions (23), probably because of the technical difficulty and safety and liability risks associated with measuring large emissions from, for example, venting tanks such as those observed in aerial surveys (24).

Abnormal conditions causing high CH₄ emissions have been observed in studies across the O/NG supply chain. An analysis of site-scale emission measurements in the Barnett Shale concluded that equipment behaving as designed could not explain the number of high-emitting production sites in the region (23). An extensive aerial infrared camera survey of ~8000 production sites in seven U.S. O/NG basins found that ~4% of surveyed sites had one or more observable high-emission rate plumes (24) (detection threshold of ~3 to 10 kg CH₄/hour was two to seven times higher than mean production site emissions estimated in this work). Emissions released from liquid storage tank hatches and vents represented 90% of these sightings. It appears that abnormal operating conditions must be largely responsible, because the observation frequency was too high to be attributed to routine operations like condensate flashing or liquid unloadings alone (24). All other observations were due to anomalous venting from dehydrators, separators, and flares. Notably, the two largest sources of aggregate emissions in the EPA GHGI—pneumatic controllers and equipment leaks—were never observed from these aerial surveys. Similarly, a national survey of gathering facilities found that emission rates were four times higher at the 20% of facilities where substantial tank venting emissions were observed, as compared to the 80% of facilities without such venting (25). In addition, very large emissions from leaking isolation valves at transmission and storage facilities were quantified by means of downwind measurement but could not be accurately (or safely) measured by on-site methods (26). There is an urgent need to complete equipment-based measurement campaigns that capture these large-emission events, so that their causes are better understood.

In contrast to abnormal operational conditions, alternative explanations such as outdated component emission factors are unlikely to explain the magnitude of the difference between our facility-based BU estimate and the GHGI. First, an equipment-level inventory analogous to the EPA GHGI but updated with recent direct measurements of component emissions (materials and methods, section S1.4) predicts total production emissions that are within ~10% of the EPA GHGI, although the contributions of individual source categories differ significantly (table S3). Second, we consider unlikely an alternative hypothesis that systematically higher emissions during daytime sampling cause a high bias in TD methods (materials and methods, section S1.6). Two other factors may lead to low bias in EPA GHGI and similar inventory

Table 1. Summary of this work's bottom-up estimates of CH₄ emissions from the U.S. oil and natural gas (O/NG) supply chain (95% confidence interval) and comparison to the EPA Greenhouse Gas Inventory (GHGI).

Industry segment	2015 CH ₄ emissions (Tg/year)	
	This work (bottom-up)	EPA GHGI (17)
Production	7.6 (+1.9/−1.6)	3.5
Gathering	2.6 (+0.59/−0.18)	2.3
Processing	0.72 (+0.20/−0.071)	0.44
Transmission and storage	1.8 (+0.35/−0.22)	1.4
Local distribution*	0.44 (+0.51/−0.22)	0.44
Oil refining and transportation*	0.034 (+0.050/−0.008)	0.034
U.S. O/NG total	13 (+2.1/−1.7)	8.1 (+2.1/−1.4) [†]

*This work's emission estimates for these sources are taken directly from the GHGI. The local distribution estimate is expected to be a lower bound on actual emissions and does not include losses downstream of customer meters due to leaks or incomplete combustion (materials and methods, section S1.5).
[†]The GHGI only reports industry-wide uncertainties.

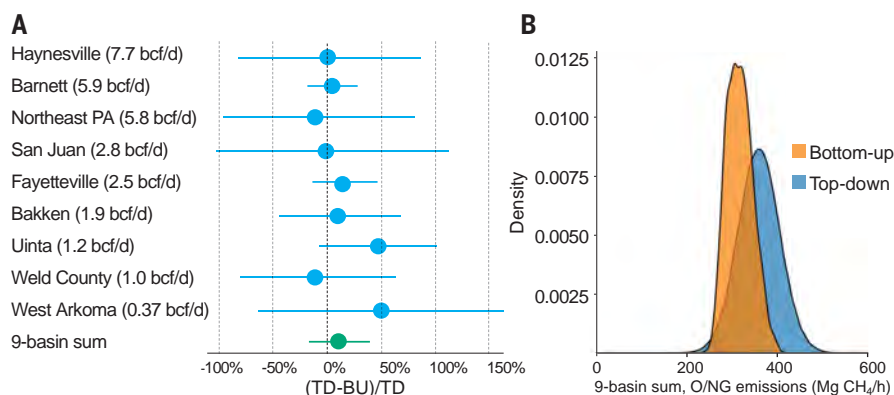


Fig. 1. Comparison of this work's bottom-up (BU) estimates of methane emissions from oil and natural gas (O/NG) sources to top-down (TD) estimates in nine U.S. O/NG production areas. (A) Relative differences of the TD and BU mean emissions, normalized by the TD value, rank ordered by natural gas production in billion cubic feet per day (bcf/d, where 1 bcf = 2.8×10^7 m³). Error bars represent 95% confidence intervals. **(B)** Distributions of the nine-basin sum of TD and BU mean estimates (blue and orange probability density, respectively). Neither the ensemble of TD-BU pairs (A) nor the nine-basin sum of means (B) are statistically different [$p = 0.13$ by a randomization test, and mean difference of 11% (95% confidence interval of −17 to 41%)].

estimates. Operator cooperation is required to obtain site access for emission measurements (8). Operators with lower-emitting sites are plausibly more likely to cooperate in such studies, and workers are likely to be more careful to avoid errors or fix problems when measurement teams are on site or about to arrive. The potential bias due to this “opt-in” study design is very challenging to determine. We therefore rely primarily on site-level, downwind measurement methods with limited or no operator forewarning to construct our BU estimate. Another possible source of bias is measurement error. It has been suggested that malfunction of a measurement instrument widely used in the O/NG industry contributes to underestimated emissions in inventories (27); however, this cannot explain the more than twofold difference in production emissions (28).

The tail-heavy distribution for many O/NG CH₄ emission sources has important implications for mitigation because it suggests that most sources—whether they represent whole facilities or individual pieces of equipment—can have lower emissions when they operate as designed. We anticipate that significant emissions reductions could be achieved by deploying well-designed emission detection and repair systems that are capable of identifying abnormally operating facilities or equipment. For example, pneumatic controllers and equipment leaks are the largest emission sources in the O/NG production segment exclusive of missing emission sources (38 and 21%, respectively; table S3), with malfunctioning controllers contributing 66% of total pneumatic controller emissions (materials and methods, section S1.4) and equipment leaks 60% higher than the GHGI estimate.

Gathering operations, which transport unprocessed natural gas from production sites to processing plants or transmission pipelines, produce ~20% of total O/NG supply chain CH₄ emissions. Until the publication of recent measurements (29), these emissions were largely unaccounted for by the EPA GHGI. Gas processing, transmission and storage together contribute another ~20% of total O/NG supply chain emissions, most of which come from ~2500 processing and compression facilities.

Our estimate of emissions from the U.S. O/NG supply chain (13 Tg CH₄/year) compares to the EPA estimate of 18 Tg CH₄/year for all other anthropogenic CH₄ sources (17). Natural gas losses are a waste of a limited natural resource (~\$2 billion/year), increase global levels of surface ozone pollution (30), and substantially erode the potential climate benefits of natural gas use. Indeed, our estimate of CH₄ emissions across the supply chain, per unit of gas consumed, results in roughly the same radiative forcing as does the CO₂ from combustion of natural gas over a 20-year time horizon (31% over 100 years). Moreover, the climate impact of 13 Tg CH₄/year over a 20-year time horizon roughly equals that from the annual CO₂ emissions from all U.S. coal-fired power plants operating in 2015 (31% of the impact over a 100-year time horizon) (materials and methods, section S1.7).

We suggest that inventory methods would be improved by including the substantial volume of missing O/NG CH₄ emissions evident from the large body of scientific work now available and synthesized here. Such empirical adjustments based on observed data have been previously used in air quality management (31).

The large spatial and temporal variability in CH₄ emissions for similar equipment and facilities (due to equipment malfunction and other abnormal operating conditions) reinforces the conclusion that substantial emission reductions are feasible. Key aspects of effective mitigation include pairing well-established technologies and best practices for routine emission sources with economically viable systems to rapidly detect the root causes of high emissions arising from abnormal conditions. The latter could involve combinations of current technologies such as on-site leak surveys by company personnel using optical gas imaging (32), deployment of passive sensors at individual facilities (33, 34) or mounted on ground-based work trucks (35), and in situ remote-sensing approaches using

tower networks, aircraft, or satellites (36). Over time, the development of less failure-prone systems would be expected through repeated observation of and further research into common causes of abnormal emissions, followed by re-engineered design of individual components and processes.

REFERENCES AND NOTES

1. G. Myhre *et al.*, in *Climate Change 2013: The Physical Science Basis. Contribution of Working Group I to the Fifth Assessment Report of the Intergovernmental Panel on Climate Change* (Cambridge Univ. Press, Cambridge, UK, 2013); www.ipcc.ch/pdf/assessment-report/ar5/wgl/WGIAR5_Chapter08_FINAL.pdf.
2. J. K. Shoemaker, D. P. Schrag, M. J. Molina, V. Ramanathan, *Science* **342**, 1323–1324 (2013).
3. U.S. Energy Information Administration (EIA), "Annual Energy Outlook 2017" (EIA, 2017); www.eia.gov/outlooks/aeo/.
4. R. W. Howarth, R. Santoro, A. Ingraffea, *Clim. Change* **106**, 679–690 (2011).
5. R. A. Alvarez, S. W. Pacala, J. J. Winebrake, W. L. Chameides, S. P. Hamburg, *Proc. Natl. Acad. Sci. U.S.A.* **109**, 6435–6440 (2012).
6. U.S. Department of Energy (DOE), "Ninety-day report of the Secretary of Energy Advisory Board's Shale Gas Subcommittee" (2011); <https://energy.gov/downloads/90-day-interim-report-shale-gas-production-secretary-energy-advisory-board>.
7. National Petroleum Council (NPC), "Prudent Development: Realizing the Potential of North America's Abundant Natural Gas and Oil Resources" (NPC, 2011); www.npc.org.
8. A. R. Brandt *et al.*, *Science* **343**, 733–735 (2014).
9. D. T. Allen, *J. Air Waste Manag. Assoc.* **66**, 549–575 (2016).
10. P. Balcombe, K. Anderson, J. Speirs, N. Brandon, A. Hawkes, *ACS Sustain. Chem. & Eng.* **5**, 3–20 (2017).
11. J. A. Littlefield, J. Marriot, G. A. Schivley, T. J. Skone, *J. Clean. Prod.* **148**, 118–126 (2017).
12. See supplementary materials.
13. Drillinginfo, Inc., Drillinginfo Production Query (2015); <https://info.drillinginfo.com/>.
14. D. Zavala-Araiza *et al.*, *Proc. Natl. Acad. Sci. U.S.A.* **112**, 1941–1946 (2015).
15. B. K. Lamb *et al.*, *Environ. Sci. Technol.* **50**, 8910–8917 (2016).
16. D. Wunch *et al.*, *Atmos. Chem. Phys.* **16**, 14091–14105 (2016).
17. U.S. Environmental Protection Agency (EPA), "Inventory of U.S. Greenhouse Gas Emissions and Sinks: 1990–2015" (EPA, 2017); www.epa.gov/ghgemissions/inventory-us-greenhouse-gas-emissions-and-sinks-1990-2015.
18. D. Zavala-Araiza *et al.*, *Proc. Natl. Acad. Sci. U.S.A.* **112**, 15597–15602 (2015).
19. C. W. Rella, T. R. Tsai, C. G. Botkin, E. R. Crosson, D. Steele, *Environ. Sci. Technol.* **49**, 4742–4748 (2015).
20. M. Omara *et al.*, *Environ. Sci. Technol.* **50**, 2099–2107 (2016).
21. A. M. Robertson *et al.*, *Environ. Sci. Technol.* **51**, 8832–8840 (2017).
22. A. R. Brandt, G. A. Heath, D. Cooley, *Environ. Sci. Technol.* **50**, 12512–12520 (2016).
23. D. Zavala-Araiza *et al.*, *Nat. Commun.* **8**, 14012 (2017).
24. D. R. Lyon *et al.*, *Environ. Sci. Technol.* **50**, 4877–4886 (2016).
25. A. L. Mitchell *et al.*, *Environ. Sci. Technol.* **49**, 3219–3227 (2015).
26. D. J. Zimmerman *et al.*, *Environ. Sci. Technol.* **49**, 9374–9383 (2015).
27. T. Howard, T. W. Ferrara, A. Townsend-Small, *J. Air Waste Manag. Assoc.* **65**, 856–862 (2015).

28. R. A. Alvarez, D. R. Lyon, A. J. Marchese, A. L. Robinson, S. P. Hamburg, *Elem. Sci. Anth.* **4**, 000137 (2016).
29. A. J. Marchese *et al.*, *Environ. Sci. Technol.* **49**, 10718–10727 (2015).
30. A. M. Fiore *et al.*, *Geophys. Res. Lett.* **29**, 21-1–25-4 (2002).
31. Texas Commission on Environmental Quality (TCEQ), "Houston-Galveston-Brazoria Attainment Demonstration State Implementation Plan Revision for the 1997 Eight-Hour Ozone Standard" (2010), pp. 3–18; www.tceq.texas.gov/assets/public/implementation/air/sip/hgb/hgb_sip_2009/09017SIP_completeNarr_ado.pdf.
32. A. P. Ravikumar, J. Wang, A. R. Brandt, *Environ. Sci. Technol.* **51**, 718–724 (2017).
33. U.S. Department of Energy (DOE) Advanced Research Projects Agency – Energy (ARPA-E, 2014), "ARPA-E MONITOR Program" (ARPA-E); <https://arpa-e.energy.gov/?q=programs/monitor>.
34. Environmental Defense Fund (EDF), "Methane Detectors Challenge" (EDF, 2014); www.edf.org/energy/natural-gas-policy/methane-detectors-challenge.
35. J. D. Albertson *et al.*, *Environ. Sci. Technol.* **50**, 2487–2497 (2016).
36. D. J. Jacob *et al.*, *Atmos. Chem. Phys.* **16**, 14371–14396 (2016).

ACKNOWLEDGMENTS

The authors are grateful to R. Harriss for support in the design and conduct of studies. We thank D. Zimmerle, A. Robertson, and A. Pintar for helpful discussions, and the scores of researchers that contributed to the body of work assessed here. **Funding:** Alfred P. Sloan Foundation, Fiona and Stan Druckenmiller, Heising-Simons Foundation, Bill and Susan Oberndorf, Betsy and Sam Reeves, Robertson Foundation, TomKat Charitable Trust, and the Walton Family Foundation (for EDF authors as well as support of related studies involving D.T.A., S.C.H., A.K., E.A.K., B.K.L., A.J.M., A.L.R., P.B.S., C.S., A.T.-S., S.C.W.); DOE National Energy Technology Laboratory (Z.R.B., K.J.D., T.L., A.L.R.); NASA Earth Science Division (D.J.J., E.A.K., J.D.M.); NOAA Climate Program Office (E.A.K., J.P., A.L.R., C.S.). **Author contributions:** R.A.A., D.Z.-A., D.R.L., and S.P.H. conceived the study; R.A.A., D.Z.-A., D.R.L., E.A.K., S.W.P. and S.P.H. designed the study and interpreted results with input from all authors; each author contributed to the collection, analysis, or assessment of one or more datasets necessary to perform this study; D.Z.-A., D.R.L., and S.W.P. performed the analysis, with contributions from R.A.A., A.R.B., A.K., and M.O.; R.A.A., D.Z.-A., D.R.L., S.W.P., S.C.W., and S.P.H. wrote the manuscript with input from all authors. **Competing interests:** None declared. **Data and materials availability:** All data and methods needed to reproduce the results in the paper are provided in the paper or as supplementary materials. Additional author disclosures (affiliations, funding sources, financial holdings) are provided in the supplementary materials.

SUPPLEMENTARY MATERIALS

www.sciencemag.org/content/361/6398/186/suppl/DC1
Materials and Methods
Additional Author Disclosures
Figs. S1 to S11
Tables S1 to S12
References (37–77)
Databases S1 and S2

19 December 2017; accepted 18 May 2018
Published online 21 June 2018
10.1126/science.aar7204

Assessment of methane emissions from the U.S. oil and gas supply chain

Ramón A. Alvarez, Daniel Zavala-Araiza, David R. Lyon, David T. Allen, Zachary R. Barkley, Adam R. Brandt, Kenneth J. Davis, Scott C. Herndon, Daniel J. Jacob, Anna Karion, Eric A. Kort, Brian K. Lamb, Thomas Lauvaux, Joannes D. Maasakkers, Anthony J. Marchese, Mark Omara, Stephen W. Pacala, Jeff Peischl, Allen L. Robinson, Paul B. Shepson, Colm Sweeney, Amy Townsend-Small, Steven C. Wofsy and Steven P. Hamburg

Science **361** (6398), 186-188.

DOI: 10.1126/science.aar7204 originally published online June 21, 2018

A leaky endeavor

Considerable amounts of the greenhouse gas methane leak from the U.S. oil and natural gas supply chain. Alvarez *et al.* reassessed the magnitude of this leakage and found that in 2015, supply chain emissions were ~60% higher than the U.S. Environmental Protection Agency inventory estimate. They suggest that this discrepancy exists because current inventory methods miss emissions that occur during abnormal operating conditions. These data, and the methodology used to obtain them, could improve and verify international inventories of greenhouse gases and provide a better understanding of mitigation efforts outlined by the Paris Agreement.

Science, this issue p. 186

ARTICLE TOOLS

<http://science.sciencemag.org/content/361/6398/186>

SUPPLEMENTARY MATERIALS

<http://science.sciencemag.org/content/suppl/2018/06/20/science.aar7204.DC1>

REFERENCES

This article cites 60 articles, 8 of which you can access for free
<http://science.sciencemag.org/content/361/6398/186#BIBL>

PERMISSIONS

<http://www.sciencemag.org/help/reprints-and-permissions>

Use of this article is subject to the [Terms of Service](#)

Science (print ISSN 0036-8075; online ISSN 1095-9203) is published by the American Association for the Advancement of Science, 1200 New York Avenue NW, Washington, DC 20005. The title *Science* is a registered trademark of AAAS.

Copyright © 2018 The Authors, some rights reserved; exclusive licensee American Association for the Advancement of Science. No claim to original U.S. Government Works

Exhibit 18

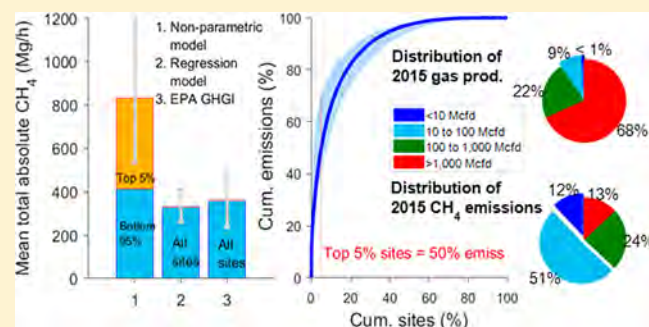
Methane Emissions from Natural Gas Production Sites in the United States: Data Synthesis and National Estimate

Mark Omara,^{*,†} Naomi Zimmerman,[‡] Melissa R. Sullivan, Xiang Li,[§] Aja Ellis, Rebecca Cesa, R. Subramanian, Albert A. Presto,^{||} and Allen L. Robinson^{||}

Center for Atmospheric Particle Studies, Department of Mechanical Engineering, Carnegie Mellon University, 5000 Forbes Avenue, Pittsburgh, Pennsylvania 15213, United States

Supporting Information

ABSTRACT: We used site-level methane (CH₄) emissions data from over 1000 natural gas (NG) production sites in eight basins, including 92 new site-level CH₄ measurements in the Uinta, northeastern Marcellus, and Denver-Julesburg basins, to investigate CH₄ emissions characteristics and develop a new national CH₄ emission estimate for the NG production sector. The distribution of site-level emissions is highly skewed, with the top 5% of sites accounting for 50% of cumulative emissions. High emitting sites are predominantly also high producing (>10 Mcfd). However, low NG production sites emit a larger fraction of their CH₄ production. When combined with activity data, we predict that this creates substantial variability in the basin-level CH₄ emissions which, as a fraction of basin-level CH₄ production, range from 0.90% for the Appalachian and Greater Green River to >4.5% in the San Juan and San Joaquin. This suggests that much of the basin-level differences in production-normalized CH₄ emissions reported by aircraft studies can be explained by differences in site size and distribution of site-level production rates. We estimate that NG production sites emit total CH₄ emissions of 830 Mg/h (95% CI: 530–1200), 63% of which come from the sites producing <100 Mcfd that account for only 10% of total NG production. Our total CH₄ emissions estimate is 2.3 times higher than the U.S. Environmental Protection Agency's estimate and likely attributable to the disproportionate influence of high emitting sites.



INTRODUCTION

Natural gas (NG) extracted from shale and tight oil reservoirs has transformed the U.S. energy landscape resulting in rapid increases in total NG production and consumption.¹ While NG combustion emits less than half the carbon dioxide (CO₂) of other fossil fuels,² it is primarily composed of methane (CH₄), which produces 86 times more radiative forcing than CO₂ over a 20-year time frame.³ Therefore, CH₄ emitted from the NG system represents wasted resources, lost revenue, and erodes the potential climate benefits of NG relative to other fossil fuels.

There has been a major effort over the last five years to quantify CH₄ emissions from the oil and NG supply chain. Dozens of recent measurement-based studies^{4–32} have exposed the magnitude and scope of the CH₄ emissions problem, highlighting the following common themes: (i) Government inventories often significantly underestimate CH₄ emissions, (ii) a small fraction of high-emitting sites or sources account for a disproportionately large fraction of total CH₄ emissions, and (iii) there are significant basin-to-basin differences in production-normalized CH₄ emissions (i.e., CH₄ emissions expressed as a fraction of CH₄ produced).

We focus on CH₄ emissions from NG production sites. The U.S. EPA³³ attributes two-thirds of the 6.5 Tg of total CH₄

emissions from the NG supply chain to the NG production sector, which includes 2 Tg of CH₄ emissions associated with NG production from more than 400 000 NG wells. Herein, we define NG production sites to include any NG-producing well pad with one or more wellheads and ancillary surface equipment (e.g., NG separators, pneumatic pumps/controllers, and/or storage vessels). Such onsite processing equipment are often significant sources of elevated CH₄ emissions.^{4,8,29} These high emissions are often the result of abnormal process conditions (e.g., equipment malfunctions); they can be persistent or episodic and are difficult to predict.^{4,27–29} The stochastic characteristics of high-emitting sites appear to contribute, at least in part, to the orders-of-magnitude variability in measured absolute site-level CH₄ emissions (Figure 1). Furthermore, top-down aircraft studies report widely varying estimates of basin-level, production-normalized CH₄ emissions.^{19–24} The causative factors for site- and basin-level variability in CH₄ emissions are not well-understood. It has been suggested that differences in the composition of the

Received: June 27, 2018

Revised: August 29, 2018

Accepted: September 26, 2018

Published: September 26, 2018

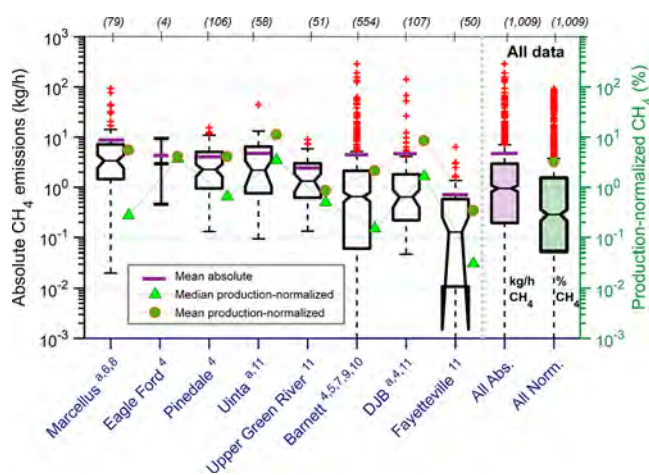


Figure 1. Site-level measurement data synthesized in this study. Numbers in parentheses indicate the number of sites with emissions data for each basin; the citations to the original studies are indicated as superscripts after basin names. New measurements are indicated with an (a) in the Denver-Julesburg (DJB; $n = 18$, or 17% of all DJB sites), Marcellus (NE PA unconventional sites, $n = 45$, or 57% of all Marcellus data), and Uinta ($n = 29$, or 50% of all Uinta sites). The boxes represent the 25th and 75th percentiles, while the whiskers extend to $1.5\times$ the interquartile range, and values outside this range are the outliers, marked with red crosses. The black horizontal line inside each box represents the median while means are shown in purple. The notches visually depict the 95% confidence interval on the median. For Eagle Ford, measurement data for the four sites are represented with an error bar indicating the minimum and maximum. For Fayetteville, the notch extends beyond the 25th percentile as a result of the sample size and the data spread in this basin. “All Abs.” and “All Norm.” represent combined data set for all absolute and production-normalized CH_4 emission rates ($n = 1009$), respectively.

extracted NG (e.g., dry versus wet gas), operator practices, and/or differences in NG production rates may be important.^{11,24,29} Additionally, several states have recently proposed or enacted oil and NG CH_4 regulations,^{34–38} which may yield pronounced differences in future regional/basin-level CH_4 emissions when compared against regions/basins without similar regulatory actions.

To better understand CH_4 emissions among NG production sites and across multiple basins, we compiled and analyzed recently measured site-level CH_4 emissions data for more than 1000 NG production sites in eight U.S. basins^{4–11} (Figure 1). We use this large data set of site-level CH_4 emissions (both absolute and production-normalized emissions) and site-level NG production to test the hypothesis that there are no significant basin-to-basin differences in the distribution of site-level CH_4 emissions and that, on average, site-level emissions correlate with their NG production characteristics. We then combine these site-level CH_4 emissions data with a national database on NG production site characteristics (i.e., site-level NG production rate) to estimate (i) total CH_4 emissions from U.S. NG production sites, (ii) major sources and distributions of CH_4 emissions, including CH_4 from high-emitting sites, and (iii) variability in CH_4 emissions among basins.

MATERIALS AND METHODS

Overview of Site-Level Measurement Data. We analyzed measured site-level CH_4 emissions data from 1009 NG production sites located in eight different basins. This includes recently published data from eight independent

studies,^{4–11} supplemented with new data for 92 additional sites sampled in the Denver-Julesburg (DJB), Uinta, and Marcellus (northeastern PA, Figure 1, Supporting Information (SI) Section S1). These new measurements targeted production regions with unique site-level production characteristics, that is, unconventional dry gas production sites with high site-level production rates in northeastern Marcellus and low-producing, mixed oil and gas sites in Uinta and DJB. The new measurement data help diversify site-level production characteristics and measured production regions/basins in the consolidated data set.

We focus on routinely producing sites with known NG production and assumed that measured CH_4 emissions resulted from routine operations (e.g., equipment leaks, venting from pneumatic controllers and storage tanks) or were unplanned (e.g., unintended emissions from malfunctioning equipment). Thus, the combined data set does not include CH_4 emissions from completion flowback⁸ or liquids unloadings.¹¹ Additionally, site-level CH_4 emissions rates were unavailable for storage or coalbed CH_4 well sites, and emissions from these sites were not assessed in the present study. For measured sites with reported NG production rates, the CH_4 measurements were performed between 2010 and 2016 and used a variety of onsite and downwind ground-based site-level CH_4 measurement techniques that can be broadly grouped into three categories:

- Direct onsite measurements (henceforth, “onsite measurements”), which involved optical gas imaging for leak identification followed by direct quantification of all identified leaks.⁵ These component-specific measurements are then summed to estimate site-level emission rate. Onsite measurements accounted for 28% of all site-level measurement data.
- Downwind tracer flux (TF) measurements of downwind plumes of CH_4 and intentionally released tracers (e.g., acetylene and nitrous oxide).^{6,8} TF sites accounted for 6.7% of the total data.
- Downwind CH_4 plume measurements combined with inverse Gaussian modeling. This includes both downwind stationary measurements using EPA’s Other Test Method (OTM-33A^{4,11}), and downwind mobile measurements followed by Gaussian modeling (MM-Gaussian^{7,9,10}). Sites sampled using these techniques accounted for 65% of the total sites.

There are limitations with each method. For example, onsite measurement (method (a)) requires site access and proper operation and performance of both the plume imaging (for leaks survey) and leak rate measurement devices.^{5,39} Even with site access, some onsite emission sources may be present at locations that are not safely accessible for leak rate quantification (e.g., see Subramanian et al.¹⁶). Additionally, all stationary and mobile downwind measurements require sites with downwind road access and favorable meteorological conditions. These measurement methods have different uncertainties, which range from approximately $\pm 20\%$ to $\pm 60\%$ (TF and OTM-33A) to a factor of 3 for the MM-Gaussian approach.^{4–11}

We use the site-level production-normalized CH_4 emissions as reported by Robertson et al.¹¹ and Omara et al.⁸ For Rella et al.,¹⁰ Yacovitch et al.,⁹ and Lan et al.⁷ we use the site-level CH_4 emissions, NG production, and production-normalized CH_4 emissions as consolidated and reported by Zavala-Araiza et

Table 1. Ten NG Production Bins Used in the Nonparametric Model (Developed Based on Deciles of NG Production for the Measured Sites) And Their Estimated Mean Site-Level Production-Normalized CH₄ Emissions

production bin (Mcf/d)	<0.4–31	31–73	73–147	147–254	254–390	390–616	616–1047	1047–1699	1699–3342	>3342
no. measured sites ^a	101	101	101	101	101	101	101	101	101	100
national sites (%) ^b	65%	15%	8.3%	3.9%	2.1%	1.7%	1.4%	0.90%	0.83%	0.81%
national prod. (%) ^c	3.2%	4.2%	5.2%	4.5%	3.97%	4.9%	6.7%	7.2%	11.7%	48.4%
mean (% CH ₄) ^d	20	5.4	2.8	1.6	1.9	1.4	0.89	1.2	0.23	0.17
lower bound on mean (% CH ₄)	16	3.3	1.6	1.1	0.96	0.7	0.38	0.45	0.14	0.12
upper bound on mean (% CH ₄)	25	7.9	4.4	2.2	3.3	2.5	1.7	2.2	0.34	0.24

^aDenotes the number of measured sites in each production bin (total = 1009). ^bTotal U.S. NG production sites = 498 000. ^cNG production for these 498 000 sites was 83 billion cubic feet per day (Bcf/d). ^dThe mean production-normalized CH₄ emission rate in each bin was obtained by randomly drawing, with replacement, an emission rate from the empirical distribution until a randomly sampled emission rate was assigned to each of the sampled sites. This was repeated 10 000 times and the mean obtained from the average of averages of each simulation, while the 2.5th and 97.5th percentiles characterized the lower and upper bounds on the mean, respectively (SI Figure S18).

al.²⁹ For onsite measurements in the Barnett,⁵ we calculated site-level production-normalized CH₄ emissions based on the study's reported site-specific CH₄ mole fraction in NG and site-level NG production; sites without NG production rates were excluded from this analysis. For Brantley et al.⁴ and measurements performed as part of the present study, we estimated site-specific production-normalized CH₄ emissions based on the average county-specific or region-specific CH₄ mole fractions from the EPA's Oil and Gas Tool.⁴⁰

We excluded data for eight sites with production-normalized CH₄ emissions >100%. These eight sites were sampled offsite using the downwind plume measurements approaches utilizing Gaussian plume inverse modeling. It is possible that the measured CH₄ emissions exceeding 100% of CH₄ production was due to offsite CH₄ sources (e.g., biogenic CH₄ source, CH₄ from collocated equipment such as abandoned well, etc.). The exclusion of these eight sites from the consolidated data set does not change our results: if we include them in our analysis, the total production CH₄ emissions increases by <7%, well within the overall 95% confidence interval.

Overall, the 1009 measured sites were located in the Barnett ($n = 554$ sites), Denver-Julesburg (DJB, $n = 107$), Pinedale ($n = 106$), Marcellus ($n = 79$), Uinta ($n = 58$), Upper Green River ($n = 51$), Fayetteville ($n = 50$), and Eagle Ford ($n = 4$) basins (Figure 1). Site-specific NG production rates ranged from 0.4 Mcfd (1 Mcfd = 1000 cubic feet per day) to 78 000 Mcfd. Analysis of production data from Drillinginfo⁴¹ (further description below) indicates that in 2015, 94% of U.S. NG production sites had site-level NG production rates that fell within this range. Additional site information (e.g., number of wells onsite, gas processing and emissions control equipment in use, conventional or unconventional well type, and site age) were generally unavailable or not reported.

National Activity Data. We used well-level NG production data reported by Drillinginfo (DI Desktop⁴¹), a commercial platform that aggregates publicly available and proprietary well-level data, including monthly NG production, first reported production date, drilling configuration, operator name, and location. Using geospatial analysis with ArcGIS, we aggregated well-level information into site-level (well-pad) information (see SI Section S2). In total, 498 000 NG producing well pad sites were identified, with total 2015 NG production of approximately 27 Tcf (trillion cubic feet). As of March 2017, Drillinginfo did not report 2015 well-level production data for wells in Kentucky, Tennessee, Missouri, Oregon, Illinois, and Indiana. These states were not included in our analyses. The EIA⁴² estimates that these states

contributed <0.5% of total national NG production. Using the EPA's county-specific and basin-specific estimates of mean CH₄ content in NG,⁴⁰ we estimated total CH₄ production of 23 Tcf from these sites in 2015. The distribution of sites based on their NG production characteristics is shown in Table 1.

Extrapolation of Measured Site-Level Emissions to Total Population of Sites. We used two methods for extrapolating the measured site-level CH₄ emissions to the total population of sites: (i) a robust regression model, and (ii) a nonparametric model. These two approaches allow us to explore the influence of high-emitting sites on predicted total CH₄ emissions; whereas the first approach downweights their contribution, the second approach fully incorporates them. As described further in detail below, both of these approaches utilize the site-level production-normalized CH₄ emissions data. In the first approach, we estimated site-level CH₄ emissions for each of the 498 000 NG production sites in 2015 by fitting a robust weighted least-squares quadratic regression model of the production-normalized CH₄ emission as a function of NG production. The robust fit was performed using a MATLAB Statistics Toolbox algorithm that uses an iteratively reweighted least-squares approach with a bisquare weighting function,⁴³ $wfun(wfun = (abs(r) < 1) \times (1 - r^2)^2; r = resid/(tune \times s \times (1 - h)^{0.5}); s = \frac{1}{0.6745} \times \text{median absolute deviation of the residuals (resid) from the median}; h \text{ is a vector of leverage values for the least-squares fit and tune is a tuning constant} = 4.685)$. Thus, for each site, its production-normalized CH₄ emission rate (%) was estimated based on the fit obtained from the robust regression, which is a function of the site's NG production rate. The site's absolute CH₄ emission rate (kg/h) was then calculated by multiplying its production-normalized CH₄ emission rate with its CH₄ production rate.

In the second approach, we estimate site-level CH₄ emissions using nonparametric bootstrap resampling methods in order to adequately characterize the asymmetrical distributions of the empirical data. We first developed 10 empirical production-normalized CH₄ emissions distributions by grouping measured emissions into 10 bins based on deciles of NG production for the 1009 sites with emissions data (Table 1). We then grouped all 498 000 U.S. NG production sites into the same 10 bins based on the measured site-level NG production deciles. Among sites with emissions data, the site-level NG production rates ranged from 0.4 Mcfd to 78 000 Mcfd; however, among the total population of U.S. NG production sites, site-level NG production ranged from 0.001 Mcfd to 138 000 Mcfd (SI Figure S21). In grouping the

national population of sites, the 28 900 sites (5.8% of all sites) producing <0.4 Mcfd were placed in the same bin as the sites producing 0.4 to 31 Mcfd, which describes the first decile. Similarly, the six sites (0.0012% of all sites) that produced >78 000 Mcfd were placed in the last bin as the sites producing 3342 to 78 000 Mcfd. As shown in Table 1, the mean production-normalized CH₄ emissions in each bin decreases consistently with increases in site-level NG production. Our analysis shows that this grouping for national sites with NG production outside of the measured production is robust: if, for example, sites producing <0.4 Mcfd were assigned a production-normalized CH₄ emissions of 100%, the resulting national CH₄ emissions would increase by only 0.33%. Furthermore, we find that the distribution of site-level NG production rates for the sampled sites is statistically similar to that for the national population of sites across all production bins, except for the low production sites in the first bin which are undersampled (SI Figure S17).

For each site in each production bin, we estimate its site-level CH₄ emissions (kg/h/site) by randomly drawing, with replacement, a production-normalized CH₄ emission rate from the bin-specific empirical distribution. We then multiply this randomly sampled production-normalized CH₄ emission rate with the site-specific CH₄ production rate, repeat this process for every site, and then sum across all sites. We repeat this simulation 5000 times for each site in order to estimate the mean total CH₄ emissions; the 2.5th and the 97.5th percentiles were then used to characterize the 95% confidence interval on mean total CH₄ emissions.

Our overall estimated uncertainty on mean total CH₄ emissions, obtained from the 2.5th and 97.5th percentiles based on the nonparametric resampling, was +40%/−36% and was dominated by variability in mean site-level CH₄ emissions. These are influenced by study-specific sample sizes, site representativeness, and/or method accuracy. There are also uncertainties associated with activity data from Drillinginfo⁴¹ but they are difficult to quantify as these data are aggregated from publicly available sources that may be subject to reporting errors. These uncertainties include uncertainties in well location and production data. All Drillinginfo data were used as reported without any modifications. Finally, there are uncertainties associated with county/basin-level CH₄ mole fractions from the EPA's Oil and Gas Tool.⁴⁰ However, the impact of these uncertainties on estimated total CH₄ emissions are expected to be small. For example, in the Appalachian Basin, we used an average CH₄ content of 83%.⁴⁰ Increasing this to 95% or decreasing it to 75% yields results that are within 15% of the mean estimated total CH₄ for this basin, well within the overall method uncertainty of +40%/−36%.

Two-Sample Kolmogorov–Smirnov Tests. We compared the distributions of site-level absolute and production-normalized CH₄ emissions among different basins using the two-sample Kolmogorov–Smirnov (K–S) test, with significance established at $p < 0.01$. These statistical comparisons were performed using MATLAB.

RESULTS AND DISCUSSION

Variability in Empirical Site-Level and Basin-Level Methane Emission Rates. Figure 1 shows that both the absolute and production-normalized CH₄ emission rates are highly variable. Nearly three-quarters (74%) of sites exhibited site-level CH₄ emissions between 0.1 and 10 kg/h but, overall, site-specific absolute CH₄ emission rates varied by more than 5

orders of magnitude, ranging from 0 to 300 kg/h. There are basin-to-basin differences in emissions with mean basin-specific absolute CH₄ emission rate ranging from 0.61 kg/h/site (95% confidence interval, henceforth CI: 0.33–0.95) to 7.9 kg/h/site (CI: 4.9–12) in the Fayetteville and Marcellus basins, respectively. The overlap, or lack thereof, in the length of the boxplot notches in Figure 1 suggests basins cluster into three groups with statistically different measured median absolute CH₄ emission rates: (i) A group of basins with high site-level emissions: Marcellus (median = 3.4 kg/h/site), Pinedale (2.3 kg/h/site), Uinta (2.2 kg/h/site); (ii) A group of basins with moderate site-level emissions: Barnett (0.65 kg/h/site) and Denver-Julesburg (DJB) (0.64 kg/h/site); and (iii) Fayetteville, with low site-level emissions (0.13 kg/h/site). The Upper Green River basin falls between the high and moderate emissions groups with a median emissions of 1.3 kg/h/site.

Site-specific production-normalized CH₄ emission rates ranged from 0% to 91%, while the mean basin-specific production-normalized CH₄ emission rates ranged from 0.34% (CI: 0.07–0.74%) to 11% (CI: 6.9–16%) in the Fayetteville and Uinta, respectively (SI Table S8). Within 95% confidence intervals, four groups of basins have measured median production-normalized CH₄ emissions that are statistically different (SI Figure S19): (i) DJB (median = 1.6%) and Uinta (3.5%) have high production-normalized emissions; (ii) Marcellus (0.27%), Pinedale (0.65%), and Upper Green River (0.50%) have moderate production-normalized emissions; (iii) Barnett (0.15%) and (iv) Fayetteville (0.031%) both have low emissions. Thus, at the basin level, the measured mean or median site-level production-normalized CH₄ emissions vary by one to 2 orders of magnitude, while the measured mean or median site-level absolute CH₄ emissions vary by at least an order of magnitude.

Comparison of Empirical Site-Level Methane Emissions Distributions among Basins. Figure 2 shows the empirical cumulative distributions of both the absolute and production-normalized CH₄ emissions sorted by basins. The site-level emissions are highly skewed; for example, among all sampled sites in the Barnett, the top 5% of high-emitting sites accounted for 66% of cumulative absolute CH₄ emissions. The skewness of CH₄ emissions distributions are determined, in part, by the sample size.¹⁸ A concern is representativeness of the sample population, including the magnitude and frequency of extreme emitters.⁴⁴ Representative distributions are difficult to capture in part because of the stochastic characteristics of site-level CH₄ emissions and the logistical limitations of common site-level measurement techniques (see Materials and Methods). To compare CH₄ emissions distributions among basins, we attempted to control for these potential sampling artifacts by stratifying basin-specific CH₄ emissions based on the median site-level NG production rate (390 Mcfd) and, in each group, limiting our comparison to only include basins with $n \geq 50$.

We used the two-sample Kolmogorov–Smirnov test (i.e., six paired tests for the <390 Mcfd group and three paired tests for the >390 Mcfd group) to compare the different basin-specific emissions distributions shown in Figure 2 (SI Table S13). The absolute CH₄ emissions distributions are generally statistically different among basins at the 1% significance level (Figure 2a). Indeed, the two-sample K–S test suggests only the absolute site-level CH₄ emissions distributions for the <390 Mcfd sites in the Pinedale and Uinta basins came from similar continuous distributions ($p = 0.24$).

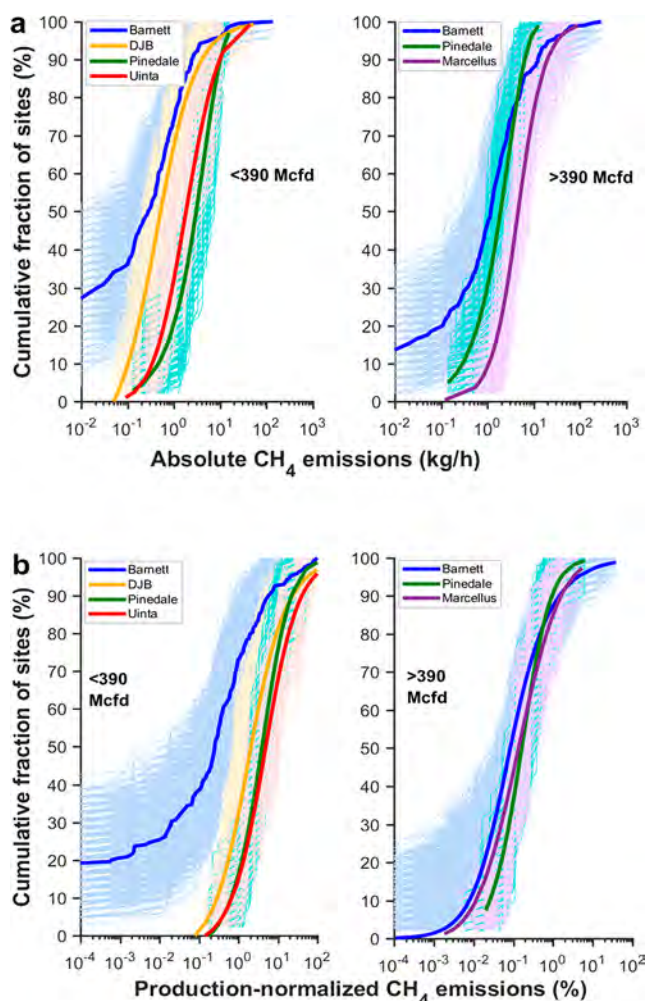


Figure 2. Comparison of CH₄ emissions distributions among basins. (a) absolute and (b) production-normalized emissions. Only basins with $n \geq 50$ sites were evaluated. For the <390 Mcfd bin, comparisons were made among the Barnett ($n = 245$), DJB ($n = 95$), Pinedale ($n = 50$), and Uinta ($n = 50$) Basins. For the >390 Mcfd bin, comparisons were made among the Barnett ($n = 309$), Pinedale ($n = 56$), and the Marcellus ($n = 57$) Basins. The lightly colored lines indicate the 10 000 bootstrap distributions obtained by randomly sampling 50 sites, with replacement, from the empirical distributions (shown in bold solid lines). Differences in distributions were assessed using the 2-sample Kolmogorov–Smirnov test with significance established at $p < 0.01$.

In contrast, the distributions of production-normalized CH₄ emissions were generally statistically similar among all paired basins ($p > 0.01$, SI Table S13), except for the Barnett sites producing <390 Mcfd (Figure 2b). The Barnett data for the <390 Mcfd sites are skewed low compared to the other basins partly because 20% of all the sampled sites in this bin had nondetectable emissions,¹⁰ and nearly one-third were obtained from short-term onsite measurements.⁵ The sites with reported zero emissions were sampled using mobile downwind plume measurements but had no independent measure to verify sites with undetectable plumes (e.g., the use of an intentionally released tracer from the site). Additionally, component-level measurements,⁵ which are typically completed in minutes, may be biased low as periodic emission events (e.g., tank flashing) may be missed. Given this uncertainty, it is possible that high-emitting sites are underrepresented among sites producing

<390 Mcfd in the Barnett, thus increasing the uncertainty in the scaled-up CH₄ emissions. This potential sampling artifact was not observed among sites producing >390 Mcfd (Figure 2b). However, the 10 000 bootstrap distributions (recreated from the empirical distribution) for the Barnett indicate overlap with the Denver-Julesburg (DJB), Pinedale, and Uinta CH₄ distributions, particularly at the high end of the distribution (Figure 2).

Relationship between Measured Site-Level Methane Emissions and NG Production. Recent studies report weak relationships between absolute CH₄ emissions and site-level characteristics, including NG production, oil production, water production, and/or site age.^{4,8,11,29} Given the limited information for individual sites, we can only examine the relationship between site-level CH₄ emissions and NG production.

Figure 3 shows the site-level absolute and production-normalized CH₄ emissions as functions of NG production. Figure 3b shows a strong trend of decreasing production-normalized CH₄ emissions with increases in site-level NG production. To quantify the trend, we fit the entire data set with quadratic robust weighted least-squares regression with bisquare weighting (see Materials and Methods):

$$\log_{10} \left[\% \text{CH}_4 \left(\frac{\text{kg/h}}{\text{kg/h}} \right) \right] = 0.072 \pm 0.056 (95\% \text{CI}) \times \log_{10} [\text{Prod}(\text{Mcf/d})]^2 - 1.1 \pm 0.28 \times \log_{10} [\text{Prod}(\text{Mcf/d})] + 1.96 \pm 0.34; r_{\text{adj}}^2 = 0.74.$$

On average, low NG producing sites emit a larger fraction of their CH₄ production than high NG producing sites and up to 74% of the variability is explained by variability in NG production rates (Figure 3). This implies that basins in which total NG production are dominated by high NG production sites are likely to have lower production-normalized CH₄ emissions and vice versa.

Figure 3 also shows modest increases in absolute CH₄ emissions with site-level NG production (quadratic robust weighted least-squares regression with bisquare weighting):

$$\log_{10} [\text{CH}_4(\text{kg/h})] = 0.071 \pm 0.056 (95\% \text{CI}) \times \log_{10} [\text{Prod}(\text{Mcf/d})]^2 - 0.097 \pm 0.28 \times \log_{10} [\text{Prod}(\text{Mcf/d})] - 0.23 \pm 0.33; r_{\text{adj}}^2 = 0.74)$$

High NG production sites (e.g., > 1000 Mcfd/site) are generally newer facilities (SI Figure S3); they may have optimally performing equipment and components, and are likely subjected to more frequent on-site inspection and maintenance than old, low producing sites.⁸ Because of their high NG production rates, exceptionally high CH₄ emissions (e.g., > 10% of site-level CH₄ production) at these sites would likely be audible and/or visible, increasing the possibility for detection and repair if routine inspections are performed.

Both Figure 1 and Figure 3 highlight the significant scatter in CH₄ emissions within basins and within NG production bins; this underscores the stochastic character of emissions at any given site, which may result from sources that include malfunctions (e.g., separator dump valve stuck open), operational errors (e.g., storage tank venting from thief hatch accidentally left open), and/or process and design issues (e.g., overpressurized separators).^{27–29} Therefore, the fits in Figure 3 predict the emissions of an average site as a function of production but do not predict the emissions for any specific site. Fortunately, trends in average emissions are what is needed to develop national or basin-level emission estimates,

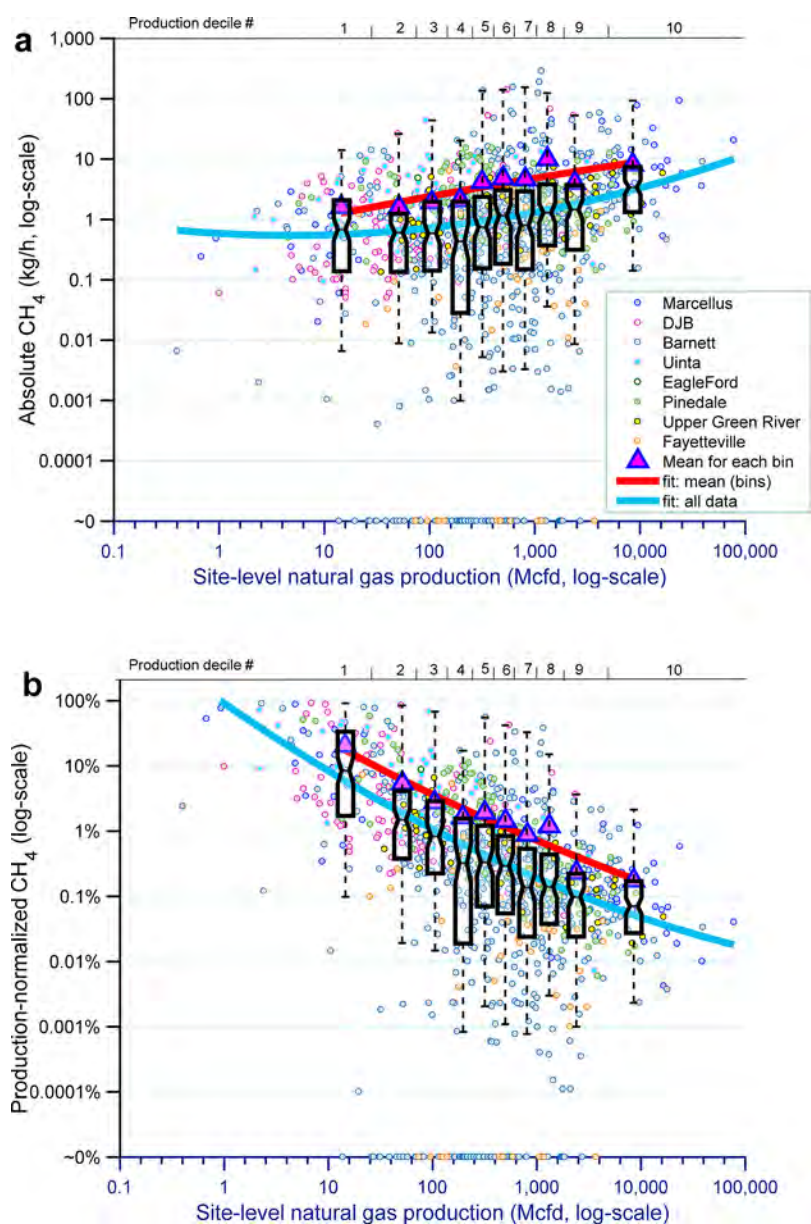


Figure 3. Relationship between site-level CH₄ emissions and NG production. (a) absolute and (b) production-normalized CH₄ emissions. Solid cyan lines show quadratic robust weighted least-squares regressions with bisquare weighting (see *Materials and Methods*) performed on the entire data set. Measured site-level CH₄ emissions were also binned by deciles of their site-level NG production, which are numbered sequentially on the top *x* axis. The notched box plots (outliers not shown) visually depict the data spread in each production decile. The black horizontal line in each notched box shows the median. The triangular purple symbols show the mean CH₄ emission rate in each production decile and the solid red lines show the polynomial fit through the mean CH₄ emission rate in each decile. These regression equations are (a) $\log_{10}[\text{CH}_4 \text{ (kg/h)}] = 0.30 \pm 0.14 \times \log_{10}[\text{Prod (Mcf/d)}] - 0.23 \pm 0.38$; $r_{\text{adj}}^2 = 0.72$) and (b) $\log_{10}[\% \text{CH}_4 \text{ (kg/h/kg/h)}] = -0.71 \pm 0.15 \times \log_{10}[\text{Prod (Mcf/d)}] + 2.0 \pm 0.41$; $r_{\text{adj}}^2 = 0.93$) for the absolute and production-normalized CH₄ emissions, respectively.

which integrate an average emission factor with activity data reflecting the total number of well sites.

Influence of High-Emitting Sites on Total Methane Emissions. Within each basin (Figure 1) and production bin (Figure 3, notched box plots), the mean CH₄ emission rate is higher than the median because of the disproportionate influence of low frequency, high emitting sites. The high CH₄ emitters are commonly referred to as “super emitters”; since we lack information on the site-level CH₄ sources, we denote them simply as “high emitters” and identify them as the top 5% of sites based on the cumulative fraction of CH₄ emissions. Figure 4a shows, empirically, that the top 5% of high-emitting

sites account for 57% (CI: 40–70%) of cumulative CH₄ emissions, with each of these sites having site-level CH₄ emissions >13 kg/h/site. Furthermore, their cumulative CH₄ emissions are equivalent to 1.6% (CI: 1.1–2.2%) of their total CH₄ production. This result is consistent with the observation by Brandt et al.⁴⁴ that the largest 5% of leaks from NG systems typically contribute over 50% of total leakage volume. Overall, our results suggest that CH₄ emission models (or CH₄ emission factors) that do not adequately capture the disproportionate contribution of high emitters may significantly underestimate total emissions.

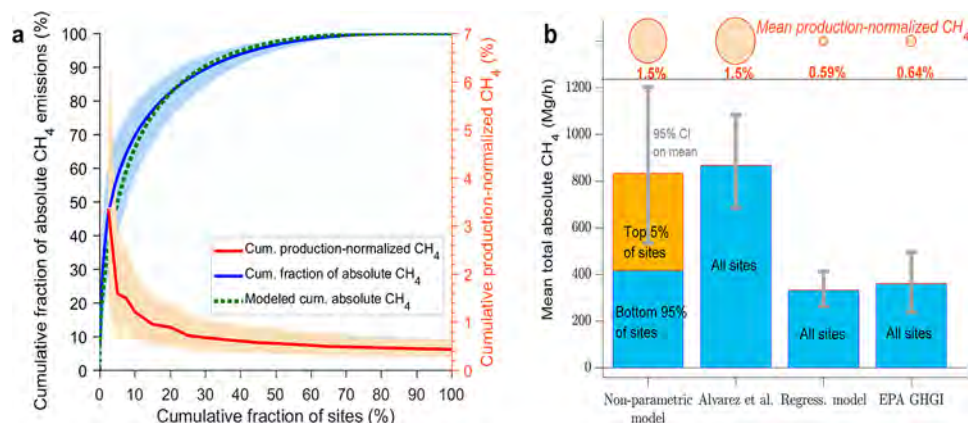


Figure 4. Total CH₄ emissions are dominated by a small fraction of high-emitting sites. (a) Site-level absolute CH₄ emissions distribution plotted in descending rank-order. Empirically ($n = 1009$), the top 5% of sites contribute 57% of total absolute CH₄ emissions (solid blue line); their cumulative CH₄ emissions are equivalent to 1.6% of their total CH₄ production (solid red line). The light blue and orange bands visually depict the 95% confidence intervals on the cumulative fraction of absolute and production-normalized CH₄ emissions, respectively. The dotted green line shows the predicted CH₄ distribution for all 498 000 U.S. onshore NG production sites as obtained from the nonparametric model—the top 5% of sites account for 50% of total CH₄ and have mean site-level CH₄ emissions of 17 kg/h/site (CI: 10–25). (b) Comparison of estimated total U.S. production CH₄ emissions based on (i) nonparametric model, (ii) total CH₄ emission estimate for all production sources reported by Alvarez et al.,⁴⁵ (iii) a regression model approach, and (iv) total onshore CH₄ emissions from the 2017 EPA GHGI (see Main Text). The top bubble plots visually depict the differences in production-normalized CH₄ emissions (see SI Section 2.2).

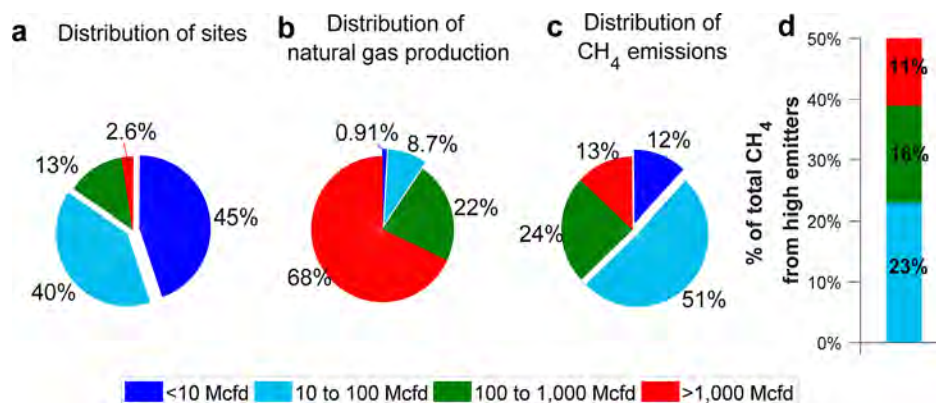


Figure 5. Distribution of sites, NG production, and CH₄ emissions based on four cohorts of site-level NG production. (a) Distribution of U.S. NG production sites in 2015 ($n = 498\,000$). (b) Distribution of their NG production (total = 83 Bcf/d). (c) Distribution of their estimated CH₄ emissions (total = 830 Mg/h). (d) CH₄ emissions from the high-emitting sites (none of the 220 000 sites producing <10 Mcfd was estimated to be a high emitter). High-emitting sites are defined as the top 5% of U.S. sites (based on the cumulative fraction of site-level CH₄ emissions ($n = 25\,000$)) and that emit >7.2 kg/h/site. Total CH₄ from high-emitting sites were estimated to be 420 Mg/h (95% CI: 260–630 Mg/h).

To quantify the importance of accurate accounting of high-emitters on national emission estimates such as the EPA GHGI,³³ we estimated, for the year 2015, the total U.S. CH₄ emissions from NG production using the two approaches previously described (see Materials and Methods). In the first approach, we use a robust regression model that captures the average site-level CH₄ emissions behavior and simulates a bottom-up inventory approach in which the full effect of extreme CH₄ emitters are not accounted for. Second, we use a nonparametric model that fully incorporates the disproportionate influence of high-emitting sites. For this analysis, we use the combined production-normalized CH₄ emissions data given the strong similarities in basin-specific distributions (Figure 2b) and robust trend with site-level NG production (Figure 3b). We include site-level production-normalized CH₄ data from all basins, including those where small sample sizes precluded a comparative assessment of their CH₄ distribution. We acknowledge that this and other potential sampling

artifacts discussed above likely increase the overall uncertainty in total estimated CH₄ emissions.

When combined with activity data from Drillinginfo's DI Desktop,⁴¹ the regression model approach estimates total CH₄ emissions of 330 Mg/h (95% CI on mean: 260–410; or 0.67 kg/h/site and equivalent to production-normalized emissions of 0.59%; Figure 4b) in 2015. In contrast, the nonparametric model yields an estimate that is more than two times the regression model results, that is, total CH₄ emissions of 830 Mg/h (CI: 530–1200; or 1.7 kg/h/site and equivalent to production-normalized emissions of 1.5%).

The regression model approach is similar, in principle, to the bottom-up inventory methods in which an average CH₄ emission factor is applied to activity data, which may include count of wells, components, and/or equipment at a site or region. This is the approach typically used in government inventories such as the EPA GHGI.³³ Our estimated total CH₄ emissions based on the regression model (330 Mg/h) is similar to the 360 Mg/h of total CH₄ emissions for onshore oil and

Methane emissions from natural gas production sites in the United States (2015)

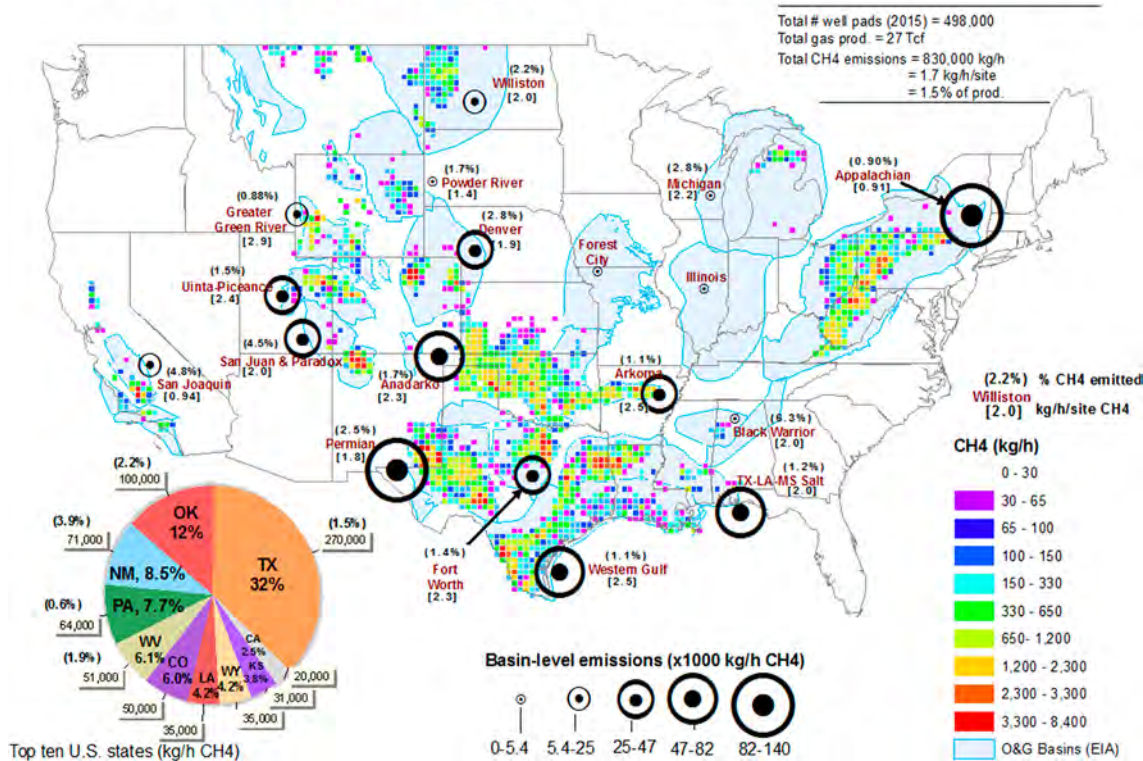


Figure 6. Spatial distribution of CH₄ emissions, plotted on 35km × 35km grid cells. Percentages and numbers in parentheses above and below basin names indicate the basin-level production-normalized and average site-level CH₄ emission rates, respectively. Pie chart labels indicate the predicted mean total CH₄ emissions (kg/h); percentages above the labels indicate the production-normalized CH₄ emissions for the top five states, while percentages inside each pie indicate the predicted fraction of total U.S. CH₄ contributed by that state. Additional data can be found in SI Tables S7, S9, and S11 and in the provided Google Earth kmz file. The oil and gas basin boundaries are from the U.S. EIA.⁴⁶ Map data source: ArcUSA, U.S. Census, and ESRI. The map was created using ArcGIS software by ESRI (www.esri.com) and used herein under license.

NG production sites as reported in the 2017 EPA GHGI for 2015 emissions (Figure 4b). Furthermore, the EPA GHGI estimate is similar to our mean estimate of 420 Mg/h (CI: 300–570; or 0.88 kg/h/site (CI: 0.61–1.2)) for the lowest-emitting 95% of all U.S. sites (based on cumulative fraction of emissions) as obtained from the nonparametric model (Figure 4b). The robust regression fit (cyan line in Figure 3b) essentially passes through the median CH₄ emission rate in each production bin as the effect of extreme CH₄ outliers are downweighed in favor of tracing the underlying trend through the bulk of the data. Thus, total emissions estimates based on the robust regression model and the results for the lowest-emitting 95% of sites do not fully account for the CH₄ emissions from the exceptionally high emitters.

Our nonparametric model incorporates high emitters (i.e., the top 5% of sites). Its estimate of the total CH₄ emissions is 2.3 times higher than the EPA GHGI’s estimate for total CH₄ from the oil and NG production sites (Figure 4b). Similar discrepancies between bottom-up inventories and measurements have been reported in recent studies.^{17,18,25,26,30,45} Herein, our results suggest that CH₄ emissions from the high emitters (national mean: 17 kg/h/site (CI: 10–25); range: 7.2–1100), which account for 50% (CI: 32–75%) of cumulative emissions (Figure 4a), are primarily responsible for the discrepancy between our predicted total CH₄ and the EPA GHGI estimate. That is, the nonparametric model results match the EPA GHGI only when we exclude the contribution of the top 5% of high emitting sites. As reported in the 2017

GHGI,³³ the 2015 national CH₄ emissions for the NG gathering and processing (2.8 Tg), transmission and storage (1.3 Tg), and distribution (0.44 Tg) sectors already incorporate data from skewed emissions distributions obtained in recent sector-specific measurement-based campaigns.^{14,17,18} Our analysis supports a similar adjustment of CH₄ emissions for the NG production sector.

Distribution of Methane Emissions among Natural Gas Production Sites. Figure 5 summarizes the total CH₄ predictions stratified by production level. We define low, intermediate, and high NG production sites as sites producing <100 Mcfd, 100 to 1000 Mcfd, and >1000 Mcfd, respectively. Low NG production sites account for 85% of the total number of sites but only 9.6% of total NG production (Figure 5a,b). Although their mean site-level CH₄ emissions are low (0.46 and 2.1 kg/h/site for the <10 Mcfd and 10 to 100 Mcfd sites, respectively; SI Table S10), their very large number makes them an important source of CH₄ emissions nationally, contributing nearly two-thirds (63% (CI: 45–83%)) of the total CH₄ emissions. In contrast, high NG production sites (>1000 Mcfd/site) contribute two-thirds of total U.S. NG production and have higher mean site-level CH₄ emissions (8.3 kg/h/site; SI Table S10). However, they are few in number (i.e., they account for only 2.6% of the total number of sites) and contribute only 13% (CI: 7–21%) of the total CH₄ emissions.

We estimate that none of the 220 000 sites (45% of all sites) producing <10 Mcfd/site are high emitters; these low-

production sites had mean site-level CH₄ emission estimate of 0.46 kg/h/site (CI: 0.35–0.58; SI Table S10). In contrast, we estimate that 47% of the total CH₄ from high-emitting sites came from 8.3% of sites producing 10–100 Mcfd/site. High emitters in this cohort accounted for 23% of the total CH₄ from all sites (Figure 5d, SI Table S10). The remainder of the emissions from high emitters are contributed by sites with intermediate (16% of total CH₄ from all sites) and high NG production (11% of total CH₄ from all sites, Figure 5d).

Spatial Distribution of Methane Emissions. Figure 6 shows the estimated spatial distribution of site-level CH₄ emissions calculated from the nonparametric model, as previously discussed (i.e., the site-level CH₄ emissions distributions for all 498 000 NG production sites plotted in Figure 6 is the same distribution shown in Figure 4a (dotted green line)). Using site-specific location data from Drillinginfo,⁴¹ the estimated emissions were then geo-spatially joined to 35 km × 35 km grid cells and summed to give the grid-specific total CH₄ (Figure 6).

We predict production CH₄ hotspots in the liquids-rich fairway of the Appalachian Basin (southwestern Pennsylvania and northern West Virginia), and in northwestern (San Juan Basin) and southeastern (Permian Basin) New Mexico, and in Weld County, Colorado (Denver Basin; Figure 6). Methane hotspots are not necessarily areas with high NG production. For example, Weld County (CO) was the eighth largest NG producing county in 2015 but is predicted to be the highest CH₄ emitting county in 2015 (26 Mg/h (CI: 16–34 Mg/h)). The emissions in Weld County are four times greater than that from Susquehanna (PA), the highest NG producing county. This is due to the very large number of sites with relatively low NG production in Weld County (13 000 sites) compared to Susquehanna (400 high producing sites).

Our analysis predicts wide variability in CH₄ emissions among states and among basins. For example, we predict that Texas contributes approximately one-third (32% (95% CI: 20–48%); Figure 6, SI Table S11) of total CH₄ emissions from NG production sites, roughly equivalent to the contribution of the combined CH₄ emissions from NG production sites in Oklahoma, New Mexico, and Pennsylvania (28% (95% CI: 19–39%)). Additionally, predicted basin-specific mean absolute CH₄ emissions per site ranged from 0.91 kg/h/site (CI: 0.62–1.2) in the Appalachian to 2.9 kg/h/site (CI: 1.6–3.9) in the Greater Green River Basin (SI Table S9). Mean production-normalized CH₄ emissions ranged from 0.88% (CI: 0.48–1.2%) in the Greater Green River Basin to 4.5% (CI: 3.3–6.6%) in the San Juan Basin (Figure 6; Table S9). These trends are caused by differences in the distributions of both the number of sites and their NG production characteristics. For example, the Appalachian Basin has the highest basin-level CH₄ emissions (140 Mg/h (CI: 95–180 Mg/h) or 17% of total CH₄ emissions (Figure 6). However, the Appalachian and Greater Green River Basins have the lowest estimated production-normalized CH₄ emissions of approximately 0.90% (Figure 6). NG production in both of these basins are dominated by high-producing sites with relatively low estimated production-normalized emission rates. These sites account for 94% and 72% of total NG production in the Appalachian and Greater Green River Basins, respectively. Similarly, the high estimated production-normalized CH₄ emissions of 4.5% (CI: 2.9–6.0%) in the San Juan Basin (Figure 6; SI Table S9) reflects the large contribution to total

NG production (90%) from sites producing <1000 Mcfd/site in this basin.

Comparison with Previous Literature Estimates. Two previously published studies used site-level CH₄ emissions data that are part of the consolidated data set in the present study to estimate basin-level²⁶ or state-level CH₄ emissions.⁸ Zavala-Araiza et al.²⁶ reported 2013 site-level CH₄ emissions of 1.8 (CI: 1.3–2.5) kg/h/site for the Barnett; the 2015 site-level CH₄ emissions estimates in the present study of 2.4 (CI: 1.4–3.6) kg/h/site for the Fort Worth Basin are in good agreement with their study. Similarly, our estimate of 115 Mg/h (CI: 78–150) for 2015 CH₄ emissions for NG producing sites in Pennsylvania and West Virginia overlaps with a previous estimate by Omara et al.⁸ for these sources in 2014 (144 Mg/h (CI: 70–190)). Finally, our national estimate for total CH₄ emissions from NG production sites (830 Mg/h (CI: 530–1200)) compares well with recent estimates by Alvarez et al.⁴⁵ (870 Mg/h (CI: 680–1080, Figure 5b) that were based on site-level measurements but utilized a different extrapolation approach incorporating parametrized nonlinear models.²⁶

Recent aircraft studies estimated the total CH₄ emissions from different NG production regions.^{19–24,31,32} These studies report widely varying mean production-normalized CH₄ estimates, ranging from approximately 0.3–9% in northeastern PA (Marcellus) and Uinta Basin, respectively. Our analysis predicts that the distribution of sites and their NG production levels are important contributors to these trends. For example, basins in which low producing sites dominate site count and NG production (e.g., San Juan) have much higher production-normalized CH₄ emissions than basins where NG production are dominated by high NG producing sites (e.g., Greater Green River). We compared our new bottom-up estimates with these top-down studies (SI Section 3.6; Figure S20), which estimate CH₄ emissions from all oil and NG sources. Our predictions explain, on average, 58% of the airborne top-down CH₄ emissions (20–129% of basin-specific airborne CH₄ emissions (SI Table S12)). There are uncertainties in both estimates. For aircraft measurements, CH₄ source attribution and mass balance closure are uncertain, while the uncertainties in our bottom-up estimates were dominated by variability in study-specific mean site-level emissions.

Other factors (beyond number of sites and site production characteristics) such as new state/local regulations^{34–38} or voluntary emissions reductions programs performed by specific operators, likely also contribute to basin-to-basin variability, but we could not assess those factors in this analysis. Additionally, our approach assumes that the large and diverse ensemble of sites considered here reproduces the distribution of emissions across the NG production system at any given point in time. However, there are uncertainties on CH₄ emissions distributions that are difficult to quantify based on available data. Future studies are needed to specifically address these factors.

■ ASSOCIATED CONTENT

📄 Supporting Information

The Supporting Information is available free of charge on the ACS Publications website at DOI: 10.1021/acs.est.8b03535.

A Google Earth kmz file showing the data presented in Figure 6, and documentation that describes the measurement results obtained in the present study, characteristics and distribution of natural gas production

sites, and additional study results, figures, and tables (PDF, ZIP)

AUTHOR INFORMATION

Corresponding Author

*Phone: +1-512-691-3432; e-mail: momara@edf.org.

ORCID

Mark Omara: 0000-0002-8933-1927

Xiang Li: 0000-0001-6797-7340

Albert A. Presto: 0000-0002-9156-1094

Allen L. Robinson: 0000-0002-1819-083X

Present Addresses

[†]Environmental Defense Fund, 301 Congress Avenue, Austin, Texas 78701, United States.

[‡]Department of Mechanical Engineering, University of British Columbia, 2054–6250 Applied Science Lane, Vancouver, British Columbia, Canada, V6T 1Z4.

[§]Department of Soil, Water, and Climate, University of Minnesota, St Paul, Minnesota 55108, United States.

Author Contributions

A.L.R., R.S., and A.A.P. designed the research. M.O., N.Z., M.R.S., X.L., A.E., R.C., and R.S. performed the field measurements. M.O. and N.Z. analyzed data. M.O. prepared the manuscript with feedback from all authors.

Notes

The authors declare no competing financial interest.

ACKNOWLEDGMENTS

Funding for this study was provided by the National Oceanic Atmospheric Administration Climate Program Office, Award No. NA14OAR4310135 and by the Department of Energy, National Energy Technology Laboratory, funding opportunity #DE-FOA-0000894. N.Z.'s work was supported in part by the NSERC postdoctoral fellowship, No. PDF-487660-2016. X.L.'s work was supported in part by the NASA Earth and Space Science Fellowship Program, Grant 15-EARTH15F-181. We thank Dr. Eben Thoma for providing the OTM-33A site-level measurement data presented in Brantley et al.⁴ The views expressed herein are solely those of the authors and do not necessarily reflect those of the project funders or Environmental Defense Fund.

REFERENCES

- (1) U.S. Energy Information Administration. Annual Energy Outlook 2017. Available at: [https://www.eia.gov/outlooks/aeo/pdf/0383\(2017\).pdf](https://www.eia.gov/outlooks/aeo/pdf/0383(2017).pdf) (accessed on August 29, 2018).
- (2) U.S. Energy Information Administration. Carbon Dioxide Emissions Coefficients. Available at: https://www.eia.gov/environment/emissions/co2_vol_mass.php (accessed on August 29, 2018).
- (3) IPCC. Intergovernmental Panel on Climate Change: *Fifth Assessment Report*; Geneva, 2014.
- (4) Brantley, H. L.; Thoma, E. D.; Squier, W. C.; Guven, B. B.; Lyon, D. Assessment of methane emissions from oil and gas production pads using mobile measurements. *Environ. Sci. Technol.* **2014**, *48*, 14508–14515.
- (5) ERG. Eastern Research Group, Inc. City of Fort Worth Natural Gas Air Quality Study. Final Report. July, 2011. Available at <http://fortworthtexas.gov/gaswells/air-quality-study/final/> (accessed on August 29, 2018).
- (6) Goetz, J. D.; Floerchinger, C.; Fortner, E. C.; Wormhoudt, J.; Massoli, P.; Knighton, W. B.; Herndon, S. C.; Kolb, C. E.; Knipping, E.; Shaw, S. L.; DeCarlo, P. F. Atmospheric emission characterization

of Marcellus Shale natural gas development sites. *Environ. Sci. Technol.* **2015**, *49*, 7012–7020.

(7) Lan, X.; Talbot, R.; Laine, P.; Torres, A. Characterizing fugitive methane emissions in the Barnett Shale area using a mobile laboratory. *Environ. Sci. Technol.* **2015**, *49*, 8139–8146.

(8) Omara, M.; Sullivan, M.; Li, X.; Subramanian, R.; Robinson, A. L.; Presto, A. A. Methane emissions from conventional and unconventional natural gas production sites in the Marcellus Shale region. *Environ. Sci. Technol.* **2016**, *50*, 2099–2107.

(9) Yacovitch, T. I.; Herndon, S. C.; Petron, G.; Kofler, J.; Lyon, D.; Zahniser, M. S.; Kolb, C. E. Mobile laboratory observations of methane emissions in the Barnett Shale region. *Environ. Sci. Technol.* **2015**, *49*, 7889–7895.

(10) Rella, C. W.; Tsai, T. R.; Botkin, C. G.; Crosson, E. R.; Steele, D. Measuring emissions from oil and natural gas well pads using the mobile flux plane technique. *Environ. Sci. Technol.* **2015**, *49*, 4742–4748.

(11) Robertson, A. M.; Edie, R.; Snare, D.; Soltis, J.; Field, R. A.; Burkhart, M. D.; Bell, C. S.; Zimmerle, D.; Murphy, S. M. Variation in methane emission rates from well pads in four oil and gas basins with contrasting production volumes and composition. *Environ. Sci. Technol.* **2017**, *51*, 8832–8840.

(12) Allen, D. T.; Torres, V. M.; Thomas, J.; Sullivan, D. W.; Harrison, M.; Hendler, A.; Herndon, S. C.; Kolb, C. E.; Fraser, M. P.; Hill, A. D.; Lamb, B. K.; Miskimins, J.; Sawyer, R. F.; Seinfeld, J. H. Measurements of methane emissions at natural gas production sites in the United States. *Proc. Natl. Acad. Sci. U. S. A.* **2013**, *110*, 17768–17773.

(13) Allen, D. T.; Sullivan, D. W.; Zavala-Araiza, D.; Pacsi, A. P.; Harrison, M.; Keen, K.; Fraser, M. P.; Hill, A. D.; Lamb, B. K.; Sawyer, R. F.; Seinfeld, J. H. Methane emissions from process equipment at natural gas production sites in the United States: pneumatic controllers. *Environ. Sci. Technol.* **2015**, *49*, 633–640.

(14) Lamb, B. K.; Edburg, S. L.; Ferrara, W. W.; Howard, T.; Harrison, M. R.; Kolb, C. E.; Townsend-Small, A.; Dyck, W.; Possolo, A.; Whetstone, J. R. Direct measurements show decreasing methane emissions from natural gas local distribution systems in the United States. *Environ. Sci. Technol.* **2015**, *49*, 5161–5169.

(15) Mitchell, A. L.; Tkacik, D. S.; Roscioli, J. R.; Herndon, S. C.; Yacovitch, T. I.; Martinez, D. M.; Vaughn, T. L.; Williams, L. L.; Sullivan, M. R.; Floerchinger, C.; Omara, M.; Subramanian, R.; Zimmerle, D.; Marchese, A. J.; Robinson, A. L. Measurements of methane emissions from natural gas gathering facilities and processing plants: measurement results. *Environ. Sci. Technol.* **2015**, *49*, 3219–3227.

(16) Subramanian, R.; Williams, L. L.; Vaughn, T. L.; Zimmerle, D.; Roscioli, J. R.; Herndon, S. C.; Yacovitch, T. I.; Floerchinger, C.; Tkacik, D. S.; Mitchell, A. L.; Sullivan, M. R.; Dallmann, T. R.; Robinson, A. L. Methane emissions from natural gas compressor stations in the transmission and storage sector: measurements and comparisons with the EPA Greenhouse Gas Reporting Program protocol. *Environ. Sci. Technol.* **2015**, *49*, 3252–3261.

(17) Marchese, A. J.; Vaughn, T. L.; Zimmerle, D. J.; Martinez, D. M.; Williams, L. L.; Robinson, A. L.; Mitchell, A. L.; Subramanian, R.; Tkacik, D. S.; Roscioli, J. R.; Herndon, S. C. Methane emissions from United States natural gas gathering and processing. *Environ. Sci. Technol.* **2015**, *49*, 3219–3227.

(18) Zimmerle, D. J.; Williams, L. L.; Vaughn, T. L.; Quinn, C.; Subramanian, R.; Duggan, G. P.; Wilson, B.; Opsomer, J. D.; Marchese, A. J.; Martinez, D. M.; Robinson, A. L. Methane emissions from the natural gas transmission and storage system in the United States. *Environ. Sci. Technol.* **2015**, *49*, 9374–9383.

(19) Caulton, D. R.; Shepson, P. B.; Santoro, R. L.; Sparks, J. P.; Howarth, R. W.; Ingraffea, A. R.; Cambaliza, M. O. L.; Sweeney, C.; Karion, A.; Davis, K. J.; Stirm, B. H.; Montzka, S. A.; Miller, B. R. Toward a better understanding and quantification of methane emissions from shale gas development. *Proc. Natl. Acad. Sci. U. S. A.* **2014**, *111*, 6237–6242.

- (20) Petron, G.; Karion, A.; Sweeney, C.; Miller, B. R.; Montzka, S. A.; Frost, G. J.; Trainer, M.; Tans, P.; Andrew, A.; Kofler, J.; Helmig, D.; Guenther, D.; Dlugokencky, E.; Lang, P.; Newberger, T.; Wolter, S.; Hall, B.; Novelli, P.; Brewer, A.; Conley, S.; Hardesty, M.; Banta, R.; White, A.; Noone, D.; Wolfe, D.; Schnell, R. A new look at methane and nonmethane hydrocarbon emissions from oil and natural gas operations in the Colorado Denver-Julesburg Basin: hydrocarbon emissions in oil & gas basin. *J. Geophys. Res. Atmospheres* **2014**, *119*, 6836–6852.
- (21) Karion, A.; Sweeney, C.; Petron, G.; Frost, G.; Hardesty, R. M.; Kofler, J.; Miller, B. R.; Newberger, T.; Wolter, S.; Banta, R.; Brewer, A.; Dlugokencky, E.; Lang, P.; Montzka, S. A.; Schnell, R.; Tans, P.; Trainer, M.; Zamora, R.; Conley, S. Methane emissions estimate from airborne measurements over a western United States natural gas field. *J. Geophys. Res. Lett.* **2013**, *40*, 4393–4397.
- (22) Karion, A.; Sweeney, C.; Kort, E. A.; Shepson, P. B.; Brewer, A.; Cambaliza, M.; Conley, S. A.; Davis, K.; Deng, A.; Hardesty, M.; Herndon, S. C.; Lauvaux, T.; Lavoie, T.; Lyon, D.; Newberger, T.; Petron, P.; Rella, C.; Smith, M.; Wolter, S.; Yacovitch, T. I.; Tans, P. Aircraft-based estimate of total methane emissions from the Barnett Shale region. *Environ. Sci. Technol.* **2015**, *49*, 8124–8131.
- (23) Peischl, J.; Ryerson, T. B.; Aikin, K. C.; de Gouw, J. A.; Gilman, J. B.; Holloway, J. S.; Lerner, B. M.; Nadkarni, R.; Neuman, J. A.; Nowak, J. B.; Trainer, M.; Warneke, C.; Parrish, D. D. Quantifying atmospheric methane emissions from Haynesville, Fayetteville, and northeastern Marcellus shale gas production regions. *J. Geophys. Res. Atmospheres* **2015**, *120*, 2119–2139.
- (24) Peischl, J.; Karion, A.; Sweeney, C.; Kort, E. A.; Smith, M. L.; Brandt, A. R.; Yeskoo, T.; Aikin, K. C.; Conley, S. A.; Gvakharia, A.; Trainer, M.; Wolter, S.; Ryerson, T. B. Quantifying atmospheric methane emissions from oil and natural gas production in the Bakken shale region of North Dakota. *J. Geophys. Res. Atmospheres* **2016**, *121*, 6101–6111.
- (25) Lyon, D. R.; Zavala-Araiza, D.; Alvarez, R. A.; Harris, R.; Palacios, V.; Lan, X.; Talbot, R.; Lavoie, T.; Shepson, P.; Yacovitch, T. I.; Herndon, S. C.; Marchese, A. J.; Zimmerle, D.; Robinson, A. L.; Hamburg, S. P. Constructing a spatially resolved methane emission inventory for the Barnett Shale region. *Environ. Sci. Technol.* **2015**, *49*, 8147–8157.
- (26) Zavala-Araiza, D.; Lyon, D. R.; Alvarez, R. A.; Davis, K. J.; Harris, R.; Herndon, S. C.; Karion, A.; Kort, E. A.; Lamb, B. K.; Lan, X.; Marchese, A. J.; Pacala, S. W.; Robinson, A. L.; Shepson, P. B.; Sweeney, C.; Talbot, R.; Townsend-Small, A.; Yacovitch, T. I.; Zimmerle, D. J.; Hamburg, S. P. Reconciling divergent estimates of oil and gas methane emissions. *Proc. Natl. Acad. Sci. U. S. A.* **2015**, *112*, 15597–15602.
- (27) Zavala-Araiza, D.; Alvarez, R. A.; Lyon, D. R.; Allen, D. T.; Marchese, A. J.; Zimmerle, D. J.; Hamburg, S. P. Super-emitters in natural gas infrastructure are caused by abnormal process conditions. *Nat. Commun.* **2017**, *8*, 14012–1421.
- (28) Zavala-Araiza, D.; Lyon, D.; Alvarez, R. A.; Palacios, V.; Harris, R.; Lan, X.; Talbot, R.; Hamburg, S. P. Toward a functional definition of methane super-emitters: application to natural gas production sites. *Environ. Sci. Technol.* **2015**, *49*, 8167–8174.
- (29) Lyon, D. R.; Alvarez, R. A.; Zavala-Araiza, D.; Brandt, A. R.; Jackson, R. B.; Hamburg, S. P. Aerial surveys of elevated hydrocarbon emissions from oil and gas production sites. *Environ. Sci. Technol.* **2016**, *50*, 4877–4886.
- (30) Brandt, A. R.; Heath, G. A.; Kort, E. A.; O'Sullivan, F.; Petron, G.; Jordaan, S. M.; Tans, P.; Wilcox, J.; Gopstein, A. M.; Arent, D.; Wofsy, S.; Brown, N. J.; Bradley, R.; Stucky, G. D.; Eardley, D.; Harris, R. Methane leaks from North American natural gas systems. *Science* **2014**, *343*, 733–735.
- (31) Barkley, Z. R.; Lauvaux, T.; Davis, K. J.; Deng, A.; Miles, N. L.; Richardson, S. J.; Cao, Y.; Sweeney, C.; Karion, A.; Smith, M.; Kort, E. A.; Schwietzke, S.; Murphy, T.; Cervone, G.; Martins, D.; Maasakkers, J. D. Quantifying methane emissions from natural gas production in northeastern Pennsylvania. *Atmos. Chem. Phys.* **2017**, *17*, 13941–13966.
- (32) Smith, M. L.; Gvakharia, A.; Kort, E. A.; Sweeney, C.; Conley, S. A.; Faloon, I.; Newberger, T.; Schnell, R.; Schwietzke, S.; Wolter, S. Airborne quantification of methane emissions over the Four Corners Region. *Environ. Sci. Technol.* **2017**, *51*, 5832–5837.
- (33) U.S. Environmental Protection Agency. Inventory of U.S. Greenhouse Gas Emissions and Sinks: 1990–2015 (2017). Available at <https://www.epa.gov/ghgemissions/inventory-us-greenhouse-gas-emissions-and-sinks-1990-2015> (accessed on August 29, 2018).
- (34) California Air Resources Board, Oil and Gas Regulation (2017). Available at: <https://www.arb.ca.gov/regact/2016/oilandgas2016/oilandgas2016.htm> (accessed on August 29, 2018).
- (35) Wyoming Oil and Gas Conservation Commission. Administrative Rules Chapter 3, Section 39. Authorization for Flaring and Venting of Gas (2016). Available at: <https://rules.wyo.gov/> (accessed on August 29, 2018).
- (36) Colorado Department of Public Health and Environment. Oil and gas emissions requirements (Regulation 7, Section XVII) (2016). Available at: <https://www.colorado.gov/pacific/cdphe/summary-oil-and-gas-emissions-requirements> (accessed on August 29, 2018).
- (37) Pennsylvania Methane Reduction Strategy (2016). Available at: <http://www.dep.pa.gov/business/air/pages/methane-reduction-strategy.aspx> (accessed on August 29, 2018).
- (38) Ohio Oil and Gas Laws (2016). Available at: <http://oilandgas.ohiodnr.gov/laws-regulations/oil-gas-law-summary> (accessed on August 29, 2018).
- (39) Ravikumar, A. P.; Wang, J.; Brandt, A. R. Are optical gas imaging technologies effective for methane leak detection? *Environ. Sci. Technol.* **2017**, *51*, 718–724.
- (40) U.S. Environmental Protection Agency. EPA Oil and Gas Tool, 2014 NEI Version 1.5—Production Activities Module. Updated July, 2016. Available at: <ftp://ftp.epa.gov/EmisInventory/2014nei/doc/> (accessed on August 29, 2018).
- (41) Drillinginfo DI Desktop; Austin, TX (2015). <http://www.didesktop.com/> (accessed on August 29, 2018).
- (42) U.S. Energy Information Administration. Natural Gas Gross Withdrawals and Production. Available at: https://www.eia.gov/dnav/ng/ng_prod_sum_dc_NUS_mmcf_a.htm (accessed on August 29, 2018).
- (43) Street, J. O.; Carrol, R. J.; Ruppert, D. A note on computing robust regression estimates via iteratively reweighted least squares. *Am. Stat.* **1988**, *42*, 152–154.
- (44) Brandt, A. R.; Heath, G. A.; Cooley, D. Methane leaks from natural gas systems follow extreme distributions. *Environ. Sci. Technol.* **2016**, *50*, 12512–12520.
- (45) Alvarez, R. A.; Zavala-Araiza, D.; Lyon, D. R.; Allen, D. T.; Barkley, A. R.; Brandt, A. R.; Davis, K. J.; Herndon, S. C.; Jacob, D. J.; Karion, A.; Kort, E. A.; Lamb, B. K.; Lauvaux, T.; Maasakkers, J. D.; Marchese, A. J.; Omara, M.; Pacala, S. W.; Peischl, J.; Robinson, A. L.; Shepson, P. B.; Sweeney, C.; Townsend-Small, A.; Wofsy, S. C.; Hamburg, S. P. Assessment of methane emissions from the U.S. oil and gas supply chain. *Science* **2018**, *361*, 186–188.
- (46) U.S. Energy Information Administration. Maps: Exploration, resources, reserves, and production. Available online at: <https://www.eia.gov/maps/maps.htm> (accessed August 29, 2018).

Exhibit 19



Remote sensing of methane leakage from natural gas and petroleum systems revisited

Oliver Schneising, Michael Buchwitz, Maximilian Reuter, Steffen Vanselow, Heinrich Bovensmann, and John P. Burrows

Institute of Environmental Physics (IUP), University of Bremen FB1, Bremen, Germany

Correspondence: Oliver Schneising (oliver.schneising@iup.physik.uni-bremen.de)

Received: 23 March 2020 – Discussion started: 14 April 2020

Revised: 25 June 2020 – Accepted: 3 July 2020 – Published: 3 August 2020

Abstract. The switch from the use of coal to natural gas or oil for energy generation potentially reduces greenhouse gas emissions and thus the impact on global warming and climate change because of the higher energy creation per CO₂ molecule emitted. However, the climate benefit over coal is offset by methane (CH₄) leakage from natural gas and petroleum systems, which reverses the climate impact mitigation if the rate of fugitive emissions exceeds the compensation point at which the global warming resulting from the leakage and the benefit from the reduction of coal combustion coincide. Consequently, an accurate quantification of CH₄ emissions from the oil and gas industry is essential to evaluate the suitability of natural gas and petroleum as bridging fuels on the way to a carbon-neutral future.

We show that regional CH₄ release from large oil and gas fields can be monitored from space by using dense daily recurrent measurements of the TROPOspheric Monitoring Instrument (TROPOMI) onboard the Sentinel-5 Precursor satellite to quantify emissions and leakage rates. The average emissions for the time period 2018/2019 from the five most productive basins in the United States, the Permian, Appalachian, Eagle Ford, Bakken, and Anadarko, are estimated to be 3.18 ± 1.13 , 2.36 ± 0.88 , 1.37 ± 0.63 , 0.89 ± 0.56 , and 2.74 ± 0.74 Mt yr⁻¹, respectively. This corresponds to CH₄ leakage rates relative to the associated production between 1.2% and 1.4% for the first four production regions, which are consistent with bottom-up estimates and likely fall below the break-even leakage rate for immediate climate benefit. For the Anadarko Basin, the fugitive emission rate is larger and amounts to 3.9 ± 1.1 %, which likely exceeds the break-even rate for immediate benefit and roughly corresponds to the break-even rate for a 20-year time horizon. The deter-

mined values are smaller than previously derived satellite-based leakage rates for the time period 2009–2011, which was an early phase of hydraulic fracturing, indicating that it is possible to improve the climate footprint of the oil and gas industry by adopting new technologies and that efforts to reduce methane emissions have been successful. For two of the world's largest natural gas fields, Galkynysh and Dauletabad in Turkmenistan, we find collective methane emissions of 3.26 ± 1.17 Mt yr⁻¹, which corresponds to a leakage rate of 4.1 ± 1.5 %, suggesting that the Turkmen energy industry is not employing methane emission avoidance strategies and technologies as successfully as those currently widely used in the United States. The leakage rates in Turkmenistan and in the Anadarko Basin indicate that there is potential to reduce fugitive methane emissions from natural gas and petroleum systems worldwide. In particular, relatively newly developed oil and gas plays appear to have larger leakage rates compared to more mature production areas.

1 Introduction

Methane (CH₄) is an important greenhouse gas, which accounts for the second-largest share of radiative forcing caused by human activities since preindustrial times. It has a much shorter atmospheric lifetime and a considerably higher global warming potential than the most important anthropogenically modified greenhouse gas, carbon dioxide (CO₂) (Holmes et al., 2013). Hence, a combined climate change mitigation strategy, aiming at reducing both CO₂ and CH₄ emissions in parallel, addresses long-term and near-term effects of global warming and is required to achieve climate

goals most efficiently (Shindell et al., 2012; Shoemaker et al., 2013).

An integral contribution to anthropogenic methane emissions originates from the exploitation of natural gas and oil for energy generation (i.e. the production of natural gas and oil, the refining of oil, and the subsequent storage, distribution, and combustion of these fuels). To assess the climate impact of the production of natural gas or oil in comparison to coal, the fugitive emission rate relative to production is a key parameter. Although the combustion of natural gas or oil produces less CO₂ than coal at the same energy content, methane emissions during the production and distribution process offset the climate benefit over coal. Hence, there is a compensation point, the break-even rate, at which the climate impacts of the relevant gas–oil mix and coal coincide. The exact break-even rate depends on the time horizon, the climate impact metric (e.g. global warming potential or technology warming potential), and the considered fuel-switching scenario. It has been estimated that an immediate climate benefit of switching from coal-fired to gas-fired power plants requires life-cycle methane emissions to stay below 3% (Alvarez et al., 2012). For a time horizon of 20 years the corresponding break-even rate is about 4%, which drops to 2% if carbon capture and sequestration becomes available (Farquharson et al., 2016).

The latest official bottom-up estimate of methane emissions from natural gas and petroleum systems reported by the United States Environmental Protection Agency (EPA) is 8.13 Mt [5.12–11.54; 2 σ] in 2017, corresponding to 0.9% [0.5–1.2; 2 σ] of aggregated gross production (U.S. Environmental Protection Agency, 2019a), which is very likely below the break-even emission rate. As in all leakage rate estimations presented here, combined oil and gas production in terms of energy content is the reference value of the calculation, and a methane content of 93% in natural gas (U.S. Environmental Protection Agency, 2019b) is used to determine the mass fraction of methane in the produced natural gas. Alternative bottom-up estimates (Alvarez et al., 2018) find total US oil and gas emissions of 13.0 Mt [11.3–15.1; 2 σ] in 2015, which is 63% higher than the EPA estimate and corresponds to a fugitive emission rate of 1.4% [1.1–1.6; 2 σ] (relative to combined oil and gas production).

However, several top-down studies suggest that the oil and gas industry leaks substantially more methane than assumed in official inventories, at least locally or temporally, with highly variable regional leakage rates occasionally reaching several multiples of the expected bottom-up estimates (Pétron et al., 2012; Karion et al., 2013; Caulton et al., 2014; Brandt et al., 2014; Schneising et al., 2014; Peischl et al., 2015, 2016, 2018; Alvarez et al., 2018). This points to a heterogeneity of the methane leakage and complicates the specification of typical emission rates, which are necessary to reliably assess the climate footprint of the natural gas and petroleum industry as a whole.

In the past, the satellite-based detection of CH₄ emissions from the oil and gas industry was mostly limited to long-term averages typically yielding emission rates with large associated uncertainties (Schneising et al., 2014; Turner et al., 2016; Buchwitz et al., 2017). Exceptional emissions of superemitters have also been observed in single satellite overpasses (Thompson et al., 2016). The recently launched Tropospheric Monitoring Instrument (TROPOMI) onboard the Sentinel-5 Precursor satellite, with its unique combination of high precision, accuracy, and spatiotemporal coverage (Veefkind et al., 2012), now enables the systematic detection of sufficiently large emission sources in a single satellite overpass. This has already been demonstrated for daily CH₄ enhancements from the energy sector for specific source regions in North America, Europe, and Turkmenistan (Varon et al., 2019; Schneising et al., 2019; Pandey et al., 2019; de Gouw et al., 2020). Here we use dense daily recurrent TROPOMI observations to reassess the emissions of petroleum- and gas-producing basins. The presented analysis includes emission estimates of the five most prolific basins in the United States as well as for two of the world's largest natural gas fields in Turkmenistan. The corresponding locations of these production regions are shown in Fig. 1.

2 Data and methods

In this study, atmospheric methane abundances are retrieved from radiance measurements in the shortwave infrared (SWIR) spectral range of the TROPOMI instrument onboard the Sentinel-5 Precursor (Sentinel-5P) satellite using the latest version of the Weighting Function Modified DOAS (WFM-DOAS) algorithm (Buchwitz et al., 2006; Schneising et al., 2011) optimised to retrieve methane and carbon monoxide simultaneously (TROPOMI/WFMD v1.2) (Schneising et al., 2019).

Sentinel-5P was launched in October 2017 into a sun-synchronous orbit with an Equator crossing time of 13:30 local solar time. TROPOMI is a spaceborne nadir-viewing imaging spectrometer measuring solar radiation reflected by the Earth in a push-broom configuration. It has a swath width of 2600 km and combines high spatial resolution with daily global coverage. The nadir measurements in the SWIR have a horizontal resolution of $7 \times 7 \text{ km}^2$ and are sensitive to all altitude levels including the planetary boundary layer, which makes them well suited for the investigation of emissions from oil and gas fields. The retrieved TROPOMI/WFMD column-averaged dry air mole fractions of methane, XCH₄, are characterised by a random error (precision) of 14.0 ppb and a systematic error (relative accuracy) of 4.3 ppb after quality filtering (Schneising et al., 2019).

The methane emission estimation is based on daily TROPOMI observations and a Gaussian integral method. For a fixed source region, quality-filtered daily XCH₄ retrievals are automatically processed as described below. First the data

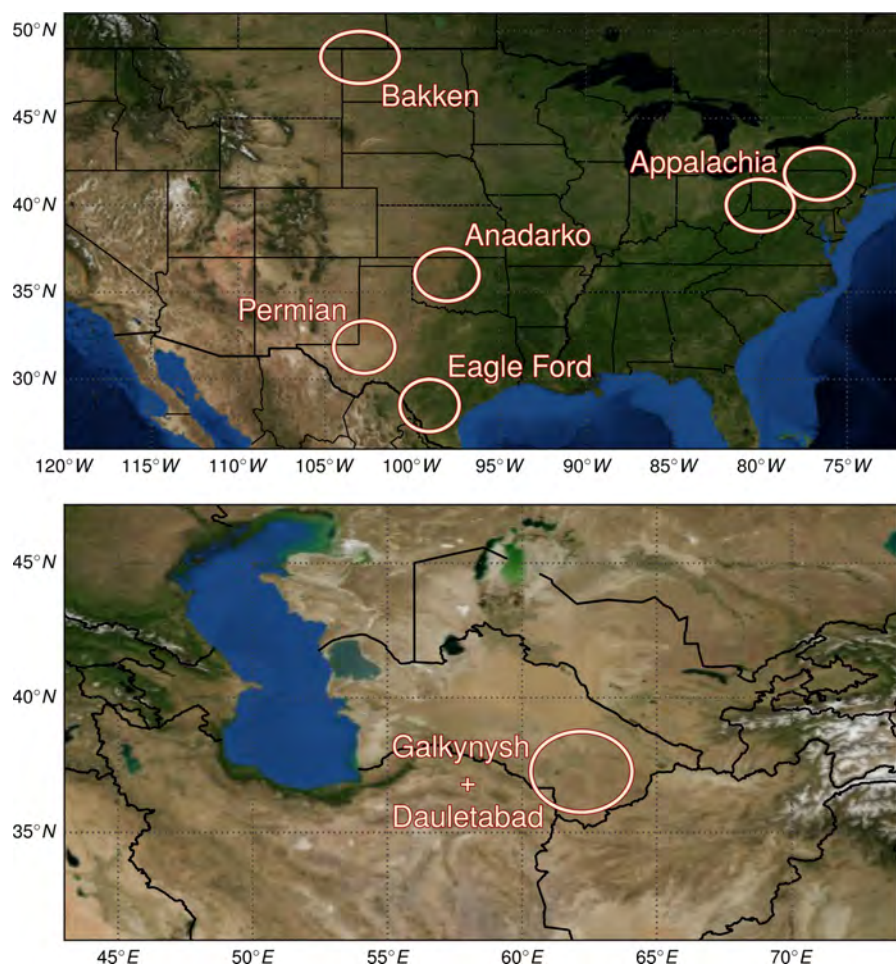


Figure 1. Location of the analysed natural gas and oil production regions. Due to its large and elongated extent, the Appalachia region is split into two subregions. All circles have a radius of 166.5 km, corresponding to 1.5° after the coordinate transformation described in Sect. 2.

given on geographical longitude and latitude are transformed to rotated coordinates so that zero meridian and Equator pass through the centre of the analysed region with the zonal direction matching the mean wind direction. The mean wind is defined as the average of all boundary layer winds within the region (as defined by the circles in Figs. 1, 4, 5, 7, 8, 10, and 11) and within the time window between 11:00 and 13:00 local time to take the wind history into account. Thereby, the boundary layer wind at a given time and place is defined as the pressure-weighted mean of winds for all layers within the boundary layer as obtained from the hourly European Centre for Medium-Range Weather Forecasts (ECMWF) ERA5 re-analysis product (Hersbach et al., 2018). The corresponding transformation of the coordinates and wind components is described in detail in Doms and Baldauf (2018). Similar approaches based on rotating individual satellite observations according to wind direction have also been used in the analysis of other atmospheric species (Valin et al., 2013; Pommier et al., 2013; Fioletov et al., 2015).

After rotating the coordinate system, the transformed daily data are gridded on a $0.05^\circ \times 0.05^\circ$ grid, and boxes with XCH₄ below the 10th percentile within a radius of 700 km around the pivotal point are additionally excluded due to potential residual cloud cover that may occur occasionally (Schneising et al., 2019). The rotated coordinates have the following advantages: (1) the new grid is nearly rectangular, leading to an almost homogeneous distribution of grid points, (2) it is straightforward to compute the integral perpendicular to wind direction, which is needed in our flux estimation, and (3) multiple daily grid files can be easily combined into long-term averages because the wind always has the same orientation (left to right).

After subtracting a mean background upwind of the source, the data look like the example shown in Fig. 2. The corresponding background region, which is highlighted in the figure, has the same position for all days and all investigated regions in the transformed coordinate system, and its suitability to enable a reliable emission estimate of the source region for a given day is automatically evaluated using cer-

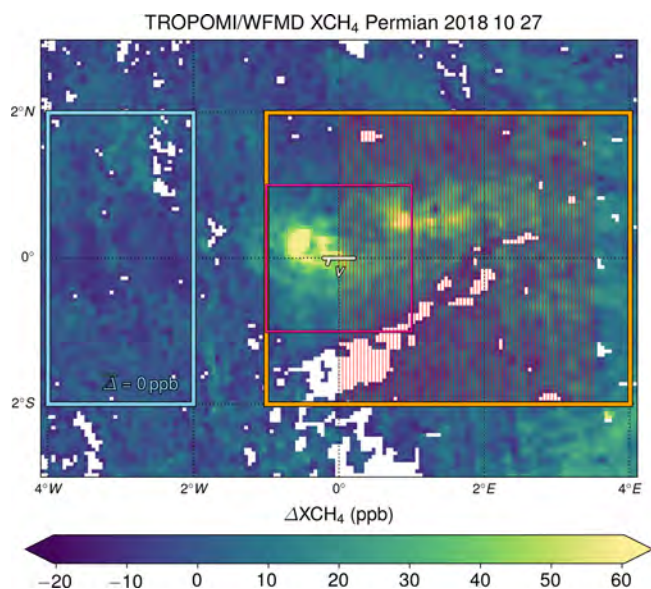


Figure 2. Example daily data to illustrate the estimation of the emission. The coordinate system has been transformed so that the wind direction lies along the Equator. The background region is shown in sky blue, the plume region in orange, and the hot-spot region in pink. The extent of these regions is fixed for all analysed days in the rotated coordinate system. By design, the background region has a mean abundance of 0 ppb. The meridional sections used to calculate the daily flux are displayed in red.

tain selection criteria introduced below (see also Sect. 3.7 for an assessment of the exclusionary power of the filter criteria, including those concerning the background region). Let E be the total column enhancement (in units of mass per area) and v the mean boundary layer wind speed. To estimate the daily emission rate Φ , we calculate fluxes of the vector field $E\mathbf{v}$ through cross sections perpendicular to wind direction (meridional red lines in Fig. 2) according to the divergence theorem; the flux through the other three sides of a rectangle surrounding the source region is assumed to be negligible (unit normals of the zonal boundaries are perpendicular to wind direction, and the upwind meridional boundary is in the background with $E = 0$). The flux through the k th cross section is

$$\begin{aligned} \Phi_k &= \int_V (\nabla \cdot E\mathbf{v}) dV = \oint_{\partial V=S} E\mathbf{v} \cdot d\mathbf{S} = \sum_i E_i v \Delta l_i \\ &= v \Delta l \sum_i E_i = \frac{v \cdot \Delta l \cdot M_{\text{CH}_4} \cdot \rho_{\text{dry}}}{N_A \cdot A_{\text{CH}_4}} \sum_i (\Delta X_{\text{CH}_4})_i. \end{aligned} \quad (1)$$

Thereby, Δl is the size of a grid box (0.05° is equivalent to about 5 km near the Equator) and i corresponds to meridional summation along the k th red line. The molar mass of methane $M_{\text{CH}_4} = 16.04 \text{ g mol}^{-1}$, the Avogadro constant $N_A = 6.022 \cdot 10^{23} \text{ molec mol}^{-1}$, and the mean dry air column ρ_{dry} (in units of molecules per area) within a radius corresponding to 3° after the coordinate transformation are used to

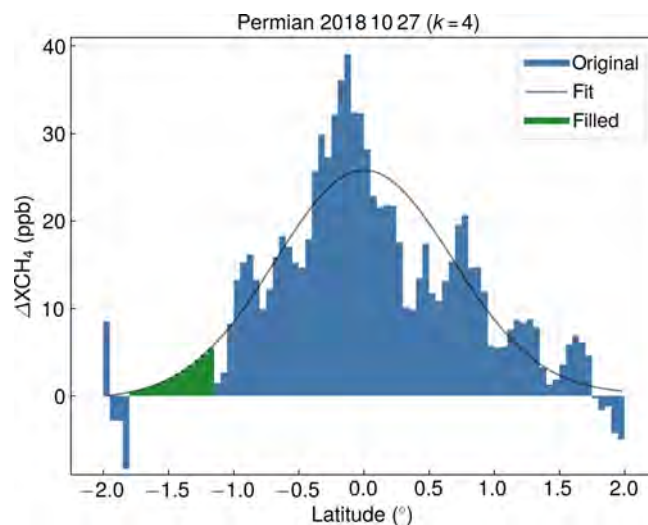


Figure 3. Demonstration of the gap-filling procedure. For Φ_k with at least 60% of all maximum available grid boxes along the meridional section, the gaps in the original data (blue) are filled (green) according to a fitted linear combination of a Gaussian and a linear polynomial (grey). The Φ_k values with less than 60% of data are not used in the estimation of the daily emissions. Shown here are the results for a specific k on an example day.

convert between the enhancement in X_{CH_4} and the total column enhancement E ; A_{CH_4} is the dimensionless near-surface averaging kernel (which is about 1.02 for all source regions analysed here) characterising the boundary layer sensitivity of the retrieval valid for the present mean altitude.

The average over all Φ_k then yields the final daily flux estimate Φ . Thereby, all Φ_k values with at least 60% of all maximum available grid boxes existing along the k th meridional section are selected. If there are no such Φ_k values to average, there is no flux estimate for this specific day. Before averaging, the gaps of the selected Φ_k are filled according to a fitted linear combination of a Gaussian and a linear polynomial (see Fig. 3 for an example meridional section).

The corresponding total 1σ uncertainty u_Φ is determined by the individual uncertainty components relative to the respective means via

$$\left(\frac{u_\Phi}{\Phi}\right)^2 = \frac{u_{v,\text{abs}}^2 + u_{v,\text{dir}}^2}{v^2} + \left(\frac{u_{\rho_{\text{dry}}}}{\rho_{\text{dry}}}\right)^2 + \left(\frac{u_E}{E}\right)^2, \quad (2)$$

with $u_{v,\text{abs}}$ being the standard deviation of all absolute boundary layer wind speed values over the selected region between 11:00 and 13:00 local time and $u_{v,\text{dir}}$ quantifying the uncertainty due to the maximal mean wind direction change in the considered 2 h time window of wind history; $u_{\rho_{\text{dry}}}$ is the standard deviation of the dry air columns within the same region used to determine the mean value, and u_E is the standard deviation of the enhancement integrals along the different meridional sections. For the regions under consideration in this study, the impact of topography (via $u_{\rho_{\text{dry}}}$)

is small compared to the other parameters contributing to the flux uncertainty (see Sect. 3.7).

Of all available days, those with a sufficient amount of data are selected to calculate the averaged long-term emission rate $\bar{\Phi}$ of the corresponding source region and the regional mean enhancement distribution. Thereby, at least 25 % of the background, plume, and hot-spot regions (see Fig. 2) must be filled with data after quality filtering in each case, and there have to be at least four cross sections with more than 60 % of data to average. As scenes with low wind speed may be dominated by diffusion and scenes with large wind velocity exhibit smaller column enhancements, additional criteria require that $v \in (2 \text{ m s}^{-1}, 10 \text{ m s}^{-1})$. Moreover, the enhancement distribution is required to be sufficiently uniform with respect to the Equator and in the background ($|\bar{E}_b^N - \bar{E}_b^S| < 10 \text{ ppb}$, $|\bar{E}_p^N - \bar{E}_p^S| < 15 \text{ ppb}$, $\sigma(E_b) < 10 \text{ ppb}$) to minimise scenarios with potential residual cloudiness or a considerably wrong wind direction, where $\bar{E}_{b,p}^{N,S}$ is the mean enhancement on the northern and southern half of the background and plume region, and $\sigma(E_b)$ is the standard deviation of the enhancements in the background region. Furthermore, days with mean wind direction changes during the considered 2 h time window that are larger than 30° or with uncertainty estimates larger than 5 Mt yr⁻¹ are additionally excluded. The corresponding uncertainty $u_{\bar{\Phi}}$ of the mean long-term emission rate is given via error propagation by the root sum square of the individual daily uncertainties $u_{\Phi,j}$ divided by the number of effectively contributing days n_{eff} , which is smaller than the actual number of days due to expected correlation of neighbouring data points,

$$u_{\bar{\Phi}} = \frac{\sqrt{\sum_j u_{\Phi,j}^2}}{n_{\text{eff}}} \quad (3)$$

We assume uncorrelated data blocks with a length of 1 month; i.e. n_{eff} is the number of months containing emission estimates contributing to the mean.

The associated long-term leakage rate is then calculated by normalising the estimated emissions $\bar{\Phi}$ by the combined oil and gas gross production of the considered region in terms of energy content (Schneising et al., 2014). In order to express the leakage rate as a percentage, emission (dividend) and production (divisor) are converted to the same units (energy per time, see Table 1). To quantify the combined production, the natural gas is converted to barrel of oil equivalent (BOE) by using a factor depending on its energy content. Although the exact conversion factor varies slightly with the specific composition of the natural gas, we use the widely used relationship of 6000 cubic feet per BOE (U.S. Energy Information Administration, 2019). To convert between emitted CH₄ mass and natural gas volume in cubic feet via the ideal gas law, we assume standard natural gas reference conditions (International Organization for Standardization, 1996) ($T = 288.15 \text{ K}$, $p = 1013.25 \text{ hPa}$) and a CH₄ content of 93 % in natural gas (U.S. Environmental Protec-

tion Agency, 2019b) with a realistic range of 87 %–99 % for high-caloric gas. Please note that all comparative leakage rates presented here (e.g. the bottom-up and airborne-based estimates) were also calculated as or converted to combined energy loss rates to make them comparable to our estimates.

For a production mixture of oil and gas the break-even rate of about 3 % estimated in the literature for gas-only production (Alvarez et al., 2012; Farquharson et al., 2016) has to be reduced as oil produces more CO₂ per unit of energy than natural gas. The fuel-related emission factors for bituminous coal, crude oil, and natural gas are 95, 73, and 56 tCO₂ TJ⁻¹ (Intergovernmental Panel on Climate Change, 2006). Thus, oil has about 56 % of the emission-saving potential of natural gas when replacing coal. As the maximal share of oil in the production mixtures of the analysed production regions is 75 % (see Sect. 3 and Table 1), the smallest occurring compensation value of all considered mixtures is assumed to be $(0.75 \cdot 0.56 + 0.25) \cdot 3 \% = 2 \%$. Consequently, we assume a break-even range of 2 %–3 % to achieve immediate climate benefit when switching from coal-based to a typical mixture of gas- and petroleum-based energy generation for a natural gas share between 25 % and 100 %.

3 Results and discussion

The top five producing basins in the United States during 2018/2019 in order of combined oil and gas production in terms of energy content were the Permian, Appalachian, Eagle Ford, Bakken, and Anadarko (U.S. Energy Information Administration, 2020), which are therefore potential candidates for our approach. As rotation in wind direction is an important element in the presented method, nearly rotation-symmetrical basins such as the Permian, Bakken, and Anadarko are best suited for the analysis. Due to its large and elongated extent, the Appalachia region is split into two subregions. The tubular shape of Eagle Ford, with almost linearly arranged sources, and its proximity to the offshore sources in the Gulf of Mexico complicate the analysis for this region. We also consider Galkynysh and Dauletabad, which are two of the world's largest natural gas fields located in Turkmenistan, to put the American results into a global context.

3.1 Permian

The Permian is a sedimentary basin in western Texas and eastern New Mexico. It has become one of the most productive oil-producing regions in the world and is by far the most prolific oil field in the United States. In the recent past, the share of natural gas has been increasing as wells get older and fewer new wells are drilled. The average production in the period 2018/2019 was 3897 thousand barrels of oil (Mbbbl) and 13 182 million cubic feet (MMcf) of natural gas per day (U.S. Energy Information Administration,

2020), corresponding to a total combined energy production of 6094 kBOE d⁻¹ (kilo barrel of oil equivalent per day). Thus, the production mix consists of about 65 % oil and 35 % natural gas. The Permian is subdivided into two major lobes with unconventional oil and gas production, the Delaware and the Midland Basin, which are separated by the Central Basin Platform dominated by conventional production. The qualitative detection of daily methane enhancements for the Permian has recently been demonstrated using TROPOMI measurements (de Gouw et al., 2020). Usually, the methane emissions of the Delaware Basin and Midland Basin are detected independently in daily satellite data (for example in Fig. 2). The averaged enhancement distribution for the period 2018/2019 and the daily emission estimates are shown in Fig. 4. The associated mean emission estimate for this period is $3.18 \pm 1.13 \text{ Mt yr}^{-1}$, corresponding to a fugitive emission rate of $1.3 \pm 0.5 \%$ relative to combined oil and gas energy production, which is slightly larger than the national bottom-up estimate of the EPA (0.9 % [0.5–1.2; 2σ]) but consistent with Alvarez et al. (2018) (1.4 % [1.1–1.6; 2σ]) and likely below the break-even leakage rate for immediate climate benefit.

Concurrent with our study, Zhang et al. (2020) also quantified methane emissions from the Permian Basin using a different data set and an alternative inversion method combining information from the operational TROPOMI methane product and prior emission estimates within a Bayesian framework. Despite these quite distinct approaches, their total emission estimate of $2.9 \pm 0.5 \text{ Mt yr}^{-1}$ based on satellite observations from May 2018 to March 2019 agrees within uncertainties with our estimate. If we restrict our analysis to this specific period, the consistency becomes even better and we get the almost identical estimate of 2.8 Mt yr^{-1} with our method, which is independent of prior knowledge. Therefore, the corresponding absolute results are considered very robust. However, there is a crucial difference in the calculation and subsequent interpretation of the leakage rate: while our rate (1.3 %) is calculated relative to combined oil and gas production in terms of energy content (Schneising et al., 2014), the rate of Zhang et al. (2020) is larger (3.7 %) and appears more alarming because it is put in relation to natural gas production only. With this alternative divisor we would also get a leakage rate of 3.7 % (as can be determined from Table 1). But as the Permian is dominated by oil production, we consider the total energy approach to be better suited to assess the climate impact compared to coal in general. Otherwise, the energy content of the extracted oil would be neglected and a pure oil play (with an infinitesimal fraction of not marketed but vented natural gas) would have a leakage rate of 100 %. For a pure natural gas play, however, both approaches to determine the leakage rate coincide.

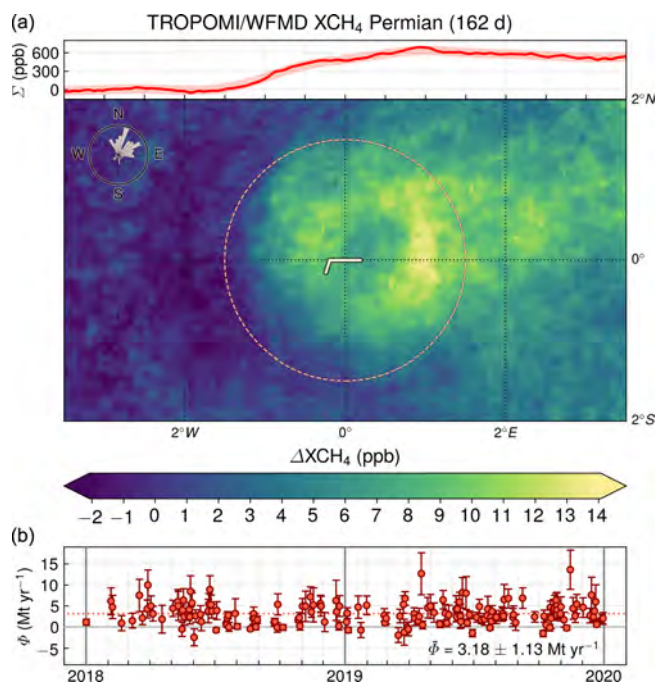


Figure 4. Averaged enhancement distribution with associated integrated enhancement along the meridional sections (a) and daily emission estimates Φ (b) for the Permian Basin. The coordinates of the pivotal point are 31.85° N and 102.75° W ; the radius of the circle highlighting the approximate basin extent is 166.5 km, corresponding to 1.5° after the coordinate transformation. The daily Φ values are used to determine the mean emission Φ , which corresponds to a fugitive emission rate of $1.3 \pm 0.5 \%$. The distribution of the associated original daily wind directions (defined as the direction in which the wind blows) can be seen in the overlaid wind rose in the upper left corner.

3.2 Bakken

The Bakken formation is the second-largest oil-producing region in the United States, with production mainly concentrated in North Dakota. The oil and natural gas in the Bakken are locked in rock reservoirs with low permeability, and unconventional drilling methods were necessary to transform the formation into a prolific production region. The production mix consists of about 75 % oil and 25 % natural gas, and the average production in the period 2018/2019 was 1361 Mbbbl of oil and 2661 MMcf of natural gas per day (U.S. Energy Information Administration, 2020), corresponding to a total combined energy production of 1805 kBOE d⁻¹. The determined mean emission estimate for the period 2018/2019 is $0.89 \pm 0.56 \text{ Mt yr}^{-1}$. As can be seen in Fig. 5, the associated averaged enhancement distribution is noisier due to fewer contributing days and does not show a plume structure as clear as in the case of the Permian. Together with the large relative uncertainty, this suggests that the emissions of the Bakken are close to the detection limit for daily data. The estimated emissions correspond to a fugitive emission rate

of $1.3 \pm 0.8\%$ relative to combined oil and gas energy production, which is consistent with Alvarez et al. (2018) and slightly larger than the national EPA bottom-up estimate. The rate is likely below the break-even rate, but the error bars extend into the break-even range. The derived leakage rate is also consistent with the energy loss rates of $1.6 \pm 0.5\%$ and $1.4 \pm 0.5\%$ estimated for the Bakken from airborne data taken in May 2014 (Peischl et al., 2016) and April 2015 (Peischl et al., 2018). The respective airborne-based estimates were originally specified as leakage rates relative to natural gas production only and have been converted to rates relative to combined oil and gas production in terms of energy content in each case by considering the natural gas fraction of 25% in the production mix of the Bakken to make the estimates directly comparable to our estimates. The Bakken estimate from this study is smaller than previously derived satellite-based leakage rates for the time period 2009–2011, which were estimated to be $10.1 \pm 7.3\%$ for this early phase of hydraulic fracturing (Schneising et al., 2014). Although the corresponding uncertainties of both satellite studies for the Bakken are large, the reduction of relative leakage over time suggests that the climate footprint of the oil and gas industry can be improved by adopting new technologies and that efforts to reduce fugitive methane emissions have been successful. The systematic measures proactively implemented by coalitions of oil and gas companies since 2014 to continuously reduce methane emissions include additional leak detection and repair campaigns, replacement or upgrade of high-emitting devices, and reduction of venting or flaring toward the ambitious goal of achieving a leakage rate not exceeding 1% across the natural gas supply chain (including a maximum of 0.3% from upstream operations) by 2025 (ONE Future, 2019; Oil and Gas Climate Initiative, 2019). An illustration of the decreasing leakage rates derived from satellite and airborne measurements in the discussed publications is shown together with the assumed break-even range for immediate climate benefit in Fig. 6.

3.3 Appalachia

The Appalachia region in eastern North America consists of several stacked formations, most prominently the Marcellus and Utica shale plays. The region drives the overall increase in United States natural gas production. The Marcellus shale is a unit of sedimentary rock and the most productive natural-gas-producing formation in the Appalachian Basin. The older Utica and Point Pleasant formations extend below the Marcellus shale and the Upper Devonian shale above it. Unconventional drilling in the Appalachian is mainly focused on two hot-spot regions in the southwestern and northeastern part of Pennsylvania. These two regions are analysed separately due to the large and elongated extent of the basin. The average production of the Appalachia region during 2018/2019 was 30 312 MMcf of natural gas and 127 Mbbl of oil per day (U.S. Energy Information Admin-

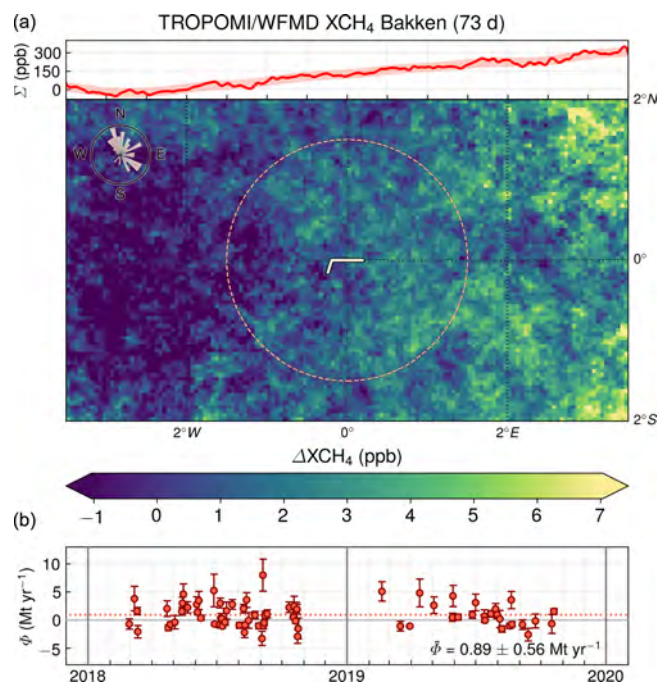


Figure 5. As Fig. 4 but for the Bakken formation. The coordinates of the pivotal point are 48.5° N, 103° W. The mean emission estimate $\bar{\Phi}$ corresponds to a fugitive emission rate of $1.3 \pm 0.8\%$.

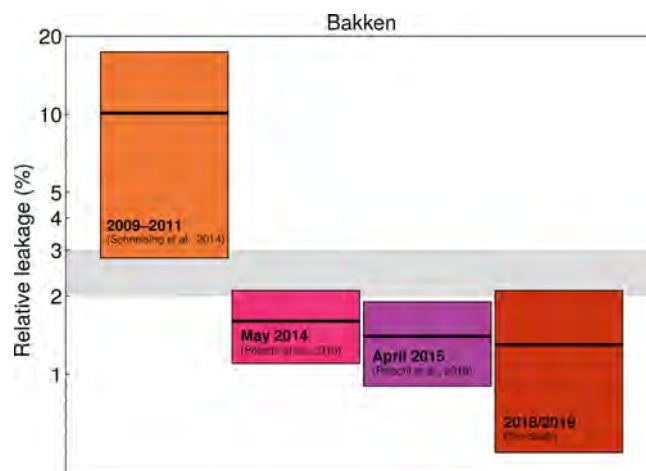


Figure 6. Comparison of fugitive emission rates for the Bakken formation from different studies with a reduction of relative leakage over time. See main text for details. The assumed break-even range for immediate climate benefit is shown in grey.

istration, 2020), corresponding to a total combined energy production of 5179 kBOE d^{-1} . Thus, the production mix is strongly gas driven, with 98% natural gas and only 2% oil. The averaged enhancement distribution during 2018/2019 for the southwestern part of the Appalachia region and the daily emission estimates are shown in Fig. 7. The associated mean emission estimate is $1.07 \pm 0.45 \text{ Mt yr}^{-1}$. The corresponding estimation for the northeastern part is 1.29 ± 0.43

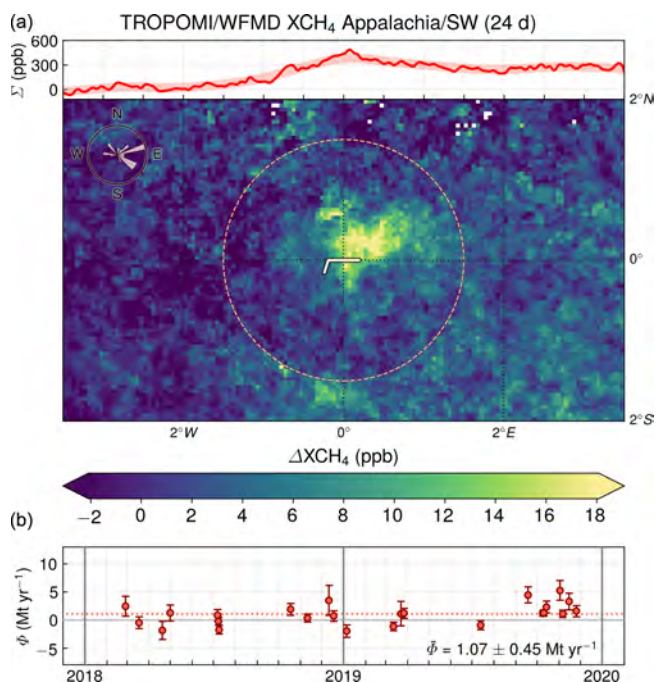


Figure 7. As Figs. 4 and 5 but for the southwestern part of the Appalachia region. The coordinates of the pivotal point are 40° N, 80° W. The pivotal point of the second subregion not shown here is located at 41.8° N, 76.6° W.

Mt yr⁻¹. Thus, the mean emission for the complete Appalachia region amounts to 2.36 ± 0.88 Mt yr⁻¹. However, it has to be noted that there are only a few days contributing to this emission estimate, namely 24 d for the southwestern and 10 d for the northeastern part of the Appalachian. The derived emissions are equivalent to a fugitive emission rate of 1.2 ± 0.4 %, which is consistent with the bottom-up estimates and likely below the compensation point for a climate benefit on all time frames. The leakage rate inferred from satellite measurements of XCH₄ is higher than the loss rate of 0.3 ± 0.1 % estimated for the northeastern Marcellus from airborne data taken in July 2013 (Peischl et al., 2015). Although this airborne estimate was specified as a leakage rate relative to natural gas production only, it can be compared directly to our estimate because the Appalachia region is strongly gas driven (98 %), and conversion to a rate relative to combined oil and gas production in terms of energy content thus has only a marginal impact.

3.4 Eagle Ford

The Eagle Ford Shale is a geological formation in southern Texas, which extends from the Mexican border to the northeast in a tubular shape. The brittleness of the rock in the high-carbonate areas in the western part of the formation makes it more conducive to hydraulic fracturing, and a lot of capital has been invested to develop its unconventional hydrocarbon extraction. The production mix consists

of about 55 % oil and 45 % natural gas, and the average production in the period 2018/2019 was 1344 Mbbl of oil and 6674 MMcf of natural gas per day (U.S. Energy Information Administration, 2020), corresponding to a total combined energy production of 2456 kBOE d⁻¹. Due to its shape, with almost linearly arranged sources and proximity to significant offshore sources in the Gulf of Mexico (Yacovitch et al., 2020), the introduced approach is challenging in the case of Eagle Ford. To avoid the background being impacted by the offshore sources, wind directions blowing towards the north-west (between north and west) were additionally excluded. As a consequence, almost all summer days on which the winds mainly blow off the sea are filtered out, leaving only 25 d for analysis (see Fig. 8). The associated mean emission estimate for the period 2018/2019 is 1.37 ± 0.63 Mt yr⁻¹, corresponding to a leakage rate of 1.4 ± 0.7 %, which is consistent with Alvarez et al. (2018) and slightly larger than the national EPA bottom-up estimate. Although the estimated fugitive emission rate is below 2 %, the error bars extend into the break-even range. The derived leakage rate is also consistent with estimates based on airborne data taken in April 2015 (Peischl et al., 2018), which report a mean loss rate of 2.6 ± 0.9 % relative to natural gas production. This corresponds to an energy loss rate of 1.2 ± 0.4 % when taking the natural gas share of 45 % in the production mix into account. As in the case of the Bakken, the Eagle Ford estimate from this study is smaller than previously derived satellite-based leakage rates for the time period 2009–2011, which were estimated to be 9.1 ± 6.2 % (Schneising et al., 2014), suggesting that the emissions have been reduced by improving the technological standards since the early phase of hydraulic fracturing. An illustration of the decreasing leakage rates derived from satellite and airborne measurements in the discussed publications is shown together with the assumed break-even range for immediate climate benefit in Fig. 9.

3.5 Anadarko

The Anadarko Basin is located in the western part of Oklahoma and the bordering states. It is one of the most prolific natural gas production regions in North America and is just beginning to exploit its unconventional production potential. It is an attractive target for operators as it contains many stacked plays overlapping in large parts of the basin, allowing access to multiple targets from one well pad. The average production in the period 2018/2019 was 7421 MMcf of natural gas and 548 Mbbl of oil per day (U.S. Energy Information Administration, 2020), which corresponds to a total production of 1785 kBOE d⁻¹ and a production mix of about 70 % natural gas and 30 % oil. The averaged enhancement distribution for the period 2018/2019 and the daily emission estimates are shown in Fig. 10. The mean emission estimate of 2.74 ± 0.74 Mt yr⁻¹ corresponds to a leakage rate of 3.9 ± 1.1 %, which is considerably larger than for the other analysed production regions in the United States and likely

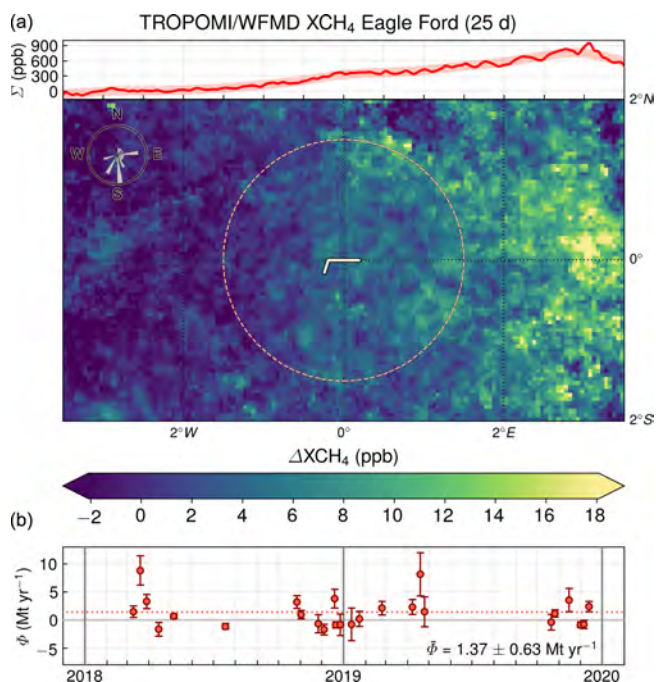


Figure 8. As Figs. 4, 5, and 7 but for the Eagle Ford formation. The coordinates of the pivotal point are 28.5° N, 99° W. To avoid the background being impacted by offshore sources, wind directions blowing towards the northwest were additionally excluded.

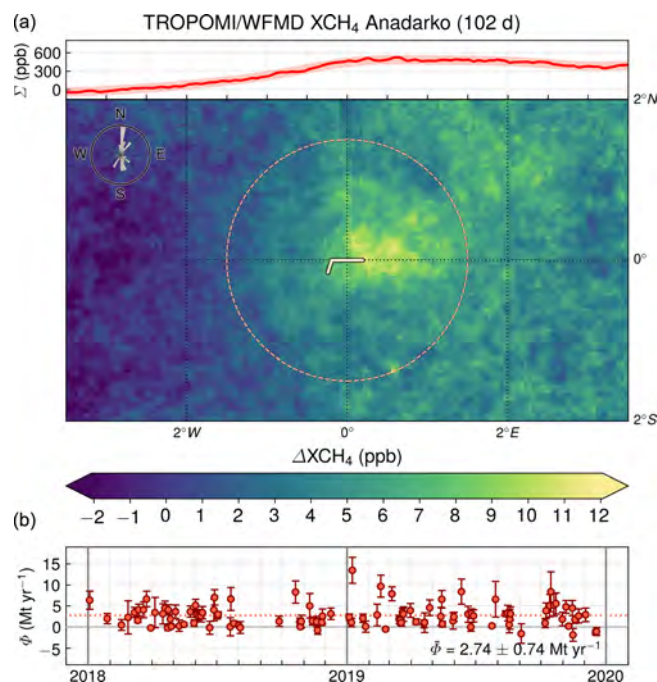


Figure 10. As Figs. 4, 5, 7, and 8 but for the Anadarko Basin. The coordinates of the pivotal point are 36° N, 98° W. The mean emission estimate $\bar{\Phi}$ corresponds to a fugitive emission rate of $3.9 \pm 1.1\%$.

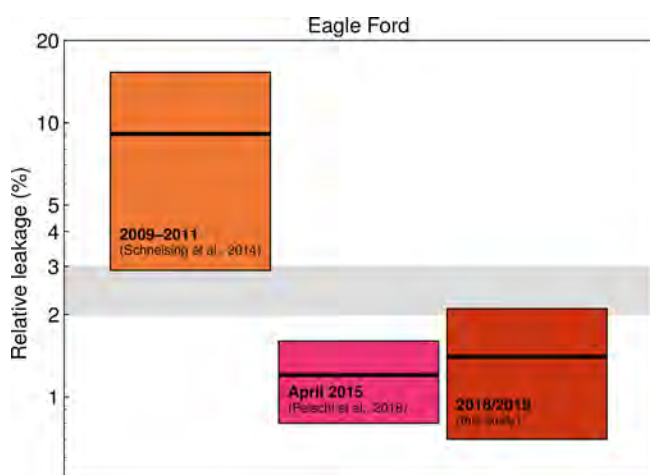


Figure 9. Comparison of fugitive emission rates for the Eagle Ford Shale from different studies with a reduction of relative leakage over time. See main text for details. The assumed break-even range for immediate climate benefit is shown in grey.

exceeds the break-even rate for immediate climate benefit. It rather corresponds to the break-even rate for a 20-year time horizon and a scenario without carbon capture and sequestration (Farquharson et al., 2016).

3.6 Galkynysh and Dauletabad

Besides the discussed production regions in the United States, we also analysed methane emissions from two of the world's largest natural gas fields, Galkynysh and Dauletabad in Turkmenistan. Galkynysh is a cluster of conventional oil and gas deposits that have been combined under a common name. Galkynysh started production in 2013 and was planned to be developed in three stages by adding capacities of about 2900, 2900, and 3400 MMcf d⁻¹ in the respective stages (AidData, 2013; U.S. Energy Information Administration, 2016). As the last stage was expected to start in late 2015, we assume that the field production was close to the envisaged total quantity of 9200 MMcf d⁻¹ in the analysed period 2018/2019, although official production figures are not available. Dauletabad is also a large natural gas field in Turkmenistan, which is located between Galkynysh and the Iranian border, with assumed gas production of 2900 MMcf d⁻¹ (Mammadov, 2015). This corresponds to a total collective production for Galkynysh and Dauletabad of 2017 kBOE d⁻¹ because there is no reference to commercial oil production from either field. The qualitative detection of daily methane enhancements for the Galkynysh field has already been demonstrated using TROPOMI measurements (Schneising et al., 2019). The quantitative reinforcement in this study (see Fig. 11) provides a joint emission estimate together with Dauletabad of 3.26 ± 1.17 Mt yr⁻¹, correspond-

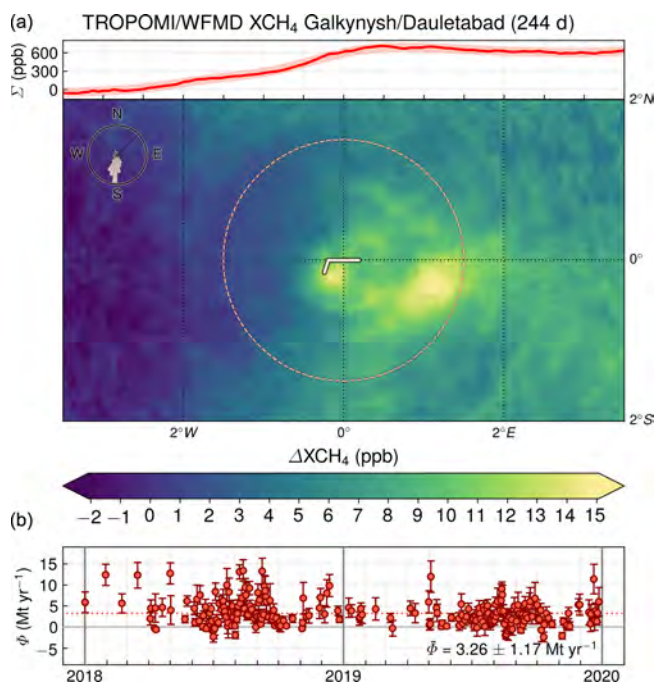


Figure 11. As Figs. 4, 5, 7, 8, and 10 but for the Galkynysh and Dauletabad fields in Turkmenistan. The coordinates of the pivotal point are 37.25° N, 62.2° E.

ing to a fugitive emission rate of $4.1 \pm 1.5\%$, which is comparable to the leakage rate for the Anadarko Basin and roughly corresponds to the break-even rate for a 20-year time horizon (Farquharson et al., 2016). Due to the lack of official production reporting, it is possible that the actual leakage rate for these Turkmen fields may be somewhat smaller (e.g. if there is also some oil production) or larger (e.g. if the targeted production of Galkynysh was not achieved in 2018/2019).

3.7 Uncertainty contributions and breakdown of selection criteria

As described in Sect. 2, the total daily uncertainty u_ϕ is determined from individual uncertainty components quantifying the impact of the enhancement patterns in the context of systematic biases or single-measurement precision (u_E), absolute wind speed and wind direction knowledge or variability ($u_{v, \text{abs}}$ and $u_{v, \text{dir}}$), and pressure or topography ($u_{\rho_{\text{dry}}}$) on the emission estimates (see Eq. 2). The mean percentage variance contribution for a given component c is defined as the mean of all contributing days of the daily $(\frac{u_c}{c})^2 / (\frac{u_\phi}{\phi})^2$. Besides the emission and production values used to determine the leakage rates, the individual mean percentage variance contributions to the emission estimates are summarised in Table 1 for the regions under consideration in this study. As can be seen, the main sources of uncertainty are given by the variable enhancement patterns related to precision and accuracy and by the spatial and temporal variability of the

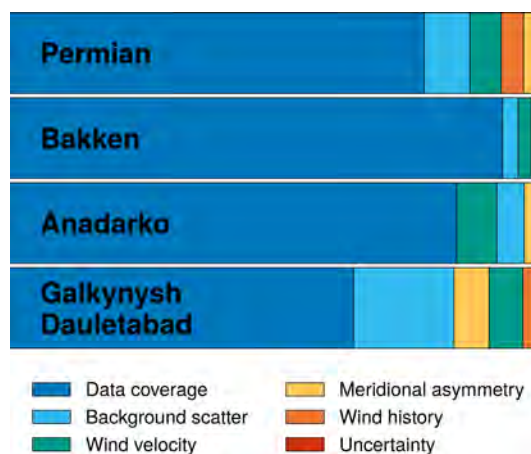


Figure 12. Relative contributions of the selection criteria sorted by importance for different regions. See main text for details.

absolute wind speed. Due to the exclusion of days with mean wind direction changes larger than 30° during the considered 2 h time window of wind history, the contribution of wind direction variability is small. The same is true for the relative impact of topography on the emission estimates, at least for the regions analysed here.

Section 2 also describes the filter criteria for selecting the data in order to ensure reliable emission estimates. Most excluding are the ones that filter out days with too few data coverage over the corresponding region. To determine the subsequent order of the leftover filters, the criteria excluding the most days of the remaining data set are successively identified. The results are summarised in Fig. 12 for different oil and gas plays under consideration. The filter criteria ordered by exclusionary power for all regions combined are (1) too few data, (2) background scatter $\sigma(E_b)$ that is too high, (3) wind velocity v that is too high or too low, (4) asymmetry $|\overline{E}_{b,p}^N - \overline{E}_{b,p}^S|$ that is too large with respect to the Equator, (5) considerable wind direction change within the 2 h time window of wind history, and (6) daily uncertainty u_ϕ that is too large. For the individual regions, the respective filter sequences are similar, with a maximum permutation of two criteria compared to the overall sequence.

4 Conclusions

We have analysed regional atmospheric methane enhancements over large oil and gas production areas derived from daily measurements in the shortwave infrared spectral range of the TROPOMI instrument onboard the Sentinel-5 Precursor satellite to estimate the mean emissions for the analysed regions during the period 2018/2019. The analysis benefits from TROPOMI's unique combination of high precision, accuracy, and spatiotemporal coverage, allowing for the sys-

Table 1. Summary of the emission and production values used to determine the leakage rates (emissions divided by combined oil and gas production). All values have been converted (kBOE d⁻¹) as described in Sect. 2. Also shown are the mean percentage variance contributions to the emission estimates for the relative uncertainty components of Eq. (2).

Region	Emissions (kBOE d ⁻¹)	Production			Leakage (%)	Variance contributions					
		Oil (kBOE d ⁻¹)	Gas (kBOE d ⁻¹)	Oil+gas (kBOE d ⁻¹)		<i>E</i>	<i>v</i> , abs	<i>v</i> , dir	ρ_{dry}		
Permian	81	3897	2197	64	36	6094	1.3	59.9	38.9	0.6	0.6
Appalachia	60	127	5052	2	98	5179	1.2	73.2	26.4	0.2	0.2
Eagle Ford	35	1344	1112	55	45	2456	1.4	65.0	34.0	0.5	0.5
Bakken	23	1361	444	75	25	1805	1.3	64.9	34.5	0.4	0.2
Anadarko	70	548	1237	31	69	1785	3.9	70.5	28.7	0.4	0.4
Galkynysh– Dauletabad	83	0	1533	0	100	2017	4.1	74.1	22.6	0.5	2.8

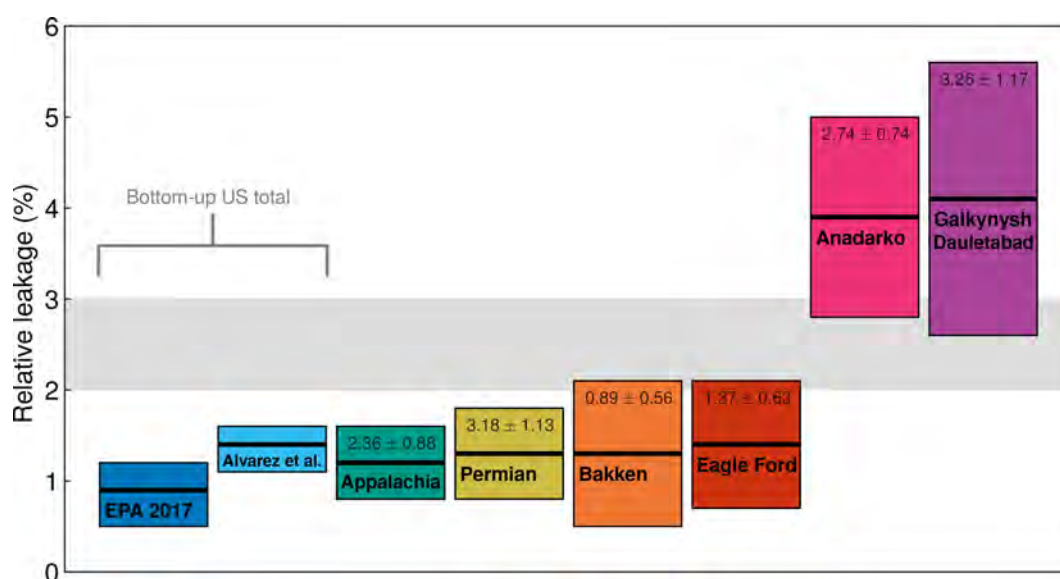


Figure 13. Summary of the results for the different regions analysed in this study and a comparison to bottom-up estimates for the entire United States. All leakage rates are calculated relative to combined oil and gas production in terms of energy content. The respective absolute emissions (Mt yr⁻¹) are shown in the upper area of the bars for the individual regions. The assumed break-even range for immediate climate benefit is shown in grey.

tematic detection of sufficiently large emission sources in a single satellite overpass.

To assess the climate impact of the oil and gas industry, the determined emission estimates were related to the combined oil and gas production of the considered regions in terms of energy content to infer the respective fugitive emission rates. A summary of the results is given in Table 1 and illustrated in Fig. 13, showing the leakage rates for the different regions analysed in comparison to bottom-up estimates for the entire United States. In addition to regions where the inferred fugitive emission rates are reasonably consistent with the bottom-up estimates and likely below the break-even rate for immediate climate benefit (Appalachian, Permian, Bakken, and Eagle Ford), we have also identified regions that probably exceed this range (Anadarko and Galkynysh–Dauletabad), ren-

dering a climate benefit over all time frames for these production areas questionable. The results suggest that it is possible to reduce methane emissions below the break-even leakage rate at which the climate impacts of the gas–oil mix and coal coincide if sufficient technological efforts are undertaken and appropriate industrial practices are employed. On the other hand, this does not seem to have been achieved in all production regions yet. In particular, relatively newly developed oil and gas plays appear to have larger leakage rates compared to more mature production areas. As a consequence, there is still potential to reduce fugitive methane emissions from natural gas and petroleum systems worldwide. The self-imposed goal of many oil and gas companies to reduce the leakage rate below 1% has probably not yet been achieved in the measured regions.

Due to the inherent heterogeneity of methane leakage in the energy sector depending on operating conditions and procedures, it is difficult to specify typical leakage rates and to reliably assess the climate footprint of the natural gas and petroleum industry as a whole, which is essential for developing a sagacious environmental and energy policy. Further studies including other regions and longer time series are needed to unambiguously evaluate the sustainability of the oil and gas industry by obtaining a better sampling of the leakage distribution. Better knowledge of the relationships between leakage and production practices or basin development would also serve to improve current spatially and temporally resolved emission databases. In order to achieve these objectives, satellite measurements, ideally supplemented by frequent aircraft and ground-based measurements, can make an important contribution. An analysis of the main sources of uncertainty in satellite-based emission and leakage estimates suggests that future missions with improved precision and spatial resolution may have the potential to refine the current capabilities of emission monitoring from space by further reducing uncertainties. However, any emission estimation requires accurate knowledge of the wind speed and direction at an adequate horizontal and vertical resolution, which is not directly available by satellite observations and has to be provided by external sources.

Data availability. The methane data set presented in this publication can be accessed via http://www.iup.uni-bremen.de/carbon_ghg/products/tropomi_wfmd/ (Schneising, 2019).

Author contributions. OS designed and operated the TROPOMI/WFMD satellite retrievals, performed the data analysis, interpreted the results, and wrote the paper. MB, MR, SV, HB, and JPB provided significant conceptual input to the design of the TROPOMI/WFMD satellite retrievals, the interpretation, and the improvement of the paper. All authors discussed the results and commented on the paper.

Competing interests. The authors declare that they have no conflict of interest.

Special issue statement. This article is part of the special issue “TROPOMI on Sentinel-5 Precursor: first year in operation (AMT/ACP inter-journal SI)”. It is not associated with a conference.

Acknowledgements. This publication contains modified Copernicus Sentinel data (2018, 2019). Sentinel-5 Precursor is an ESA mission implemented on behalf of the European Commission. The TROPOMI payload is a joint development by the ESA and the Netherlands Space Office (NSO). Sentinel-5 Precursor ground-

segment development has been funded by the ESA and with national contributions from the Netherlands, Germany, and Belgium.

We acknowledge the use of the meteorological ERA5 reanalysis from the European Centre for Medium-Range Weather Forecasts (ECMWF) and the oil and natural gas production data from the U.S. Energy Information Administration (EIA).

Financial support. The research leading to the presented results has in part been funded by the ESA projects GHG-CCI, GHG-CCI+, and Methane+, the Federal Ministry of Education and Research project AIRSPACE (grant 01LK1701B), the DLR project “S5P Datennutzung” (50EE1811A), and the State and the University of Bremen.

The article processing charges for this open-access publication were covered by the University of Bremen.

Review statement. This paper was edited by Ben Veihelmann and reviewed by two anonymous referees.

References

- AidData: China CDB Agree Financing for Turkmenistan Gas Fields, available at: <https://china.aiddata.org/projects/43168> (last access: 17 February 2020), 2013.
- Alvarez, R. A., Pacala, S. W., Winebrake, J. J., Chameides, W. L., and Hamburg, S. P.: Greater focus needed on methane leakage from natural gas infrastructure, *P. Natl. Acad. Sci. USA*, 109, 6435–6440, <https://doi.org/10.1073/pnas.1202407109>, 2012.
- Alvarez, R. A., Zavala-Araiza, D., Lyon, D. R., Allen, D. T., Barkley, Z. R., Brandt, A. R., Davis, K. J., Herndon, S. C., Jacob, D. J., Karion, A., Kort, E. A., Lamb, B. K., Lauvaux, T., Maasakkers, J. D., Marchese, A. J., Omara, M., Pacala, S. W., Peischl, J., Robinson, A. L., Shepson, P. B., Sweeney, C., Townsend-Small, A., Wofsy, S. C., and Hamburg, S. P.: Assessment of methane emissions from the U.S. oil and gas supply chain, *Science*, 361, 186–188, <https://doi.org/10.1126/science.aar7204>, 2018.
- Brandt, A. R., Heath, G. A., Kort, E. A., O’Sullivan, F., Pétron, G., Jordaan, S. M., Tans, P., Wilcox, J., Gopstein, A. M., Arent, D., Wofsy, S., Brown, N. J., Bradley, R., Stucky, G. D., Eardley, D., and Harriss, R.: Methane Leaks from North American Natural Gas Systems, *Science*, 343, 733–735, <https://doi.org/10.1126/science.1247045>, 2014.
- Buchwitz, M., de Beek, R., Noël, S., Burrows, J. P., Bovensmann, H., Schneising, O., Khlystova, I., Bruns, M., Bremer, H., Bergamaschi, P., Körner, S., and Heimann, M.: Atmospheric carbon gases retrieved from SCIAMACHY by WFM-DOAS: version 0.5 CO and CH₄ and impact of calibration improvements on CO₂ retrieval, *Atmos. Chem. Phys.*, 6, 2727–2751, <https://doi.org/10.5194/acp-6-2727-2006>, 2006.
- Buchwitz, M., Schneising, O., Reuter, M., Heymann, J., Krautwurst, S., Bovensmann, H., Burrows, J. P., Boesch, H., Parker, R. J., Somkuti, P., Detmers, R. G., Hasekamp, O. P., Aben, I., Butz, A., Frankenberg, C., and Turner, A. J.: Satellite-derived methane hotspot emission estimates using a

- fast data-driven method, *Atmos. Chem. Phys.*, 17, 5751–5774, <https://doi.org/10.5194/acp-17-5751-2017>, 2017.
- Caulton, D. R., Shepson, P. B., Santoro, R. L., Sparks, J. P., Howarth, R. W., Ingraffea, A. R., Cambaliza, M. O. L., Sweeney, C., Karion, A., Davis, K. J., Stirm, B. H., Montzka, S. A., and Miller, B. R.: Toward a better understanding and quantification of methane emissions from shale gas development, *P. Natl. Acad. Sci. USA*, 111, 6237–6242, <https://doi.org/10.1073/pnas.1316546111>, 2014.
- de Gouw, J. A., Veefkind, J. P., Roosenbrand, E., Dix, B., Lin, J. C., Landgraf, J., and Levelt, P. F.: Daily Satellite Observations of Methane from Oil and Gas Production Regions in the United States, *Sci. Rep.*, 10, 1379, <https://doi.org/10.1038/s41598-020-57678-4>, 2020.
- Doms, G. and Baldauf, M.: A Description of the Nonhydrostatic Regional COSMO-Model, Part I: Dynamics and Numerics, Core documentation of the COSMO-model, available at: <http://www.cosmo-model.org/content/model/documentation/core/cosmoDynNumcs.pdf> (last access: 2 December 2019), 2018.
- Farquharson, D., Jaramillo, P., Schivley, G., Klima, K., Carlson, D., and Samaras, C.: Beyond Global Warming Potential: A Comparative Application of Climate Impact Metrics for the Life Cycle Assessment of Coal and Natural Gas Based Electricity, *J. Ind. Ecol.*, 21, 857–873, <https://doi.org/10.1111/jiec.12475>, 2016.
- Fioletov, V. E., McLinden, C. A., Krotkov, N., and Li, C.: Lifetimes and emissions of SO₂ from point sources estimated from OMI, *Geophys. Res. Lett.*, 42, 1969–1976, <https://doi.org/10.1002/2015GL063148>, 2015.
- Hersbach, H., de Rosnay, P., Bell, B., Schepers, D., Simmons, A., Soci, C., Abdalla, S., Alonso-Balmaseda, M., Balsamo, G., Bechtold, P., Berrisford, P., Bidlot, J.-R., de Boissésion, E., Bonavita, M., Browne, P., Buizza, R., Dahlgren, P., Dee, D., Dragani, R., Diamantakis, M., Flemming, J., Forbes, R., Geer, A. J., Haiden, T., Hólm, E., Haimberger, L., Hogan, R., Horányi, A., Janiskova, M., Laloyaux, P., Lopez, P., Muñoz-Sabater, J., Peubey, C., Radu, R., Richardson, D., Thépaut, J.-N., Vitart, F., Yang, X., Zsótér, E., and Zuo, H.: Operational global reanalysis: progress, future directions and synergies with NWP, ERA Report Series, European Centre for Medium Range Weather Forecasts, Reading, England, <https://doi.org/10.21957/tkic6g3wm>, 2018.
- Holmes, C. D., Prather, M. J., Søvde, O. A., and Myhre, G.: Future methane, hydroxyl, and their uncertainties: key climate and emission parameters for future predictions, *Atmos. Chem. Phys.*, 13, 285–302, <https://doi.org/10.5194/acp-13-285-2013>, 2013.
- Intergovernmental Panel on Climate Change: IPCC Guidelines for National Greenhouse Gas Inventories, Volume 2 Energy, Chapter 2 Stationary Combustion, available at: https://www.ipcc-nggip.iges.or.jp/public/2006gl/pdf/2_Volume2/V2_2_Ch2_Stationary_Combustion.pdf (last access: 12 March 2020), 2006.
- International Organization for Standardization: Natural gas – Standard reference conditions (ISO 13443), available at: <https://www.iso.org/standard/20461.html> (last access: 17 February 2020), 1996.
- Karion, A., Sweeney, C., Pétron, G., Frost, G., Hardesty, R. M., Kofler, J., Miller, B. R., Newberger, T., Wolter, S., Banta, R., Brewer, A., Dlugokencky, E., Lang, P., Montzka, S. A., Schnell, R., Tans, P., Trainer, M., Zamora, R., and Conley, S.: Methane emissions estimate from airborne measurements over a western United States natural gas field, *Geophys. Res. Lett.*, 40, 4393–4397, <https://doi.org/10.1002/grl.50811>, 2013.
- Mammadov, Q.: Turkmenistan positions itself as Eurasian natural gas power, *Oil Gas J.*, 113, 76–84, <http://digital.ogj.com/ogjournal/20151207>, 2015.
- Oil and Gas Climate Initiative: Scaling up action – A report from the Oil and Gas Climate Initiative, available at: <https://oilandgasclimateinitiative.com/annual-report/> (last access: 2 June 2020), 2019.
- ONE Future: 2018 Methane Emission Intensities – A Progress Report, available at: <https://onefuture.us/wp-content/uploads/2019/11/ONE-Future-2018-Final-Report-LN.pdf> (last access: 2 June 2020), 2019.
- Pandey, S., Gautam, R., Houweling, S., van der Gon, H. D., Sadavarte, P., Borsdorff, T., Hasekamp, O., Landgraf, J., Tol, P., van Kempen, T., Hoogeveen, R., van Hees, R., Hamburg, S. P., Maasakkers, J. D., and Aben, I.: Satellite observations reveal extreme methane leakage from a natural gas well blowout, *P. Natl. Acad. Sci. USA*, 116, 26376–26381, <https://doi.org/10.1073/pnas.1908712116>, 2019.
- Peischl, J., Ryerson, T. B., Aikin, K. C., de Gouw, J. A., Gilman, J. B., Holloway, J. S., Lerner, B. M., Nadkarni, R., Neuman, J. A., Nowak, J. B., Trainer, M., Warneke, C., and Parrish, D. D.: Quantifying atmospheric methane emissions from the Haynesville, Fayetteville, and northeastern Marcellus shale gas production regions, *J. Geophys. Res.*, 120, 2119–2139, <https://doi.org/10.1002/2014JD022697>, 2015.
- Peischl, J., Karion, A., Sweeney, C., Kort, E. A., Smith, M. L., Brandt, A. R., Yeskoo, T., Aikin, K. C., Conley, S. A., Gvakharia, A., Trainer, M., Wolter, S., and Ryerson, T. B.: Quantifying atmospheric methane emissions from oil and natural gas production in the Bakken shale region of North Dakota, *J. Geophys. Res.*, 121, 6101–6111, <https://doi.org/10.1002/2015JD024631>, 2016.
- Peischl, J., Eilerman, S. J., Neuman, J. A., Aikin, K. C., de Gouw, J., Gilman, J. B., Herndon, S. C., Nadkarni, R., Trainer, M., Warneke, C., and Ryerson, T. B.: Quantifying Methane and Ethane Emissions to the Atmosphere From Central and Western U.S. Oil and Natural Gas Production Regions, *J. Geophys. Res.*, 123, 7725–7740, <https://doi.org/10.1029/2018JD028622>, 2018.
- Pétron, G., Frost, G., Miller, B. R., Hirsch, A. I., Montzka, S. A., Karion, A., Trainer, M., Sweeney, C., Andrews, A. E., Miller, L., Kofler, J., Bar-Ilan, A., Dlugokencky, E. J., Patrick, L., Moore, C. T., Ryerson, T. B., Siso, C., Kolodzey, W., Lang, P. M., Conway, T., Novelli, P., Masarie, K., Hall, B., Guenther, D., Kitzis, D., Miller, J., Welsh, D., Wolfe, D., Neff, W., and Tans, P.: Hydrocarbon emissions characterization in the Colorado Front Range: A pilot study, *J. Geophys. Res.*, 117, D04304, <https://doi.org/10.1029/2011JD016360>, 2012.
- Pommier, M., McLinden, C. A., and Deeter, M.: Relative changes in CO emissions over megacities based on observations from space, *Geophys. Res. Lett.*, 40, 3766–3771, <https://doi.org/10.1002/grl.50704>, 2013.
- Schneising, O.: TROPOMI/WFMD XCH₄ and XCO v1.2, available at: http://www.iup.uni-bremen.de/carbon_ghg/products/tropomi_wfmd/ (last access: 24 July 2020), 2019.
- Schneising, O., Buchwitz, M., Reuter, M., Heymann, J., Bovensmann, H., and Burrows, J. P.: Long-term analysis of car-

- bon dioxide and methane column-averaged mole fractions retrieved from SCIAMACHY, *Atmos. Chem. Phys.*, 11, 2863–2880, <https://doi.org/10.5194/acp-11-2863-2011>, 2011.
- Schneising, O., Burrows, J. P., Dickerson, R. R., Buchwitz, M., Reuter, M., and Bovensmann, H.: Remote sensing of fugitive methane emissions from oil and gas production in North American tight geologic formations, *Earth's Future*, 2, 548–558, <https://doi.org/10.1002/2014EF000265>, 2014.
- Schneising, O., Buchwitz, M., Reuter, M., Bovensmann, H., Burrows, J. P., Borsdorff, T., Deutscher, N. M., Feist, D. G., Griffith, D. W. T., Hase, F., Hermans, C., Iraci, L. T., Kivi, R., Landgraf, J., Morino, I., Notholt, J., Petri, C., Pollard, D. F., Roche, S., Shiomi, K., Strong, K., Sussmann, R., Velasco, V. A., Warneke, T., and Wunch, D.: A scientific algorithm to simultaneously retrieve carbon monoxide and methane from TROPOMI onboard Sentinel-5 Precursor, *Atmos. Meas. Tech.*, 12, 6771–6802, <https://doi.org/10.5194/amt-12-6771-2019>, 2019.
- Shindell, D., Kuylensstierna, J. C. I., Vignati, E., van Dingenen, R., Amann, M., Klimont, Z., Anenberg, S. C., Müller, N., Janssens-Maenhout, G., Raes, F., Schwartz, J., Faluvegi, G., Pozzoli, L., Kupiainen, K., Höglund-Isaksson, L., Emberson, L., Streets, D., Ramanathan, V., Hicks, K., Oanh, N. T. K., Milly, G., Williams, M., Demkine, V., and Fowler, D.: Simultaneously Mitigating Near-Term Climate Change and Improving Human Health and Food Security, *Science*, 335, 183–189, <https://doi.org/10.1126/science.1210026>, 2012.
- Shoemaker, J. K., Schrag, D. P., Molina, M. J., and Ramanathan, V.: What Role for Short-Lived Climate Pollutants in Mitigation Policy?, *Science*, 342, 1323–1324, <https://doi.org/10.1126/science.1240162>, 2013.
- Thompson, D. R., Thorpe, A. K., Frankenberg, C., Green, R. O., Duren, R., Guanter, L., Hollstein, A., Middleton, E., Ong, L., and Ungar, S.: Space-based remote imaging spectroscopy of the Aliso Canyon CH₄ superemitter, *Geophys. Res. Lett.*, 43, 6571–6578, <https://doi.org/10.1002/2016GL069079>, 2016.
- Turner, A. J., Jacob, D. J., Benmergui, J., Wofsy, S. C., Maasakkers, J. D., Butz, A., Hasekamp, O., and Biraud, S. C.: A large increase in U.S. methane emissions over the past decade inferred from satellite data and surface observations, *Geophys. Res. Lett.*, 43, 2218–2224, <https://doi.org/10.1002/2016GL067987>, 2016.
- U.S. Energy Information Administration: International Energy Statistics – Turkmenistan Analysis, available at: <https://www.eia.gov/international/analysis/country/TKM> (last access: 17 February 2020), 2016.
- U.S. Energy Information Administration: The Distribution of U.S. Oil and Natural Gas Wells by Production Rate, available at: https://www.eia.gov/petroleum/wells/pdf/full_report.pdf (last access: 17 February 2020), 2019.
- U.S. Energy Information Administration: Drilling Productivity Report, January 2020, available at: <https://www.eia.gov/petroleum/drilling/pdf/dpr-full.pdf> and <https://www.eia.gov/petroleum/drilling/xls/dpr-data.xlsx>, last access: 31 January 2020.
- U.S. Environmental Protection Agency: Inventory of U.S. Greenhouse Gas Emissions and Sinks 1990–2017, available at: <https://www.epa.gov/sites/production/files/2019-04/documents/us-ghg-inventory-2019-main-text.pdf>, last access: 2 December 2019a.
- U.S. Environmental Protection Agency: Inventory of U.S. Greenhouse Gas Emissions and Sinks 1990–2017, All Annexes, available at: <https://www.epa.gov/sites/production/files/2019-04/documents/us-ghg-inventory-2019-annexes.pdf>, last access: 2 December 2019b.
- Valin, L. C., Russell, A. R., and Cohen, R. C.: Variations of OH radical in an urban plume inferred from NO₂ column measurements, *Geophys. Res. Lett.*, 40, 1856–1860, <https://doi.org/10.1002/grl.50267>, 2013.
- Varon, D. J., McKeever, J., Jervis, D., Maasakkers, J. D., Pandey, S., Houweling, S., Aben, I., Scarpelli, T., and Jacob, D. J.: Satellite Discovery of Anomalously Large Methane Point Sources From Oil/Gas Production, *Geophys. Res. Lett.*, 46, 13507–13516, <https://doi.org/10.1029/2019GL083798>, 2019.
- Veefkind, J. P., Aben, I., McMullan, K., Förster, H., de Vries, J., Otter, G., Claas, J., Eskes, H. J., de Haan, J. F., Kleipool, Q., van Weele, M., Hasekamp, O., Hoogeveen, R., Landgraf, J., Snel, R., Tol, P., Ingmann, P., Voors, R., Kruizinga, B., Vink, R., Visser, H., and Levelt, P. F.: TROPOMI on the ESA Sentinel-5 Precursor: A GMES mission for global observations of the atmospheric composition for climate, air quality and ozone layer applications, *Remote Sens. Environ.*, 120, 70–83, <https://doi.org/10.1016/j.rse.2011.09.027>, 2012.
- Yacovitch, T. I., Daube, C., and Herndon, S. C.: Methane Emissions from Offshore Oil and Gas Platforms in the Gulf of Mexico, *Environ. Sci. Technol.*, 54, 3530–3538, <https://doi.org/10.1021/acs.est.9b07148>, 2020.
- Zhang, Y., Gautam, R., Pandey, S., Omara, M., Maasakkers, J. D., Sadavarte, P., Lyon, D., Nesser, H., Sulprizio, M. P., Varon, D. J., Zhang, R., Houweling, S., Zavala-Araiza, D., Alvarez, R. A., Lorente, A., Hamburg, S. P., Aben, I., and Jacob, D. J.: Quantifying methane emissions from the largest oil-producing basin in the United States from space, *Science Advances*, 6, eaaz5120, <https://doi.org/10.1126/sciadv.aaz5120>, 2020.

Exhibit 20

New Mexico Permian Basin Measured Well Pad Methane Emissions Are a Factor of 5–9 Times Higher Than U.S. EPA Estimates

Anna M. Robertson, Rachel Edie, Robert A. Field, David Lyon, Renee McVay, Mark Omara, Daniel Zavala-Araiza, and Shane M. Murphy*



Cite This: *Environ. Sci. Technol.* 2020, 54, 13926–13934



Read Online

ACCESS |



Metrics & More

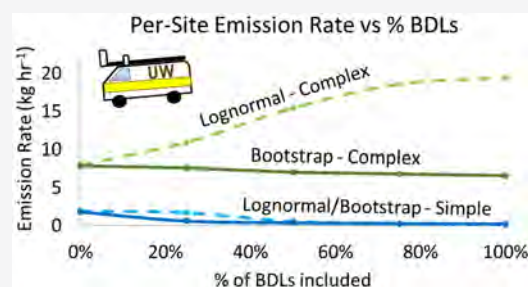


Article Recommendations



Supporting Information

ABSTRACT: Methane emission fluxes were estimated for 71 oil and gas well pads in the western Permian Basin (Delaware Basin), using a mobile laboratory and an inverse Gaussian dispersion method (OTM 33A). Sites with emissions that were below detection limit (BDL) for OTM 33A were recorded and included in the sample. Average emission rate per site was estimated by bootstrapping and by maximum likelihood best log-normal fit. Sites had to be split into “complex” (sites with liquid storage tanks and/or compressors) and “simple” (sites with only wellheads/pump jacks/separators) categories to achieve acceptable log-normal fits. For complex sites, the log-normal fit depends heavily on the number of BDL sites included. As more BDL sites are included, the log-normal distribution fit to the data is falsely widened, overestimating the mean, highlighting the importance of correctly characterizing low end emissions when using log-normal fits. Basin-wide methane emission rates were estimated for the production sector of the New Mexico portion of the Permian and range from ~520 000 tons per year, TPY (bootstrapping, 95% CI: 300 000–790 000) to ~610 000 TPY (log-normal fit method, 95% CI: 330 000–1 000 000). These estimates are a factor of 5.5–9.0 times greater than EPA National Emission Inventory (NEI) estimates for the region.



INTRODUCTION

Production of oil and natural gas in the United States has increased by over 200% and 150%, respectively, since 2005.¹ This boom has primarily been driven by the increased use of hydraulic fracturing combined with directional drilling technologies, allowing the extraction of fossil fuels from formations that were not economically feasible with prior drilling practices. Natural gas has been proposed as a bridge fuel toward a lower carbon economy with less carbon dioxide emissions than coal.² However, natural gas is primarily comprised of methane, a powerful greenhouse gas that has a global warming potential 86 times that of carbon dioxide over a 20 year period.³ According to the most recent estimates from the U.S. Environmental Protection Agency (EPA), natural gas and petroleum systems are the largest anthropogenic source of methane emissions in the United States, accounting for 31% of man-made methane emissions. The production sector alone accounts for over 70% of emissions from natural gas and petroleum systems.⁴

A 2018 study by Alvarez et al.⁵ used observations from several U.S. oil and gas (O&G) basins to determine that observed methane emissions are ~60% higher than EPA emission estimates for the O&G sector, and observed emissions from the production sector alone are 2.2 times higher than EPA estimates, while a study by Howarth et al. suggests even larger underestimates of O&G sector emissions.⁶

One explanation for this low bias in emission inventories is that they do not account for the “heavy-tail” or “fat-tail” of the emission distributions commonly observed in O&G basins. This “fat-tail” is caused by a small percentage of sites, a.k.a., “super-emitters,” that disproportionately account for a large majority of emissions.^{7–15} These high emissions can be the result of routine maintenance (e.g., liquid unloadings, well blowdowns) as well as equipment malfunctions that occur stochastically at any given site.¹³ Due to the random nature of some of these larger leaks, they are difficult to account for in an emission inventory, but recent studies have demonstrated that using a more statistically robust method to estimate O&G emission distributions in emission inventories can successfully represent observed methane emissions.^{5,7}

The Permian Basin is a highly active O&G basin spanning western Texas and southeastern New Mexico. Since 2007, oil and gas production have more than quadrupled and doubled in the basin, respectively. Currently, the basin has the highest oil production in the U.S., and gas production is second only to

Received: May 7, 2020

Revised: September 25, 2020

Accepted: October 2, 2020

Published: October 15, 2020



the Marcellus Shale.¹ However, despite it being an important O&G basin, the current study is the first to report ground-based methane flux estimates in the Permian. Aircraft mass-balance flights have not yet successfully estimated a basin-wide emission rate due to the immense size of the basin¹⁶ (~200 000 km²), although current attempts are ongoing. This study examines the use of two different widely used statistical methods (bootstrapping and maximum likelihood log-normal fit) to estimate average emission rates that are then used to scale up facility-level methane emission rates to a basin-level estimate for well pad emissions.

MATERIALS AND METHODS

Mobile Laboratory Platform. Measurements were performed using the University of Wyoming Atmospheric Science Mobile Research Laboratory (Mobile Lab, Supporting Information (SI) Figure S1).^{17–19} A mast extends out beyond the front bumper of the Mobile Lab and is 4 m off the ground to minimize wind interference/wake effects from the body of the vehicle or the ground. The mast houses meteorological instruments, including a 3D sonic anemometer, an AirMar GPS/2D wind sensor, and a 2D compact weather station. An inlet is also attached to the front of the mast which pulls air through approximately 7 m of 1/4 in. Teflon tubing into instruments inside the lab at a rate of 7 LPM. During this project, a Picarro Cavity Ringdown Spectrometer (CRDS) was used to measure methane and water vapor mixing ratios (model G2204, modified by Picarro Inc. to sample at 2-Hz). The calibration of the Picarro was performed by sampling a NIST traceable ($\pm 1\%$) methane in ultrapure air mixture with a methane concentration of 2.576 ppm. The 2-Hz Picarro CRDS calibration fluctuated less than ± 6 ppb over the course of the project and was always in agreement with the NIST standard.

Emission Flux Quantification. Methane emission fluxes were calculated using the Gaussian dispersion approach within the U.S. EPA's Other Test Method (OTM) 33A. This method has been described in detail in Brantley et al., Robertson et al., and EPA documentation.^{19–21} The 1-sigma error for OTM 33A, verified by test releases performed under a wide variety of real-world conditions, is $\pm 35\%$ relative to a known release rate, which translates to an error of $+54\%/-26\%$ for measurement of an unknown emission rate in the field.²² Results using this method have been used in a measurement-based inventory to estimate emissions from other O&G production regions.^{5,12} Briefly, this method uses rapid wind and methane mixing ratio measurements (~ 2 Hz) downwind of a site to calculate average methane enhancements for each wind direction over a minimum 20 min period. An advantage of OTM 33A is that it does not require site access from operators and therefore can limit the so-called "operator opt-in bias." During a measurement, as the plume wafts back and forth over the inlet, a plot of the time-averaged in-plume concentrations versus wind direction forms a Gaussian distribution.²³ The peak of a Gaussian fit to the data gives C_{peak} in eq 1 while the horizontal and vertical dispersion parameters (σ_y and σ_z) are determined from a lookup table based on distance from the source and atmospheric stability determined by variation in the horizontal and vertical winds. An emission flux (Q) is calculated by

$$Q = 2\pi \times \bar{U} \times \sigma_y \times \sigma_z \times C_{\text{peak}} \quad (1)$$

Where, \bar{U} is the mean wind speed during the measurement (SI Section 1.2 gives further detail). The limit of detection

(LOD) for the OTM 33A method was empirically determined to be 0.036 kg hr⁻¹ (0.01 g/s).²⁰ While we have no empirical evidence that this is not a valid LOD at all distances, we agree that the LOD could vary with distance and meteorological conditions. Therefore, we ran sensitivity tests using varying detection limits (up to an order of magnitude greater, 0.36 kg hr⁻¹), but saw no significant effect on final results (detailed in SI Section 1.4).

Of the 111 measurements performed in the Permian Basin during this study, 47 yielded a quantified flux estimate with the OTM 33A technique and 29 sites were measured to be below detection limit (BDL) (number of measurements detailed further in SI Section 7.0). A measurement yields a flux estimate if it passes a series of data quality flags that are part of the OTM 33A analysis method, including flags for atmospheric stability, poor Gaussian fit of the emission plume, excessive wind variance, and others (see SI Section 1.3). An infrared optical gas imaging camera (FLIR GF300) was used at measurement sites to check for any large conflicting emission sources nearby (such as pipeline leaks) and to pinpoint emission sources on the well pad. A measurement may also be removed from the final data set during postprocessing if satellite imagery (from Google Earth) or analysis of the wind direction during the measurement suggest that there may have been an interfering source upwind.

Study Area. The Permian Basin is located in western Texas (TX) and southeastern New Mexico (NM). The Permian is broken into two main geologic basins: the Midland Basin on the eastern side, and the Delaware Basin (DB) on the western side, separated by the Central Basin Platform (SI Figure S3). For this study, 111 ground-based, facility-level methane emission measurements were collected in the DB during August 2018. Out of the 111 measurements, 71 were collected in NM and 40 were collected in TX. The sample number was lower in TX mostly due to lighter and more variable winds. Measurements were attempted in the Midland Basin, but due to lack of public road access the measurements were not successful. As of August 2018, there were approximately 144 000 active wells in the Permian Basin, roughly half (73 000) of which were located in the DB.²⁴

Sampling Strategy. Due to the large size of the basin, a clustered random sampling strategy was implemented - clustered by production fields with the densest population of wells in the basin (SI Figure S4 and S5). This resulted in 8 original clusters, which were then stratified by production magnitude and age of wells to try to obtain a sample set that represented the large age and production range in the basin, including older/low producing wells, newer/high producing wells and those in-between. After a cluster was chosen for the day, we randomly selected sites based on wind direction and downwind road access. This strategy was chosen to minimize transit time between potential sites and to maximize sample size. As the field campaign progressed and the number of measurable sites in each of the original clusters began to dwindle (sites with good downwind road access for given winds had already been measured), 3 more clusters were added in areas that had a sufficient number of well pads that could be targeted. The end result was that the measurements collected in this study leaned more toward the newer/high producing end of the spectrum with an average age of 8 years, average gas production of 680 thousands of cubic feet per day (mcf/d), and average oil production of 170 barrels per day (bpd). Whereas basin-average values for the DB in 2018 were 17 years, 160

mcf, and 41 bpd (SI Figure S6). Since newer/higher-producing wells tend to have higher methane emission rates than older/lower-producing wells, this sampling bias may have resulted in an overestimation of the average emission rate per well by up to 20% (details of this analysis are in SI Section 2.3). However, due to the low sample number and limited confidence in the robustness of the relationship between emissions and age/production, as well as the possibility that we may have underestimated the fat-tail (discussed more in the Section “Well Site Classification: Simple Vs Complex”), no correction factor was applied to the data.

Once a site was chosen for measurement, several transects downwind of the site were performed to locate the approximate center of the emission plume, where the Mobile Lab was then parked and the engine turned off to avoid exhaust interference. To check for interfering sources upwind several methods were employed either alone or in combination including performing transects upwind of the site when possible, using the FLIR camera to check pipeline junctions or other nearby sources, and using Google Earth imagery to ensure that there were no large sources nearby that we visually missed. If there was a large site directly upwind of the site of interest and we could not confirm that there were no conflicting emissions coming from that site then we did not measure. Wind direction and speed (10 Hz) and methane mixing ratios (2 Hz) were then measured for a period of at least 20 min to allow the plume to average out into a Gaussian. Sites where the Mobile Lab was clearly downwind, but where no emission plume was detected or emissions were below the detection limit for OTM 33A were recorded as below detection limit (BDL). All measurements were performed within 40–200 m of the source, with distance to source measured using a laser range finder.

Sites Below Detection Limit (BDL). In an effort to make the measurements as representative of the emission distribution in the DB as possible, sites where emissions were below the OTM 33A method's detection limit (0.036 kg hr^{-1}) were also recorded and will be referred to as below detection limit (BDL) sites. A site was recorded as BDL if, while sitting within 150 m downwind, maximum observed methane enhancements were below 50–100 ppb. This is the minimum enhancement distinguishable from background fluctuations that is necessary for an accurate flux estimate. Lofted plumes are a limitation of OTM 33A since measurements are performed from a ground-based vehicle at relatively close distances, so to verify that there were not plumes that were lofted over the inlet at these sites, each site was also verified to have no visible emissions using the FLIR camera from near the edge of the well pad. A site was also only recorded as BDL if the winds were consistent enough to ensure that we were directly downwind of all potential sources on the site. The lowest quantified emission with OTM 33A during this campaign was 0.068 kg hr^{-1} .

To include the BDL sites in the final statistics, first a “success fraction” was applied to the total number of BDL sites. The success fraction represents the fraction of total OTM measurements that passed data quality criteria and is applied to the number of BDL sites to include the same fraction of BDLs as OTM measurements. If this were not done the BDL sites would be statistically over-represented. Not including the success fraction decreases the final basin-level estimate by 5–7%. This success fraction was 72%, resulting in a total of 29 BDL sites counted in the final data set, 17 in NM, and 12 in TX. To estimate the emissions from these sites, values were

chosen randomly with equal probability between 0 kg hr^{-1} and the method minimum detection limit (0.036 kg hr^{-1}). This approach likely underestimates the leakage rate assuming the BDLs actually follow the tail of the data set's log-normal distribution (which would result in the majority of BDL sites having an emission rate close to the LOD), but was chosen to be conservative. One caveat for the number of BDL sites is that the majority of them were measured for less than 5 min, and therefore some low frequency intermittent emissions could have been missed.

Well Site Classification: Simple Vs Complex. The oil and gas extracted at well pads needs to be separated (into oil, gas, and water) and sometimes further processed (e.g., dehydration of the gas), before it is stored on site or sent to a gathering pipeline. Typically, these processes occur at the well pad, where produced water and oil/condensate are sent to atmospheric storage tanks on site that flash gas (though some have controls that combust flashed emissions). However, the majority of sites in the DB have only wellheads or oil pump jacks on site with their production routed offsite to central gathering sites/tank batteries for processing and storage. These “simple” sites therefore have either no, or minimal, liquids storage or processing equipment on site, which have been shown to be the primary emission sources on well pads.^{13,25} During analysis, it became apparent that these “simple” sites have a very different emission profile (median emission rate of 0.03 kg hr^{-1}) than sites with one or more compressors or liquids storage tanks on site (median emission rate of 2.6 kg hr^{-1}). Therefore, sites are broken into two categories for analysis: simple and complex sites. A complex site is defined in this study as any well pad with one or more oil/water storage tank(s) and/or compressor(s) on-site. All other sites are defined as simple, which includes well pads with only one or more wellhead(s), pump jack(s), and/or separator(s)/other simple equipment on-site. Of the 46 sites with flux estimates in NM, 30 were complex and 16 were simple. Of the 25 sites with flux estimates in TX, 17 were complex and 8 were simple.

This classification is especially important when estimating emission distributions and extrapolating facility-level emissions to a basin-level estimate. To extrapolate our measured emissions per site to a basin-level estimate for the NM portion of the DB, the number of wells in the basin during the month of measurement that were actively producing (August 2018:25 000 wells) was divided by the average number of wells per site (1.2) to get an approximate number of sites.²⁴ Wells that were listed as suspended/abandoned/etc. were not included in the scale-up. Then, the number of simple and complex well pads was calculated based on the results from human classification of satellite imagery (Airbus SPOT) that $\sim 2/3$ of the well pads in the NM DB are “simple” with the remaining $1/3$ being “complex” ($\sim 97\%$ of the sites had imagery from 2018 or 2019). This classification only includes well pads with at least one wellhead or pump jack on site. In our sample set, this ratio was reversed, with $\sim 2/3$ of our sites that passed QA/QC being complex sites. A major focus of this field campaign was to capture the high-end of the emission distribution to avoid underestimating the fat-tail, which played into the sampling strategy. There was much less variation in emissions from simple sites (with a large majority of them being BDL) than complex sites so we began preferentially targeting the complex sites to better nail down their contribution to the emission distribution. Importantly, since we estimate average emissions for simple and complex sites

separately, and then scale them up separately to a basin-level estimate, this complex-bias does not contribute to an overestimation of basin-level emissions. Also, although there are twice as many simple sites than complex sites in the basin, emissions from the complex sites dominate the emissions, representing 91% of total emissions.

A similar extrapolation for the TX portion of the basin was not performed due to the lower number of measurements on the TX side, and therefore less confidence in scaling up the data there, and because the classification of satellite imagery was only available for the NM side of the basin. There were only 13 successful site-level measurements (using OTM 33A) and 12 BDL sites from the TX side of the DB (0.05% of active wells in TX DB), as opposed to 29 successful site-level measurements and 17 BDLs on the NM side (0.18% of active wells in NM DB).

It is also important to note that although BDL sites were accounted for and included in the analysis, several sites with large methane enhancements that were either too spread out or too close to the road to sample due to the limitations of OTM 33A¹⁷ were not accounted for/included in the analysis because we do not have approximate mass emission rates for them (similar sites with no emissions were recorded under the BDL category for complex sites). Often, the sites with large observed methane enhancements (15–20 PPM CH₄ from over 100 m away) were gathering facilities/tank batteries that only had tanks and processing equipment on-site but no wells or pump jacks and therefore were not quantified with OTM 33A, identified in the Google Earth analysis, or included in the basin-wide scale up. Since these sites do not have a well or pump jack on-site, they are also not listed in either the NM or TX production databases and there is no publicly available data on their throughput or which wells/pump jacks have production routed to them. Thus, these are likely a significant but currently unaccounted for emission source that requires further study to fully characterize the emissions in the basin. Furthermore, because we have production information for the simple sites but no information on where their production is sent, we may be underestimating their total emissions if their production is being sent to one of these unaccounted for central gathering facilities/tank batteries.

Statistical Techniques for Emission Estimation. Two common methods used for extrapolating facility- or well-level emissions data to a basin-wide estimate are bootstrapping and maximum likelihood best log-normal fit.^{5,7,8,10,12,14,20,26–28} Each of these methods are a way to predict the average emission rate per well/site for a given data set. The average emission rate can then be multiplied by the total number of wells/sites to obtain a total emission rate for a basin or region. One of the objectives of this study is to compare the average emission rate calculated using these two methods and explore how and why they may differ.

$$\text{GMP} \left(\frac{\text{kg}}{\text{h}} \right) = \text{NGP} \left(\frac{\text{mcf}}{\text{mo}} \right) \times \left[\frac{\left(1000 \frac{\text{ft}^3}{\text{mcf}} \right) \times \left(1.19804 \frac{\text{molgas}}{\text{ft}^3} \right) \times \left(x \frac{\text{molCH}_4}{\text{molgas}} \right) \times \left(0.01604 \frac{\text{kg}}{\text{molCH}_4} \right)}{(\# \text{days}/\text{mo})(24 \text{h}/\text{day})} \right] \quad (2)$$

The Permian Basin is a wet gas basin, and publicly available composition data for natural gas produced in the DB is sparse but existing reports cite a methane content (mol CH₄/mol

gas) of 60–75%.^{31,32} For this study, methane content for each site was randomly chosen from a normal distribution centered on 70%, with 95% of values falling between 64 and 76%. Bootstrapping is a proven method used to approximate statistics (and their confidence intervals) of a population without assuming that the data come from any specific distribution. This method estimates statistics of the underlying population by resampling the measured data set (with replacement) a large number of times,²⁹ that is, “pulling the data up by its bootstraps”. For this study, bootstrapping is used to estimate average emission rates per well pad (i.e., per site) and to investigate the production characteristics of different subsections of the DB. The bootstrapping method used in this study is described in detail in Robertson et al. 2017. Briefly, the error distribution for each measurement is first created using a normal distribution with the measured emission rate as the mean and the 1-sigma error estimate for OTM 33A (+54%/–26%)²² as the standard deviation. The measurements with incorporated error are resampled with replacement 100 000 times, creating 100 000 new sample sets of the original sample size (e.g., $n = 71$ for all successful well pad measurements in the DB, $n = 46$ for NM, and $n = 25$ for TX). From these 100 000 sample sets one can calculate 100 000 estimates of the mean and the distribution of all the possible means can be used to determine the 95% CI.

Another popular method to estimate emissions from O&G basins is to assume the data follow a log-normal distribution and use the best log-normal fit to estimate population statistics.^{5,7,12} It has been shown throughout U.S. O&G basins that a small fraction of sites account for a large fraction of the emissions resulting in a “fat-tail”/“heavy-tail” in the emission distribution. However, because this heavy-tail is caused by a small percentage of sites, it is difficult to make enough measurements to capture a significant fraction of these sites during a two- or three-week ground campaign.³⁰ Trying to accurately approximate the heavy-tail of the emissions distribution is critical because it drives the mean emission rate per well/site and therefore the extrapolation to a basin-level estimate. For this reason, studies have fit a log-normal distribution to measured emissions to estimate the heavy-tail. Notably, past studies of O&G basins have revealed that measured emission distributions often exhibit even more extreme distributions than a log-normal fit.⁹ For this study, Matlab’s (version R2018b) log-normal fitting routine, based on maximum likelihood estimation (MLE), was used to evaluate the best log-normal fit to the emission distribution, fitting complex and simple sites as two separate distributions. The lognormality of the data sets is explored more in the [Results and Discussion](#).

Converting Gas Production to Methane Production. Monthly oil and gas production data for measured sites were obtained from the DrillingInfo database.²⁴ The monthly natural gas production (NGP) rates are converted from thousands of cubic feet of natural gas per month (mcf/mo) to kilograms of gross methane produced (GMP) per hour (kg hr⁻¹) using eq 2:

gas) of 60–75%.^{31,32} For this study, methane content for each site was randomly chosen from a normal distribution centered on 70%, with 95% of values falling between 64 and 76%.

was done to be as robust as possible with any potential errors involved in the calculation, but pulling random values versus using the same methane content (e.g., 70%) for each measurement had a negligible effect on the final results.

TNMA, ENMA, and Oil Fraction. A throughput-normalized mass average (TNMA) emission, often referred to as the average fraction of methane produced that was emitted to the atmosphere, is calculated following eq 3:

$$\text{TNMA}(\%) = \frac{\sum \text{MMER} \left(\frac{\text{kg}}{\text{h}} \right)}{\sum \text{GMP} \left(\frac{\text{kg}}{\text{h}} \right)} \times 100 \quad (3)$$

Where MMER is the measured methane emission rate (either using OTM 33A or estimated for BDLs), and GMP is the gross methane produced as defined in eq 2. As opposed to separate throughput-normalized emissions for each facility, TNMA represents a basin-average throughput-normalized emission rate.

As mentioned earlier, the DB also produces considerable quantities of oil and therefore all methane emissions from a site cannot be attributed entirely to natural gas production. Average oil fraction, that is, the fraction of total energy production at the site that can be attributed to oil, is calculated as follows:

$$\text{average oil fraction} = \frac{\sum \text{OP} \left(\frac{\text{bbl}}{\text{d}} \right)}{\sum \text{totalBOE} \left(\frac{\text{bbl}}{\text{d}} \right)} = \frac{\sum \text{OP} \left(\frac{\text{bbl}}{\text{d}} \right)}{\sum \left[\text{OP} \left(\frac{\text{bbl}}{\text{d}} \right) + \text{OEGP} \left(\frac{\text{bbl}}{\text{d}} \right) \right]} \quad (4)$$

Where OP is oil production, OEGP is the oil equivalent gas production, and BOE is the barrels of oil equivalent. Gas production is converted to equivalent barrels of oil (OEGP) using the Society of Petroleum Engineer's (SPE) conversion ratio of 5.8 mcf of gas = 1 BOE.³³ Since some sites primarily produce oil with some associated gas, an energy-normalized mass average (ENMA), or the fraction of energy produced (oil plus gas) that is emitted to the atmosphere as methane, is calculated following the same method as Robertson et al. 2017.¹⁹

$$\text{ENMA}(\%) = \frac{\sum \text{MEER} \left(\frac{\text{Btu}}{\text{d}} \right)}{\sum \text{EEP} \left(\frac{\text{Btu}}{\text{d}} \right)} \times 100 \quad (5)$$

where MEER is the measured energy emission rate, and EEP is the equivalent energy production. Total energy production (oil plus gas) was converted to units of Btu using the standard values from the SPE of 5.8×10^6 Btu per barrel of oil and 1×10^6 Btu per mcf of gas.³⁴

RESULTS AND DISCUSSION

Raw Emissions Distribution. Plotting the cumulative emission distribution for measurements of individual well pads using OTM 33A and estimated emissions for BDLs reveals that, similar to results from other basins,^{7–12} the emission distribution in the DB exhibits a skewed, or heavy-tailed, distribution (SI Figure S8). In the DB, the top 15% of emitters had emissions of at least 7 kg hr⁻¹ and accounted for over 70% of total emissions. The top 5% of emitters had emissions of at least 20 kg hr⁻¹ and accounted for over 30% of total emissions, both in NM and TX. The lognormality of the data set is explored further in the “Per-Site Emission Rate” section.

Bootstrapped Mass Emission Rate, TNMA, Oil Fraction, and ENMA. The results from bootstrapping the emission and production data in the DB are shown in Figure 1

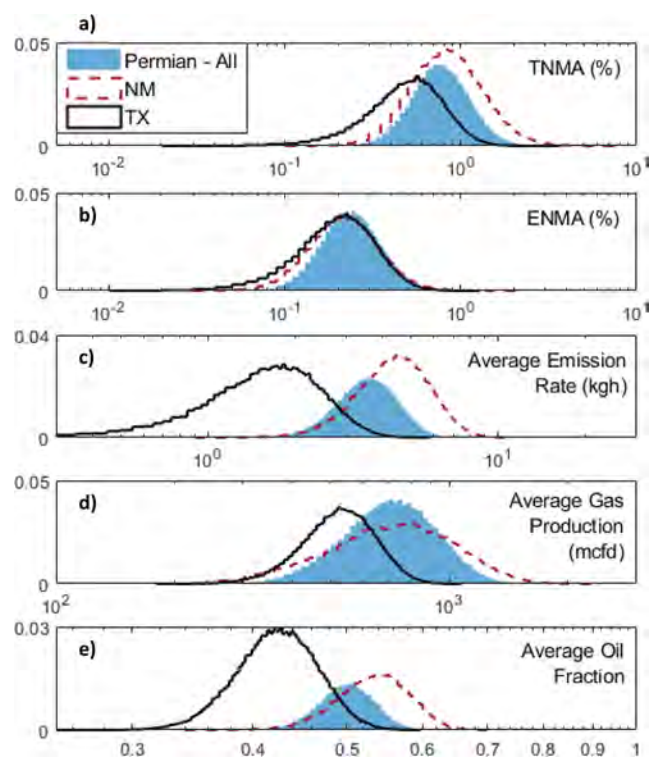


Figure 1. Probability density functions of average emission rates derived by bootstrapping measurements. Panels show all well pads in the DB (blue, filled in), well pads in the NM portion of the DB (red dashed line), and well pads in the TX portion of the DB (black solid line). Panels are (a) throughput-normalized mass average (TNMA, %), (b) energy-normalized mass average (ENMA, %), (c) average mass emission rate per facility (kg hr⁻¹), and (d) average gas production per facility (mcf/d), and (e) average oil fraction per facility.

and Table 1. Measurements performed in NM and TX are separated to compare differences at the state level. Notably, there were only 13 OTM and 12 BDL measurements on the TX side versus 29 OTM and 17 BDL measurements on the NM side (SI Section 7.0), so the results from TX may be skewed by the lower sample size. Statistics are also presented combining measurements from both states, represented as “DB” in Figure 1 and Table 1. To provide context for the current work, results from the DB are compared to statistics from other US basins calculated using the same methods (past work refers to Robertson et al. 2017¹⁹). In these previous studies there was never a statistical reason to separate sites into simple and complex sites. The central estimate for mean TNMA emission rate (Figure 1a) for well pads in the DB is 0.88% (0.42–1.83, 95% CI), which puts the basin midway between previous well pad TNMA emission estimates for the Upper Green River (UGR) Basin and Fayetteville (FV) gas play of 0.1–0.2% and the Denver-Julesburg (DJ) and Uinta Basins of 2–3% (previous estimates shown in SI Figure S9). The central estimate of mean facility-level mass emission rates (Figure 1c) in the DB is 3.8 kg hr⁻¹ of methane (2.2–5.7, 95% CI), which is comparable to the average emission rate measured in the Uinta Basin (3.7 kg hr⁻¹), which is the highest we observed from previously measured basins. The

Table 1. Summary of Central Estimates for Facility-Level Mean Emissions (Bootstrapped Distributions Shown in Figure 1)

portion of basin	mean TNMA—% (95% CI)	mean ENMA—% (95% CI)	mean mass emission rate—kg hr ⁻¹ (95% CI)	mean gas production—mcf (95% CI)	mean oil fraction (95% CI)
DB	0.89 (0.42–1.83)	0.26 (0.12–0.56)	3.76 (2.24–5.71)	762 (435–1210)	0.50 (0.44–0.57)
NM	1.03 (0.42–2.69)	0.26 (0.11–0.66)	4.74 (2.58–7.61)	818 (377–1470)	0.54 (0.45–0.62)
TX	0.61 (0.22–1.30)	0.25 (0.09–0.55)	1.89 (0.70–3.52)	551 (352–786)	0.43 (0.35–0.51)

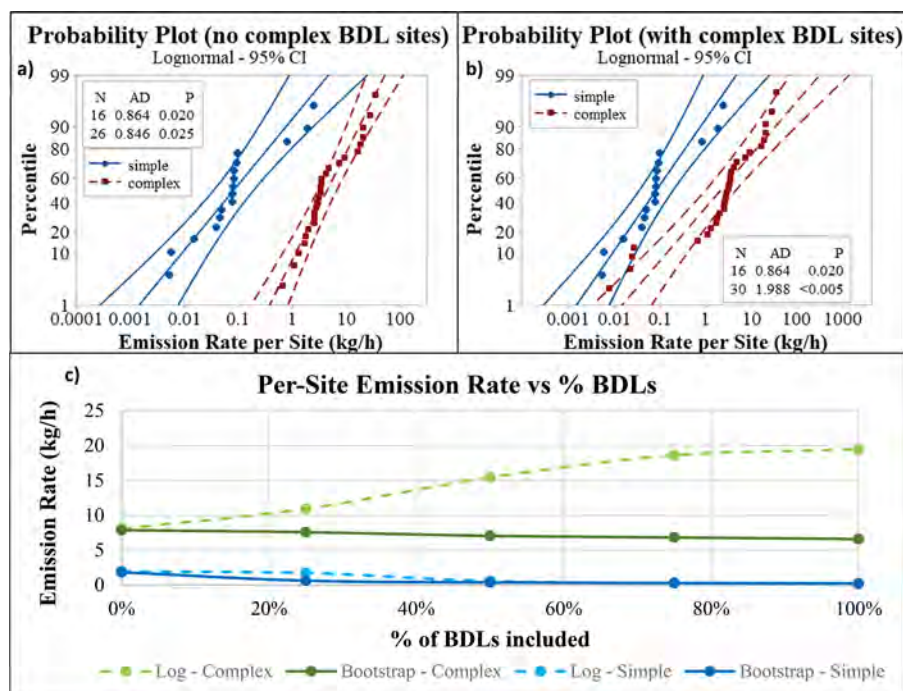


Figure 2. Top two panels show probability plots (emission rate versus percentile) to illustrate how well the measured emission rate data follow a log-normal fit with (a) no complex BDL sites included, and (b) with complex BDL sites included. The distribution for the simple sites is the same in panels a and b (both include BDL sites). The complex BDL sites in panel b are the four data points below 0.1 kg h⁻¹, denoted here as kg/h. Blue circle markers are simple sites and red squares are complex sites. The central lines show the best log-normal fit with outside lines showing 95% confidence bounds (solid lines for the simple site distribution, dashed lines for the complex sites distribution). In the legend, N is the sample size, AD is the Anderson-Darling statistic, and P is the corresponding *p*-value, with the values for simple sites on the top row and the values for complex sites on the bottom row. The bottom panel shows estimated per-site emission rate (kg/h) for wells measured in the NM portion of the DB, estimated with both the bootstrapping and log-normal methods using different fractions of the total measured number of below detection limit (BDL) sites. Numbers of BDLs are plotted at increments of 25%, from 0% (0 BDLs) to 100% (28 BDLs).

distributions of measured mass emission rates and TNMA are broken down further into simple and complex sites for both NM and TX in SI Figure S10. Average gas production per well pad (Figure 1d) is approximately 820 mcf in NM, similar to the relatively high production rate seen in FV and UGR, and about 50% higher than the average production observed at the TX well pads (550 mcf). Well counts for NM and TX well pads were similar with an average of 1.2 and 1.1 wells per site, respectively. Wells in the DB overall have a much higher oil fraction (Figure 1e) than has been observed in other basins with a median value of 0.50 (0.44–0.57, 95% CI). For reference, the DJ Basin in Colorado, which also produces a considerable amount of oil along with its gas production, has an oil fraction of 0.2–0.3. Accordingly, emission rates were also normalized by total energy production (ENMA). The median ENMA (Figure 1b) for the DB is 0.29% (0.14–0.60%, 95% CI).

Per-Site Emission Rate: Lognormal Versus Bootstrapping. To scale measured methane mass emission rates up to a basin-level estimate for the NM portion of the basin, first a per-site emission rate was estimated separately for complex and simple sites using two different methods: (1)

bootstrapping and (2) best log-normal fit. Then, a basin-level estimate was calculated using the number of actively producing simple and complex sites on the NM side of the DB at the time of measurement and their respective average emission rates per site. In August 2018, there were approximately 21 000 active sites in the DB.²⁴ Using the estimate from the manual counting of satellite imagery that ~66% of well pads in the basin were simple and ~33% were complex results in approximately 14 000 simple sites and 7000 complex sites. For the bootstrap method, the per-site emission rate was estimated to be 0.37 kg CH₄ site⁻¹ hr⁻¹ (0.03–0.87, 95% CI) for simple sites, and 7.5 kg CH₄ site⁻¹ hr⁻¹ (4.1–12, 95% CI) for complex sites. Resulting in a basin-level estimate of 520 000 tons per year, TPY (300 000–790 000, 95% CI).

Figure 2 illustrates how well the measured simple and complex sites follow a log-normal distribution. When fitting a log-normal distribution to the simple site emission rates (with estimates for the 13 simple BDL sites included), the resulting *p*-value is 0.02 and the Anderson-Darling (AD) statistic is moderate (0.9), indicating that the null hypothesis that the data come from a log-normal distribution cannot be rejected at the $\alpha = 0.01$ level and that the log-normal assumption is

reasonable for estimating an average emission rate. On the other hand, trying to fit a log-normal distribution to the complex sites (with the four complex BDL sites included), results in a p -value $\ll 0.01$ and a relatively high AD statistic of 2.0 (Figure 2b), indicating that the null hypothesis is rejected and the data do not follow a log-normal distribution. The probability plot (Figure 2b) also suggests that there is a very low probability that the complex BDL sites actually belong on the same distribution as the rest of the complex sites since they are either right on or just outside of the 95% confidence bounds. This may indicate that the complex sites are more likely to have emissions above the detection limit. Undoubtedly, the complex BDL sites are more likely than the simple sites to have intermittent emissions that may have been missed because of the large number of operations occurring on site. The probability plots in Figure 2 also reveal that if the complex BDL sites are included (Figure 2b), it widens the log-normal distribution fit to the data (compared to Figure 2a). Therefore, including these low emitting sites actually increases the mean emission rate for complex sites when estimated using a log-normal distribution. This behavior is explored further in SI Table S1. If the complex BDL sites are excluded from the complex site distribution (Figure 2a), the p -value and AD statistic are similar to those for the simple site distribution, indicating that assuming a log-normal distribution for the emission rates from complex sites is more valid if the complex BDL sites are not included.

As a result, the following analysis will present results using three different approaches: (1) the four complex BDL sites are excluded from the log-normal fit to the complex sites, (2) the four complex BDL sites are excluded from the fit but are factored into the final basin-level emission estimate by assuming the same ratio of BDL complex sites ($4/30 = 13\%$) while using $0.036 \text{ kg CH}_4 \text{ hr}^{-1}$ as their emission rate, and (3) the four complex BDL sites are included in the log-normal fit (with BDL values chosen randomly between 0.01 and $0.036 \text{ kg CH}_4 \text{ hr}^{-1}$ to match the BDL estimation for simple sites). Note, the third method, as discussed above, results in an invalid log-normal fit but is included here for illustrative purposes.

Using the first approach, the best log-normal fit resulted in per-site emission estimates of $0.43 \text{ kg CH}_4 \text{ site}^{-1} \text{ hr}^{-1}$ for simple sites (0.03–1.93, 95% CI) and $8.8 \text{ kg CH}_4 \text{ site}^{-1} \text{ hr}^{-1}$ for complex sites (4.6–15, 95% CI). The log-normal parameters for the fit to simple sites are $\mu = -3.1$, $\sigma = 1.8$, mode = 0.0016; and for the complex sites: $\mu = 1.5$, $\sigma = 1.1$, mode = 1.4. This results in a basin-level emission estimate of 610 000 TPY (330 000–1 000 000, 95% CI). The log-normal method results in a larger emission estimate than the bootstrapping method (520 000 TPY) since it includes a larger fat-tail in its estimated emission distribution. The second approach results in the same per-site emission rates and log-normal parameters as the first approach, but factoring the fraction of BDL sites into the basin-level roll-up results in a smaller basin-level estimate of 540 000 TPY (290 000–940 000, 95% CI). The third approach results in a similar average per-site emission rate for the simple sites of $0.47 \text{ kg CH}_4 \text{ hr}^{-1} \text{ site}^{-1}$ (0.03–1.7, 95% CI), but a much higher emission rate for complex sites since the log-normal fit is incorrectly widened with the inclusion of the BDL sites: $29 \text{ kg CH}_4 \text{ hr}^{-1} \text{ site}^{-1}$ (7.9–56, 95% CI). Using this approach results in a basin-level estimate of 1 900 000 TPY (540 000–3 600 000, 95% CI).

The sensitivity of the log-normal fit to the number and emission estimates chosen for the BDLs is explored further in Figure 2c and SI Section 6.0. In summary, as an increasing number of BDLs are included in the complex site emission distribution, the best log-normal fit to the data increasingly widens, resulting in larger and larger average emission rates and an increasing divergence from bootstrapping estimates. Therefore, although log-normal fits have been widely used to better characterize the heavy-tail of emission distributions in O&G basins to avoid underestimating total emissions, it is also important to ensure the low end of emissions is representative of the population so that average emission rates are not overestimated when using this approach.

Comparison to EPA Emission Inventories. Since production, and consequently emissions, has changed so drastically in the Permian in the last 5 years, comparisons were only made to the most recently available emission inventories, the EPA's Greenhouse Gas Reporting Program (GHGRP) and National Emission Inventory (NEI). All operators that emit more than 25 000 tons (t) CO_2 -equivalent (CO_2e) per year must report their emissions through the GHGRP. However, although the EPA states that the GHGRP accounts for 85–90% of total U.S. emissions compared to their greenhouse gas inventory (GHGI), the majority of the O&G well pads in the basin likely are not included in the total since they do not meet the 25 000 t CO_2e annual emission threshold. The emission estimate for the O&G production sector (i.e., no gathering, boosting, or transmission) is only reported at the basin-level in the GHGRP. For the Permian Basin in 2018, 68 operators reported their annual production sector emissions for a total of $\sim 216\,000 \text{ TPY CH}_4$. To estimate emissions from just the NM portion of the basin so that our measurements could be more directly compared, total emissions from the Permian were divided based on the fraction of total basin production from NM in 2018 ($\sim 21\%$).²⁴ Taking 21% of the total results in approximately 45 000 TPY of methane from the NM portion of the basin. Comparing this value to our basin-level estimate of 520 000 TPY (using the bootstrapping method) to 610 000 TPY (using the first approach to the log-normal method), suggests that the inventory is over an order of magnitude low for this region.

To generate an estimate from the EPA's NEI 2017 data, the 2017 NEI Production Oil and Gas Tool was used (v1_1). For all O&G production activities in the NM portion of the basin, the NEI 2017 estimates total methane emissions of 91 000 TPY. Excluding truck loading and blowdown emissions from the NEI 2017 estimate, which were not included in our basin-level scale-up, yields a methane emission rate of 67 000 TPY (a factor of 7.8–9.0 times lower than our estimate). However, as mentioned previously, the Permian Basin reported large increases in oil and gas production from 2017 to 2018, with oil production increasing by $\sim 40\%$ and gas production by $\sim 30\%$.³⁵ Because NEI 2018 emissions are not available, we scale the NEI emission estimates by the larger change in production (40%), yielding total methane emissions of 127 000 TPY, and 94 000 TPY if truck loading and blowdown emissions are excluded. Suggesting that the NEI is underestimating methane emissions by a factor of 5.5–6.5.

Comparison to Other Basins. To put methane emissions from the Permian into perspective, estimated basin-wide emissions from only well pads in just the NM portion of the basin (520 000–610 000 TPY CH_4) exceed total basin-wide emissions (i.e., all O&G operations) estimated using aircraft

mass balance techniques in almost every other O&G basin in the U.S. (Alvarez et al. (2018)⁵ demonstrated that bottom-up estimates using OTM 33A give statistically similar results to aircraft mass balance techniques). The one exception is the Eagle Ford Shale region in southern TX with total emissions estimated to be 730 000 ($\pm 190\,000$) TPY CH₄.¹⁶ The same study that measured the Eagle Ford (Peischl et al. 2018) also estimated basin-wide methane emissions from O&G operations in several other U.S. basins and reported (TPY CH₄): 250 000 ($\pm 61\,000$) in the Bakken; 370 000 ($\pm 160\,000$) in Haynesville; and 400 000 ($\pm 260\,000$) in the Barnett. Basin-wide methane emissions for the Denver-Julesburg Basin were estimated in two separate studies (2012 and 2015) to be 160 000 ($\pm 70\,000$) – 170 000 ($\pm 60\,000$) TPY CH₄.^{16,36} Lastly, Karion et al. (2013) estimated emissions from the Uinta Basin to be 480 000 ($\pm 130\,000$) TPY CH₄.

Future Studies. As this is the first ground-based study of the PB, and only the western portion of the PB, many questions remain and further research is needed to fully characterize emissions in the basin. One important question is how methane emissions in the eastern portion of the basin (Midland Basin) compare to those measured in the DB. Another important question is what fraction of total methane emissions in the basin are contributed by well pad emissions? Comparing our results to a recent satellite study by Zhang et al. (2020) which reported total methane emissions from O&G operations in the DB to be 1.7×10^6 TPY,³⁷ suggests this ratio may be 31–35%. There are several other significant emission sources in the basin not measured in this study, including but not limited to, gathering facilities/tank batteries, compressor stations, leaks along gathering pipelines (including in-line compressors), processing plants, and emissions from unlit or inefficient flare stacks. Emissions from gathering facilities/tank batteries would be particularly informative in trying to gain more information about total emissions from the simple sites measured in this study. Lastly, the measurement of older/low-producing wells should be a priority for future studies to gain a better understanding of the relationship between emissions and age/production of wells in the basin.

■ ASSOCIATED CONTENT

SI Supporting Information

The Supporting Information is available free of charge at <https://pubs.acs.org/doi/10.1021/acs.est.0c02927>.

Details of the OTM 33A methodology; study region and sampling strategy; comparison to previous measurements and subcategories of data presented here; further analysis of the log-normal fit method used; and additional data for all measurements (PDF)

■ AUTHOR INFORMATION

Corresponding Author

Shane M. Murphy – Department of Atmospheric Science, University of Wyoming, Wyoming 82071, United States; orcid.org/0000-0002-6415-2607; Phone: 1-307-766-6408; Email: Shane.Murphy@uwyo.edu

Authors

Anna M. Robertson – Department of Atmospheric Science, University of Wyoming, Wyoming 82071, United States

Rachel Edie – Department of Atmospheric Science, University of Wyoming, Wyoming 82071, United States; orcid.org/0000-0001-7959-4232

Robert A. Field – Department of Atmospheric Science, University of Wyoming, Wyoming 82071, United States

David Lyon – Environmental Defense Fund, Austin, Texas 78701, United States

Renee McVay – Environmental Defense Fund, Austin, Texas 78701, United States

Mark Omara – Environmental Defense Fund, Austin, Texas 78701, United States; orcid.org/0000-0002-8933-1927

Daniel Zavala-Araiza – Environmental Defense Fund, Austin, Texas 78701, United States; orcid.org/0000-0002-8394-5725

Complete contact information is available at:

<https://pubs.acs.org/10.1021/acs.est.0c02927>

Notes

The authors declare no competing financial interest.

■ ACKNOWLEDGMENTS

We acknowledge the Environmental Defense Fund (EDF) for providing funding and guidance on this work. We also acknowledge the University of Wyoming's School of Energy Resources who provided funding for the equipment used during this project and for funding of the Center of Excellence in Air Quality. We also thank the University of Wyoming Department of Atmospheric Science team of engineers for keeping our mobile laboratory running smoothly.

■ REFERENCES

- (1) U.S. Energy Information Administration. No Title <https://www.eia.gov/>.
- (2) Hausfather, Z. Bounding the Climate Viability of Natural Gas as a Bridge Fuel to Displace Coal. *Energy Policy* **2015**, *86*, 286–294.
- (3) Myhre, G.; Shindell, D.; Bre' on, F.-M.; Collins, W.; Fuglestvedt, J. ; Huang, J.; Koch, D.; Lamarque, J.-F.; Lee, D.; Mendoza, B.; Nakajima, T.; Robock, A.; Stephens, G.; Takemura, T.; Zhan, H. Anthropogenic and Natural Radiative Forcing. In *Climate Change 2013: The Physical Science Basis*; Contribution of Working Group I to the Fifth Assessment Report of the Intergovernmental Panel on Climate Change, 2013; pp 659–740 DOI: [10.1017/CBO9781107415324.018](https://doi.org/10.1017/CBO9781107415324.018).
- (4) U.S. Environmental Protection Agency. *Inventory of U.S. Greenhouse Gas Emissions and Sinks: 1990–2014*, 2016.
- (5) Alvarez, R. A.; Zavala-Araiza, D.; Lyon, D. R.; Allen, D. T.; Barkley, Z. R.; Brandt, A. R.; Davis, K. J.; Herndon, S. C.; Jacob, D. J.; Karion, A.; Kort, E. A. Assessment of Methane Emissions from the U.S. Oil and Gas Supply Chain. *Science* **2018**, *361*, 186–188.
- (6) Howarth, R. W. Ideas and Perspectives: Is Shale Gas a Major Driver of Recent Increase in Global Atmospheric Methane? *Biogeosciences* **2019**, *16* (15), 3033–3046.
- (7) Zavala-Araiza, D.; Lyon, D. R.; Alvarez, R. A.; Davis, K. J.; Harriss, R.; Herndon, S. C.; Karion, A.; Kort, E. A.; Lamb, B. K.; Lan, X.; Marchese, A. J. Reconciling Divergent Estimates of Oil and Gas Methane Emissions. *Proc. Natl. Acad. Sci. U. S. A.* **2015**, *112* (S1), 15597–15602.
- (8) Rella, C. W.; Tsai, T. R.; Botkin, C. G.; Crosson, E. R.; Steele, D. Measuring Emissions from Oil and Natural Gas Well Pads Using the Mobile Flux Plane Technique. *Environ. Sci. Technol.* **2015**, *49*, 4742–4748.
- (9) Brandt, A. R.; Heath, G. A.; Cooley, D. Methane Leaks from Natural Gas Systems Follow Extreme Distributions. *Environ. Sci. Technol.* **2016**, *50*, 12512–12520.
- (10) Omara, M.; Sullivan, M. R.; Li, X.; Subramanian, R.; Robinson, A. L.; Presto, A. A. Methane Emissions from Conventional and

Unconventional Natural Gas Production Sites in the Marcellus Shale Basin. *Environ. Sci. Technol.* **2016**, *50* (4), 2099–2107.

(11) Bell, C. S.; Vaughn, T. L.; Zimmerle, D.; Herndon, S. C.; Yacovitch, T. I.; Heath, G. A.; Petron, G.; Edie, R.; Field, R. A.; Murphy, S. M.; Robertson, A. M. Comparison of Methane Emission Estimates from Multiple Measurement Techniques at Natural Gas Production Pads. *Elementa Science of the Anthropocene* **2017**, *5* (79).79

(12) Omara, M.; Zimmerman, N.; Sullivan, M. R.; Li, X.; Ellis, A.; Cesa, R.; Subramanian, R.; Presto, A. A.; Robinson, A. L. Methane Emissions from Natural Gas Production Sites in the United States: Data Synthesis and National Estimate. *Environ. Sci. Technol.* **2018**, *52* (21), 12915–12925.

(13) Lyon, D. R.; Alvarez, R. A.; Zavala-Araiza, D.; Brandt, A. R.; Jackson, R. B.; Hamburg, S. P. Aerial Surveys of Elevated Hydrocarbon Emissions from Oil and Gas Production Sites. *Environ. Sci. Technol.* **2016**, *50*, 4877–4886.

(14) Zavala-Araiza, D.; Alvarez, R. A.; Lyon, D. R.; Allen, D. T.; Marchese, A. J.; Zimmerle, D. J.; Hamburg, S. P. Super-Emitters in Natural Gas Infrastructure Are Caused by Abnormal Process Conditions. *Nat. Commun.* **2017**, *8* (1), 1–10.

(15) Allen, D. T. Emissions from Oil and Gas Operations in the United States and Their Air Quality Implications. *J. Air Waste Manage. Assoc.* **2016**, *66* (6), 549–575.

(16) Peischl, J.; Eilerman, S. J.; Neuman, J. A.; Aikin, K. C.; de Gouw, J.; Gilman, J. B.; Herndon, S. C.; Nadkarni, R.; Trainer, M.; Warneke, C.; Ryerson, T. B. Quantifying Methane and Ethane Emissions to the Atmosphere From Central and Western U.S. Oil and Natural Gas Production Regions. *J. Geophys. Res. Atmos.* **2018**, *123*, 7725–7740.

(17) Edie, R.; Robertson, A. M.; Field, R. A.; Soltis, J.; Snare, D. A.; Zimmerle, D.; Bell, C. S.; Vaughn, T. L.; Murphy, S. M. Constraining the Accuracy of Flux Estimates Using OTM 33A. *Atmos. Meas. Tech.* **2020**, *13* (1), 341–353.

(18) Edie, R.; Robertson, A. M.; Soltis, J.; Field, R. A.; Snare, D.; Burkhart, M. D.; Murphy, S. M. Off-Site Flux Estimates of Volatile Organic Compounds from Oil and Gas Production Facilities Using Fast-Response Instrumentation. *Environ. Sci. Technol.* **2020**, *54*, 1385–1394.

(19) Robertson, A. M.; Edie, R.; Snare, D.; Soltis, J.; Field, R. A.; Burkhart, M. D.; Bell, C. S.; Zimmerle, D.; Murphy, S. M. Variation in Methane Emission Rates from Well Pads in Four Oil and Gas Basins with Contrasting Production Volumes and Compositions. *Environ. Sci. Technol.* **2017**, *51*, 8832–8840.

(20) Brantley, H. L.; Thoma, E. D.; Squier, W. C.; Guven, B. B.; Lyon, D. Assessment of Methane Emissions from Oil and Gas Production Pads Using Mobile Measurements. *Environ. Sci. Technol.* **2014**, *48* (24), 14508–14515.

(21) U.S. Environmental Protection Agency. Other Test Method (OTM) 33 and 33A Geospatial Measurement of Air Pollution-Remote Emissions Quantification Direct Assessment (GMAP-REQ-DA). <http://www.epa.gov/%0Attn/emc/prelim.html>.

(22) Edie, R.; Robertson, A.; Field, R.; Soltis, J.; Snare, D.; Zimmerle, D.; Bell, C.; Vaughn, T.; Murphy, S. Constraining the Accuracy of Flux Estimates Using OTM 33A. *Atmos. Meas. Tech.* **2020**, *13*, 341–353.

(23) Turner, D. B. Workbook of Atmospheric Dispersion Estimates. Publication No. 999-AP-26. 1969.

(24) DrillingInfo DI Desktop. No Title enverus.com.

(25) Allen, D. T. Emissions from Oil and Gas Operations in the United States and Their Air Quality Implications. *J. Air Waste Manage. Assoc.* **2016**, *66* (6), 549–575.

(26) Brantley, H. L.; Thoma, E. D.; Eisele, A. P. Assessment of VOC and HAP Emissions from Oil and Natural Gas Well Pads Using Mobile Remote and Onsite Direct Measurements. *J. Air Waste Manage. Assoc.* **2015**, *65* (9), 1072–1082.

(27) Allen, D. T.; Pacsi, A. P.; Sullivan, D. W.; Zavala-araiza, D.; Harrison, M.; Keen, K.; Fraser, M. P.; Hill, a D.; Sawyer, R. F.; Seinfeld, J. H. Methane Emissions from Process Equipment at Natural

Gas Production Sites in the United States: Pneumatic Controllers. *Environ. Sci. Technol.* **2015**, *49* (1), 630–640.

(28) Yacovitch, T. I.; Daube, C.; Vaughn, T. L.; Bell, C. S.; Roscioli, J. R.; Knighton, W. B.; Nelson, D. D.; Zimmerle, D.; Pétron, G.; Herndon, S. C. Natural Gas Facility Methane Emissions: Measurements by Tracer Flux Ratio in Two US Natural Gas Producing Basins. *Elementa Science of the Anthropocene* **2017**, *5* (69).69

(29) Efron, B.; Tibshirani, R. Bootstrap Methods for Standard Errors, Confidence Intervals, and Other Measures of Statistical Accuracy. *Stat. Sci.* **1986**, *1* (1), 54–77.

(30) Caulton, D. R.; Lu, J. M.; Lane, H. M.; Buchholz, B.; Fitts, J. P.; Golston, L. M.; Guo, X.; Li, Q.; McSpirtt, J.; Pan, D.; Wendt, L. Importance of Superemitter Natural Gas Well Pads in the Marcellus Shale. *Environ. Sci. Technol.* **2019**, *53*, 4747–4754.

(31) Howard, T.; Ferrara, T. W.; Townsend-Small, A. Sensor Transition Failure in the High Flow Sampler: Implications for Methane Emission Inventories of Natural Gas Infrastructure. *J. Air Waste Manage. Assoc.* **2015**, *65* (7), 856–862.

(32) Broadhead, R. F.; Mansell, M.; Jones, G. *Carbon Dioxide in New Mexico: Geologic Distribution of Natural Occurrences*, Report No. 514; New Mexico Bureau of Geology and Mineral Resources A Division of New Mexico Tech: Socorro, NM, 2009.

(33) Society of Petroleum Engineers. Guidelines for the evaluation of petroleum reserves and resources http://www.spe.org/%0Aindustry/docs/GuidelinesEvaluationReservesResources_2001.pdf.

(34) Society of Petroleum Engineers. Unit Conversion Factors www.spe.org/industry/unit-conversion-factors.php.

(35) New Mexico Oil Conservation Division. <http://www.emrd.state.nm.us/ocd/>.

(36) Petron, G.; Karion, A.; Sweeney, C.; Miller, B. R.; Montzka, S. A.; Frost, G. J.; Trainer, M.; Tans, P.; Andrews, A.; Kofler, J.; Helmig, D. A New Look at Methane and Nonmethane Hydrocarbon Emissions from Oil and Natural Gas Operations in the Colorado Denver-Julesburg Basin. *J. Geophys. Res.: Atmos.* **2014**, *119*, 6836–6852.

(37) Zhang, Y.; Gautam, R.; Pandey, S.; Omara, M.; Maasakkers, J. D.; Sadavarte, P.; Lyon, D.; Nesser, H.; Sulprizio, M. P.; Varon, D. J.; Zhang, R. Quantifying Methane Emissions from the Largest Oil-Producing Basin in the United States from Space. *Sci. Adv.* **2020**, *6* (17).eaaz5120

Exhibit 21

Closing the gap: Explaining persistent underestimation by US oil and natural gas production-segment methane inventories

Jeffrey S. Rutherford¹, Evan D. Sherwin¹, Arvind P. Ravikumar², Garvin A. Heath³, Jacob Englander⁴, Daniel Cooley⁵, David Lyon⁶, Mark Omara⁶, Quinn Langfitt⁴, Adam R. Brandt¹

¹ Department of Energy Resources Engineering, Stanford University, Stanford CA 94305; jruth@stanford.edu (J.S.R.); evands@stanford.edu (E.D.S.); abrandt@stanford.edu (A.R.B.).

² Department of Systems Engineering, Harrisburg University of Science and Technology, Harrisburg, PA 17101; ARavikumar@HarrisburgU.edu.

³ National Renewable Energy Laboratory, Golden, CO 80401; Joint Institute for Strategic Energy Analysis (JISEA); Garvin.Heath@nrel.gov.

⁴ Industrial Strategies Division, California Air Resources Board, Sacramento CA 95814; jacob.english@arb.ca.gov (J.G.E.); Quinn.Langfitt@arb.ca.gov (Q.L.).

⁵ Department of Statistics, Colorado State University, Ft. Collins CO 80523; cooleyd@rams.colostate.edu.

⁶ Environmental Defense Fund, Austin TX; dlyon@edf.org (D.L.); momara@edf.org (M.O.).

Abstract

Methane (CH₄) emissions from oil and natural gas (O&NG) systems are an important contributor to greenhouse gas emissions. In the United States (US), recent synthesis studies of field measurements of CH₄ emissions at different spatial scales are ~1.5x-2x greater compared to official Environmental Protection Agency (EPA) greenhouse gas inventory (GHGI) estimates. Site-level field studies have isolated the production-segment as the dominant contributor to this divergence. Based on an updated synthesis of measurements from component-level field studies, we develop a new inventory-based model for CH₄ emissions using bootstrap resampling that agrees within error with recent syntheses of site-level field studies and allows for isolation of differences between our inventory and the GHGI at the equipment-level. We find that venting and malfunction-related emissions from tanks and other equipment leaks are the largest contributors to divergence with the GHGI. To further understand this divergence, we decompose GHGI equipment-level emission factors into their underlying component-level data. This decomposition shows that GHGI inventory methods are based on measurements of emission rates that are systematically lower compared with our updated synthesis of more recent measurements. If our proposed method were adopted in the US and other jurisdictions, inventory estimates could become more accurate, helping to guide methane mitigation policy priorities.

Methane (CH₄) is the principle constituent of natural gas and is also a potent greenhouse gas (GHG) [1]. During production of oil and natural gas (O&NG), some processes are designed to vent CH₄ to the air, and CH₄ is also emitted unintentionally via leaks in the system. According to the official United States (US) GHG inventory, CH₄ from O&NG operations are estimated to contribute ~3% of national GHG emissions (with 100 year GWP = 25, [2]). At the international level the contribution is approximately 5% (based on estimates from [3] and [4]). However, the uncertainty in this estimate, data gaps, and inconsistency with alternative approaches suggested a need for further evidence [5]–[8]. To this end, significant research in the past decade has investigated CH₄ emissions from the O&NG system.

The US Environmental Protection Agency (EPA) estimates O&NG CH₄ emissions in an annual Greenhouse Gas Inventory (GHGI) [9]. The GHGI uses a data-rich, “bottom-up” approach to estimate national CH₄ emissions by scaling up CH₄ emissions measurements from activities like well completions and gas handling components like valves or seals. However, a recurrent theme consistently found in the literature is that the GHGI underestimates total US O&NG CH₄ emissions compared to observed values [10]. Brandt et al. [11] summarize the literature, and observe that national-scale estimates from large-scale field studies exceed the GHGI by ~1.5 times. This difference is sometimes referred to as the “top-down/bottom-up” gap [11]–[17], based on the differences in approach between the GHGI and the conflicting studies. “Top-down” studies determine total emissions from multiple sites via measurements from aircraft, satellites, or weather stations (e.g. [14]–[16], [18]–[20]).

Some recent studies have used a meso-scale “site-level” approach which measures CH₄ downwind of facilities (e.g., well-pads) to estimate total emissions of an entire site or facility (e.g. [21]–[24]). A recent synthesis of site-level data by Alvarez et al. [13] finds agreement between site-level results and top-down results, with a best estimate of supply chain emissions (including all equipment from production to distribution) ~1.8 times that of the component-level GHGI [25] (up to ~2.1x in the production-segment).

Most emissions sources in the GHGI are derived using bottom-up methods. The bottom-up approach estimates overall CH₄ emissions by combining counts of individual components (or activities) with emissions per component/activity (the “emission factor”). The bottom-up approach allows for representation of sources at a high resolution, with 67 and 45 separate sources for the O&NG production segments, respectively [25]. Because of this high resolution, the GHGI is useful for development of CH₄ mitigation policies. For example, the Obama administration’s Climate Action Plan developed recommendations using the relative contribution of emissions sources in the GHGI [26]. Also, the bottom-up framework of the GHGI is recommended for reporting national emissions under the United Nations Framework Convention on Climate Change (UNFCCC, [27]), under which participating countries report their inventory of GHG emissions.

This study aims to answer two questions. First, why does the bottom-up EPA GHGI underestimate CH₄ emissions compared to both site-level and large-scale top-down studies? Second, is this underestimation due to an inherent problem with the bottom-up methods used in the GHGI? Previous studies have noted that the underlying data sources of the GHGI were

published in the 1990s and may be outdated [11], [28], [29]. The site-level synthesis study of Alvarez et al. [13] suggested that the divergence is likely due to a systematic bias in the bottom-up methodology that misses “super-emitters”, a finding supported by others (e.g., [11] [30]). Recent work suggests that top-down measurement campaigns are capturing systematically higher emissions during daytime hours from episodic events. However, this may not be true at a national level, as it has been noted that the upward bias of top-down measurements was likely explained by unusually high liquids-unloadings in the Fayetteville shale [13], [31]. Some have attempted to construct alternative inventories (e.g., [13], [32], [33]), however these attempts have not taken full advantage of the robust set of component-level data now available.

In this study, for the first time, we explain with source-level specificity the underestimation of O&NG CH₄ emissions in the GHGI as compared to top-down studies. Our analysis boundary is the O&NG production segment which includes all active, onshore well pads and tank batteries (excluding inactive and offshore wells) and ends prior to centralized gathering and processing facilities (**Figure S1**). We focus on the production segment given its significant emissions (~58% of total supply chain CH₄ emissions in Alvarez et al. [13]) and the large difference between site-level estimates and the GHGI [13] (~70% of difference between Alvarez et al. [13] and the GHGI, **Figure S2**). This study develops and validates approaches that can be applied to other segments in the O&NG supply chain.

Our novel contributions are threefold. First, we construct a bottom-up, O&NG production-segment CH₄ emissions estimation tool based on the most comprehensive public database of component-level activity and emissions measurements yet assembled. Our approach differs from the GHGI in that it applies modern statistical approaches (bootstrap resampling) to allow for inclusion of infrequent, large emitters, thus robustly addressing the issue of super-emitters. Second, we use this tool to produce an inventory of US O&NG production segment CH₄ emissions and compare this with the GHGI and previous site-level results, showing that much of the divergence between different methods at different scales vanishes when we apply our improved dataset and statistical approaches. As mentioned earlier, site-level synthesis studies have been validated against even larger-scale top-down studies, so improved alignment between our method and site-level results suggests much better agreement with top-down results [13], [34]. Third, to isolate specific sources of disagreement between the GHGI and other studies, we reconstruct the GHGI emission factors beginning with the underlying datasets and uncover some possible sources of disagreement between inventory methods and top-down studies. Based on these results, we suggest a strategy for improving the accuracy of the GHGI, and likewise any country using a similar approach in reporting O&NG CH₄ emissions to the UNFCCC.

A new bottom-up approach

Bottom-up approaches extrapolate component or equipment emissions rates to large (e.g., national) scales by multiplying emission factors (emissions per component or equipment per unit time) by activity factors (counts of components per equipment, and equipment per well) (**Figure 1**). Our estimation tool requires two sequential extrapolations, first from the component to the equipment-level, and second from the equipment to the national or regional-level.

The approach utilized in our bottom-up estimation tool begins with a database of component-level direct emissions measurements (e.g., component-level emission factors). We generate component-level emission factor distributions for this study from a literature review building on prior work [11], [30] and adding new publicly available quantified measurements (**Table 1** in Methods). Our resulting tool's database includes ~3200 measurements from 6 studies across a 12-fold component classification scheme (see SI-3.2 for further description of this classification scheme). We applied emission factors as reported in the individual studies, with no modifications beyond unit conversion (noting that there are some differences between studies in High Flow Sampler bias correction for gas concentration and flow rate, which may introduce uncertainty to our results). Data for component counts and fraction of components emitting (the ratio of emitting components to all components counted) was scarce, with only 3 studies containing useful information for both ([35]–[37] for component counts and [35], [36], [38] for fraction of components emitting).

We derive equipment-level emission factors for our tool by random re-sampling (i.e., bootstrapping, with replacement) from our component-level database according to component counts per equipment and fraction of components emitting. Source-specific approaches were required for infrequent events (i.e., completions, workovers, liquids unloadings), methane slip from reciprocating engines, and liquid storage tanks (see SI-3.3).

We then perform a second extrapolation, using our equipment-level emission and activity factors to calculate a 2015 US O&NG production-segment CH₄ emissions estimate. For this step, our tool is integrated into the Oil Production and Greenhouse Gas Emissions Estimator (further description of OPGEE can be found in SI-3.1) and parameterized using 2015 domestic well count and O&NG production data (same dataset as Alvarez et al. [13]). A total of ~1 million wells and associated equipment are partitioned and analyzed across 74 analysis bins (SI-4.1). We performed a Monte Carlo uncertainty analysis repeating the bootstrapping algorithm 100 times across all ~1 million wells (SI-4.4). It is worth mentioning that emission factors are often themselves only measured in a few locations, and thus in our extrapolation we assume applicability to other regions.

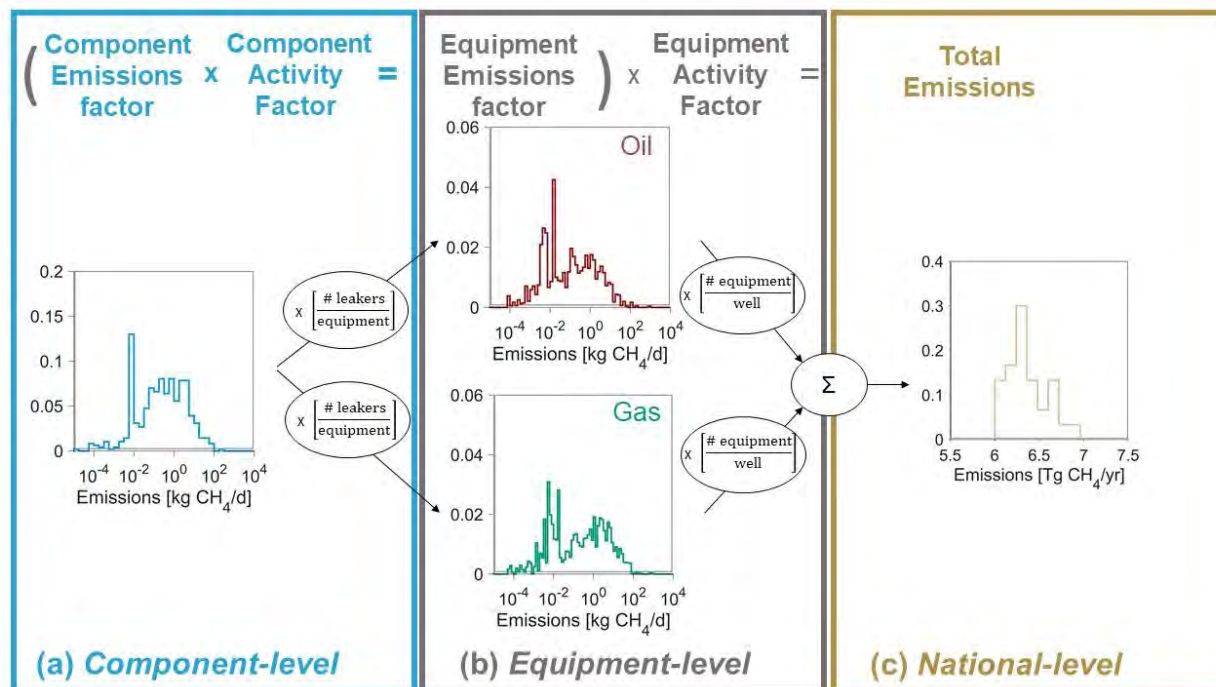


Figure 1: Schematic of this study’s bottom-up CH₄ emissions estimation tool which involves multiplication of emission factors (e.g., emissions per valve) by activity factors (e.g., number of valves per wellhead). Two sequential extrapolations are performed using an iterative bootstrapping approach. First, our database of component-level (e.g., valve, connector) emissions measurements (a) is extrapolated using component-level activity factors to generate equipment-level (e.g., wellhead, separator) emission factors (b). Second, these equipment-level emission factor distributions are extrapolated using equipment-level activity factors to generate a 2015 US O&NG production-segment CH₄ emissions estimate. This extrapolation is performed 100 times to generate a distribution of national-level CH₄ emissions (c) and estimate a 95% confidence interval (CI).

Comparison of US production-segment CH₄ emissions with site-level studies and the GHGI

We first compare our resulting US 2015 O&NG production-segment CH₄ emissions estimate with the GHGI’s estimate for 2015 produced in their most recent 2020 inventory [25]. We also validate our bottom-up tool by comparing total emissions and emissions distributions with those generated in site-level synthesis studies (total emissions are compared with Alvarez et al. [13], site-level distributions are compared with Omara et al.[34]).

We estimate mean O&NG production-segment CH₄ emissions of 6.3 Tg/yr (5.8-6.9 Tg/yr, at 95% confidence-interval, CI) (Fig. 2a, Note that the CI is relatively narrow given that this only captures uncertainty due to resampling). Our mean, production-normalized emissions rate from the production segment is 1.3% (1.2-1.4% at 95% CI, based on gross NG production of 32 trillion cubic feet and an average CH₄ content of 82% [39], [40]), slightly lower than Alvarez et al.[13], [34], who estimate 1.5% (applying the same denominator as above). Both our bottom-up component-level inventory results and the Alvarez site-level results are approximately 2x those of the GHGI estimate of 3.6 Tg/yr (year 2015 data [25], excludes offshore systems) for the

O&NG production segment. Interestingly, the difference in US production-segment emissions between this study and the GHGI is approximately the same volume as our estimate of contribution from super-emitters (top 5% of emissions events). Given that our results match the Alvarez et al. site-level results, we conclude that the divergence between the GHGI and top-down/site-level studies is not likely to be due to any inherent issue with the bottom-up approach.

Figure 2(b-c) show that site-level distributions developed using our model match empirical distributions from the site-level synthesis study of Omara et al. [34]. To report our results on a basis consistent with site-level studies (recalling that sites can contain more than one well), we cluster equipment-level emissions outputs into production sites (SI-4.3). Several other observations from our simulations are of interest. First, our modeled emissions per site are higher at liquids-rich sites versus gas-rich sites (**Figure S29**), in alignment with recent field measurement campaigns in both Canada and the United States [41], [42]. Second, our model recreates the trend demonstrated by Omara et al. wherein low-producing sites exhibit higher production-normalized emissions rates [34] (**Figure S30**). Finally, the tail of our modeled distribution closely matches the tail of the empirical Omara et al. distribution (**Figure 2b** and **Figure S28**). This is of particular interest, given that recent papers assert the divergence between the GHGI and site-level studies is mostly due to an inability of the bottom-up methods to capture super-emitters [32], [42]. Our results clearly show that a modern dataset with proper bootstrap resampling techniques can recreate observed super-emitters.

Because our approach uses a component-level, bottom-up approach, we can investigate the source of differences with the GHGI. This cannot be done with site-level data. Relative to the GHGI, contributions from equipment leaks in our estimate are larger by ~ 1.3 Tg CH₄ and tank leaks and venting by ~ 2.1 Tg CH₄ (**Figure 3**). Together, these two sources contribute over half of total O&NG production-segment CH₄ emissions. The increase in estimated emissions from equipment leaks compared to the GHGI are due to our updated emission factor; we know that the difference is not due to equipment-level activity factors because ours are nearly identical to the GHGI (see SI-2.3). In the next section we will perform a deeper investigation into both component-level emissions data for equipment leaks and tank modelling as underlying contributors to differences between our results and the GHGI.

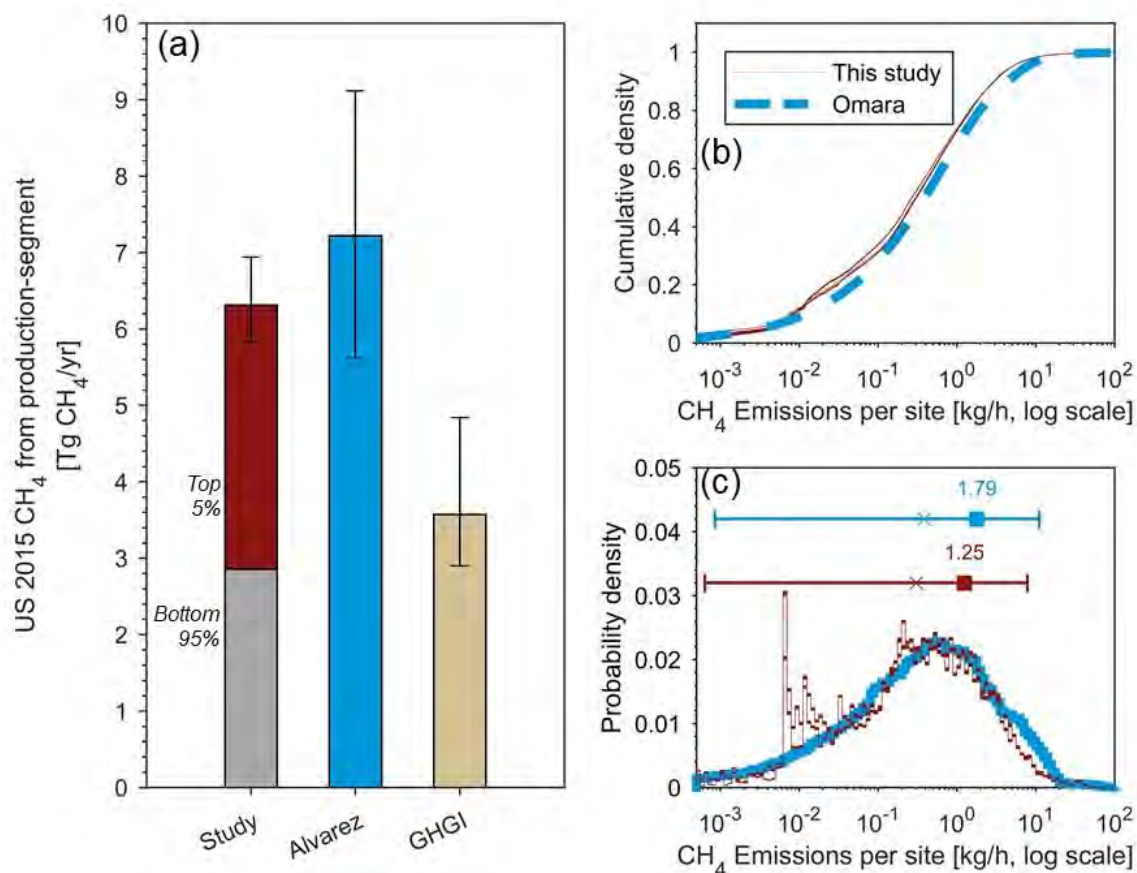


Figure 2: (a) Comparison of this study’s aggregate US 2015 CH₄ emissions from O&NG production-segment with site-level results of Alvarez et al. (see Table S3 in [13] minus contributions from offshore platforms and abandoned wells) and the GHGI [25] including fraction estimated from super-emitters (top 5% of sources) and 95% confidence interval. We also compare probability distributions of our component-level simulations (red lines), aggregated into site-level emissions, with site-level results of Omara (blue line): (b) Cumulative distribution plot (CDF) describing the fraction of well-sites with emissions below a given amount, and (c) probability distribution of emissions rate per well-site with the mean (filled square), median (x), and 95% confidence intervals shown above the plots. Results of this study are presented using 100 Monte Carlo simulations. Because of the large number of sampled sites, the Monte Carlo simulations all converge toward the same size distribution in panels (b) and (c).

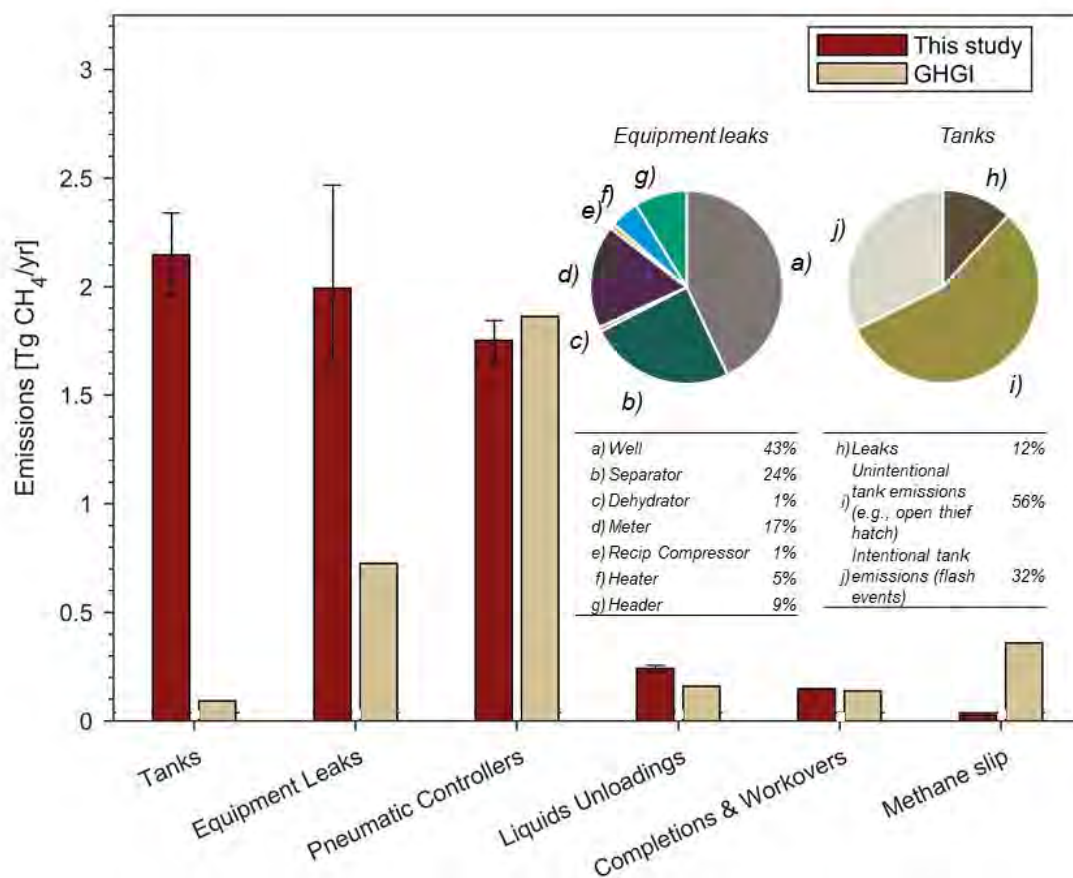


Figure 3: Contributions of emissions sources to our US 2015 O&NG production-segment inventory (and 95% confidence interval) compared with 2020 GHGI [25]. Inset pie charts illustrate individual source-specific contributions of our inventory to equipment leaks (left pie chart) and tanks (right pie chart). Discrepancies with the GHGI are dominated by liquid hydrocarbon tank leaks and venting (“tanks”, ~2.1 Tg/yr CH₄) and equipment leaks (~1.3 Tg/yr CH₄). Details regarding the modelling of tank emissions sources is given in SI-3.3. Results in tabular form are given in Table S2 and Table S3.

Main sources of GHGI underestimation

Given that our new component-level method is validated by the empirical results from site-level field studies, can we explain why the GHGI produces lower O&NG production-segment CH₄ emissions estimates? Results from our modelling (Figure 3), in addition to recent revisions by the GHGI and other analyses (SI- 5.1), suggest that the downward bias of the GHGI is not due to pneumatic controllers, liquids unloadings, or completions and workovers because either the divergence is small or absolute emissions are small, or both. Methane slip in reciprocating engines is higher in the GHGI, although the overall magnitude in difference is small. The combustion emission factor used in the GHGI for methane slip from reciprocating gas engines is based on a 1991 TRANSDAT dataset published by the Gas Research Institute [43]. The difference compared to our study is probably explained by substantial improvement in engine emissions since publication of that report (based on manufacturer reported specifications for

reciprocating gas engines [44]). For these reasons, this paper focuses its analysis of the two largest sources of GHGI underestimation compared to our validated method: equipment leakage and liquid hydrocarbon storage tanks, whose emissions are 1.3 and 2.1 Tg CH₄ lower than our estimates, respectively. See SI-1.1 for definitions of each emissions source.

The GHGI constructs emission factors for equipment-level leaks using an approach very similar to ours, where emission factors of individual components are aggregated according to estimated counts of components per piece of equipment. To explore differences in equipment leak estimates, we decompose equipment-level emission factors into the constituent parts: Component-level emissions data, component counts, and fraction of components emitting (the relationship between these parameters is defined in **Figure 4**).

Reconstructing equipment-level, equipment leakage emission factors from the GHGI is complicated by the fact that the underlying studies from the 1990s [35], [45] are at a more detailed level than the GHGI itself. For example, the underlying data for natural gas system emission factors are subdivided by region (e.g., Western gas versus Eastern gas), and for petroleum systems data are subdivided by product stream (e.g., light oil versus heavy oil). Equipment-level emission factors for gas systems, for example, are a weighted average of both Western emission factors and Eastern emission factors. The GHGI approach to aggregating these factors to overall values for natural gas and petroleum systems is described in SI-5.2.

We demonstrate differences in equipment-level emission factors for equipment leaks via a decomposition into constituent factors for a single example (equipment type and region) – leakage from gas wells in the West (**Figure 4**) – with equipment leaks from all other sources similarly described in the SI (**Figure S18 – Figure S26**). The difference between our study’s equipment-level equipment leakage emission factor for Western natural gas wells and the GHGI – the difference to be explained by decomposition – is ~5x (3.4 kg/day versus 0.7 kg/day). The underlying factors are plotted in **Figure 4**.

First, we compare component-level emission factors, defined as the average emissions rate of leaking components (**Figure 4a**). (Note that the “average emission rate of leaking components” is not the same as an average emission rate for all components.) For Western gas and petroleum systems in the GHGI, component-level leakage emission factors are constructed using a method referred to by the EPA [46] as the “EPA correlation approach” (defined in detail in SI-5.2.2). In this approach, emission factors are constructed from a dataset of various facilities including oil and gas production sites, refineries, and marketing terminals (n = 445, data compiled in the EPA Protocol document [46]). The difference between our study’s component-level emission factors and the GHGI for connectors, valves, and open-ended lines (the components comprising the wells) is ~7x, 6x, and 5x respectively (**Figure 4a**). Note that the decomposition in **Figure 4a** is limited to connectors, valves, and open-ended lines (the three components inventoried by the GHGI) although our inventory also accounts for pressure relief valves, regulators, and other (miscellaneous) components on wells. The fact that GHGI equipment-level emission factors are based upon only three component types (when more component classes exist, according to our database) will contribute to some underestimation.

Figure 4b compares the fraction of components emitting (the ratio of emitting components to all components counted), while **Figure 4c** shows component counts (number of components counted per piece of equipment). These have offsetting effects, where component-level emission factors and component counts contribute to higher emissions in our study versus the GHGI, and fraction of components emitting contributing to lower emissions in our study. The resulting total emissions per well (**Figure 4d**) are the product of these factors, summed across all components.

Similar results are found across all equipment categories compared to the GHGI. In general, in our dataset, component-level emission factors are higher [5x to 46x comparing our emission factors for connectors, valves, and open-ended lines across all GHGI categories, see **Figure S18 – Figure S26**], the fraction of components emitting is lower [1x to 0.05x], and the number of components per piece of equipment is generally, but not always, higher [0.2x to 20x comparing our emission factors for wells, separators, and meters across all GHGI categories, see **Figure S18 – Figure S26**]. Considering the decomposition presented here, along with the rest in the SI (**Figure S18 – Figure S26**, plus some discussion of smaller factors not described here), we can explain much of the overall underestimation of the GHGI compared to our results for the equipment leaks source category.

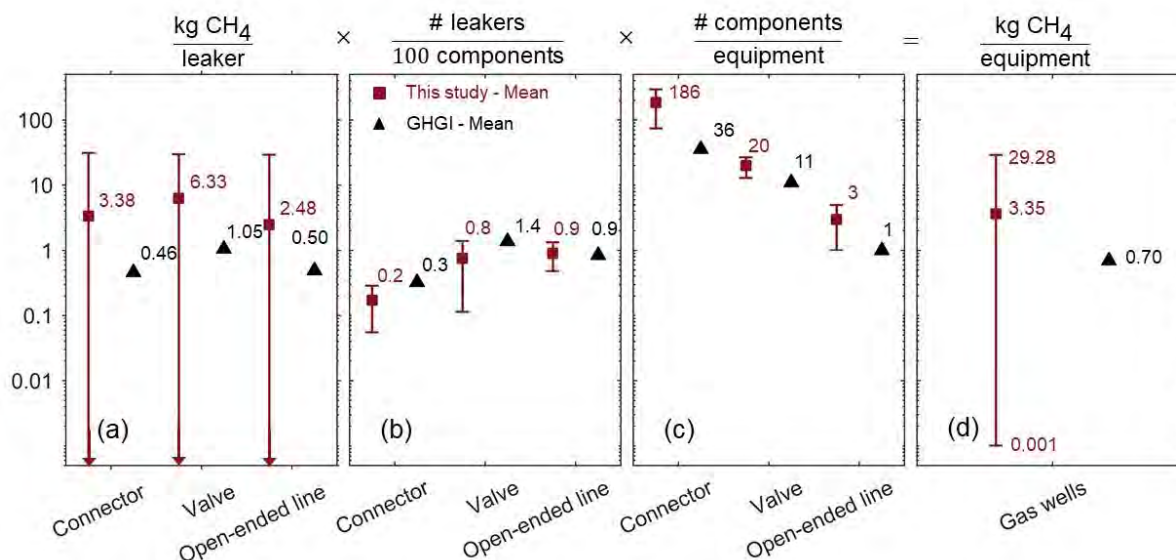


Figure 4: Example decomposition of the equipment-level emission factor for Western US gas wells (Note that units differ for each panel, and also the logarithmic scale meaning that visible differences between points often span orders of magnitude). This study's equipment-level emission factor (d) is decomposed into constituent parts and compared with the GHGI. Constituent parts include: component-level emission factors (a), fraction of components emitting (b), and component counts (c). When multiplied together, these factors have counteracting biases, with component-level emission factors and component counts contributing to higher emissions in our study versus the GHGI, and fraction of components emitting contributing to lower emissions in our study. Note that in actual usage in the GHGI, equipment-level emission factors for gas systems are a weighted average of both Western systems (API 4598, [47]) and Eastern gas systems (Star Environmental, [45]). Here, for illustration purposes, we only show constituent data for Western gas systems; results for Eastern gas system are reported in SI Section 5.2. Further, we also limit this figure to connectors, valve, and open-ended lines (the three components inventoried by the GHGI) although our inventory also accounts for pressure relief valves, regulators, and other (miscellaneous) components on wells.

The second source of significant divergence between this study and the GHGI for US CH₄ emissions in the O&NG production-segment is with emissions from liquid hydrocarbon storage tanks. The EPA GHGI constructs storage tank emissions estimates using Greenhouse Gas Reporting Program (GHGRP) data. The GHGRP is a program which collects emissions data from industrial facilities, where requirements for natural gas and petroleum systems are specified by the Code of Federal Regulations Section 40 Subpart W [48]. Based on GHGRP data for storage tanks (see methods in SI-5.3), we decompose total emissions for the GHGI into tank counts and emission factors allowing us to draw comparisons to results from this study.

Before presenting our decompositions, it is worth noting two key differences in modelling of emissions from liquid hydrocarbon storage tanks between our study and the GHGI (see further description of how our model estimates tank emissions in SI-3.3.2). First, whereas our model is based on direct measurements, the GHGI is based on operator reported simulations from software programs such as API E&P Tank or AspenTech HYSYS [49], [50]. Second, as a consequence of these differing approaches, whereas our emissions are classified based on measurement source (e.g., vent stack, thief hatch, etc.) GHGI emissions are classified according

to the simulated process (e.g., flash emissions). As a consequence of these differences in emissions classification, comparisons between decompositions of our study versus the GHGI will be imperfect.

With this in mind, we define emission factors in our decomposition as the summation of intentional emission factors and unintentional emission factors (**Figure 5**). Here, intentional (flash related) emission factors are based on direct emission measurements at the vent stack for our study, and simulations of uncontrolled and controlled tanks in the GHGI (see details in SI-5.3). Our comparison of unintentional emission factors is less precise. In the GHGI, unintentional emissions are limited to what is reported under “malfunctioning separator dump valves” (although it is unclear if additional unintentional emissions are reported alongside flash emissions in the other tank categories, see SI-5.3). Conversely, unintentional emission factors in our study are based on direct measurements of emissions from open thief hatches, rust-related holes, and malfunctioning pressure-relief valves.

We demonstrate the decomposition in **Figure 5** for petroleum systems (see **Figure S28** in the SI for natural gas systems). Note that flash emissions will only occur at controlled tanks, while unintentional emissions from thief hatches, holes, or pressure-relief valves could occur at either controlled or uncontrolled tanks. **Figure 5** and **Figure S28** demonstrate that, while several factors contribute to differences, difference in emission factors for various unintentional emissions sources are the greatest source of difference between this study and the GHGI. Unintentional emission factors are the product of (i) average emissions rate per event, and (ii) frequency of unintentional emissions events per tank. Both of these values are approximately an order of magnitude higher for our study as compared to the GHGI, contributing to the nearly two orders of magnitude difference in total emissions.

Our findings suggest that both the magnitude and frequency of unintentional emissions sources could contribute to significant underestimation in the GHGI. Due to the limited quantified, component-level data available on tank emissions (based upon safety and accessibility issues) our tank emissions measurements come from a single study in a single geographic area (Eastern Research Group in the Barnett shale,[51]). Therefore, more studies are required to provide a comprehensive view of tank emissions.

However, while quantified emissions data for tank sources are scarce, the *existence* of unintentional emissions from tanks (due to open thief hatches, rust-related holes, pressure-relief valves, etc.) has been corroborated by numerous ground and aerial surveys [42], [52]–[54]. Several of these studies are summarized in **Table S26**. Taken together, these studies provide further evidence that: (i) high emissions events are frequently observed at storage tanks, not just from vents but also at open thief hatches and pressure relief valves, (ii) these high emissions events are common at both controlled tanks and uncontrolled tanks, (iii) the frequency (events/tank) of unintentional emissions events is much higher than the rate suggested by the EPA (2%, see **Figure 5c**) for malfunctioning separator dump valves.

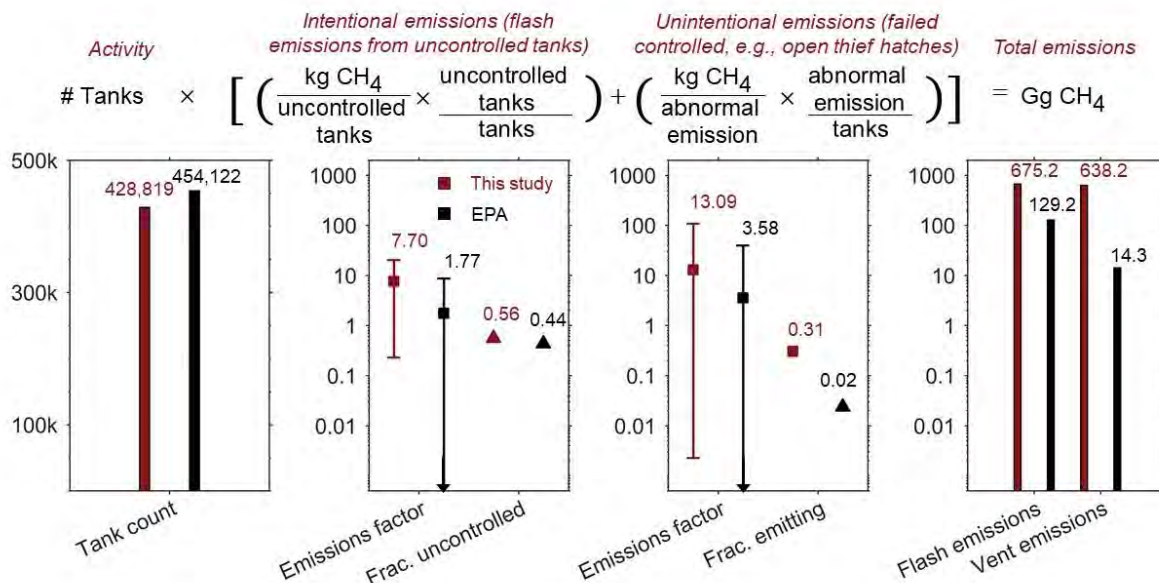


Figure 5: Decomposition of total emissions for oil tanks (far right panel) into constituent parts, with comparison of this study’s dataset to those of the GHGI. From left to right: Total activity, intentional (flash-related) emission factor, unintentional emission factor, and total emissions. Flash and unintentional emission factors are decomposed into emission factors (kg CH₄/ emitting tanks) and control rates (emitting tanks/ total tanks). Note the log scale for the right three panels.

Discussion

Development of accurate inventories at the equipment-level is critical for targeting CH₄ mitigation strategies. US government agencies [26], environmental groups [55], [56], and researchers [57] rely on inventory data for policy design, cost analysis, formulation of leak detection and repair programs, and life-cycle assessment research. However, recent studies have emphasized a ~1.5x-2x divergence between the EPA GHGI estimates of CH₄ emissions from O&NG and those estimated from field measurements at different spatial scales. This suggests an opportunity for improvement in the GHGI approach.

In this study we develop a component-level, bottom-up approach validated by previous site-level estimates of US 2015 CH₄ emissions from the production segment of the O&NG sector. Consistent with site-level findings, our estimate is ~1.8 times that of the GHGI. The strength of our approach is that by developing our estimate using component-level data, we can diagnose at the equipment-level the key sources contributing to the GHGI underestimation. Our detailed decomposition identifies (i) underlying equipment-leak measurements and (ii) neglect of the contribution of unintentional emissions events at tanks (e.g., liquid hydrocarbon tank “thief hatches”) as the most important contributors to the underestimation.

These results demonstrate that the bottom-up methodology is a valid approach to produce accurate emissions estimates and that improvements to inventory methods are possible. We make several recommendations:

- Improvements to equipment leak emission factors can be implemented relatively easily. This study applies a very similar approach to the GHGI, albeit using a more comprehensive set of data on component-level emission factors, fraction of components emitting, and component counts. We can only speculate on why differences exist between our dataset and the GHGI dataset, but based on the fact that our dataset is larger and contains more recent measurements, we suggest that it is likely to be more representative of today's conditions.
- Improvements to crude and condensate storage tank emission factors will be more difficult. Differences between our emissions estimate and the emissions estimate of the GHGI is believed to be largely a result of the GHGI neglecting emissions from failed tank controls (e.g., open thief hatches). Although we attempt to estimate their contribution, and reference supporting site-level surveys, a significant data gap exists in this area.
- Regular efforts to validate equipment-level emission factors by comparing existing or new emission factors with measurements from randomly sampled sources at different spatial scales would also improve accuracy and “build in” to inventory efforts the ability to correct data over time.

The results of this study are also relevant globally. All parties to the UNFCCC submit annual inventories, generated using a bottom-up approach, to report on progress towards GHG targets. The IPCC's Guidance Document on Emission factors outlines three approaches towards producing an inventory, with the simplest approach (Tier 1) based on IPCC default emission factors [27], [58]. Default emission factors for the petroleum and natural gas systems production-segment are based upon the same underlying data sets as the GHGI. This means that, in addition to the US-submitted GHGI, other countries using Tier 1 emission factors will be contributing CH₄ estimates according to data that we have found likely to be underestimating of actual emissions, and thus the recommendations offered herein, if implemented, would improve emissions estimates globally.

Improvements offered in this study are thus potentially directly applicable to the UNFCCC inventory method and any country directly reporting emissions estimates to the UNFCCC. Our study suggests an approach which can be applied to prepare a more accurate inventory.

Methods:

Here, we describe the methodological aspects of each of this study’s three key contributions: (i) tool development, (ii) generating a US CH₄ estimate for the O&NG production-segment, and (iii) decomposing GHGI emission factors. Our methods are also described in greater detail in the Supplementary Information (SI). Datasets and code are available in a Github repository: https://github.com/JSRuthe/O-G_Methane_Supporting_Code

Tool development

Tool structure

The analysis platform for this study is the methane venting and fugitives (VF) subroutine embedded within the Oil and Gas Production Greenhouse Gas Emissions Estimator (OPGEE version 3.0). This subroutine processes equipment-level emissions distributions and well and production values and produces gross emissions estimates.

The following equation describes the methane VF subroutine:

$$Q_{population} = \sum_{i=1}^{n_{field}} \left\{ \sum_{j=1}^{n_{wells,i}} \left[\sum_{k=1}^{n_{equip}} EF_{i,j,k} * af_k \right] \right\}$$

Here, a “field” represents a subpopulation (or bin) of wells that share similar production characteristics (e.g., gas to oil ratio). This binning was necessary because OPGEE generates outputs (carbon intensity or methane leakage rate) on a “field” basis. For each field, i , emissions are calculated well-by-well. For a single well, j , equipment-level emissions are calculated by multiplying a randomly drawn emission factor, $EF_{i,j,k}$ [kg/equipment/day], by its respective activity scaling factor, af_k [# equipment/well]. Because we iterate across wells, there is no need to explicitly multiply the activity scaling factor by well count (see SI section 3.4). Emissions are calculated across all equipment classes, k .

Database on component level studies

Our equipment-level emission factors are generated with a component-level measurement database. We conducted a detailed literature review to inform the database for this study. This review built on prior work done for Brandt et al. [11], [30] and adds new publicly available component-level measurements. Studies were reviewed for information regarding: (i) data on quantified emissions volumes per emitting component or source, (ii) activity counts for numbers of components per piece of equipment or per site, and (iii) data on fraction of components found to be emitting in a survey.

Quantified emissions data was further filtered for: (i) data collected within the production (upstream) segment, (ii) and data collected in the United States (although we do include some component count and fraction leaking data from Canada, see further details in SI-3.2). A total of 6 studies and ~ 3200 measurements met our inclusion criteria (see Table 1).

To aggregate the data from the various studies, we developed a 12-category component classification and 11-category equipment schemes. For components these include: Threaded connections and flanges, valves, open-ended lines, pressure-relief valves, compressor seals, regulators, pneumatic controllers/ actuators, chemical injection pumps, tank vents, tank thief hatches, tank pressure-relief valves, and other (miscellaneous) components. For equipment these include: Well, header, heater, separator, meter, tanks – leaks, tanks – vents, reciprocating compressor, dehydrator, chemical injection pump, and pneumatic controller/actuator (note that the “tanks – leaks” category tracks all non-vent/hatch emissions on a tank (e.g., connectors, valves, etc.) while the “tank – vent” category tracks all vent/hatch related emissions).

To align the categories of components used by the authors of a study to our common component definitions, we create a set of “correspondence matrices” to perform consistent matrix transformations (see SI-3.2.5).

Table 1: Oil and gas methane emission measurement studies that reported raw data for quantified emissions measurements, fraction of components emitting, and component counts. These studies are a subset of all studies that were examined closely, meeting inclusion criteria described. Detailed summary of each study’s results are reported in SI-6.

Study ID	Location	Number of quantified leaks	Number of components screened	Leak volumes used	Component counts used	Components screened
Allen 2013 [33]	Various	645	NR ¹	Y	N	Various components
Allen 2014 [59]	Various	377	377	Y	N	Pneum. controllers
Bell 2017 [60]	Fayetteville	322	NR	Y	N	Various components
ERG 2011 [38]	Barnett	1949	NR	Y	N	Various components
Thoma 2017 [61]	Uintah	80	80	Y	N	Pneum. controllers
Pasci 2019 [36]	Various	192	54,618	Y	Y	Various components
API 1993 [35]	Various	4794	182,833	N	Y	Various components
Clearstone 2018 ¹ [37]	Canada			N	Y	

NR = not reported

¹Given that leakage data was taken in Canada, we limit usage of this data to component counts

In addition to component-level emissions measurements, we also require component counts and fraction of components emitting. A total of 3 studies contained information on component counts [35]–[37], and we aligned the data into our standard categories. Data on fraction of components emitting was also scarce, with 3 studies containing useful information [35], [36], [51]. The fraction emitting rate is an important parameter in deriving equipment-level emission factors, but varies greatly by study due to (i) differences in screening methods between studies (e.g., Method 21 vs. infrared camera) and (ii) use of different screening sensitivity to assign a component to the emitting state (10 ppmv vs. 10,000 ppmv). Therefore, based on the technologies employed different studies may be sampling different parts of the “true” population emissions distribution. In order to ensure that we are not over or under-sampling a subset of the true distribution, we split our dataset at 10,000 ppmv (see reasons for this threshold in SI-3.2.4). Different quantified emissions bins and fraction emitting values were derived for the two halves.

Equipment-level emission factors

We required a variety of approaches to describe the different sources of emissions. The most common approach taken by this study, utilized for fugitive leaks and most vents, is a “stochastic failure” approach. In the stochastic failure approach we combine component-level emissions data, component counts, and fraction emitting values to produce equipment-level emission factors. These emission factors take the form of distributions which are generated by iteratively resampling our emissions datasets (see SI-3.3.1).

For each equipment category, we iterate across component categories and draw emissions measurements according to a probability specified by the fraction emitting value. Given that we split our dataset at 10,000 ppmv (describing quantified emitters that were missed by optical gas imaging but caught with Method 21 below the threshold, and emitters that were caught with optical gas imaging above the threshold), we develop two sets of emission factors. These two emission factor distributions are superposed to form our best approximation of the true emissions distribution (SI-3.2.4).

We applied separate approaches for flashing emission from tanks, methane slip from reciprocating compressors, and intermittent and startup losses from liquids unloading, completions, and workovers. These approaches are described in SI sections 3.3.2, 3.3.3, and 3.3.4 respectively.

Equipment-level activity factors

In the GHGI, direct equipment counts are not available for every year. As an approximation, the GHGI uses “activity drivers” such as gas production, number of producing wells, or system throughput. Activity drivers are multiplied by a scaling factor (e.g., separators per well) derived from a subsample of the population. For each piece of equipment, we employ well counts as the activity driver. Since the 2018 GHGI, the EPA has calculated activity factors for most equipment using scaling factors based on GHGRP data. Scaling factors based upon reporting year 2015 equipment counts are multiplied by year-specific wellhead counts to calculate year-specific equipment counts [62].

Extrapolation to US oil and gas wells*Development of representative “fields” for analysis*

In OPGEE, fields are described with over 50 primary input parameters, and numerous secondary parameters. Given that we are restricting our analysis to methane leaks and vents in the upstream sector, however, we only concern ourselves with a handful of inputs: Oil production, well count, gas-to-oil ratio (GOR), and methane mole fraction. The 2015 well count and production data (**Table S31**) were based on the dataset from Alvarez et al. [13], which were originally derived from Enverus and filtered to remove offshore and inactive wells (~6,000).

In order to account for the heterogeneous nature of petroleum and NG systems, the total population was divided into several simulation sub-populations (or “bins”) according to the production GOR (where gas wells have a GOR > 100 mscf/bbl, [63]), gas productivity, and

liquids unloadings method. 60 bins were developed for natural gas systems while 14 bins were developed for petroleum systems (see SI-4.1).

Uncertainty analysis

This study applies the Monte Carlo method to estimate uncertainty. Input parameters – component-level emission factors, component counts, and fraction of components emitting – are assigned distributions, and the range of uncertainty in these distributions is propagated through the model. Therefore, the full range of uncertainty is captured to the extent that these distributions encompass the full set of possible values.

A single OPGEE simulation will produce an estimate of total US CH₄, but it will not output a distribution. We run OPGEE 100 times (100 Monte Carlo iterations), each using a different set of equipment-level emission factor distributions (further description in SI section 4.2.1). In producing variable equipment level emission factor distributions, component counts and fraction of components emitting are approximated as uniform distributions between the maximum and minimum values found in our surveyed studies (see **Table S5** and **Table S6** for component counts and **Table S10** for fraction leaking). Unfortunately, our sparse dataset does not allow us to determine a likely distribution shape for these parameters.

Comparison with the EPA GHGI

Equipment leakage

The construction of equipment-level emission factors in the GHGI is rooted in several studies conducted in the 1990s. We review these studies and trace how emission factors in today's GHGI are derived from these earlier analyses. The modelling approach of the early 1990s studies is closely related to the approach in this paper, in that equipment-level emission factors are calculated from component-level emissions measurements and counts. By gathering the underlying datasets used to construct the GHGI's equipment-level emission factors we can generate component-level distributions for comparison with the distributions of our study.

The GHGI relies on a 1996 report by the Gas Research Institute [[64], henceforth referred to as the “GRI report”] for natural gas systems and a 1996 calculation workbook by the American Petroleum Institute [[65], henceforth referred to as “API 4638”] for petroleum systems. These reports were not measurement campaigns, rather these reports summarized the results of multiple earlier works. The GRI report references API 4589 ([35], sites 9-12) for the Western US natural gas system and Star Environmental [45] for the Eastern US natural gas system. API 4638 references data from API 4598 (sites 1 – 8). Therefore, only two measurement campaigns underlie GHGI equipment leakage: the API 4589 and the Star Environmental datasets.

We first analyze the screening data in API 4598 and Star Environmental and follow the methodologies outlined in SI sections 5.2.2 – 5.2.4. In API 4598, screening concentrations from Appendix C were scanned and tabulated. Unfortunately, it was not possible to re-derive the component-level emission factors in the Star Environmental dataset. This was for two reasons. First, in the Eastern leak quantification data (provided in Appendix F, [45]), information is not provided on components measured. Therefore, quantified emissions cannot be connected to the

screening values contained in Appendix E. Second, the Eastern dataset does not report how they assigned leak volumes to the 81 instrument readings > 10,000 ppmv which were not quantified with the Hi Flow sampler. Therefore, component-by-component distributions can only be generated for API 4598.

After digitization and re-engineering of the GHGI methods, we can compare the distributions of the resulting component-level estimates with our dataset (**Figure 4**, with additional comparisons in SI Section 5.2.5).

Tank emissions

To reconstruct emission factors for crude and condensate storage tanks, we begin by downloading GHGRP data from the “Envirofacts GHG Customized Search” tool [66]. After gathering the data, we divide the dataset by product stream (natural gas, petroleum systems) and tank class. However, before making any comparisons with this study, we need to adjust how emissions-factors are reported by the GHGI. The GHGI reports storage tank emission factors on a throughput-basis (kgCH₄/bbl/year) and our study reports emission factors on a tank basis (kgCH₄/tank/day). Fortunately, in addition to tank throughput, atmospheric storage tank counts per sub-basin are also reported to the GHGRP by tank class.

Emissions-factor distributions (**Figure 5**) are calculated by dividing total emissions by tank count for every sub-basin (or row in the downloaded dataset). See SI Section 5.3 for additional details on this calculation. In SI Section 5.3, we validate this approach by calculating and comparing throughput-basis emission factors with those reported in the GHGI.

Acknowledgements

This work was funded by the California Air Resources Board, grant 18ISD011. Support for the work was also provided by Novim under a Limited Sponsorship Agreement with the Joint Institute for Strategic Energy Analysis of NREL.

References

- [1] T. F. Stocker *et al.*, *Climate change 2013 the physical science basis: Working Group I contribution to the fifth assessment report of the intergovernmental panel on climate change*. 2013.
- [2] (EPA) Environmental Protection Agency, “Overview of Greenhouse Gases.” <https://www.epa.gov/ghgemissions/overview-greenhouse-gases>.
- [3] Q. Saunio, M., Stavert, A. R., Poulter, B., Bousquet, P., Canadell, J. G., Jackson, R. B., Raymond, P. A., Dlugokencky, E. J., Houweling, S., Patra, P. K., Ciais, P., Arora, V. K., Bastviken, D., Bergamaschi, P., Blake, D. R., Brailsford, G., Bruhwiler, L., “The Global Methane Budget 2000–2017,” *Earth Syst. Sci. Data Discuss*, doi: <https://doi.org/10.5194/essd-2019-128>.
- [4] P. Friedlingstein *et al.*, “Global carbon budget 2019,” *Earth Syst. Sci. Data*, 2019, doi: 10.5194/essd-11-1783-2019.
- [5] R. W. Howarth, R. Santoro, and A. Ingraffea, “Methane and the greenhouse-gas footprint of natural gas from shale formations,” *Clim. Change*, vol. 106, no. 4, p. 679, 2011.

- [6] R. W. Howarth, “A bridge to nowhere: methane emissions and the greenhouse gas footprint of natural gas,” *Energy Sci. Eng.*, vol. 2, no. 2, pp. 47–60, 2014.
- [7] L. M. Cathles, L. Brown, M. Taam, and A. Hunter, “A commentary on ‘The greenhouse-gas footprint of natural gas in shale formations’ by R.W. Howarth, R. Santoro, and Anthony Ingraffea,” *Clim. Change*, 2012, doi: 10.1007/s10584-011-0333-0.
- [8] R. A. Alvarez, S. W. Pacala, J. J. Winebrake, W. L. Chameides, and S. P. Hamburg, “Greater focus needed on methane leakage from natural gas infrastructure,” *Proc. Natl. Acad. Sci.*, 2012.
- [9] (EPA) Environmental Protection Agency, “Inventory of Greenhouse Gas Emissions and Sinks,” 2019.
- [10] B. Hmiel *et al.*, “Preindustrial 14CH₄ indicates greater anthropogenic fossil CH₄ emissions,” *Nature*, 2020, doi: 10.1038/s41586-020-1991-8.
- [11] A. R. Brandt *et al.*, “Methane leaks from North American natural gas systems,” *Science (80-.)*, vol. 343, no. 6172, pp. 733–735, 2014.
- [12] D. Zavala-Araiza *et al.*, “Reconciling divergent estimates of oil and gas methane emissions,” *Proc. Natl. Acad. Sci. U. S. A.*, 2015, doi: 10.1073/pnas.1522126112.
- [13] R. A. Alvarez *et al.*, “Assessment of methane emissions from the US oil and gas supply chain,” *Science (80-.)*, p. eaar7204, 2018.
- [14] A. Karion *et al.*, “Methane emissions estimate from airborne measurements over a western United States natural gas field,” *Geophys. Res. Lett.*, 2013, doi: 10.1002/grl.50811.
- [15] J. Peischl *et al.*, “Quantifying atmospheric methane emissions from oil and natural gas production in the Bakken shale region of North Dakota,” *J. Geophys. Res.*, 2016, doi: 10.1002/2015JD024631.
- [16] J. Peischl *et al.*, “Quantifying atmospheric methane emissions from the Haynesville, Fayetteville, and northeastern Marcellus shale gas production regions,” *J. Geophys. Res.*, 2015, doi: 10.1002/2014JD022697.
- [17] S. M. Miller *et al.*, “Anthropogenic emissions of methane in the United States,” *Proc. Natl. Acad. Sci. U. S. A.*, 2013, doi: 10.1073/pnas.1314392110.
- [18] S. Schwietzke *et al.*, “Improved Mechanistic Understanding of Natural Gas Methane Emissions from Spatially Resolved Aircraft Measurements,” *Environ. Sci. Technol.*, 2017, doi: 10.1021/acs.est.7b01810.
- [19] G. Pétron *et al.*, “A new look at methane and nonmethane hydrocarbon emissions from oil and natural gas operations in the Colorado Denver-Julesburg Basin,” *J. Geophys. Res.*, 2014, doi: 10.1002/2013JD021272.
- [20] A. Karion *et al.*, “Aircraft-Based Estimate of Total Methane Emissions from the Barnett Shale Region,” *Environ. Sci. Technol.*, 2015, doi: 10.1021/acs.est.5b00217.
- [21] R. Harriss, R. A. Alvarez, D. Lyon, D. Zavala-Araiza, D. Nelson, and S. P. Hamburg, “Using Multi-Scale Measurements to Improve Methane Emission Estimates from Oil and Gas Operations in the Barnett Shale Region, Texas,” *Environmental Science and Technology*. 2015, doi: 10.1021/acs.est.5b02305.
- [22] T. I. Yacovitch *et al.*, “Mobile Laboratory Observations of Methane Emissions in the Barnett Shale Region,” *Environ. Sci. Technol.*, 2015, doi: 10.1021/es506352j.
- [23] C. W. Rella, T. R. Tsai, C. G. Botkin, E. R. Crosson, and D. Steele, “Measuring emissions from oil and natural gas well pads using the mobile flux plane technique,” *Environ. Sci. Technol.*, 2015, doi: 10.1021/acs.est.5b00099.
- [24] H. L. Brantley, E. D. Thoma, W. C. Squier, B. B. Guven, and D. Lyon, “Assessment of methane emissions from oil and gas production pads using mobile measurements,” *Environ. Sci. Technol.*, 2014, doi: 10.1021/es503070q.
- [25] (EPA) Environmental Protection Agency, “Inventory of U.S. Greenhouse Gas Emissions and Sinks: 1990 - 2018,” 2020.

- [26] The White House, “Climate action plan: Strategy to reduce methane emissions,” in *Methane: Emission Sources and Reduction Strategies*, 2015.
- [27] J. Penman, M. Gytarsky, T. Hiraishi, W. Irving, and T. Krug, *2006 IPCC - Guidelines for National Greenhouse Gas Inventories*. 2006.
- [28] Heath, G., Warner, E., Steinberg, D., Brandt, A.R., “Estimating U.S. Methane Emissions from the Natural Gas Supply Chain: Approaches, Uncertainties, Current Estimates, and Future Studies,” Golden, CO, 2015.
- [29] Office of Inspector General EPA, “EPA Needs to Improve Air Emissions Data for the Oil and Natural Gas Production Sector,” 2013.
- [30] A. R. Brandt, G. A. Heath, and D. Cooley, “Methane Leaks from Natural Gas Systems Follow Extreme Distributions,” *Environ. Sci. Technol.*, 2016, doi: 10.1021/acs.est.6b04303.
- [31] T. L. Vaughn *et al.*, “Temporal variability largely explains top-down/bottom-up difference in methane emission estimates from a natural gas production region,” *Proc. Natl. Acad. Sci. U. S. A.*, 2018, doi: 10.1073/pnas.1805687115.
- [32] D. Zavala-Araiza *et al.*, “Super-emitters in natural gas infrastructure are caused by abnormal process conditions,” *Nat. Commun.*, 2017, doi: 10.1038/ncomms14012.
- [33] D. T. Allen *et al.*, “Measurements of methane emissions at natural gas production sites in the United States,” *Proc. Natl. Acad. Sci. U. S. A.*, 2013, doi: 10.1073/pnas.1304880110.
- [34] M. Omara *et al.*, “Methane Emissions from Natural Gas Production Sites in the United States: Data Synthesis and National Estimate,” *Environ. Sci. Technol.*, vol. 52, no. 21, pp. 12915–12925, 2018.
- [35] Star Environmental, “Fugitive hydrocarbon emissions from oil and gas production operations. API Publication 4589,” 1993.
- [36] A. P. Pacsi *et al.*, “Equipment leak detection and quantification at 67 oil and gas sites in the Western United States,” *Elementa*, 2019, doi: 10.1525/elementa.368.
- [37] Clearstone Engineering Ltd., “Update of Equipment, Component and Fugitive Emission Factors for Alberta Upstream Oil and Gas,” Calgary, AB, 2018.
- [38] (ERG) Eastern Research Group, “City of Fort Worth Natural Gas Air Quality Study,” Morrisville, NC, 2011.
- [39] Gas Technology Institute, “Gas Resource Database: Unconventional Natural Gas and Gas Composition Databases,” 2001.
- [40] Enervus, “Enervus Exploration and Production.” <https://www.enverus.com/industry/exploration-and-production/>.
- [41] D. Zavala-Araiza *et al.*, “Toward a Functional Definition of Methane Super-Emitters: Application to Natural Gas Production Sites,” *Environ. Sci. Technol.*, 2015, doi: 10.1021/acs.est.5b00133.
- [42] D. R. Lyon, R. A. Alvarez, D. Zavala-Araiza, A. R. Brandt, R. B. Jackson, and S. P. Hamburg, “Aerial Surveys of Elevated Hydrocarbon Emissions from Oil and Gas Production Sites,” *Environ. Sci. Technol.*, 2016, doi: 10.1021/acs.est.6b00705.
- [43] J. Campbell, L., Campbell, M., Cowgill, M., Epperson, D., Hall, M., Harrison, M., Hummel, K., Myers, D., Shires, T., Stapper, B., Stapper, C., Wessel, “Methane emissions from the natural gas industry. Volume 11: Compressor driver exhaust,” 1996.
- [44] New Source Performance Standard, “Stationary Engines: SI Engines (NSPS). C.F.R., Title 40, Part 60, Subpart JJJJ.” 2008, [Online]. Available: https://www.dieselnet.com/standards/us/stationary_nsps_si.php#ng.
- [45] Star Environmental, “Fugitive Hydrocarbon Emissions: Eastern Gas Wells,” 1995.

- [46] (EPA) Environmental Protection Agency, “Protocol for Equipment Leak Emission Estimates. Report No. EPA-453/R-95-017,” 1995.
- [47] Star Environmental, “Emission factors for oil and gas production operations. API Publication 4615,” 1995.
- [48] Code of Federal Regulations, *Title 40 Part 98 Subpart W, Petroleum and Natural Gas Systems*. 2010.
- [49] (API) American Petroleum Institute, “PRODUCTION TANK EMISSIONS MODEL - A PROGRAM FOR ESTIMATING EMISSIONS FROM HYDROCARBON PRODUCTION TANKS - E&P TANK VERSION 2.0,” 2000.
- [50] aspentech, “HYSYS 2004 Simulation basis,” 2004.
- [51] (ERG) Eastern Research Group, “Condensate Tank Oil and Gas Activities,” 2012.
- [52] S. N. Lyman, T. Tran, M. L. Mansfield, and A. P. Ravikumar, “Aerial and ground-based optical gas imaging survey of Uinta Basin oil and gas wells,” *Elementa*, 2019, doi: 10.1525/elementa.381.
- [53] B. Mansfield, Marc L., Lyman, S., O’Neil, T., Anderson, R., Jones, C., Tran, H., Mathis, J., Barickman, P., Oswald, W., LeBaron, “STORAGE TANK EMISSIONS PILOT PROJECT (STEPP): FUGITIVE ORGANIC COMPOUND EMISSIONS FROM LIQUID STORAGE TANKS IN THE UINTA BASIN,” 2017.
- [54] J. G. Englander, A. R. Brandt, S. Conley, D. R. Lyon, and R. B. Jackson, “Aerial Interyear Comparison and Quantification of Methane Emissions Persistence in the Bakken Formation of North Dakota, USA,” *Environ. Sci. Technol.*, 2018, doi: 10.1021/acs.est.8b01665.
- [55] A. Bradbury, J., Obeiter, M., Draucker, L., Wang, W., Stevens, “Clearing the air: reducing upstream greenhouse gas emissions from US natural gas systems,” 2013.
- [56] ICF International, “Economic Analysis of Methane Emission Reduction Opportunities in the US Onshore Oil and Natural Gas Industries,” Fairfax, VA, 2014.
- [57] Y. Gan *et al.*, “Carbon footprint of global natural gas supplies to China,” *Nat. Commun.*, 2020, doi: 10.1038/s41467-020-14606-4.
- [58] G. et al Domke, “2019 Refinement to the 2006 IPCC Guidelines for National Greenhouse Gas Inventories. Vol 4. Chapter 4. Forest Land,” *Forestry*, 2019, doi: 10.1016/j.phrs.2011.03.002.
- [59] D. T. Allen *et al.*, “Methane emissions from process equipment at natural gas production sites in the United States: Pneumatic controllers,” *Environ. Sci. Technol.*, 2015, doi: 10.1021/es5040156.
- [60] C. S. Bell *et al.*, “Comparison of methane emission estimates from multiple measurement techniques at natural gas production pads,” *Elementa*, 2017, doi: 10.1525/elementa.266.
- [61] E. D. Thoma, P. Deshmukh, R. Logan, M. Stovern, C. Dresser, and H. L. Brantley, “Assessment of Uinta Basin Oil and Natural Gas Well Pad Pneumatic Controller Emissions,” *J. Environ. Prot. (Irvine, Calif.)*, 2017, doi: 10.4236/jep.2017.84029.
- [62] (EPA) Environmental Protection Agency, “Additional Revisions Considered for 2018 and Future GHGIs,” 2018. [Online]. Available: www.epa.gov/sites/production/files/2018-04/documents/ghgemissions_additional_revisions_2018.pdf.
- [63] (EPA) Environmental Protection Agency, “Revision to Well Counts Data,” 2015. <https://www.epa.gov/sites/production/files/2015-12/documents/revision-data-source-well-counts-4-10-2015.pdf>.
- [64] M. R. Hummel, K.E., Campbell, L.M. and Harrison, “Methane Emissions from the Natural Gas Industry. Volume 8. Equipment Leaks,” 1996.
- [65] Star Environmental, “Calculation Workbook for Oil and Gas Production Equipment Fugitive Emissions. API Publication 4638,” 1996.

- [66] (EPA) Environmental Protection Agency, “Greenhouse gas customized search.”
<https://www.epa.gov/enviro/greenhouse-gas-customized-search>.